

INTERNATIONAL SERIES OF MONOGRAPHS IN  
THE SCIENCE OF THE SOLID STATE  
GENERAL EDITOR: B. R. PAMPLIN

---

VOLUME 8

**ELECTRONIC STATES  
AND OPTICAL TRANSITIONS IN SOLIDS**

INTRODUCTION TO VOLUME 8  
Ecole Polytechnique Fédérale de Lausanne  
PHB  
M. GELLMAN  
1971

OTHER TITLES IN THE SERIES IN THE SCIENCE OF THE SOLID STATE

- VOL. 1. GREENAWAY AND HARBEKE—Optical Properties and Band Structures of Semiconductors.
- VOL. 2. RAY—II-VI Compounds.
- VOL. 3. NAG—Theory of Electrical Transport in Semiconductors.
- VOL. 4. JARZEBSKI—Oxide Semiconductors
- VOL. 5. SHARMA AND PUROHIT—Semiconductor Heterojunctions
- VOL. 6. PAMPLIN—Crystal Growth
- VOL. 7. SHAY AND WERNICK—Ternary Chalcopyrite Semiconductors. Growth, Electronic Properties and Applications

BIBLIOTHÈQUE DU  
DÉPARTEMENT DE PHYSIQUE  
Ecole Polytechnique Fédérale  
PHB - Ecole poly  
CH - 1015 LAUSANNE SUISSE

TAT

# ELECTRONIC STATES AND OPTICAL TRANSITIONS IN SOLIDS

by

F. BASSANI

Professor of Solid State Physics, University of Rome

and

**G. PASTORI PARRAVICINI**

Professor of Solid State Physics, University of Pisa

Edited by

**R. A. BALLINGER**

Senior Lecturer in Mathematical Physics, University of Bath

BIBLIOTHÈQUE DU  
DÉPARTEMENT SCIENTIFIQUE  
Ecole Polytechnique  
PHYSIQUE  
C. J. M. - 1971  
1971



**PERGAMON PRESS**  
OXFORD · NEW YORK · TORONTO  
SYDNEY · BRAUNSCHWEIG

Pergamon Press Ltd., Headington Hill Hall, Oxford  
Pergamon Press Inc., Maxwell House, Fairview Park, Elmsford,  
New York 10523  
Pergamon of Canada Ltd., 207 Queen's Quay West, Toronto 1  
Pergamon Press (Aust.) Pty. Ltd., 19a Boundary Street,  
Rushcutters Bay, N.S.W. 2011, Australia  
Pergamon Press GmbH, Burgplatz 1, Braunschweig 3300, West Germany

---

Copyright © 1975 F. Bassani and G. Pastori Parravicini

*All Rights Reserved. No part of this publication may be  
reproduced, stored in a retrieval system, or transmitted, in any  
form or by any means, electronic, mechanical, photocopying,  
recording or otherwise, without the prior permission of  
Pergamon Press Ltd.*

First edition 1975

Library of Congress Cataloging in Publication Data

Bassani, Giuseppe Franco, 1929-  
Electronic states and optical transitions in solids.  
(International series of monographs in the science  
of the solid state, v. 8)  
Includes bibliographical references.  
1. Energy-band theory of solids. 2. Solids-  
Optical properties. I. Parravicini, G. Pastori,  
joint author. II. Title.  
QC176.8.E4B37 530.4'1 74-8112  
ISBN 0-08-016846-9

BIBLIOTHÈQUE DU  
DÉPARTEMENT DE PHYSIQUE  
Ecole Polytechnique Fédérale  
PHB - Ecublens  
**CH-1015 LAUSANNE** Suisse  
TÉL. 021-47 11 11

## CONTENTS

<b>1 USE OF SYMMETRY IN QUANTUM MECHANICS</b>	<b>1</b>
1-1 Groups and their properties	1
1-2 Group representations	5
1-2a Definitions and basic theorems	5
1-2b Rules for constructing the character table of a group	8
1-2c Further relationships among representations	12
1-3 Representations and eigenfunctions	15
1-3a Classification of the eigenstates	15
1-3b Projection operators and orthogonality theorems on partner functions	17
1-3c Further relationships between representations and basis functions	19
1-4 Rotation and rotation-inversion groups	20
1-4a Irreducible representations of rotation and rotation-inversion groups	20
1-4b Decomposition of the irreducible representations of the rotation-inversion group into irreducible representations of finite groups	22
1-5 Spin dependent functions and double groups	23
1-5a Transformation of spin functions under proper and improper rotations	23
1-5b Irreducible representations of double groups	26
1-5c Decomposition of the states of a simple group into the states of a double group	30
1-6 Time reversal symmetry	31
1-6a The time reversal operator	31
1-6b Essential degeneracies due to time reversal symmetry	35
1-7 Selection rules	38
References and notes	39
 <b>2 SYMMETRY PROPERTIES OF THE ELECTRONIC STATES IN CRYSTALS</b>	<b>41</b>
2-1 Translation group and Brillouin zone	41
2-2 Space groups	46
2-2a Irreducible representations of the space groups	46
2-2b Additional irreducible representations of the space groups and spin-orbit splitting	56
2-3 Additional degeneracies required by time reversal symmetry	58
2-4 Selection rules	63
2-4a Selection rules at a given point of the Brillouin zone	63
2-4b Selection rules connecting different points of the Brillouin zone	64
References and notes	66
 <b>3 METHODS OF CALCULATING THE ELECTRONIC BAND STRUCTURES OF CRYSTALS</b>	<b>67</b>
3-1 The basic approximations	67
3-2 The tight binding method	71
3-2a Description of the method	71
3-2b Matrix elements of the secular equation appearing in the tight binding method	72
3-2c Symmetrized combinations of Bloch sums	75
3-2d Discussion of the tight binding method	76
3-3 The orthogonalized plane wave method	77
3-3a Description of the method	77
3-3b Matrix elements of the secular equation appearing in the OPW method	78
3-3c Use of crystal symmetry in the OPW method	79

## CONTENTS

3-3 d Discussion of the OPW method	80
3-3 e Perturbative approach to the OPW method	81
3-4 The pseudopotential method	83
3-4 a Formulation of the pseudopotential method	83
3-4 b Pseudopotential approximation	85
3-5 The cellular method	86
3-5 a Description of the method	86
3-5 b Relevant aspects of the cellular method	87
3-6 The augmented plane wave method	89
3-6 a Description of the method	89
3-6 b Discussion of the APW method	90
3-7 Green's function method	91
3-8 The quantum defect method	93
3-9 The $k \cdot p$ method	94
3-10 Relativistic effects	97
3-10 a General considerations	97
3-10 b Relativistic effects in atoms	98
3-10 c Relativistic effects in crystals	100
References and notes	102
<b>4 ELECTRONIC BAND STRUCTURE IN SOME CRYSTALS</b>	104
4-1 Energy bands of isoelectronic semiconductors with the diamond and zincblende structure	104
4-1 a Symmetry properties of the diamond lattice	104
4-1 b Electronic state calculations in diamond, silicon, germanium, and grey tin	108
4-1 c Symmetry properties of the zincblende lattice	115
4-1 d Electronic states in isoelectronic semiconductors with zincblende structure	117
4-2 Energy bands of layer type crystals	120
4-2 a Symmetry properties of graphite and hexagonal BN in the two-dimensional approximation	120
4-2 b Electronic state calculations for graphite and BN in the two-dimensional approximation	125
4-2 c Electronic states of graphite and BN in the three-dimensional case	129
4-2 d Considerations on other layer structures	130
4-3 Energy bands of linear chain type crystals: selenium and tellurium	134
4-3 a Symmetry properties of the selenium structure	134
4-3 b Energy bands for selenium and tellurium	137
4-4 Considerations on the band structure of some large gap insulators	138
4-5 Considerations on the band structure of some molecular crystals	142
4-6 Considerations on the band structure of simple metals	143
References and notes	146
<b>5 INTERBAND TRANSITIONS AND OPTICAL PROPERTIES</b>	149
5-1 General theoretical analysis of band-to-band optical transitions	149
5-1 a Basic approximations	149
5-1 b Quantum theory of band-to-band transitions	150
5-1 c Connection with the optical constants	153
5-2 Structure of the optical constants at critical points	155
5-2 a Theoretical discussion	155
5-2 b Experimental evidence. Two examples: germanium and graphite	160
5-3 Multiphoton transitions	164
5-4 Indirect band-to-band transitions	168
5-4 a General remarks and electron-phonon interaction	168
5-4 b Properties of indirect transitions	170
Appendix 5A Matrix elements of one-electron and two-electron operators between determinantal states	172

## CONTENTS

Appendix 5B Koopmans' approximation	174
References and notes	176
<b>6 EXCITONS IN CRYSTALS</b>	<b>177</b>
<b>6-1 General considerations</b>	<b>177</b>
<b>6-2 Tight binding excitons</b>	<b>178</b>
6-2a Tight binding excitons in a two-band model	178
6-2b Relevant aspects of the tight binding exciton theory	182
6-2c Optical transitions with exciton effects	183
<b>6-3 Weak binding excitons</b>	<b>184</b>
6-3a Weak binding excitons in a two-band model	184
6-3b Examples of solution of the effective mass equation	187
6-3c Optical properties with exciton effects in a two-band model semiconductor	190
6-3d Excitons at the edge of degenerate bands. Two examples	196
<b>6-4 Intermediately bound excitons</b>	<b>201</b>
6-4a Theory and general considerations	201
6-4b An example: solid argon	203
6-4c Comments on polarization screening	204
<b>6-5 Two-photon exciton transitions</b>	<b>205</b>
<b>6-6 Indirect exciton transitions</b>	<b>206</b>
<b>6-7 Interband mixing and high energy excitons</b>	<b>210</b>
Appendix 6A Evaluation of matrix elements appearing in the tight binding exciton theory	211
Appendix 6B Effective mass equation for weakly bound excitons	213
References and notes	216
<b>7 IMPURITY STATES IN INSULATORS AND SEMICONDUCTORS</b>	<b>218</b>
<b>7-1 Introduction</b>	<b>218</b>
<b>7-2 Tightly bound impurity states</b>	<b>219</b>
7-2a General remarks and classification of the states	219
7-2b Many-electron states	223
7-2c Computation of the splittings	225
7-2d Selection rules for optical transitions—Ligand field mixing	230
<b>7-3 Shallow impurity states</b>	<b>231</b>
7-3a Introduction	231
7-3b General formulation of the impurity problem	232
7-3c Effective mass approximation and applications	235
7-3d Intervalley mixing and degenerate bands	240
7-3e Band mixing and resonant states	244
<b>7-4 Intermediately bound impurity states. Isoelectronic impurities</b>	<b>248</b>
<b>7-5 Considerations on optical transition processes involving impurities</b>	<b>251</b>
References and notes	253
<b>8 EFFECTS OF EXTERNAL PERTURBATIONS</b>	<b>255</b>
<b>8-1 Introduction and general remarks</b>	<b>255</b>
<b>8-2 Effect of hydrostatic pressure and alloying</b>	<b>256</b>
<b>8-3 Effect of uniaxial stresses</b>	<b>263</b>
<b>8-4 Electronic states and optical constants of crystals in an electric field</b>	<b>267</b>
8-4a General remarks	267
8-4b Theory of electric field effects on interband transitions	269

## CONTENTS

8-5 Electronic states and optical constants in a magnetic field	276
8-5a General remarks and effective mass formulation	276
8-5b Magnetic quantum levels	277
8-5c Interband transitions in a magnetic field and selection rules	281
8-5d Degenerate bands and interband coupling	284
8-6 Excitons in a magnetic field	286
Appendix 8A Electron in a uniform electric field	291
References and notes	292
Subject index	295

BIBLIOTHÈQUE DU  
DÉPARTEMENT DE PHYSIQUE  
Ecole Polytechnique Fédérale  
PHB - LIBRAIRIE  
CH - 1015 LAUSANNE SUISSE  
Tél. 021-47 11 11

## PREFACE

THE aim of this book is to give a self-contained account of the theoretical foundations and of the basic data relating to the electronic energy levels and wave functions in solids.

Our original idea, when Dr. B. R. Pamplin invited us to write a monograph as the theoretical counterpart of the book by Greenaway and Harbeke on optical properties, was to review the band structure of crystals, emphasizing the role of symmetry. The reasons why crystals with the same number of valence electrons per unit cell and the same symmetry have similar energy band properties began to be understood in the early sixties. As more sophisticated band structure calculations became available in an increasing variety of materials, simple criteria to determine the sequence of the energy levels maintained their usefulness, and their validity was confirmed. It turns out that the full symmetry of the space group is the essential feature in determining the structure of the electronic levels; the available electrons then fill the frame and this accounts for the basic properties of the material.

As in atomic physics, the most precise and direct analysis of the electronic structure is provided by the optical excitation spectrum and it seemed that a band structure monograph without an account of the interaction of electrons with the electromagnetic field would be lifeless. This prompted us to expand our scope to interband transitions and to exciton states, keeping the symmetry determined properties as our guidelines.

Impurity states and the effect of external perturbations were then considered, as further probes for the band structure, as well as for their intrinsic interest. We tried here to emphasize the connection between states of the perfect lattice and states of the perturbed lattice and found again the symmetry arguments extremely useful.

As a final result, what was originally intended as a monograph developed into a textbook. Though its domain is not as extended as that of the classical textbooks in the theory of solids (those of Seitz, Slater, Kittel, and Ziman for instance) it is nevertheless sufficiently wide to be used in advanced courses. This book is self-contained and does not require outside references for comprehension. The pedagogical novelty may be the frequent use of group theoretical arguments, but we found from experience that one quickly learns to master group theory as a simple algebra without perhaps having to understand all its subtleties; this we tried to teach from the beginning. No previous knowledge is implied except for the basic quantum mechanical foundations as are taught in undergraduate courses. Information on elementary crystallography and descriptive facts about solids can be of help, but are not essential.

A problem we had to face was how to move in the wide forests of the literature. We could have refrained from all quotations except to books, monographs, and to some review articles, but we are aware that many readers are interested to learn more on some specific topics and like to find a guide to original papers. We decided then

## PREFACE

to refer to some articles, and by necessity we mentioned only some of those we are most familiar with because of our specific research interests at one time or another. We do not claim to have been fair or accurate and we must apologize to our colleagues on this account.

The final manuscript was completed at the École Polytechnique Fédérale of Lausanne, where one of us (Franco Bassani) was invited to lecture on this subject within the post-graduate programme of Swiss Western Universities (CICP). The list of friends and colleagues who helped us is too long to quote here. We are grateful to all of them. Acknowledgements are due to Dr. R. A. Ballinger for his pains in correcting an earlier version of the manuscript and for his constructive criticisms and suggestions.

Before closing, we owe special thanks to Professor F. Seitz who encouraged us in this field; we consider ourselves very fortunate to have been at the University of Illinois in the early years of our professional life.

*Lausanne 1973*

FRANCO BASSANI

G. PASTORI PARRAVICINI

BIBLIOTHÈQUE DU  
DÉPARTEMENT DE PHYSIQUE  
Ecole Polytechnique Fédérale  
PHYSIQUE  
CH-1015 LAUSANNE Suisse  
Tél. 021-471111

## CHAPTER 1

### USE OF SYMMETRY IN QUANTUM MECHANICS

THE fundamental problem of quantum mechanics is to solve the Schrödinger equation or the Dirac equation, to determine energy levels and eigenfunctions. Except for some standard problems (such as the harmonic oscillator, hydrogenic atoms, and so on) the solutions of an eigenvalue problem cannot be obtained exactly; in general, rather laborious approximation procedures are required. The symmetry properties of the Hamiltonian operator can be used in these cases to simplify the problem and to obtain the symmetry properties of the exact solutions. In particular, the group theoretical study of an operator's symmetry properties makes it possible to classify its eigenstates, to determine essential degeneracies, to derive selection rules, and to reduce the order of the secular determinants which must be diagonalized in order to compute approximate eigenvalues. Though all group theoretical results are contained in the basic equations of quantum mechanics, in practice group theory is an essential tool for the quantum mechanical study of atoms, molecules, and crystals.

In this chapter we wish to present elements of group theory which are required for classifying electronic states and which are useful in computing them. We will give only the basic elements emphasizing the operational point of view, and will refer to some of the standard books on group theory for demonstrating most of the results. The purpose is not that of adding to the excellent existing literature on group theory, but rather of providing non-experts with a working knowledge of it. We believe that this chapter will also be useful to people who already know some group theory but have not applied it extensively to problems of solid state physics.

#### 1-1 Groups and their properties<sup>[1]</sup>

A group is an ensemble  $\mathcal{G}$  of elements among which a multiplication operation is defined which associates a third element with any ordered pair and which satisfies the following requirements:

- (i) The product of any two elements in  $\mathcal{G}$  is also an element of  $\mathcal{G}$ .
- (ii) The associative law of multiplication holds for any three elements  $R_i, R_j, R_l$  of  $\mathcal{G}$ .

$$R_i(R_jR_l) = (R_iR_j)R_l.$$

- (iii) There is in  $\mathcal{G}$  only one identity or unit element  $E$  such that

$$ER_i = R_iE = R_i$$

for any  $R_i$  of  $\mathcal{G}$ .

## ELECTRONIC STATES AND OPTICAL TRANSITIONS

- (iv) Every element  $R_i$  of  $\mathcal{G}$  has a unique inverse  $R_i^{-1}$  which is a member of the ensemble and satisfies:

$$R_i R_i^{-1} = R_i^{-1} R_i = E.$$

The number of elements in the group is called the *order* of the group. For our purposes we will mainly consider finite order groups, i.e. groups containing a finite number of elements.

If the products are commutative so that

$$R_i R_j = R_j R_i$$

for any element  $R_i$ ,  $R_j$  of  $\mathcal{G}$ , the group is said to be commutative or *abelian*.

A group constituted from the sequence of elements  $R, R^2, \dots, R^n = E$  is said to form a *cyclic group* of order  $n$  generated by  $R$ . We note that all cyclic groups are also abelian.

Two groups  $\mathcal{G}(R)$  and  $\mathcal{G}(R')$  are said to be *isomorphic* when it is possible to establish a one-to-one correspondence between their elements so that  $R_i R_j = R_l$  implies  $R'_i R'_j = R'_l$ , and vice versa.

Any subset of elements within a group  $\mathcal{G}$ , which in itself forms a group, is called a *subgroup* of  $\mathcal{G}$ .

It is useful at this point to introduce the notion of *complex* as a collection  $\mathcal{A} = A_1, A_2, \dots, A_n$  of elements in a group. In a complex, a given element may appear more than once. We define as *product*  $\mathcal{A} \cdot \mathcal{B}$  of two complexes  $\mathcal{A} = A_1, A_2, \dots, A_n$  and  $\mathcal{B} = B_1, B_2, \dots, B_m$  the complex containing the set of elements

$$A_1 B_1, A_2 B_1, \dots, A_n B_1; \dots; A_1 B_m, A_2 B_m, \dots, A_n B_m.$$

The elements of the complex  $\mathcal{A} \cdot \mathcal{B}$  are thus obtained when all the elements of  $\mathcal{A}$  are multiplied on the right by all the elements of  $\mathcal{B}$ .

We define as *inner product* ( $\mathcal{A} \cdot \mathcal{B}$ ) of two complexes the complex obtained by listing *only once* the distinct elements of the complex  $\mathcal{A} \cdot \mathcal{B}$ .

Two elements  $R_i$  and  $R_j$  of a group  $\mathcal{G}(R)$  are said to be *conjugate* if we can find an element  $X$  in  $\mathcal{G}$  so that

$$R_i = X^{-1} R_j X.$$

The ensemble of all mutually conjugate elements of a group constitute a *class* of the group. The elements of a group can be separated into classes by considering for every element  $R_i$  all its conjugate elements  $X^{-1} R_i X$ , obtained by letting  $X$  range over all the elements of the group. The distinct elements so obtained form a class. We note that the identity  $E$  always forms a class by itself. If a group is abelian, the number of classes is equal to the number of elements in the group.

Let  $\mathcal{C}_i$  and  $\mathcal{C}_j$  indicate two classes of a group and  $\mathcal{C}_i \cdot \mathcal{C}_j$  the complex obtained by multiplying all the elements of  $\mathcal{C}_i$  by all the elements of  $\mathcal{C}_j$ . It can be proved<sup>[11]</sup> that the product of two classes is composed of a number of classes in the group. Thus we can write

$$\mathcal{C}_i \cdot \mathcal{C}_j = \sum_s c_{ijs} \mathcal{C}_s, \quad (1-1)$$

where  $c_{ijs}$  are integer numbers (including zero).

Let  $\mathcal{S} = E, S_2, S_3, \dots$ , be a subgroup of a group  $\mathcal{G}$ . We call *right coset*  $\mathcal{S} \cdot X$  the set of elements  $EX, S_2 X, S_3 X, \dots$ , obtained by multiplying all the elements of the subgroup  $\mathcal{S}$  by an element  $X$  of the group  $\mathcal{G}$ . In a similar way we define the set of ele-

## USE OF SYMMETRY IN QUANTUM MECHANICS

ments  $XE$ ,  $XS_2$ ,  $XS_3$ , ..., as being the *left coset*  $X \cdot \mathcal{S}$ . Two right (or left) cosets of a subgroup  $\mathcal{S}$  are either identical or have no elements in common. A subgroup and all its *distinct* right (or left) cosets contain all the elements of the group once and only once. From this it follows that the order of a subgroup is a divisor of the order of the group.

If a subgroup  $\mathcal{S}$  of a group  $\mathcal{G}$  consists of complete classes of  $\mathcal{G}$  it is called an *invariant* or a *normal subgroup*. An invariant subgroup is characterized by the fact that its right and left cosets are identical. An invariant subgroup  $\mathcal{S}$  and its distinct cosets considered as entities in themselves, constitute a group when the multiplication operation is defined as the *inner product* among the above complexes. Such a group is called *factor group* of the normal subgroup.

Let  $\mathcal{G}_1(R)$  and  $\mathcal{G}_2(S)$  be two groups in which all the elements of the first group commute with all the elements of the second, and the groups have in common only the identity  $E$ . It can be shown that all possible elements  $RS$  constitute a group  $\mathcal{G}_1 \times \mathcal{G}_2$  called the *direct product* of  $\mathcal{G}_1$  and  $\mathcal{G}_2$ . The order of the direct product of two groups is equal to the product of the order of the two composing groups.

### *Illustrative examples*

As an example of how the definitions and results so far described may be applied, we consider the group of transformations which leave the figure of a cube coincident with its original position. The symmetry group of a cube<sup>[1]</sup> (called  $O_h$ ) is very important in crystal physics, and throughout this book we will often refer to this group to illustrate operational applications of general results of group theory. With the aid of Fig. 1-1

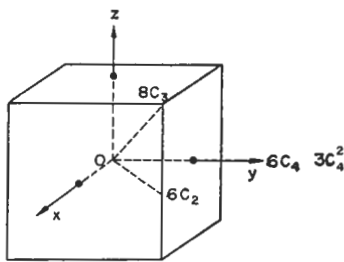


FIG. 1-1. The symmetry elements of a cube.

CH-ABU  
 DÉPARTEMENT DE LA  
 Ecole Polytechnique Fédérale de Lausanne  
 CH-1015 LAUSANNE SWITZERLAND  
 Tél. 021-417 11 11

it is possible to determine the symmetry operations for the cubic group  $O_h$ . There are a total of 48 symmetry operations, namely:

- The identity ( $E$ ).
- The rotations by  $\pi$  about the axes  $x, y, z (3C_4^2)$ .
- The rotations by  $\pm\pi/2$  about the axes  $x, y, z (6C_4)$ .
- The rotations by  $\pi$  about the bisectrices in the planes  $xy, yz, xz (6C_2)$ .
- The rotations by  $\pm 2\pi/3$  about the four diagonals of the cube ( $8C_3$ ).
- The combination of the inversion ( $I$ ) with the above 24 symmetry operations.

The symbols  $E$ ,  $I$ , and  $C_n$  have been used to indicate the identity, the spatial inversion through the centre and a rotation by  $2\pi/n$  respectively. In Table 1-1 all the 48 symmetry operations of the group  $O_h$  are listed, using crystallographic notations and co-

## ELECTRONIC STATES AND OPTICAL TRANSITIONS

ordinate transformations. The mathematical description of the symmetry operations by means of coordinate transformation is particularly convenient for obtaining rapidly the product of two (or more) elements in the group and analysing the group structure in that way.

TABLE 1-1. Symmetry operations of cubic group  $O_h$ . The notations for the 48 operations of the group are given in columns 2 and 5. For example,  $I\delta_{2yz}$  indicates a rotation by  $2\pi/2$  about the axis whose director cosines on the  $x$ ,  $y$ ,  $z$  axis are in the ratio  $0:1:\bar{1}$ , followed by the inversion. Notations for the classes are given in columns 1 and 4; columns 3 and 6 indicate the coordinate transformations

Class	Symmetry operation	Coordinate transformation			Class	Symmetry operation	Coordinate transformation		
		$x$	$y$	$z$		$I$	$\bar{x}$	$\bar{y}$	$\bar{z}$
$C_4^2$	$\delta_{2z}$	$\bar{x}$	$\bar{y}$	$z$	$IC_4^2$	$I\delta_{2z}$	$x$	$y$	$\bar{z}$
	$\delta_{2x}$	$x$	$\bar{y}$	$\bar{z}$		$I\delta_{2x}$	$\bar{x}$	$y$	$z$
	$\delta_{2y}$	$\bar{x}$	$y$	$\bar{z}$		$I\delta_{2y}$	$x$	$\bar{y}$	$z$
$C_4$	$\delta_{4z}^{-1}$	$\bar{y}$	$x$	$z$	$IC_4$	$I\delta_{4z}^{-1}$	$y$	$\bar{x}$	$\bar{z}$
	$\delta_{4z}$	$y$	$\bar{x}$	$z$		$I\delta_{4z}$	$\bar{y}$	$x$	$\bar{z}$
	$\delta_{4x}^{-1}$	$x$	$\bar{z}$	$y$		$I\delta_{4x}^{-1}$	$\bar{x}$	$z$	$\bar{y}$
	$\delta_{4x}$	$x$	$z$	$\bar{y}$		$I\delta_{4x}$	$\bar{x}$	$\bar{z}$	$y$
	$\delta_{4y}^{-1}$	$z$	$y$	$\bar{x}$		$I\delta_{4y}^{-1}$	$\bar{z}$	$\bar{y}$	$x$
	$\delta_{4y}$	$\bar{z}$	$y$	$x$		$I\delta_{4y}$	$z$	$\bar{y}$	$\bar{x}$
$C_2$	$\delta_{2xy}$	$y$	$x$	$\bar{z}$	$IC_2$	$I\delta_{2xy}$	$\bar{y}$	$\bar{x}$	$z$
	$\delta_{2xz}$	$z$	$\bar{y}$	$x$		$I\delta_{2xz}$	$\bar{z}$	$y$	$\bar{x}$
	$\delta_{2yz}$	$\bar{x}$	$z$	$y$		$I\delta_{2yz}$	$x$	$\bar{z}$	$\bar{y}$
	$\delta_{2x\bar{y}}$	$\bar{y}$	$\bar{x}$	$\bar{z}$		$I\delta_{2x\bar{y}}$	$y$	$x$	$z$
	$\delta_{2\bar{x}z}$	$\bar{z}$	$\bar{y}$	$\bar{x}$		$I\delta_{2\bar{x}z}$	$z$	$y$	$x$
	$\delta_{2y\bar{z}}$	$\bar{x}$	$\bar{z}$	$\bar{y}$		$I\delta_{2y\bar{z}}$	$x$	$z$	$y$
$C_3$	$\delta_{3xyz}^{-1}$	$z$	$x$	$y$	$IC_3$	$I\delta_{3xyz}^{-1}$	$\bar{z}$	$\bar{x}$	$\bar{y}$
	$\delta_{3xyz}$	$y$	$z$	$x$		$I\delta_{3xyz}$	$\bar{y}$	$\bar{z}$	$\bar{x}$
	$\delta_{3x\bar{y}z}^{-1}$	$z$	$\bar{x}$	$\bar{y}$		$I\delta_{3x\bar{y}z}^{-1}$	$\bar{z}$	$x$	$y$
	$\delta_{3x\bar{y}z}$	$\bar{y}$	$\bar{z}$	$x$		$I\delta_{3x\bar{y}z}$	$y$	$z$	$\bar{x}$
	$\delta_{3x\bar{y}\bar{z}}^{-1}$	$\bar{z}$	$\bar{x}$	$y$		$I\delta_{3x\bar{y}\bar{z}}^{-1}$	$z$	$x$	$\bar{y}$
	$\delta_{3x\bar{y}\bar{z}}$	$\bar{y}$	$z$	$\bar{x}$		$I\delta_{3x\bar{y}\bar{z}}$	$y$	$\bar{z}$	$x$
	$\delta_{3xy\bar{z}}^{-1}$	$\bar{z}$	$x$	$\bar{y}$		$I\delta_{3xy\bar{z}}^{-1}$	$z$	$\bar{x}$	$y$
	$\delta_{3xy\bar{z}}$	$y$	$\bar{z}$	$\bar{x}$		$I\delta_{3xy\bar{z}}$	$\bar{y}$	$z$	$x$

Now we would like to show how to separate the 48 elements of  $O_h$  into classes. We note that the identity  $E$  forms a class by itself. The inversion  $I$  commutes with all the elements of  $O_h$  and thus constitutes a class by itself. The elements ( $\delta_{2x}, \delta_{2y}, \delta_{2z}$ ) form a class because we have

$$X^{-1}\delta_{2x}X = \delta_{2x}, \quad \text{or} \quad \delta_{2y}, \quad \text{or} \quad \delta_{2z},$$

depending on the choice of the element  $X$  of  $O_h$ . In a similar way one can divide all the elements of the group into classes. We find that the elements of  $O_h$  are divided into 10 classes (which we can denote as  $\mathcal{C}_1, \mathcal{C}_2, \dots, \mathcal{C}_{10}$  following the order of Table 1-1).

As an example of multiplication among classes, we give

$$\begin{aligned}\mathcal{C}_2 \cdot \mathcal{C}_2 &= (\delta_{2x}, \delta_{2y}, \delta_{2z})(\delta_{2x}, \delta_{2y}, \delta_{2z}) \\ &= E, \delta_{2z}, \delta_{2y}, \delta_{2z}, E, \delta_{2x}, \delta_{2y}, \delta_{2x}, E = 3E + 2(\delta_{2x}, \delta_{2y}, \delta_{2z}).\end{aligned}$$

Thus

$$\mathcal{C}_2 \cdot \mathcal{C}_2 = 3\mathcal{C}_1 + 2\mathcal{C}_2.$$

Similarly

$$\mathcal{C}_2 \cdot \mathcal{C}_3 = \mathcal{C}_3 + 2\mathcal{C}_4,$$

and so forth.

We will now give examples of subgroups of  $O_h$ . If we consider the rotations only, we obtain a subgroup  $O$  composed of the 24 operations listed on the left part of Table 1-1. The subgroup  $O$  is an invariant subgroup of  $O_h$  because it consists of complete classes of  $O_h$ . It can be verified immediately that another invariant subgroup  $T_d$  of order 24 exists and is formed by the classes  $E, C_4^2, IC_4, IC_2, C_3$  of Table 1-1. The symmetry operations of  $O_h$  that interchange  $x, y, z$  among themselves constitute a subgroup (called  $C_{3v}$ ). If we add the inversion to the symmetry operations of group  $C_{3v}$ , we obtain a group called  $D_{3d}$  containing a double number of elements. The rotations  $(E, \delta_{4x}, \delta_{2x}, \delta_{4x}^{-1})$  about the  $x$  axis constitute a subgroup called  $C_4$ ; this is a cyclic group generated by  $\delta_{4x}$ . The subgroup of the elements that change  $x$  into itself is  $C_{4v}$ . The subgroup of the elements that change  $x$  into  $-x$  or  $x$  is called  $D_{4h}$ . The elements  $E$  and  $I$  constitute a subgroup of  $O_h$  that is designated by  $C_t$ . We notice that the group  $O_h$  can be considered as the direct product of the subgroup  $O$  and  $C_t: O_h = O \times C_t$ . In a similar way we have  $D_{3d} = C_{3v} \times C_t$ ;  $D_{4h} = C_{4v} \times C_t$ . The subdivision into classes of the above mentioned groups is different for each one of them, even when a number of operations are common to different groups. We leave to the reader the simple exercise of obtaining the classes of all the above-mentioned groups.

## 1-2 Group representations

In this section we give an outline of the mathematical properties of the representations of groups; this is preliminary to the classification of the electronic states which will be developed in the following section. The basic theorems are stated and working examples are given. For a more detailed discussion of the theory of representations we refer to the standard books on group theory.<sup>[1,2]</sup>

### 1-2a Definitions and basic theorems

By a *representation* of a group we mean a collection of square non-singular matrices associated with the elements of a group and obeying the group multiplication rules. If we indicate with  $\mathbf{D}(R)$  the matrix that corresponds to the operation  $R$ , in a given representation  $D$ , from

$$R_i R_j = R_i$$

it follows

$$\mathbf{D}(R_i) \cdot \mathbf{D}(R_j) = \mathbf{D}(R_i),$$

where the multiplication operation among matrices is defined by the usual row by column multiplication rule. In particular, from  $E E = E$  it follows  $\mathbf{D}(E) \cdot \mathbf{D}(E) = \mathbf{D}(E)$

## ELECTRONIC STATES AND OPTICAL TRANSITIONS

and then  $D(E) = 1$ . In any representation the unit matrix is assigned to the identity element  $E$ . If all the matrices of a representation are different the representation is said to be *faithful*. If some of the matrices of a representation are equal, the representation is said to be *unfaithful*. If we assign the identity matrix to all the elements of a group, we obtain an unfaithful representation called the *identical representation*. The number of rows (or columns) of the matrices of a representation is called the *dimension* of the representation.

Given a representation  $D$  of a group  $\mathcal{G}(R)$  and a nonsingular matrix  $S$ , the ensemble of matrices  $S^{-1} \cdot D(R) \cdot S = D'(R)$  constitutes a representation  $D'$  of the group  $\mathcal{G}(R)$ . We say that the two representations  $D$  and  $D'$  are connected by a *similarity transformation*, defined by the matrix  $S$ . Two representations are *equivalent* if they are related one to the other by a similarity transformation. We recall at this point that any two matrices connected by a similarity transformation have the same *trace* (sum of diagonal elements). Two representations are *inequivalent* if it is impossible to find a similarity transformation that connects one of them to the other. As will be shown clearly in the following Section 1-3, only inequivalent representations are different from a physical point of view, and therefore we need to consider only one among all the infinite equivalent representations.

A representation  $D$  is said to be *reducible* if it is equivalent to a representation having the block form

$$\begin{pmatrix} D^{(1)}(R) & O \\ O & D^{(2)}(R) \end{pmatrix}$$

where  $D^{(1)}(R)$  and  $D^{(2)}(R)$  are square matrices and  $O$  represents a block of zeros. It is easily verified that the matrices  $D^{(1)}(R)$  (or  $D^{(2)}(R)$ ) constitute a representation  $D^{(1)}$  (or  $D^{(2)}$ ) of the group  $\mathcal{G}(R)$ . The representation  $D$  is said to be reducible in the representations  $D^{(1)}$  and  $D^{(2)}$ ,

$$D = D^{(1)} + D^{(2)}.$$

A representation is called *irreducible* if it is impossible to reduce all the matrices representing the elements of the group to block form by a similarity transformation. We note that a reducible representation can always be decomposed by an appropriate similarity transformation into a number of irreducible representations. In what follows it will be important to establish how a reducible representation can be decomposed into irreducible representations, to determine whether or not two representations are equivalent, and to find all the inequivalent, irreducible representations. These results can be derived as a consequence of some fundamental properties of the representations of a group whose proofs can be found in classical books on group theory.<sup>[2]</sup> Here we report the basic theorems in order to emphasize the implied consequences and to derive operational procedures.

First we mention a lemma which applies both to reducible and irreducible representations of a group and allows the use of only those representations with unitary matrices:<sup>\*</sup>

*Any representation is equivalent to a representation with unitary matrices.*

\* We recall that a matrix  $U$  is said to be unitary if  $U^+ U = 1$ , where  $U^+$  indicates the conjugate of the transpose of  $U$ . The elements of a unitary matrix satisfy the equations  $\sum_i U_{ij}^* U_{il} = \delta_{jl}$ , i.e. columns (or rows) of unitary matrices are orthonormals.

Next we consider two theorems which are appropriate to irreducible representations with unitary matrices.

**SCHUR'S LEMMA:** *Any matrix which commutes with all the matrices of an irreducible representation must be a constant matrix (i.e. a matrix of the form  $c\delta_{ik}$ , where  $c$  is a constant and  $\delta_{ik}$  the Kronecker symbol).*

We point out as an immediate application that if an element commutes with all the other elements of the group it forms a class by itself, and the matrix that represents this element commutes with all matrix representatives. Thus in any irreducible representation such an element of the group must be represented by a constant matrix.

**THE ORTHOGONALITY THEOREM:** *The non-equivalent, irreducible, and unitary representations of a group satisfy the relation*

$$\sum_R D^{(\alpha)}(R)^* D^{(\alpha')}(R)_{mn'} = \frac{h}{l_\alpha} \delta_{\alpha\alpha'} \delta_{mm'} \delta_{nn'}, \quad (1-2)$$

where  $R$  runs over all the elements of the group,  $h$  is the order of the group, and  $l_\alpha$  is the dimension of the representation  $D^{(\alpha)}$ .

The orthogonality theorem and its consequences are fundamental in group representation theory. To demonstrate a first important consequence we can observe that the matrix elements  $D^{(\alpha)}(R)_{mn}$ , when  $R$  runs over the  $h$  elements of a group, constitute a number  $\sum_\alpha l_\alpha^2$  of independent and mutually orthogonal vectors. Since in any  $h$ -dimensional space there can exist at most  $h$ -orthogonal vectors, it follows that  $\sum_\alpha l_\alpha^2 \leq h$ .

Actually it can be proved<sup>[2]</sup> that the sum of the squares of the dimensions of the irreducible representations is equal to the order of the group; i.e.

$$\sum_\alpha l_\alpha^2 = h. \quad (1-3)$$

A second important consequence follows from (1-2) when applied to the traces  $\chi^{(\alpha)}(R)$  of the matrices  $D^\alpha(R)$ :

$$\chi^{(\alpha)}(R) = \sum_{m=1}^{l_\alpha} D^{(\alpha)}(R)_{mm}. \quad (1-4)$$

The traces  $\chi^{(\alpha)}(R)$  satisfy the orthogonality relation

$$\sum_R \chi^{(\alpha)}(R)^* \chi^{(\alpha')}(R) = h\delta_{\alpha\alpha'}. \quad (1-5a)$$

The set of numbers  $\chi^{(\alpha)}(R)$ , when  $R$  runs over the  $h$  elements of the group, is called the *character* of the representation  $D^{(\alpha)}(R)$ . We note explicitly that the character  $\chi(E)$  of the identity element equals the dimension of the representation. Performing a similarity transformation does not change the trace of a matrix, so that representations that are equivalent have the same character. The specification of a representation by means of complete matrices presents a high degree of arbitrariness (due to the fact that all matrix representations related to each other through a similarity transformation are equivalent). Instead, the specification of a representation by means of the character is unique for any of the equivalent representations. Only non-equivalent representations have different characters. We also note that, for the same reason, all the elements which belong to the same class have the same character, and we can therefore rewrite (1-5a) as

$$\sum_{C_i} \chi^{(\alpha)}(C_i)^* \chi^{(\alpha')}(C_i) n_i = h\delta_{\alpha\alpha'}. \quad (1-5b)$$

## ELECTRONIC STATES AND OPTICAL TRANSITIONS

where the sum now runs over the classes and  $n_i$  is the number of elements of the class  $\mathcal{C}_i$ . From (1-5b) the following theorem<sup>[1,2]</sup> is obtained: *The number of irreducible representations of a group is equal to the number of classes in the group.*

The orthogonality relation (1-5a) provides a simple method of decomposing a reducible representation into irreducible representations. A reducible representation  $D$  can always be decomposed in the form

$$D = \sum_{\alpha} n_{\alpha} D^{(\alpha)}, \quad (1-6a)$$

where  $n_{\alpha}$  indicates the number of times the irreducible representation  $D^{(\alpha)}$  is contained in  $D$ . To determine  $n_{\alpha}$  we note that the character  $\chi(R)$  of  $D$  can be expressed in the form

$$\chi(R) = \sum_{\alpha} n_{\alpha} \chi^{(\alpha)}(R), \quad (1-6b)$$

where  $\chi^{(\alpha)}(R)$  is the character of the irreducible representation  $D^{(\alpha)}$ . Multiplying (1-6b) by  $\chi^{(\alpha')}(R)^*$  summing on  $R$ , and using (1-5a),

$$n_{\alpha} = \frac{1}{h} \sum_R \chi^{(\alpha)}(R)^* \chi(R). \quad (1-7)$$

### 1-2 b Rules for constructing the character table of a group

It is convenient to display in table form the characters of the irreducible representations of a group. Such a table gives less information than a complete set of matrices would, but it is sufficient for classifying the electronic states and allows us to derive an explicit set of unitary matrices, as will be explained in Section 1-3. From the results described above a number of practical rules can be given which are sufficient for constructing the character table of finite symmetry groups.

1. The number of irreducible representations equals the number of classes in the group.
2. The sum of the squares of the dimensions  $l_{\alpha}$  of the irreducible representations is equal to the number of elements in the group

$$\sum_{\alpha} l_{\alpha}^2 = h.$$

3. The characters of the irreducible representations must be mutually orthogonal and normalized to the order of the group

$$\sum_R \chi^{(\alpha)}(R)^* \chi^{(\alpha')}(R) = h \delta_{\alpha\alpha'}.$$

4. Every group admits the one-dimensional identical representation in which each element in the group is represented by the number 1. The orthogonality relation between characters then shows that for any irreducible representation, except the identical representation,  $\sum_R \chi^{(\alpha)}(R)$  is zero.
5. The characters of the irreducible representations satisfy the relation<sup>[1]</sup>

$$\sum_{\alpha} \chi^{(\alpha)}(\mathcal{C}_i)^* \chi^{(\alpha)}(\mathcal{C}_j) = \frac{h}{n_i} \delta_{ij},$$

where the sum is over the irreducible representations and  $n_i$  indicates the number of elements in the class  $\mathcal{C}_i$ .

6. We recall, from Section 1-1, that the class product  $\mathcal{C}_i \cdot \mathcal{C}_j$  can be decomposed in the form

$$\mathcal{C}_i \cdot \mathcal{C}_j = \sum_s c_{ijs} \mathcal{C}_s,$$

with  $c_{ijs}$  integer numbers. It follows<sup>[11]</sup> that the characters of an irreducible representation  $D^{(\alpha)}$  satisfy the relation

$$n_i n_j \chi^{(\alpha)}(\mathcal{C}_i) \chi^{(\alpha)}(\mathcal{C}_j) = l_\alpha \sum_s c_{ijs} n_s \chi^{(\alpha)}(\mathcal{C}_s), \quad (1-8)$$

where  $n_i$ ,  $n_j$ ,  $n_s$  indicate the number of elements of classes  $\mathcal{C}_i$ ,  $\mathcal{C}_j$ ,  $\mathcal{C}_s$  respectively, and  $l_\alpha$  is the dimension of the irreducible representation  $D^{(\alpha)}$ .

### Illustrative examples

The above rules are sufficient to enable the character tables of all finite symmetry groups of interest in crystal physics to be derived. We wish to illustrate the application of the above rules with several examples.

**Group  $C_1$ .** Group  $C_1$  (also called parity group) has two elements — the identity  $E$  and the inversion  $I$  — and two classes. Thus it has two irreducible one-dimensional representations—an even and an odd one, which are given in Table 1-2.

TABLE 1-2. Character table for group  $C_1$ . The identical representation is labelled with symbol  $g$  and the other with symbol  $u$

	$E$	$I$
$g$	1	1
$u$	1	-1

TABLE 1-3. Character table for group  $O$

$\mathcal{C}_1$	$\mathcal{C}_2$	$\mathcal{C}_3$	$\mathcal{C}_4$	$\mathcal{C}_5$
$E$	$3C_4^2$	$6C_4$	$6C_2$	$8C_3$
1	1	1	1	1
1	1	-1	-1	1
2	2	0	0	-1
3	-1	-1	1	0
3	-1	1	-1	0

**Group  $O$ .** Group  $O$  contains 24 symmetry rotations of a cube. These 24 symmetry elements, which have been reported on the left side of Table 1-1, are collected in 5 classes that we call  $\mathcal{C}_1, \mathcal{C}_2, \dots, \mathcal{C}_5$ , in the order given in Table 1-3. Because of rule 1 we have five irreducible representations. Because of rule 2, the equation for the dimensions of the irreducible representations

$$\sum_{\alpha=1}^5 l_\alpha^2 = 24$$

## ELECTRONIC STATES AND OPTICAL TRANSITIONS

holds. Its only solution in integer numbers is  $1^2 + 1^2 + 2^2 + 3^2 + 3^2 = 24$ . As a consequence, group  $O$  has two one-dimensional, one two-dimensional, and two three-dimensional irreducible representations. Since the character of  $E$  equals the dimension of the representation, we can write the first column of Table 1-3, and since any group has the one-dimensional identical representation, we can immediately write the first row of Table 1-3. The other rows of the table can be obtained by inspection, using orthogonality rules 3 and 5, with the condition that the characters are all real. This condition follows from the fact that an element and its inverse belong to the same class.

We can also use an alternative procedure which is really required only for more complicated cases. It consists in using the properties of class multiplication. For instance, from

$$\mathcal{C}_2 \cdot \mathcal{C}_2 = 3\mathcal{C}_1 + 2\mathcal{C}_2$$

it follows, because of (1-8),

$$3 \cdot 3 \chi^{(\alpha)}(\mathcal{C}_2) \cdot \chi^{(\alpha)}(\mathcal{C}_2) = l_\alpha [3\chi^{(\alpha)}(\mathcal{C}_1) + 2 \cdot 3\chi^{(\alpha)}(\mathcal{C}_2)]. \quad (1-9)$$

For the one-dimensional representations  $\chi^{(\alpha)}(\mathcal{C}_1) = l_\alpha = 1$ , and we obtain the relation

$$9[\chi^{(\alpha)}(\mathcal{C}_2)]^2 = 3 + 6\chi^{(\alpha)}(\mathcal{C}_2)$$

whose solutions are 1 and  $-1/3$ . The value of  $\chi^{(\alpha)}(\mathcal{C}_2)$  must be chosen among these solutions. The solution  $\chi^{(\alpha)}(\mathcal{C}_2) = -1/3$  must be rejected because unitary one-dimensional matrices have modulus 1. Thus the character of the class  $\mathcal{C}_2$  in a one-dimensional representation must be +1. For the three-dimensional representations eq. (1-9) gives

$$9[\chi^{(\alpha)}(\mathcal{C}_2)]^2 = 27 + 18\chi^{(\alpha)}(\mathcal{C}_2)$$

whose solutions are  $-1$  and  $+3$ . We exclude solution  $\chi^{(\alpha)}(\mathcal{C}_2) = 3$  because it does not allow the normalization to  $h = 24$  required by rule 3. Therefore the character of class  $\mathcal{C}_2$  in the three-dimensional representations must be  $-1$ . For the two-dimensional representation we have roots 2 and  $-2/3$ . The condition of orthogonality among the first and second column implied by rule 5 excludes root  $-2/3$ . Thus we can write the entire second column of Table 1-3. We point out that this column is correctly normalized to  $8 = h/n_2 = 24/3$ , as required by rule 5.

If we apply similar arguments to the class multiplication

$$\mathcal{C}_2 \cdot \mathcal{C}_3 = \mathcal{C}_3 + 2\mathcal{C}_4$$

we find that  $\chi^{(\alpha)}(\mathcal{C}_3) = \chi^{(\alpha)}(\mathcal{C}_4)$  for the one- and two-dimensional representations, while  $\chi^{(\alpha)}(\mathcal{C}_3) = -\chi^{(\alpha)}(\mathcal{C}_4)$  for the three-dimensional representations. By continuing in a similar manner one can complete the whole Table 1-3.

*Group  $O_h$ .* Group  $O_h$  contains the 48 symmetry operations which are given in Table 1-1. The character table of group  $O_h$  can be easily worked out by noting that in this group inversion  $I$  commutes with all the other elements. As a consequence of Shur's lemma in any irreducible representation, the matrix  $D(I)$  assigned to the inversion  $I$  must have the form

$$D(I) = c\mathbf{1}.$$

Since  $I^2 = E$  it follows  $D(I) \cdot D(I) = D(E)$ . This implies  $c^2 = 1$  and  $c = \pm 1$ . The irreducible representations with  $c = 1$  are such that  $D(R) = D(IR)$  and  $\chi(R) = \chi(IR)$ ,

## USE OF SYMMETRY IN QUANTUM MECHANICS

while the irreducible representations with  $c = -1$  are such that

$$\mathbf{D}(R) = -\mathbf{D}(IR) \quad \text{and} \quad \chi(R) = -\chi(IR).$$

The irreducible representations for  $O_h$  are in this way obtained from those of group  $O$  by assigning to all the products of a rotation by  $I$  either the character of the rotation in group  $O$  or its negative. They are displayed in Table 1-4, where we have used the notations from the classical paper by Bouckaert *et al.*<sup>[3]</sup>

TABLE 1-4. Character table for cubic group  $O_h$ . The notations for this and for the following four tables are those of reference [3]

	$E$	$3C_4^2$	$6C_4$	$6C_2$	$8C_3$	$I$	$3IC_4^2$	$6IC_4$	$6IC_2$	$8IC_3$
$\Gamma_1$	1	1	1	1	1	1	1	1	1	1
$\Gamma_2$	1	1	-1	-1	1	1	1	-1	-1	1
$\Gamma_{12}$	2	2	0	0	-1	2	2	0	0	-1
$\Gamma'_{25}$	3	-1	-1	1	0	3	-1	-1	1	0
$\Gamma'_{15}$	3	-1	1	-1	0	3	-1	1	-1	0
$\Gamma'_1$	1	1	1	1	1	-1	-1	-1	-1	-1
$\Gamma'_2$	1	1	-1	-1	1	-1	-1	1	1	-1
$\Gamma'_{12}$	2	2	0	0	-1	-2	-2	0	0	1
$\Gamma_{25}$	3	-1	-1	1	0	-3	1	1	-1	0
$\Gamma_{15}$	3	-1	1	-1	0	-3	1	-1	1	0

TABLE 1-5. Character table for group  $C_{3v}$

	$E$	$\delta_{3xyz}^{-1}\delta_{3xyz}$	$I\delta_{2xy}I\delta_{2xz}I\delta_{2yz}$
$A_1$	1	1	1
$A_2$	1	1	-1
$A_3$	2	-1	0

TABLE 1-6. Character table for group  $D_{3d}$

	$E$	$\delta_{3xyz}^{-1}\delta_{3xyz}$	$I\delta_{2xy}I\delta_{2xz}I\delta_{2yz}$	$I$	$I\delta_{3xyz}^{-1}\delta_{3xyz}$	$\delta_{2xy}\delta_{2xz}\delta_{2yz}$
$L_1$	1	1	1	1	1	1
$L_2$	1	1	-1	1	1	-1
$L_3$	2	-1	0	2	-1	0
$L'_1$	1	1	1	-1	-1	-1
$L'_2$	1	1	-1	-1	-1	1
$L'_3$	2	-1	0	-2	1	0

*Groups  $C_{3v}$  and  $D_{3d}$ .* These two groups have been described in Section 1-1, and we recall the relation  $D_{3d} = C_{3v} \times C_t$ . The character table for each group can easily be obtained using the standard procedures described above, and the results are reported in Tables 1-5 and 1-6.

## ELECTRONIC STATES AND OPTICAL TRANSITIONS

*Groups  $C_{4v}$  and  $D_{4h}$ .* These groups have also been described in Section 1-1. The characters of the irreducible representations, obtained by standard procedures, are given in Tables 1-7 and 1-8.

TABLE 1-7. Character table for group  $C_{4v}$

	$E$	$\delta_{2x}$	$\delta_{4x}^{-1}\delta_{4x}$	$I\delta_{2z}I\delta_{2y}$	$I\delta_{2yz}I\delta_{2y\bar{z}}$
$A_1$	1	1	1	1	1
$A'_1$	1	1	1	-1	-1
$A_2$	1	1	-1	1	-1
$A'_2$	1	1	-1	-1	1
$A_5$	2	-2	0	0	0

TABLE 1-8. Character table for group  $D_{4h}$

	$E$	$\delta_{2x}$	$\delta_{4x}^{-1}\delta_{4x}$	$I\delta_{2z}I\delta_{2y}$	$I\delta_{2yz}I\delta_{2y\bar{z}}$	$I$	$I\delta_{2x}$	$I\delta_{4x}^{-1}I\delta_{4x}$	$\delta_{2z}\delta_{2y}$	$\delta_{2yz}\delta_{2y\bar{z}}$
$M_1$	1	1	1	1	1	1	1	1	1	1
$M_2$	1	1	1	-1	-1	1	1	1	-1	-1
$M_3$	1	1	-1	1	-1	1	1	-1	1	-1
$M_4$	1	1	-1	-1	1	1	1	-1	-1	1
$M_5$	2	-2	0	0	0	2	-2	0	0	0
$M'_1$	1	1	1	1	1	-1	-1	-1	-1	-1
$M'_2$	1	1	1	-1	-1	-1	-1	-1	1	1
$M'_3$	1	1	-1	1	-1	-1	-1	1	-1	1
$M'_4$	1	1	-1	-1	1	-1	-1	1	1	-1
$M'_5$	2	-2	0	0	0	-2	2	0	0	0

*Group  $C_4$ .* This is a cyclic group of order 4 generated by  $\delta_{4x}$ . Since a cyclic group is abelian, the number of classes equals the order of the group, and we have as many one-dimensional irreducible representations as the number of elements in the group. The irreducible representations are obtained by assigning to the generator element all the fourth order roots of unity. The irreducible representations thus obtained are given in Table 1-9.

TABLE 1-9. Character table for group  $C_4$

$E$	$\delta_{4x}$	$\delta_{2x}$	$\delta_{4x}^{-1}$
1	1	1	1
1	-1	1	-1
1	$i$	-1	$-i$
1	$-i$	-1	$i$

In the same manner we can obtain the irreducible representations of all symmetry groups of crystals which can be found, for instance, in ref. [4].

### 1-2c Further relationships among representations

We wish here to summarize briefly some properties which we will use in the following chapters and which can be derived from the basic theorems described above.

*Product representations and their decomposition into irreducible representations*

As will be shown in Section 1-7, the notion of product representation is basic to the discussion of selection rules. Here are some definitions and results which can be verified immediately without any difficulty.

The direct product of two matrices  $\mathbf{A}$  and  $\mathbf{B}$  of order  $n_a$  and  $n_b$  is a matrix  $\mathbf{C} = \mathbf{A} \times \mathbf{B}$  of order  $n_c = n_a n_b$ , whose elements are

$$C_{ik,jl} = A_{ij}B_{kl}, \quad (1-10)$$

where indexes  $ik$  label the rows and  $jl$  the columns. Matrix  $C$  can be written in the block form

$$\mathbf{C} = \mathbf{A} \times \mathbf{B} = \begin{pmatrix} A_{11}\mathbf{B} & A_{12}\mathbf{B} \dots \\ A_{21}\mathbf{B} & A_{22}\mathbf{B} \dots \\ \dots & \dots \\ \dots & \dots \end{pmatrix}.$$

We note in particular that the character of the product matrix  $\mathbf{C}$  is equal to the product of the characters of matrices  $\mathbf{A}$  and  $\mathbf{B}$ .

Let us now consider two (reducible or irreducible) representations  $D^{(\alpha)}$  and  $D^{(\nu)}$  of a group  $\mathcal{G}(R)$ . As a consequence of the definition of product matrix, it can be verified<sup>[4]</sup> that the matrices  $D^{(\alpha)}(R) \times D^{(\nu)}(R)$  constitute a representation  $D^{(\alpha \times \nu)}$  of the group  $\mathcal{G}(R)$  called a *product representation*. The character  $\chi^{(\alpha \times \nu)}(R)$  of the product representation equals the product of the characters of the composing representations

$$\chi^{(\alpha \times \nu)}(R) = \chi^{(\alpha)}(R) \chi^{(\nu)}(R). \quad (1-11)$$

It is often useful to decompose the product representation  $D^{(\alpha \times \nu)}$  into irreducible representations  $D^{(\mu)}$  of the group. Working with (1-7) we find that the number of times the irreducible representation  $D^{(\mu)}$  appears in the product  $D^{(\alpha \times \nu)}$  is given by

$$c(\mu, \alpha, \nu) = \frac{1}{h} \sum_R \chi^{(\mu)}(R)^* \chi^{(\alpha)}(R) \chi^{(\nu)}(R). \quad (1-12)$$

For some examples of product representations, let us consider group  $O_h$  (Table 1-4). Using (1-12) we can readily obtain, for instance, the decomposition

$$\Gamma_{12} \times \Gamma_{12} = \Gamma_1 + \Gamma_2 + \Gamma_{12},$$

$$\Gamma_{12} \times \Gamma_{25} = \Gamma'_{25} + \Gamma'_{15}, \quad \text{etc.}$$

As a further example which will be useful for the optical selection rules, we give in Table 1-10 the decomposition of the representations obtained as the product of the irreducible representations of group  $O_h$  by the irreducible representation  $\Gamma_{15}$ .

TABLE 1-10. Examples of decomposition of product representations for group  $O_h$

$\Gamma_1$	$\Gamma_1$	$\Gamma_2$	$\Gamma_{12}$	$\Gamma'_{25}$	$\Gamma'_{15}$
$\Gamma_1 \times \Gamma_{15}$	$\Gamma_{15}$	$\Gamma_{25}$	$\Gamma_{25} + \Gamma_{15}$	$\Gamma'_2 + \Gamma'_{12} + \Gamma_{25} + \Gamma_{15}$	$\Gamma'_1 + \Gamma'_{12} + \Gamma_{25} + \Gamma_{15}$
$\Gamma_1$	$\Gamma'_1$	$\Gamma'_2$	$\Gamma'_{12}$	$\Gamma_{25}$	$\Gamma_{15}$
$\Gamma_1 \times \Gamma_{15}$	$\Gamma'_{15}$	$\Gamma'_{25}$	$\Gamma'_{25} + \Gamma'_{15}$	$\Gamma_2 + \Gamma_{12} + \Gamma'_{25} + \Gamma'_{15}$	$\Gamma_1 + \Gamma_{12} + \Gamma'_{25} + \Gamma'_{15}$

*Complex conjugate representations*

It will be shown in Section 1-6 that complex conjugate representations are important in discussing the operation of time reversal.

We wish now to establish the relationship between an irreducible representation  $D$  and its complex conjugate  $D^*$ . First of all we want to determine whether they are equivalent or nonequivalent. Since the character of  $D^*$  is the complex conjugate of the character of  $D$ , it follows that  $D$  and  $D^*$  are equivalent if and only if the character of  $D$  is real. In this case there exists a unitary matrix  $M$  that transforms  $D$  into  $D^*$ :

$$D^*(R) = M^{-1}D(R)M. \quad (1-13)$$

It can be proved<sup>[4]</sup> that the matrix  $M$  is either symmetric or antisymmetric. If the matrix  $M$  is antisymmetric, it also follows<sup>[4]</sup> that  $D$  cannot be transformed into *real form* (i.e. with all matrix elements real) by a similarity transformation. If instead the matrix  $M$  is symmetric, then  $D$  can be transformed into real form by an appropriate similarity transformation.

The relationships between an irreducible representation and its complex conjugate can be summarized as follows:

Case a:  $D$  and  $D^*$  are equivalent to the same real irreducible representation.

Case b:  $D$  and  $D^*$  are non-equivalent.

Case c:  $D$  and  $D^*$  are equivalent to each other but cannot be made real.

For a finite group there exists a criterion introduced by Frobenius and Schur<sup>[5]</sup> that enables us to distinguish between cases a, b, and c by inspecting the characters of the irreducible representations. Consider the sum  $\sum_R \chi(R^2)$  of the characters of the *squares* of the elements in the group. It can be proved that this sum takes on the values  $h$ , 0,  $-h$  when the irreducible representation  $D$  belongs to case a, b, or c, respectively:

$$\sum_R \chi(R^2) = \begin{cases} h & \text{case a,} \\ 0 & \text{case b,} \\ -h & \text{case c.} \end{cases} \quad (1-14)$$

As an application of (1-14) let us consider group  $O_h$  (Table 1-4). All the irreducible representations have real characters, so only cases a or c may occur. The one-dimensional representations  $\Gamma_1, \Gamma_2, \Gamma'_1, \Gamma'_2$  obviously belong to case a because they are already in real form. By applying the test (1-14) it can be seen, moreover, that the other irreducible representations of group  $O_h$  also belong to case a.

As a second example, let us take group  $C_4$  (Table 1-9). It can be immediately verified by applying (1-14) that the first two representations belong to case a and the last two to case b.

*Irreducible representations of a product group*

We will show in Section 1-5 that these concepts are important for discussing spin degeneracy and the effect of spin-orbit coupling.

We recall from Section 1-1 that a group  $G$  is said to be the direct product of two groups  $G_1(R)$  and  $G_2(S)$  when the elements of  $G$  are obtained as products of all the elements of  $G_1$  by those of  $G_2$ , and all the elements of  $G_1$  commute with the elements of  $G_2$ , the identity being the only element common to  $G_1$  and  $G_2$ .

The irreducible representations of group  $\mathcal{G}$  can be obtained very easily from the irreducible representations of  $\mathcal{G}_1$  and  $\mathcal{G}_2$ . It can in fact be proved<sup>[4]</sup> that if  $D^{(\alpha)}(R)$  is any irreducible representation of the group  $\mathcal{G}_1$  and  $D^{(\beta)}(S)$  is any irreducible representation of  $\mathcal{G}_2$ , the product matrices

$$D^{(\alpha \times \beta)}(RS) = D^{(\alpha)}(R) \times D^{(\beta)}(S)$$

form an irreducible representation of group  $\mathcal{G}$ , with characters

$$\chi^{(\alpha \times \beta)}(RS) = \chi^{(\alpha)}(R)\chi^{(\beta)}(S). \quad (1-15)$$

Furthermore it can be proved that all the irreducible representations of group  $\mathcal{G}$  are obtained by multiplying all the different irreducible representations of  $\mathcal{G}_1$  by all the different irreducible representations of  $\mathcal{G}_2$ .

As an example consider group  $O_h$ . This group can be written as the direct product  $O_h = O \times C_i$ . The characters of the irreducible representations of groups  $C_i$  and  $O$  are given in Table 1-2 and 1-3 respectively. The character table of the group  $O_h$  can therefore be obtained by multiplying the characters of groups  $O$  and  $C_i$ , and it can be immediately verified that the result gives character Table 1-4, which was previously obtained by a different procedure.

### Compatibility relations

Let us consider a group  $\mathcal{G}$  and a subgroup  $\mathcal{S}$ . Given a representation of  $\mathcal{G}$ , let us choose from these matrices only those matrices corresponding to the elements of subgroup  $\mathcal{S}$ ; we obtain in this way a set of matrices that constitute a representation of  $\mathcal{S}$ . The representation obtained for the subgroup is in general reducible, even when the original representation of the full group is irreducible. It may be decomposed, by using (1-7), into a number of irreducible representations of the subgroup that are said to be *compatible* with the given irreducible representation of  $\mathcal{G}$ .

To give an example, let us take group  $O_h$  (Table 1-4) and subgroup  $C_{4v}$  (Table 1-7). The decomposition of the irreducible representations  $\Gamma_i$  of group  $O_h$  into the irreducible representations  $\Delta_j$  of subgroup  $C_{4v}$  is immediately obtained using (1-7), and we give the results in Table 1-11.

TABLE 1-11. Decomposition of the irreducible representations  $\Gamma_i$  of group  $O_h$  into the irreducible representations  $\Delta_j$  of subgroup  $C_{4v}$

$\Gamma_1$	$\Gamma_2$	$\Gamma_{12}$	$\Gamma'_{25}$	$\Gamma'_{15}$
$\Delta_1$	$\Delta_2$	$\Delta_1 + \Delta_2$	$\Delta'_2 + \Delta_5$	$\Delta'_1 + \Delta_5$
$\Gamma'_1$	$\Gamma'_2$	$\Gamma'_{12}$	$\Gamma_{25}$	$\Gamma_{15}$
$\Delta'_1$	$\Delta'_2$	$\Delta'_1 + \Delta'_2$	$\Delta_2 + \Delta_5$	$\Delta_1 + \Delta_5$

## 1-3 Representations and eigenfunctions

### 1-3a Classification of the eigenstates

In the previous section we considered the mathematical treatment of the representations of a group. In this section we illustrate the close relationship between the representation theory previously discussed and an eigenvalue problem.

An operation of symmetry with respect to an operator  $H(\mathbf{r})$  is defined as a linear transformation of coordinates  $\mathbf{r}' = \mathbf{R}\mathbf{r}$  (with  $\mathbf{R}$  real and unitary matrix) that does not

change the form of the operator, i.e.  $H(\mathbf{r}') = H(\mathbf{r})$ .\* The collection of all distinct operations of symmetry constitutes a symmetry group because the identity operation, the product of two operations, and the inverse of any operation are all operations of symmetry. Given a real and unitary matrix  $\mathbf{R}$ , let us consider the operator  $O_R$  defined thus:  $O_R$  transforms a function  $f(\mathbf{r})$  into a new function  $O_R f(\mathbf{r})$ , which assumes in the point  $\mathbf{R}\mathbf{r}$  the same value that  $f(\mathbf{r})$  has in  $\mathbf{r}$ . This means

$$O_R f(\mathbf{R}\mathbf{r}) = f(\mathbf{r})$$

and consequently

$$O_R f(\mathbf{r}) = f(\mathbf{R}^{-1}\mathbf{r}), \quad (1-16)$$

which is the form usually adopted to define the operator  $O_R$ . The ensemble of the operations  $O_R$  associated with every element  $R$  of a symmetry group  $\mathcal{G}(R)$  constitutes a group isomorphous to the symmetry group  $\mathcal{G}(R)$ .

Let us consider an eigenvalue problem

$$H(\mathbf{r})f(\mathbf{r}) = Ef(\mathbf{r}) \quad (1-17)$$

and let  $\mathcal{G}(R)$  denote the symmetry group of the operator  $H$ . By applying to both members of (1-17) the operator  $O_R$  defined above,

$$O_R H(\mathbf{r})f(\mathbf{r}) = EO_R f(\mathbf{r}),$$

$$H(\mathbf{r}) O_R f(\mathbf{r}) = EO_R f(\mathbf{r}).$$

This means that  $f(\mathbf{r})$  and  $O_R f(\mathbf{r})$  are both eigenfunctions belonging to the same eigenvalue.

Now let us take a set of linearly independent eigenfunctions  $(f_1, f_2, \dots, f_l)$  associated with an eigenvalue of degeneracy  $l$ . The functions  $O_R f_i$  are also eigenfunctions belonging to the eigenvalue  $E$  and can thus be expressed as linear combinations of  $(f_1, f_2, \dots, f_l)$ :

$$O_R f_j = \sum_i \mathbf{D}(R)_{ij} f_i \quad (i, j = 1, 2, \dots, l). \quad (1-18)$$

The matrices  $\mathbf{D}(R)$  follow the multiplication rules of the group, and thus constitute the matrices for a representation  $D$  of the symmetry group. The representation  $D$  so obtained is said to have  $(f_1, f_2, \dots, f_l)$  as *basis functions*. Instead of assuming such basis functions, one can consider a new set  $(f'_1, f'_2, \dots, f'_l)$  made up of  $l$  independent linear combinations of  $(f_1, f_2, \dots, f_l)$ . It can be proved<sup>[6]</sup> that the representation  $D'$  of basis functions  $(f'_1, f'_2, \dots, f'_l)$  is related to the representation  $D$  of basis functions  $(f_1, f_2, \dots, f_l)$  by the equation  $\mathbf{D}'(R) = \mathbf{M}^{-1} \mathbf{D}(R) \mathbf{M}$ , where  $\mathbf{M}$  is the matrix that transforms the set  $f_i$  ( $i = 1, \dots, l$ ) into  $f'_i$  ( $i = 1, \dots, l$ ). The representation  $D'$  is thus equivalent to  $D$ , i.e. *only one distinct representation of the symmetry group  $\mathcal{G}(R)$  is associated with a given eigenstate*. The space of the functions  $(f_1, f_2, \dots, f_l)$  is said to be irreducible (reducible) if the representation  $D$  is irreducible (reducible). If  $D$  is irreducible and has dimension  $l$  it is impossible to choose a number  $< l$  of functions or linear combinations of  $f_i$  ( $i = 1, \dots, l$ ), that transform only among themselves under the operations of the group. If the basis functions  $(f_1, f_2, \dots, f_l)$  are orthogonal and normalized, the corresponding representation is unitary. We thus

\* The more general case of linear transformations of the type  $\mathbf{r}' = \mathbf{R}\mathbf{r} + \mathbf{a}$  which appear in crystals, and the case in which spin coordinates are included, will be considered in detail later, though the general concepts of this section apply to these cases also.

obtain a simple physical interpretation of the lemma of Section 1-2a which shows the equivalence of any representation to an appropriate representation with unitary matrices.

The results so far obtained provide a classification of the eigenvalues of an operator. In fact each eigenvalue can be labelled with a representation of the operator's symmetry group whose bases are the corresponding eigenfunctions. Furthermore, if the group contains *all* of the operator's symmetry operations, the representation associated with an eigenvalue is in general *irreducible*. (In the exceptional cases in which the representation associated with a given eigenvalue is reducible, we say that there is *accidental degeneracy* not determined from the symmetry properties.) The dimensions of the irreducible representations determine the *essential degeneracies* of the eigenvalues.

### 1-3b Projection operators and orthogonality theorems on partner functions

Given an irreducible *unitary* representation  $D^{(\alpha)}$  of a symmetry group  $\mathcal{G}(R)$ , any set  $(f_1^{(\alpha)}, f_2^{(\alpha)}, \dots, f_l^{(\alpha)})$  of functions that transform into each other according to the relation

$$O_R f_j^{(\alpha)} = \sum_i D^{(\alpha)}(R)_{ij} f_i^{(\alpha)} \quad (1-19)$$

is called a set of partner functions for the irreducible representation  $D^{(\alpha)}$ . We also say that  $f_j^{(\alpha)}$  belongs to the  $j$ th row of the irreducible representation  $D^{(\alpha)}$ . If we multiply by  $D^{(\beta)}(R)_{ii}^*$  both members of (1-19), sum over  $R$ , and use (1-2),

$$\sum_R D^{(\beta)}(R)_{ii}^* O_R f_j^{(\alpha)} = \sum_i \frac{h}{l_\alpha} \delta_{ii} \delta_{ij} \delta_{\alpha\beta} f_i^{(\alpha)} = \frac{h}{l_\alpha} \delta_{ij} \delta_{\alpha\beta} f_i^{(\alpha)}. \quad (1-20)$$

The above equation suggests how to define a projection operator which projects from any function its part which belongs to the  $j$ th row of the irreducible representation. We define:

$$P_j^{(\alpha)} = \frac{l_\alpha}{h} \sum_R D^{(\alpha)}(R)_{jj}^* O_R, \quad (1-21)$$

and eq. (1-20) can be written as

$$P_j^{(\alpha)} f_{j'}^{(\alpha')} = f_j^{(\alpha)} \delta_{jj'} \delta_{\alpha\alpha'}. \quad (1-22)$$

Any function can always be expanded in a sum of functions belonging to the different rows of the irreducible representations of a group  $\mathcal{G}(R)$ . In fact, given a function  $\psi$  let us consider the  $h$ -functions  $(\psi, O_{R_1}\psi, \dots, O_{R_h}\psi)$  and take only those which are linearly independent. They constitute a basis for a representation  $D$  of the group  $\mathcal{G}(R)$ . With similarity transformations we can always decompose  $D$  into one or more irreducible representations of  $\mathcal{G}(R)$ , and this corresponds to an appropriate new choice of basis functions. Consequently the function  $\psi$  can be expressed in terms of the new basis functions as

$$\psi = \sum_\alpha \sum_{j=1}^{l_\alpha} \psi_j^{(\alpha)}, \quad (1-23)$$

where  $\psi_j^{(\alpha)}$  is the part of the function  $\psi$  that belongs to the  $j$ th row of the irreducible representation  $D^{(\alpha)}$ . Because of (1-22),

$$\psi_j^{(\alpha)} = P_j^{(\alpha)} \psi. \quad (1-24)$$

## ELECTRONIC STATES AND OPTICAL TRANSITIONS

This last relationship explicitly allows us to decompose an arbitrary function into parts belonging to the different rows of the various irreducible representations, thereby justifying the definition of 'a' or 'the' projection operator given in (1-21).

The projection operators defined by (1-21) require a knowledge of the diagonal matrix elements of the irreducible representations. This can be somewhat inconvenient, since we have not yet given procedures to obtain the matrices of the irreducible representations, but only the characters. We can overcome this difficulty by summing (1-20) with respect to  $l$ , to obtain

$$\sum_R \chi^{(\beta)}(R)^* O_R f_j^{(\alpha)} = \frac{h}{l_\alpha} \delta_{\alpha\beta} f_j^{(\alpha)}.$$

It is convenient to define a projection operator  $P^{(\alpha)}$  in terms of the characters of the irreducible representation  $D^{(\alpha)}$  as follows:

$$P^{(\alpha)} = \frac{l_\alpha}{h} \sum_R \chi^{(\alpha)}(R)^* O_R. \quad (1-25)$$

We have the fundamental relation

$$P^{(\alpha)} f^{(\alpha')} = f^{(\alpha)} \delta_{\alpha\alpha'}, \quad (1-26)$$

where  $f^{(\alpha)}$  indicates a function which belongs to the irreducible representation  $D^{(\alpha)}$  because it is a linear combinations of  $f_i^{(\alpha)}$ . Since any function  $\psi$  can be decomposed into functions belonging to irreducible representations of the group as shown above,

$$\psi = \sum_\alpha \psi^{(\alpha)}, \quad (1-27)$$

we obtain from (1-26)

$$\psi^{(\alpha)} = P^{(\alpha)} \psi. \quad (1-28)$$

The relations (1-27) and (1-28) can be used to construct the matrices of the irreducible representations explicitly. Given a function  $\psi$ , we can use the projection operator  $P^{(\alpha)}$  (1-25) (whose construction requires only the knowledge of the characters of representation  $D^{(\alpha)}$ ) to determine the function  $\psi^{(\alpha)}$ . We can then apply to  $\psi^{(\alpha)}$  (supposedly different from zero) the operations of the symmetry group, to obtain the  $h$ -functions ( $\psi^{(\alpha)}, O_{R_1}\psi^{(\alpha)}, \dots, O_{R_h}\psi^{(\alpha)}$ ). Only  $l_\alpha$  linearly independent functions, which can be made orthonormal, are obtained. These functions constitute a basis for the irreducible representation  $D^{(\alpha)}$ . This is in practice the procedure adopted in crystal physics to obtain the matrix representatives of the irreducible representations.

We also wish to note that if a function belongs to an irreducible representation, it belongs to all equivalent representations related to it by a unitary transformation. On the contrary, the property of a function to belong to a row of a given irreducible representation is valid only for one particular representation among all the equivalent unitary representations.

The following are central orthogonality theorems for basis functions which have wide application.

*Two functions belonging to different irreducible representations, or to different rows of the same irreducible representation, are orthogonal.* In formula,

$$\langle f_i^{(\alpha)} | \varphi_j^{(\alpha')} \rangle = C_\alpha \delta_{ij} \delta_{\alpha\alpha'}. \quad (1-29)$$

We observe that the matrix element of two partner functions does not depend on the particular row to which the functions belong. Similarly,

*Matrix elements of an operator  $H$  can be different from zero only among functions belonging to the same row of the same irreducible representation of the symmetry group of  $H$ . In formula,*

$$\langle f_i^{(\alpha)} | H | \varphi_j^{(\alpha')} \rangle = C'_\alpha \delta_{ij} \delta_{\alpha\alpha'}. \quad (1-30)$$

$C'_\alpha$  being a constant independent of  $i$ . The proofs of the above orthogonality theorems can be easily obtained by applying to both terms of the cross products in the left side of eq. (1-29) and (1-30) the operator  $O_R$ , as in (1-19), and summing over  $R$ . As an immediate consequence of the results (1-29) and (1-30), we need to include in the expansion of an eigenfunction in a complete set of functions only those which belong to the same row of the same irreducible representation as the exact eigenfunction. Since, in general, the number of terms of the expansion is limited by practical reasons, the use of symmetry greatly improves the accuracy of the results, besides allowing a classification of the states.

### Examples

(i) Let us consider group  $C_1$  whose characters are given in Table 1-2. By means of (1-25) and (1-28) we project an arbitrary function  $\psi(\mathbf{r})$  on the irreducible representations  $g$  and  $u$  of group  $C_1$ , and we obtain the well-known results

$$\frac{1}{2}[\psi(\mathbf{r}) + \psi(-\mathbf{r})] \quad \text{and} \quad \frac{1}{2}[\psi(\mathbf{r}) - \psi(-\mathbf{r})] \quad (1-31)$$

for the even and the odd representation respectively.

(ii) Next, let us consider group  $C_{4v}$  of Table 1-7 and the functions  $x, y, z$ . Using the projection operators (1-25) we verify that  $x$  belongs to the irreducible representation  $A_1$ , while  $y$  and  $z$  belong to the irreducible representation  $A_5$ . Since  $y$  and  $z$  are independent and orthonormal functions, we can take them as basis functions and apply the symmetry operation to them to obtain, for  $A_5$ , the matrices

$E$	$\delta_{2x}$	$\delta_{4x}$	$\delta_{4x}^{-1}$	$I\delta_{2y}$	$I\delta_{2z}$	$I\delta_{2yz}$	$I\delta_{2yz}$
$\begin{pmatrix} 1 & 0 \\ 0 & 1 \end{pmatrix}$	$\begin{pmatrix} 1 & 0 \\ 0 & 1 \end{pmatrix}$	$\begin{pmatrix} 0 & 1 \\ 1 & 0 \end{pmatrix}$	$\begin{pmatrix} 0 & 1 \\ 1 & 0 \end{pmatrix}$	$\begin{pmatrix} 1 & 0 \\ 0 & 1 \end{pmatrix}$	$\begin{pmatrix} 1 & 0 \\ 0 & 1 \end{pmatrix}$	$\begin{pmatrix} 0 & 1 \\ 1 & 0 \end{pmatrix}$	$\begin{pmatrix} 0 & 1 \\ 1 & 0 \end{pmatrix}$

(1-32)

(iii) Now let us consider group  $O_h$  of Table 1-4. Using the projection operators (1-25) we verify that the independent functions  $x, y, z$  belong to the irreducible representation  $I_{15}$ . Since they are orthonormal, they can be taken as basis functions to obtain all the matrices for the representation  $I_{15}$ . For instance, we have

$$E = \begin{pmatrix} 1 & 0 & 0 \\ 0 & 1 & 0 \\ 0 & 0 & 1 \end{pmatrix}, \quad \delta_{2z} = \begin{pmatrix} 1 & 0 & 0 \\ 0 & 1 & 0 \\ 0 & 0 & 1 \end{pmatrix}, \quad \text{etc.,}$$

which can be obtained immediately using the coordinate transformations of Table 1-1.

### 1-3c Further relationships between representations and basis functions<sup>[6]</sup>

A close relationship between representations and basis functions can be shown to apply also to the results described in Section 1-2c. The statements which follow can be verified without any difficulty.

By multiplying among themselves two linearly independent sets of functions which are the basis for two representations of the group, one obtains a set of basis functions for the product representation.

If a set of functions constitutes a basis for a representation  $D$  of a group, the set of complex conjugate functions constitutes a basis for the complex conjugate representation  $D^*$ .

Consider the product group  $\mathcal{G} = \mathcal{G}_1 \times \mathcal{G}_2$  and let  $f_i^{(\alpha)} (i = 1, \dots, l_\alpha)$  and  $\varphi_j^{(\beta)} (j = 1 \dots l_\beta)$  be basis functions for the irreducible representations  $D^{(\alpha)}$  and  $D^{(\beta)}$  of  $\mathcal{G}_1$  and  $\mathcal{G}_2$  respectively. Then the  $l_\alpha l_\beta$  functions  $f_i^{(\alpha)} \varphi_j^{(\beta)}$  form a basis for the irreducible representation  $D^{(\alpha)} \times D^{(\beta)}$  of the group  $\mathcal{G}$ .

A perturbation which lowers the symmetry of the Hamiltonian will split the level of a given symmetry into sublevels which belong to the irreducible representations of subgroup  $\mathcal{S}$  defined by the symmetry operations of the new Hamiltonian. This splitting is determined by the compatibility relations between the irreducible representations of group  $\mathcal{G}$  and those of the subgroup  $\mathcal{S}$ .

#### 1-4 Rotation and rotation-inversion groups<sup>[7]</sup>

##### 1-4a Irreducible representations of rotation and rotation-inversion groups

Up to this point our review of the results of group theory has been devoted to finite groups. Now we want to consider briefly the main results concerning the continuous rotation group in three dimension which is used to classify atomic states, as we will be using these results extensively.

Group  $O^+(3)$  of *proper rotations* in three dimensions is defined as the ensemble of 3 by 3 real, unitary matrices (orthogonal matrices) each with determinant equal to +1. The group contains an infinite number of elements and an infinite number of classes. The rotations of the same angle about any axis belong to the same class.

The irreducible representations of group  $O^+(3)$  can be obtained in many ways. We can simply use the fact that a Hamiltonian with spherically symmetric potential is invariant under the group  $O^+(3)$ . Thus the spherical harmonics  $Y_{lm}(\theta, \varphi)$  ( $m = -l \dots +l$ ) that are solutions of the angular part of the Schrödinger equation, can be taken as basis functions in order to generate a representation  $D^{(l)}$  of the rotational group. All the representations so obtained are irreducible. A rotation through an angle  $\alpha$  about the z-axis transforms  $Y_{lm}(\theta, \varphi)$  into  $e^{-im\alpha} Y_{lm}(\theta, \varphi)$  and is thus represented in the irreducible representation  $D^{(l)}$  by the diagonal matrix

$$\begin{pmatrix} e^{-il\alpha} & 0 & . & 0 \\ 0 & e^{-i(l-1)\alpha} & . & 0 \\ . & . & . & . \\ 0 & 0 & . & e^{il\alpha} \end{pmatrix} \quad (1-33)$$

with character

$$\chi^{(l)}(\alpha) = \sum_{m=-l}^l e^{im\alpha} = 1 + 2 \cos \alpha + \dots + 2 \cos l\alpha \quad (1-34)$$

## USE OF SYMMETRY IN QUANTUM MECHANICS

Since all the rotations of the same angle belong to the same class, the character of any rotation of angle  $\alpha$  in the irreducible representations  $D^{(l)}$  is given by (1-34). The characters

$$\chi^{(0)}(\alpha), \chi^{(1)}(\alpha), \dots, \chi^{(l)}(\alpha), \quad (1-35)$$

constitute a complete set of functions in the interval  $0 \leq \alpha \leq 2\pi$  and are the only irreducible representations of the proper rotation group  $O^+(3)$ . They are given for convenience in Table 1-12.

TABLE 1-12. Characters of the irreducible representations of proper rotations group  $O^+(3)$

	$E$	Rotations through $\alpha$
$D^{(0)}$	1	1
$D^{(1)}$	3	$1 + 2 \cos \alpha$
$D^{(l)}$	$2l + 1$	$\sum_{m=-l}^{+l} e^{im\alpha}$

The direct product of two representations of the proper rotation group may be decomposed into irreducible representations as described in Section 1-2c for finite groups. With the aid of expression (1-34)

$$D^{(l_1)} \times D^{(l_2)} = \sum_{|l_1 - l_2|}^{l_1 + l_2} D^{(l)}. \quad (1-36)$$

Consider also the rotation-inversion group  $O(3)$  which is the ensemble of the orthogonal 3 by 3 matrices with determinant +1 (proper rotations) and determinant -1 (*improper rotations*). This group is the direct product of group  $O^+(3)$  and group  $C_i$ , which contains identity  $E$  and spatial inversion  $I$ . The irreducible representations of the rotation-inversion group can be obtained from the irreducible representations of groups  $O^+(3)$  and  $C_i$ . From any irreducible representation  $D^{(l)}$  of the rotation group, one obtains an even representation  $D^{(l+)}$  and an odd representation  $D^{(l-)}$  of the rotation-inversion group by attributing equal and opposite characters to proper and improper rotations respectively. The characters of the irreducible representations of the rotation-inversion group  $O(3)$  are reported in Table 1-13.

TABLE 1-13. Characters of the irreducible representations of rotation-inversion group  $O(3)$

	$E$	Rotations through $\alpha$	$I$	$I \cdot$ Rotations through $\alpha$
$D^{(0+)}$	1	1	1	1
$D^{(0-)}$	1	1	-1	-1
$D^{(1+)}$	3	$1 + 2 \cos \alpha$	3	$1 + 2 \cos \alpha$
$D^{(1-)}$	3	$1 + 2 \cos \alpha$	-3	$-(1 + 2 \cos \alpha)$
$D^{(l+)}$	$2l + 1$	$\sum_{m=-l}^{+l} e^{im\alpha}$	$2l + 1$	$\sum_{m=-l}^{+l} e^{im\alpha}$
$D^{(l-)}$	$2l + 1$	$\sum_{m=-l}^{+l} e^{im\alpha}$	$-(2l + 1)$	$-\sum_{m=-l}^{+l} e^{im\alpha}$

## ELECTRONIC STATES AND OPTICAL TRANSITIONS

**1-4b Decomposition of the irreducible representations of the rotation-inversion group into irreducible representations of finite groups**

For this purpose one must compute the characters of the irreducible representations  $D^{(l+)}$  or  $D^{(l-)}$  for the symmetry operations of the finite group and see how they decompose into the characters of the irreducible representations of the finite symmetry group. As an example, Table 1-14 gives the characters of representations  $D^{(l+)}$  and

TABLE 1-14. Characters of representations  $D^{(l+)}$  and  $D^{(l-)}$ , with  $l$  up to 5, for the operations of symmetry group  $O_h$

	$E$	$3C_4^2$	$6C_4$	$6C_2$	$8C_3$	$I$	$3IC_4^2$	$6IC_4$	$6IC_2$	$8IC_3$
$D^{(0+)}$	1	1	1	1	1	1	1	1	1	1
$D^{(0-)}$	1	1	1	1	1	-1	-1	-1	-1	-1
$D^{(1+)}$	3	-1	1	-1	0	3	-1	1	-1	0
$D^{(1-)}$	3	-1	1	-1	0	-3	1	-1	1	0
$D^{(2+)}$	5	1	-1	1	-1	5	1	-1	1	-1
$D^{(2-)}$	5	1	-1	1	-1	-5	-1	1	-1	1
$D^{(3+)}$	7	-1	-1	-1	1	7	-1	-1	-1	1
$D^{(3-)}$	7	-1	-1	-1	1	-7	1	1	1	-1
$D^{(4+)}$	9	1	1	1	0	9	1	1	1	0
$D^{(4-)}$	9	1	1	1	0	-9	-1	-1	-1	0
$D^{(5+)}$	11	-1	1	-1	-1	11	-1	1	-1	-1
$D^{(5-)}$	11	-1	1	-1	-1	-11	1	-1	1	1

$D^{(l-)}$  for the operations of symmetry group  $O_h$  up to  $l = 5$ . A finite symmetry group can be considered as a subgroup of the rotation-inversion group. It is useful to work out the compatibility relations between the irreducible representations of the rotation-inversion group and the irreducible representations of a finite symmetry group in order to find the splittings of atomic states in a crystal field. The decomposition of the irreducible representations of group  $O(3)$  with  $l$  up to 5 (Table 1-14), into the irreducible representations of group  $O_h$  (Table 1-4), can be carried out using (1-7) and is reported in Table 1-15.

Note that the spherical harmonics  $Y_{lm}(\theta, \varphi)$  ( $m = -l \dots +l$ ) with even (odd)  $l$  constitute a basis for the irreducible representation  $D^{(l+)}(D^{(l-)})$  of group  $O(3)$ . Hence the spherical harmonics  $Y_{lm}(\theta, \varphi)$  ( $m = -l \dots +l$ ) constitute a basis for a representation of a finite symmetry group. The appropriate combinations of spherical harmonics that belong to the irreducible representations of a symmetry point group can be obtained by applying the projection operators (1-21) or (1-25) to the spherical harmonics.<sup>[8]</sup>

For example, consider the states of an atom split by a perturbation with the cubic symmetry  $O_h$ . Using Table 1-15 one can immediately write:

$$\text{State } s \text{ } (l = 0) = \Gamma_1.$$

$$\text{State } p \text{ } (l = 1) = \Gamma_{15}.$$

$$\text{State } d \text{ } (l = 2) = \Gamma'_{25} + \Gamma_{12}.$$

$$\text{State } f \text{ } (l = 3) = \Gamma_{15} + \Gamma_{25} + \Gamma'_2.$$

$$\text{State } g \text{ } (l = 4) = \Gamma'_{25} + \Gamma'_{15} + \Gamma_{12} + \Gamma_1.$$

$$\text{State } h \text{ } (l = 5) = \Gamma_{25} + 2\Gamma_{15} + \Gamma'_{12}.$$

TABLE 1-15. Decomposition of the irreducible representations of group  $O(3)$  with  $l$  up to 5 into the irreducible representations of group  $O_h$

$D^{(0+)}$ $\Gamma_1$	$D^{(0-)}$ $\Gamma'_1$	$D^{(1+)}$ $\Gamma'_{15}$	$D^{(1-)}$ $\Gamma_{15}$	$D^{(2+)}$ $\Gamma_{12} + \Gamma'_{25}$	$D^{(2-)}$ $\Gamma'_{12} + \Gamma_{25}$
$D^{(3+)}$ $\Gamma_2 + \Gamma'_{25} + \Gamma'_{15}$	$D^{(3-)}$ $\Gamma'_2 + \Gamma_{25} + \Gamma_{15}$	$D^{(4+)}$ $\Gamma_1 + \Gamma_{12} + \Gamma'_{25} + \Gamma'_{15}$	$D^{(4-)}$ $\Gamma'_1 + \Gamma'_{12} + \Gamma_{25} + \Gamma_{15}$	$D^{(5+)}$ $\Gamma_{12} + \Gamma'_{25} + 2\Gamma'_{15}$	$D^{(5-)}$ $\Gamma'_{12} + \Gamma_{25} + 2\Gamma_{15}$

It is sometimes convenient to label the irreducible representations of a finite symmetry group with the name of the lowest order spherical harmonic that transforms according to the given representation. In the case of group  $O_h$ , for instance, state  $\Gamma_1$  is said to be *s*-like, because the spherical harmonic  $Y_{00}$  belongs to it. Similarly, representation  $\Gamma_{15}$  is said to be *p*-like, while  $\Gamma_{12}$  and  $\Gamma'_{25}$  are *d*-like representations.

The linear combinations of spherical harmonics that are partner functions of the irreducible representations of point group  $O_h$  can be obtained using the standard projection operators defined by (1-21) and (1-25) on the spherical harmonics expressed in cartesian coordinates. The linear combinations for *s*, *p*, *d*, and *f* atomic states are reported for convenience in Table 1-16. These symmetry-adapted linear combinations are known as cubic harmonics.

## 1-5 Spin dependent functions and double groups

### 1-5a Transformation of spin functions under proper and improper rotations<sup>[9]</sup>

In the symmetry groups so far considered we have implicitly limited the symmetry elements to include rotations through an angle  $\alpha$  with  $0 \leq \alpha < 2\pi$  (and the product of such rotations by  $I$ ) because of the basic assumption that any rotation by  $2\pi$  or multiple of  $2\pi$  coincides with the identity. A rotation by  $2\pi$  automatically leaves a function  $f(\mathbf{r})$  unchanged, and eq. (1-16) defines the effect of a symmetry operation on this function.

Let us extend the results of the previous sections to an eigenvalue problem in which spin is included. It is known that electrons are half-spin particles. The natural way to treat particles with spin is within the frame of the relativistic quantum theory. However, for symmetry problems and for the approximate treatment of a number of problems, it is sufficient to define the spin space containing two linearly independent states and to consider an electron as described by wave functions depending on both space and spin coordinates. In spin space the intrinsic angular momentum operator of the electron is  $\mathbf{s} = \frac{1}{2}\hbar\boldsymbol{\sigma}$ ;  $\sigma_x, \sigma_y, \sigma_z$  are represented by the Pauli matrices

$$\sigma_x = \begin{pmatrix} 0 & 1 \\ 1 & 0 \end{pmatrix}, \quad \sigma_y = \begin{pmatrix} 0 & -i \\ i & 0 \end{pmatrix}, \quad \sigma_z = \begin{pmatrix} 1 & 0 \\ 0 & -1 \end{pmatrix}, \quad (1-37)$$

in the representation in which  $\sigma_z$  is diagonal. The eigenstates of operator  $\sigma_z$ , which we denote as  $u_+$  and  $u_-$ , are

$$u_+ = \begin{pmatrix} 1 \\ 0 \end{pmatrix} \quad \text{and} \quad u_- = \begin{pmatrix} 0 \\ 1 \end{pmatrix}.$$

TABLE I-16. Linear combination of spherical harmonics up to  $l=3$  that are partner functions for the irreducible representations of point group  $O_h$ . The expression of spherical harmonics in cartesian coordinates is given on the left side of the table. The phase convention is that of Condon and Shortley after C. J. Ballhausen, *Ligand Field Theory* (McGraw-Hill, 1962)

$s$ state	$\left\{ Y_{00} = \frac{1}{\sqrt{4\pi}} \right.$	$\Gamma_1 \quad \left\{ s = \frac{1}{\sqrt{4\pi}} = Y_{00} \right.$
$p$ state	$\begin{cases} Y_{11} = -\sqrt{\left(\frac{3}{8\pi}\right)} \frac{x+iy}{r} \\ Y_{10} = \sqrt{\left(\frac{3}{4\pi}\right)} \frac{z}{r} \\ Y_{1-1} = \sqrt{\left(\frac{3}{8\pi}\right)} \frac{x-iy}{r} \end{cases}$	$\begin{cases} p_x = \sqrt{\left(\frac{3}{4\pi}\right)} \frac{x}{r} = \frac{1}{\sqrt{2}} (-Y_{11} + Y_{1-1}) \\ p_y = \sqrt{\left(\frac{3}{4\pi}\right)} \frac{y}{r} = \frac{i}{\sqrt{2}} (Y_{11} + Y_{1-1}) \\ p_z = \sqrt{\left(\frac{3}{4\pi}\right)} \frac{z}{r} = Y_{10} \end{cases}$
$d$ state	$\begin{cases} Y_{22} = \sqrt{\left(\frac{15}{32\pi}\right)} \frac{(x+iy)^2}{r^2} \\ Y_{21} = -\sqrt{\left(\frac{15}{8\pi}\right)} \frac{(x+iy)z}{r^2} \\ Y_{20} = \sqrt{\left(\frac{5}{16\pi}\right)} \frac{3z^2-r^2}{r^2} \\ Y_{2-1} = \sqrt{\left(\frac{15}{8\pi}\right)} \frac{(x-iy)z}{r^2} \\ Y_{2-2} = \sqrt{\left(\frac{15}{32\pi}\right)} \frac{(x-iy)^2}{r^2} \end{cases}$	$\begin{cases} d_{xx} = \sqrt{\left(\frac{15}{4\pi}\right)} \frac{xz}{r^2} = \frac{1}{\sqrt{2}} (-Y_{21} + Y_{2-1}) \\ d_{xy} = \sqrt{\left(\frac{15}{4\pi}\right)} \frac{xy}{r^2} = \frac{-i}{\sqrt{2}} (Y_{22} - Y_{2-2}) \\ d_{yz} = \sqrt{\left(\frac{15}{4\pi}\right)} \frac{yz}{r^2} = \frac{i}{\sqrt{2}} (Y_{21} + Y_{2-1}) \\ d_{3z^2-r^2} = \sqrt{\left(\frac{5}{16\pi}\right)} \frac{3z^2-r^2}{r^2} = Y_{20} \\ d_{x^2-y^2} = \sqrt{\left(\frac{15}{16\pi}\right)} \frac{x^2-y^2}{r^2} = \frac{1}{\sqrt{2}} (Y_{22} + Y_{2-2}) \end{cases}$
$f$ state	$\begin{cases} Y_{33} = -\sqrt{\frac{7}{4}} \sqrt{\left(\frac{5}{16\pi}\right)} \frac{(x+iy)^3}{r^3} \\ Y_{32} = \sqrt{\frac{7}{4}} \sqrt{\left(\frac{15}{8\pi}\right)} \frac{(x+iy)^2 z}{r^3} \\ Y_{31} = -\sqrt{\frac{7}{4}} \sqrt{\left(\frac{3}{16\pi}\right)} \frac{(x+iy)(5z^2-r^2)}{r^3} \\ Y_{30} = \sqrt{\frac{7}{4}} \sqrt{\left(\frac{1}{4\pi}\right)} \frac{(5z^2-3r^2)z}{r^3} \\ Y_{3-1} = \sqrt{\frac{7}{4}} \sqrt{\left(\frac{3}{16\pi}\right)} \frac{(x-iy)(5z^2-r^2)}{r^3} \\ Y_{3-2} = \sqrt{\frac{7}{4}} \sqrt{\left(\frac{15}{8\pi}\right)} \frac{(x-iy)^2 z}{r^3} \\ Y_{3-3} = \sqrt{\frac{7}{4}} \sqrt{\left(\frac{5}{16\pi}\right)} \frac{(x-iy)^3}{r^3} \end{cases}$	$\begin{cases} f_{(5x^2-3y^2)x} = \sqrt{\frac{7}{4}} \sqrt{\left(\frac{1}{4\pi}\right)} \frac{(5x^2-3r^2)x}{r^3} = \sqrt{\left(\frac{3}{16}\right)} (Y_{31} - Y_{3-1}) - \sqrt{\left(\frac{5}{16}\right)} (Y_{33} - Y_{3-3}) \\ f_{(5y^2-3r^2)y} = \sqrt{\frac{7}{4}} \sqrt{\left(\frac{1}{4\pi}\right)} \frac{(5y^2-3r^2)y}{r^3} = -i\sqrt{\left(\frac{3}{16}\right)} (Y_{31} + Y_{3-1}) - i\sqrt{\left(\frac{5}{16}\right)} (Y_{33} + Y_{3-3}) \\ f_{(5z^2-3r^2)z} = \sqrt{\frac{7}{4}} \sqrt{\left(\frac{1}{4\pi}\right)} \frac{(5z^2-3r^2)z}{r^3} = Y_{30} \\ f_{(x^2-y^2)xy} = \sqrt{\frac{7}{4}} \sqrt{\left(\frac{15}{4\pi}\right)} \frac{(x^2-y^2)z}{r^3} = -i\sqrt{\left(\frac{5}{16}\right)} (Y_{31} + Y_{3-1}) + i\sqrt{\left(\frac{3}{16}\right)} (Y_{33} + Y_{3-3}) \\ f_{(x^2-z^2)yz} = \sqrt{\frac{7}{4}} \sqrt{\left(\frac{15}{4\pi}\right)} \frac{(x^2-y^2)z}{r^3} = \frac{1}{\sqrt{2}} (Y_{32} + Y_{3-2}) \\ f_{(y^2-z^2)zx} = \sqrt{\frac{7}{4}} \sqrt{\left(\frac{15}{4\pi}\right)} \frac{(y^2-z^2)x}{r^3} = \sqrt{\left(\frac{5}{16}\right)} (Y_{31} - Y_{3-1}) + \sqrt{\left(\frac{3}{16}\right)} (Y_{33} - Y_{3-3}) \\ f_{xyz} = \sqrt{\frac{7}{4}} \sqrt{\left(\frac{15}{\pi}\right)} \frac{xyz}{r^3} = -\frac{i}{\sqrt{2}} (Y_{32} - Y_{3-2}) \end{cases}$

Any other state in spin space may be expressed as a linear combination of  $u_+$  and  $u_-$ . In order to be able to extend ordinary group theoretical techniques, we consider the transformation properties of spin functions under the rotation-inversion operations. Let us first investigate the effect of a proper rotation  $R$  on the states  $(u_+, u_-)$ . The states  $Ru_+$  and  $Ru_-$  obtained by applying a rotation  $R$  on  $u_+$  and  $u_-$  can be expressed as

$$\left. \begin{aligned} Ru_+ &= au_+ + cu_- \\ Ru_- &= bu_+ + du_- \end{aligned} \right\} \quad (1-38)$$

The spin functions  $(u_+, u_-)$  constitute a basis for a representation of the rotation group in which rotation  $R$  is represented by the matrix  $\begin{pmatrix} a & b \\ c & d \end{pmatrix}$ . To determine this matrix, let us introduce the infinitesimal rotation operator  $I_\xi$  about the  $\xi$ -axis, so that the rotation  $R(\alpha, \xi)$  can be written as

$$R(\alpha, \xi) = I - i\alpha I_\xi \quad (1-39)$$

for small  $\alpha$ .

Any rotation of a finite angle about the  $\xi$ -axis can be expressed in terms of  $I_\xi$ . In fact, any rotation of angle  $\alpha$  may be considered as the product of  $n$  infinitesimal rotations of angle  $\alpha/n$  so that for large  $n$  we have

$$R(\alpha, \xi) = \lim_{n \rightarrow \infty} \left( I - \frac{i\alpha}{n} I_\xi \right)^n = \sum_n \frac{(-i\alpha I_\xi)^n}{n!}. \quad (1-40)$$

Let  $l, m, n$  be the direction cosines of the  $\xi$ -axis and  $s_\xi$  the component along the  $\xi$ -axis of the intrinsic angular momentum operator, which from (1-37) is

$$s_\xi = ls_x + ms_y + ns_z = \frac{\hbar}{2} \begin{pmatrix} n & l - im \\ l + im & -n \end{pmatrix}.$$

One can show<sup>[10]</sup> that the infinitesimal rotation operator  $I_\xi$  is related to  $s_\xi$  by the expression  $\hbar I_\xi = s_\xi$  so that

$$I_\xi = \frac{1}{2} \begin{pmatrix} n & l - im \\ l + im & -n \end{pmatrix}.$$

Substituting the above expression for  $I_\xi$  into (1-40),

$$R(\alpha, \xi) = \sum_{n \text{ even}} \frac{(-i\alpha I_\xi)^n}{n!} + \sum_{n \text{ odd}} \frac{(-i\alpha I_\xi)^n}{n!} = I \cos \frac{\alpha}{2} - 2iI_\xi \sin \frac{\alpha}{2}$$

or

$$R(\alpha, \xi) = \begin{pmatrix} \cos \frac{\alpha}{2} - in \sin \frac{\alpha}{2} & (-il - m) \sin \frac{\alpha}{2} \\ (-il + m) \sin \frac{\alpha}{2} & \cos \frac{\alpha}{2} + in \sin \frac{\alpha}{2} \end{pmatrix}. \quad (1-41)$$

Equation (1-41) gives the transformation properties of spin functions under any proper rotation. Note in particular that any rotation of angle  $\alpha = 2\pi$  changes the sign of the spin functions. Thus in spin space, a rotation by  $2\pi$  is not equivalent to the identity operation;

only rotations by  $4\pi$  or a multiple of  $4\pi$  coincide with the identity. Consequently, when we treat an eigenvalue problem with explicit inclusion of spin, we must enlarge the symmetry group  $\mathcal{G}(R)$  of the operator by adding the symmetry element  $\bar{E}$ , corresponding to a rotation by  $2\pi$ , and the product of  $\bar{E}$  with all the other symmetry elements of  $\mathcal{G}(R)$ : we obtain a *double group*  $\mathcal{G}'(R)$  which has twice as many elements as  $\mathcal{G}(R)$ .

Note that the spin functions  $(u_+, u_-)$  constitute a basis for the irreducible representation, referred to as  $D^{(1/2)}$ , of the double group  $O^+(3)'$  of the pure rotation group  $O^+(3)$ . The matrix representatives are given by (1-41). If we take two independent linear combinations of  $(u_+, u_-)$  as basis functions, the representation  $D^{(1/2)}$  is transformed into  $\mathbf{M}^{-1} \mathbf{D}^{(1/2)}(R) \mathbf{M}$ , where  $\mathbf{M}$  is the matrix defining the linear combination (see Section 1-3a). In particular, if we take  $\mathbf{M} = i\sigma_y \equiv \begin{pmatrix} 0 & 1 \\ -1 & 0 \end{pmatrix}$ , we can easily verify that

$$\left. \begin{array}{l} (i\sigma_y) u_+ = -u_- \\ (i\sigma_y) u_- = u_+ \end{array} \right\} \quad (1-42)$$

and

$$(i\sigma_y)^{-1} \mathbf{D}^{(1/2)}(R) (i\sigma_y) = \mathbf{D}^{(1/2)}(R)^*. \quad (1-43)$$

We thus obtain the following important result to be used in the discussion of time-reversal symmetry: *the functions  $(u_+, u_-)$  constitute a basis for the representation  $D^{(1/2)}$  of the rotation double group, and the functions  $(-u_-, u_+)$  constitute a basis for the complex conjugate representation  $D^{(1/2)*}$ .*

So far our considerations have been limited to proper rotations. To extend the theory to improper rotations, one must consider the effect of inversion  $I$  on spin functions. The states  $Iu_+$  and  $Iu_-$  must be linear combinations of  $u_+$  and  $u_-$ , and the coefficients of these linear combinations determine the matrix representative of  $I$ . Since  $I$  commutes with any rotation, the matrix that represents it must, according to Schur's lemma, be a constant matrix:

$$\mathbf{D}(I) = c\mathbf{1}.$$

Physical considerations require that  $\langle Iu_+ | Iu_+ \rangle = \langle u_+ | u_+ \rangle = 1$  (and a similar relation for  $u_-$ ). This gives

$$c^*c = 1.$$

The effect of inversion therefore is to multiply any possible spin function by a phase factor. It can be shown that this phase factor is real by noting that the basis functions of the complex conjugate representation are multiplied by  $c^*$  that must be equal to  $c$ . One is thus left with the two possibilities  $c = \pm 1$ . Since the introduction of  $I$  automatically implies the introduction of  $I = I\bar{E}$ , without loss of generality one can assume  $c = 1$ . This gives the result

$$\left. \begin{array}{l} Iu_+ = u_+ \\ Iu_- = u_- \end{array} \right\} \quad (1-44)$$

### 1-5b Irreducible representations of double groups

Let us consider a finite symmetry group  $\mathcal{G}(R)$  constituted by an appropriate collection of proper and improper rotations of angles  $\alpha$  with  $0 \leq \alpha < 2\pi$ , and the double group  $\mathcal{G}'$  obtained by adding the operation  $\bar{E}$  (rotation by  $2\pi$ ) and the product of it

by any other operation. The double group  $\mathcal{G}'$  is obtained associating to every element of  $\mathcal{G}(R)$  the matrix (1-41) for proper rotations  $R(\alpha, \xi)$  of an angle  $\alpha < 2\pi$  and the product  $IR(\alpha, \xi)$  for improper rotations and including the operation  $\bar{E}$ . The multiplications of all elements and the separation into classes can then be easily worked out, as explained in Section 1-1. The irreducible representations are then derived by applying the standard procedures of Section 1-2b. A simple but important observation on the irreducible representations of the double group is that the element  $\bar{E}$ , which indicates the rotation by  $2\pi$ , commutes with every element of the group, and forms a class by itself. The representations of the double group may be separated into representations with  $c = 1$  or  $c = -1$ . In those with  $c = 1$  the elements  $E$  and  $\bar{E}$  (and in general  $R$  and  $\bar{R} = R\bar{E}$ ) are represented by the same matrices; these representations can be obtained directly from the representations of the simple group  $\mathcal{G}(R)$ . In the representations characterized by  $c = -1$  the elements  $E$  and  $\bar{E}$  (and in general  $R$  and  $\bar{R} = R\bar{E}$ ) are represented by opposite matrices. These new representations are called the additional representations of the double group and are used to classify the eigenstates when spin is included because, as has been shown, spinors change their sign under  $\bar{E}$ .

### Illustrative examples

**Group  $C'_1$ .** The simple group  $C_1$  contains the identity  $E$ . The double group contains  $E$  and  $\bar{E}$ . There are two classes and two one-dimensional irreducible representations, shown in Table 1-17.

TABLE 1-17. Irreducible representations of double group  $C'_1$

$E$	$\bar{E}$	
1	1	Representation corresponding to the simple group
1	-1	Additional representation of the double group

**Group  $C'_i$ .** The simple group  $C_i$  contains the identity  $E$  and the inversion  $I$  (Table 1-2). The double group  $C'_i$  contains the four elements  $E, \bar{E}, I, \bar{I}$ . Because all these elements commute, there are four classes and four one-dimensional irreducible representations given in Table 1-18.

TABLE 1-18. Irreducible representations of double group  $C'_i$

$E$	$\bar{E}$	$I$	$\bar{I}$	
1	1	1	1	Representations corresponding to the simple group
1	1	-1	-1	
1	-1	1	-1	Additional representations of the double group
1	-1	-1	1	

**Group  $C'_{3v}$ .** The simple group  $C_{3v}$  contains six elements:  $E, \delta_{3xyz}, \delta_{3xyz}^{-1}, I\delta_{2xy}, I\delta_{2xz}, I\delta_{2yz}$  (Table 1-5). Recall that  $\delta_{3xyz}$  means a rotation by an angle  $2\pi/3$  around an axis with director cosines on the ratio  $1:1:1$ . To find the matrix (1-41) corresponding

## ELECTRONIC STATES AND OPTICAL TRANSITIONS

to  $\delta_{3xyz}$ , one must take  $\alpha = 2\pi/3$  and  $l = m = n = 1/\sqrt{3}$ :

$$\delta_{3xyz} = \begin{pmatrix} \frac{1-i}{2} & -\frac{1+i}{2} \\ \frac{1-i}{2} & \frac{1+i}{2} \end{pmatrix}.$$

Similarly,  $I\delta_{2xy}$  means the product of the inversion  $I$  by the rotation of  $2\pi/2$  around an axis with director cosines in the ratio  $1:1:0$ . To find the matrix (1-41) corresponding to  $\delta_{2xy}$ , take  $\alpha = \pi$  and  $l = 1/\sqrt{2}$ ,  $m = -1/\sqrt{2}$ ,  $n = 0$ . One thus obtains

$$I\delta_{2xy} = I \begin{pmatrix} 0 & \frac{1-i}{\sqrt{2}} \\ -\frac{1+i}{\sqrt{2}} & 0 \end{pmatrix}.$$

TABLE 1-19. List of the elements of double group  $C'_{3v}$  and its separation into classes

$\mathcal{C}_1$	$E = \begin{pmatrix} 1 & 0 \\ 0 & 1 \end{pmatrix}$	$\mathcal{C}_2$	$\bar{E} = \begin{pmatrix} -1 & 0 \\ 0 & -1 \end{pmatrix}$
$\mathcal{C}_3$	$\delta_{3xyz} = \begin{pmatrix} \frac{1-i}{2} & -\frac{1+i}{2} \\ \frac{1-i}{2} & \frac{1+i}{2} \end{pmatrix}$	$\mathcal{C}_4$	$\bar{\delta}_{3xyz} = \begin{pmatrix} \frac{-1+i}{2} & \frac{1+i}{2} \\ \frac{-1+i}{2} & \frac{-1-i}{2} \end{pmatrix}$
	$\delta_{3xyz}^{-1} = \begin{pmatrix} \frac{1+i}{2} & \frac{1+i}{2} \\ -\frac{1-i}{2} & \frac{1-i}{2} \end{pmatrix}$		$\bar{\delta}_{3xyz}^{-1} = \begin{pmatrix} -\frac{1+i}{2} & -\frac{1+i}{2} \\ \frac{1-i}{2} & \frac{-1+i}{2} \end{pmatrix}$
$\mathcal{C}_5$	$I\delta_{2xy} = I \begin{pmatrix} 0 & \frac{1-i}{\sqrt{2}} \\ -\frac{1+i}{\sqrt{2}} & 0 \end{pmatrix}$	$\mathcal{C}_6$	$I\bar{\delta}_{2xy} = I \begin{pmatrix} 0 & -\frac{1-i}{\sqrt{2}} \\ \frac{1+i}{\sqrt{2}} & 0 \end{pmatrix}$
	$I\delta_{2xz} = I \begin{pmatrix} -\frac{i}{\sqrt{2}} & \frac{i}{\sqrt{2}} \\ \frac{i}{\sqrt{2}} & \frac{i}{\sqrt{2}} \end{pmatrix}$		$I\bar{\delta}_{2xz} = I \begin{pmatrix} \frac{i}{\sqrt{2}} & -\frac{i}{\sqrt{2}} \\ -\frac{i}{\sqrt{2}} & -\frac{i}{\sqrt{2}} \end{pmatrix}$
	$I\delta_{2yz} = I \begin{pmatrix} \frac{i}{\sqrt{2}} & -\frac{1}{\sqrt{2}} \\ \frac{1}{\sqrt{2}} & -\frac{i}{\sqrt{2}} \end{pmatrix}$		$I\bar{\delta}_{2yz} = I \begin{pmatrix} -\frac{i}{\sqrt{2}} & \frac{1}{\sqrt{2}} \\ -\frac{1}{\sqrt{2}} & \frac{i}{\sqrt{2}} \end{pmatrix}$

Proceeding in this way for all the six elements of group  $C_{3v}$ , and then multiplying by  $E$  and  $\bar{E}$ , one obtains the 12 elements for double group  $C'_{3v}$ , indicated in Table 1-19. The elements of group  $C'_{3v}$  can now be divided into classes. It is to be noted immediately that  $E$  and  $\bar{E}$  commute with all the elements of the group and thus constitute two classes. The two elements  $\delta_{3xyz}$  and  $\delta_{3xyz}^{-1}$  belong to the same class. In fact

$$(I\delta_{2\bar{x}z})\delta_{3xyz}(I\delta_{2\bar{x}z})^{-1}$$

$$= I \begin{pmatrix} -i & i \\ \sqrt{2} & \sqrt{2} \end{pmatrix} \begin{pmatrix} 1-i & -1+i \\ 2 & 2 \end{pmatrix} I \begin{pmatrix} i & -i \\ \sqrt{2} & \sqrt{2} \end{pmatrix}$$

$$= \begin{pmatrix} 1+i & 1+i \\ 2 & 2 \end{pmatrix} = \delta_{3xyz}^{-1}.$$

By a continuance of this procedure, we find that the 12 elements of group  $C'_{3v}$  can be divided into six classes, and these are also supplied for convenience in Table 1-20.

TABLE 1-20. Irreducible representations of double group  $C'_{3v}$ 

	$\mathcal{C}_1$	$\mathcal{C}_2$	$\mathcal{C}_3$	$\mathcal{C}_4$	$\mathcal{C}_5$	$\mathcal{C}_6$	
	$E$	$E$	$\delta_{3xyz}^{-1}\delta_{3xyz}$	$\bar{\delta}_{3xyz}^{-1}\bar{\delta}_{3xyz}$	$I\delta_{2xy}I\delta_{2\bar{x}z}I\delta_{2yz}$	$I\bar{\delta}_{2xy}I\bar{\delta}_{2\bar{x}z}I\bar{\delta}_{2yz}$	
$A_1$	1	1	1	1	1	1	Representations corresponding to the simple group
$A_2$	1	1	1	1	-1	-1	
$A_3$	2	2	-1	-1	0	0	
<hr/>							
$A_4$	1	-1	-1	1	$i$	$-i$	Additional representations of the double group
$A_5$	1	-1	-1	1	$-i$	$i$	
$A_6$	2	-2	1	-1	0	0	

Since there are 12 elements in six classes, the dimensions of the irreducible representations are

$$\sum_{\alpha=1}^6 l_{\alpha}^2 = 12$$

with the solution  $1^2 + 1^2 + 1^2 + 1^2 + 2^2 + 2^2 = 12$ . Thus there are a total of four one-dimensional and two two-dimensional representations. Since the three irreducible representations of  $C_{3v}$  of Table 1-5 are also irreducible representations of  $C'_{3v}$ , there remain three additional representations to be found—two one-dimensional and one two-dimensional. The best way to proceed is to use multiplication of classes, obtaining immediately

$$\mathcal{C}_3\mathcal{C}_3 = 2\mathcal{C}_1 + \mathcal{C}_4.$$

## ELECTRONIC STATES AND OPTICAL TRANSITIONS

By using formula (1-8)

$$2\chi^{(\alpha)}(\mathcal{C}_3) 2\chi^{(\alpha)}(\mathcal{C}_3) = l_\alpha [2\chi^{(\alpha)}(\mathcal{C}_1) + 2\chi^{(\alpha)}(\mathcal{C}_4)].$$

Since  $R$  and  $\bar{R}$  have opposite matrices, for the additional irreducible representations  $\chi^{(\alpha)}(\mathcal{C}_4) = -\chi^{(\alpha)}(\mathcal{C}_3)$ , which gives the acceptable solution  $\chi^{(\alpha)}(\mathcal{C}_3) = -1$  when substituted into the preceding expression with  $l_\alpha = 1$ . The acceptable solution  $\chi^{(\alpha)}(\mathcal{C}_3) = +1$  is obtained when  $l_\alpha = 2$ . Similarly, the relation

$$\mathcal{C}_5 \mathcal{C}_5 = 3\mathcal{C}_2 + 3\mathcal{C}_3$$

gives

$$3\chi^{(\alpha)}(\mathcal{C}_5) 3\chi^{(\alpha)}(\mathcal{C}_5) = l_\alpha [3\chi^{(\alpha)}(\mathcal{C}_2) + 6\chi^{(\alpha)}(\mathcal{C}_3)].$$

In a one-dimensional irreducible representation  $\chi^{(\alpha)}(\mathcal{C}_3) = \chi^{(\alpha)}(\mathcal{C}_2) = -l_\alpha = -1$ , and we obtain the solutions  $\chi^{(\alpha)}(\mathcal{C}_5) = \pm i$ . In a two-dimensional representation,  $\chi^{(\alpha)}(\mathcal{C}_3) = 1$   $\chi^{(\alpha)}(\mathcal{C}_2) = -2$ ; it follows that  $\chi^{(\alpha)}(\mathcal{C}_5) = 0$ . All the irreducible representations of group  $C_{3v}'$  are given in Table 1-20.

*Group  $O^+(3)$ .* The simple group  $O^+(3)$  contains all proper rotations. For the procedures to obtain additional irreducible representations of the infinite group  $O^+(3)'$  we refer the reader to standard books on group theory.<sup>[7]</sup> In the additional irreducible representations  $D^{(j)}$  of the double group it is worth noting that the character corresponding to a rotation through an angle  $\alpha$  is given by

$$\chi^{(j)}(\alpha) = \sum_{m=-j}^j e^{im\alpha} = \frac{\sin(j + \frac{1}{2})\alpha}{\sin\alpha/2},$$

with  $j$  a semi-integer used to label the irreducible representations. The characters of the irreducible representations of group  $O^+(3)'$  are given in Table 1-21.

### 1-5c Decomposition of the states of a simple group into the states of a double group

Now let us consider how the states of a simple group are related to the states of a double group. For this purpose, take an eigenvalue  $E$  and the eigenfunctions  $(f_1, f_2, \dots, f_{l_\alpha})$

TABLE 1-21. Irreducible representations of double group  $O^+(3)'$ . Representations  $D^{(l)}$ , with integer  $l$ , correspond to the representations of the simple group. Representations  $D^{(j)}$ , with  $j$  half integer, are the additional irreducible representations of the double group

	$E$	Rotations through $\alpha$	$E$	$E \cdot$ Rotations through $\alpha$
$D^{(0)}$	1	1	1	1
$D^{(\frac{1}{2})}$	2	$2 \cos \frac{\alpha}{2}$	-2	$-2 \cos \frac{\alpha}{2}$
$D^{(1)}$	3	$1 + 2 \cos \alpha$	3	$1 + 2 \cos \alpha$
$D^{(j)}$	$(2j+1)$	$\sum_{m=-j}^j e^{im\alpha}$	$-(2j+1)$	$-\sum_{m=-j}^j e^{im\alpha}$
$D^{(l)}$	$(2l+1)$	$\sum_{m=-l}^l e^{im\alpha}$	$(2l+1)$	$\sum_{m=-l}^l e^{im\alpha}$

which act as a basis for representation  $D^{(\alpha)}$  of the Hamiltonian's symmetry group  $\mathcal{G}(R)$ , when spin is neglected. The product of the functions  $f_i$  ( $i = 1 \dots l_\alpha$ ) with the functions  $(u_+, u_-)$  which are the basis for representation  $D^{(1/2)}$ , constitutes a basis for a representation of the double group  $\mathcal{G}'(R)$  with characters  $\chi^{(\alpha)}(R) \chi^{(1/2)}(R)$ . We can reduce the product representation to a sum of additional irreducible representations of the double group by using (1-7). The number of irreducible representations contained in it and the dimension of the representations give the splitting of the eigenvalue and the degeneracy of the sublevels when spin dependent terms—like spin-orbit interaction—are included in the Hamiltonian.

The following example illustrates the procedure for the decomposition of states of the simple group into states of the double group, for group  $C_{3v}$ . Table 1-22 gives the

TABLE 1-22. Decomposition of the states of the simple group into the states of the double group, for symmetry group  $C_{3v}$

	$E$	$\bar{E}$	$\delta_{3xyz}^{-1} \delta_{3xyz}$	$\bar{\delta}_{3xyz}^{-1} \bar{\delta}_{3xyz}$	$I\delta_{2xy} I\delta_{2xz} I\delta_{2yz}$	$I\bar{\delta}_{2xy} I\bar{\delta}_{2xz} I\bar{\delta}_{2yz}$
$A_1$	1	1	1	1	1	1
$A_2$	1	1	1	1	-1	-1
$A_3$	2	2	-1	-1	0	0
$D^{(1/2)}$	2	-2	1	-1	0	0
$A_1 \times D^{(1/2)}$	2	-2	1	-1	0	0
$A_2 \times D^{(1/2)}$	2	-2	1	-1	0	0
$A_3 \times D^{(1/2)}$	4	-4	-1	1	0	0

characters of the representations  $A_1$ ,  $A_2$ , and  $A_3$  of group  $C_{3v}$ , the character of the symmetry elements in representation  $D^{(1/2)}$  and the products  $A_1 \times D^{(1/2)}$ ,  $A_2 \times D^{(1/2)}$ , and  $A_3 \times D^{(1/2)}$ . From the characters of the additional representations of Table 1-20, one sees that  $A_1 \times D^{(1/2)} = A_6$ ,  $A_2 \times D^{(1/2)} = A_6$ ,  $A_3 \times D^{(1/2)} = A_4 + A_5 + A_6$ .

As a second example, consider a Hamiltonian invariant under rotation group  $O^+(3)$ . Its eigenvalues are classified by the irreducible representations  $D^{(l)}$  ( $l = 0, 1, \dots$ ) of the rotation group. To study the splitting of the states when spin is included and spin-dependent terms of the Hamiltonian are considered, note that<sup>[7]</sup>

$$D^{(l)} \times D^{(1/2)} = \sum_{j=|l-1/2|}^{j=l+1/2} D^{(j)}. \quad (1-45)$$

The result obtained is that an  $s$ -state does not split for spin-orbit effects, while all other states split into two sublevels. Specifically, a  $p$ -state separates into two sublevels with degeneracy 6 and 4, and so on.

Other cases will be discussed when we give the electronic states of specific crystals.

## 1-6 Time reversal symmetry

### 1-6a The time reversal operator<sup>[11]</sup>

Before considering the time reversal symmetry in quantum mechanics, we wish to call to mind the principle of time reversal in classical mechanics for an isolated system.

## ELECTRONIC STATES AND OPTICAL TRANSITIONS

In classical mechanics the state of a system is specified from the values of the generalized coordinates and momenta  $q$  and  $p$  of the system. Given a state of the system, let us consider the state described by the same generalized coordinates but with opposite moments. This state is called the *time reversed conjugate* of the other. There is a close relationship between a state and its time-reversed conjugate but, in general, they are not exactly the same.

Suppose we consider over a certain interval of time the succession of states  $q(t), p(t)$  as determined by Hamilton's equations

$$\dot{q} = \frac{\partial H(p, q)}{\partial p} \quad \text{and} \quad \dot{p} = -\frac{\partial H(p, q)}{\partial q}.$$

Because of the principle of time reversal symmetry, the laws of motion and interactions are such that the sequence of time-reversed states in reversed chronological order constitutes a succession of states in its own right. Hamilton's equations in fact do not change their form under the transformation  $t \rightarrow -t, p \rightarrow -p$ , because  $H(p, q) = H(p, q)$  for an isolated system; therefore if  $q(t), p(t)$  are solutions of Hamilton's equations, so are  $q(-t), -p(-t)$ . The correspondence between these two solutions is schematically represented in Fig. 1-2.

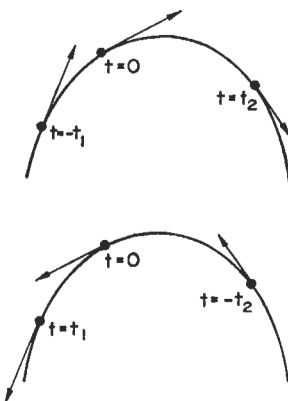


FIG. 1-2. Schematic representations of a trajectory  $q(t), p(t)$  and its time reversal  $q(-t), -p(-t)$ .

Now let us consider time reversal symmetry in quantum mechanics. In quantum mechanics the state of a system is specified by a wave function, the Hamiltonian function of classical mechanics is replaced by the Hamiltonian operator, and the evolution law is the time dependent Schrödinger equation. Let us first deal with the case of a spinless particle. The time dependent Schrödinger equation is

$$H(\mathbf{r}, \mathbf{p}) \psi(\mathbf{r}, t) = i\hbar \frac{\partial}{\partial t} \psi(\mathbf{r}, t),$$

and  $\mathbf{p} = -i\hbar\nabla$ . Changing  $t \rightarrow -t$  and taking the complex conjugate of the above relation gives

$$H(\mathbf{r}, -\mathbf{p}) \psi^*(\mathbf{r}, -t) = i\hbar \frac{\partial}{\partial t} \psi^*(\mathbf{r}, -t). \quad (1-46)$$

In an isolated system  $H(\mathbf{r}, -\mathbf{p}) = H(\mathbf{r}, \mathbf{p})$ . Equation (1-46) shows that if  $\psi(\mathbf{r}, t)$  represents a succession of states, the succession  $\psi^*(\mathbf{r}, -t)$  of complex conjugate states in reversed chronological order constitutes a possible succession of states. Given a state  $\psi$ , one calls  $\psi^*$  the *time-reversed conjugate of  $\psi$* . For a spinless particle, one is led to define a transformation in which wave function  $\psi$  transforms into its complex conjugate  $\psi^*$ .  $T$  indicates the operator effecting this transformation, and it will be called the *time reversal operator*. By definition,

$$T\psi(\mathbf{r}) = \psi^*(\mathbf{r}). \quad (1-47)$$

From definition (1-47) it follows that the operator  $T$  is antilinear, i.e.

$$T(a\psi + b\varphi) = a^*T\psi + b^*T\varphi$$

and anti-unitary, i.e.

$$\langle \psi | \varphi \rangle = \langle T\varphi | T\psi \rangle.$$

From definition (1-47) it also follows that

$$\left. \begin{aligned} \langle \psi | \mathbf{r} | \psi \rangle &= \langle T\psi | \mathbf{r} | T\psi \rangle, \\ \langle \psi | \mathbf{p} | \psi \rangle &= -\langle T\psi | \mathbf{p} | T\psi \rangle, \end{aligned} \right\} \quad (1-48a)$$

where, in the last relation, the minus sign appears because

$$\int \psi^* \nabla \psi \, d\mathbf{r} = - \int \psi \nabla \psi^* \, d\mathbf{r}.$$

The above equation (1-48a) implies the commutation rules

$$\left. \begin{aligned} T\mathbf{r}T^{-1} &= \mathbf{r}, \\ T\mathbf{p}T^{-1} &= -\mathbf{p}. \end{aligned} \right\} \quad (1-48b)$$

Equations (1-48) show that the expectation values of coordinates on a state and on its time-reversed conjugate state are equal, while the expectation values of momenta on a state and on its time-reversed conjugate state are opposite. A close relationship between time reversal symmetry in classical and quantum mechanics is thus established. One should note that for spinless particles

$$T^2\psi(\mathbf{r}) = \psi(\mathbf{r}). \quad (1-49)$$

Similar considerations can be made in the case of half-spin particles. In this case, we consider the Pauli equation

$$H(\mathbf{r}, \mathbf{p}, \sigma_x, \sigma_y, \sigma_z) \begin{pmatrix} \psi_1(\mathbf{r}, t) \\ \psi_2(\mathbf{r}, t) \end{pmatrix} = i\hbar \frac{\partial}{\partial t} \begin{pmatrix} \psi_1(\mathbf{r}, t) \\ \psi_2(\mathbf{r}, t) \end{pmatrix}, \quad (1-50)$$

where the dependence of  $H$  on the spin operators  $\sigma_x, \sigma_y, \sigma_z$  defined in (1-37) must be understood as a way to write a system of two differential equations in compact form. Changing  $t \rightarrow -t$  and taking the complex conjugate of (1-50) gives

$$H(\mathbf{r}, -\mathbf{p}, \sigma_x, -\sigma_y, \sigma_z) \begin{pmatrix} \psi_1^*(\mathbf{r}, -t) \\ \psi_2^*(\mathbf{r}, -t) \end{pmatrix} = i\hbar \frac{\partial}{\partial t} \begin{pmatrix} \psi_1^*(\mathbf{r}, -t) \\ \psi_2^*(\mathbf{r}, -t) \end{pmatrix}.$$

It is convenient to pre-multiply by the operator  $i\sigma_y$  both members of the above equation:

$$(i\sigma_y) H(\mathbf{r}, -\mathbf{p}, \sigma_x, -\sigma_y, \sigma_z) (i\sigma_y)^{-1} (i\sigma_y) \begin{pmatrix} \psi_1^*(\mathbf{r}, -t) \\ \psi_2^*(\mathbf{r}, -t) \end{pmatrix} = i\hbar \frac{\partial}{\partial t} (i\sigma_y) \begin{pmatrix} \psi_1^*(\mathbf{r}, -t) \\ \psi_2^*(\mathbf{r}, -t) \end{pmatrix}.$$

## ELECTRONIC STATES AND OPTICAL TRANSITIONS

Since  $\sigma_y$  anticommutes with  $\sigma_x$  and  $\sigma_z$ ,

$$H(\mathbf{r}, -\mathbf{p}, -\sigma)(i\sigma_y) \begin{pmatrix} \psi_1^*(\mathbf{r}, -t) \\ \psi_2^*(\mathbf{r}, -t) \end{pmatrix} = i\hbar \frac{\partial}{\partial t} (i\sigma_y) \begin{pmatrix} \psi_1^*(\mathbf{r}, -t) \\ \psi_2^*(\mathbf{r}, -t) \end{pmatrix}, \quad (1-51)$$

where for brevity  $H(\mathbf{r}, -\mathbf{p}, -\sigma)$  is written for  $H(\mathbf{r}, -\mathbf{p}, -\sigma_x, -\sigma_y, -\sigma_z)$ . In an isolated system,  $H(\mathbf{r}, -\mathbf{p}, -\sigma) = H(\mathbf{r}, \mathbf{p}, \sigma)$ . Thus (1-51) shows that when

$$\begin{pmatrix} \psi_1(\mathbf{r}, t) \\ \psi_2(\mathbf{r}, t) \end{pmatrix}$$

represents a succession of states, the succession of states

$$(i\sigma_y) \begin{pmatrix} \psi_1^*(\mathbf{r}, -t) \\ \psi_2^*(\mathbf{r}, -t) \end{pmatrix}$$

in reversed chronological order constitutes a possible succession of states.

Given a state  $\begin{pmatrix} \psi_1(\mathbf{r}) \\ \psi_2(\mathbf{r}) \end{pmatrix}$ , one calls  $(i\sigma_y) \begin{pmatrix} \psi_1^*(\mathbf{r}) \\ \psi_2^*(\mathbf{r}) \end{pmatrix}$  the *time-reversed conjugate* of  $\begin{pmatrix} \psi_1(\mathbf{r}) \\ \psi_2(\mathbf{r}) \end{pmatrix}$ , and for half-spin particles the *time reversal operator*  $T$  is defined as

$$T \begin{pmatrix} \psi_1(\mathbf{r}) \\ \psi_2(\mathbf{r}) \end{pmatrix} = (i\sigma_y) \begin{pmatrix} \psi_1^*(\mathbf{r}) \\ \psi_2^*(\mathbf{r}) \end{pmatrix} = \begin{pmatrix} \psi_2^*(\mathbf{r}) \\ -\psi_1^*(\mathbf{r}) \end{pmatrix}, \quad (1-52)$$

where both complex conjugate and multiplication by  $(i\sigma_y)$  is required for half-spin particles.

Note in particular that the time reversal operator applied to spin functions  $u_+$  and  $u_-$  gives

$$\left. \begin{array}{l} Tu_+ = -u_- \\ Tu_- = u_+ \end{array} \right\} \quad (1-53)$$

From definition (1-52) it is easily proved that  $T$  is an antilinear and anti-unitary operator. We also have

$$\left. \begin{array}{l} \left\langle \begin{pmatrix} \psi_1 \\ \psi_2 \end{pmatrix} \middle| \mathbf{r} \middle| \begin{pmatrix} \psi_1 \\ \psi_2 \end{pmatrix} \right\rangle = \left\langle T \begin{pmatrix} \psi_1 \\ \psi_2 \end{pmatrix} \middle| \mathbf{r} \middle| T \begin{pmatrix} \psi_1 \\ \psi_2 \end{pmatrix} \right\rangle, \\ \left\langle \begin{pmatrix} \psi_1 \\ \psi_2 \end{pmatrix} \middle| \mathbf{p} \middle| \begin{pmatrix} \psi_1 \\ \psi_2 \end{pmatrix} \right\rangle = - \left\langle T \begin{pmatrix} \psi_1 \\ \psi_2 \end{pmatrix} \middle| \mathbf{p} \middle| T \begin{pmatrix} \psi_1 \\ \psi_2 \end{pmatrix} \right\rangle, \\ \left\langle \begin{pmatrix} \psi_1 \\ \psi_2 \end{pmatrix} \middle| \sigma \middle| \begin{pmatrix} \psi_1 \\ \psi_2 \end{pmatrix} \right\rangle = - \left\langle T \begin{pmatrix} \psi_1 \\ \psi_2 \end{pmatrix} \middle| \sigma \middle| T \begin{pmatrix} \psi_1 \\ \psi_2 \end{pmatrix} \right\rangle, \end{array} \right\} \quad (1-54a)$$

which imply the commutation rules

$$\left. \begin{array}{l} T \mathbf{r} T^{-1} = \mathbf{r}, \\ T \mathbf{p} T^{-1} = -\mathbf{p}, \\ T \sigma T^{-1} = -\sigma. \end{array} \right\} \quad (1-54b)$$

## USE OF SYMMETRY IN QUANTUM MECHANICS

Equations (1-54) show that the expectation values of the coordinates in a state and on its reversed conjugate are equal, while the expectation values of momenta and spin on a state and on its reversed conjugate are opposite. Also

$$T^2 \begin{pmatrix} \psi_1(\mathbf{r}) \\ \psi_2(\mathbf{r}) \end{pmatrix} = - \begin{pmatrix} \psi_1(\mathbf{r}) \\ \psi_2(\mathbf{r}) \end{pmatrix}. \quad (1-55)$$

Let us now establish for which systems operator  $T$  commutes with the Hamiltonian, so that the relation

$$H(\mathbf{r}, -\mathbf{p}, -\sigma) = TH(\mathbf{r}, \mathbf{p}, \sigma) T^{-1} = H(\mathbf{r}, \mathbf{p}, \sigma)$$

is satisfied. It should be noted that the time reversal operator, because of (1-48b) or (1-54b), commutes with the potential energy terms and with the kinetic energy term, which is quadratic in  $\mathbf{p}$ . It also commutes with terms containing spin-orbit and spin-spin interactions, and in general with the Hamiltonian of any isolated system. Time reversal symmetry may not apply if the system being considered is not isolated; for instance, operator  $T$  does not commute with the Hamiltonian of a charged particle in an *external magnetic field* because in such a case the Hamiltonian is a linear function of the operators  $\mathbf{p}$  and  $\sigma$ .

### 1-6b Essential degeneracies due to time reversal symmetry

Let us consider the eigenvalue problem

$$H\psi = E\psi$$

and suppose that Hamiltonian  $H$  is invariant under time reversal symmetry. We then have:

$$HT\psi = ET\psi.$$

Function  $T\psi$  is therefore an eigenfunction of  $H$  as  $\psi$ . There will be degeneracy due to time reversal if the two functions are linearly independent. In a quantum system, where Hamiltonian  $H$  has time reversal symmetry, additional systematic degeneracies among eigenfunctions may be expected.

As an example of a systematic degeneracy introduced by the time reversal operator, consider the case of half-spin particles and note that the spinor eigenfunctions  $\psi$  and  $T\psi$  cannot be linearly dependent. If this were not so, we could write

$$T\psi = c\psi$$

and

$$T^2\psi = c^*T\psi = c^*c\psi = |c|^2\psi,$$

which would be incompatible with (1-55). Thus  $T\psi$  and  $\psi$  must be linearly independent, and there is at least a double degeneracy for half-spin particles when the Hamiltonian is invariant under time reversal. This essential degeneracy is the famous Kramers theorem<sup>[12]</sup> of quantum mechanics. The Kramers degeneracy does not apply to quantum systems for which the time reversal operator is not a symmetry operator. For instance, an atomic state with total angular momentum  $J$  is split by an external magnetic field into  $2J + 1$  non-degenerate levels. Also  $S$  states ( $L = 0, J = \frac{1}{2}$ ) are split by an external magnetic field into two non-degenerate sublevels.

Let us consider an operator with space symmetry group  $\mathcal{G}(R)$  and invariant under time reversal symmetry. To discuss the effect of time reversal one can try to add  $T$  to group  $\mathcal{G}(R)$ . But this procedure presents the basic difficulty that space symmetry operators are linear operators, while  $T$  is antilinear. An appropriate generalization of the usual results of group theory, to deal with a group containing unitary as well as anti-unitary operations, ought therefore to be considered. (See, for example, Wigner.<sup>[11]</sup>) For simplicity, one can study the effect of time reversal by means of the following alternative procedure. Suppose that the set of eigenfunctions  $(\psi_1, \psi_2, \dots, \psi_l)$  belonging to eigenvalue  $E$  are required by space symmetry to be degenerate, and belong to an irreducible representation of the space symmetry group  $\mathcal{G}(R)$ . Then the set of functions  $(T\psi_1, T\psi_2, \dots, T\psi_l)$  also belongs to eigenvalue  $E$  and one must be able to decide whether or not the new set is linearly dependent on the previous one. *We note that if a set of functions belongs to the irreducible representation  $D$  of the Hamiltonian's symmetry group, the set of time reversal conjugate functions belongs to the complex conjugate representation  $D^*$ .* This result is immediate in the case of spinless particles because of definition (1-47); it also holds for half-spin particles because of (1-53) and because  $(-u_-, u_+)$  constitute a basis for representation  $D^{(1/2)*}$  of the rotation group, as shown in Section 1-5a.

It can now be decided whether the two sets of functions  $(\psi_1, \psi_2, \dots, \psi_l)$  and  $(T\psi_1, T\psi_2, \dots, T\psi_l)$  are or are not linearly dependent on the properties of corresponding representations  $D$  and  $D^*$  as discovered by Wigner.<sup>[11]</sup> The relationship between an irreducible representation and its complex conjugate was discussed in Section 1-2c, and it was seen that three different cases may occur:

- Case a:  $D$  and  $D^*$  are equivalent to the same real irreducible representation.
- Case b:  $D$  and  $D^*$  are inequivalent.
- Case c:  $D$  and  $D^*$  are equivalent to each other but not to a real representation.

In cases a and c time reversal may or may not give additional degeneracies, depending on the spin of the particle. In case b, the functions obtained by time reversal are linearly independent, and an additional degeneracy is introduced by time reversal for both spinless and half-spin particles. For irreducible representations which belong to case a, an additional degeneracy is introduced only for half-spin particles, while for those which belong to case c, an additional degeneracy is introduced only for spinless particles. The above-discussed effects of time reversal in introducing additional degeneracies are summarized in Table 1-23 and are known as Wigner's rules. To establish which of the three cases occurs for each irreducible representation, one uses the Frobenius-Schur test (1-14). A simple proof of the above conclusions is given below to clarify the physical reasons for the systematic degeneracies introduced by time reversal.

#### *Proof of Wigner's rules<sup>[11]</sup>*

*Case a.*  $D$  and  $D^*$  are equivalent to the same real irreducible representation. By an appropriate change of basis functions one gets a set of partner functions  $(\psi_1, \psi_2, \dots, \psi_l)$  for the irreducible representation  $D$ , with real matrix elements. Because  $D$  is real  $(T\psi_1, T\psi_2, \dots, T\psi_l)$  are partner functions for the irreducible representation  $D$ . Because of the orthogonality theorem of Section 1-3b one has, for partner functions of the same irreducible representation,

$$\langle \psi_i | T\psi_j \rangle = 0 \quad \text{if } i \neq j.$$

Now let us examine the possibility that  $T\psi_i$  is linearly dependent on  $\psi_i$ :

$$T\psi_i = c\psi_i.$$

## USE OF SYMMETRY IN QUANTUM MECHANICS

TABLE 1-23. Effect of time reversal symmetry

Case	Relation between $D$ and $D^*$	Frobenius-Schur test	Spinless particle	Half-spin particle
Case a	$D$ and $D^*$ are equivalent to the same real irreducible representation	$\sum_R \chi(R^2) = h$	No extra degeneracy	Doubled degeneracy
Case b	$D$ and $D^*$ are inequivalent	$\sum_R \chi(R^2) = 0$	Doubled degeneracy	Doubled degeneracy
Case c	$D$ and $D^*$ are equivalent to each other but not to a real representation	$\sum_R \chi(R^2) = -h$	Doubled degeneracy	No extra degeneracy

By applying operator  $T$ ,

$$T^2\psi_i = c^*T\psi_i = |c|^2 \psi_i.$$

For a half-spin particle this last relation is incompatible with (1-55); it follows that the functions  $\psi_i$  ( $i = 1 \dots l$ ) and the time reversed conjugate  $T\psi_i$  ( $i = 1 \dots l$ ) cannot be linearly dependent, and consequently the representation  $D$  appears twice with the same energy. For a spinless particle however, the above relation is compatible with (1-49), and therefore time-reversal symmetry does not imply any additional degeneracy.

*Case b.*  $D$  and  $D^*$  are inequivalent. The two sets of functions  $(\psi_1, \psi_2, \dots, \psi_l)$  and  $(T\psi_1, T\psi_2, \dots, T\psi_l)$  are linearly independent because basis functions of non-equivalent irreducible representations are orthogonal. Thus an additional degeneracy is introduced by the time reversal operator.

*Case c.*  $D$  and  $D^*$  are equivalent to each other but not to a real representation. Let us examine the possibility that the set of functions  $(T\psi_1, T\psi_2, \dots, T\psi_l)$  is linearly dependent on the set  $(\psi_1, \psi_2, \dots, \psi_l)$ , i.e.

$$T\psi_i = \sum_j M_{ij} \psi_j. \quad (1-56)$$

Pre-multiplication by the operator  $T$  gives

$$\pm \psi_i = \sum_j M_{ij}^* T\psi_j,$$

where the + sign refers to spinless particles, and the - sign to half-spin particles. Using expression (1-56) one has

$$\pm \psi_i = \sum_{ji} M_{ij}^* M_{ji} \psi_i.$$

Using the orthogonality of the functions  $\psi_i$  ( $i = 1 \dots l$ ) gives

$$\sum_j M_{ij}^* M_{ji} = \pm \delta_{ii},$$

or, equivalently,

$$\mathbf{M}^* \cdot \mathbf{M} = \pm \mathbf{1},$$

which implies that  $\mathbf{M}$  is either symmetric or antisymmetric. In the case of spinless particles, the relation  $\mathbf{M} \cdot \mathbf{M}^* = 1$  implies that we can transform representation  $D$  into  $D^*$  with a symmetric matrix, but this is impossible (see Section 1-2c). Relation (1-56) is also impossible and  $T\psi_i$  ( $i = 1 \dots l$ ) cannot be linearly dependent on  $\psi_i$  ( $i = 1 \dots l$ ). Thus the equivalent representations  $D$  and  $D^*$  always appear together, and the number of independent functions belonging to the same eigenvalue is doubled. In the case of particles with spin, the relation  $\mathbf{M} \cdot \mathbf{M}^* = -1$  implies that we can transform representation  $D$  into  $D^*$  with an antisymmetric matrix, with no additional degeneracy being introduced by time reversal.

### *Illustrative examples*

First let us consider the case of total absence of symmetry. The irreducible representations of group  $C'_1$  are given in Table 1-17. The identity representation refers to states without spin. Since it belongs to case a, the time reversal symmetry does not introduce any additional degeneracy. The additional representation of the double group belongs to case a and always appears twice, in agreement with Kramer's theorem.

Next consider the case of group  $C'_3$  (Table 1-20). All the representations of simple group  $A_1, A_2, A_3$  belong to case a and no additional degeneracy occurs. It can be seen that representations  $A_4$  and  $A_5$  of the double group belong to case b and are degenerate among themselves by time reversal symmetry. Representation  $A_6$  belongs to case c and no additional degeneracy is required by time reversal.

As a final example, let us consider the rotation group  $O^+(3)'$  (Table 1-21). Since the characters are real, the representations belong either to case a or to case c. The distinction between these two alternatives cannot be established by the Frobenius-Schur test, which applies only to finite groups. However, it would be easy to prove<sup>[11]</sup> that representations  $D^{(l)}$  with integer  $l$  can be put in real form (case a), while representations  $D^{(j)}$  with half integer  $j$  cannot be put in real form (case c). Consequently time reversal does not imply any further degeneracy.

## 1-7 Selection rules

In Section 1-3b it was seen that an operator with symmetry group  $\mathcal{G}(R)$  has vanishing matrix elements among functions belonging to different irreducible representations of the group or to different rows of the same irreducible representation. This is just a simple case of selection rules. In general one must calculate matrix elements of the type

$$\langle \varphi_m^{(\mu)} | V_i^{(\alpha)} | \psi_n^{(\nu)} \rangle, \quad (1-57)$$

where  $\varphi_m^{(\mu)}$  ( $m = 1, 2, \dots, l_\mu$ ) is a set of eigenfunctions transforming as the irreducible representation  $D^{(\mu)}$  of symmetry group  $\mathcal{G}(R)$ ,  $\psi_n^{(\nu)}$  ( $n = 1, 2, \dots, l_\nu$ ) is another set of eigenfunctions belonging to a different eigenvalue, and  $V_i^{(\alpha)}$  is a set of a perturbation functions that transform according to the irreducible representation  $D^{(\alpha)}$ . Remember (Section 1-3c) that the set of product functions obtained by multiplying among themselves two independent sets, are basis functions for the product representation and the products  $V_i^{(\alpha)} \psi_n^{(\nu)}$  ( $i = 1 \dots l_\alpha, n = 1 \dots l_\nu$ ) can be expressed as an appropriate combination of basis functions of the irreducible representations contained in the product representation. If irreducible representation  $D^{(\mu)}$  does not appear in the decomposition

of product representation  $D^{(\alpha)} \times D^{(\nu)}$  the matrix elements (1-57) are zero because of the orthogonality theorem (Section 1-3b). If  $c(\mu, \alpha, \nu)$  indicates the number of times irreducible representation  $D^{(\mu)}$  appears in the decomposition of product representation  $D^{(\alpha)} \times D^{(\nu)}$  then all matrix elements (1-57) can be expressed in terms of only  $c(\mu, \alpha, \nu)$  independent parameters. The number  $c(\mu, \alpha, \nu)$  is determined by equation (1-12) as

$$c(\mu, \alpha, \nu) = \frac{1}{h} \sum_{\mathbf{R}} \chi^{(\mu)*}(\mathbf{R}) \chi^{(\alpha)}(\mathbf{R}) \chi^{(\nu)}(\mathbf{R}). \quad (1-58)$$

It is to be emphasized here that the derivation of formula (1-58) implies that the two sets of functions  $\varphi_m^{(\mu)}$  and  $\psi_n^{(\nu)}$  are completely independent of each other. This is automatically satisfied if  $\varphi_m^{(\mu)}$  and  $\psi_n^{(\nu)}$  belong to different eigenvalues. When we consider matrix elements of a perturbation function among sets of degenerate eigenfunctions, selection rules may become more stringent than (1-58). Namely, in (1-58) the product character of initial and final states must be substituted by the symmetric or antisymmetric product.<sup>[13]</sup>

As an example let us consider the selection rules for optical transitions. Within the dipole approximation, the perturbation function  $V$  is proportional to  $\mathbf{e} \cdot \mathbf{r}$  where  $\mathbf{e}$  is the polarization vector of the radiation field. Let  $D^{(\alpha)}$  indicate the representation to which function  $\mathbf{e} \cdot \mathbf{r}$  belongs. The selection rules are obtained by multiplying  $D^{(\alpha)}$  by the irreducible representations of group  $\mathcal{G}(R)$  and then decomposing the product representations. The results for group  $C_{4v}$  are given in Table 1-24. Note that in this case selection rules are different when light is polarized  $\parallel$  or  $\perp$  to the fourfold  $x$ -axis. In fact, for light polarized parallel to the  $x$  axis the perturbation function  $\mathbf{e} \cdot \mathbf{r}$  has symmetry  $A_1$ , while for light polarized perpendicular to the  $x$ -axis the perturbation function  $\mathbf{e} \cdot \mathbf{r}$  has symmetry  $A_5$ . For instance, transition  $A_1 \rightarrow A_1$ , is allowed for light polarized  $\parallel$  to the  $x$ -axis, while it is forbidden for light polarized  $\perp$  to the  $x$ -axis.

TABLE 1-24. Allowed optical transitions in the dipole approximation for group  $C_{4v}$ . The case in which light is polarized  $\perp$  or  $\parallel$  to the fourfold axis has been separately indicated

$x \in A_1$	$A_1$ $A_1 \times A_1$	$A_1$ $A_1$	$A'_1$ $A'_1$	$A_2$ $A_2$	$A'_2$ $A'_2$	$A_5$ $A_5$
$(y, z) \in A_5$	$A_1$ $A_1 \times A_5$	$A_1$ $A_5$	$A'_1$ $A_5$	$A_2$ $A_5$	$A'_2$ $A_5$	$A_5$ $A_1 + A'_1 + A_2 + A'_2$

The optical selection rules for states of group  $O_h$  can be obtained in a similar way, and are basically contained in Table 1-10. We point out that in the case of group  $O_h$ , function  $\mathbf{e} \cdot \mathbf{r}$  belongs to representation  $\Gamma_{15}$  and selection rules do not depend on the polarization of the light, which is not surprising since the system has cubic symmetry.

## References and notes

[1] See, for instance M.TINKHAM, *Group Theory and Quantum Mechanics* (McGraw-Hill, 1964). This book contains a clear review of the definitions and properties of abstract groups, and many physical applications to atoms, molecules and solids. The reader may also consult the excellent book of J. S. LOMONT, *Applications of Finite Groups* (Academic Press, 1959). (It contains a very complete bibliography.)

## ELECTRONIC STATES AND OPTICAL TRANSITIONS

- [2] The general theory of representations of finite groups is dealt with in the classical book of E. P. WIGNER, *Group Theory and its Applications to the Quantum Mechanics of Atomic Spectra* (Academic Press, 1959), chapter 9. The reader more interested in physical applications can consult the books in ref. [1].
- [3] L. BOUCKAERT, R. SMOLUCHOWSKI and E. WIGNER, *Phys. Rev.* **50**, 58 (1936).
- [4] The derivation of the irreducible representations of all point symmetry groups of interest in crystal physics can be found in chapter 4 of the book by M. HAMERMESH, *Group Theory and its Applications to Physical Problems* (Addison-Wesley, 1962). We refer to the same book for a detailed analysis of complex conjugate representations and the direct product representation.
- [5] G. FROBENIUS and I. SCHUR, *Berliner Berichte*, p. 186 (1906). The demonstration of the test is also contained in the book by Hamermesh, ref. [4] chapter 5.
- [6] For the detailed proof of theorems on the relationship between representations and eigenfunctions we refer to Wigner's book, ref. [2], chapters 11, 12, and 16.
- [7] For the properties of continuous groups, and in particular for the properties of continuous rotation and rotation-inversion groups we refer to the book by Hamermesh, ref. [4], chapter 9. Other important topics, such as the effect of a crystalline field on atomic levels, are also discussed here.
- [8] A thorough discussion of symmetrized combinations of spherical harmonics that are partner functions of a number of symmetry point groups is contained in the article by D. G. BELL, *Rev. Mod. Phys.* **26**, 311 (1953). An even more manageable procedure, mainly for spherical harmonics at high values of  $l$ , is described in the works of S. L. ALTMANN and A. P. CRACKNELL, *Rev. Mod. Phys.* **37**, 19 (1965), and in S. L. ALTMANN and C. J. BRADLEY, *Rev. Mod. Phys.* **37**, 33 (1965).
- [9] The transformation properties of spin functions under proper or improper rotations are dealt with in the book by V. HEINE, *Group Theory in Quantum Mechanics* (Pergamon Press, 1960). In our basic relation (1-41) we preferred the specification of the rotation by the director cosines of the rotation axis to the standard specification by Euler angles. In the same chapter of Heine's book, one can find some simple but convenient rules to simplify the procedure for separating the elements of a double group into classes and for determining the additional irreducible representations of a number of groups.
- [10] For a clear demonstration of the relation  $\hbar I \xi = s \xi$  we refer to the book by P. M. DIRAC, *The Principles of Quantum Mechanics* (Clarendon Press, 1958), chapter 4.
- [11] A thorough discussion of time reversal symmetry can be found in the books by WIGNER, ref. [2], chapter 26, and HEINE, ref. [9], chapter 4.
- [12] H. KRAMERS, *Proc. Acad. Sci., Amsterdam* **33**, 959 (1936).
- [13] M. LAX, *Phys. Rev.* **138 A**, 793 (1965).

## CHAPTER 2

### SYMMETRY PROPERTIES OF THE ELECTRONIC STATES IN CRYSTALS

IN THE previous chapter we summarized some general results of group theory as applied to quantum mechanics and we considered symmetry groups containing coordinate transformations with a fixed origin and time reversal symmetry. However, a crystal consists of a regular array of identical unit cells, and space displacement operations also occur. In this chapter we shall apply the general results described in Chapter 1 to the discussion of crystal symmetry and to the classification of the electronic states in crystals. We will base our treatment on a geometrical analysis of the Brillouin zone, which fully exploits crystal symmetry and at the same time provides a remarkable simplification of rather complicated problems, such as the effect of time reversal symmetry on indirect transitions.

#### 2-1 Translation group and Brillouin zone<sup>[1]</sup>

A crystal has the basic property of remaining unchanged by the translations

$$\tau_n = n_1 \tau_1 + n_2 \tau_2 + n_3 \tau_3, \quad (2-1a)$$

where the subscript  $n$  on  $\tau$  indicates a collection of three integers  $n_1, n_2, n_3$ , and  $\tau_1, \tau_2, \tau_3$  are the primitive translation vectors. The translations (2-1a) can be indicated by the symbol introduced by Seitz,

$$\{E|\tau_n\}, \quad (2-1b)$$

where  $E$  indicates the identity operation and specifies that we are considering a pure translation.

In practice one has to deal with crystals of finite dimensions  $N_1 \tau_1, N_2 \tau_2, N_3 \tau_3$ , where  $N_1, N_2, N_3$  are large but finite integers. In order to preserve translational symmetry, cyclic boundary conditions are adopted,

$$\{E|\tau_{N_1 0 0}\} = \{E|\tau_{0 N_2 0}\} = \{E|\tau_{0 0 N_3}\} = \{E|0\}, \quad (2-2)$$

which implies neglecting the break in symmetry produced by the surface.

The ensemble of translations (2-1) with the condition (2-2) constitutes a finite translation group  $\mathcal{T}$  with as many elements as the number of unit cells of the crystal, i.e.  $N_1 N_2 N_3 = N$ . The translation group is an abelian group because all elements commute; consequently, every element of the group forms a class by itself. The representations

are one-dimensional and can be immediately obtained by taking into account that the translation group is the direct product of three cyclic groups of order  $N_1, N_2, N_3$  generated by the primitive translations  $\tau_1, \tau_2, \tau_3$  respectively. We recall from Section 1-2 that in a cyclic group of order  $N_i$  the matrices of the irreducible representations are given by the  $N_i$  roots of unity, and that the representations of a product group are the products of the representations of the member groups. As a consequence the translation  $\{E|\tau_n\}$  defined in (2-1) is represented by

$$\exp \left[ -i2\pi \left( \frac{n_1}{N_1} m_1 + \frac{n_2}{N_2} m_2 + \frac{n_3}{N_3} m_3 \right) \right], \quad (2-3a)$$

where the set of numbers  $(m_1, m_2, m_3)$  with  $(m_i = 0, 1, \dots, N_i - 1)$ , labels the irreducible representations. It is convenient to introduce the reciprocal lattice with vectors  $\mathbf{h}_m$  defined by the equation

$$e^{i\mathbf{h}_m \cdot \tau_n} = 1 \quad (2-4)$$

and having solutions

$$\mathbf{h}_m = m_1 \mathbf{h}_1 + m_2 \mathbf{h}_2 + m_3 \mathbf{h}_3,$$

with  $\mathbf{h}_1, \mathbf{h}_2, \mathbf{h}_3$  the primitive reciprocal lattice vectors

$$\mathbf{h}_1 = 2\pi \frac{\tau_2 \times \tau_3}{\tau_1 \cdot (\tau_2 \times \tau_3)}, \quad \mathbf{h}_2 = 2\pi \frac{\tau_3 \times \tau_1}{\tau_1 \cdot (\tau_2 \times \tau_3)}, \quad \mathbf{h}_3 = 2\pi \frac{\tau_1 \times \tau_2}{\tau_1 \cdot (\tau_2 \times \tau_3)}. \quad (2-5)$$

Equation (2-3a) can now be written in a much more effective form since

$$\{E|\tau_n\} \text{ is represented by } e^{-i\mathbf{k} \cdot \tau_n}, \quad (2-3b)$$

where the vectors

$$\mathbf{k} = \frac{m_1}{N_1} \mathbf{h}_1 + \frac{m_2}{N_2} \mathbf{h}_2 + \frac{m_3}{N_3} \mathbf{h}_3 \quad (2-3c)$$

label the irreducible representations; it now follows from (2-3b) and (2-4) that two  $\mathbf{k}$  vectors differing by a reciprocal lattice vector label the same irreducible representation. The irreducible representations of the translation group are provided in Table 2-1.

In order to classify the eigenvalues one needs to consider only those  $\mathbf{k}$  vectors which differ in magnitude by amounts less than the magnitude of a reciprocal lattice vector. It is therefore convenient to define a volume of  $\mathbf{k}$  space inside which this condition is satisfied. A particularly convenient volume is the so-called first Brillouin zone, which is the smallest region enclosed after bisecting the reciprocal lattice vectors with per-

TABLE 2-1. Irreducible representations of the translation group of a crystal. The representations  $D^{(\mathbf{k})}$  and  $D^{(-\mathbf{k})}$  ( $\mathbf{k} \neq 0$ ) are degenerate by time reversal symmetry

	$\{E 0\}$	$\{E \tau_n\}$
$D^{(\mathbf{k}=0)}$	1	1
$\{D^{(\mathbf{k})}$	1	$e^{-i\mathbf{k} \cdot \tau_n}$
$D^{(-\mathbf{k})}$	1	$e^{i\mathbf{k} \cdot \tau_n}$

pendicular planes. It is not necessary to limit the values of  $\mathbf{k}$  inside this first Brillouin zone; we could just as well consider all possible values of  $\mathbf{k}$  in other regions of  $\mathbf{k}$  space, keeping in mind that two values of  $\mathbf{k}$  which differ by a reciprocal lattice vector label the same irreducible representation of the translational group. In most cases we shall use the *reduced zone scheme* and label the electronic states in the first Brillouin zone, but sometimes we may find it convenient to consider all possible values of  $\mathbf{k}$  and then we shall specify that the *extended zone scheme* is being used.

Since a translation  $\tau_n$  is represented by  $e^{-i\mathbf{k} \cdot \tau_n}$ , the basis functions for the irreducible representations of the translation group satisfy the relation

$$O_{\{E|\tau_n\}}\psi(\mathbf{r}) = \psi(\mathbf{r} - \tau_n) = e^{-i\mathbf{k} \cdot \tau_n}\psi(\mathbf{r}), \quad (2-6a)$$

where we have used (1-16) to operate on the function. By multiplying eq. (2-6a) by the factor  $e^{i\mathbf{k} \cdot (\mathbf{r} - \tau_n)}$ ,

$$e^{-i\mathbf{k} \cdot (\mathbf{r} - \tau_n)}\psi(\mathbf{r} - \tau_n) = e^{-i\mathbf{k} \cdot \mathbf{r}}\psi(\mathbf{r}), \quad (2-6b)$$

which shows that  $e^{-i\mathbf{k} \cdot \mathbf{r}}\psi(\mathbf{r}) = u(\mathbf{r})$  is a periodic function. The basis functions of the translation group can then be written in the familiar form first obtained by Bloch,<sup>[2]</sup>

$$\psi(\mathbf{r}) = e^{i\mathbf{k} \cdot \mathbf{r}}u(\mathbf{r}), \quad (2-6c)$$

where  $u(\mathbf{r}) = u(\mathbf{r} + \tau_n)$ . Equations (2-6a) and (2-6c) are equivalent expressions of what is known as the Bloch theorem, which in this case has been derived from symmetry properties alone.

The eigenfunctions of the electrons of a crystal must satisfy conditions (2-6) and are called Bloch functions. Eigenfunctions and eigenvalues corresponding to a vector  $\mathbf{k}$  can be indicated with  $\psi_n(\mathbf{k}, \mathbf{r})$  and  $E_n(\mathbf{k})$ , where the subscript  $n$  specifies a given eigenstate. The electronic energies  $E_n(\mathbf{k})$ , when  $\mathbf{k}$  varies over the whole Brillouin zone, constitute the energy bands of the crystal which are occupied by the electrons according to Fermi-Dirac statistics. The boundary conditions (2-2) are sufficient to prove that the number of  $\mathbf{k}$  values as given by (2-3c) inside the reduced zone is equal to the number of unit cells of the lattice  $N$ ; consequently every energy band can accommodate  $2N$  electrons.

So far we have neglected the spin of the electron. In order to classify the electronic states when spin is included, we must consider the additional irreducible representations of the double group  $\mathcal{T}'$  obtained by adding the operation  $\{E|0\}$  (rotation by  $2\pi$ ) to the translation group  $\mathcal{T}$ . Since this operation commutes with all translations, the double group can be seen to be the direct product of the translation group and the group formed by  $\{E|0\}$ ,  $\{\bar{E}|0\}$ . This latter group has only two irreducible representations—one even and one odd under  $\{\bar{E}|0\}$ . The irreducible representations of the double translation group can be derived from (2-3b) by giving to the operations of the type  $\{E|\tau_n\}$  the character of  $\{E|\tau_n\}$  or its negative. To classify the states of particles with semi-integer spin we must use only the irreducible representations which are odd in  $\{\bar{E}|0\}$ . They are provided in Table 2-2. It can be observed that the additional irreducible representations of the double translation group  $\mathcal{T}'$  are one-dimensional, so that in general a splitting of all states should occur when spin dependent terms are included in the Hamiltonian.

The effect of time reversal symmetry can be studied according to the rules given in Table 1-23. Let us first consider the simple group  $\mathcal{T}$ , whose representations are given in Table 2-1. For  $\mathbf{k} \neq 0$ , case b of Table 1-23, occurs because the irreducible representa-

## ELECTRONIC STATES AND OPTICAL TRANSITIONS

TABLE 2-2. Additional irreducible representations of the translation group of a crystal

The representations  $D'(\mathbf{k})$  and  $D'(-\mathbf{k})$  ( $\mathbf{k} \neq 0$ ) are degenerate by time reversal symmetry, and  $D'(\mathbf{k}=0)$  always appears twice

	$\langle E   0 \rangle$	$\langle E   0 \rangle$	$\langle E   \tau_n \rangle$	$\langle E   \tau_n \rangle$
$D'(\mathbf{k}=0)$	1	-1	1	-1
$D'(\mathbf{k})$	1	-1	$e^{-i\mathbf{k} \cdot \tau_n}$	$-e^{-i\mathbf{k} \cdot \tau_n}$
$D'(-\mathbf{k})$	1	-1	$e^{i\mathbf{k} \cdot \tau_n}$	$-e^{i\mathbf{k} \cdot \tau_n}$

tion with character  $e^{i\mathbf{k} \cdot \tau_n}$  is not equivalent to its complex conjugate representation  $e^{-i\mathbf{k} \cdot \tau_n}$ . Consequently the eigenvalues corresponding to the irreducible representation  $\mathbf{k}$  and  $-\mathbf{k}$  are degenerate, i.e.  $E(\mathbf{k}) = E(-\mathbf{k})$ . The irreducible representation with  $\mathbf{k} = 0$  is real and belongs to case a, so that no additional degeneracy is introduced by time reversal. Let us now consider group  $\mathcal{T}'$  whose additional representations are given in Table 2-2. The additional irreducible representations with  $\mathbf{k} \neq 0$  are not equivalent to their com-

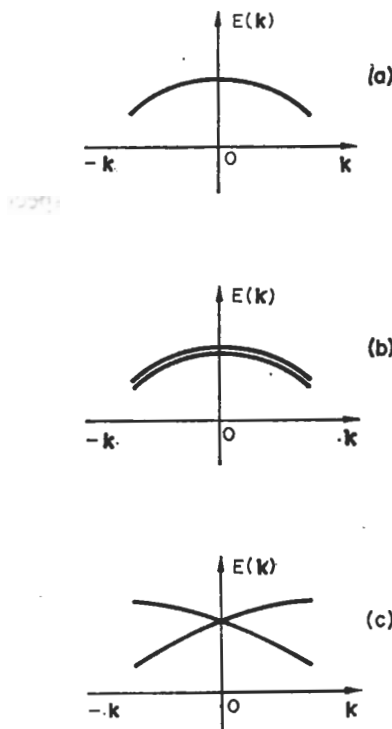


FIG. 2-1. Schematic diagram of the energy as a function of wave vector  $\mathbf{k}$  in the vicinity of  $\mathbf{k} = 0$ . The essential degeneracies required by translational and time reversal symmetry are displayed. (a) Refers to spinless particles. All states at a given  $\mathbf{k}$  have degeneracy one. (b) Refers to the case in which spin is considered but spin dependent terms are neglected in the Hamiltonian. For any  $\mathbf{k}$  vector there is degeneracy. (c) Refers to the case where spin dependent terms are included in the Hamiltonian.

The degeneracy is removed at every  $\mathbf{k}$  except at  $\mathbf{k} = 0$ .

## SYMMETRY PROPERTIES OF THE ELECTRONIC STATES IN CRYSTALS

plex conjugate representations and consequently, also for semi-integer spin  $E(\mathbf{k}) = E(-\mathbf{k})$ . The additional irreducible representation with  $\mathbf{k} = 0$  is real and belongs to case a, so that we have a twofold degeneracy. Thus for the case of particles with semi-integer spin every state is at least twice degenerate, in agreement with Kramer's theorem (see Section 1-6b). The essential degeneracies imposed by translation and time reversal symmetry in the vicinity of  $\mathbf{k} = 0$  are schematically shown in Fig. 2-1. We notice that the condition  $E(\mathbf{k}) = E(-\mathbf{k})$  implies

$$\left( \frac{\partial E}{\partial \mathbf{k}} \right)_{\mathbf{k}=0} = 0 \quad (2-7a)$$

for a non-degenerate band at  $\mathbf{k} = 0$ , or

$$\left( \frac{\partial E_1}{\partial \mathbf{k}} \right)_{\mathbf{k}=0} + \left( \frac{\partial E_2}{\partial \mathbf{k}} \right)_{\mathbf{k}=0} = 0 \quad (2-7b)$$

for a twofold degenerate band at  $\mathbf{k} = 0$ . We also note that further symmetry operations cannot remove the essential degeneracies imposed by translation and time reversal symmetry; on the contrary, they may introduce other systematic degeneracies.

*Example*

To illustrate the above results we will consider the case appropriate to crystals with the diamond structure shown in Fig. 2-2. It can be seen that the three primitive trans-

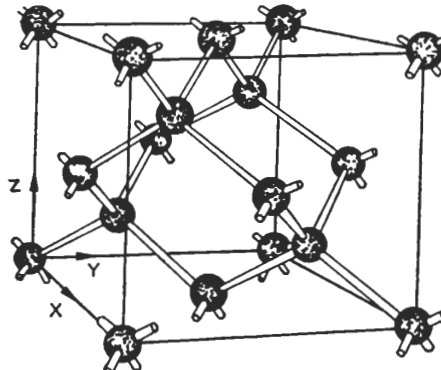


FIG. 2-2. Perspective view of diamond structure.

lation vectors join the corner of a cube with the midpoints of its adjacent faces, so that the translation symmetry is face-centred cubic. We have, then,

$$\left. \begin{aligned} \tau_1 &= \frac{a}{2} (0, 1, 1), \\ \tau_2 &= \frac{a}{2} (1, 0, 1), \\ \tau_3 &= \frac{a}{2} (1, 1, 0), \end{aligned} \right\} \quad (2-8)$$

where  $a$  is the length of the cube edge. From (2-5) we obtain, for the primitive reciprocal lattice vectors,

$$\left. \begin{aligned} \mathbf{h}_1 &= \frac{2\pi}{a} (1, 1, 1), \\ \mathbf{h}_2 &= \frac{2\pi}{a} (1, -1, 1), \\ \mathbf{h}_3 &= \frac{2\pi}{a} (1, 1, -1). \end{aligned} \right\} \quad (2-9)$$

The first Brillouin zone is obtained by bisecting the reciprocal lattice vectors with perpendicular planes and considering the smallest volume enclosed. It turns out to be the truncated octahedron shown in Fig. 2-3.

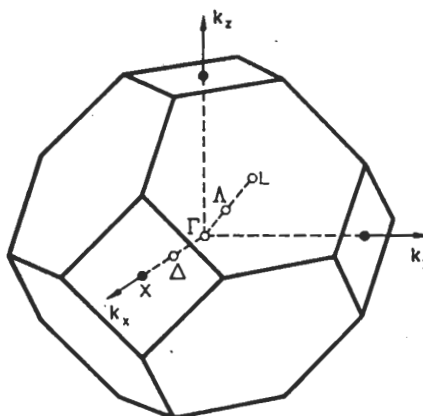


FIG. 2-3. Brillouin zone for a face-centred cubic lattice. Standard notations are used for the symmetry points and the symmetry lines.

## 2-2 Space groups

### 2-2a Irreducible representations of the space groups<sup>[3]</sup>

Crystal structure is fully specified by the primitive vectors  $\tau_1, \tau_2, \tau_3$  of the translation group and by a basis of vectors  $\mathbf{d}_1, \mathbf{d}_2, \dots, \mathbf{d}_j$ , which determine the position of the atoms (or ions) in the unit cell. All the symmetry operations which leave a crystal unchanged constitute a space group. Besides the translation symmetry operations, a space group contains proper or improper rotations, followed by an appropriate spatial displacement. The elements of the space group can be denoted by  $\{R|\mathbf{a}\}$ , where  $R$  is a real orthogonal matrix indicating the (proper or improper) rotational part, and  $\mathbf{a}$  is an appropriate space displacement vector. All possible vectors  $\mathbf{a}$  associated with  $R$  have the form  $\mathbf{a} = \tau_n + \mathbf{f}$ , where  $\tau_n$  is a translation defined by (2-1) and  $\mathbf{f}$  is a fractional translation required for some rotations. The application of a symmetry operation  $\{R|\mathbf{a}\}$  to a vector  $\mathbf{d}_j$ , determining the position of an atom in the unit cell, gives

$$\{R|\mathbf{a}\} \mathbf{d}_j = \mathbf{d}_{j'} + \tau', \quad (2-10)$$

where  $\mathbf{d}_j$ , also individuates an atom in the unit cell (and may coincide with  $\mathbf{d}_j$ ) and  $\tau'$  is a suitable translation vector (including zero). Since  $\{R|\mathbf{a}\}$  is a symmetry operation of the crystal, the positions  $\mathbf{d}_j$  and  $\mathbf{d}_{j'}$  are occupied by the same type of atoms. Skilful use of eq. (2-10) easily enables us to determine explicitly all the symmetry operations of a space group when the primitive translation vectors and the basis vectors are known.

It can easily be verified that

$$\{R|\mathbf{a}\} \cdot \{S|\mathbf{b}\} = \{RS|R\mathbf{b} + \mathbf{a}\}, \quad (2-11a)$$

$$\{R|\mathbf{a}\}^{-1} = \{R^{-1}| - R^{-1}\mathbf{a}\}, \quad (2-11b)$$

and therefore the rotational parts  $R$  of the space group symmetry elements constitute a group which is called the point group of the lattice. Only 32 point groups are possible because of the limitations imposed by translational symmetry.<sup>[1]</sup>

The translations  $\{E|\tau_n\}$  form an invariant subgroup because they transform into each other by a similarity transformation; in fact, by applying (2-11a) and (2-11b),

$$\{R|\mathbf{a}\}^{-1} \{E|\tau_n\} \{R|\mathbf{a}\} = \{E|R^{-1}\tau_n\} = \{E|\tau_{n'}\}.$$

Thus the elements of space group  $\mathcal{G}_{\text{space}}$  can be separated into the various cosets of the invariant translation subgroup  $\mathcal{T}$  and we can write

$$\mathcal{G}_{\text{space}} = \mathcal{T} \times [\{E|0\} \{R_2|\mathbf{f}_2\}, \dots, \{R_h|\mathbf{f}_h\}]. \quad (2-12)$$

The  $Nh$  elements of  $\mathcal{G}_{\text{space}}$  are thus obtained by multiplying the  $N$  elements of  $\mathcal{T}$  by the  $h$  elements  $\{E|0\}, \{R_2|\mathbf{f}_2\}, \dots, \{R_h|\mathbf{f}_h\}$ . If all the fractional translations are zero, space group  $\mathcal{G}_{\text{space}}$  is said to be *symmorphic*.  $\mathcal{G}(R)$  indicates the point group formed by the rotational parts  $E, R_2, \dots, R_h$  of operations  $\{E|0\}, \{R_2|\mathbf{f}_2\}, \dots, \{R_h|\mathbf{f}_h\}$ . It must be stressed that even in the case of a symmorphic group, space group  $\mathcal{G}_{\text{space}}$  is not the direct product of  $\mathcal{T}$  and  $\mathcal{G}(R)$  because the elements of  $\mathcal{T}$  and  $\mathcal{G}(R)$  in general do not commute.

We wish now to determine the irreducible representations of space group  $\mathcal{G}_{\text{space}}$  in order to classify the eigenvalues and eigenfunctions of the crystal Hamiltonian. To simplify the procedure we shall use results previously established for the translation group. Since the basis functions for the irreducible representations of the space group are also basis functions for the irreducible representations of the translation group, we can always choose the Bloch functions discussed in the preceding section as basis functions for any irreducible representation of the space group. We also note that an operation  $\{R|\mathbf{a}\}$  of the space group transforms a Bloch function of vector  $\mathbf{k}$  into a Bloch function of vector  $R\mathbf{k}$ . In fact, applying (2-11b) and (1-16),

$$\begin{aligned} O_{\{R|\mathbf{a}\}} e^{i\mathbf{k} \cdot \mathbf{r}} u(\mathbf{r}) &= e^{i\mathbf{k} \cdot (R^{-1}\mathbf{r} - R^{-1}\mathbf{a})} u(R^{-1}\mathbf{r} - R^{-1}\mathbf{a}) \\ &= e^{iR\mathbf{k} \cdot \mathbf{r}} e^{-i\mathbf{k} \cdot R^{-1}\mathbf{a}} u(R^{-1}(\mathbf{r} - \mathbf{a})) = e^{iR\mathbf{k} \cdot \mathbf{r}} u^{(1)}(\mathbf{r}), \end{aligned} \quad (2-13)$$

where  $u(\mathbf{r})$  and  $u^{(1)}(\mathbf{r})$  are both periodic functions.

Given a vector  $\mathbf{k}$  in the first Brillouin zone, it is convenient to choose from  $\mathcal{G}(R)$  the symmetry elements satisfying the relation

$$R\mathbf{k} = \mathbf{k} + \mathbf{h}, \quad (2-14a)$$

where  $\mathbf{h}$  is a reciprocal lattice vector (including zero). Let  $R_{\mathbf{k}}$  indicate the symmetry operations which leave  $\mathbf{k}$  unchanged (modulo  $\mathbf{h}$ ). The operations  $R_{\mathbf{k}}$  form a group  $\mathcal{G}_{\mathbf{k}}$

called the *small point group of  $\mathbf{k}$* , and all the symmetry operations of the form  $\{R_{\mathbf{k}}|\mathbf{a}\}$  constitute a group  $\mathcal{G}_{\mathbf{k}\text{space}}$  called the *little group of  $\mathbf{k}$*  or simply the group of  $\mathbf{k}$ . We note that at a general point  $\mathbf{k}$  only the identity satisfies the condition (2-14a). At special points in the first Brillouin zone one can have a number of symmetry operations satisfying (2-14a): in particular, at  $\mathbf{k} = 0$  the small point group  $\mathcal{G}_{\mathbf{k}}$  coincides with the point group of the lattice.

Let us now consider a set of basis functions for an irreducible representation of space group  $\mathcal{G}_{\text{space}}$ . Let us choose from the functions in this set the subset of functions with a given  $\mathbf{k}$  vector. As a consequence of the transformation property (2-13), this subset constitutes a basis for an irreducible representation of the little group of  $\mathbf{k}$ . The irreducible representations of the little group of the  $\mathbf{k}$  vector (whose basis functions are Bloch functions of vector  $\mathbf{k}$ ) allow the classification of the eigenvalues at any given  $\mathbf{k}$  vector.

There is a general procedure for obtaining the irreducible representations at a given  $\mathbf{k}$  vector when  $\mathbf{k}$  is inside the first Brillouin zone. In this case the small point group  $\mathcal{G}_{\mathbf{k}}$  is selected from  $\mathcal{G}(R)$  by choosing the symmetry operations for which

$$R\mathbf{k} = \mathbf{k}. \quad (2-14b)$$

From any irreducible representation  $\mathbf{D}^{(\alpha)}(R_{\mathbf{k}})$  of the small point group  $\mathcal{G}_{\mathbf{k}}$  an irreducible representation  $D^{(\mathbf{k}, \alpha)}$  of the little group of  $\mathbf{k}$  is obtained by associating to every element  $\{R_{\mathbf{k}}|\mathbf{a}\}$  of little group  $\mathcal{G}_{\mathbf{k}\text{space}}$  the matrix  $e^{-i\mathbf{k} \cdot \mathbf{a}} \mathbf{D}^{(\alpha)}(R_{\mathbf{k}})$ . To show that these matrices follow the same multiplication rules as the space group, we compare the product of the operations of the space group,

$$\{R_{\mathbf{k}}|\mathbf{a}\} \{S_{\mathbf{k}}|\mathbf{b}\} = \{R_{\mathbf{k}}S_{\mathbf{k}}|R_{\mathbf{k}}\mathbf{b} + \mathbf{a}\} \quad (2-15)$$

with the product of the corresponding matrices,

$$e^{-i\mathbf{k} \cdot \mathbf{a}} \mathbf{D}^{(\alpha)}(R_{\mathbf{k}}) e^{-i\mathbf{k} \cdot \mathbf{b}} \mathbf{D}^{(\alpha)}(S_{\mathbf{k}}) = e^{-i\mathbf{k} \cdot (\mathbf{a} + \mathbf{b})} \mathbf{D}^{(\alpha)}(R_{\mathbf{k}}S_{\mathbf{k}}). \quad (2-16)$$

The matrix which corresponds to the operation of the space group on the right hand side of (2-15) is

$$e^{-i\mathbf{k} \cdot (R_{\mathbf{k}}\mathbf{b} + \mathbf{a})} \mathbf{D}^{(\alpha)}(R_{\mathbf{k}}S_{\mathbf{k}}) = e^{-iR_{\mathbf{k}}^{-1}\mathbf{k} \cdot \mathbf{b}} e^{-i\mathbf{k} \cdot \mathbf{a}} \mathbf{D}^{(\alpha)}(R_{\mathbf{k}}S_{\mathbf{k}}). \quad (2-17)$$

The phase factors in expressions (2-16) and (2-17) always coincide when  $\mathbf{k}$  is inside the first Brillouin zone because  $R_{\mathbf{k}}^{-1}\mathbf{k} = \mathbf{k}$ .

When  $\mathbf{k}$  is at the surface of the first Brillouin zone the same procedure can be applied if the  $\mathbf{f}$  vectors are zero. However, in the case of non-symmorphic groups, the phase factors of eqs. (2-16) and (2-17) do not coincide if we have  $R_{\mathbf{k}}^{-1}\mathbf{k} = \mathbf{k} + \mathbf{h}$  and  $e^{-i\mathbf{h} \cdot \mathbf{f}} \neq 1$ . Then the above-described procedure is not valid and one must use a different method.

We consider first the case  $\mathbf{k} = \frac{1}{2}\mathbf{h}_m$ , which may occur only at the centres, edges, or corners of the Brillouin surface. We collect the translations of little group  $\mathcal{G}_{\mathbf{k}\text{space}}$  into two sets, each set including all translations having the same value  $+1$  or  $-1$  of  $e^{i\mathbf{k} \cdot \mathbf{r}_n}$ . In a similar way one collects the elements  $\{R_{\mathbf{k}}|\mathbf{r}_n + \mathbf{f}\}$  of the little group of the  $\mathbf{k}$  vector in a number of sets, each corresponding to different values of  $e^{i\mathbf{k} \cdot \mathbf{r}_n}$  or of  $R_{\mathbf{k}}$ . Then one considers a new group whose elements are the sets so obtained and whose multiplication rule is the inner product of two sets. This group is still manageable because its order is twice the order of the small point group of  $\mathbf{k}$ . From all the irreducible

representations of the new group one must consider only those appropriate to Bloch functions of vector  $\mathbf{k}$ .

At a general  $\mathbf{k}$  vector of the Brillouin surface we write  $\mathbf{k} = \frac{1}{2}\mathbf{h}_m + \mathbf{k}'$  with  $\mathbf{k}'$  inside the Brillouin zone; the irreducible representations are obtained by a straightforward combination of the procedures appropriate for the case  $\mathbf{k} = \frac{1}{2}\mathbf{h}_m$  and for the case  $\mathbf{k}'$  inside the Brillouin zone.

So far we have considered only those symmetry operations of the space group satisfying the condition  $R\mathbf{k} = \mathbf{k} + \mathbf{h}$ . In general the effect of the point group symmetry operations is to send  $\mathbf{k}$  into a *star* of vectors  $\mathbf{k}_1 = \mathbf{k}, \mathbf{k}_2, \dots, \mathbf{k}_s$ . The eigenvalues at all points of the star are the same and the eigenfunctions at all points of the star are obtained by applying the symmetry operations of the space group to the eigenfunctions of vector  $\mathbf{k}$ . It is convenient to define the *restricted volume* inside the first Brillouin zone as a volume containing all points that do not belong to the same star. The restricted volume is equal to the volume of the Brillouin zone divided by  $h$ , the number of elements of  $\mathcal{G}(R)$ . The basis eigenfunctions

$$\psi_k^{(1)}, \psi_k^{(2)}, \dots, \psi_k^{(l_\alpha)} \quad (2-18)$$

of the irreducible representation  $D^{(\mathbf{k}, \alpha)}$  of  $\mathcal{G}_{\mathbf{k}, \text{space}}$  and the corresponding eigenfunctions at the vectors of the star of  $\mathbf{k}$  constitute a basis for an irreducible representation  $D_{\text{space}}^{(\mathbf{k}, \alpha)}$  of space group  $\mathcal{G}_{\text{space}}$ . Its dimension is  $s_k l_\alpha$ , where  $s_k$  is the number of points in the star of  $\mathbf{k}$ . Note that the sum of the square of the dimensions of the irreducible non-equivalent representations so obtained is

$$\sum_{\mathbf{k} \in \text{restricted volume}} \sum_{\alpha} (s_k l_\alpha)^2 = \sum_{\mathbf{k} \in \text{restricted volume}} s_k^2 h_k,$$

where  $h_k$  is the order of the small point group of  $\mathbf{k}$ . Since  $s_k \cdot h_k$  equals the order  $h$  of the crystal point group,

$$\sum_{\mathbf{k} \in \text{restricted volume}} s_k \cdot h = \sum_{\mathbf{k} \in \text{Brillouin zone}} h = Nh.$$

We have thus obtained all the irreducible representations of space group  $\mathcal{G}_{\text{space}}$ .

As will be apparent later, we never need to know explicitly the representations of  $\mathcal{G}_{\text{space}}$ ; it is sufficient to know the irreducible representations of the little groups of  $\mathbf{k}$ . It should also be noted that in order to specify irreducible representations it is sufficient to list the characters of the  $h_k$  elements of the form  $\{R_{\mathbf{k}}|\mathbf{f}\}$  since the character of  $\{R_{\mathbf{k}}|\mathbf{f} + \tau_n\}$  is  $e^{-i\mathbf{k} \cdot \tau_n}$  times the character of  $\{R_{\mathbf{k}}|\mathbf{f}\}$ .

### Example

As an example we consider the case of the diamond lattice (Fig. 2-2). The diamond crystal is invariant for translations  $\{\mathbf{E}|\tau_n\}$  with

$$\tau_n = n_1 \tau_1 + n_2 \tau_2 + n_3 \tau_3 \quad (2-19)$$

and  $\tau_1, \tau_2, \tau_3$  defined by (2-8). There are two equal atoms in the unit cell in the positions

$$\left. \begin{aligned} \mathbf{d}_1 &= (0, 0, 0), \\ \mathbf{d}_2 &= \frac{a}{4}(1, 1, 1). \end{aligned} \right\} \quad (2-20)$$

## ELECTRONIC STATES AND OPTICAL TRANSITIONS

The diamond lattice can be thought of as consisting of two face-centred cubic sublattices displaced with respect to each other by the vector  $\frac{a}{4}(1, 1, 1)$ . The point group of the diamond structure is the cubic group  $O_h$ . The diamond group is not symmorphic because some of the symmetry operations of cubic group  $O_h$  appear in the space group associated with the fractional translation  $\mathbf{f} = \frac{a}{4}(1, 1, 1) = \frac{1}{4}(\tau_1 + \tau_2 + \tau_3)$ . By choosing a lattice point as origin, as indicated in Fig. 2-2, we obtain for the symmetry operations the explicit expressions given in Table 2-3. Following are the irreducible representations of  $k$  group at some symmetry points of interest.

*Point  $\Gamma$  ( $k = (0, 0, 0)$ ).* This is the point at the origin of the first Brillouin zone. The small point group of  $k$  is the entire point group  $O_h$ . Since we are inside the Brillouin zone and  $e^{ik \cdot f} = 1$ , the characters of the irreducible representations at  $\Gamma$  (Table 2-4) are simply given by the characters of point group  $O_h$  (Table 1-4), without any modification.

TABLE 2-3. Symmetry operations of the factor group of the translation group of the diamond structure  
The origin is at a lattice point and  $\mathbf{f} = \frac{a}{4}(1, 1, 1)$ . The notations used are similar to those of Table 1-1,  
but we have recorded on the right hand side the operations associated with  $\mathbf{f}$

Class	Symmetry operation	Coordinate transformation	Class	Symmetry operation	Coordinate transformation
$E$	$\{E 0\}$	$x \ y \ z$	$I$	$\{I \mathbf{f}\}$	$\bar{x} + \frac{1}{4}a \ \bar{y} + \frac{1}{4}a \ \bar{z} + \frac{1}{4}a$
$C_4^2$	$\{\delta_{2z} 0\}$	$\bar{x} \ \bar{y} \ z$	$IC_4^2$	$\{I\delta_{2z} \mathbf{f}\}$	$x + \frac{1}{4}a \ y + \frac{1}{4}a \ \bar{z} + \frac{1}{4}a$
	$\{\delta_{2x} 0\}$	$x \ \bar{y} \ \bar{z}$		$\{I\delta_{2x} \mathbf{f}\}$	$\bar{x} + \frac{1}{4}a \ y + \frac{1}{4}a \ z + \frac{1}{4}a$
	$\{\delta_{2y} 0\}$	$\bar{x} \ y \ \bar{z}$		$\{I\delta_{2y} \mathbf{f}\}$	$x + \frac{1}{4}a \ \bar{y} + \frac{1}{4}a \ z + \frac{1}{4}a$
$IC_4$	$\{I\delta_{4z}^{-1} 0\}$	$y \ \bar{x} \ \bar{z}$	$C_4$	$\{\delta_{4z}^{-1} \mathbf{f}\}$	$\bar{y} + \frac{1}{4}a \ x + \frac{1}{4}a \ z + \frac{1}{4}a$
	$\{I\delta_{4z} 0\}$	$\bar{y} \ x \ \bar{z}$		$\{\delta_{4z} \mathbf{f}\}$	$y + \frac{1}{4}a \ \bar{x} + \frac{1}{4}a \ z + \frac{1}{4}a$
	$\{I\delta_{4x}^{-1} 0\}$	$\bar{x} \ z \ \bar{y}$		$\{\delta_{4x}^{-1} \mathbf{f}\}$	$x + \frac{1}{4}a \ \bar{z} + \frac{1}{4}a \ y + \frac{1}{4}a$
	$\{I\delta_{4x} 0\}$	$\bar{x} \ \bar{z} \ y$		$\{\delta_{4x} \mathbf{f}\}$	$x + \frac{1}{4}a \ z + \frac{1}{4}a \ \bar{y} + \frac{1}{4}a$
	$\{I\delta_{4y}^{-1} 0\}$	$\bar{z} \ \bar{y} \ x$		$\{\delta_{4y}^{-1} \mathbf{f}\}$	$z + \frac{1}{4}a \ y + \frac{1}{4}a \ \bar{x} + \frac{1}{4}a$
	$\{I\delta_{4y} 0\}$	$z \ \bar{y} \ \bar{x}$		$\{\delta_{4y} \mathbf{f}\}$	$\bar{z} + \frac{1}{4}a \ y + \frac{1}{4}a \ x + \frac{1}{4}a$
	$\{I\delta_{2xy} 0\}$	$\bar{y} \ \bar{x} \ z$	$C_2$	$\{\delta_{2xy} \mathbf{f}\}$	$y + \frac{1}{4}a \ x + \frac{1}{4}a \ \bar{z} + \frac{1}{4}a$
$IC_2$	$\{I\delta_{2xz} 0\}$	$\bar{z} \ y \ \bar{x}$		$\{\delta_{2xz} \mathbf{f}\}$	$z + \frac{1}{4}a \ \bar{y} + \frac{1}{4}a \ x + \frac{1}{4}a$
	$\{I\delta_{2yz} 0\}$	$x \ \bar{z} \ \bar{y}$		$\{\delta_{2yz} \mathbf{f}\}$	$\bar{x} + \frac{1}{4}a \ z + \frac{1}{4}a \ y + \frac{1}{4}a$
	$\{I\delta_{2xy} 0\}$	$y \ x \ z$		$\{\delta_{2xy} \mathbf{f}\}$	$\bar{y} + \frac{1}{4}a \ \bar{x} + \frac{1}{4}a \ \bar{z} + \frac{1}{4}a$
	$\{I\delta_{2\bar{x}z} 0\}$	$z \ y \ x$		$\{\delta_{2\bar{x}z} \mathbf{f}\}$	$\bar{z} + \frac{1}{4}a \ \bar{y} + \frac{1}{4}a \ \bar{x} + \frac{1}{4}a$
	$\{I\delta_{2\bar{y}z} 0\}$	$x \ z \ y$		$\{\delta_{2\bar{y}z} \mathbf{f}\}$	$\bar{x} + \frac{1}{4}a \ \bar{z} + \frac{1}{4}a \ \bar{y} + \frac{1}{4}a$
	$\{I\delta_{3xyz} 0\}$	$z \ x \ y$	$IC_3$	$\{I\delta_{3xyz}^{-1} \mathbf{f}\}$	$\bar{z} + \frac{1}{4}a \ \bar{x} + \frac{1}{4}a \ \bar{y} + \frac{1}{4}a$
$C_3$	$\{\delta_{3xyz} 0\}$	$y \ z \ x$		$\{I\delta_{3xyz} \mathbf{f}\}$	$\bar{y} + \frac{1}{4}a \ \bar{z} + \frac{1}{4}a \ \bar{x} + \frac{1}{4}a$
	$\{\delta_{3x\bar{y}z}^{-1} 0\}$	$z \ \bar{x} \ \bar{y}$		$\{I\delta_{3x\bar{y}z}^{-1} \mathbf{f}\}$	$\bar{z} + \frac{1}{4}a \ x + \frac{1}{4}a \ y + \frac{1}{4}a$
	$\{\delta_{3x\bar{y}z} 0\}$	$\bar{y} \ \bar{z} \ x$		$\{I\delta_{3x\bar{y}z} \mathbf{f}\}$	$y + \frac{1}{4}a \ z + \frac{1}{4}a \ \bar{x} + \frac{1}{4}a$
	$\{\delta_{3x\bar{y}z}^{-1} 0\}$	$\bar{z} \ \bar{x} \ y$		$\{I\delta_{3x\bar{y}z}^{-1} \mathbf{f}\}$	$z + \frac{1}{4}a \ x + \frac{1}{4}a \ \bar{y} + \frac{1}{4}a$
	$\{\delta_{3x\bar{y}z} 0\}$	$\bar{y} \ z \ \bar{x}$		$\{I\delta_{3x\bar{y}z} \mathbf{f}\}$	$y + \frac{1}{4}a \ \bar{z} + \frac{1}{4}a \ x + \frac{1}{4}a$
	$\{\delta_{3x\bar{y}z}^{-1} 0\}$	$\bar{z} \ x \ \bar{y}$		$\{I\delta_{3x\bar{y}z}^{-1} \mathbf{f}\}$	$z + \frac{1}{4}a \ \bar{x} + \frac{1}{4}a \ y + \frac{1}{4}a$
	$\{\delta_{3x\bar{y}z} 0\}$	$y \ \bar{z} \ \bar{x}$		$\{I\delta_{3x\bar{y}z} \mathbf{f}\}$	$\bar{y} + \frac{1}{4}a \ z + \frac{1}{4}a \ x + \frac{1}{4}a$

## SYMMETRY PROPERTIES OF THE ELECTRONIC STATES IN CRYSTALS

TABLE 2-4. Irreducible representations at symmetry point  $\Gamma$  of the diamond structure  
 The notations are taken from L. Bouckaert *et al.*, *Phys. Rev.* **50**, 58 (1936)

Point $\Gamma$	$E$	$3C_4^2$	$6C_4$	$6C_2$	$8C_3$	$I$	$3IC_4^2$	$6IC_4$	$6IC_2$	$8IC_3$
$\Gamma_1$	1	1	1	1	1	1	1	1	1	1
$\Gamma_2$	1	1	-1	-1	1	1	1	-1	-1	1
$\Gamma_{12}$	2	2	0	0	-1	2	2	0	0	-1
$\Gamma'_{25}$	3	-1	-1	1	0	3	-1	-1	1	0
$\Gamma'_{15}$	3	-1	1	-1	0	3	-1	1	-1	0
$\Gamma'_1$	1	1	1	1	1	-1	-1	-1	-1	-1
$\Gamma'_2$	1	1	-1	-1	1	-1	-1	1	1	-1
$\Gamma'_{12}$	2	2	0	0	-1	-2	-2	0	0	1
$\Gamma_{25}$	3	-1	-1	1	0	-3	1	1	-1	0
$\Gamma_{15}$	3	-1	1	-1	0	-3	1	-1	1	0

TABLE 2-5. Irreducible representations on symmetry line  $A$  of the diamond structure  
 The notations are taken from L. Bouckaert *et al.*, *Phys. Rev.* **50**, 58 (1936)

Line $A$	$\{E 0\}$	$\{\delta_{3xyz}^{-1} 0\}$ $\{\delta_{3xyz} 0\}$	$\{I\delta_{2xy} 0\}$ $\{I\delta_{2xz} 0\}$ $\{I\delta_{2yz} 0\}$
$A_1$	1	1	1
$A_2$	1	1	-1
$A_3$	2	-1	0

TABLE 2-6. Irreducible representations on symmetry line  $\Delta$  of the diamond structure  
 The notations are taken from L. Bouckaert *et al.*, *Phys. Rev.* **50**, 58 (1936)

Line $\Delta$	$\{E 0\}$	$\{\delta_{2x} 0\}$	$\{\delta_{4x}^{-1} f\rangle \langle \delta_{4x} f\}$	$\{I\delta_{2x} f\rangle \langle I\delta_{2y} f\}$	$\{I\delta_{2y} 0\}$ $\{I\delta_{2yz} 0\}$
$\Delta_1$	1	1	$e^{-i(\pi/2)\delta}$	$e^{-i(\pi/2)\delta}$	1
$\Delta'_1$	1	1	$e^{-i(\pi/2)\delta}$	$-e^{-i(\pi/2)\delta}$	-1
$\Delta_2$	1	1	$-e^{-i(\pi/2)\delta}$	$e^{-i(\pi/2)\delta}$	-1
$\Delta'_2$	1	1	$-e^{-i(\pi/2)\delta}$	$-e^{-i(\pi/2)\delta}$	1
$\Delta_5$	2	-2	0	0	0

*Line A* ( $\mathbf{k} = \pi/a (\lambda, \lambda, \lambda)$  with  $0 < \lambda < 1$ ). This is a point on the line joining the centre of the Brillouin zone to the midpoint of a hexagonal face. The small point group of  $\mathbf{k}$  is made up by the operations of Table 2-3 whose rotational parts interchange ( $x, y, z$ ) among themselves, because these are the only operations which leave  $\mathbf{k}$  unchanged. The small point group of  $\mathbf{k}$  is thus  $C_{3v}$ . Since no fractional translation  $\mathbf{f}$  is associated with the elements of  $C_{3v}$ , the characters of the irreducible representations at  $A$  (Table 2-5) are the characters of group  $C_{3v}$  (Table 1-5) without any modification.

*Line  $\Delta$*  ( $\mathbf{k} = 2\pi/a (\delta, 0, 0)$  with  $0 < \delta < 1$ ). This is a point on the line joining the centre of the Brillouin zone to the midpoint of the square face. The small point group of  $\mathbf{k}$  is given by the operations of Table 2-3 whose rotational parts leave  $x$  unchanged. The small point group of  $\mathbf{k}$  is thus  $C_{4v}$ . The irreducible representations at  $\Delta$  (Table 2-6) are obtained by multiplying the characters of the irreducible representations of group  $C_{4v}$  (Table 1-7) by the phase factor  $e^{-i\mathbf{k} \cdot \mathbf{f}} = e^{-i(\pi/2)\delta}$ .

## ELECTRONIC STATES AND OPTICAL TRANSITIONS

We will now consider points on the surface of the Brillouin zone. Since the space group of the diamond structure is not symmorphic, the procedure for obtaining representations here is not always as straightforward as that for points inside the Brillouin zone. Let us illustrate the procedure with some examples.

**Point X ( $\mathbf{k} = 2\pi/a(1, 0, 0)$ ).** This point is the centre of the square face at the surface of the Brillouin zone. The symmetry operations of the small point group of  $\mathbf{k}$  are those which change  $x$  into itself or into  $-x$ . The small point group of  $\mathbf{k}$  is  $D_{4h} = C_{4h} \times C_1$ . In fact, the operations of group  $C_{4v}$  leave  $\mathbf{k}$  unchanged, and inversion  $I$  gives

$$I\mathbf{k} = \frac{2\pi}{a}(1, 0, 0) = \mathbf{k} - (\mathbf{h}_2 + \mathbf{h}_3),$$

where  $\mathbf{h}_2, \mathbf{h}_3$  are defined in (2-9). In the diamond structure, the inversion is associated with the fractional translation  $\mathbf{f}$ , and  $e^{-i(\mathbf{h}_2 + \mathbf{h}_3) \cdot \mathbf{f}} = -1$ . The irreducible representations of the little group of  $\mathbf{k}$  cannot be derived from the irreducible representations of group  $D_{4h}$  (Table 1-8) because we have symmetry operations (for instance  $\{I|\mathbf{f}\}$ ) for which the phase factor in (2-16) differs from the phase factor in (2-17). To derive the irreducible representations of the little group in this case, we consider the expression  $e^{i\mathbf{k} \cdot \tau_n}$  at  $X$ . From (2-19) we see that  $e^{i\mathbf{k} \cdot \tau_n} = e^{i(n_2 + n_3)\pi} = \pm 1$  depending on the parity of the sum  $n_2 + n_3$  in  $\tau_n$ . We next consider a new group whose elements are given in Table 2-7. The set of translations  $\tau_n$  for which  $e^{i\mathbf{k} \cdot \tau_n}$  is equal to  $+1$  or  $-1$  is indicated by  $\{E|0\}$  or  $\{E|1\}$  respectively. Similarly,  $\{R|\mathbf{f}\}$  (or  $\{R|\mathbf{f} + 1\}$ ) indicates the set of elements  $\{R|\mathbf{f} + \tau_n\}$  for which  $e^{i\mathbf{k} \cdot \tau_n}$  is equal to  $+1$  (or  $-1$ ). The new group contains 32 elements which we now separate into classes using the inner product notion of Section 1-1. The elements  $\{E|0\}$  and  $\{E|1\}$  commute with all the elements of the group, and each forms a class. The elements  $\{I|\mathbf{f}\}$  and  $\{I|\mathbf{f} + 1\}$  belong to the same class because, for example

$$\{\delta_{2z}|0\}^{-1} \{I|\mathbf{f}\} \{\delta_{2z}|0\} = \{I|\delta_{2z}\mathbf{f}\} \quad (2-21)$$

and

$$\delta_{2z}\mathbf{f} = \frac{a}{4}(1, 1, 1) = \mathbf{f} - \tau_3.$$

Then  $\{I|\delta_{2z}\mathbf{f}\} = \{I|\mathbf{f} - \tau_3\}$  belongs to the set of elements  $\{I|\mathbf{f} + 1\}$  and (2-21) shows that  $\{I|\mathbf{f}\}$  and  $\{I|\mathbf{f} + 1\}$  belong to the same class. In a similar manner it can be shown that the 32 elements of the new group are divided into 14 classes, and we must thus have 14 irreducible representations. Since  $\{E|1\}$  commutes with all the elements of the group, the matrix  $\mathbf{D}(\{E|1\})$  representing it must be a constant matrix

$$\mathbf{D}(\{E|1\}) = c\mathbf{1}.$$

Since  $\{E|1\}^2 = \{E|0\}$  we have  $c^2 = 1$  and  $c = \pm 1$ . In the representations characterized by  $c = +1$ ,  $\{E|0\}$  and  $\{E|1\}$  are represented by the same matrix and so are the elements  $\{R|\mathbf{f}\}$  and  $\{R|\mathbf{f} + 1\}$  or  $\{S|0\}$  and  $\{S|1\}$ . The irreducible representations with  $c = 1$  coincide with the 10 irreducible representations of Table 1-8. It remains for us to find the irreducible representations characterized by  $c = -1$ . We must have  $14 - 10 = 4$  such irreducible representations and, since from Table 1-8 we have  $\sum_{\alpha=1}^{10} l_{\alpha}^2 = 16$  and the order of the group is 32, they will satisfy

$$\sum_{\alpha=1}^4 l_{\alpha}^2 = 16 \quad (2-22)$$

because of eq. (1-3).

TABLE 2-7. Irreducible representations of the group of  $\mathbf{k}$  at symmetry point  $X$  of the diamond structure  
The representations  $X_1, X_2, X_3, X_4$  are the only acceptable representations to classify the electronic states at point  $X$

$\{E 0\}$	$\{E 1\}$	$\{\delta_{2x} 0\}$	$\{\delta_{2x} 1\}$	$\{\delta_{4x}^{-1}, \delta_{4x} f\}$ $\{\delta_{4x}^{-1}, \delta_{4x} f+1\}$	$\{I\delta_{2z}, I\delta_{2z} f\}$ $\{I\delta_{2z}, I\delta_{2z} f+1\}$	$\{I\delta_{2zx} 0\}$ $\{I\delta_{2zx} 1\}$	$\{I\delta_{2zx} f\}$ $\{I\delta_{2zx} f+1\}$	$\{I \mathbf{f}\}$ $\{I \mathbf{f}+1\}$	$\{I\delta_{2xz} 0\}$ $\{I\delta_{2xz} 1\}$	$\{I\delta_{2xz} f\}$ $\{I\delta_{2xz} f+1\}$	$\{\delta_{2z}, \delta_{2z} 0\}$ $\{\delta_{2z}, \delta_{2z} 1\}$	$\{\delta_{2yz} f\}$ $\{\delta_{2yz} f+1\}$	
$M_1$	1	1	1	1	1	1	1	1	1	1	1	1	1
$M_2$	1	1	1	1	-1	-1	-1	1	1	-1	-1	-1	-1
$M_3$	1	1	1	-1	1	-1	-1	1	1	-1	-1	-1	-1
$M_4$	1	1	1	-1	-1	1	1	1	-1	-1	-1	1	1
$M_5$	2	-2	-2	0	0	0	2	-2	0	0	0	0	0
$M'_1$	1	1	1	1	1	1	1	-1	-1	-1	-1	-1	-1
$M'_2$	1	1	1	1	-1	-1	-1	-1	-1	-1	-1	-1	-1
$M'_3$	1	1	1	-1	-1	-1	-1	1	1	1	1	1	1
$M'_4$	1	1	1	-1	-1	1	1	-1	-1	1	1	-1	-1
$M'_5$	2	-2	-2	0	0	0	-2	2	0	0	0	0	0
$X_1$	2	-2	2	-2	0	0	2	-2	0	0	0	0	0
$X_2$	2	-2	2	-2	0	0	-2	2	0	0	0	0	0
$X_3$	2	-2	-2	2	0	0	0	0	0	0	0	2	-2
$X_4$	2	-2	-2	2	0	0	0	0	0	0	0	-2	2

École Polytechnique Fédérale de Lausanne  
PHB - Institut de Physique  
CH-1015 Lausanne, Suisse  
Tél. 021-626 71 11

TABLE 2-8. Irreducible representations for Bloch functions at symmetry point  $X$  of the diamond structure  
 The notations are taken from C. Herring, *J. Franklin Inst.* 233, 525 (1942).

Point $X$	$\{E 0\}$	$\{\delta_{2x} 0\}$	$\{\delta_{4x}^{-1} f\}$ $\{\delta_{4x} f\}$	$\{\delta_{2z} f\}$ $\{\delta_{2y} f\}$	$\{I\delta_{2yz} 0\}$ $\{I\delta_{2xy} 0\}$	$\{I f\}$	$\{I\delta_{2x} f\}$	$\{I\delta_{4x}^{-1} 0\}$ $\{I\delta_{4x} 0\}$	$\{\delta_{2z} 0\}$ $\{\delta_{2y} 0\}$	$\{\delta_{2y} f\}$
$X_1$	2	2	0	0	2	0	0	0	0	0
$X_2$	2	2	0	0	-2	0	0	0	0	0
$X_3$	2	-2	0	0	0	0	0	0	2	-2
$X_4$	2	-2	0	0	0	0	0	0	-2	2

TABLE 2-9. Irreducible representations at symmetry point  $L$  of the diamond structure  
 The notations are taken from L. Bouckaert *et al.*, *Phys. Rev.* 50, 58 (1936)

Point $L$	$\{E 0\}$	$\{\delta_{3xyz}^{-1}, \delta_{3xyz} 0\}$	$\{I\delta_{2xy}, I\delta_{2yz}, I\delta_{2zx} 0\}$	$\{I f\}$	$\{I\delta_{3xyz}^{-1}, I\delta_{3xyz} f\}$	$\{I\delta_{3xyz}, I\delta_{3xyz} 0\}$
$L_1$	1	1	1	1	1	1
$L_2$	1	1	-1	1	1	-1
$L_3$	2	-1	0	2	-1	0
$L'_1$	1	1	1	-1	-1	-1
$L'_2$	1	1	-1	-1	-1	1
$L'_3$	2	-1	0	-2	1	0

The only solution of (2-22) is  $2^2 + 2^2 + 2^2 + 2^2 = 16$ , and we thus obtain four two-dimensional irreducible representations. The determination of the characters is immediate if we note that elements labelled with 0 and 1 are represented by matrices with opposite signs, and when they appear in the same class their characters must be zero. In Table 2-7 we list all the irreducible representations (both with  $c = 1$  and  $c = -1$ ) thus obtained. We note that only the representations with  $c = -1$  are acceptable as representations of the little group of  $\mathbf{k}$ , since  $O_{\{E|1\}}\psi_{\mathbf{k}} = e^{-i\mathbf{k} \cdot \tau_n}\psi_{\mathbf{k}} = -\psi_{\mathbf{k}}(\tau_n$  translation with  $n_2 + n_3$  odd). In Table 2-8 we report the characters of the acceptable representations of the little group of  $\mathbf{k}$ .

Since all the irreducible representations of the group of  $\mathbf{k}$  are two-dimensional, it follows that the energy levels at  $X$  are at least doubly degenerate. The reason for this is essentially due to the fractional translation which is associated with some symmetry operations because there are two equal atoms per unit cell. (In a symmorphic group, irreducible representations of the group of  $\mathbf{k}$  would be derived from the irreducible representations of the small group of  $\mathbf{k}$ , and among them there is at least the one-dimensional identity representation.)

*Point L* ( $\mathbf{k} = \pi/a(1, 1, 1)$ ). This point is the centre of the hexagonal face at the surface of the Brillouin zone. The small point group of  $\mathbf{k}$  is  $D_{3d} = C_{3v} \times C_1$ . In this case we also have symmetry operations (for instance  $\{I|\mathbf{f}\}$ ) for which the factor in (2-16) differs from the phase factor in (2-17). We must thus follow a procedure similar to that of point  $X$ , and we list the results in Table 2-9. In this case there is a close similarity between Table 2-9 and Table 1-6 (note, however, that the characters of Table 2-9 are not obtained from Table 1-6 simply by multiplying by  $e^{-i\mathbf{k} \cdot \mathbf{f}}$ ).

TABLE 2-10. Compatibility relations between the irreducible representations at symmetry points  $\Gamma, L, X$  and on symmetry lines  $A, \Delta$  of the diamond structure

Point $\Gamma$	$\Gamma_1$	$\Gamma_2$	$\Gamma_{12}$	$\Gamma'_{25}$	$\Gamma'_{15}$	$\Gamma'_1$	$\Gamma'_2$	$\Gamma'_{12}$	$\Gamma_{25}$	$\Gamma_{15}$
Line $A$	$A_1$	$A_2$	$A_3$	$A_1 + A_3$	$A_2 + A_3$	$A_2$	$A_1$	$A_3$	$A_2 + A_3$	$A_1 + A_3$
Point $\Gamma$	$\Gamma_1$	$\Gamma_2$	$\Gamma_{12}$	$\Gamma'_{25}$	$\Gamma'_{15}$	$\Gamma'_1$	$\Gamma'_2$	$\Gamma'_{12}$	$\Gamma_{25}$	$\Gamma_{15}$
Line $\Delta$	$\Delta_1$	$\Delta_2$	$\Delta_1 + \Delta_2$	$\Delta'_2 + \Delta_5$	$\Delta'_1 + \Delta_5$	$\Delta'_1$	$\Delta'_2$	$\Delta'_1 + \Delta'_2$	$\Delta_2 + \Delta_5$	$\Delta_1 + \Delta_5$
Point $X$			$X_1$		$X_2$		$X_3$		$X_4$	
Line $\Delta$			$\Delta_1 + \Delta'_2$		$\Delta'_1 + \Delta_2$		$\Delta_5$		$\Delta_5$	
Point $L$			$L_1$		$L_2$		$L_3$		$L'_1$	
Line $A$			$A_1$		$A_2$		$A_3$		$A_1$	
									$A_2$	
										$A_3$

*Compatibility relations.* We note that the group of  $\mathbf{k}$  along a symmetry line must be a subgroup of the group of  $\mathbf{k}$  at a special symmetry point on the line. The irreducible representations at the symmetry points can be decomposed into a number of irreducible representations of the group of  $\mathbf{k}$  along symmetry lines. Compatibility relations between the states along symmetry lines and the states at symmetry points can thus be established. As an example, the compatibility relations for the points  $\Gamma, L, X$  and lines  $A$  and  $\Delta$  are given in Table 2-10 for the diamond lattice.

2-2 b Additional irreducible representations of the space groups and spin-orbit splitting<sup>[1]</sup>

As explained in Section 1-5, in order to include the spin dependence of the electronic wave functions we must find the irreducible representations of the double space group, which is obtained by extending the space group (2-12) with the operation  $\{\bar{E}|0\}$  (rotation by  $2\pi$ ). The double space group can then be written as

$$\mathcal{G}'_{\text{space}} = \mathcal{T} \times [\{E|0\}, \{\bar{E}|0\}, \{R_2|\mathbf{f}_2\}, \{\bar{R}_2|\mathbf{f}_2\}, \dots, \{R_h|\mathbf{f}_h\}, \{\bar{R}_h|\mathbf{f}_h\}].$$

We recall that the double group of a symmetry group is isomorphic to the group of matrices which represent the symmetry operations in the representation  $D^{(1/2)}$  of the rotation group [see eq. (1-41)]. Inversion can be treated as an element that commutes with all other elements and satisfies  $I^2 = E$ . In the double group the multiplication rules are

$$\{\bar{R}|\mathbf{a}\} \{S|\mathbf{b}\} = \{\bar{R}S|R\mathbf{b} + \mathbf{a}\},$$

$$\{\bar{R}|\mathbf{a}\}^{-1} = \{\bar{R}^{-1}\} - R^{-1}\mathbf{a},$$

where the product of the rotation parts follows the multiplication rules of the double group and the associate vector is determined by the rules of the simple group.

One can extend the procedure of Section 2-2a and obtain all the irreducible representations of the double group. It turns out that all irreducible representations of the simple group are also irreducible representations of the double group with the same character for  $\{E|0\}$  and  $\{\bar{E}|0\}$ . These representations have to be discarded because we know that the spin dependent part of the wave function changes its sign under  $\{\bar{E}|0\}$ . There are additional representations where the matrix corresponding to  $\{E|0\}$  is the negative of that corresponding to  $\{\bar{E}|0\}$ . These are used to classify the energy states when spin is not neglected.

It is of interest to see how the spin degeneracy is removed by the spin-orbit interaction. To determine this effect, we must decide how the states of the simple group of the previous section are decomposed into the states of the double group. This can be done by considering the product of a given irreducible representation of the simple group by the representation  $D^{(1/2)}$  of the spin functions, whose character is  $2 \cos \alpha/2$  for any proper or improper rotation of angle  $\alpha$ . The product representation can be decomposed into the sum of irreducible representations of the double group: the number and dimensions of the component irreducible representations give the number and the degeneracy of the sublevels produced by spin-orbit interaction.

*Illustrative example*

For the case of the diamond structure, we wish to find the additional irreducible representations of the group of  $\mathbf{k}$  at several symmetry points and symmetry lines.

*Point  $\Gamma$*  ( $\mathbf{k} = (0, 0, 0)$ ). The small point group of  $\mathbf{k}$  is the cubic group  $O_h$ . Since we are inside the Brillouin zone and  $e^{-i\mathbf{k} \cdot \mathbf{f}}$  is one, the characters of the additional irreducible representations at  $\Gamma$  (Table 2-11) are obtained from the additional characters<sup>[1]</sup> of the point group  $O'_h$  without any modification.

*Line  $A$*  ( $\mathbf{k} = \pi/a(\lambda, \lambda, \lambda)$  with  $0 < \lambda < 1$ ). The small point group of  $\mathbf{k}$  is  $C_{3v}$ . Since no fractional translation  $\mathbf{f}$  is associated with the elements of  $C_{3v}$ , the characters of the additional irreducible representations at  $A$  (Table 2-12) are obtained from the additional characters of the double group  $C'_{3v}$  (Table 1-20) without any modification.

TABLE 2-11. Additional irreducible representations of the double group of  $\mathbf{k}$  at point  $\Gamma$  of the diamond structure  
 The notations are taken from R. J. Elliott, *Phys. Rev.* **96**, 130 (1954)

Point $\Gamma$	$E$	$E$	$3C_4^2$	$3C_4$	$6C_4$	$6C_2$	$6C_2$	$8C_3$	$8C_3$	$I$	$\bar{I}$	$3IC_4^2$	$3IC_4^2$	$6IC_4$	$6IC_4$	$6IC_2$	$6IC_2$	$8IC_3$	$8IC_3$
$\Gamma_6^+$	2	-2	0	$\sqrt{2}$	$-\sqrt{2}$	0	$\sqrt{2}$	1	-1	2	-2	0	$\sqrt{2}$	$-\sqrt{2}$	0	1	1	-1	
$\Gamma_7^+$	2	-2	0	$-\sqrt{2}$	$\sqrt{2}$	0	$-\sqrt{2}$	1	-1	2	-2	0	$-\sqrt{2}$	$\sqrt{2}$	0	1	1	-1	
$\Gamma_8^+$	4	-4	0	0	0	$\sqrt{2}$	$-\sqrt{2}$	0	1	4	-4	0	0	0	0	-1	-1	1	
$\Gamma_6^-$	2	-2	0	$\sqrt{2}$	$-\sqrt{2}$	0	$-\sqrt{2}$	0	1	-1	-2	2	0	$-\sqrt{2}$	$\sqrt{2}$	0	-1	1	
$\Gamma_7^-$	2	-2	0	$-\sqrt{2}$	$\sqrt{2}$	0	$\sqrt{2}$	0	1	-1	-2	2	0	$\sqrt{2}$	$-\sqrt{2}$	0	-1	1	
$\Gamma_8^-$	4	-4	0	0	0	0	0	-1	1	-4	4	0	0	0	0	1	1	-1	

## ELECTRONIC STATES AND OPTICAL TRANSITIONS

TABLE 2-12. Additional irreducible representations of the double group of  $\mathbf{k}$  on line  $A$  of the diamond structure

The notations are taken from R. H. Parmenter, *Phys. Rev.* **100**, 573 (1955). The irreducible representations  $A_4 A_5$  are degenerate by time reversal symmetry

Line $A$	$\{E 0\}$	$\{\bar{E} 0\}$	$\{\delta_{3xyz}^{-1}, \delta_{3xyz} 0\}$	$\{\bar{\delta}_{3xyz}^{-1}, \bar{\delta}_{3xyz} 0\}$	$\{I\delta_{2xy}, I\delta_{2\bar{x}\bar{z}}, I\delta_{2y\bar{z}} 0\}$	$\{I\bar{\delta}_{2xy}, I\bar{\delta}_{2\bar{x}\bar{z}}, I\bar{\delta}_{2y\bar{z}} 0\}$
$A_4$	1	-1	-1	1	$i$	$-i$
$A_5$	1	-1	-1	1	$-i$	$i$
$A_6$	2	-2	1	-1	0	0

*Line A* ( $\mathbf{k} = 2\pi/a(\delta, 0, 0)$  with  $0 < \delta < 1$ ). The small point group of  $\mathbf{k}$  is  $C_{4v}$ . The additional irreducible representations at  $A$  (Table 2-13) are obtained from the characters of the additional representations<sup>[1]</sup> of the group  $C'_4$ , by multiplying by the phase factor  $e^{-i\mathbf{k}\cdot\mathbf{t}} = e^{-i(\pi/2)\delta}$  the character of symmetry operations associated with fractional translation.

*Point X* ( $\mathbf{k} = 2\pi/a(1, 0, 0)$ ). The small point group of  $\mathbf{k}$  is  $D_{4h}$ . The additional irreducible representations at the point  $X$  cannot be derived from the additional irreducible representations of the double group  $D'_{4h}$  for the reasons given in Section 2-2a. We thus extend the procedure adopted for the simple group irreducible representations, and we consider a group whose elements are obtained by multiplying the elements of Table 2-7 by  $\{E|0\}$  and  $\{\bar{E}|0\}$ . The double group at point  $X$  now has 64 elements. Elements  $\{E|0\}$ ,  $\{\bar{E}|0\}$ ,  $\{E|1\}$ , and  $\{\bar{E}|1\}$  form separate classes, and all 64 elements can be collected into 16 classes. With the standard methods described in Section 1-5 we obtain a unique acceptable additional irreducible representation  $X_5$  in which the character of  $\{E|0\}$  and  $\{\bar{E}|1\}$  is 4, that of  $\{\bar{E}|0\}$  and  $\{E|1\}$  is -4, and all remaining elements have character 0.

*Point L* ( $\mathbf{k} = \pi/a(1, 1, 1)$ ). The small point group of  $\mathbf{k}$  is  $D_{3d}$ . The additional representations (Table 2-14) for the group of  $\mathbf{k}$  are obtained by a procedure similar to that used for point  $X$ . As in the case of the simple group there is a close similarity between Table 2-14 and the additional characters<sup>[1]</sup> of group  $D'_{3d}$ .

*Compatibility relations.* We can decompose the additional irreducible representations at the symmetry points into the additional irreducible representations at symmetry lines, and we can obtain compatibility relations between the states along symmetry lines and the states at symmetry points. The compatibility relations for the additional irreducible representations for the points  $L$ ,  $X$  and lines  $A$  and  $\bar{A}$  are given in Table 2-15.

*Spin-orbit splitting.* To establish how the states of the simple group of the previous section are decomposed into the states of the double group, we must consider the product of a given irreducible representation of the simple group with representation  $D^{(1/2)}$  of the rotation group. The product representation can be decomposed into a sum of irreducible representations of the double group, as shown in Table 2-16. We note in particular that no splitting is introduced at point  $X$  of the diamond structure by spin-orbit interaction.

### 2-3 Additional degeneracies required by time reversal symmetry

In the previous sections we constructed the irreducible representations of the space groups, both in the case of spinless particles and for particles with semi-integer spin. In addition to the space group symmetry operations, the Hamiltonian of an isolated

TABLE 2-13. Additional irreducible representations of the double group of  $\mathbf{k}$  on line  $\Delta$  of the diamond structure  
 The notations are taken from R. J. Elliott, *Phys. Rev.* 96, 130 (1954)

Line $\Delta$	$\langle E 0\rangle$	$\langle E 0\rangle$	$\langle \delta_{2x}, \bar{\delta}_{2x} 0\rangle$	$\langle \delta_{4x}^{-1}, \delta_{4x} f\rangle$	$\langle \bar{\delta}_{4x}^{-1}, \bar{\delta}_{4x} f\rangle$	$\langle I\delta_{2z}, \bar{I}\delta_{2z}, I\bar{\delta}_{2z}, \bar{I}\bar{\delta}_{2z} f\rangle$	$\langle \bar{I}\delta_{2z}, I\delta_{2z}, \bar{I}\bar{\delta}_{2z}, \bar{I}\bar{\delta}_{2z} 0\rangle$
$\Delta_6$	2	-2	0	$\frac{1}{2} e^{-i(\pi/2)\delta}$	$-\frac{1}{2} e^{-i(\pi/2)\delta}$	0	0
$\Delta_7$	2	-2	0	$-\frac{1}{2} e^{-i(\pi/2)\delta}$	$\frac{1}{2} e^{-i(\pi/2)\delta}$	0	0

TABLE 2-14. Additional irreducible representations of the double group of  $\mathbf{k}$  at point  $L$  of the diamond structure  
 The notations are taken from R. H. Parmenter, *Phys. Rev.* 100, 573 (1955). The representations  $L_4^+L_5^+$  and  $L_4^-L_5^-$  are degenerate by time reversal symmetry

Point $L$	$\langle E 0\rangle$	$\langle E 0\rangle$	$\langle \delta_{3xy}^{-1} 0\rangle$	$\langle \bar{\delta}_{3xy}^{-1} 0\rangle$	$\langle I\delta_{2xy} 0\rangle$	$\langle \bar{I}\delta_{2xy} 0\rangle$	$\langle I f\rangle$	$\langle \bar{I} f\rangle$	$\langle I\delta_{3xy}^{-1} f\rangle$	$\langle \bar{I}\delta_{3xy}^{-1} f\rangle$	$\langle \delta_{2xy} f\rangle$	$\langle \bar{\delta}_{2xy} f\rangle$
$L_4^+$	1	-1	-1	1	$i$	$-i$	1	$-i$	-1	-1	1	$-i$
$L_5^+$	1	-1	1	-1	$-i$	$i$	1	$-i$	-1	1	$-i$	$i$
$L_6^+$	2	-2	1	-1	0	0	2	-2	1	-1	0	0
$L_4^-$	1	-1	-1	1	$i$	$-i$	-1	1	1	-1	$i$	$-i$
$L_5^-$	1	-1	-1	1	$-i$	$i$	-1	1	1	-1	$i$	$-i$
$L_6^-$	2	-2	1	-1	0	0	-2	2	-1	1	0	0

BIBLIOTHÈQUE DU  
 DÉPARTEMENT DE PHYSIQUE  
 Ecole Polytechnique Fédérale de Lausanne  
 PHB - Ecublens  
 CH - 1015 LAUSANNE SUISSE

## ELECTRONIC STATES AND OPTICAL TRANSITIONS

TABLE 2-15. Compatibility relations between the additional irreducible representations of the double groups of  $\mathbf{k}$  at symmetry points  $\Gamma$ ,  $L$ ,  $X$  and symmetry lines  $A$ ,  $\Delta$  of the diamond structure

Point $\Gamma$	$\Gamma_6^+$	$\Gamma_7^+$	$\Gamma_8^+$	$\Gamma_6^-$	$\Gamma_7^-$	$\Gamma_8^-$
Line $A$	$A_6$	$A_6$	$A_4 + A_5 + A_6$	$A_6$	$A_6$	$A_4 + A_5 + A_6$
Point $\Gamma$	$\Gamma_6^+$	$\Gamma_7^+$	$\Gamma_8^+$	$\Gamma_6^-$	$\Gamma_7^-$	$\Gamma_8^-$
Line $\Delta$	$\Delta_6$	$\Delta_7$	$\Delta_6 + \Delta_7$	$\Delta_6$	$\Delta_7$	$\Delta_6 + \Delta_7$
Point $X$				$X_5$		
Line $\Delta$				$\Delta_6 + \Delta_7$		
Point $L$	$L_4^+$	$L_5^+$	$L_6^+$	$L_4^-$	$L_5^-$	$L_6^-$
Line $A$	$A_4$	$A_5$	$A_6$	$A_4$	$A_5$	$A_6$

TABLE 2-16. Decomposition of the states of the simple group into the states of the double group at symmetry points  $\Gamma$ ,  $L$ ,  $X$  and symmetry lines  $A$ ,  $\Delta$  of the diamond structure

$\Gamma_1$ $\Gamma_t \times D^{(1/2)}$	$\Gamma_1$	$\Gamma_2$	$\Gamma_{12}$	$\Gamma'_{25}$	$\Gamma'_{15}$	$\Gamma'_1$	$\Gamma'_2$	$\Gamma'_{12}$	$\Gamma_{25}$	$\Gamma_{15}$
$\Gamma_6^+$ $\Gamma_t \times D^{(1/2)}$	$\Gamma_6^+$	$\Gamma_7^+$	$\Gamma_8^+$	$\Gamma_7^+ + \Gamma_8^+$	$\Gamma_7^+ + \Gamma_8^+$	$\Gamma_6^-$	$\Gamma_7^-$	$\Gamma_8^-$	$\Gamma_7^- + \Gamma_8^-$	$\Gamma_7^- + \Gamma_8^-$
$A_1$				$A_1$		$A_2$			$A_3$	
$A_1$ $A_t \times D^{(1/2)}$				$A_6$		$A_6$			$A_4 + A_5 + A_6$	
$\Delta_1$				$\Delta_1$		$\Delta'_1$		$\Delta_2$		$\Delta'_2$
$\Delta_1$ $\Delta_t \times D^{(1/2)}$				$\Delta_6$		$\Delta_6$		$\Delta_7$		$\Delta_5$
$X_1$				$X_1$		$X_2$		$X_3$		$X_4$
$X_1$ $X_t \times D^{(1/2)}$				$X_5$		$X_5$		$X_5$		$X_5$
$L_1$	$L_1^+$	$L_2^+$		$L_3^+$		$L_1^-$	$L_2^-$		$L_3^-$	
$L_1$ $L_t \times D^{(1/2)}$	$L_6^+$	$L_6^+$		$L_4^+ + L_5^+ + L_6^+$		$L_6^-$	$L_6^-$		$L_4^- + L_5^- + L_6^-$	

crystal exhibits time reversal symmetry. To discuss the systematic degeneracies imposed by time reversal symmetry we must apply the general theory outlined in Section 1-6 and the Wigner criterion for additional degeneracies given in Table 1-23.

From translation symmetry alone we have shown that  $E(\mathbf{k}) = E(-\mathbf{k})$  because of time reversal. Other symmetry operations in addition to the translation group do not remove this essential degeneracy. To study the effect of the other symmetry operations we must distinguish the case in which  $\mathbf{k}$  and  $-\mathbf{k}$  belong to the same or to different stars.

If  $\mathbf{k}$  and  $-\mathbf{k}$  do not belong to the same star, i.e.  $\mathbf{k}$  and  $-\mathbf{k}$  are not related one to another by a space symmetry operation, the irreducible representations of the space group constructed starting from the irreducible representations of the group of  $\mathbf{k}$  cannot be equivalent to their complex conjugate representations (constructed starting from the group of  $-\mathbf{k}$ ). An additional degeneracy occurs among the eigenvalues of the stars of  $\mathbf{k}$  and  $-\mathbf{k}$ , but no further degeneracy occurs at a given  $\mathbf{k}$  vector.

If  $\mathbf{k}$  and  $-\mathbf{k}$  belong to the same star, the relation  $E(\mathbf{k}) = E(-\mathbf{k})$  is already needed by space symmetry, and the time reversal operator may introduce new degeneracies at a given  $\mathbf{k}$  vector. One may or may not obtain additional degeneracies at a given  $\mathbf{k}$  vector depending on which of the three cases of Table 1-23 actually occurs. Herring<sup>[4]</sup>

has brought the test of Frobenius-Schur (Table 1-23) into a form which is particularly suitable for the irreducible representations of the space groups. The Herring test, which can be used to determine whether or not an irreducible representation of the space group can (i) be reduced to real form (case a), (ii) is not equivalent to its complex conjugate (case b), or (iii) cannot be brought into real form although equivalent to its complex conjugate (case c), is given as

$$\sum_{\{Q|\mathbf{q}\}} \chi^{(\mathbf{k}, \alpha)} (\{Q|\mathbf{q}\}^2) = \begin{cases} h_k & \text{case a,} \\ 0 & \text{case b,} \\ -h_k & \text{case c.} \end{cases} \quad (2-23)$$

In (2-23) the sum extends only to the operations  $\{Q|\mathbf{q}\}$ , elements in the square brackets of (2-12), for which  $Q\mathbf{k} = -\mathbf{k} + \mathbf{h}$  and  $\mathbf{q}$  is the fractional translation associated with  $Q$ .  $h_k$  indicates the number of operations of the small point group of  $\mathbf{k}$  and  $\chi^{(\mathbf{k}, \alpha)}$  the character of representation  $D^{(\mathbf{k}, \alpha)}$  of the little group of  $\mathbf{k}$ . The main advantage of (2-23) is that we can carry out the test using the character table of the little group of  $\mathbf{k}$  because  $\{Q|\mathbf{q}\}^2$  belongs to it. The effect of time reversal symmetry in the different cases has been discussed in Section 1-6.

For convenience we summarize in Table 2-17 the systematic degeneracies among space group representations required by time reversal symmetry.

TABLE 2-17. Effect of time reversal symmetry for space groups

$\mathbf{k}$ and $-\mathbf{k}$ do not belong to the same star				
Case	Relation between $D_{\text{space}}^{(\mathbf{k}, \alpha)}$ and $D_{\text{space}}^{(\mathbf{k}, \alpha)*}$	Herring's test	Spinless particle	Half-spin particle
Case b	$D_{\text{space}}^{(\mathbf{k}, \alpha)}$ and $D_{\text{space}}^{(\mathbf{k}, \alpha)*}$ are inequivalent	$\sum_{\{Q_m \mathbf{q}_m\}} \chi^{(\mathbf{k}, \alpha)} (\{Q_m \mathbf{q}_m\}^2) = 0$	No extra degeneracy at $\mathbf{k}$	No extra degeneracy at $\mathbf{k}$

 $\mathbf{k}$  and  $-\mathbf{k}$  belong to the same star

Case	Relation between $D_{\text{space}}^{(\mathbf{k}, \alpha)}$ and $D_{\text{space}}^{(\mathbf{k}, \alpha)*}$	Herring's test	Spinless particle	Half-spin particle
Case a	$D_{\text{space}}^{(\mathbf{k}, \alpha)}$ and $D_{\text{space}}^{(\mathbf{k}, \alpha)*}$ are equivalent to the same real irreducible representation	$\sum_{\{Q_m \mathbf{q}_m\}} \chi^{(\mathbf{k}, \alpha)} (\{Q_m \mathbf{q}_m\}^2) = h_k$	No extra degeneracy at $\mathbf{k}$	Doubled degeneracy at $\mathbf{k}$
Case b	$D_{\text{space}}^{(\mathbf{k}, \alpha)}$ and $D_{\text{space}}^{(\mathbf{k}, \alpha)*}$ are inequivalent	$\sum_{\{Q_m \mathbf{q}_m\}} \chi^{(\mathbf{k}, \alpha)} (\{Q_m \mathbf{q}_m\}^2) = 0$	Doubled degeneracy at $\mathbf{k}$	Doubled degeneracy at $\mathbf{k}$
Case c	$D_{\text{space}}^{(\mathbf{k}, \alpha)}$ and $D_{\text{space}}^{(\mathbf{k}, \alpha)*}$ are equivalent to each other but not to a real representation	$\sum_{\{Q_m \mathbf{q}_m\}} \chi^{(\mathbf{k}, \alpha)} (\{Q_m \mathbf{q}_m\}^2) = -h_k$	Doubled degeneracy at $\mathbf{k}$	No extra degeneracy at $\mathbf{k}$

*Proof of Herring's test*

The proof of Herring's test can be obtained by applying the Frobenius-Schur test to the irreducible representation  $D_{\text{space}}^{(\mathbf{k}, \alpha)}$  of the space group constructed starting from the irreducible representation  $D^{(\mathbf{k}, \alpha)}$  of the group of  $\mathbf{k}$ . We have

$$\sum_{\{R|\mathbf{a}\}} \chi_{\text{space}}^{(\mathbf{k}, \alpha)} (\{R|\mathbf{a}\}^2) = \begin{cases} Nh & \text{case a,} \\ 0 & \text{case b,} \\ -Nh & \text{case c,} \end{cases} \quad (2-24)$$

where  $Nh$  is the order of the space group and  $\chi_{\text{space}}^{(\mathbf{k}, \alpha)}$  the character of the irreducible representation  $D_{\text{space}}^{(\mathbf{k}, \alpha)}$ . We can write (2-24) in the form

$$\sum_{\{R|\mathbf{a}\}} \chi_{\text{space}}^{(\mathbf{k}, \alpha)} (\{R|\mathbf{a}\}^2) = s_k \sum_{\{R|\mathbf{a}\}} \sum_{j=1}^{l_a} \langle \psi_k^{(j)} | O_{\{R|\mathbf{a}\}^2} | \psi_k^{(j)} \rangle,$$

where  $s_k$  indicates the number of points of the star of  $\mathbf{k}$ , and  $\psi_k^{(j)}$  ( $j = 1 \dots l_a$ ) denote the basis function for  $D^{(\mathbf{k}, \alpha)}$ . We observe that  $\{R|\mathbf{a}\}$  can be written as  $\{E|\tau_n\} \{R|\mathbf{f}\}$  and, furthermore, that

$$\{R|\mathbf{a}\}^2 = \{E|\tau_n\} \{R|\mathbf{f}\} \{E|\tau_n\} \{R|\mathbf{f}\}^{-1} \{R|\mathbf{f}\}^2 = \{E|R\tau_n + \tau_n\} \{R|\mathbf{f}\}^2.$$

Consequently,

$$\begin{aligned} \sum_{\{R|\mathbf{a}\}} \chi_{\text{space}}^{(\mathbf{k}, \alpha)} (\{R|\mathbf{a}\}^2) &= s_k \sum_{\{E|\tau_n\}} \sum_{\{R|\mathbf{f}\}} \sum_{j=1}^{l_a} \langle \psi_k^{(j)} | O_{\{E|R\tau_n + \tau_n\}} O_{\{R|\mathbf{f}\}^2} | \psi_k^{(j)} \rangle \\ &= s_k \sum_{j=1}^{l_a} \sum_{\{R|\mathbf{f}\}} \sum_{\{E|\tau_n\}} e^{i(\mathbf{k} + R^{-1}\mathbf{k}) \cdot \tau_n} \langle \psi_k^{(j)} | O_{\{R|\mathbf{f}\}^2} | \psi_k^{(j)} \rangle. \end{aligned}$$

The sum over  $\{E|\tau_n\}$  gives

$$\sum_{\{E|\tau_n\}} e^{i(\mathbf{k} + R^{-1}\mathbf{k}) \cdot \tau_n} = \begin{cases} 0 & \text{when } R^{-1}\mathbf{k} \neq -\mathbf{k} + \mathbf{h}, \\ N & \text{when } R^{-1}\mathbf{k} = -\mathbf{k} + \mathbf{h}. \end{cases} \quad (2-25)$$

Let  $\{Q|\mathbf{q}\}$  indicate those elements of  $\{R|\mathbf{f}\}$  whose rotational part changes  $\mathbf{k}$  into  $-\mathbf{k} + \mathbf{h}$ ,  $\mathbf{h}$  being a reciprocal lattice vector and  $\mathbf{q}$  the fractional translation associated with  $Q$ . These are the only elements which give a non-vanishing contribution to the sum in (2-25). Equation (2-24) thus becomes

$$\sum_{\{Q|\mathbf{q}\}} \chi_{\text{space}}^{(\mathbf{k}, \alpha)} (\{Q|\mathbf{q}\}^2) = \begin{cases} h/s_k & \text{case a,} \\ 0 & \text{case b,} \\ -h/s_k & \text{case c.} \end{cases}$$

Since  $h/s_k = h_k$ , the Herring test (2-23) is thus proved.

*Example*

We wish now to apply the above considerations to the case of the diamond structure. At the points  $\Gamma$ ,  $X$ , and  $\Delta$  it is easily verified that case a always obtains for the simple group representations and case c for the double group representations. Time reversal does not introduce additional degeneracy at these points. However, along line  $A$ ,  $A_4$ , and  $A_5$  belong to case b and are degenerate by time reversal. At the point  $L$ ,  $L_4^+ L_5^+$  and  $L_4^- L_5^-$  are degenerate by time reversal symmetry.

At a general point, the small point group of  $\mathbf{k}$  contains only the identity  $\{E|0\}$ , and its irreducible representations are listed in Table 1-17. The only operation that changes  $\mathbf{k}$  into  $-\mathbf{k}$  is the inversion  $\{I|\mathbf{f}\}$ . Since  $\{I|\mathbf{f}\}^2 = \{E|0\}$ , case a of Table 2-17 occurs both for the irreducible representation of the simple group  $C_1$  and for the irreducible representation of the double group  $C'_1$ ; thus an additional degeneracy is required by time reversal symmetry for particles with semi-integer spin. The energy bands of any space group with spatial inversion symmetry are (at least) doubly degenerate at every  $\mathbf{k}$  vector when spin is included.

## 2-4 Selection rules

### 2-4 a Selection rules at a given point of the Brillouin zone

The general theory of selection rules has been considered in Section 1-7, and we now apply it to crystal states.

Let us first discuss matrix elements of the type

$$\langle \varphi_m^{(\mathbf{k}_2, \mu)} | V | \psi_n^{(\mathbf{k}_1, \nu)} \rangle, \quad (2-26)$$

where  $V$  is a periodic function having the periodicity of the lattice,  $\varphi_m^{(\mathbf{k}_2, \mu)}$  ( $m = 1, 2, \dots, l_\mu$ ) is a set of functions transforming as the irreducible representation  $D^{(\mathbf{k}_2, \mu)}$  of the group of  $\mathbf{k}_2$ , and  $\psi_n^{(\mathbf{k}_1, \nu)}$  ( $n = 1, 2, \dots, l_\nu$ ) is a different set of functions transforming as the irreducible representation  $D^{(\mathbf{k}_1, \nu)}$  of the group of  $\mathbf{k}_1$ . The translation symmetry of the crystal determines the first important selection rule. The product functions  $V\psi_n^{(\mathbf{k}_1, \nu)}$  are Bloch functions of vector  $\mathbf{k}_1$ . Thus the matrix elements (2-26) are zero unless

$$\mathbf{k}_2 \doteq \mathbf{k}_1, \quad (2-27)$$

where  $\doteq$  implies that the two members of (2-27) either are equal or differ by a reciprocal lattice vector. A periodic function (for instance the crystal potential) having the periodicity of the lattice may have non-vanishing matrix elements only among Bloch functions with the same  $\mathbf{k}$  vector. Once (2-27) is satisfied, the other symmetry operations of the group of  $\mathbf{k}_1$  ( $\mathbf{k}_1$  is equivalent to  $\mathbf{k}_2$ ) may determine further selection rules. Let  $D^{(\alpha)}(R_{\mathbf{k}_1})$  denote the (reducible or irreducible) representation of the small point group of vector  $\mathbf{k}_1$  to which function  $V$  belongs. The product functions  $V\psi_n^{(\mathbf{k}_1, \nu)}$  belong to the product representation  $D^{(\alpha)}(R_{\mathbf{k}_1}) \times D^{(\mathbf{k}_1, \nu)}(\{R_{\mathbf{k}_1}|\mathbf{a}\})$  of the group of  $\mathbf{k}_1$ . Using (1-58) we find that the number of times the representation  $D^{(\mathbf{k}_1, \nu)}$  appears in the product representation is given by

$$c(\mathbf{k}_1 \mu; \alpha; \mathbf{k}_1 \nu) = \frac{1}{h_{\mathbf{k}_1}} \sum_{\{R_{\mathbf{k}_1}|\mathbf{f}\}} \chi^{(\mathbf{k}_1, \mu)}(\{R_{\mathbf{k}_1}|\mathbf{f}\})^* \chi^{(\alpha)}(R_{\mathbf{k}_1}) \chi^{(\mathbf{k}_1, \nu)}(\{R_{\mathbf{k}_1}|\mathbf{f}\}), \quad (2-28)$$

where the sum is extended to the operations of the small point group of  $\mathbf{k}_1$ . The occurrence  $c(\mathbf{k}_1 \mu; \alpha; \mathbf{k}_1 \nu) = 0$  determines the selection rules as discussed in Section (1-7).

#### Example

As an example of the application of (2-28), we consider the selection rules for optical transitions in the diamond structure. In the dipole approximation, function  $V$  for the radiation field is proportional to  $\mathbf{e} \cdot \mathbf{r}$  where  $\mathbf{e}$  is the polarization vector of the electric

## ELECTRONIC STATES AND OPTICAL TRANSITIONS

field. Given a vector  $\mathbf{k}$ , let  $D^{(\alpha)}(R_{\mathbf{k}})$  be the representation of the small point group of  $\mathbf{k}$  to which function  $e \cdot r$  belongs. Selection rules can be found by decomposing the product representation

$$D^{(\alpha)}(R_{\mathbf{k}}) \times D^{(\mathbf{k}, \mu)}(\{R_{\mathbf{k}}|\mathbf{a}\})$$

into irreducible representations  $D^{(\mathbf{k}, \mu)}$  of the group of  $\mathbf{k}$ , using (2-28). Results for symmetry lines and symmetry points of interest in the diamond lattice are given in Table 2-18.

TABLE 2-18. Allowed optical transitions at high symmetry points and lines of the Brillouin zone for the diamond structure

In the first column the representation of the small group of  $\mathbf{k}$  according to which  $(x, y, z)$  transform is given. In the second column the decomposition of the product representation is listed. Selection rules are then obtained by inspection. We see, for instance that the transitions allowed from  $\Gamma_{12}$  are those to  $\Gamma_{15}$  and  $\Gamma_{25}$

Point $\Gamma$	$\Gamma_1 : \Gamma_1$	$\Gamma_2 : \Gamma_{25} + \Gamma_{15}$	$\Gamma_{12} : \Gamma_6^+ + \Gamma_7^+$	$\Gamma'_{25} : \Gamma_2' + \Gamma_{12}' + \Gamma_{25} + \Gamma_{15}$
$\Gamma_{15}$	$\Gamma_1 \times \Gamma_{15} : \Gamma_{15}$	$\Gamma_{25}$	$\Gamma_{25} + \Gamma_{15}$	$\Gamma_2' + \Gamma_{12}' + \Gamma_{25} + \Gamma_{15}$
	$\Gamma_1 : \Gamma'_{15}$		$\Gamma_6^+$	$\Gamma_7^+$
	$\Gamma_1 \times \Gamma_{15} : \Gamma'_1 + \Gamma'_{12} + \Gamma_{25} + \Gamma_{15}$	$\Gamma_6^- + \Gamma_8^-$	$\Gamma_7^- + \Gamma_8^-$	$\Gamma_6^- + \Gamma_7^- + 2\Gamma_8^-$
Line $A$	$A_1 : A_1 \ A_2 \ A_3 \ A_4 \ A_5 \ A_6$			
	$A_1 \times A_1 : A_1 \ A_2 \ A_3 \ A_4 \ A_5 \ A_6$			
$A_1 + A_3$	$A_1 \times A_3 : A_3 \ A_3 \ A_1 + A_2 + A_3 \ A_6 \ A_6 \ A_4 + A_5 + A_6$			
Line $A'$	$A_1 : A_1 \ A'_1 \ A_2 \ A'_2 \ A_5 \ A_6 \ A_7$			
	$A_1 \times A_1 : A_1 \ A'_1 \ A_2 \ A'_2 \ A_5 \ A_6 \ A_7$			
$A_1 + A_5$	$A_1 \times A_5 : A_5 \ A_5 \ A_5 \ A_1 + A'_1 + A_2 + A'_2 \ A_6 + A_7 \ A_6 + A_7$			
Point $X$	$X_1 : X_1 \ X_2 \ X_3 \ X_4 \ X_5$			
	$X_1 \times M'_1 : X_1 \ X_2 \ X_3 \ X_4 \ X_5$			
$M'_1 + M'_5$	$X_1 \times M'_5 : X_3 + X_4 \ X_3 + X_4 \ X_1 + X_2 \ X_1 + X_2 \ 2X_5$			
Point $L$	$L_1 : L_1 \ L_2 \ L_3 \ L_4^+ \ L_5^+ \ L_6^+$			
	$L_1 \times L'_1 : L'_1 \ L'_2 \ L'_3 \ L'_4 \ L'_5 \ L'_6$			
$L'_1 + L'_3$	$L_1 \times L'_3 : L'_3 \ L'_3 \ L'_1 + L'_2 + L'_3 \ L'_6 \ L'_6 \ L'_4 + L'_5 + L'_6$			

### 2-4b Selection rules connecting different points of the Brillouin zone<sup>[5]</sup>

We wish to discuss the matrix elements

$$\langle \varphi_m^{(k_2, \mu)} | V_i^{(q, \alpha)} | \psi_n^{(k_1, \nu)} \rangle, \quad (2-29)$$

where  $\psi_n^{(k_1, \nu)}$  ( $n = 1 \dots l_\nu$ ),  $\varphi_m^{(k_2, \mu)}$  ( $m = 1 \dots l_\mu$ ), and  $V_i^{(q, \alpha)}$  ( $i = 1 \dots l_\alpha$ ) are partner functions for the irreducible representation  $D^{(k_1, \nu)}$ ,  $D^{(k_2, \mu)}$ , and  $D^{(q, \alpha)}$  respectively. The three sets of functions are supposed not to be related to one another by a symmetry operation.

The translation symmetry determines the first important selection rule. The product functions  $V_i^{(q, \alpha)} \psi_n^{(k_1, \nu)}$  are Bloch functions of vector  $\mathbf{q} + \mathbf{k}_1$ . The integrals (2-29) are zero, unless

$$\mathbf{k}_2 \doteq \mathbf{k}_1 + \mathbf{q}. \quad (2-30)$$

Once (2-30) is satisfied, the other symmetry operations common to the little group of  $\mathbf{k}_2$  and  $\mathbf{k}_1$  (and hence of  $\mathbf{q}$ ) may determine further selection rules. Note that  $D^{(k_1, \nu)}$ ,  $D^{(k_2, \mu)}$ ,  $D^{(q, \alpha)}$  provide a representation (in general reducible) of the common group

## SYMMETRY PROPERTIES OF THE ELECTRONIC STATES IN CRYSTALS

(a group of operations that are common to the little groups of  $\mathbf{k}_2$ ,  $\mathbf{k}_1$ , and  $\mathbf{q}$ ). The product functions  $V_i^{(q,\alpha)}\psi_n^{(k_1,\nu)}$  belong to the product representation

$$\mathbf{D}^{(q,\alpha)}(\{R_c|\mathbf{a}\}) \times \mathbf{D}^{(k_1,\nu)}(\{R_c|\mathbf{a}\})$$

of the common group. Using (1-58) we find that the number of times the representation  $D^{(k_2,\mu)}$  appears in the product representation is given by

$$c(k_2\mu, q\alpha, k_1\nu) = \frac{1}{h_c} \sum_{\{R_c|\mathbf{f}_c\}} \chi^{(k_2,\mu)}(\{R_c|\mathbf{f}_c\})^* \chi^{(q,\alpha)}(\{R_c|\mathbf{f}_c\}) \chi^{(k_1,\nu)}(\{R_c|\mathbf{f}_c\}), \quad (2-31)$$

where the sum is extended to the operations of the common group. The occurrence  $c(k_2\mu, q\alpha, k_1\nu) = 0$  determines the selection rules. It is easy to verify that (2-31) reduces to (2-28) when  $q = 0$ .

Let us consider, for instance, the product of the representations  $L_1 \times L_1$  at point  $L$  of the diamond structure. As a result of the product, irreducible representations for point  $\Gamma$  are obtained. Using Tables 2-4 and 2-9, and eq. (2-31), we find that  $\Gamma_1$  and  $\Gamma'_{25}$  are contained once in the product representation, and we thus write

$$L_1 \times L_1 = \Gamma_1 + \Gamma'_{25}.$$

$\Gamma_1$  and  $\Gamma'_{25}$  therefore are the only states which interact with a state of symmetry  $L_1$  via a perturbation of symmetry  $L_1$ . Similarly,

$$L_3 \times L_3 = \Gamma_1 + \Gamma_2 + \Gamma_{12} + 2\Gamma'_{15} + 2\Gamma'_{25}.$$

Let us consider the product of representation  $L_1$  and  $\Gamma_1$ . We obtain irreducible representations for point  $L$ . Using (2-31) we have

$$\Gamma_1 \times L_1 = L_1$$

and, similarly,

$$L_3 \times \Gamma_{15} = L_1 + L_2 + 2L_3.$$

It is interesting to mention that selection rules more stringent than (2-31) are obtained when the periodic part of the perturbation operator  $V_i^{(q,\alpha)}$  is even or odd under time reversal symmetry (i.e.

$$TV_i^{(q,\alpha)} e^{-i\mathbf{q} \cdot \mathbf{r}} = a V_i^{(q,\alpha)} e^{-i\mathbf{q} \cdot \mathbf{r}} T$$

with  $a = \pm 1$ ) and the set of functions  $\psi_m^{(k_2,\mu)}$  are connected to the set of functions  $\psi_n^{(k_1,\nu)}$  by the relation

$$\psi_m^{(k_2,\mu)} = TO_{\{R|\mathbf{f}\}} \psi_n^{(k_1,\nu)};$$

this happens when  $\mathbf{k}_1$  and  $-\mathbf{k}_2$  belong to the same star. Doni and Pastori Parravicini<sup>[5]</sup> have shown that the selection rules are given in this case by the expression

$$\begin{aligned} c(k_2\mu; q\alpha; k_1\mu) &= \frac{1}{2h_c} \sum_{\{R_c|\mathbf{f}_c\}} \chi^{(k_2,\mu)}(\{R|\mathbf{f}\}^{-1} \{R_c|\mathbf{f}_c\} \{R|\mathbf{f}\}) \chi^{(q,\alpha)}(\{R_c|\mathbf{f}_c\}) \chi^{(k_1,\mu)}(\{R_c|\mathbf{f}_c\}) \\ &\quad + b \frac{1}{2h_c} \sum_{\{S|\mathbf{s}\}} \chi^{(k_1,\mu)}(\{S|\mathbf{s}\}^2) \chi^{(q,\alpha)}(\{S|\mathbf{s}\}). \end{aligned} \quad (2-32)$$

In (2-32)  $\{R_c|\mathbf{f}_c\}$  are the operations common to the little groups of  $\mathbf{k}_2$ ,  $\mathbf{k}_1$ , and  $\mathbf{q}$ ;  $\{S|\mathbf{s}\}$  is the set of operations (if any) such that  $S\mathbf{k}_1 \doteq -\mathbf{k}_2$  and  $S\mathbf{k}_2 \doteq -\mathbf{k}_1$ ;  $b$  equals  $+a$  or  $-a$  for spinless particles and for half-spin particles respectively.

## References and notes

- [1] All possible translation groups and Brillouin zones are described in the article by G. F. KOSTER, *Solid State Physics* **5**, 173 (1957). This article includes a detailed and useful collection of the irreducible representations at symmetry points and symmetry lines in the Brillouin zone of many common crystal structures. The irreducible representations of all the 230 space groups are tabulated in the very useful book by C. J. BRADLEY and A. P. CRACKNELL, *The Mathematical Theory of Symmetry in Solids* (Clarendon Press, 1972).
- [2] F. BLOCH, *Z. Physik* **52**, 555 (1928).
- [3] The basic papers concerning symmetry analysis of crystal states are: F. SEITZ, *Ann. Math.* **37**, 17 (1936) for the irreducible representations of space groups; L. P. BOUCKAERT, R. SMOLUCHOWSKI, and E. P. WIGNER, *Phys. Rev.* **50**, 58 (1936) for the small groups of the  $\mathbf{k}$  vector; H. BETHE, *Ann. Physik* **3**, 133 (1929) and W. OPECHOWSKI, *Physica* **7**, 552 (1940) for the irreducible representations of double groups. See also ref. [1].
- [4] C. HERRING, *Phys. Rev.* **52**, 361 (1937).
- [5] The selection rules connecting different points of the Brillouin zone were first discussed by R. J. ELLIOTT and R. LOUDON, *J. Phys. Chem. Solids* **15**, 146 (1960), and M. LAX and J. J. HOPFIELD, *Phys. Rev.* **124**, 115 (1961). Besides the familiar selection rules, expressed by eq. (2-31), more stringent selection rules are obtained in the particular case when the basis functions at the vectors  $\mathbf{k}_1$ ,  $\mathbf{k}_2$ , or  $\mathbf{q}$  are related to one another by a symmetry operation. In this case, a symmetric or antisymmetric product of space group representations has to be considered, as shown by M. LAX, *Phys. Rev.* **138A**, 793 (1965). For an alternative and very simple derivation of selection rules connecting different points of the Brillouin zone, we refer to N. O. FOLLAND and F. BASSANI, *J. Phys. Chem. Solids* **29**, 281 (1968); E. DONI and G. PASTORI PARRAVICINI, *J. Phys.* **C6**, 2859 (1973); **C7**, 1786 (1974). For further applications of symmetry to physical problems in crystals we recommend the book by R. S. KNOX and A. GOLD, *Symmetry in the Solid State* (Benjamin, 1964). This book also includes a useful collection of reprints.

## CHAPTER 3

### METHODS OF CALCULATING THE ELECTRONIC BAND STRUCTURES OF CRYSTALS

IN THIS chapter we briefly describe methods for calculating electronic states in crystals, and discuss the physical reasons that recommend a given method for a given crystal or class of crystals. Each method has its own difficulties due to the inadequacy of the approximations required and to the unavoidable inaccuracies of the crystal potential used. For these reasons, emphasis will be put on results which depend more on the symmetry than on the actual value of the potential. Interpolation schemes and semi-empirical approaches will also be described because they simplify the calculation of measurable quantities to be compared with the experiment, thus allowing an interpretation of the optical properties of crystals, as will be illustrated in the following chapters.

#### 3-1 The basic approximations

A crystal is made up of a large number of interacting particles, and consequently the theoretical treatment of the energy levels and wave functions of a solid cannot be attempted without a number of simplifying approximations. One can describe the crystal as an ensemble of mutually interacting electrons and nuclei, and we can write the total Hamiltonian of the system in the form

$$H_t = T_e + T_L + V_{ee} + V_{eL} + V_{LL} \quad (3-1a)$$

where  $T_e$  and  $T_L$  indicate the kinetic energy of the electrons and nuclei respectively, and  $V_{ee}$ ,  $V_{eL}$ ,  $V_{LL}$  the electron-electron, electron-nuclei, and nuclei-nuclei interactions respectively. Since by far the strongest interactions between particles are those due to coulomb forces, we use the following expression for  $H_t$ :

$$\begin{aligned} H_t = & - \sum_i \frac{\hbar^2}{2m} \nabla_i^2 - \sum_I \frac{\hbar^2}{2M_I} \nabla_I^2 + \sum_{i < j} \frac{e^2}{|\mathbf{r}_i - \mathbf{r}_j|} - \sum_{I,i} \frac{Z_I e^2}{|\mathbf{R}_I - \mathbf{r}_i|} \\ & + \sum_{I < J} \frac{Z_I Z_J e^2}{|\mathbf{R}_I - \mathbf{R}_J|}, \end{aligned} \quad (3-1b)$$

where the indices  $i, j$  and  $I, J$  refer to the electrons and nuclei respectively, and  $Z$  indicates the nuclear charge. Note that eq. (3-1 b) is only an approximation of (3-1 a) since it does not contain all possible interactions (e.g. spin-spin interactions are not included)

and the non-relativistic expression of the kinetic energy is assumed (the role of relativistic effects will be discussed later).

We now consider the Schrödinger equation

$$H_t \Psi(\mathbf{R}, \mathbf{r}) = E \Psi(\mathbf{R}, \mathbf{r}), \quad (3-2)$$

where  $\mathbf{R}$  represents the space and spin coordinates of all the nuclei and  $\mathbf{r}$  those of the electrons, and  $H_t$  is the Hamiltonian (3-1a) or (3-1b). The eigenvalue problem (3-2) can be reduced to a workable one for electronic states in crystals by means of some basic approximations which we now describe.

(i) *The adiabatic approximation*

The system we are dealing with is made up of nuclei and electrons which have very different masses. We can use the Born–Oppenheimer approximation<sup>[1]</sup> to split the eigenvalue problem (3-2) into two separate, though interdependent, eigenvalue problems for electrons and nuclei. For this purpose, let us consider the electron Hamiltonian defined by

$$H_e = T_e + V_{ee} + V_{eL} \quad (3-3a)$$

or

$$H_e = - \sum_i \frac{\hbar^2}{2m_i} \nabla_i^2 + \sum_{i < j} \frac{e^2}{|\mathbf{r}_i - \mathbf{r}_j|} - \sum_{I,i} \frac{Z_I e^2}{|\mathbf{R}_I - \mathbf{r}_i|}. \quad (3-3b)$$

The Hamiltonian (3-3) depends parametrically on the coordinates of the nuclei. For each nuclear configuration  $\mathbf{R}$  we consider the eigenvalue problem

$$[T_e + V_{ee} + V_{eL}] \psi_n(\mathbf{R}, \mathbf{r}) = E_n(\mathbf{R}) \psi_n(\mathbf{R}, \mathbf{r}), \quad (3-4)$$

where  $n$  indicates the quantum numbers for the electronic coordinates  $\mathbf{r}$ . Because of the large difference between electronic and nuclear masses, we assume that the electrons will adiabatically follow the motion of the nuclei and that the eigenvalues  $E_n(\mathbf{R})$  and eigenfunctions  $\psi_n(\mathbf{R}, \mathbf{r})$  will depend on the nuclear coordinates  $\mathbf{R}$  in a smooth and continuous way. We look for eigenfunctions of the total Hamiltonian  $H_t$  of the form

$$\Psi_{n,v}(\mathbf{R}, \mathbf{r}) = \chi_{n,v}(\mathbf{R}) \psi_n(\mathbf{R}, \mathbf{r}), \quad (3-5)$$

where the dependence on  $\mathbf{r}$  is confined to  $\psi_n(\mathbf{R}, \mathbf{r})$  and  $v$  indicates the quantum numbers for the nuclear coordinates  $\mathbf{R}$ . We must have

$$[T_e + T_L + V_{ee} + V_{eL} + V_{LL}] \chi_{n,v}(\mathbf{R}) \psi_n(\mathbf{R}, \mathbf{r}) = E_{n,v} \chi_{n,v}(\mathbf{R}) \psi_n(\mathbf{R}, \mathbf{r}). \quad (3-6)$$

Let us consider the quantity  $\nabla_{\mathbf{R}}^2 [\chi_{n,v}(\mathbf{R}) \psi_n(\mathbf{R}, \mathbf{r})]$  needed for the explicit calculation of  $T_L$ . We have

$$\begin{aligned} \nabla_{\mathbf{R}}^2 [\chi_{n,v}(\mathbf{R}) \psi_n(\mathbf{R}, \mathbf{r})] &= \psi_n(\mathbf{R}, \mathbf{r}) \nabla_{\mathbf{R}}^2 \chi_{n,v}(\mathbf{R}) + 2 \nabla_{\mathbf{R}} \psi_n(\mathbf{R}, \mathbf{r}) \cdot \nabla_{\mathbf{R}} \chi_{n,v}(\mathbf{R}) \\ &\quad + \chi_{n,v}(\mathbf{R}) \nabla_{\mathbf{R}}^2 \psi_n(\mathbf{R}, \mathbf{r}). \end{aligned} \quad (3-7)$$

Because of the smooth dependence of  $\psi_n(\mathbf{R}, \mathbf{r})$  on  $\mathbf{R}$ , the first term on the right hand side of eq. (3-7) is expected to be the dominant one, and we make the basic approximation of considering only this term. As a consequence of this assumption, the nuclear kinetic operator  $T_L$  can be written as

$$T_L [\chi_{n,v}(\mathbf{R}) \psi_n(\mathbf{R}, \mathbf{r})] \approx \psi_n(\mathbf{R}, \mathbf{r}) T_L \chi_{n,v}(\mathbf{R}). \quad (3-8)$$

Substituting (3-8) and (3-4) into the general equation (3-6) and dividing by  $\psi_n(\mathbf{R}, \mathbf{r})$ ,

$$[T_L + V_{LL} + E_n(\mathbf{R})] \chi_{n,v}(\mathbf{R}) = E_{n,v} \chi_{n,v}(\mathbf{R}). \quad (3-9)$$

Equations (3-4) and (3-9) are the fundamental equations of the adiabatic approximation. Equation (3-4) gives the energy values of the electronic states  $E_n(\mathbf{R})$  when the nuclei have fixed positions  $\mathbf{R}$ . These energy values then appear as a potential function in the eigenvalue equation for nuclear motion (3-9). In this way (3-4) and (3-9) permit a separate, though interdependent, calculation of the energy values of the electronic states and the lattice vibrational states. In some cases it is necessary to go outside this approximation and consider electron-lattice coupling by taking into account the second and third terms on the right hand side of eq. (3-7).

To determine the electronic states of crystals, we use only eq. (3-4) with the nuclei in their equilibrium positions.

### (ii) The one-electron approximation<sup>[2]</sup>

Equation (3-4) represents a very complicated many-body problem which our present mathematical knowledge cannot deal with. To simplify its solution, one uses the so-called one-electron approximation, which represents the electronic states of the whole crystal by "determinantal wave functions", antisymmetrized products of one-electron functions. A determinantal state is specified by giving the one-electron functions that enter the determinant. The variational principle shows that the best one-electron functions in the determinantal state satisfy the Hartree-Fock equations

$$H_{HF} \psi_n(\mathbf{r}) = E_n \psi_n(\mathbf{r}) \quad (3-10a)$$

with

$$H_{HF} = -\frac{\hbar^2 \nabla^2}{2m} - \sum_I \frac{Z_I e^2}{|\mathbf{r} - \mathbf{R}_I|} + V_{coul} + V_{exch} \quad (3-10b)$$

and

$$V_{coul}(\mathbf{r}) = e^2 \sum_J \int \frac{|\psi_J(\mathbf{r}_1)|^2}{|\mathbf{r} - \mathbf{r}_1|} d\mathbf{r}_1, \quad (3-10c)$$

$$V_{exch} \psi_n(\mathbf{r}) = -e^2 \sum_J \psi_J(\mathbf{r}) \int \frac{\psi_J^*(\mathbf{r}_1) \psi_n(\mathbf{r}_1)}{|\mathbf{r} - \mathbf{r}_1|} d\mathbf{r}_1. \quad (3-10d)$$

In (3-10) the integrations also imply summation over the spin variables.

The Hartree-Fock Hamiltonian operator  $H_{HF}$  of (3-10b) is a one-electron operator which depends on its own eigenfunctions, the functions of the determinantal state. The coulomb potential  $V_{coul}$  is a local potential since it is simply a product operator, whereas the exchange potential is non-local since it is an integral operator. To reduce mathematical difficulties one often approximates the exchange potential with a local potential along the lines suggested by Slater.<sup>[2]</sup>

It should be pointed out that the replacement of the many-body equation (3-4) by the one-electron Hartree-Fock equation (3-10) may be a poor approximation in certain types of problems. It is well known that one cannot obtain reliable results for the total ground state energy of atoms from the Hartree-Fock approximation. This approximation is known to be unreliable in the case of free electron gas also, and it has been shown that higher order corrections produce a screening of the exchange interaction by the other electrons of the system. It also seems likely that a better approximation

to (3-4) in crystals would require a "screened Hartree-Fock approximation" in which the coulomb interaction (3-10c) is left unchanged, but the exchange interaction (3-10d) is screened with an appropriate dielectric function.<sup>[2]</sup> By analogy with the results obtained for atoms and for free electron gas, we expect that the Hartree-Fock approximation or the screened Hartree-Fock approximation will reproduce the differences in energies of the electronic states of the system accurately enough, though the actual value of the energy of each state separately may be considerably inaccurate. In the last resort, only comparison with the experiment can test the approximations used. Since the optical constants are related to the energy differences of the electrons, they are expected to be interpreted accurately in the one-electron approximation. Other experimental data, such as the cohesive energy, involve the total ground state energy of the system and cannot be obtained accurately in this approximation.

### (iii) *The band approximation*

The solution of the self-consistent equation (3-10) is still a very difficult mathematical problem. For this reason one often adopts the band approximation, i.e. one solves the Schrödinger equation with an assumed crystal potential, hoping that such a potential is accurate enough to give meaningful results. The basic equation of the "band approximation" is then

$$\left[ -\frac{\hbar^2 \nabla^2}{2m} + V(\mathbf{r}) \right] \psi_n(\mathbf{k}, \mathbf{r}) = E_n(\mathbf{k}) \psi_n(\mathbf{k}, \mathbf{r}), \quad (3-11)$$

where the crystal potential  $V(\mathbf{r})$  is invariant for all symmetry operations of the space group described in Chapter 2. As an approximate crystal potential one usually considers a sum of atomic-like potentials derived from the self-consistent potentials for the free atoms. The physical quantities which depend strongly on the details of the potential are not expected to be given reliably by the band approximation, but the eigenvalues for the electronic states depend to a large extent on the symmetry properties of the lattice and are not very sensitive to small changes in the crystal potential. This seems to be the main reason why many calculations of electronic states are successful despite the approximations involved. In some electronic state calculations, mainly the more recent ones, attempts are made to achieve some degree of self-consistency by successively and iteratively recomputing the crystal potential from the electronic wave functions in the crystal.

There are two distinctly different though equivalent procedures for obtaining crystal states within the band approximation. On the one hand, one can expand the crystal states on a complete set of Bloch type functions and then determine the coefficients of the expansion by requiring that the crystal states satisfy the appropriate Schrödinger equation. On the other hand, one can expand the crystal states on a complete set of functions that are solutions of the Schrödinger equation within a unit cell, and then determine the coefficients of the expansion by requiring that the crystal states satisfy appropriate boundary conditions. Different methods of band calculations can be classified depending on which of the two above approaches is followed. The tight binding method, the orthogonalized plane wave method, and pseudopotential formalism are based on the first point of view, while the cellular method, the augmented plane wave method, and Green's function method, are based on the second. As a practical matter one has to choose, from physical considerations, the method whose set of basis functions is sufficiently close to the exact eigenfunctions, so that one can obtain meaningful results

with a small number of terms in the expansion. The availability of large computers and the full use of symmetry to simplify the calculations makes it possible in most practical cases to obtain accurate results within the stated approximations.

A band structure calculation is generally quite laborious. Semi-empirical approaches and interpolation schemes are often used as subsidiary tools for a band structure calculation. Semi-empirical approaches make use of experimental data to determine quantities difficult to compute *a priori*; among these, the semi-empirical pseudopotential approach and the quantum defect approach are particularly important. Interpolation schemes use the knowledge of the band structure at one or more values of  $\mathbf{k}$  to obtain the band structure throughout the Brillouin zone; of these methods, particular emphasis will be given to the  $\mathbf{k} \cdot \mathbf{p}$  interpolation procedure.

We will also consider relativistic effects. These can be inserted into the band approximation by using the Dirac equation instead of the Schrödinger equation with an assumed model potential. In the last few years the relativistic generalization of all methods for calculating band structures has been established.

### 3-2 The tight binding method

#### 3-2a Description of the method

We will first describe the tight binding method, originally suggested by Bloch<sup>[3]</sup> in 1928. The atomic orbitals of the atoms (or ions) inside the unit cell of a given crystal are used as the basic expansion set for the Bloch functions. This procedure, as we shall explain, is convenient only for low energy states.

We can always write the Bloch functions  $\psi_n(\mathbf{k}, \mathbf{r})$ , which are the solutions of eq.(3-11), in the form

$$\psi_n(\mathbf{k}, \mathbf{r}) = \frac{1}{\sqrt{N}} \sum_{\tau_v} e^{i\mathbf{k} \cdot \tau_v} a_n(\mathbf{r} - \tau_v), \quad (3-12)$$

where  $\tau_v$  indicates a lattice translation vector of type (2-1) and  $a_n(\mathbf{r} - \tau_v)$  indicate localized functions on each cell; these are called Wannier functions<sup>[4]</sup> and can be expressed in turn as

$$a_n(\mathbf{r} - \tau_v) = \frac{1}{\sqrt{N}} \sum_{\mathbf{k}} e^{-i\mathbf{k} \cdot \tau_v} \psi_n(\mathbf{k}, \mathbf{r}). \quad (3-13)$$

In (3-12) the sum is over the lattice translations of the crystal and in (3-13) the sum is over the wave vectors of the Brillouin zone;  $N$  indicates the number of unit cells of the crystal. It is easy to prove that the Wannier functions with different band indices  $n$  or different cell indices  $v$  are orthogonal:

$$\int a_n^*(\mathbf{r} - \tau_{v'}) a_n(\mathbf{r} - \tau_v) d\mathbf{r} = \delta_{nn'} \delta_{vv'}. \quad (3-14)$$

Let  $\varphi_{\mu\nu}(\mathbf{r} - \mathbf{d}_\mu)$  indicate the atomic orbital defined by quantum numbers  $v$  for an atom located in position  $\mathbf{d}_\mu$  of the unit cell. It is convenient to define, for any atomic orbital  $\varphi_{\mu\nu}(\mathbf{r} - \mathbf{d}_\mu)$ , the corresponding Bloch sum  $\Phi_{\mu\nu}(\mathbf{k}, \mathbf{r})$  of vector  $\mathbf{k}$ ,

$$\Phi_{\mu\nu}(\mathbf{k}, \mathbf{r}) = \frac{1}{\sqrt{N}} \sum_{\tau_v} e^{i\mathbf{k} \cdot \tau_v} \varphi_{\mu\nu}(\mathbf{r} - \mathbf{d}_\mu - \tau_v). \quad (3-15)$$

## ELECTRONIC STATES AND OPTICAL TRANSITIONS

Since in (3-12) we can always expand  $a_n$  as a linear combination of atomic orbitals (LCAOs), we can also express the crystal wave functions of wave vector  $\mathbf{k}$  as linear combinations of Bloch sums (3-15) with this same wave vector,

$$\psi_n(\mathbf{k}, \mathbf{r}) = \sum_{\mu\nu} c_{\mu\nu}(\mathbf{k}) \Phi_{\mu\nu}(\mathbf{k}, \mathbf{r}). \quad (3-16)$$

We can convert the one-electron Schrödinger equation (3-11) into a secular problem by minimizing the expectation value of the crystal Hamiltonian with respect to the coefficients  $c_{\mu\nu}$  of (3-16). It is directly shown that the coefficients  $c_{\mu\nu}(\mathbf{k})$  of the expansion (3-16) and the energies can then be obtained as the eigenvectors and eigenvalues of the matrix whose determinantal compatibility equation is

$$\| \langle \Phi_{\mu'\nu'}(\mathbf{k}, \mathbf{r}) | H - E | \Phi_{\mu\nu}(\mathbf{k}, \mathbf{r}) \rangle \| = 0, \quad (3-17)$$

$H = (\mathbf{p}^2/2m) + V(\mathbf{r})$  being the crystal Hamiltonian.

This procedure is useful in those cases for which only a small number of terms are important in the expansion (3-16), and the corresponding determinant (3-17) can be solved. This applies to atomic orbitals of low energy for which the wave functions are well localized near the nucleus and are expected to change very little when atoms are joined to form the crystal. In fact, these states are very close to being eigenfunctions of the crystal Hamiltonian, since the difference between the crystal and the atomic potential is nearly constant in the small region into which the wave functions extend. Corresponding to each inner atomic orbital, we obtain for the crystal a very narrow energy band  $E_n(\mathbf{k})$  and eigenfunctions which coincide with the Bloch sum (3-15). Such crystal states are called "core states".

To illustrate the criterion used in choosing the expansion functions, we consider the case of layer compound graphite made up of hexagons of carbon atoms. The graphite layer structure has two atoms per unit cell, as will be shown in detail in Chapter 4. The atomic configuration of the ground state of the carbon atom is  $1s^2, 2s^2, 2p^2$ . The energies of the states  $1s, 2s, 2p$  are  $-21.37, -1.29, -0.66$  Rydberg respectively. The lowest energy bands of the crystal can be obtained by solving a secular problem limited to the ten Bloch sums, which are obtained from the atomic orbitals  $1s, 2s, 2p_x, 2p_y, 2p_z$  of the two atoms in the unit cell. In practice, one usually ignores the mixing of Bloch sums derived from  $1s$  states with those derived from  $2s$  and  $2p$  states because of the large differences in atomic energies. Corresponding to the  $1s$  carbon orbitals, for every  $\mathbf{k}$  vector we have two crystal core states which can accommodate four core electrons per unit cell. Higher energy bands are obtained by considering the eight Bloch sums built up from the atomic orbitals  $2s$  and  $2p$ ; the eight valence electrons will occupy half of these bands, leaving the others as empty conduction states.

### 3-2b Matrix elements of the secular equation appearing in the tight binding method

We now consider how to compute the matrix elements of the tight binding secular equation (3-17). Let us first consider the overlap integrals between two Bloch sums. We have

$$\begin{aligned} \langle \Phi_{\mu'\nu'}(\mathbf{k}, \mathbf{r}) | \Phi_{\mu\nu}(\mathbf{k}, \mathbf{r}) \rangle &= \frac{1}{N} \sum_{\tau_\nu \tau_{\nu'}} e^{i\mathbf{k} \cdot (\tau_\nu - \tau_{\nu'})} \int \varphi_{\mu'\nu'}^*(\mathbf{r} - \mathbf{d}_{\mu'} - \tau_{\nu'}) \varphi_{\mu\nu}(\mathbf{r} - \mathbf{d}_\mu - \tau_\nu) d\mathbf{r} \\ &= \sum_{\tau_\nu} e^{i\mathbf{k} \cdot \tau_\nu} \int \varphi_{\mu'\nu'}^*(\mathbf{r} - \mathbf{d}_{\mu'}) \varphi_{\mu\nu}(\mathbf{r} - \mathbf{d}_\mu - \tau_\nu) d\mathbf{r}, \end{aligned} \quad (3-18)$$

## METHODS OF CALCULATING THE ELECTRONIC BAND STRUCTURES OF CRYSTALS

where the summation over  $\tau_s$  cancels the factor  $(1/N)$ . Since the atomic functions are localized, the overlap between them decreases sharply with increasing distance, and one can limit the sum in eq. (3-18) to a given order of neighbours. The integrals on the same centre which appear in (3-18) are immediately seen to be one or zero because of the properties of atomic orbitals. The two-centre integrals appearing in (3-18) can be expressed in terms of a small number of independent integrals, as shown by Slater and Koster.<sup>[5]</sup> Let us consider two-centre integrals of the type

$$\int \varphi_{\mu'n'l'm'}^*(\mathbf{r}) \varphi_{\mu n l m}(\mathbf{r} - \mathbf{R}) d\mathbf{r}, \quad (3-19)$$

where  $\mathbf{R}$  is the relative distance between the centres, and  $n'l'm'$ ,  $nlm$  are the quantum numbers of the atomic orbitals. We consider first the case where  $\mathbf{R}$  is along the quantization axis. The integral (3-19) is then non-zero only if  $m = m'$ , because of cylindrical symmetry. Furthermore, changing the sign of  $m$  and  $m'$  does not change the integral because of time reversal symmetry. The independent integrals are labelled with the symbols  $\sigma$ ,  $\pi$ ,  $\delta$ , etc., corresponding to the values  $m = 0, \pm 1, \pm 2$ , etc., respectively. For instance, the overlap integrals between two  $s$  functions can be expressed in terms of one independent integral  $S(ss\sigma)$ ; the overlap integrals between an  $s$  function and a  $p$  function can be expressed in terms of one independent integral  $S(sp\sigma)$ , and the overlap integrals between two  $p$  functions can be expressed in terms of two independent integrals  $S(pp\sigma)$  and  $S(pp\pi)$ , etc.

In the general case in which the vector  $\mathbf{R}$  has direction cosines  $l_x, l_y, l_z$  with respect to the axis  $x, y, z$ , the overlap integral (3-19) can be expressed directly in terms of the independent integrals previously discussed. In Table 3-1 we list the expressions for two-

TABLE 3-1. Expressions of two-centre integrals involving  $s, p_x, p_y, p_z$  atomic orbitals

The other expressions of interest are obtained by cyclically permutating  $x, y, z$ , and  $l_x, l_y, l_z$ . Expressions of two-centre integrals for  $d$  and  $f$  atomic orbitals can be found in ref. [5]

$\langle s s \rangle$	$S(ss\sigma)$
$\langle s p_x \rangle$	$l_x S(sp\sigma)$
$\langle p_x p_x \rangle$	$l_x^2 S(pp\sigma) + (1 - l_x^2) S(pp\pi)$
$\langle p_x p_y \rangle$	$l_x l_y S(pp\sigma) - l_x l_y S(pp\pi)$
$\langle p_x p_z \rangle$	$l_x l_z S(pp\sigma) - l_x l_z S(pp\pi)$

BIBLIOTHÈQUE  
 DÉPARTEMENT DE PHYSIQUE  
 Ecole Polytechnique Fédérale  
 CH-1015 LAUSANNE Suisse  
 Tél. 021-471111

centre integrals involving  $s$  and  $p_x, p_y, p_z$  atomic functions as given by Slater and Koster<sup>[5]</sup>. Two-centre integrals between atomic functions with higher angular momenta can be treated in a similar way.<sup>[5]</sup> With the results thus established, the overlap integrals (3-19) can be expressed in terms of a small number of independent integrals, the expressions depending on the positions of neighbouring atoms as given by the symmetry of the lattice.

We next consider the matrix elements of the crystal Hamiltonian. We can write the Hamiltonian of the crystal in the form

$$H = \frac{\mathbf{p}^2}{2m} + V(\mathbf{r}) = \frac{\mathbf{p}^2}{2m} + \sum_{\tau_\nu} \sum_{\mathbf{d}_\mu} V_\mu(\mathbf{r} - \mathbf{d}_\mu - \tau_\nu), \quad (3-20)$$

## ELECTRONIC STATES AND OPTICAL TRANSITIONS

where the vectors  $\mathbf{d}_\mu + \boldsymbol{\tau}_v$  describe the positions of the atoms and  $V_\mu(\mathbf{r} - \mathbf{d}_\mu - \boldsymbol{\tau}_v)$  represents the corresponding atomic-like potential. We have

$$\begin{aligned} \langle \Phi_{\mu'v'}(\mathbf{k}, \mathbf{r}) | H | \Phi_{\mu v}(\mathbf{k}, \mathbf{r}) \rangle &= E_{\mu'v'} \langle \Phi_{\mu'v'}(\mathbf{k}, \mathbf{r}) | \Phi_{\mu v}(\mathbf{k}, \mathbf{r}) \rangle \\ &+ \sum_{\boldsymbol{\tau}_v} e^{i\mathbf{k} \cdot \boldsymbol{\tau}_v} \int \varphi_{\mu'v'}^*(\mathbf{r} - \mathbf{d}_{\mu'}) V'(\mathbf{r}) \varphi_{\mu v}(\mathbf{r} - \mathbf{d}_\mu - \boldsymbol{\tau}_v) d\mathbf{r}, \end{aligned} \quad (3-21)$$

where  $V'(\mathbf{r}) = V(\mathbf{r}) - V_{\mu'}(\mathbf{r} - \mathbf{d}_{\mu'})$  and use has been made of the fact that the atomic orbitals  $\varphi_{\mu'v'}$  satisfy the relation

$$\left[ \frac{\mathbf{p}^2}{2m} + V_{\mu'}(\mathbf{r} - \mathbf{d}_{\mu'}) \right] \varphi_{\mu'v'}(\mathbf{r} - \mathbf{d}_{\mu'}) = E_{\mu'v'} \varphi_{\mu'v'}(\mathbf{r} - \mathbf{d}_{\mu'}). \quad (3-21)$$

The first expression on the right hand side of (3-21) can be calculated using (3-18). The second expression contains two- and three-centre integrals. The two-centre integrals have the form

$$\int \varphi_{\mu'n'l'm'}^*(\mathbf{r}) V_\mu(\mathbf{r} - \mathbf{R}) \varphi_{\mu n l m}(\mathbf{r} - \mathbf{R}) d\mathbf{r}, \quad (3-22)$$

where  $\mathbf{R}$  is the relative distance between the centres. Because of the spherical symmetry of the atomic-like potential, the two-centre integrals (3-22) can be expressed in terms of a small number of independent integrals using the same techniques as those applied to the case of overlap integrals (3-19). Three-centre integrals can be evaluated in a similar way, though the computational techniques are somewhat more complicated. Lafon *et al.*<sup>[6]</sup> have shown how to compute multicentre integrals if one adopts simple analytic forms for the potential; Ellis and Painter<sup>[7]</sup> have developed a discrete variational method for their computation. In many cases, however, three-centre integrals are neglected because, in the tight binding limit, they are at least one order of magnitude smaller than two-centre integrals.

In the tight binding method, the eigenvalues are the zeros of the secular determinant (3-17). For the special case of a unique Bloch function  $\Phi_{\mu v}(\mathbf{k}, \mathbf{r})$  we obtain the following expression for the corresponding crystal states:

$$\begin{aligned} E(\mathbf{k}) &= \frac{\langle \Phi_{\mu v}(\mathbf{k}, \mathbf{r}) | H | \Phi_{\mu v}(\mathbf{k}, \mathbf{r}) \rangle}{\langle \Phi_{\mu v}(\mathbf{k}, \mathbf{r}) | \Phi_{\mu v}(\mathbf{k}, \mathbf{r}) \rangle} \\ &= E_{\mu v} + \frac{\sum_{\boldsymbol{\tau}_v} e^{i\mathbf{k} \cdot \boldsymbol{\tau}_v} \int \varphi_{\mu v}^*(\mathbf{r} - \mathbf{d}_\mu) V'(\mathbf{r}) \varphi_{\mu v}(\mathbf{r} - \mathbf{d}_\mu - \boldsymbol{\tau}_v) d\mathbf{r}}{\sum_{\boldsymbol{\tau}_v} e^{i\mathbf{k} \cdot \boldsymbol{\tau}_v} \int \varphi_{\mu v}^*(\mathbf{r} - \mathbf{d}_\mu) \varphi_{\mu v}(\mathbf{r} - \mathbf{d}_\mu - \boldsymbol{\tau}_v) d\mathbf{r}} \end{aligned} \quad (3-23)$$

In the case of core states we can ignore in (3-23) the overlap and potential integrals between atomic functions centred on different atoms; this is equivalent to considering only terms with  $\boldsymbol{\tau}_v = 0$  in the summation. The energy in this case does not depend explicitly on  $\mathbf{k}$ , and we obtain for the core states

$$E_c = E_{\mu v} + \int |\varphi_{\mu v}(\mathbf{r} - \mathbf{d}_\mu)|^2 V'(\mathbf{r}) d\mathbf{r}. \quad (3-24)$$

The second term on the right hand side of (3-24) is the so-called crystal field integral; it gives the splittings and the shifts of the core energy states from the corresponding states of the free atom, due to the potential of the other atoms of the lattice. Expression

(3-24) would also give, to the first order of perturbation theory, the energy of a foreign impurity state in a lattice as discussed in Chapter 7. When the terms with  $\tau_s \neq 0$  cannot be neglected, (3-23) gives a spreading of each atomic level into a corresponding energy band. More generally, we require mixing between different atomic functions to obtain the crystal eigenstates.

### 3-2c Symmetrized combinations of Bloch sums

The secular equation (3-17) of the tight binding approach can be simplified at high symmetry points of the Brillouin zone by taking symmetry-adapted Bloch sums as basis functions. We recall (Section 2-2) that, for a given  $\mathbf{k}$  vector, the eigenvalues can be classified according to the irreducible representations of the little group of vector  $\mathbf{k}$ . In order to use the standard methods of group theory, we consider the transformation properties of a Bloch sum (3-15) under an operation of the space group. We obtain

$$\begin{aligned} O_{\{R|\mathbf{a}\}} \Phi_{\mu\nu}(\mathbf{k}, \mathbf{r}) &= \Phi_{\mu\nu}(\mathbf{k}, R^{-1}\mathbf{r} - R^{-1}\mathbf{a}) \\ &= \frac{1}{\sqrt{N}} \sum_{\tau_s} e^{i\mathbf{k} \cdot \tau_s} \varphi_{\mu\nu}[R^{-1}(\mathbf{r} - \{R|\mathbf{a}\} \mathbf{d}_\mu - R\tau_s)]. \end{aligned} \quad (3-25)$$

Since  $\{R|\mathbf{a}\}$  is a symmetry operation, we have

$$\{R|\mathbf{a}\} \mathbf{d}_\mu = \mathbf{d}_{\mu'} + \tau',$$

where  $\mathbf{d}_{\mu'}$  is a vector defining the position of an atom in the unit cell (and may coincide with  $\mathbf{d}_\mu$ ) and  $\tau'$  is a suitable translation vector (including zero). Furthermore, the positions  $\mathbf{d}_\mu$  and  $\mathbf{d}_{\mu'}$  in the unit cell are occupied by the same type of atom. Equation (3-25) then becomes

$$O_{\{R|\mathbf{a}\}} \Phi_{\mu\nu}(\mathbf{k}, \mathbf{r}) = e^{-iR\mathbf{k} \cdot \tau'} \frac{1}{\sqrt{N}} \sum_{\tau_s} e^{iR\mathbf{k} \cdot (\tau_s + \tau')} \varphi_{\mu\nu}[R^{-1}(\mathbf{r} - \mathbf{d}_{\mu'} - \tau' - R\tau_s)].$$

Making use of the fact that  $R_k \mathbf{k} = \mathbf{k} + \mathbf{h}$  and that  $R\tau_s + \tau'$  is still a translation, we obtain for the symmetry operations of the little group of  $\mathbf{k}$ :

$$O_{\{R_k|\mathbf{a}\}} \Phi_{\mu\nu}(\mathbf{k}, \mathbf{r}) = e^{-i\mathbf{k} \cdot \tau'} \frac{1}{\sqrt{N}} \sum_{\tau_s} e^{i\mathbf{k} \cdot \tau_s} \varphi_{\mu\nu}[R_k^{-1}(\mathbf{r} - \mathbf{d}_{\mu'} - \tau_s)]. \quad (3-26)$$

This shows that Bloch sums of a given  $\mathbf{k}$  vector, derived from degenerate atomic states, form a basis for the little group of vector  $\mathbf{k}$ . Symmetrized combinations of Bloch sums\* can be obtained by applying projection operations and by using the standard methods of group theory described in Chapter 1. The secular equation of the tight binding approach can thus be factorized into a number of determinantal equations obtained by considering in the expansion (3-16) only those basis functions which belong to the same row of the same irreducible representation.

The use of group theory both to obtain symmetrized combinations of Bloch sums and to express the matrix elements as functions of a few parameters gives some insight into the sequence of the energy levels of the crystal without performing detailed cal-

\* Note that at any  $\mathbf{k}$  vector the phonon states (we shall discuss them in Section 5-4) have the symmetry of the symmetrized combinations of Bloch sums derived from  $p$  orbitals centred on the atomic positions in the unit cell.

## ELECTRONIC STATES AND OPTICAL TRANSITIONS

culations. The sequence can be determined by relating a crystal state of a given symmetry to the atomic states of the same symmetry and by estimating the corrections due to the crystal field and to the two-centre overlap and potential integrals. Usually it is convenient to perform this analysis at  $\mathbf{k} = 0$ . At other symmetry points, similar considerations and compatibility relations (see Section 2-2) give information on the expected sequence of the levels.

### 3-2d Discussion of the tight binding method

We have already remarked that the tight binding method is expected to give reliable results only for bands originating from well-localized atomic states. The main criticism of the method when applied to valence and conduction states lies in the fact that it is difficult to test its convergence. In principle, this could be done by adding more and more atomic states in the expansion (3-16) and studying the stability of the lower eigenvalues. However, excited states for atoms extend over a large number of neighbours, and in fact they have a continuous spectrum above the ionization energy. Even ignoring the problem of convergence, there may be difficulties associated with the high sensitivity of some matrix elements to the crystal potential. From eq. (3-21) we can see that the diagonal matrix elements of the crystal Hamiltonian contain integrals of the type

$$\int |\varphi_{\mu\nu}(\mathbf{r} - \mathbf{d}_\mu)|^2 V'(\mathbf{r}) d\mathbf{r}$$

referred to as crystal field integrals. *Ab initio* calculations of these parameters depend very critically on the tail of the atomic-like potentials, which are expected to be different from the potentials of free atoms. Bassani *et al.*<sup>[8]</sup> have shown how to overcome this difficulty, at least in the case of AgCl and AgBr, by correcting the exchange part of the atomic potentials with a density dependent screening factor.

Another difficulty arises when the atomic wave functions are extended as compared with the lattice constant, so that the overlap matrix elements between nearest atoms are very large. In this case, the higher eigenvalues may be so sensitive to them as to be unreliable. This difficulty is a more fundamental one and limits the applicability of the method. We also want to mention a possible modification of the tight binding approach which should greatly improve the reliability of the results in those cases where it has some applicability. This modification has been suggested by Gilbert<sup>[9]</sup> as a result of a detailed study of the Hartree-Fock method in crystals. Instead of using atomic orbitals in the expansion (3-16), one could use a different type (distorted orbitals), given as solutions of the Schrödinger equation for a given atom, but with a potential that allows for other atoms of the lattice. Such basis orbitals have the symmetry of the lattice and may be significantly different from the original atomic orbitals in their behaviour far from the nucleus. The same formalism as that of the previous sections applies, but the crystal potential and distorted orbitals should be computed self-consistently. Since distorted orbitals will be less extended in the direction of the bonds than the simple atomic orbitals, a consequent improvement of the reliability of the computed matrix elements is expected.

When the results of first principles calculations are not reliable, one can adopt the interpolation scheme suggested by Slater and Koster.<sup>[5]</sup> In such a scheme, three-centre integrals are ignored and all matrix elements are expressed in terms of independent two-centre integrals involving a given number of neighbours (usually the nearest and

next-nearest neighbours). When the theoretical values of the integrals are not completely reliable, for the reasons we have discussed, one can allow variations from their computed values in order to fit experimental data or theoretical results obtained using different methods of calculation. In a simple way, such an interpolation scheme relates the states of the atoms to the states of the crystal, and in some cases has proved useful in giving a semiquantitative picture of the band structure of crystals.

Finally, we mention briefly a generalization of the tight binding approach that is convenient for treating molecular crystals, i.e. crystals made up of an ensemble of weakly interacting molecules. In this case it is convenient to consider as an expansion set the Bloch sums obtained from molecular orbitals. This approach is equivalent to the tight binding method with atomic orbitals, and is preferable when a small number of basis functions can be considered.<sup>[10]</sup>

### 3-3 The orthogonalized plane wave method

#### 3-3a Description of the method

Plane waves appear to provide a simple and convenient set of basis functions for the expansion of crystal states. The choice of plane waves as basis functions was suggested by Sommerfeld and Bethe<sup>[11]</sup> (1933).

Since a Bloch function  $\psi(\mathbf{k}, \mathbf{r})$  belongs to the representation  $\mathbf{k}$  of the translation group, it can be expanded in plane waves of vectors  $\mathbf{k} + \mathbf{h}_j$ , where  $\mathbf{h}_j$  indicates a reciprocal lattice vector. We may write

$$\psi(\mathbf{k}, \mathbf{r}) = \sum_j a_j(\mathbf{k}) \frac{1}{\sqrt{N\Omega}} e^{i(\mathbf{k} + \mathbf{h}_j) \cdot \mathbf{r}} \quad (3-27)$$

where  $\Omega$  is the volume of the unit cell. If we substitute expression (3-27) into the expectation value of the crystal Hamiltonian and minimize it with respect to the expansion parameters  $a_j(\mathbf{k})$ , we immediately find that the coefficients  $a_j(\mathbf{k})$  of expansion (3-27) and the energies  $E(\mathbf{k})$  are given by the eigenvectors and eigenvalues of the determinantal equation

$$\| \langle W_{\mathbf{k}_i} | H - E | W_{\mathbf{k}_j} \rangle \| = 0, \quad (3-28)$$

where

$$W_{\mathbf{k}_j} = \frac{1}{\sqrt{N\Omega}} e^{i(\mathbf{k} + \mathbf{h}_j) \cdot \mathbf{r}}.$$

Physical considerations indicate that a simple expansion in plane waves is impractical because of its slow convergence. In fact, if we set up the secular equation using  $n$  plane waves, then as  $n \rightarrow \infty$  the lowest root of the secular equation approaches the energy of the lowest core state of the crystal whose wave function closely coincides with that of an atomic orbital. A large number of plane waves is needed, however, to describe crystal states originating from strongly localized atomic orbitals. (In the limiting case of the expansion of function  $\delta(\mathbf{r})$ , all plane waves appear with the same coefficient.) Thus the determinants (3-28) do not converge quickly enough to the exact solutions for the lowest energy states, and the variational principle implies that the results obtained for higher energy states are consequently not reliable either.

Herring<sup>[11]</sup> (1940) suggested the way to overcome this fundamental difficulty by using at the outset the information already known about the core states. The wave

functions and eigenvalues of the core states are assumed to be given by the tight binding approximation of the previous section. The crystal states of higher energy (valence and conduction states) must be orthogonal to the core states because they are eigenfunctions of the same crystal Hamiltonian and can be expanded in plane waves orthogonalized to the core states. Given a plane wave  $W(\mathbf{k}_j, \mathbf{r})$  of vector  $\mathbf{k}_j = \mathbf{k} + \mathbf{h}_j$ , we consider the orthogonalized plane wave (OPW)  $\chi(\mathbf{k}_j, \mathbf{r})$  defined as

$$\chi(\mathbf{k}_j, \mathbf{r}) = W(\mathbf{k}_j, \mathbf{r}) - \sum_c \langle \psi_c | W_{\mathbf{k}_j} \rangle \psi_c, \quad (3-29)$$

where the Schmidt procedure has been used to orthogonalize the plane waves to the core functions  $\psi_c(\mathbf{k}, \mathbf{r})$  of type (3-15). A valence or conduction function  $\psi_v(\mathbf{k}, \mathbf{r})$  of vector  $\mathbf{k}$  can be expanded in the form

$$\psi_v(\mathbf{k}, \mathbf{r}) = \sum_j a_j(\mathbf{k}) \chi(\mathbf{k}_j, \mathbf{r}). \quad (3-30)$$

By substituting expansion (3-30) into the Schrödinger equation, or equivalently by making use of the variational principle, we obtain for the eigenvalues the determinantal compatibility equation

$$\| \langle \chi_{\mathbf{k}_i} | H - E | \chi_{\mathbf{k}_j} \rangle \| = 0, \quad (3-31)$$

where  $\chi(\mathbf{k}, \mathbf{r})$  is denoted by  $\chi_{\mathbf{k}}$  for brevity.

Matrix equation (3-31) has the advantage over the matrix equation (3-28) in that it gives only the eigenvalues of the valence and conduction states, since the basis functions of the expansion (3-30) are automatically orthogonal to the core states. If we set up the secular equation using  $n$  OPWs, then for  $n \rightarrow \infty$  the lowest root of the secular equation approaches the energy of the lowest valence state, and a reasonably rapid convergence is expected.

### 3-3 b Matrix elements of the secular equation appearing in the OPW method

We now show how the matrix elements of the determinant equation (3-31) can be evaluated. Their explicit form is

$$\langle \chi_{\mathbf{k}_i} | H - E | \chi_{\mathbf{k}_j} \rangle = \langle W_{\mathbf{k}_i} | H - E | W_{\mathbf{k}_j} \rangle + \sum_c (E - E_c) \langle \psi_c | W_{\mathbf{k}_j} \rangle \langle W_{\mathbf{k}_i} | \psi_c \rangle, \quad (3-32a)$$

where use has been made of (3-29) and of the fact that  $\psi_c$  is an eigenfunction of  $H$  with eigenvalue  $E_c$ . Using expression (3-20) for the crystal Hamiltonian, the first term on the right hand side of (3-32a) becomes

$$\langle W_{\mathbf{k}_i} | H - E | W_{\mathbf{k}_j} \rangle = \left( \frac{\hbar^2 \mathbf{k}_i^2}{2m} - E \right) \delta_{ij} + \left\langle W_{\mathbf{k}_i} \left| \sum_{\tau_v} \sum_{\mathbf{d}_{\mu}} V_{\mu}(\mathbf{r} - \mathbf{d}_{\mu} - \boldsymbol{\tau}_v) \right| W_{\mathbf{k}_j} \right\rangle,$$

which can be further simplified by adopting a local expression for the atomic-like potential  $V_{\mu}(\mathbf{r})$  and considering its Fourier transform

$$V_{\mu}(\mathbf{h}_i - \mathbf{h}_j) = V_{\mu}(|\mathbf{h}_i - \mathbf{h}_j|) = \int e^{-i(\mathbf{h}_i - \mathbf{h}_j) \cdot \mathbf{r}} \tilde{V}_{\mu}(\mathbf{r}) d\mathbf{r}.$$

We obtain

$$\langle W_{\mathbf{k}_i} | H - E | W_{\mathbf{k}_j} \rangle = \left( \frac{\hbar^2 \mathbf{k}_i^2}{2m} - E \right) \delta_{ij} + \frac{1}{Q} \sum_{\mathbf{d}_{\mu}} e^{-i(\mathbf{h}_i - \mathbf{h}_j) \cdot \mathbf{d}_{\mu}} V_{\mu}(\mathbf{h}_i - \mathbf{h}_j). \quad (3-32b)$$

## METHODS OF CALCULATING THE ELECTRONIC BAND STRUCTURES OF CRYSTALS

To compute the second term in (3-32a) we must calculate the orthogonality coefficients between plane waves and core states. Let

$$\psi_c(\mathbf{k}, \mathbf{r}) = \frac{1}{\sqrt{N}} \sum_{\tau_v} e^{i\mathbf{k} \cdot \tau_v} \varphi_{\mu nlm}(\mathbf{r} - \mathbf{d}_\mu - \tau_v)$$

indicate the core state derived from the atomic function

$$\varphi_{\mu nlm}(\mathbf{r}) = R_{\mu nl}(r) Y_{lm}(\theta, \varphi),$$

with radial function  $R_{\mu nl}(r)$  and angular dependence given by the spherical harmonic  $Y_{lm}(\theta, \varphi)$ . We obtain for  $\langle \psi_c | W_{k_j} \rangle$  the expression

$$\begin{aligned} \langle \psi_c | W_{k_j} \rangle &= \frac{1}{N\sqrt{\Omega}} \sum_{\tau_v} \int e^{-i\mathbf{k} \cdot \tau_v} \varphi_{\mu nlm}^*(\mathbf{r} - \mathbf{d}_\mu - \tau_v) e^{i(\mathbf{k} + \mathbf{h}_j) \cdot \mathbf{r}} d\mathbf{r} \\ &= \frac{1}{N\sqrt{\Omega}} e^{i(\mathbf{k} + \mathbf{h}_j) \cdot \mathbf{d}_\mu} \sum_{\tau_v} \int e^{i(\mathbf{k} + \mathbf{h}_j) \cdot (\mathbf{r} - \mathbf{d}_\mu - \tau_v)} \varphi_{\mu nlm}^*(\mathbf{r} - \mathbf{d}_\mu - \tau_v) d\mathbf{r} \\ &= \frac{1}{\sqrt{\Omega}} e^{i(\mathbf{k} + \mathbf{h}_j) \cdot \mathbf{d}_\mu} \int e^{i(\mathbf{k} + \mathbf{h}_j) \cdot \mathbf{r}} R_{\mu nl}^*(r) Y_{lm}^*(\theta, \varphi) dr. \end{aligned}$$

The integral in the above equation can be computed by expanding the plane wave  $e^{i\mathbf{k}_j \cdot \mathbf{r}}$  in spherical harmonics

$$e^{i\mathbf{k}_j \cdot \mathbf{r}} = 4\pi \sum_{l'=0}^{\infty} \sum_{m'=-l'}^{l'} i^{l'} j_{l'}(k_j r) Y_{l'm'}(\theta, \varphi) Y_{l'm'}^*(\theta_{k_j}, \varphi_{k_j}),$$

where  $\theta, \varphi$  and  $\theta_{k_j}, \varphi_{k_j}$  are the polar angles of  $\mathbf{r}$  and  $\mathbf{k}_j$ , respectively, and  $j_{l'}$  is the spherical Bessel function. We obtain

$$\int e^{i\mathbf{k}_j \cdot \mathbf{r}} R_{\mu nl}^*(r) Y_{lm}^*(\theta, \varphi) dr = 4\pi Y_{lm}^*(\theta_{k_j}, \varphi_{k_j}) i^l \int_0^\infty R_{\mu nl}^*(r) j_l(k_j r) r^2 dr.$$

The orthogonality coefficients, denoted by  $A_{\mu nl}(k_j)$  are given by

$$A_{\mu nl}(k_j) = i^l \left[ \frac{4\pi(2l+1)}{\Omega} \right]^{1/2} \int_0^\infty R_{\mu nl}^*(r) j_l(k_j r) r^2 dr,$$

and we obtain the final result

$$\langle \psi_c | W_{k_j} \rangle = \left( \frac{4\pi}{2l+1} \right)^{1/2} e^{i(\mathbf{k} + \mathbf{h}_j) \cdot \mathbf{d}_\mu} Y_{lm}^*(\theta_{k_j}, \varphi_{k_j}) A_{\mu nl}(k_j). \quad (3-32c)$$

With the use of (3-32b) and (3-32c), the matrix element (3-32a) of the OPW method can now be explicitly computed from the Fourier transforms of the atomic-like potential and from the orthogonality coefficients.

### 3-3c Use of crystal symmetry in the OPW method

The secular equation (3-31) of the OPW method can be simplified at high symmetry  $\mathbf{k}$  vectors using standard group theory procedures. For this purpose, let us consider the transformation properties of plane waves of vector  $\mathbf{k} + \mathbf{h}_l$  under symmetry oper-

ations

$$O_{\{R|a\}} \frac{1}{\sqrt{N\Omega}} e^{i(\mathbf{k} + \mathbf{h}_j) \cdot \mathbf{r}} = \frac{1}{\sqrt{N\Omega}} e^{i(\mathbf{k} + \mathbf{h}_j) \cdot (R^{-1}\mathbf{r} - R^{-1}\mathbf{a})} = e^{-iR(\mathbf{k} + \mathbf{h}_j) \cdot \mathbf{a}} \frac{1}{\sqrt{N\Omega}} e^{iR(\mathbf{k} + \mathbf{h}_j) \cdot \mathbf{r}}.$$

Since  $R$  is a unitary matrix and does not change the length of a vector, the plane waves with a given modulus  $|\mathbf{k} + \mathbf{h}_j|$  constitute a basis for a representation of the little group of vector  $\mathbf{k}$ . The symmetrized combinations  $S_i^{(\alpha)}$  of plane waves which are partner functions for irreducible representations of the group of  $\mathbf{k}$  can then be obtained by the standard procedures of Section 1-3b. The symmetry-adapted combinations  $\psi_c^{(\alpha)}(\mathbf{k}, \mathbf{r})$  of core states can also be obtained as described in Section 3-2c. The symmetrized combinations  $\chi_i^{(\alpha)}(\mathbf{k}, \mathbf{r})$  of orthogonalized plane waves are then given by

$$\chi_i^{(\alpha)}(\mathbf{k}, \mathbf{r}) = S_i^{(\alpha)}(\mathbf{k}, \mathbf{r}) - \sum_c \langle \psi_c^{(\alpha)} | S_i^{(\alpha)} \rangle \psi_c^{(\alpha)}.$$

Consequently the secular equation of the OPW method can be factorized into a number of determinantal equations obtained by considering in the expansion (3-30) only basis functions with the same symmetry. Matrix elements of  $H$  between symmetrized combinations of OPWs can be set up explicitly because we have seen in Section 3-3b how to compute matrix elements between two OPWs, and group theory determines coefficients with which an OPW appears in a symmetrized combination.

### 3-3d Discussion of the OPW method<sup>[12]</sup>

The OPW method has been widely applied to determine valence and conduction states of a large number of crystals, such as group IV semiconductors, group III-V semiconductors, alkali halides, rare gas solids, etc.

A rewarding feature of the OPW method is the possibility it gives of testing the convergence of the method. The standard procedure is to consider all OPWs (or symmetrized combinations of OPWs) with wave vectors up to a given value, and to solve the secular determinant; one then adds a few more OPWs (or symmetrized combinations of OPWs), repeats the procedure, and compares the lowest eigenvalues with the previous ones. This process of adding more OPWs is stopped when the eigenvalues in the energy range of interest are stable. In general, a reasonable number of OPWs (varying from several to a few hundred) is sufficient to give a satisfactory convergence. The use of symmetrized combinations of OPWs remarkably simplifies the determinantal problem. The satisfactory convergence of the method can be seen from the fact that the OPWs used in the expansion (3-30) behave like atomic functions near the nuclei and like plane waves far from the nuclei, and this is the expected behaviour of the crystal wave functions. From a mathematical point of view, the convergence of the method can be seen from the fact that, when the values of the momentum transfer  $|\mathbf{h}_i - \mathbf{h}_j|$  are large, the terms arising from the orthogonalization to the core states tend to cancel the terms due to the Fourier transforms of the crystal potential, thus decreasing the values of the off-diagonal matrix elements.

In the OPW method, the quantities more sensitive to the tails of atomic potentials are the energies  $E_c$  of the core states, given by expression (3-24) and the Fourier transform  $V(0)$  of the crystal potential  $V(\mathbf{r})$ , i.e. the space average of  $V(\mathbf{r})$ . However, a change of  $V(0)$  and core energies  $E_c$  by the same amount would result in a rigid shift of all crystal states, as can be seen from (3-32). For this reason, in some calculations, one prefers to assume as core energies the energy of the corresponding atomic states

and then to fix the relative position of valence and conduction states by regarding  $V(0)$  as a disposable parameter in fitting some experimental data such as the energy gap. The other Fourier transforms of the potential are less affected by the tail of the atomic-like potentials because of the oscillatory character of  $e^{i\mathbf{h}\cdot\mathbf{r}}$  when  $\mathbf{h} \neq 0$ .

The OPW method assumes that the crystal core wave functions are the same as the corresponding wave functions of the atomic states. In the cases in which Bloch sums derived from atomic core states are not accurate eigenfunctions of the crystal Hamiltonian, the convergence of the OPW method to the valence states becomes questionable. In such cases the crystal core wave functions should be recomputed with the crystal potential, but this poses a very complicated self-consistency problem.

Another difficulty of the OPW method is that it requires the separation of the energy levels of the crystal into core states and valence and conduction states. Core states are assumed to be well-localized spatially in the unit cell and well-separated in energy from valence states. In several practical cases there may exist difficulties in setting up such a separation. This happens, for instance, in the case of crystals containing atoms with incomplete  $d$  shells. The energies of atomic  $d$  states, in fact, are not very different from those of  $s$  or  $p$  atomic states with the same principal quantum number, so that  $d$  wave functions cannot be included among core states. On the other hand,  $d$  states are in general well-localized around the nucleus, so that a large number of plane waves would be required to reproduce them. For such situations, the OPW method is not expected to give rapid convergence.

A modification of the OPW method to overcome the basic difficulties concerning core states and the separation of the energy levels between core states and valence and conduction states has been proposed by Kunz<sup>[13]</sup> (1969). Kunz suggests an expansion of crystal wave functions in Bloch sums corresponding to atomic wave functions and plane waves. No *a priori* restriction about the fact that Bloch sums are to be eigenfunctions of the crystal Hamiltonian is introduced. The method (called the mixed basis method) appears to be a significant and workable improvement with respect to the OPW method. The mixed basis method has already been applied successfully to describe energy levels in crystals.<sup>[13]</sup>

### 3-3e Perturbative approach to the OPW method

When the non-diagonal matrix elements of a secular determinant are small, perturbation theory can be applied and gives equivalent results. The main advantage of using perturbation theory, as opposed to solving the secular problem, is in its simplicity and in the qualitative considerations it allows. Starting from the observation that the off-diagonal matrix elements of the OPW method are usually small because of the cancellation previously discussed, Bassani and Celli<sup>[14]</sup> have developed a perturbative approach to the OPW method which is very simple to use.

The total crystal Hamiltonian is written in the form

$$H = H_0 + V_1$$

with

$$H_0 = -\frac{\hbar^2 \nabla^2}{2m} + V(0) \quad \text{and} \quad V_1 = V(\mathbf{r}) - V(0).$$

The zero order Hamiltonian is taken to be  $-(\hbar^2 \nabla^2 / 2m) + V(0)$ . The average crystal potential  $V(0)$  may be a relatively large quantity, subtracted from the crystal potential,

so that the term  $V_1$  can be considered a small perturbation. The solutions of the unperturbed Hamiltonian are plane waves which may be formed into symmetrized combinations  $S_i^{(\alpha)}(\mathbf{k}, \mathbf{r})$ . (Accidental degeneracies are assumed to be fully removed by the symmetry analysis, so that we can apply standard perturbation theory for non-degenerate states.) A crystal valence or conduction state  $\psi_i^{(\alpha)}(\mathbf{k}, \mathbf{r})$  belonging to the  $\alpha$ th irreducible representation of the group of  $\mathbf{k}$  can be expanded in the form

$$\begin{aligned}\psi_i^{(\alpha)}(\mathbf{k}, \mathbf{r}) &= S_i^{(\alpha)}(\mathbf{k}, \mathbf{r}) - \sum_c \langle \psi_c^{(\alpha)} | S_i^{(\alpha)} \rangle \psi_c^{(\alpha)} \\ &\quad + \sum_j [a_j^{(1)} + a_j^{(2)} + \dots] [S_j^{(\alpha)}(\mathbf{k}, \mathbf{r}) - \sum_c \langle \psi_c^{(\alpha)} | S_j^{(\alpha)} \rangle \psi_c^{(\alpha)}],\end{aligned}\quad (3-33a)$$

where  $a_j^{(n)}$  indicates the  $n$ th order coefficient of the expansion. We also expand the energy  $W_i$  of the crystal state in the series

$$W_i = W_i^{(0)} + W_i^{(1)} + W_i^{(2)} + \dots \quad (3-33b)$$

to the various orders of approximation. If we substitute the expansions (2-33a) and (3-33b) into the Schrödinger equation, and we consistently retain the terms of the same order, we obtain for the eigenvalues to second order:

$$W_i^{(0)} = \frac{\hbar^2 |\mathbf{k} + \mathbf{h}_i|^2}{2m} + V(0), \quad (3-34a)$$

$$W_i^{(1)} = \langle S_i^{(\alpha)} | V_1 | S_i^{(\alpha)} \rangle + \sum_c (W_i^{(0)} - E_c) |\langle \psi_i^{(\alpha)} | S_i^{(\alpha)} \rangle|^2, \quad (3-34b)$$

$$\begin{aligned}W_i^{(2)} &= W_i^{(1)} \sum_c |\langle \psi_c^{(\alpha)} | S_i^{(\alpha)} \rangle|^2, \\ &\quad + \sum_{j \neq i} \frac{\left| \langle S_i^{(\alpha)} | V_1 | S_j^{(\alpha)} \rangle + \sum_c (W_i^{(0)} - E_c) \langle \psi_c^{(\alpha)} | S_i^{(\alpha)} \rangle \langle S_j^{(\alpha)} | \psi_c^{(\alpha)} \rangle \right|^2}{W_i^{(0)} - W_j^{(0)}}.\end{aligned}\quad (3-34c)$$

In crystals in which the non-diagonal matrix elements of the OPW secular problem are much smaller than the separation of the unperturbed eigenvalues the results of the perturbation approach and those of the OPW method are practically the same. Even when these conditions are not well satisfied, the perturbation approach is useful to obtain qualitative results on the sequence of the energy states. We note that the zero order eigenstates in our perturbation approach are the solutions of a Schrödinger equation with a constant crystal potential. Such a fictitious crystal was originally introduced by Shockley<sup>[15]</sup> and is called the "empty lattice". The eigenfunction  $S_i^{(\alpha)}(\mathbf{k}, \mathbf{r})$  of the empty lattice are classified according to the crystal symmetry, but the constant potential produces accidental degeneracies between the plane waves of the same modulus  $|\mathbf{k} + \mathbf{h}|$ .

The first rule which follows in cases where the perturbative approach has any applicability at all, is that the order of the "empty lattice" eigenvalues is generally maintained, though the accidental degeneracies are removed when the actual crystal potential is considered. To establish the way in which the degeneracies in the empty lattice are removed, we consider the first order correction (3-34b). Calculations show that the leading term in  $W^{(1)}$  is due to the effect of orthogonalization. This term is always repulsive and is determined from the symmetry of the core states. For symmetrized

combinations of plane waves of a given  $|\mathbf{k} + \mathbf{h}|$  it turns out that the effect of orthogonalization is more important for those which are *s*-like, rather than those which are *p*-like and *d*-like. This is basically due to the *l*-dependence of the orthogonalization coefficients and to the structure of the matrix elements.

Next we consider the second order correction (3-34c). The first term of (3-34c) is again repulsive. The effect of the second term in (3-34c) can be understood qualitatively by realizing that the interaction between two states with different energies tends to decrease (increase) the energy of the state with lower (higher) energy, and that states whose unperturbed energies are close are expected to repel more strongly as the perturbation is turned on.

In conclusion, the expected sequence of the valence or conduction states is mainly determined from the symmetry of the empty lattice eigenstates. The order of the levels of the empty lattice is generally maintained. Degeneracies in the empty lattice are removed in first order because of the repulsive effect of core states of the same symmetry, and in second order because of interaction with other states of the empty lattice of the same symmetry. In this way it can be shown that the sequence of energy levels is generally the same for a given crystal symmetry in spite of differences in the atomic potentials. We will discuss detailed applications of this analysis in Chapter 4.

### 3-4 The pseudopotential method

#### 3-4a Formulation of the pseudopotential method

The basic concepts of pseudopotential formalism in crystals were formulated by Phillips and Kleinman (1959) and by Bassani and Celli (1961), and were then extended by a number of authors.<sup>[16]</sup> Pseudopotential formalism, like the OPW method, makes use of the fact that valence and conduction crystal states must be orthogonal to core states. However, in pseudopotential formalism, the effect of orthogonality is included in a form particularly meaningful and suitable for the development of approximate procedures or interpolation schemes.

A valence or conduction crystal state  $\psi_v(\mathbf{k}, \mathbf{r})$  satisfies the Schrödinger equation

$$\left[ \frac{\mathbf{p}^2}{2m} + V(\mathbf{r}) \right] \psi_v(\mathbf{k}, \mathbf{r}) = E_v(\mathbf{k}) \psi_v(\mathbf{k}, \mathbf{r}) \quad (3-35a)$$

with the orthogonality condition

$$\langle \psi_c | \psi_v \rangle = 0 \quad (3-35b)$$

for every core state  $\psi_c$ . We can always write the valence state  $\psi_v(\mathbf{k}, \mathbf{r})$  in the form

$$\psi_v(\mathbf{k}, \mathbf{r}) = \varphi_v(\mathbf{k}, \mathbf{r}) - \sum_c \langle \psi_c | \varphi_v \rangle \psi_c. \quad (3-36)$$

Substituting (3-36) in (3-35a) we obtain the following equation for  $\varphi_v(\mathbf{k}, \mathbf{r})$ :

$$\left[ \frac{\mathbf{p}^2}{2m} + V(\mathbf{r}) \right] \varphi_v(\mathbf{k}, \mathbf{r}) + \sum_c [E_v(\mathbf{k}) - E_c] \langle \psi_c | \varphi_v \rangle \psi_c = E_v(\mathbf{k}) \varphi_v(\mathbf{k}, \mathbf{r}). \quad (3-37a)$$

The Schrödinger equation (3-35a) with the true crystal potential  $V(\mathbf{r})$  and orthogonality conditions (3-35b) has the same eigenvalues as equation (3-37a), in which the crystal potential  $V(\mathbf{r})$  is replaced by the operator

$$V(\mathbf{r}) + \sum_c [E_v(\mathbf{k}) - E_c] \langle \psi_c | \dots \rangle \psi_c = V(\mathbf{r}) + V_R \equiv V_p. \quad (3-37b)$$

## ELECTRONIC STATES AND OPTICAL TRANSITIONS

This was termed pseudopotential by Phillips and Kleinmann. Equation (3-37) is as difficult to solve as eqs. (3-35a) and (3-35b) because  $V_p$  is a non-local, eigenvalue dependent operator, and an expansion of  $\varphi_v$  in plane waves would lead to the same equations as the OPW method described in Section 3-3.

It is immediate to verify that if  $\varphi_v(\mathbf{k}, \mathbf{r})$  satisfies (3-37a) also the functions

$$\Phi_v = \varphi_v + \sum_c a_c \psi_c$$

obtained by adding to  $\varphi_v(\mathbf{k}, \mathbf{r})$  a linear combination of core states with arbitrary coefficients  $a_c$ , satisfy (3-37a). This arbitrariness in the eigenfunctions of (3-37a) can be transferred into the pseudopotential operator by introducing an arbitrary operator  $A$  and by defining a general non-local pseudopotential

$$V_p = V(\mathbf{r}) + \sum_c \langle \psi_c | A | \dots \rangle \psi_c. \quad (3-38a)$$

The pseudopotential equation becomes

$$\left[ \frac{\mathbf{p}^2}{2m} + V(\mathbf{r}) \right] \phi_v(\mathbf{k}, \mathbf{r}) + \sum_c \langle \psi_c | A | \phi_v \rangle \psi_c = E_v(\mathbf{k}) \phi_v(\mathbf{k}, \mathbf{r}), \quad (3-38b)$$

where the choice of the arbitrary operator  $A$  determines the particular choice of  $\phi_v$ , but the eigenvalues  $E_v(\mathbf{k})$  are the same as those of eq. (3-37), in spite of the arbitrariness of operator  $A$ . As shown by Bassani and Celli,<sup>[16]</sup> in fact, multiplication of (3-38b) by a core wave function  $\psi_c^*$  and integration gives the condition

$$\langle \psi_c | A | \phi_v \rangle = [E_v(\mathbf{k}) - E_c] \langle \psi_c | \phi_v \rangle, \quad (3-38c)$$

which proves the equivalence of (3-38) and (3-37). The formulation with the arbitrary operator (3-38) is more convenient and has led to useful developments. It was also hoped that by an appropriate choice of  $A$  one could reduce  $V_p$  to a simple and easily soluble form, but this attempt was doomed to failure by condition (3-38c), which is automatically satisfied by the exact solutions of (3-38b), but must be imposed on the approximate solutions to any order of approximation. Equation (3-38), however, can be considered as the fundamental of pseudopotential formalism and gives the energies of the valence and conduction states of the crystal, their eigenfunctions being related to the true wave functions by orthogonalization to the core states (3-36). To illustrate the significance of (3-38) let us consider some particular choices of  $A$ . The choice  $A = 0$  immediately reduces (3-38) to (3-35) and (3-38c) assures that condition (3-35b) is satisfied. Choice  $A = E_v(\mathbf{k}) - H$  automatically satisfies eq. (3-38c) and reduces (3-38a) to form (3-37) of Phillips and Kleinmann.<sup>[16]</sup> An interesting form of the pseudopotential equations can be obtained from choice

$$A = -V(\mathbf{r}) = -\left[ \frac{\mathbf{p}^2}{2m} + V(\mathbf{r}) \right] + \frac{\mathbf{p}^2}{2m}$$

as discussed by Cohen and Heine.<sup>[16]</sup> Equation (3-38a) shows explicitly that the effect of orthogonalization to the core states is to subtract from  $V(\mathbf{r}) \phi_v$  that part which can be expanded in the core states, thus reducing  $V_p$  in the core region and making it a smooth potential.

Approximate solutions of eqs. (3-38) can be sought by using a perturbative approach when the pseudopotential (3-38a) is very smooth. We can split off the term  $(\mathbf{p}^2/2m) + V(0)$

from the "perturbation term"

$$V(\mathbf{r}) = V(0) + \sum_c \langle \psi_c | A | \dots \rangle \psi_c$$

and then expand  $\phi_v(\mathbf{k}, \mathbf{r})$  in symmetrized combinations of plane waves to the various orders of approximation. If we consistently retain terms of the same order in eqs. (3-38b) and (3-38c) we obtain again the results (3-34) of Bassani's and Celli's perturbative approach.<sup>[14, 16]</sup>

### 3-4b Pseudopotential approximation

From all the above considerations a pseudopotential approximation to the OPW method can be formulated. In this approach one assumes that it is possible to replace the exact formulation of eq. (3-38b) and condition (3-38c) with good accuracy by a Schrödinger equation having an appropriate, greatly simplified, pseudopotential  $V_p$ . Because of the cancellation effect described above, this effective potential  $V_p$  is assumed to be weak enough to give good convergence when an expansion in plane waves is considered. The crystal pseudopotential  $V_p$  can be taken in some cases as the sum of spherically symmetric local pseudopotentials centred on the atomic sites

$$V_p = \sum_{\tau_v} \sum_{d_\mu} V_{p,\mu}(\mathbf{r} - \mathbf{d}_\mu - \boldsymbol{\tau}_v). \quad (3-39a)$$

When this is the case, the problem of diagonalizing the pseudopotential Hamiltonian  $H_p = -(\hbar^2 \nabla^2 / 2m) + V_p$  is greatly simplified, and leads to the determinantal equation

$$\| \langle W_{k_i} | H_p - E | W_{k_j} \rangle \| = 0 \quad (3-39b)$$

with matrix elements (see the analogous derivation of (3-32b))

$$\langle W_{k_i} | H_p - E | W_{k_j} \rangle = \left( \frac{\hbar^2 k_i^2}{2m} - E \right) \delta_{ij} + \frac{1}{\Omega} \sum_{d_\mu} e^{-i(\mathbf{h}_i - \mathbf{h}_j) \cdot \mathbf{d}_\mu} V_{p,\mu}(\mathbf{h}_i - \mathbf{h}_j). \quad (3-39c)$$

The Fourier coefficients  $V_{p,\mu}(\mathbf{h}_i - \mathbf{h}_j)$  are sometimes treated as disposable parameters to fit some experimental data which depend on the electronic structure. Their number can be limited by requiring that  $V(\mathbf{h}_i - \mathbf{h}_j)$  is zero when  $|\mathbf{h}_i - \mathbf{h}_j|$  is sufficiently large, as we have seen to be the case in cancelling from orthogonality terms. For instance, the valence and conduction bands of germanium have been computed by Brust *et al.*<sup>[17]</sup> using, for the Fourier transform of the pseudopotential with reciprocal lattice vectors,

$$\frac{2\pi}{a} (\pm 1, \pm 1, \pm 1), \quad \frac{2\pi}{a} (\pm 2, \pm 2, 0), \quad \frac{2\pi}{a} (\pm 3, \pm 1, \pm 1),$$

the values  $-0.23, 0.0, 0.06$  Rydberg respectively, and taking  $V_p(\mathbf{h}) = 0$  for  $[(a^2 \mathbf{h}^2)/(4\pi^2)] > 11$ . The main shortcoming of this procedure is its assumption of the same local pseudopotential for all crystal states, while it is apparent from the discussion of the perturbation approach that different pseudopotentials for *s*-like, *p*-like, or *d*-like states should be considered. The validity of this assumption has to be justified in every case.

The pseudopotential approximation can be used in a different perspective by utilizing model pseudopotentials  $V_{p,\mu}$  for atoms or ions in the crystal, to construct  $V_p$  as given by (3-39a). Pseudopotentials for valence electrons in atoms or ions can be constructed

either theoretically, using Hartree-Fock atomic calculations, or semi-empirically, by means of spectroscopically known excited states of the valence electrons.<sup>[18,19]</sup> They can show an angular momentum and an eigenvalue dependence, and thus modify the matrix elements (3-39c) by including non-local eigenvalue dependent terms. In this manner it is possible for calculations of crystal states to be performed from atomic data with an energy and angular momentum dependent pseudopotential. This is at the expense of the simplicity of the method, but offers the advantage that the atomic eigenstates will result automatically as the lattice space increases. Note, however, that in this formalism it is assumed that atomic core states and crystal core states coincide; this is not a good approximation in many cases, particularly when the lattice spacing is very small.

Calculations using the pseudopotential approach have been made for many metals, where the cancellation between the crystal potential and the terms due to the orthogonalization justifies what is referred to as "the nearly free electron" model of metals. Pseudopotential formalism has also been applied to the study of valence and conduction states in semiconductors.

### 3-5 The cellular method

#### 3-5a Description of the method

The cellular method in its original form was proposed by Wigner and Seitz<sup>[20]</sup> in 1933 to study the cohesive energy of sodium crystals. It was later extended and refined by a number of authors.<sup>[21,22,24]</sup> The important concepts on which it is based have been widely used and applied in other methods.

To illustrate the method, we first of all consider simple structures with one atom per unit cell. Following Wigner and Seitz we choose as the unit cell the polyhedron obtained from bisecting, by perpendicular planes, the lines joining an atom to its neighbours. These polyhedra fill the whole space occupied by the crystal, and each contains a single atom at the centre. The basic idea of the cellular method is to obtain the crystal states by solving the Schrödinger equation within the Wigner-Seitz cell provided that the appropriate boundary conditions of the cell are satisfied. This procedure, however, is easy to apply only if the crystal potential in the Wigner-Seitz cell is taken as a spherically symmetric potential, since the Schrödinger equation is in this case separable. In many practical cases the actual crystal potential is close to being spherically symmetric within the Wigner-Seitz cell because of the dominant contribution of the atomic core at the centre.

A crystal state  $\psi(\mathbf{k}, \mathbf{r})$  of energy  $E(\mathbf{k})$  can be conveniently expanded within the Wigner-Seitz cell in the form

$$\psi(\mathbf{k}, \mathbf{r}) = \sum_{l=0}^{\infty} \sum_{m=-l}^{l} c_{lm}(\mathbf{k}) Y_{lm}(\theta, \varphi) R_l(E, r), \quad (3-40)$$

where  $r, \theta, \varphi$  are the polar coordinates of  $\mathbf{r}$  with respect to the centre of the cell, and  $c_{lm}$  are appropriate coefficients. The function  $R_l(E, r)$  is the solution of the radial wave equation

$$\frac{1}{r^2} \frac{d}{dr} \left( r^2 \frac{dR_l}{dr} \right) + \left[ \frac{2m}{\hbar^2} (E - V(r)) - \frac{l(l+1)}{r^2} \right] R_l = 0, \quad (3-41)$$

which is regular at its origin. In (3-41)  $V(r)$  is the spherically symmetric cellular potential. For every pair of points  $\mathbf{R}_1, \mathbf{R}_2$  on opposite faces of the Wigner–Seitz cell, related to one another by a lattice translation  $\tau_{12}$ , eigenfunction (3-40) must satisfy the boundary conditions required by the Bloch theorem

$$\begin{aligned}\psi(\mathbf{k}, \mathbf{R}_1) &= e^{i\mathbf{k} \cdot \tau_{12}} \psi(\mathbf{k}, \mathbf{R}_2), \\ \mathbf{n} \cdot \nabla \psi(\mathbf{k}, \mathbf{R}_1) &= e^{i\mathbf{k} \cdot \tau_{12}} \mathbf{n} \cdot \nabla \psi(\mathbf{k}, \mathbf{R}_2),\end{aligned}\quad (3-42)$$

$\mathbf{n}$  being a unit vector normal to the pair of surfaces to which  $\mathbf{R}_1$  and  $\mathbf{R}_2$  belong. To obtain crystal states we first consider the radial wave equation (3-41) with  $E$  taken as a disposable parameter. This gives, for every value of  $l$ , a radial solution  $R_l(E, r)$  which is regular at the origin. The expansion (3-40) with arbitrary values of the coefficients is then a valid solution of the Schrödinger equation inside the Wigner–Seitz cell. However, only for particular values of  $E$  and of coefficients  $c_{lm}$  will the expansion (3-40) satisfy the boundary conditions (3-42) for every pair of points  $\mathbf{R}_1, \mathbf{R}_2$  on the Wigner–Seitz cell joined to one another by a translation lattice vector, and this determines the eigenvalues and eigenfunctions of the electronic states.

In the more complicated case where there is more than one atom per unit cell, the Wigner–Seitz cell can be divided into a number of subcells equal to the number of atoms in the unit cell. Besides considering boundary conditions (3-42) at the surface of the cell, one must now consider the appropriate continuity conditions at the surface separating the subcells.

The expansion (3-40) can be simplified at high symmetry points of the Brillouin zone by considering appropriate combinations of spherical harmonics with the symmetry of the crystal as a basis set. A complete tabulation of such symmetry-adapted functions is given for cubic symmetry by Von der Lage and Bethe<sup>[22]</sup> and, more generally, by Bell.<sup>[23]</sup> To take an example, we note that at point  $\Gamma$  of a crystal with cubic symmetry, the symmetry-adapted combinations of spherical harmonics coincide with those given in Table 1-16. From the sequence of the atomic levels and from the correspondence between spherical harmonics and symmetry-adapted combinations of spherical harmonics, some information on the expected sequence of crystal states at  $\mathbf{k}$  vectors of high symmetry can be obtained.

### 3-5b Relevant aspects of the cellular method

#### *The Wigner–Seitz approximation<sup>[20]</sup>*

The cellular method was first applied by Wigner and Seitz to study the properties of metallic sodium. This metal crystallizes in the body-centred cubic structure, with one atom per unit cell and one valence electron in the  $3s$  state. Wigner and Seitz were mainly interested in calculating the energy of the bottom of the conduction band, corresponding to  $\mathbf{k} = 0$ . The corresponding eigenfunction  $\psi_0(\mathbf{r})$  is expected to have the crystal symmetry  $\Gamma_1$ . In fact, the lowest valence state in the free atom is an  $s$ -state, and the crystal state of symmetry  $\Gamma_1$  is  $s$ -like. In expansion (3-40) for  $\psi_0(\mathbf{r})$ , we must consider only combinations of spherical harmonics of symmetry  $\Gamma_1$ . The lowest order spherical harmonics for representation  $\Gamma_1$  are those with  $l = 0, 4, 6$ , etc., as can be seen from Table 1-15. The contributions from higher harmonics ( $l = 4, 6$ , etc.) are expected to be small because in the free atom these states have energies well separated from the lowest valence state; Wigner and Seitz therefore only consider the term with

## ELECTRONIC STATES AND OPTICAL TRANSITIONS

$l = 0$  and approximate the cellular polyhedron with a sphere of equal volume and radius  $r_0$ . The eigenfunction is then spherically symmetric and is easily determined by solving the radial equation

$$\frac{1}{r^2} \frac{d}{dr} \left( r^2 \frac{d\psi_0(r)}{dr} \right) + \frac{2m}{\hbar^2} [E - V(r)] \psi_c(r) = 0$$

with the boundary condition

$$\left( \frac{d\psi_0(r)}{dr} \right)_{r=r_0} = 0.$$

The solution in this case can be explicitly obtained with very little labour.

The generalization of the Wigner-Seitz treatment to include states with different  $\mathbf{k}$  vectors has been developed in the cellular method previously described.

*Boundary conditions.* The problem of ensuring that the boundary conditions (3-42) are satisfied when the actual Wigner-Seitz polyhedron is considered is quite difficult, even in the case of simple structures with one atom per unit cell. We wish to recall here the procedure adopted by Von der Lage and Bethe<sup>[22]</sup> in their work on alkali metals because it contains some interesting aspects of the problem. In this paper the electronic states are calculated by including in the expansion (3-40) symmetrized combinations of spherical harmonics for  $l$  up to 2, in order to reproduce the  $s$ ,  $p$ , and  $d$  character of crystal states. A convenient number of points of the Wigner-Seitz cell are arbitrarily selected for the purpose of satisfying boundary conditions. For example, the midpoint of the line joining an atom with its nearest neighbour is chosen for reasons of simplicity. The accuracy of the procedure, at least for the lowest eigenvalues, is tested in a manner suggested by Shockley:<sup>[15]</sup> one first considers the case for which the crystal potential is a constant, and the solutions obtained from the cellular method can then be compared with the exact solutions constituted by plane waves (empty lattice test). Finally, detailed results for alkali metals are obtained.

The most unsatisfactory feature of any calculation based on the cellular method is the arbitrariness involved in trying to satisfy the boundary conditions when only a limited number of points are considered. Though much work has been done by several authors to establish precise variational principles,<sup>[24]</sup> there seems to be no completely satisfactory way of solving the problem, and this constitutes the main difficulty of the cellular method.

*Choice of the potential.* The potential to be used within the Wigner-Seitz cell must be spherically symmetric. This restriction is not required in the tight binding, OPW, and pseudopotential methods previously described, but appears in any method in which the functions of the expansion set satisfy the Schrödinger equation.

As a spherical potential one can use the atomic potential up to the boundary of the Wigner-Seitz cell, but one can also modify the atomic potential to take into account to some degree the contribution from the rest of the lattice. This leads to a potential which is called the muffin-tin potential; it is atomic-like up to a distance  $r_s$  from the nucleus and constant in the rest of the cell. Except for strongly covalent crystals, this approximate description of the crystal potential is likely to be accurate enough for electronic state calculations.

### 3-6 The augmented plane wave method

#### 3-6a Description of the method

The augmented plane wave method (APW method) was originally suggested by Slater<sup>[25]</sup> in 1937 to overcome the difficulty of satisfying boundary conditions inherent to the cellular method.

To describe the method we consider, for simplicity, the case of crystals containing one atom per unit cell. In the APW method the crystal potential is assumed to be spherically symmetric inside spheres surrounding the atoms (or ions) of radius  $r_s$  and constant outside (muffin-tin potential). For convenience we may take the value of the potential outside the spheres to be zero by an appropriate choice of the zero of the energy scale.

An eigenfunction  $\psi(\mathbf{k}, \mathbf{r})$  with energy  $E(\mathbf{k})$  can be expanded within the Wigner–Seitz cell in the form

$$\psi(\mathbf{k}, \mathbf{r}) = \sum_{l=0}^{\infty} \sum_{m=-l}^{+l} c_{lm}(\mathbf{k}) Y_{lm}(\theta, \varphi) R_l(E, r) \eta(r_s - r) + \sum_j b_j(\mathbf{k}) e^{i(\mathbf{k} + \mathbf{h}_j) \cdot \mathbf{r}} \eta(r - r_s), \quad (3-43)$$

where  $r, \theta, \varphi$  are the polar coordinates of  $\mathbf{r}$  with respect to the centre of the cell, and the function

$$\eta(x) = \begin{cases} 0 & \text{for } x \text{ negative,} \\ 1 & \text{for } x \text{ positive,} \end{cases}$$

is used. As in the cellular method,  $R_l(E, r)$  is the solution of the radial wave equation

$$\frac{1}{r^2} \frac{d}{dr} \left( r^2 \frac{dR_l}{dr} \right) + \left[ \frac{2m}{\hbar^2} (E - V(r)) - \frac{l(l+1)}{r^2} \right] R_l = 0,$$

which is regular at the origin.  $V(r)$  denotes the muffin-tin potential within the sphere of radius  $r_s$ . The function  $R_l(E, r)$  can be explicitly determined by numerical integration of the differential equation from the origin outwards for a range of  $E$  and  $l$  values.

In (3-43) the eigenfunction  $\psi(\mathbf{k}, \mathbf{r})$  is seen to be expanded in spherical waves within the region where the potential is atomic-like, and in plane waves in the region where the potential is constant. The boundary conditions (3-42) at the surface of the Wigner–Seitz cell are automatically satisfied, and a much easier matching problem at the sphere surface provides the eigenvalues more efficiently than in the cellular method.

To see how to match solutions inside the sphere with those outside, let us consider the function

$$\mathcal{A}(\mathbf{p}, \mathbf{r}) = \sum_{l=0}^{\infty} \sum_{m=-l}^{+l} a_{lm} Y_{lm}(\theta, \varphi) R_l(E, r) \eta(r_s - r) + e^{i\mathbf{p} \cdot \mathbf{r}} \eta(r - r_s) \quad (3-44a)$$

and choose the coefficients  $a_{lm}$  in such a way that  $\mathcal{A}(\mathbf{p}, \mathbf{r})$  is continuous. By expanding the plane wave  $e^{i\mathbf{p} \cdot \mathbf{r}}$  in spherical harmonics (see Section 3-3b) and requiring the continuity of  $\mathcal{A}(\mathbf{p}, \mathbf{r})$  at  $r = r_s$ ,

$$a_{lm} = 4\pi Y_{lm}^*(\theta_p, \varphi_p) \frac{j_l(pr_s)}{R_l(E, r_s)}. \quad (3-44b)$$

The function (3-44a) with the choice of coefficients as given in (3-44b) is called an augmented plane wave. An augmented plane wave is a continuous function but, in general, a discontinuity in the slope at  $r = r_s$  remains.

## ELECTRONIC STATES AND OPTICAL TRANSITIONS

Expansion (3-43) can now be written in the equivalent form

$$\psi(\mathbf{k}, \mathbf{r}) = \sum_j a_j(\mathbf{k}) \mathcal{A}(\mathbf{k} + \mathbf{h}_j, \mathbf{r}), \quad (3-45)$$

where  $\mathcal{A}(\mathbf{k} + \mathbf{h}_j, \mathbf{r})$  indicates the augmented plane wave of vector  $\mathbf{k} + \mathbf{h}_j$ . Though the expansion functions  $\mathcal{A}(\mathbf{k} + \mathbf{h}_j, \mathbf{r})$  are discontinuous in slope at  $r = r_s$ , the function  $\psi(\mathbf{k}, \mathbf{r})$  must be well behaved. By substituting the above expansion in the Schrödinger equation and using the variational procedure with respect to coefficients  $a_j$  of (3-45), the following matrix equation is obtained:

$$\|\langle \mathcal{A}_{\mathbf{k}_i} | H - E | \mathcal{A}_{\mathbf{k}_j} \rangle\| = 0, \quad (3-46)$$

where  $\mathcal{A}_{\mathbf{k}_i}$  is a shorthand notation for  $\mathcal{A}(\mathbf{k} + \mathbf{h}_i, \mathbf{r})$ .

The explicit evaluation of matrix elements in (3-46) requires some care because of the discontinuity in slope of the trial wave functions at  $r = r_s$ . For precise details of their evaluation we refer the reader to Loucks;<sup>[26]</sup> the matrix elements in this account are derived from rigorous variational principles developed by Schlosser and Marcus<sup>[27]</sup> for discontinuous trial functions. A more direct derivation is given in the original work of Slater,<sup>[25]</sup> whose results we record here for the case of one atom per unit cell:

$$\begin{aligned} \langle \mathcal{A}_{\mathbf{k}_i} | H - E | \mathcal{A}_{\mathbf{k}_j} \rangle &= \left( \frac{\hbar^2}{2m} \mathbf{k}_i \cdot \mathbf{k}_j - E \right) \delta_{ij} \\ &+ \frac{4\pi r_s^2}{\Omega} \left\{ \left( \frac{\hbar^2}{2m} \mathbf{k}_i \cdot \mathbf{k}_j - E \right) \frac{j_1(|\mathbf{k}_i - \mathbf{k}_j|r_s)}{|\mathbf{k}_i - \mathbf{k}_j|} \right. \\ &\left. + \sum_{l=0}^{\infty} (2l+1) P_l(\cos \theta_{ij}) j_i(k_i r_s) j_i(k_j r_s) \left[ \frac{R'_i(E, r_s)}{R_i(E, r_s)} - \frac{j'_i(k_j r_s)}{j_i(k_j r_s)} \right] \right\} \end{aligned} \quad (3-47)$$

where  $\Omega$  indicates the volume of the unit cell,  $\theta_{ij}$  indicates the angle between the wave vectors  $\mathbf{k}_i$  and  $\mathbf{k}_j$ ,  $j_i$  are the spherical Bessel functions, and  $P_l$  the Legendre polynomials. The matrix elements contain energy  $E$  both explicitly and implicitly through the logarithmic derivatives  $R'_i/R_i$  of the radial wave functions  $R_i(E, r)$  at the sphere surface. The muffin-tin potential  $V(r)$  enters expression (3-47) implicitly because it determines, for a given  $E$ , the quantity  $R'_i/R_i$ .

For practical calculations, one limits the expansion (3-45) to augmented plane waves with momenta smaller than a fixed value. The determinant (3-46) is then plotted as a function of  $E$  and eigenvalues are obtained as the zeros of the curve. The convergence of the procedure can be tested by adding more augmented plane waves in (3-45); the convergence is in general rapid, a number of 10–20 augmented plane waves being sufficient in most practical cases. As usual, group theory can be applied to obtain symmetry adapted combinations of augmented plane waves at  $\mathbf{k}$  vectors of high symmetry.

### 3-6b Discussion of the APW method

The APW method has become in recent years one of the most powerful tools for studying electronic states in crystals. Although it was developed in 1937, it is only recently that the availability of large computers has allowed extensive studies with this method. In comparison with the tight binding or OPW methods, which require only relatively simple techniques (diagonalization of determinants of the form  $\|A_{ij} - EB_{ij}\| = 0$ )

with  $A_{ij}$  and  $B_{ij}$  independent of  $E$ ), the APW method presents an additional difficulty in that the matrix elements are complicated functions of the energy, as can be seen from the expression (3-47). On the other hand, the OPW determinants are usually much larger in size than those of the APW method.

In the APW method the crystal potential has to be approximated by a muffin-tin type potential. Though in most crystals this approximation is expected to be reasonable, it is, at least in principle, the least satisfactory aspect of the method.<sup>[28]</sup> In some cases, because of the difficulties associated with the tail of the atomic-like potential, it is convenient to consider the average potential outside the spheres as a disposable parameter to fit experimental results, similar to the situation previously described concerning  $V(0)$  in the OPW method.

One good feature of the APW method with respect to the OPW (or tight binding method) is that no assumption about the core states is necessary. In cases such as transition metals, where the separation of the crystal states in well-localized core states from the spread-out valence states is questionable, the APW method can instead be applied successfully.

### 3-7 Green's function method

Green's function method was proposed originally by Korringa (1947), Kohn and Rostoker (1954), and Morse (1956), in different though equivalent forms.<sup>[29]</sup> Basically the method uses Green's function technique to transform the Schrödinger equation into an equivalent integral equation. This method avoids the difficulties concerning the problem of boundary conditions as in the cellular method, but the approximation of the crystal potential by a muffin-tin model potential is required.

For simplicity, we illustrate Green's function method in the case of crystals with one atom per unit cell. In order to calculate the crystal states of wave vector  $\mathbf{k}$  in the first Brillouin zone, we determine Green's function  $G_{\mathbf{k}}(\mathbf{r} - \mathbf{r}', E)$  which satisfies the equation

$$\left( \frac{\hbar^2}{2m} \nabla^2 + E \right) G_{\mathbf{k}}(\mathbf{r} - \mathbf{r}', E) = \delta(\mathbf{r} - \mathbf{r}') \quad (3-48)$$

and the boundary conditions:

$$G_{\mathbf{k}}(\mathbf{r} + \mathbf{r}_n, E) = e^{i\mathbf{k} \cdot \mathbf{r}_n} G_{\mathbf{k}}(\mathbf{r}, E) \quad (3-49)$$

required by the Bloch theorem. Using standard techniques<sup>[30]</sup> for a Green's function calculation, we expand  $G_{\mathbf{k}}(\mathbf{r} - \mathbf{r}', E)$  in terms of the set of eigenfunctions of the operator  $(\hbar^2/2m) \nabla^2 + E$ , satisfying the appropriate boundary conditions. We can now write

$$G_{\mathbf{k}}(\mathbf{r} - \mathbf{r}', E) = \sum_n a_n(\mathbf{k}) \frac{1}{\sqrt{\Omega}} e^{i(\mathbf{k} + \mathbf{h}_n) \cdot (\mathbf{r} - \mathbf{r}')}, \quad (3-50)$$

where  $\Omega$  is the volume of the unit cell. The coefficients of the expansion (3-50) are easily determined by direct substitution into (3-48):

$$G_{\mathbf{k}}(\mathbf{r} - \mathbf{r}', E) = - \frac{1}{\Omega} \sum_n \frac{e^{i(\mathbf{k} + \mathbf{h}_n) \cdot (\mathbf{r} - \mathbf{r}')}}{\frac{\hbar^2}{2m} (\mathbf{k} + \mathbf{h}_n)^2 - E}. \quad (3-51)$$

The Schrödinger equation

$$\left( \frac{\hbar^2}{2m} \nabla^2 + E \right) \psi(\mathbf{k}, \mathbf{r}) = V(\mathbf{r}) \psi(\mathbf{k}, \mathbf{r})$$

for crystal states of vector  $\mathbf{k}$  is transformed, as in scattering theory, into the integral equation

$$\psi(\mathbf{k}, \mathbf{r}) = \int_{\Omega} G_{\mathbf{k}}(\mathbf{r} - \mathbf{r}', E) V(\mathbf{r}') \psi(\mathbf{k}, \mathbf{r}') d\mathbf{r}'. \quad (3-52)$$

To proceed further we explicitly assume a muffin-tin form for the crystal potential and set this potential equal to zero outside the sphere. Equation (3-52) can now be written in the form

$$\psi(\mathbf{k}, \mathbf{r}) = \int_{\Omega_s} G_{\mathbf{k}}(\mathbf{r} - \mathbf{r}', E) V(r') \psi(\mathbf{k}, \mathbf{r}') dr', \quad (3-53)$$

where  $\Omega_s$  indicates the volume of the inscribed sphere and  $V(r')$  is the muffin-tin potential. We can expand  $\psi(\mathbf{k}, \mathbf{r})$  inside the sphere in the form (3-40). Substituting (3-40) into the integral equation (3-53), we obtain a determinant compatibility relation whose solutions give the eigenvalues  $E$  and the coefficients  $c_{lm}$  of the eigenfunction expansions. The derivation of the compatibility relations is somewhat laborious, and we record here (for the case of one atom per unit cell) only the results as obtained by Slater using Ziman's procedure.<sup>[31]</sup> The matrix elements of Green's function method can be written as

$$M_{ij} = \left( \frac{\hbar^2}{2m} \mathbf{k}_i \cdot \mathbf{k}_j - E \right) \delta_{ij} + \frac{4\pi r_s^2}{\Omega} \left\{ \sum_l (2l + 1) P_l(\cos \theta_{ij}) j_i(k_i r_s) j_i(k_j r_s) \times \left[ \frac{R'_i(E, r_s)}{R_i(E, r_s)} - \frac{j'_i(kr_s)}{j_i(kr_s)} \right] \right\}, \quad (3-54)$$

where  $\mathbf{k}_i = \mathbf{k} + \mathbf{h}_i$  and  $(\hbar^2/2m) k^2 = E$ ,  $E$  being the eigenvalue of the secular equation. The meaning of other symbols adopted in (3-54) is the same as in (3-47) for the APW method. This form is particularly suitable for bringing out the connection with other methods. In Green's function, as in the APW method, the muffin-tin potential enters implicitly into the expression for the matrix elements through the logarithmic derivative  $R'_i/R_i$  of the radial wave functions  $R_i(E, r)$  at the sphere radius. The term  $((\hbar^2/2m) \mathbf{k}_i \cdot \mathbf{k}_j - E) \delta_{ij}$  and the term with  $R'_i/R_i$  are identical in both expressions (3-54) and (3-47); the extra term  $j_1(|\mathbf{k}_i - \mathbf{k}_j| r_s)/|\mathbf{k}_i - \mathbf{k}_j|$  appears in (3-47), however, and the argument of  $j'_i/j_i$  is at  $k$  in (3-54) whereas it is at  $k_j$  in (3-47).

The basic principles of Green's function method are very similar to those of the APW method. Both methods can be used to solve the problem of the motion of electrons in a muffin-tin model potential. It has been established by Segall and Burdick<sup>[32]</sup> that the two methods lead to equal results when the same muffin-tin potential is considered. Furthermore a common theoretical framework for these two methods has been established by Ziman on the basis of a pseudopotential formalism,<sup>[31]</sup> similar to that described for the OPW method. In this formalism the muffin-tin potential is replaced by an "effective" potential which is zero everywhere except at the sphere surfaces, where it exhibits an energy and  $l$ -dependent singularity.

### 3-8 The quantum defect method

The quantum defect method (QDM) is a subsidiary tool in the calculation of logarithmic derivatives appearing in the cellular, APW, or Green's function methods, which makes use of experimental spectroscopic data. The QDM developed from a procedure of Kuhn and Van Vleck<sup>[33]</sup> (1950) and has since been refined by a number of authors.<sup>[34]</sup>

To describe the QDM we consider atoms, such as alkali atoms, with only one valence electron. If  $V_a(r)$  denotes the self-consistent, spherically symmetric atomic potential, the radial wave equation for atomic states becomes

$$\frac{1}{r^2} \frac{d}{dr} \left( r^2 \frac{dR_l}{dr} \right) + \left[ \frac{2m}{\hbar^2} (E - V_a(r)) - \frac{l(l+1)}{r^2} \right] R_l = 0. \quad (3-55)$$

The expression for  $V_a(r)$  outside the ion core radius  $r_c$  is  $-ze^2/r$ , where  $z$  is the difference between the nuclear and core electron charges and is equal to unity in the case of monovalent atoms.

It is convenient to consider the hydrogenic radial wave equation

$$\frac{1}{r^2} \frac{d}{dr} \left( r^2 \frac{du_l}{dr} \right) + \left[ \frac{2m}{\hbar^2} \left( E + \frac{ze^2}{r} \right) - \frac{l(l+1)}{r^2} \right] u_l = 0. \quad (3-56)$$

Let  $u_l^{(1)}(E, r)$  and  $u_l^{(2)}(E, r)$  be two linearly independent solutions of the radial wave equation with coulombic potential  $-ze^2/r$ . For any arbitrary value  $E$  and for  $r > r_c$  we can express the radial solution  $R_l(E, r)$ —regular at the origin and satisfying (3-55)—in the form

$$R_l(E, r) = \alpha(E) u_l^{(1)}(E, r) + \beta(E) u_l^{(2)}(E, r), \quad r > r_c, \quad (3-57)$$

$\alpha(E), \beta(E)$  being appropriate constants. In general, for an arbitrary value of  $E$ , eq. (3-57) is the only information we have about the function  $R_l(E, r)$  (unless we perform explicitly self-consistent atomic calculations). However, if we know *experimentally* that  $E$  is an eigenvalue of (3-55), we have the further information that  $R_l(E, r)$  must be regular at infinity. This condition implies a well-defined value of the ratio  $\alpha(E)/\beta(E)$ . When  $u_l^{(1)}(E, r)$  and  $u_l^{(2)}(E, r)$  are defined as in the paper by Ham,<sup>[34]</sup>

$$\frac{\alpha(E)}{\beta(E)} = \frac{\Gamma(n_E + l + 1)}{n_E^{2l+1} \Gamma(n_E - l) \tan(\pi n_E)}, \quad (3-58)$$

where  $n_E$  is related to the energy  $E$  by the relation  $E = -R/n_E^2$ , with  $R$  equal to 1 Rydberg. The relation (3-58) can be written in a slightly different form. We know, from the empirical Ritz law, that in alkali metals the terms of a given series (*s* or *p* or *d*, etc.) satisfy the relation

$$E = -\frac{R}{(m - \delta_E)^2},$$

where  $m$  is an integer which changes by unity from one term to the next, and  $\delta_E$  is a slowly varying quantity for the terms of a given series, called the "quantum defect". The ratio  $\alpha(E)/\beta(E)$  for a state of energy  $E$  and quantum defect  $\delta_E$  can be written in the form

$$\frac{\alpha(E)}{\beta(E)} = \frac{\Gamma(n_E + l + 1)}{n_E^{2l+1} \Gamma(n_E - l) \tan(\pi \delta_E)}. \quad (3-59)$$

Equations (3-57) and (3-59) determine, apart from a normalization factor, the function  $R_i(E, r)$  corresponding to an eigenvalue  $E$  and  $r > r_c$ . We now extend (3-59) to arbitrary energies  $E$  by extrapolating a smooth curve from the experimental quantum defect values. The success of the procedure depends on the slow dependence of the quantum defects on energy for terms of a given series; the justification has been discussed by Ham.<sup>[34]</sup> Since the analytical properties of  $u_i^{(1)}(E, r)$ ,  $u_i^{(2)}(E, r)$  are well known, the logarithmic derivative  $R'_i/R_i$  (which does not depend on the normalization) can be obtained without knowing the potential  $V_a(r)$  for  $r < r_c$ .

The QDM is used in connection with the cellular, APW, and Green's function method, and it has been mainly applied to crystals made up of monovalent atoms (such as alkali metals). In practice the method sometimes presents uncertainty in the extrapolation from atomic data, and, at times, other smooth energy dependent parameters are considered. Furthermore, the extension of the method to multivalent elements does not seem so straightforward. The application of the method also implies that crystal core states coincide with atomic core states.

Although the QDM has a restricted range of applicability because of the basic approximations involved, it is, nevertheless, a useful tool in correlating optical properties with atomic properties. Note also that the model pseudopotential method discussed at the end of Section 3-4b is another version of the same basic idea.

### 3-9 The $\mathbf{k} \cdot \mathbf{p}$ method

The  $\mathbf{k} \cdot \mathbf{p}$  method is a powerful subsidiary tool to be used in conjunction with an *a priori* calculation method. It is usually applied to determine effective masses or to calculate densities of states. The  $\mathbf{k} \cdot \mathbf{p}$  method was introduced by Bardeen (1937) and by Seitz<sup>[35]</sup> (1940) as a means of determining effective masses and crystal wave functions near high symmetry points in  $\mathbf{k}$  space. The method was extended by Shockley (1950) to include degenerate bands, and by Dresselhans *et al.* (1955) and Kane (1956) to include spin-orbit interaction.<sup>[36]</sup> The most significant use of the method is in obtaining knowledge of the band structure throughout the whole Brillouin zone from the results of detailed theoretical calculations performed only at  $\mathbf{k} = 0$ , as shown by Brinkman and Goodman<sup>[37]</sup> (1967).

To set up the  $\mathbf{k} \cdot \mathbf{p}$  method, let us suppose we know the eigenfunctions  $\psi_n(\mathbf{k}_0, \mathbf{r})$  and the eigenvalues  $E_n(\mathbf{k}_0)$  of the crystal Hamiltonian

$$\left[ \frac{\mathbf{p}^2}{2m} + V(\mathbf{r}) \right] \psi_n(\mathbf{k}_0, \mathbf{r}) = E_n(\mathbf{k}_0) \psi_n(\mathbf{k}_0, \mathbf{r})$$

- at a particular value  $\mathbf{k}_0$  of the wave vector (in many applications,  $\mathbf{k}_0$  is the highest symmetry point, i.e.  $\mathbf{k}_0 = 0$ ). The wave functions  $e^{i(\mathbf{k}-\mathbf{k}_0) \cdot \mathbf{r}} \psi_n(\mathbf{k}_0, \mathbf{r})$  are Bloch functions of vector  $\mathbf{k}$  and constitute a convenient set in which to expand the crystal wave functions  $\psi(\mathbf{k}, \mathbf{r})$ . We can thus write

$$\psi(\mathbf{k}, \mathbf{r}) = \sum_n c_n(\mathbf{k}) e^{i(\mathbf{k}-\mathbf{k}_0) \cdot \mathbf{r}} \psi_n(\mathbf{k}_0, \mathbf{r}). \quad (3-60)$$

This is equivalent to the more usual approach of expanding the periodic part of the wave function at  $\mathbf{k}$  in terms of the periodic part of the Bloch functions at  $\mathbf{k}_0$ , but we have preferred expansion (3-60) because it has some formal advantages. From the variational

## METHODS OF CALCULATING THE ELECTRONIC BAND STRUCTURES OF CRYSTALS

principle with respect to the coefficients  $c_n$  we find that the eigenvalues  $E(\mathbf{k})$  and the eigenfunctions (3-60) of the crystal Hamiltonian  $H$  are solutions of the secular problem

$$\| \langle e^{i(\mathbf{k}-\mathbf{k}_0) \cdot \mathbf{r}} \psi_{n'}(\mathbf{k}_0, \mathbf{r}) | H - E | e^{i(\mathbf{k}-\mathbf{k}_0) \cdot \mathbf{r}} \psi_n(\mathbf{k}_0, \mathbf{r}) \rangle \| = 0. \quad (3-61)$$

We note that

$$\begin{aligned} & \left[ \frac{\mathbf{p}^2}{2m} + V(\mathbf{r}) \right] e^{i(\mathbf{k}-\mathbf{k}_0) \cdot \mathbf{r}} \psi_n(\mathbf{k}_0, \mathbf{r}) \\ &= e^{i(\mathbf{k}-\mathbf{k}_0) \cdot \mathbf{r}} \left[ \frac{\hbar^2}{2m} (\mathbf{k} - \mathbf{k}_0)^2 + \frac{\hbar}{m} (\mathbf{k} - \mathbf{k}_0) \cdot \mathbf{p} + E_n(\mathbf{k}_0) \right] \psi_n(\mathbf{k}_0, \mathbf{r}), \end{aligned}$$

so that eq. (3-61) becomes

$$\left\| \left[ \left[ \frac{\hbar^2}{2m} (\mathbf{k} - \mathbf{k}_0)^2 + E_n(\mathbf{k}_0) - E \right] \delta_{n'n} + \frac{\hbar}{m} (\mathbf{k} - \mathbf{k}_0) \cdot \mathbf{M}_{n'n}(\mathbf{k}_0) \right] \right\| = 0, \quad (3-62)$$

where

$$\mathbf{M}_{n'n}(\mathbf{k}_0) = \int \psi_{n'}^*(\mathbf{k}_0, \mathbf{r}) \mathbf{p} \psi_n(\mathbf{k}_0, \mathbf{r}) d\mathbf{r}. \quad (3-63)$$

In (3-63) the integral extends over the crystal volume, where the  $\psi_n(\mathbf{k}_0, \mathbf{r})$  are normalized. Equation (3-62) determines eigenvalues and eigenfunctions throughout the whole Brillouin zone once they are known at a given vector  $\mathbf{k}_0$ .

Symmetry considerations can be used to express the matrix elements (3-63) as functions of a small number of independent parameters. By using the commutation property

$$[H, \mathbf{r}] = \frac{i\hbar}{m} \mathbf{p}$$

and by remembering that  $\psi_n(\mathbf{k}_0, \mathbf{r})$  are eigenfunctions of the crystal Hamiltonian  $H$ , we obtain, when  $E_n(\mathbf{k}_0) \neq E_{n'}(\mathbf{k}_0)$ ,

$$\mathbf{M}_{n'n}(\mathbf{k}_0) = \frac{m}{i\hbar} [E_{n'}(\mathbf{k}_0) - E_n(\mathbf{k}_0)] \int \psi_{n'}^*(\mathbf{k}_0, \mathbf{r}) \mathbf{r} \psi_n(\mathbf{k}_0, \mathbf{r}) d\mathbf{r}. \quad (3-64)$$

Let the functions  $\psi_{n'}(\mathbf{k}_0, \mathbf{r})$  and  $\psi_n(\mathbf{k}_0, \mathbf{r})$  belong, respectively, to the irreducible representations  $D^{(\mathbf{k}_0, \mu)}$  and  $D^{(\mathbf{k}_0, \nu)}$  of the group of  $\mathbf{k}_0$ , and  $\mathbf{r}$  belong to the irreducible representation  $D^{(\alpha)}(R_{\mathbf{k}_0})$  of the small point group of  $\mathbf{k}_0$ . Using relation (2-28) we find that the  $I_\mu \cdot I_\nu \cdot I_\alpha$  matrix elements

$$\langle \psi_{n'}^{(\mathbf{k}_0, \mu)} | \mathbf{r} | \psi_n^{(\mathbf{k}_0, \nu)} \rangle$$

can be expressed in terms of a reduced number of independent parameters given by

$$c(\mathbf{k}_0 \mu; \alpha; \mathbf{k}_0 \nu) = \frac{1}{h_{\mathbf{k}_0}} \sum_{\{R_{\mathbf{k}_0} | \mathbf{f}\}} \chi^{(\mathbf{k}_0, \mu)}(\{R_{\mathbf{k}_0} | \mathbf{f}\})^* \chi^{(\alpha)}(R_{\mathbf{k}_0}) \chi^{(\mathbf{k}_0, \nu)}(\{R_{\mathbf{k}_0} | \mathbf{f}\}). \quad (3-65)$$

Thus, with the use of group theory, the number of independent parameters which are needed in (3-62) is greatly reduced.

The  $\mathbf{k} \cdot \mathbf{p}$  method has been used as a subsidiary tool in band structure calculations.<sup>[37]</sup> For a given vector of high symmetry, usually vector  $\mathbf{k}_0 = 0$ , we consider a convenient number of basis states calculated by an *a priori* method. We then consider the expansion (3-60) with a sufficiently large but finite number of basis states. Using group theory,

## ELECTRONIC STATES AND OPTICAL TRANSITIONS

we express all matrix elements of operator  $\mathbf{p}$  as a function of a small number of independent parameters. These are computed, the resulting finite order secular problem (3-62) is then solved, and the energies throughout the Brillouin zone obtained. The practical advantage of the  $\mathbf{k} \cdot \mathbf{p}$  procedure is remarkable if we consider, for example, the structure of the matrix elements of the secular problem in the  $\mathbf{k} \cdot \mathbf{p}$  procedure, compared with those of the OPW, APW, or Green's function method. The  $\mathbf{k} \cdot \mathbf{p}$  procedure seems to be particularly attractive in connection with the interpretation of the optical properties of crystals because, for this purpose, the energies have to be calculated at a very large number (say several thousands) of points of the Brillouin zone. Furthermore, the matrix elements  $M_{n'n}(\mathbf{k})$  over the whole Brillouin zone (needed for the calculation of optical constants) can be obtained from the values  $M_{n'n}(\mathbf{k}_0)$  simply by considering the eigenvectors of (3-62) together with the expansion (3-60).

When *a priori* calculations are not completely reliable, the  $\mathbf{k} \cdot \mathbf{p}$  method can be applied in a semi-empirical way, with matrix elements determined so as to fit some basic experimental data (such as effective masses, energy gaps). This use of the  $\mathbf{k} \cdot \mathbf{p}$  procedure for detailed energy band calculations has been suggested by Cardona and Pollak.<sup>[38]</sup>

In many cases only the behaviour of energy bands and wave functions near high symmetry points in  $\mathbf{k}$  space need be considered. Then the non-diagonal matrix elements  $(\hbar/m)(\mathbf{k} - \mathbf{k}_0) \cdot M_{n'n}(\mathbf{k}_0)$  are small for  $\mathbf{k} \sim \mathbf{k}_0$ , and perturbation theory can be used to simplify the determinantal equation (3-62). For instance, we can calculate, for a non-degenerate band, the behaviour of energy  $E_n(\mathbf{k})$  near an extremal point  $\mathbf{k}_0$ . By considering  $(\hbar/m)(\mathbf{k} - \mathbf{k}_0) \cdot \mathbf{p}$  as a small perturbation, we obtain to second order

$$E_n(\mathbf{k} - \mathbf{k}_0) = E_n(\mathbf{k}_0) + \frac{\hbar^2}{2m} (\mathbf{k} - \mathbf{k}_0)^2 + \frac{\hbar}{m} (\mathbf{k} - \mathbf{k}_0) \cdot M_{nn}(\mathbf{k}_0) + \frac{\hbar^2}{m^2} \sum_{n' \neq n} \frac{|(\mathbf{k} - \mathbf{k}_0) \cdot M_{nn'}(\mathbf{k}_0)|^2}{E_n(\mathbf{k}_0) - E_{n'}(\mathbf{k}_0)}. \quad (3-66)$$

If  $\mathbf{k}_0$  is an extremum,  $M_{nn}(\mathbf{k}_0) = 0$ , and in this case we can express the effective mass in the direction of a principal axis of unit vector  $\mathbf{s}$  by

$$\frac{1}{m_s^*} = \frac{1}{m} + \frac{2}{m^2} \sum_{n' \neq n} \frac{|\mathbf{s} \cdot M_{nn'}(\mathbf{k}_0)|^2}{E_n(\mathbf{k}_0) - E_{n'}(\mathbf{k}_0)}. \quad (3-67)$$

This shows that the interaction with bands of lower (higher) energy tends to reduce (increase) the effective mass; it explains qualitatively why insulators with small energy gaps have small effective masses, and vice versa, and allows quite accurate calculations of effective masses.

As a typical example of the trend in the values of effective masses, we may consider the case of alkali metals which have body-centred cubic structure. An alkali atom has one valence electron in a state  $ns$ , with  $n = 2, 3, 4, 5, 6$  for lithium, sodium, potassium, rubidium, and caesium respectively, and core electrons in filled inner shells. Corresponding to core electrons we have core crystal states, while corresponding to the valence electron we have the first conduction band, with a minimum at  $\mathbf{k} = (0, 0, 0)$  and symmetry  $\Gamma_1$ . The effective masses at the bottom of the conduction band are 1.33, 0.96, 0.86, 0.78, and 0.73 in units of the electron mass, for Li, Na, K, Rb, and Cs metals respectively. In Li  $m^* > m$  because the only interactions via the operator  $\mathbf{p}$  are with

states of higher energy (the conduction state  $\Gamma_1$  cannot interact with core states, since they are  $s$ -like and have symmetry  $\Gamma_1$  and the operator  $\mathbf{p}$  has symmetry  $\Gamma_{15}$ ; eq. (3-65) immediately gives  $c(\Gamma_1, \Gamma_{15}, \Gamma_1) = 0$ ). In Na  $m^* \approx m$  because of the balance of interactions with  $p$ -like bands lower and higher in energy than the conduction band. In the other crystals the contribution to the effective mass from lower energy states is dominant and  $m^* < m$ .

In the case of degenerate bands or nearly degenerate bands at  $\mathbf{k}_0$ , the expression (3-66) for the energies must be replaced by the expression obtained from diagonalizing the appropriate determinant (3-62). A detailed procedure has been described by Kane.<sup>[39]</sup>

### 3-10 Relativistic effects

#### 3-10a General considerations

In the band approximation described in Section 3-1, one can include relativistic effects for the motion of an electron in a potential  $V(\mathbf{r})$  by considering the Dirac relativistic equation

$$[c\alpha \cdot \mathbf{p} + \beta mc^2 + V(\mathbf{r})] \psi = W\psi, \quad (3-68)$$

where  $\psi$  indicates a four-component spinor,  $\mathbf{p}$  is the operator  $-i\hbar\nabla$ ,  $\alpha = \begin{pmatrix} 0 & \sigma \\ \sigma & 0 \end{pmatrix}$ , and  $\beta = \begin{pmatrix} 1 & 0 \\ 0 & -1 \end{pmatrix}$ ;  $\sigma$  indicates the Pauli operator matrices defined in Section 1-5,  $\mathbf{1}$  is the 2 by 2 unit matrix, and  $W = E + mc^2$  is the total energy, including the rest energy  $mc^2$ .

To discuss the relationship between the Dirac wave equation (3-68) and the Schrödinger wave equation considered in the previous sections,

$$\left[ \frac{\mathbf{p}^2}{2m} + V(\mathbf{r}) \right] \psi = E\psi, \quad (3-69)$$

we make use of the Foldy-Wouthuysen transformation of the Dirac equation in which the strong and weak components of the Dirac spinor are decoupled.<sup>[40]</sup> At a low order of approximation of the ratio of the momentum to  $mc$ , the wave equation for the upper two-component spinor becomes

$$\left[ \frac{\mathbf{p}^2}{2m} + V(\mathbf{r}) - \frac{\mathbf{p}^4}{8m^3c^2} - \frac{\hbar^2}{4m^2c^2} \nabla V \cdot \nabla + \frac{\hbar}{4m^2c^2} \sigma \cdot (\nabla V \times \mathbf{p}) \right] \psi = E\psi. \quad (3-70)$$

The operator appearing in the left hand side of (3-70) is made up of the non-relativistic Hamiltonian  $(\mathbf{p}^2/2m) + V(\mathbf{r})$  and by the additional terms

$$(i) H_v = - \frac{\mathbf{p}^4}{8m^3c^2}.$$

This term is the relativistic correction to the kinetic energy, as can be seen by expanding the relativistic expression for the kinetic energy in powers of  $p$ :

$$\sqrt{(c^2\mathbf{p}^2 + m^2c^4)} = mc^2 + \frac{\mathbf{p}^2}{2m} - \frac{\mathbf{p}^4}{8m^3c^2} + \dots$$

$$(ii) H_d = -\frac{\hbar^2}{4m^2c^2} \nabla V \cdot \nabla = \frac{\hbar^2}{8m^2c^2} \nabla^2 V.$$

This term is a relativistic correction to the potential  $V(\mathbf{r})$ , known as the Darwin correction.

$$(iii) H_{so} = \frac{\hbar}{4m^2c^2} \boldsymbol{\sigma} \cdot (\nabla V \times \mathbf{p}).$$

This term is the spin-orbit coupling and mixes the two components of the Pauli spinor. Its origin is the interaction of the electron spin magnetic moment with the magnetic field “seen” by the electron. A classical analysis, however, gives twice the correct relativistic value.

The terms  $H_v$  and  $H_d$  do not depend on the spin of the electron and do not change the symmetry properties of the non-relativistic Hamiltonian. The term  $H_{so}$  couples operators in spin space and ordinary space, thus reducing the symmetry. The states of the Schrödinger equation are classified by the irreducible representations of the symmetry group of the Hamiltonian. The states of eq. (3-70) are classified by the irreducible representations of the corresponding double group. In Sections 1-5 and 2-2 we have discussed how the states of the simple group split into the states of the double group; in this way it is possible to determine how degeneracies are removed due to spin-orbit interaction. Detailed calculations need to be performed in order to assess the magnitude of the spin-orbit splittings and other relativistic effects.

### 3-10b Relativistic effects in atoms

Before considering the relativistic corrections for the electronic states of crystals, we should review, in reference to atoms, certain results which could serve as guidelines in more complex cases.

Relativistic self-consistent equations for atoms can be set up using a formalism very similar to that of the Hartree-Fock formalism except for replacing the Schrödinger with the Dirac equation.<sup>[41]</sup> For heavy atoms, self-consistent relativistic calculations are required in order to obtain theoretical results in reasonable agreement with experimental data. For light atoms, however, it is sufficient to solve the non-relativistic self-consistent equations of the Hartree-Fock method, and then treat the relativistic terms  $H_v$ ,  $H_d$ , and  $H_{so}$  by perturbation theory. Detailed calculations for atoms along these lines are described by Herman and Skillman.<sup>[42]</sup>

Now we wish to discuss some features of the relativistic corrections to the results of non-relativistic atomic calculations. Let  $\varphi_{nlm}(\mathbf{r})$ ,  $E_{nl}$ , and  $V_a(\mathbf{r})$  indicate the wave functions, the energies, and the self-consistent atomic potential obtained from the Hartree-Fock calculations; then consider the effect of the relativistic terms  $H_v$ ,  $H_d$ ,  $H_{so}$  to the first order in perturbation theory.

(i) The term  $H_v = -(\mathbf{p}^4/8m^3c^2)$  gives a negative expectation value for any atomic orbital  $\varphi_{nlm}$ . By observing that

$$\frac{\mathbf{p}^2}{2m} \varphi_{nlm} = [E_{nl} - V_a(\mathbf{r})] \varphi_{nlm}$$

and by applying again the operator  $\mathbf{p}^2/2m$ , we find that the expectation value  $\varepsilon_v = \langle \varphi_{nlm} | H_v | \varphi_{nlm} \rangle$  is given by

$$\varepsilon_v = -\frac{1}{2mc^2} \int_0^\infty r^2 R_{nl}^2(r) [E_{nl} - V_a(r)]^2 dr.$$

(ii) The term  $H_d = -(\hbar^2/4m^2c^2) \nabla V_a \cdot \nabla$  gives a correction

$$\varepsilon_d = -\frac{\hbar^2}{4m^2c^2} \int_0^\infty r^2 R_{nl}(r) \frac{dV_a(r)}{dr} \frac{dR_{nl}(r)}{dr} dr.$$

This correction is positive, and important only for  $s$  states; it is negligible for states with  $l \neq 0$ . In fact, in the special case of a simple coulombic potential, we have  $V(r) = -ze^2/r$  and  $\nabla^2 V(r) = 4\pi z e^2 \delta(\mathbf{r})$ . The Darwin term becomes  $(\pi z e^2 \hbar^2 / 2m^2 c^2) \delta(\mathbf{r})$  in this case, and has an expectation value different from zero only for  $s$  states.

(iii) Finally, we consider the term  $H_{so}$ . Since the potential  $V_a(r)$  is spherically symmetric, we can write  $\nabla V_a = (\mathbf{r}/r) dV_a(r)/dr$ . By defining  $\mathbf{l} = \mathbf{r} \times \mathbf{p}$ ,

$$H_{so} = \frac{\hbar}{4m^2c^2} \frac{1}{r} \frac{dV_a(r)}{dr} \boldsymbol{\sigma} \cdot \mathbf{l}.$$

The operator  $H_{so}$  couples the operator  $\boldsymbol{\sigma}$  in spin space with the angular momentum  $\mathbf{l}$  in ordinary space, and so is invariant only under simultaneous rotations in both spin and ordinary space. The effect of  $H_{so}$  in removing the degeneracies of non-relativistic results can be found with the aid of group theory, as explained in Section 1-5. From (1-45) we see that a state with orbital angular momentum  $l$  and degeneracy  $2(2l + 1)$  is split into a state with total angular momentum  $j = l + \frac{1}{2}$  and degeneracy  $2l + 2$ , and a state with total angular momentum  $j = l - \frac{1}{2}$  and degeneracy  $2l$ . An  $s$  state is not split.

The spin-orbit correction term can be computed easily, and turns out to be<sup>[42,43]</sup>

$$\varepsilon_{so} = \begin{cases} \frac{1}{2} l \xi_{nl} & \text{if } j = l + \frac{1}{2}, \\ -\frac{1}{2} (l + 1) \xi_{nl} & \text{if } j = l - \frac{1}{2}; \end{cases}$$

$$\xi_{nl} = \frac{\hbar^2}{2m^2c^2} \int_0^\infty dr r^2 R_{nl}^2(r) \frac{1}{r} \frac{dV_a(r)}{dr}.$$

while  $\varepsilon_{so} = 0$  for  $l = 0$ .

So far we have considered relativistic effects using first order perturbation theory. Such a procedure, however, neglects some important indirect effects. Because of the mass velocity operator  $H_v$ , the relativistic wave functions are expected to be more concentrated near the nucleus. The effect of the mass-velocity operator on the valence states is twofold: on the one hand it lowers the eigenvalues because it has negative expectation values, while, on the other, it increases them because core states are drawn nearer the nucleus and a better screening results. The latter indirect effect is obviously not included in first order perturbation theory, and in heavy atoms may compensate to a large extent for the previous effects, apart from spin-orbit splitting.

BIBLIOTHÈQUE  
DÉPARTEMENT DE PHYSIQUE  
Ecole Polytechnique Fédérale de  
PHB - Ecouteries  
CH - 1015 LAUSANNE Suisse  
Tél. 021-471111

## ELECTRONIC STATES AND OPTICAL TRANSITIONS

### 3-10c Relativistic effects in crystals

The importance of relativistic effects on the electronic states in crystals is due to the fact that the potential is very strong near the nuclei and the kinetic energy is consequently large, so that the electron velocity is comparable to the velocity of light. The corrections become more important for heavy elements; for instance, the spin-orbit separation at point  $\Gamma$  for valence bands in silicon ( $z = 14$ ) is about 0.04 eV, while for germanium ( $z = 32$ ), it is about 0.29 eV.

When accurate calculations are needed, the natural way to deal with the problem is to consider the Dirac equation directly. In the last few years all the methods of band calculations described in this chapter have been generalized to the relativistic case.<sup>[44]</sup> The relativistically generalized procedures are very similar to the corresponding non-relativistic ones. One simply considers either Bloch sums derived from relativistic atomic orbitals, or relativistic plane waves, or relativistic spherical waves, or relativistic augmented plane waves, and so on, the mathematical procedures remaining substantially the same as for non-relativistic cases. The difficulties of solving the Dirac equation directly are not very much greater than the difficulties of solving the Schrödinger equation; one has higher order secular determinants and more complicated expressions for the matrix elements, but the basic difficulty of relativistic calculations, as well as non-relativistic ones, is still that of building up a reasonable potential sufficiently close to the actual self-consistent crystal potential to give meaningful results. Within a given band structure method, the choice of whether to use the Dirac equation, or approximate perturbation procedures on the non-relativistic results, depends largely on the atomic number of the atoms forming the crystal; it depends, too, on the values of the important energy gaps of the substance when compared to the magnitude of the relativistic effects.

We shall now give a qualitative discussion of the relativistic corrections to a non-relativistic band structure calculation.

(i) The term

$$H_v = - \frac{\mathbf{p}^4}{8m^3c^2}$$

gives a negative expectation value on any electronic state. A smooth deformation of the band structure is expected, but no additional splitting is introduced.

(ii) The term

$$H_d = - \frac{\hbar^2}{4m^2c^2} \nabla V \cdot \nabla$$

gives an effect that is strongly dependent on the angular momentum. It is largest for  $s$ -like states and small for  $p$ -like or  $d$ -like states, etc. A different relative shift is thus expected, and, in some crystals, there is a resulting inversion of the order of some levels as will be shown in Chapter 4. No additional splitting is introduced.

(iii) The term

$$H_{so} = \frac{\hbar}{4m^2c^2} \boldsymbol{\sigma} \cdot (\nabla V \times \mathbf{p})$$

is spin dependent and removes some degeneracies of non-relativistic results.

When the crystal potential is taken as the sum of atomic-like, spherically symmetric potentials [as in eq. (3-20)], the  $H_{so}$  term can be written as

$$H_{so} = \frac{\hbar}{4m^2c^2} \sum_{\tau_v} \sum_{d_\mu} \frac{1}{|\mathbf{r} - \mathbf{d}_\mu - \boldsymbol{\tau}_v|} \frac{dV_\mu(\mathbf{r} - \mathbf{d}_\mu - \boldsymbol{\tau}_v)}{d(\mathbf{r} - \mathbf{d}_\mu - \boldsymbol{\tau}_v)} \boldsymbol{\sigma} \cdot \mathbf{l}(\mathbf{r} - \mathbf{d}_\mu - \boldsymbol{\tau}_v).$$

This operator is important only near the nuclei, where the crystal wave functions are atomic-like, and it explains why, for most crystals, the spin-orbit splitting can be calculated by the tight binding approach even though that approach does not give reliable results for the total energy of the electronic state.

Let us consider some relations which enable us to calculate the spin-orbit splitting in the tight binding scheme. As in (3-15), we consider Bloch sums

$$\Phi_{\mu\nu}(\mathbf{k}, \mathbf{r}) = \frac{1}{\sqrt{N}} \sum_{\tau_v} e^{i\mathbf{k} \cdot \boldsymbol{\tau}_v} \varphi_{\mu\nu}(\mathbf{r} - \mathbf{d}_\mu - \boldsymbol{\tau}_v),$$

where  $v$  now denotes the quantum numbers ( $nlms$ ), including the spin quantum number  $s$ . In computing the matrix elements of  $H_{so}$ , only one-centre integrals among degenerate Bloch sums are important in first order. Thus we obtain matrix elements of the type

$$\langle \Phi_{\mu'n'l'm's'} | H_{so} | \Phi_{\mu nlms} \rangle = \delta_{\mu'\mu} \delta_{n'n} \delta_{l'l} \langle s' | \boldsymbol{\sigma} | s \rangle \cdot \langle Y_{l'm'} | \mathbf{l} | Y_{lm} \rangle \frac{1}{2\hbar} \xi_{\mu nl},$$

where

$$\xi_{\mu nl} = \frac{\hbar^2}{2m^2c^2} \int_0^\infty dr r^2 R_{\mu nl}^2(r) \frac{1}{r} \frac{dV_\mu(r)}{dr} \quad (3-71)$$

is the same expression we found in the atomic case.

The matrix elements in both spin and angular parts can be evaluated immediately. Using the Pauli matrices (1-37) we obtain, in fact,

$$\begin{aligned} \langle u_+ | \boldsymbol{\sigma} | u_+ \rangle \cdot \langle Y_{lm} | \mathbf{l} | Y_{l'm'} \rangle &= \langle Y_{lm} | l_z | Y_{l'm'} \rangle, \\ \langle u_- | \boldsymbol{\sigma} | u_- \rangle \cdot \langle Y_{lm} | \mathbf{l} | Y_{l'm'} \rangle &= -\langle Y_{lm} | l_z | Y_{l'm'} \rangle, \\ \langle u_+ | \boldsymbol{\sigma} | u_- \rangle \cdot \langle Y_{lm} | \mathbf{l} | Y_{l'm'} \rangle &= \langle Y_{lm} | l_x - il_y | Y_{l'm'} \rangle, \\ \langle u_- | \boldsymbol{\sigma} | u_+ \rangle \cdot \langle Y_{lm} | \mathbf{l} | Y_{l'm'} \rangle &= \langle Y_{lm} | l_x + il_y | Y_{l'm'} \rangle, \end{aligned}$$

which can be immediately evaluated from the general properties of angular momentum operators<sup>[43]</sup>

$$l_z Y_{lm} = m\hbar Y_{lm}, \quad (3-72a)$$

$$(l_x + il_y) Y_{lm} = [(l - m)(l + m + 1)]^{1/2} \hbar Y_{l,m+1}, \quad (3-72b)$$

$$(l_x - il_y) Y_{lm} = [(l + m)(l - m + 1)]^{1/2} \hbar Y_{l,m-1}. \quad (3-72c)$$

The above results allows us to relate crystal spin-orbit separation to atomic spin-orbit parameters in a particularly simple way. Use of symmetry introduces simplifications at high symmetry points. In fact one can take linear combinations which transform according to the irreducible representations of the crystal double group.

## ELECTRONIC STATES AND OPTICAL TRANSITIONS

### References and notes

For excellent reviews of atomic and band structure calculations we suggest, for instance, the following books and articles: J. C. SLATER, *Quantum Theory of Atomic Structure*, vols. 1–2 (McGraw-Hill, 1960); J. CALLAWAY, *Energy Band Theory* (Academic Press, 1964); J. C. SLATER, *Quantum Theory of Molecules and Solids*, vols. 1–3 (McGraw-Hill, 1967); B. ALDER, S. FERNBACK, and M. ROTENBERG (editors), *Methods in Computational Physics*, vol. 8, *Energy Bands in Solids* (Academic Press, 1968); W. A. HARRISON, *Solid State Theory* (McGraw-Hill, 1970); G. C. FLETCHER, *Electron Band Theory of Solids* (North-Holland, 1971); J. M. ZIMAN, in *Solid State Physics* **26**, 1 (1971); P. M. MARCUS, J. F. JANAK, and A. R. WILLIAMS (editors), *Computational Methods in Band Theory* (Plenum Press, 1971).

[1] M. BORN and J. R. OPPENHEIMER, *Ann. Phys.* **84**, 457 (1927). For further reference, see J. M. ZIMAN, *Electrons and Phonons* (Oxford University Press, 1962).

[2] The derivation of the Hartree–Fock equations and their application to atoms can be found in F. SEITZ, *The Modern Theory of Solids* (McGraw-Hill, 1940). For a discussion of the Hartree–Fock equations for free electron gas, see D. PINES, *Elementary Excitations in Solids* (Benjamin, 1963). A simplified approach to the exchange potential in the Hartree–Fock equations has been considered by J. C. SLATER, *Phys. Rev.* **81**, 385 (1951). Screening corrections to the Slater exchange potential have been considered by J. E. ROBINSON, F. BASSANI, R. S. KNOX, and J. R. SCHRIEFFER, *Phys. Rev. Letters* **9**, 215 (1962). See also E. O. KANE, *Phys. Rev.* **4B**, 1910 (1971); **5B**, 1493 (1972). For a discussion of electronic correlation in crystals, see W. KOHN and L. SHAM, *Phys. Rev.* **140**, A 1133 (1965); L. HEDIN, *Phys. Rev.* **139**, A 796 (1965); W. BRINKMAN and B. GOODMAN, *Phys. Rev.* **149**, 597 (1966); N. O. LIPARI and W. B. FOWLER, *Phys. Rev.* **2B**, 3354 (1970).

[3] F. BLOCH, *Z. Physik* **52**, 555 (1928).

[4] G. WANNIER, *Phys. Rev.* **52**, 191 (1937).

[5] J. C. SLATER and G. F. KOSTER, *Phys. Rev.* **94**, 1498 (1954); K. LONDI, *Phys. Rev.* **B9**, 2433 (1974).

[6] E. E. LAFON and C. C. LIN, *Phys. Rev.* **152**, 579 (1966). R. C. CHANEY, C. C. LIN, and E. E. LAFON, *Phys. Rev. B* **3**, 459 (1971).

[7] D. E. ELLIS and G. S. PAINTER, *Phys. Rev.* **B2**, 2887 (1970).

[8] F. BASSANI, R. S. KNOX, and W. BEAL FOWLER, *Phys. Rev. A* **137**, 1217 (1965).

[9] T. L. GILBERT, in *Molecular Orbitals in Chemistry, Physics and Biology* (edited by P. O. LÖWDIN and B. PULLMAN, Academic Press, 1964), p. 405. See also A. B. KUNZ, *Phys. Rev.* **B7**, 5369, (1973); A. B. KUNZ and D. J. MICKISH, *Phys. Rev. B8*, 779 (1973).

[10] For further details on the molecular tight binding method see Section 4–5 and references quoted therein.

[11] A. SOMMERFELD and H. BETHE, *Handbuch der Physik*, vol. 24 (Berlin, 1933); C. HERRING, *Phys. Rev.* **57**, 1163 (1940).

[12] For the generalization of the OPW method to the many-body problem, see F. BASSANI, J. ROBINSON, B. GOODMAN, and J. R. SCHRIEFFER, *Phys. Rev.* **127**, 1969 (1962). For further details about the OPW method and its applications, we refer the reader to: T. O. WOODRUFF, *Solid State Physics* **4**, 367 (1957); R. S. KNOX and F. BASSANI, *Phys. Rev.* **124**, 652 (1961); F. BASSANI and M. YOSHIMINE, *Phys. Rev.* **130**, 20 (1963); F. BASSANI, in *Semiconductors and Semimetals* (edited by R. K. WILLARDSON and A. C. BEER, Academic Press, 1966), vol. 1, p. 21. N. O. LIPARI and W. B. FOWLER, *Phys. Rev.* **2B**, 3354 (1970); G. E. JURAS, J. E. MONAHAN, C. M. SHAKIN, and R. M. THALER, *Phys. Rev.* **5B**, 4000 (1972).

[13] A. B. KUNZ, *Phys. Rev.* **180**, 934 (1969); N. O. LIPARI and A. B. KUNZ, *Phys. Rev. 4B*, 4639 (1971), and references quoted therein.

[14] F. BASSANI and V. CELLI, *Nuovo Cimento* **11**, 805 (1959).

[15] W. SHOCKLEY, *Phys. Rev.* **52**, 866 (1937).

[16] For the pseudopotential formulation of the OPW method, we refer the reader to: J. C. PHILLIPS and L. KLEINMAN, *Phys. Rev.* **116**, 287 (1959); F. BASSANI and V. CELLI, *J. Phys. Chem. Solids* **20**, 64 (1961); M. H. COHEN and V. HEINE, *Phys. Rev.* **122**, 1821 (1961); B. J. AUSTIN, V. HEINE, and L. J. SHAM, *Phys. Rev.* **127**, 276 (1962). Further references and developments can be found in W. A. HARRISON, *Pseudopotentials in the Theory of Metals* (Benjamin, 1966).

[17] D. BRUST, J. C. PHILLIPS, and F. BASSANI, *Phys. Rev. Letters* **9**, 94 (1962).

[18] The earliest application of the idea of using experimental spectroscopic data of atoms or ions to give an accurate description of the atomic pseudopotential was by W. K. PROKOFJEW, *Z. Physik* **58**, 255 (1929), for the sodium atom.

[19] For pseudopotential models for atoms or ions, see, for instance: K. E. ANTONCIK, *J. Chem. Phys. Solids* **10**, 314 (1959); I. V. ABARENKOV and V. HEINE, *Phil. Mag.* **12**, 529 (1965); I. V. ABARENKOV

## METHODS OF CALCULATING THE ELECTRONIC BAND STRUCTURES OF CRYSTALS

and I. M. ANTONOVA, *Phys. Status Solidi* **20**, 643 (1967); E. S. GIULIANO and R. RUGGERI, *Nuovo Cimento* **61B**, 53 (1969). For a general review of model pseudopotentials and their developments see: V. HEINE, *Solid State Physics* **24**, 1 (1970); M. L. COHEN and V. HEINE, *Solid State Physics* **24**, 38 (1970); V. HEINE and D. WEAIKE, *Solid State Physics* **24**, 250 (1970); F. BASSANI and E. S. GIULIANO, *Nuovo Cimento* **8B**, 193 (1972).

- [20] E. WIGNER and F. SEITZ, *Phys. Rev.* **43**, 804 (1933); **46**, 509 (1934).
- [21] J. C. SLATER, *Phys. Rev.* **45**, 794 (1934).
- [22] F. C. VON DER LAGE and H. A. BETHE, *Phys. Rev.* **71**, 612 (1947).
- [23] D. G. BELL, *Rev. of Mod. Phys.* **26**, 311 (1953).
- [24] For further aspects of the cellular method, see for example, J. R. REITZ, *Solid State Physics* **1**, 1 (1955). For a discussion of boundary conditions in the cellular method see also: L. PINCHERLE, *Proc. Phys. Soc.* **72**, 281 (1958); S. L. ALTMANN and C. J. BRADLEY, *Proc. Phys. Soc.* **86**, 915 (1965); **92**, 764 (1967).
- [25] J. C. SLATER, *Phys. Rev.* **51**, 846 (1937).
- [26] For a complete discussion of the APW method, see T. LOUCKS, *Augmented Plane Wave Method* (Benjamin, 1967). See also J. O. DIMMOCK, *Solid State Physics* **26**, 103 (1971).
- [27] H. SCHLOSSER and P. M. MARCUS, *Phys. Rev.* **131**, 2529 (1963).
- [28] See: A. B. KUNZ, W. B. FOWLER, and P. M. SCHNEIDER, *Phys. Letters* **28A**, 553 (1969). For crystals with a symmorphic space group, the APW method has been generalized to deal with any crystal potential by W. E. RUDGE, *Phys. Rev.* **181**, 1024 (1969).
- [29] The original formulation of Green's function method was given by J. KORRINGA, *Physica* **13**, 392 (1947), and P. M. MORSE, *Proc. Natn. Acad. Sci. (US)* **42**, 276 (1956). In these papers the scattering of a plane wave by an atom with a spherically symmetric potential was considered. The formulation of the method in terms of standard techniques using Green's functions was done by W. KOHN and N. ROSTOKER, *Phys. Rev.* **94**, 1411 (1954).
- [30] For the basic mathematical properties of Green's function method we refer, for example, to B. FRIEDMAN, *Principles and Techniques of Applied Mathematics* (J. Wiley, 1956).
- [31] The close relationship between the APW method and Green's function method has become apparent as a result of some basic papers: J. M. ZIMAN, *Proc. Phys. Soc.* **86**, 337 (1965); J. C. SLATER, *Phys. Rev.* **145**, 599 (1966); R. LLOYD, *Proc. Phys. Soc.* **86**, 825 (1965); K. H. JOHNSON, *Phys. Rev.* **150**, 429 (1966); J. RUBIO and F. GARCIA-MOLINER, *Proc. Phys. Soc.* **91**, 739 (1967); **92**, 206 (1967).
- [32] The equivalence for practical calculations of Green's functions method and the APW method has been established, in the case of copper crystals, by B. SEGALL, *Phys. Rev.* **125**, 109 (1962), and G. A. BURDICK, *Phys. Rev.* **129**, 138 (1963).
- [33] T. S. KUHN and J. H. VAN VLEK, *Phys. Rev.* **79**, 382 (1950).
- [34] For a detailed account of the quantum defect method see F. S. HAM, *Solid State Physics* **1**, 127 (1955).
- [35] J. BARDEEN, *J. Chem. Phys.* **6**, 367 (1938); F. SEITZ, *The Modern Theory of Solids* (McGraw-Hill, 1940), p. 352.
- [36] W. SHOKLEY, *Phys. Rev.* **78**, 173 (1950); G. DRESSELHAUS, A. F. KIP, and C. KITTEL, *Phys. Rev.* **98**, 368 (1955); E. O. KANE, *J. Phys. Chem. Solids* **1**, 82 (1956).
- [37] W. BRINKMAN and B. GOODMAN, *Phys. Rev.* **149**, 597 (1966).
- [38] M. CARDONA and F. H. POLLAK, *Phys. Rev.* **142**, 530 (1966).
- [39] E. O. KANE, *J. Phys. Chem. Solids* **8**, 38 (1959).
- [40] For a discussion of the Dirac relativistic equation, see M. E. ROSE, *Relativistic Electron Theory* (Wiley, 1961).
- [41] Relativistic self-consistent calculations for a number of atoms and ions have been performed by D. LIBERMAN, J. T. WALER, and DON T. CROMER, *Phys. Rev.* **137**, A27 (1965).
- [42] Non-relativistic calculation for all atoms and inclusion of relativistic terms through perturbation theory is dealt with by F. HERMAN and S. SKILLMAN, *Atomic Structure Calculations* (Prentice-Hall, 1963).
- [43] E. U. CONDON and G. H. SHORTLEY, *The Theory of Atomic Spectra* (Cambridge University Press, 1953), p. 122.
- [44] The relativistic generalization of the OPW method has been given by P. SOREN, *Phys. Rev.* **132**, A1706 (1965). The relativistic generalization of the APW method has been given by T. L. LOUCKS, *Phys. Rev.* **139**, A1333 (1965). Green's functions method has been generalized relativistically by Y. ONODERA and M. OKAZAKI, *J. Phys. Soc. Japan* **21**, 1273 (1966). For the relativistic generalization of the pseudopotential method, see PAY-JUNE LIN-CHUNG and S. TEITLER, *Phys. Rev.* **6B**, 1419 (1972).

École Polytechnique Fédérale  
CH-1015 Lausanne Suisse  
Tél. 021-47 11 11

## CHAPTER 4

# ELECTRONIC BAND STRUCTURE IN SOME CRYSTALS

IN THIS chapter we report some examples of electronic state calculations for different types of crystals. Our principal objective is to discuss those features which depend mainly on the symmetry of the crystal rather than on the detailed crystal potential. Using crystal symmetry, in most cases it is possible to make qualitative remarks on the expected sequence of the crystal states and to understand some general trends which occur amongst crystals of a given lattice type. We shall first consider some results for cubic crystals with the diamond and zincblende structure. We shall then consider examples of anisotropic crystals. In particular, we shall discuss in some detail graphite and hexagonal boron nitride (typical examples of "layer" crystals), and selenium and tellurium (typical linear chain crystals). Finally, we shall briefly comment on the band structures of some large gap insulators, molecular crystals, and simple metals.

### 4-1 Energy bands of isoelectronic semiconductors with the diamond and zincblende structure

#### 4-1 a Symmetry properties of the diamond lattice

The diamond structure (Fig. 2-2) has been illustrated in the examples given throughout Chapter 2. We here recall that its translational symmetry is that of a face-centred cubic lattice with primitive translation vectors given by (2-8) and primitive vectors of the reciprocal lattice given by (2-9).

As can be seen in Fig. 2-2, there are two atoms per unit cell in the positions  $\mathbf{d}_1 = (0, 0, 0)$ ,  $\mathbf{d}_2 = a/4 (1, 1, 1)$ . Carbon, silicon, germanium, and grey tin crystallize in the diamond structure with lattice constant  $a$  equal to 3.56, 5.43, 5.65, and 6.46 Å, respectively.

The first Brillouin zone is the truncated octahedron of Fig. 2-3. The symmetry operations have been listed in Table 2-3. The irreducible representations of the most important symmetry points in the Brillouin zone have been obtained in Chapter 2 and are given in Tables 2-4 to 2-16.

We now consider the symmetry properties of the eigenfunctions of the diamond lattice, and we show how to construct symmetrized combinations of plane waves and symmetrized combinations of Bloch sums to be used as basis sets for expanding the exact eigenfunctions as described in Chapter 3 in connection with the different calculational methods. The classification of the diamond "empty lattice" eigenstates, which result from considering only the uniform part of the potential, can be carried out by

applying the procedures of Section 3-3c. Given a  $\mathbf{k}$  vector of the Brillouin zone, we consider plane waves of the type

$$\frac{1}{\sqrt{NQ}} e^{i(\mathbf{k} + \mathbf{h}_j) \cdot \mathbf{r}}$$

with the same modulus  $|\mathbf{k} + \mathbf{h}_j|$ . The set of plane waves so obtained forms a basis for a representation of the little group of  $\mathbf{k}$ , which can then be decomposed into a number of irreducible representations. As an example at the point  $\Gamma$ , let us consider the degenerate plane waves of modulus 3 (in units of  $(\hbar^2/2m)(4\pi^2/a^2)$ ):

$$\left. \begin{array}{ll} \psi_1 = \langle 111 \rangle, & \psi_5 = \langle \bar{1}\bar{1}\bar{1} \rangle, \\ \psi_2 = \langle 1\bar{1}\bar{1} \rangle, & \psi_6 = \langle \bar{1}11 \rangle, \\ \psi_3 = \langle \bar{1}\bar{1}\bar{1} \rangle, & \psi_7 = \langle 1\bar{1}1 \rangle, \\ \psi_4 = \langle \bar{1}\bar{1}1 \rangle, & \psi_8 = \langle 11\bar{1} \rangle, \end{array} \right\} \quad (4.1)$$

where  $\langle l_1 l_2 l_3 \rangle$  denotes the plane wave

$$\langle l_1 l_2 l_3 \rangle = \frac{1}{\sqrt{NQ}} e^{i(2\pi/a)(l_1x + l_2y + l_3z)}.$$

The eight functions (4-1) constitute a basis for a representation of the group of  $\mathbf{k}$  at  $\mathbf{k} = 0$ . The matrix representatives

$$D_{ij}(\{R | a\}) = \int \psi_i^* O_{\{R|a\}} \psi_j d\mathbf{r}$$

can be explicitly calculated operating on the plane waves (4-1) as shown in Section 3-3c. The character of the representation is the sum of the diagonal matrix elements and gives for each class of the group of Table 2-3 at  $\mathbf{k} = 0$ :

$E$	$C_4^2$	$C_3$	$IC_4$	$IC_2$	$I$	$IC_4^2$	$IC_3$	$C_4$	$C_2$
8	0	2	0	2	0	0	0	0	0

The representation with the above character can be decomposed into the irreducible representations

$$\Gamma_1 + \Gamma'_2 + \Gamma'_{25} + \Gamma_{15}$$

as can be seen by inspection using the characters of Table 2-4. Application of the projection operators (1-21) or (1-25) corresponding to the above irreducible representations on the plane waves (4-1), gives the appropriate symmetrized combinations of plane waves. A list of the symmetry combinations of plane waves is given by Herman<sup>[1]</sup> for a large number of sets of plane waves.

Similarly, the classification of the empty lattice eigenvalues at the symmetry points  $L$  and  $X$  can be obtained, and these are given, together with the classification at  $\Gamma$ , in Table 4-1. Also, for convenience, the bands for the empty diamond lattice are given in Fig. 4-1.

The classification of the Bloch sums can be carried out applying the procedure described in Section 3-2c. The Bloch sums of vector  $\mathbf{k}$ , derived from degenerate atomic orbitals, constitute a basis for a representation of the little group of  $\mathbf{k}$  which can be

## ELECTRONIC STATES AND OPTICAL TRANSITIONS

TABLE 4-1. Classification of the empty lattice eigenvalues at the symmetry points  $\Gamma$ ,  $L$ , and  $X$  of the diamond structure

	Number of plane waves	Empty lattice eigenvalues in units of $(\hbar^2/2m)(4\pi^2/a^2)$	Irreducible representations
Point $\Gamma$ $\mathbf{k} = (0, 0, 0)$	1	$(0, 0, 0)^2$	$\Gamma_1$
	8	$(1, 1, 1)^2$	$\Gamma'_{25}$
	6	$(2, 0, 0)^2$	$\Gamma'_{15}$
	12	$(2, 2, 0)^2$	$\Gamma'_{12}$
Point $L$ $\mathbf{k} = \frac{2\pi}{a} (\frac{1}{2}, \frac{1}{2}, \frac{1}{2})$	2	$(\frac{1}{2}, \frac{1}{2}, \frac{1}{2})^2$	$L_1$
	6	$(\frac{3}{2}, \frac{1}{2}, \frac{1}{2})^2$	$L'_1$
	6	$(\frac{1}{2}, \frac{3}{2}, \frac{1}{2})^2$	$L'_2$
	6	$(\frac{3}{2}, \frac{1}{2}, \frac{3}{2})^2$	$L'_3$
	2	$(\frac{3}{2}, \frac{3}{2}, \frac{3}{2})^2$	$L'_2$
Point $X$ $\mathbf{k} = \frac{2\pi}{a} (1, 0, 0)$	2	$(1, 0, 0)^2$	$X_1$
	4	$(0, 1, 1)^2$	$X_1$
	8	$(1, 2, 0)^2$	$X_2$
	8	$(2, 1, 1)^2$	$X_3$
			$2X_1$

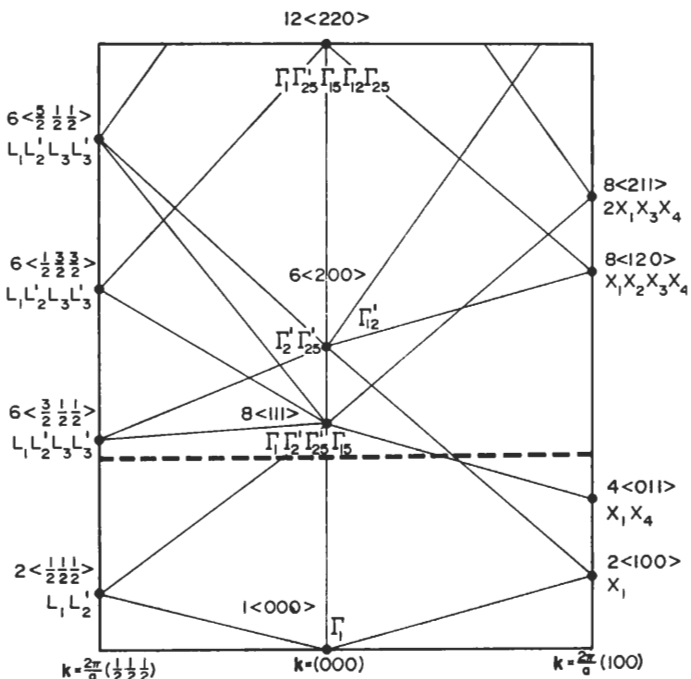


FIG. 4-1. Energy bands for the empty diamond lattice. The Fermi level corresponding to eight free electrons per unit cell is indicated with a dashed horizontal line.

reduced into a number of irreducible representations. As an example, let us consider at the point  $\Gamma$  the two Bloch sums

$$\left. \begin{aligned} s_{A_1} &= \frac{1}{\sqrt{N}} \sum_{\tau_v} e^{i\mathbf{k} \cdot \tau_v} \varphi_s(\mathbf{r} - \mathbf{d}_1 - \tau_v), \\ s_{A_2} &= \frac{1}{\sqrt{N}} \sum_{\tau_v} e^{i\mathbf{k} \cdot \tau_v} \varphi_s(\mathbf{r} - \mathbf{d}_2 - \tau_v), \end{aligned} \right\} \quad (4-2)$$

where  $\mathbf{d}_1 = (0, 0, 0)$ ,  $\mathbf{d}_2 = a/4 (1, 1, 1)$ ,  $\mathbf{k} = 0$ , and  $\varphi_s$  is a  $s$ -like function. The Bloch sums  $s_{A_1}$  and  $s_{A_2}$  transform into each other under the symmetry operations of Table 2-3 and the matrix representatives

$$D_{IJ}(\{R | a\}) = \int s_{A_1}^* O_{\{R | a\}} s_{A_2} d\mathbf{r}$$

can be explicitly evaluated using (3-26). The character of the representation based on the two functions  $s_{A_1}$  and  $s_{A_2}$  can be obtained by considering the sum of diagonal matrix elements; for each class of the group of  $\mathbf{k} = 0$ , they are:

$E$	$C_4^2$	$C_3$	$IC_4$	$IC_2$	$I$	$IC_4^2$	$IC_3$	$C_4$	$C_2$
2	2	2	2	2	0	0	0	0	0

The representation with the above characters can be decomposed into the irreducible representations  $\Gamma'_1$  and  $\Gamma'_2$ , as is immediately evident from Table 2-4. In a similar way we obtain the classification of Bloch sums formed with  $p$  and  $d$  atomic orbitals and report the results in Table 4-2 for the symmetry points  $\Gamma$ ,  $L$ , and  $X$ . Using the

TABLE 4-2. Classification of Bloch sums derived from  $s$ ,  $p$ , and  $d$  orbitals for the diamond structure

	Symmetry of the atomic state	Number of degenerate Bloch sums	Irreducible representations
Point $\Gamma$ $\mathbf{k} = (0, 0, 0)$	$s$	2	$\Gamma'_1$ $\Gamma'_2$
	$p$	6	$\Gamma'_{25}$ $\Gamma'_{15}$
	$d$	10	$\Gamma_{12}$ $\Gamma'_{12}$ $\Gamma_{15}$ $\Gamma'_{25}$
Point $L$ $\mathbf{k} = \frac{2\pi}{a} (\frac{1}{2}, \frac{1}{2}, \frac{1}{2})$	$s$	2	$L'_1$ $L'_2$
	$p$	6	$L_1$ $L'_2$ $L_3$ $L'_3$
	$d$	10	$L_1$ $L'_2$ $2L_3$ $2L'_3$
Point $X$ $\mathbf{k} = \frac{2\pi}{a} (1, 0, 0)$	$s$	2	$X_1$
	$p$	6	$X_1$ $X_3$ $X_4$
	$d$	10	$2X_1$ $X_2$ $X_3$ $X_4$

projection operators, it is easy to obtain the symmetrized combinations of Bloch sums. For example, the symmetrized combinations of Bloch sums (4-2) belonging to the irreducible representations  $\Gamma'_1$  and  $\Gamma'_2$  are

$$s_{A_1} + s_{A_2} \quad \text{and} \quad s_{A_1} - s_{A_2}$$

respectively. In a similar way, the six functions derived from degenerate  $p$  orbitals transform according to  $\Gamma'_{25} + \Gamma_{15}$ . The symmetrized combinations of Bloch sums for the above irreducible representations are

$$\Gamma'_{25} \begin{cases} p_{xA_1} - p_{xA_2}, \\ p_{yA_1} - p_{yA_2}, \\ p_{zA_1} - p_{zA_2}, \end{cases} \quad \Gamma_{15} \begin{cases} p_{xA_1} + p_{xA_2}, \\ p_{yA_1} + p_{yA_2}, \\ p_{zA_1} + p_{zA_2}. \end{cases}$$

We see that  $\Gamma_1$  and  $\Gamma'_{25}$  are states with high electronic densities in the direction of the bond midway between the atoms; they are referred to as bonding states since this is the condition for the lowering of their energy with respect to that of the free atoms in the Heitler-London theory of the chemical bond.  $\Gamma'_2$  and  $\Gamma_{15}$  are the corresponding antibonding states with small electron density in the direction of the bonds, midway between the atoms.

#### 4-1 b Electronic state calculations in diamond, silicon, germanium, and grey tin

The configuration of valence electrons in the free atoms for carbon, silicon, germanium, and tin is



with inner shells completely filled. The inner shells give rise to occupied core states with energies approximately equal to those of the atomic states. The crystal states with higher energies have been investigated using different methods, and we report here some results for diamond, silicon, germanium, and grey tin.

#### *Band structure calculations for diamond<sup>[12]</sup>*

A large number of energy band calculations has been performed on diamond because this is the basic covalent compound with tetrahedral structure and small atomic number, and can then be used as a test for the reliability of the method of calculation adopted. A line of attack is based on the tight binding method described in Section 3-2 and has been pursued, with various modifications on the crystal potentials and on the basic expansion set, for a period of 20 years, starting from the work of Hall (1952) to the new calculations of Ellis *et al.* (1971). The difficulties of the tight binding method for strongly covalent materials have been partly overcome or by using the two-centre integrals as disposable parameters, as originally suggested by Slater and Koster, or by using a larger expansion set of atomic like orbitals with freedom in the radial wave functions which can in principle be optimized by the variational principle as shown by Ellis *et al.* These authors calculated the Hamiltonian matrix elements (3-21) by direct integration on the unit cell with a numerical sampling procedure, thus including also the contribution of three-centre integrals which are usually neglected.

Another line of attack which has been particularly fruitful for understanding the basic electronic properties of a large number of tetrahedrally coordinated compounds is based on the OPW approach described in Section 3-3. It was initiated by Herman in 1952, who was able to obtain for the first time the basic band structure of diamond and germanium, and was pursued by many authors with various improvements on the choice of the crystal potential. Also the APW method of Section 3-6 has been tested on diamond by Keown, who was also able to obtain the basic band structure using

a muffin-tin potential made up of spherical atomic-like potentials around the two atoms per unit cell and treating the average potential between the spheres as a disposable parameter.

To exemplify the energy band structure of diamond, we show in Fig. 4-2 a typical result obtained with OPW method. Although the actual positions of the bands depend on the detailed nature of the individual calculations, certain features are common to any of the band structure calculations described above. At the point  $\Gamma$  the highest valence state is the triply degenerate state  $\Gamma'_{25}$  and the lowest conduction state is  $\Gamma_{15}$ . Since there are eight valence electrons per unit cell, they fully occupy the states  $\Gamma_1$  and  $\Gamma'_{25}$ . At the point  $L$  the occupied states are  $L'_2$ ,  $L_1$ , and  $L'_3$ . At the point  $X$  all representations are two-dimensional (see Table 2-8) and the states  $X_1$  and  $X_4$  are completely filled. Note that the connection between the states at the symmetry points  $\Gamma$ ,  $X$ , and  $L$  of Fig. 4-2 are determined according to the compatibility relations of Table 2-10 and obey the non-crossing rule for states of the same symmetry.

The minimum of the lowest conduction band is the state  $\Delta_1$  at a point toward the zone edge, and the energy gap between valence and conduction bands is about 5 eV. The minimum is not at the zone boundary  $X$  because the relation

$$\frac{\partial E_{\Delta_1}}{\partial \mathbf{k}} + \frac{\partial E_{\Delta_2'}}{\partial \mathbf{k}} = 0 \quad (4-3)$$

holds at  $X$  due to time reversal symmetry (see the analogous relation 2-7b).

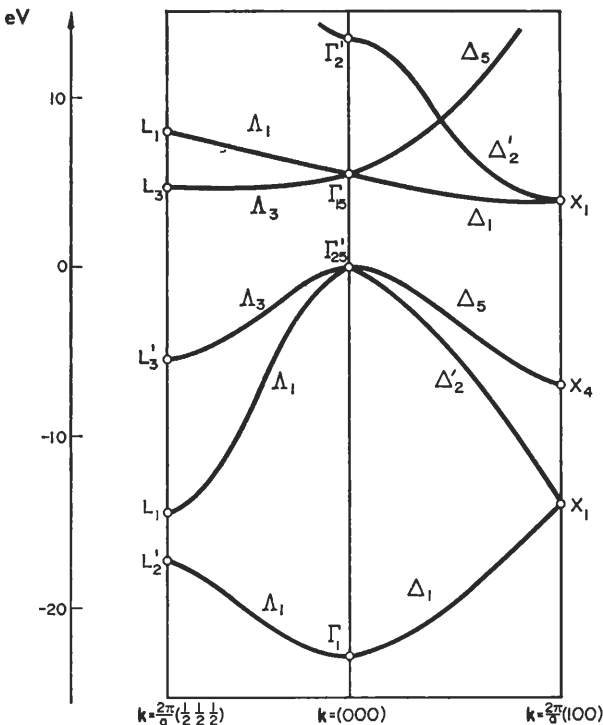


FIG. 4-2. Energy bands for diamond. (From Bassani and Yoshimine, ref. [2].) The zero of energy has been taken to lie at the top of the valence band.

## ELECTRONIC STATES AND OPTICAL TRANSITIONS

It may be instructive to compare the results of calculations performed on diamond by different authors; this is done for the relevant valence and conduction states in Table 4-3. The differences in the results indicate how sensitive the eigenvalues are to the uncertainties in the potential and/or to the approximations of the method.

TABLE 4-3. Energy eigenvalues (in eV) at the symmetry points  $\Gamma$ ,  $L$ , and  $X$  for diamond as calculated by some authors of ref. [2]. The zero of energy is taken to coincide with the lowest  $\Gamma_1$  valence state

Crystal states	Kleinman <i>et al.</i> <sup>a)</sup>	Cohan <i>et al.</i> <sup>b)</sup>	Bassani <i>et al.</i> <sup>c)</sup>	Keown <sup>d)</sup>	Painter <i>et al.</i> <sup>e)</sup>
$\Gamma_1$	0.0	0.0	0.0	0.0	0.0
$\Gamma'_{25}$	21.9	25.2	23.2	19.6	19.6
$\Gamma_{15}$	28.0	34.7	28.7	25.4	25.6
$L'_2$	5.6	8.8	5.5	5.2	5.1
$L_1(1)$	11.7	10.9	8.4	8.0	7.9
$L'_3$	17.2	24.5	17.8	17.2	17.2
$L_3$	30.9	36.7	28.0	28.2	28.5
$L_1(2)$	30.9	35.4	31.2	27.5	27.8
$X_1(1)$	10.5	12.2	9.1	8.1	8.0
$X_4$	15.2	21.8	14.7	14.4	14.3
$X_1(2)$	29.0	36.1	27.8	25.5	25.9

(a) Pseudopotential method.

(b) Tight binding method with expansion set formed with bonding and antibonding combinations of Bloch sums.

(c) OPW method.

(d) APW method.

(e) Tight binding approach associated with the discrete variational method.

It can be noticed that these differences are quite small in general and do not change the basic features of the band structure. This can be taken as another indication that the relative positions of the levels are mainly determined by symmetry and do not depend, to a large extent, on the methods of calculation used and on the details of the potential. The reason for this will be discussed at the end of this section for the tetrahedrally coordinated compounds.

### Energy band structure of silicon and germanium

The band structures of silicon and germanium have been widely investigated by a number of authors<sup>[3]</sup> with the OPW approach following the pioneering work of Herman (1954).<sup>[3]</sup> Application of the OPW method with a crystal potential constructed as the sum of Hartree-Fock atomic potentials with the Slater approximation to exchange, very soon indicated silicon and germanium to be semiconductors with small energy gaps and the minimum of the conduction band to respectively occur along the  $\Delta$  axis and at the point  $L$  of the Brillouin zone. Further improvements, which are still being made, concern the treatment of exchange, corrections to the core energies with respect to their atomic values, attempts to self-consistency; though these improvements are very important steps on the way to reliable *a priori* numerical calculations, they do not modify the basic results of Herman.<sup>[3]</sup> The pseudopotential method (see Section 3-4) has also been widely applied to obtain the energies throughout the Brillouin zone. The first application as an interpolation scheme to silicon and germanium was made

by Phillips.<sup>[4]</sup> Bassani and Celli<sup>[4]</sup> simplified the approach by showing that the Fourier transforms of the pseudopotential with large reciprocal lattice vectors could be taken equal to zero; with this simplification Brust *et al.*<sup>[4]</sup> were able to compute the density of states thus interpreting the optical constants of silicon and germanium. This approach was extended to a large number of semiconductors with tetrahedral coordination by Cohen and Bergstresser.<sup>[4]</sup> Also the  $\mathbf{k} \cdot \mathbf{p}$  method (see Section 3-9) has been used. Cardona and Pollak<sup>[5]</sup> obtain the energies throughout the Brillouin zone starting from the energies at  $\mathbf{k} = 0$  and using empirically determined values for the matrix elements of the  $\mathbf{k} \cdot \mathbf{p}$  operator; Brinkman and Goodman<sup>[6]</sup> use detailed *a priori* calculations performed at  $\mathbf{k} = 0$  with the OPW method to compute the matrix elements of the  $\mathbf{k} \cdot \mathbf{p}$  operator.

To illustrate some general features of the energy band calculations we now discuss in particular the procedure used by Cardona and Pollak<sup>[5]</sup> to obtain the band structure throughout the whole Brillouin zone from matrix elements of  $\mathbf{p}$  and energy gaps at the symmetry point  $\mathbf{k} = 0$ . Group theory selection rules allow one to simplify the number of independent parameters. The independent parameters and energy gaps are determined empirically to fit cyclotron resonance data and the position of some peaks in the experimental determination of optical constants as functions of frequency. The  $\mathbf{k} \cdot \mathbf{p}$  method is set up considering only 15 basis states corresponding to the free electron states with empty lattice eigenvalues  $(0,0,0)^2, (1,1,1)^2, (2,0,0)^2$  in units of  $(\hbar^2/2m)(4\pi^2/a^2)$  (see Table 4-1). Figure 4-3 shows their results for the energy bands of silicon. The

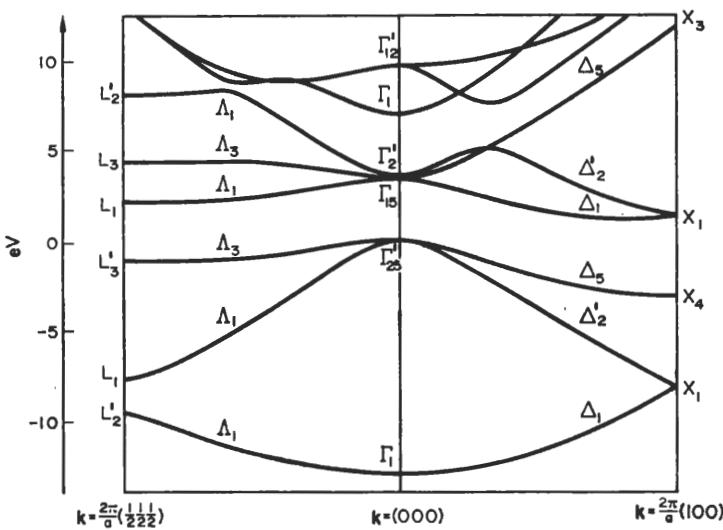


FIG. 4-3. Energy bands for silicon. (From ref. [5].)

highest valence state is  $\Gamma'_{25}$ , whilst the lowest conduction state at  $\Gamma$  is  $\Gamma_{15}$  and the minimum of the conduction band appears along the symmetry line  $\Delta$  with an indirect gap of  $\approx 1.2$  eV. In Fig. 4-4 we show the energy bands for germanium. In this case the highest valence state is still  $\Gamma'_{25}$  whilst the lowest conduction state at  $\mathbf{k} = 0$  is now  $\Gamma'_2$  and the minimum of the lowest conduction band appears at  $\mathbf{k} = (2\pi/a)(\frac{1}{2}, \frac{1}{2}, \frac{1}{2})$  and has symmetry  $L_1$ .

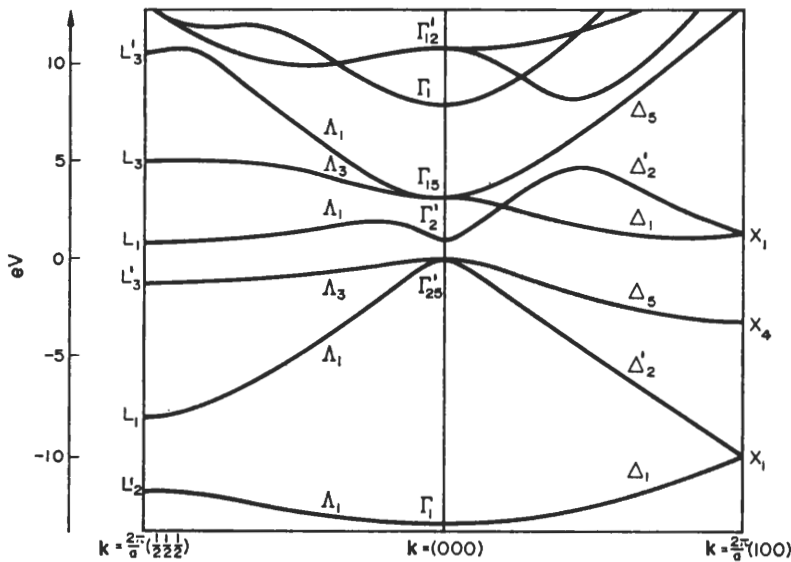


FIG. 4-4. Energy bands for germanium. (From ref. [5].)

*General trends in diamond, silicon, and germanium energy bands*

We now wish to discuss how the basic band structures and their systematic trends going from diamond to silicon to germanium can be understood on the basis of symmetry considerations.<sup>[7]</sup> For this it is sufficient to compare the free-electron energy bands of Fig. 4-1 and the energy bands structures of Fig. 4-2, 4-3, and 4-4 keeping in mind the perturbation approach of Section 3-3e which gives the relationship between the "empty lattice" eigenvalues and the crystal states.

Let us first consider the case of diamond (Fig. 4-2). The Bloch sums corresponding to the 1s core states transform as  $\Gamma_1$  and  $\Gamma'_2$ . From the classification of the empty lattice eigenvalues at the point  $\Gamma$  (Table 4-1), we thus expect a repulsive effect on the valence and conduction states  $\Gamma_1$  and  $\Gamma'_2$  because of the orthogonalization to the core wave functions of the same symmetry. The state  $\Gamma_1$  corresponding to the empty lattice eigenvalues  $(0, 0, 0)^2$  is expected to remain the lowest valence state, while the states  $\Gamma_1$  and  $\Gamma'_2$  with empty lattice eigenvalue  $(1, 1, 1)^2$  are pushed to higher energy with respect to  $\Gamma'_{25}$  and  $\Gamma_{15}$ , which do not have "core states" with the same symmetry. Furthermore, the state  $\Gamma'_{25}$  is expected to be lower in energy than  $\Gamma_{15}$  because of the interaction with the state of equal symmetry  $\Gamma'_{25}(2)$  corresponding to the empty lattice eigenvalue  $(2, 0, 0)^2$ . The expected sequence of the levels at the point  $\Gamma$  is then

$$\Gamma_1 \ll \Gamma'_{25} < \Gamma_{15} < \Gamma'_2 \quad \text{or} \quad \Gamma_1(2) \quad (4-4)$$

with the top of the valence band at  $\Gamma'_{25}$ .

In silicon the core states include also Bloch functions derived from  $p$  orbitals. There is thus also a repulsive effect for the states  $\Gamma'_{25}$  and  $\Gamma_{15}$  due to the orthogonalization to core states of the same symmetry. The repulsive effect is still larger for  $s$ -like states ( $\Gamma_1$  and  $\Gamma'_2$ ) than for  $p$ -like states ( $\Gamma'_{25}$  and  $\Gamma_{15}$ ), but the latter are raised in comparison with the case of diamond. The expected sequence is then

$$\Gamma_1 \ll \Gamma'_{25} < \Gamma_{15} \sim \Gamma'_2 \quad \text{or} \quad \Gamma_1(2) \quad \text{or} \quad \Gamma'_{12},$$

which is very similar to (4-4) except for the probability that  $\Gamma'_2$  will have an energy close to that of  $\Gamma_{15}$ .

In germanium the states  $\Gamma_1$  and  $\Gamma'_2$  must be orthogonalized to the core states  $3s$ , while  $\Gamma'_{25}$  and  $\Gamma_{15}$  must be orthogonalized to the core states  $3p$  and also  $3d$ . The presence of the new core states  $3d$  has the effect of interchanging the order of the levels  $\Gamma_{15}$  and  $\Gamma'_2$ .

At the point  $X$ , the expected sequence of the energy states in all cases is

$$X_1 \ll X_4 < X_1(2), \text{ etc.}$$

and the effect of orthogonalization is not expected to change the order of the levels which are already well separated in the empty lattice. We should just like to point out a general property of the band  $\Gamma_{15} + \Delta_1(2) - X_1(2)$ . We notice that  $X_1$  is double degenerate and splits in the  $\Delta$  direction into the irreducible representations  $\Delta_1$  and  $\Delta'_2$ . As a consequence of time reversal symmetry, eq. (4-3) holds, and the slope of the two bands  $X_1 - \Delta_1$  and  $X_1 - \Delta'_2$  must be opposite. Consequently the band  $\Gamma_{15} - \Delta_1(2) - X_1(2)$  presents a minimum along the line  $\Delta$ . This fact explains qualitatively why the band edges in silicon and diamond appear along the  $\Delta$  line.

At the point  $L$  the representations  $L_1$  and  $L'_2$  are  $s$ -like; taking into account the sequence in the empty lattice, and following a reasoning completely similar to that described at  $\Gamma$ , we see that the expected ordering of the levels is

$$L_1 \text{ and } L'_2 \ll L'_3 < L_3, L_1(2), \text{ etc.}$$

The relative position of the conduction states must be determined by performing detailed calculations. The highest occupied valence state at the point  $L$  is  $L'_3$ .

Note also that the separations among the empty lattice eigenvalues decrease when the lattice parameter is increased. This explains why diamond has an energy gap of  $\approx 5.5$  eV, silicon is a semiconductor with energy gap 1.14 eV, and germanium has a still smaller energy gap of 0.74 eV. In the same series, grey tin is a semimetal with zero energy gap as will be discussed in the following.

#### *Relativistic effects*

So far we have neglected the relativistic effects whose origin has been discussed in Section 3-10. When relativistic effects are taken into account the crystal states must be classified in accordance with the double group irreducible representations. The corrections to the non-relativistic Hamiltonian are due to the mass velocity term  $H_v$ , to the Darwin term  $H_d$  and to the spin-orbit interaction  $H_{so}$ . There exists a qualitative difference between the terms  $H_v$  and  $H_d$ , on the one hand, and the term  $H_{so}$ , on the other. The terms  $H_v$  and  $H_d$  give effects which can be interpreted as due to corrections to the crystal potential, whilst  $H_{so}$  has a different symmetry and removes some of the degeneracies. The last effect is theoretically the most important and can be compared directly with experimental results.

In Fig. 4-5 we show the band structure of germanium with the inclusion of spin-orbit interaction. For convenience, in addition to the double group notations we give the simple group notations appropriate to the non-relativistic limit. We notice that the main effect consists in the splittings of the  $\Gamma'_{25}$  valence state. It has been shown<sup>[8]</sup> that a simple relationship exists between the atomic splitting of the  $4p$  atomic state of germanium and the splitting in the crystal. At the point  $\Gamma$ , the splitting of  $\Gamma'_{25}$  is somewhat larger than the corresponding atomic splitting; at the point  $L$  it is somewhat smaller, and at  $X$  no splitting occurs at all in accordance with the symmetry analysis

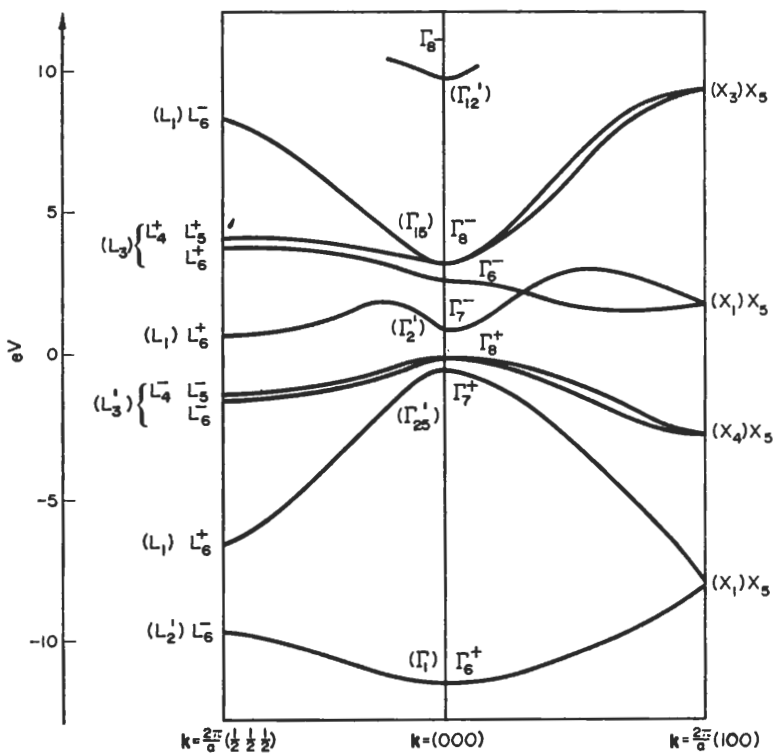


FIG. 4-5. Energy bands for germanium with the inclusion of spin-orbit interaction. In brackets we provide the irreducible representations for the states of the simple group. (From ref. [15].)

of Section 2-2b. The band structures of diamond and silicon, including relativistic effects, present features similar to those just discussed for germanium. However, carbon and silicon are elements with relatively low atomic numbers, and their energy gaps are larger than for germanium. Relativistic corrections for most practical purposes are therefore less important in the case of carbon and silicon.

Relativistic effects are even more essential instead for understanding the band structure of grey tin. The theoretical calculations of Herman<sup>[9]</sup> and Bassani and Liu<sup>[10]</sup> show the top of the valence band to have symmetry  $\Gamma_8^+$  (the state  $\Gamma_8^+$  and the low lying valence state  $\Gamma_7^+$  split from the state  $\Gamma_{25}'$  as shown in Table 2-16). The bottom of the conduction band occurs at the point  $\Gamma$  and has symmetry  $\Gamma_7^-$  ( $\Gamma_2'$  in simple group notation) and in this scheme grey tin would be an insulator with a very small energy gap. However, Bassani and Liu<sup>[10]</sup> were unable to fit the experimental effective masses and other transport measurements such as the weak pressure dependence of conductivity and Hall coefficient using the results of the calculations with a small but finite energy gap. The way to overcome these difficulties was suggested by Groves and Paul<sup>[10]</sup> as a slight modification of the band structure computed by Bassani and Liu. In this scheme the state  $\Gamma_7^-$  is put intermediate to the two states  $\Gamma_8^+$  and  $\Gamma_7^+$  with a difference between states  $\Gamma_8^+$  and  $\Gamma_7^-$  of about 0.3 eV (Fig. 4-6). Grey tin is thus given as a semi-metal with zero energy gap since the Fermi level occurs at the half-filled state  $\Gamma_8^+$ . Because of degeneracy of the state  $\Gamma_8^+$ , transport properties depend only weakly on pressure, and the same (zero) energy gap is maintained at any pressure. Also effective

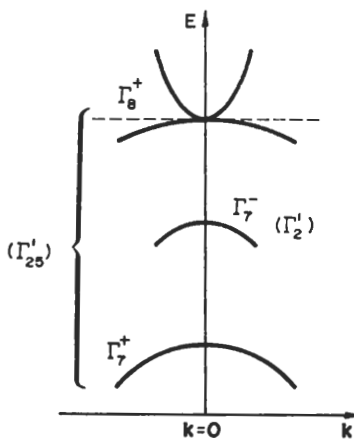


FIG. 4-6. Schematic representation of the energy bands for grey tin with the inclusion of spin-orbit interaction near the point  $k = (0,0,0)$ . In brackets we provide the irreducible representations for the states of the simple group. (From Groves and Paul, ref. [10].)

masses, dielectric function, and other properties<sup>[11]</sup> are in agreement with the model suggested by Groves and Paul.<sup>[10]</sup>

Incidentally, we notice that the trend of the band structures of germanium and grey tin at  $\Gamma$  is quite similar to the case offered by the band structures of the two compounds CdTe and HgTe. The former compound is a semiconductor with energy gap  $\approx 1$  eV, while the second is a semimetal with energy gap zero at the point  $\Gamma$ . In fact, in HgTe the s-like state  $\Gamma_6$  is intermediate to the split p-like states  $\Gamma_8$  and  $\Gamma_7$ ; this occurs because the relativistic terms  $H_s$  and  $H_d$  have the net effect of lowering the s-like conduction state  $\Gamma_6$  with respect to the p-like valence states  $\Gamma_8$  and  $\Gamma_7$ , passing from CdTe to HgTe, as shown by Kisiel and Lee.<sup>[12]</sup>

#### 4-1c Symmetry properties of the zincblende lattice

The zincblende structure can be obtained from the diamond structure (Fig. 2-2) by considering two different atoms in the positions  $\mathbf{d}_1 = (0, 0, 0)$  and  $\mathbf{d}_2 = a/4(1, 1, 1)$  in the unit cell. All operations which interchange the two sublattices among themselves are not symmetry operations of the Hamiltonian in the zincblende structure. In particular, inversion symmetry is not present and the states do not have definite parity. Only the operations to the left hand side of Table 2-3 are symmetry operations of the zincblende structure; the space group of zincblende is symmorphic and its point group is  $T_d$ . The primitive vectors of the direct and reciprocal lattice and the Brillouin zone are the same as those described for the diamond lattice. The irreducible representations of the simple group of  $\mathbf{k}$  at the symmetry points  $\Gamma$ ,  $L$ , and  $X$  and along the symmetry axes  $A$  and  $A'$  can be derived using the standard procedures described in Section 2-2; they are reported in Table 4-4. The additional irreducible representations of the double group are given in Table 4-5.

Along the  $A$  axis, the little groups of  $\mathbf{k}$  in the diamond and zincblende structure coincide, and we have the same irreducible representations. Note, however, that  $A_4$  and  $A_5$  in the zincblende structure are *not* degenerate due to time reversal as they are

## ELECTRONIC STATES AND OPTICAL TRANSITIONS

TABLE 4-4. Irreducible presentations of the simple group of  $k$  for  $\Gamma$ ,  $A$ ,  $L$ ,  $\Delta$ , and  $X$  of the zincblende structure. The irreducible representations  $\Delta_3$  and  $\Delta_4$  are degenerate by time reversal

Point $\Gamma$	$E$	$3C_4^2$	$6IC_4$	$6IC_2$	$8C_3$
$\Gamma_1$	1	1	1	1	1
$\Gamma_2$	1	1	-1	-1	1
$\Gamma_{12}$	2	2	0	0	-1
$\Gamma_{15}$	3	-1	-1	1	0
$\Gamma_{25}$	3	-1	1	-1	0

Point $A$ or $L$	$E$	$I\delta_{2xy} I\delta_{2xz} I\delta_{2yz}$	$\delta_{3xyz} \delta_{3xyz}^{-1}$
$A_1, L_1$	1	1	1
$A_2, L_2$	1	-1	1
$A_3, L_3$	2	0	-1

Point $\Delta$	$E$	$\delta_{2x}$	$I\delta_{2yz}$	$I\delta_{2y\bar{z}}$
$\Delta_1$	1	1	1	1
$\Delta_2$	1	1	-1	-1
$\{\Delta_3$	1	-1	1	-1
$\Delta_4\}$	1	-1	-1	1

Point $X$	$E$	$\delta_{2x}$	$\delta_{2y}\delta_{2z}$	$I\delta_{4x}^{-1} I\delta_{4x}$	$I\delta_{2yz} I\delta_{2y\bar{z}}$
$X_1$	1	1	1	1	1
$X_2$	1	1	1	-1	-1
$X_3$	1	1	-1	-1	1
$X_4$	1	1	-1	1	-1
$X_5$	2	-2	0	0	0

TABLE 4-5. Additional irreducible representations of the double group of  $k$  for  $\Gamma$ ,  $A$ ,  $L$ ,  $\Delta$ , and  $X$  of the zincblende structure. The irreducible representations  $L_4$  and  $L_5$  are degenerate by time reversal, but  $A_4$  and  $A_5$  are not

Point $\Gamma$	$E$	$E$	$3C_4^2 3\bar{C}_4^2$	$6IC_4$	$6I\bar{C}_4$	$6IC_2 6\bar{C}_2$	$8C_3$	$8\bar{C}_3$
$\Gamma_6$	2	-2	0	$\sqrt{2}$	$-\sqrt{2}$	0	1	-1
$\Gamma_7$	2	-2	0	$-\sqrt{2}$	$\sqrt{2}$	0	1	-1
$\Gamma_8$	4	-4	0	0	0	0	-1	1

Point $A$ or $L$	$E$	$E$	$I\delta_{2x\bar{z}} I\delta_{2x\bar{z}} I\delta_{2y\bar{z}}$	$I\bar{\delta}_{2y\bar{x}} I\bar{\delta}_{2x\bar{z}} I\bar{\delta}_{2y\bar{z}}$	$\delta_{3xyz} \delta_{3xyz}^{-1}$	$\bar{\delta}_{3xyz} \bar{\delta}_{3xyz}^{-1}$
$A_4, L_4$	1	-1	$i$	$-i$	-1	1
$A_5, L_5$	1	-1	$-i$	$i$	-1	1
$A_6, L_6$	2	-2	0	0	1	-1

Point $\Delta$	$E$	$E$	$\delta_{2x}\bar{\delta}_{2x}$	$I\delta_{2yz}\bar{I}\delta_{2yz}$	$I\delta_{2yz}\bar{I}\delta_{2y\bar{z}}$
$\Delta_5$	2	-2	0	0	0

Point $X$	$E$	$E$	$\delta_{2x}\bar{\delta}_{2x}$	$\delta_{2y}\delta_{2x}\bar{\delta}_{2y}\bar{\delta}_{2x}$	$I\delta_{4x} I\delta_{4x}^{-1}$	$I\bar{\delta}_{4x} I\bar{\delta}_{4x}^{-1}$	$I\delta_{2yz} I\delta_{2y\bar{z}} I\bar{\delta}_{2yz} I\bar{\delta}_{2y\bar{z}}$
$X_6$	2	-2	0	0	$\sqrt{2}$	$-\sqrt{2}$	0
$X_7$	2	-2	0	0	$-\sqrt{2}$	$\sqrt{2}$	0

in the diamond structure; this can be seen by applying the Herring test of Table 2-17. At the points  $\Gamma$  and  $L$ , the representations of the diamond lattice which are even or odd under inversion symmetry correspond to a unique representation for the zincblende structure. Along the  $\Delta$  axis, the states  $\Delta_1$  and  $\Delta'_2$  of the diamond structure are compatible with  $\Delta_1$  of the zincblende structure; the states  $\Delta_2$  and  $\Delta'_1$  are compatible with  $\Delta_2$ , the state  $\Delta_3$  is compatible with  $\Delta_3$  and  $\Delta_4$  degenerate by time reversal symmetry, and, finally, the state  $\Delta_6$  is compatible with  $\Delta_5$ . At the point  $X$ , the state  $X_1$  of the diamond structure is compatible with  $X_1$  and  $X_3$  of the zincblende structure, the state  $X_2$  is compatible with  $X_2$  and  $X_4$ , the states  $X_3$  and  $X_4$  are compatible with  $X_5$ , and the state  $X_5$  is compatible with  $X_6$  and  $X_7$ . Finally, at a general point  $k$  of the Brillouin zone in zincblende, we have no degeneracy irrespective of whether or not we include spin dependent terms in the Hamiltonian; at a general point of the Brillouin zone in the diamond structure we have double degeneracy when spin is included, because of inversion symmetry.

#### 4-1 d Electronic states in isoelectronic semiconductors with zincblende structure

We wish here to correlate the electronic states of group IV semiconductors with the diamond structure with the electronic states of the corresponding III-V, or II-VI, or I-VII isoelectronic semiconductors having the zincblende structure.<sup>[9, 13-15]</sup> For this purpose we can use a perturbation scheme first suggested by Herman<sup>[9]</sup> and Callaway.<sup>[13]</sup> In this scheme the potential of isoelectronic compounds is written as the sum of the potential of the corresponding IV-IV compound and a "perturbation potential" antisymmetric with respect to inversion, which increases from the III-V ones through II-VI to the I-VII ones. The method is useful for investigating a series of isoelectronic compounds with the same structure and nearly the same lattice parameter.

We first of all consider how the band structure of a III-V compound is correlated to the band structure of a IV-IV isoelectronic compound. Following the procedure of Herman,<sup>[9]</sup> we write the perturbation potential as

$$V_{\text{pert}}(\mathbf{r}) = V_{(\text{III}-\text{V})}(\mathbf{r}) - V_{(\text{IV}-\text{IV})}(\mathbf{r}),$$

where  $V_{(\text{III}-\text{V})}(\mathbf{r})$  and  $V_{(\text{IV}-\text{IV})}(\mathbf{r})$  indicate the potential of the two crystals. We split  $V_{\text{pert}}(\mathbf{r})$  into two parts which are symmetric and antisymmetric with respect to the inversion symmetry

$$V_{\text{pert}}(\mathbf{r}) = V_{\text{ant}}(\mathbf{r}) + V_{\text{symm}}(\mathbf{r})$$

with

$$V_{\text{symm}}(\mathbf{r}) = \frac{1}{2} \sum_{\tau_v} \{ [V_{\text{III}}(\mathbf{r} - \mathbf{d}_1 - \boldsymbol{\tau}_v) + V_{\text{V}}(\mathbf{r} - \mathbf{d}_1 - \boldsymbol{\tau}_v) - 2V_{\text{IV}}(\mathbf{r} - \mathbf{d}_1 - \boldsymbol{\tau}_v)] \\ + [V_{\text{III}}(\mathbf{r} - \mathbf{d}_2 - \boldsymbol{\tau}_v) + V_{\text{V}}(\mathbf{r} - \mathbf{d}_2 - \boldsymbol{\tau}_v) - 2V_{\text{IV}}(\mathbf{r} - \mathbf{d}_2 - \boldsymbol{\tau}_v)] \}$$

and

$$V_{\text{ant}}(\mathbf{r}) = \frac{1}{2} \sum_{\tau_v} \{ [V_{\text{III}}(\mathbf{r} - \mathbf{d}_1 - \boldsymbol{\tau}_v) - V_{\text{V}}(\mathbf{r} - \mathbf{d}_1 - \boldsymbol{\tau}_v)] \\ - [V_{\text{III}}(\mathbf{r} - \mathbf{d}_2 - \boldsymbol{\tau}_v) - V_{\text{V}}(\mathbf{r} - \mathbf{d}_2 - \boldsymbol{\tau}_v)] \}.$$

$V_{\text{III}}$ ,  $V_{\text{IV}}$ , and  $V_{\text{V}}$  denote the atomic-like potentials of the atoms under considerations. The average potential of III and V atoms is approximately equal to the potential of the corresponding IV atom, since these atoms appear sequentially in the Periodic Table. Thus  $V_{\text{symm}}(\mathbf{r})$  can be assumed to be zero. The term  $V_{\text{ant}}(\mathbf{r})$  is invariant under the symmetry operations of the space group of zincblende and is multiplied by  $-1$  under the inversion symmetry operation. At points of high symmetry we can easily determine

## ELECTRONIC STATES AND OPTICAL TRANSITIONS

the representation to which  $V_{\text{ant}}(\mathbf{r})$  belongs by inspection and establish when the matrix elements of  $V_{\text{ant}}(\mathbf{r})$  between states of a given symmetry may be non-vanishing. In Table 4-6 we give the states which interact via the antisymmetric term at the symmetry points  $\Gamma$ ,  $L$ , and  $X$  of the Brillouin zone.

The effect of  $V_{\text{ant}}(\mathbf{r})$  can be estimated by means of standard perturbation theory. From Table 4-6 we see that the first order corrections are zero at the symmetry points  $\Gamma$ ,  $L$ , and  $X$  except for the doubly degenerate states  $X_1$  and  $X_2$  and the fourfold degenerate state  $X_5$ . The effect of second order perturbation corrections can be realized by noting that the interaction between two states with different energy tends to decrease

TABLE 4-6. Pairs of states at the symmetry points  $\Gamma$ ,  $L$ , and  $X$  of the Brillouin zone of the diamond structure which interact via an antisymmetric potential

Point $\Gamma$	$\Gamma_1$	$\Gamma_2$	$\Gamma_{12}$	$\Gamma'_{15}$	$\Gamma'_{25}$	$\Gamma_6^+$	$\Gamma_7^+$	$\Gamma_8^+$
Point $L$	$\Gamma'_2$	$\Gamma'_1$	$\Gamma'_{12}$	$\Gamma_{25}$	$\Gamma_{15}$	$\Gamma_7^-$	$\Gamma_6^-$	$\Gamma_8^-$
Point $X$	$L_1$	$L_2$	$L_3$	$L_4$	$L_5$	$L_6$		
	$X_1$	$X_2$	$X_3$	$X_4$	$X_5$			
	$X_1$	$X_2$	$X_4$	$X_3$	$X_5$			

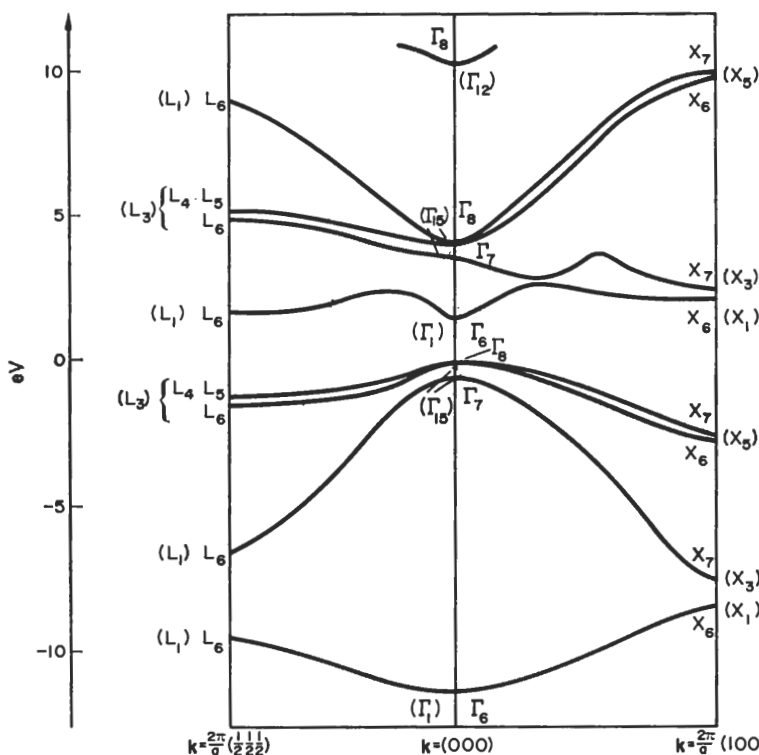


FIG. 4-7. Energy bands for GaAs with the inclusion of spin-orbit interaction. The irreducible representations for the states of the simple group are supplied in brackets. (From ref. [15].)

(increase) the energy of the state with lower (higher) energy. The interaction becomes more important the nearer in energy the states become.

As an example we apply the above considerations to discuss the band structure of GaAs, the III-V compound corresponding to germanium. Passing from the band structure of germanium (Fig. 4-4 and 4-5) to that of GaAs we expect an increase of the energy gap  $\Gamma'_{2s} - \Gamma'_2$  because of the interaction of the states  $\Gamma'_{2s}$  and  $\Gamma'_{1s}$  via the antisymmetric perturbation potential. At the point  $X$  the representation  $X_1$  is split into the representations  $X_1$  and  $X_3$  of the zincblende structure, and the representation  $X_5$  corresponds to the two states  $X_6$  and  $X_7$  in zincblende. Furthermore, the relative position of the states  $\Gamma'_2$  and  $L_1$  of the lowest conduction band tends to be interchanged because of second order corrections. All these effects are confirmed by the detailed calculations performed on GaAs<sup>[15]</sup> (Fig. 4-7).

The relationship between the band structures of a sequence of isoelectronic compounds can be established along similar lines. In general we notice that the energy gaps increase from the IV-IV compound to the other compounds of the series because of the increase of antisymmetric potential. If we tentatively and qualitatively assume that the perturbation potential is proportional to  $\lambda$  in an isoelectronic sequence, with  $\lambda = 0, 1, 2, 3$  for the IV-IV, III-V, II-VI, I-VII compounds respectively, we expect a dependence proportional to  $\lambda$  for the energy difference between states which interact to first order of perturbation theory and a dependence proportional to  $\lambda^2$  for the energy difference

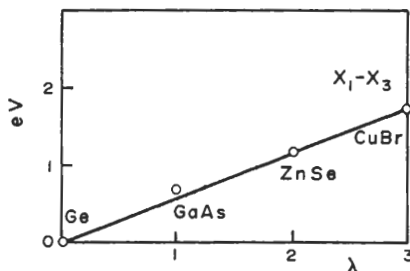
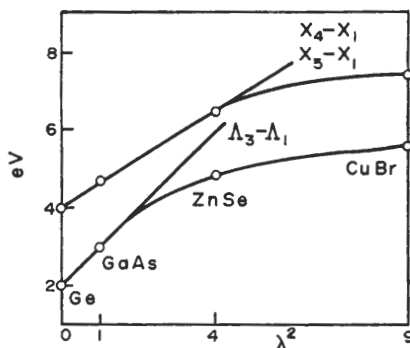


FIG. 4-8. Experimental variation of some energy gaps as function of  $\lambda$  or  $\lambda^2$  in the sequence Ge-GaAs-ZnSe-CuBr.  $A_3 - A_1$  denotes the energy threshold along the line  $A_3$ .  $X_1$  is the bottom conduction state at  $X$ ;  $X_4$  ( $X_5$ ) is the top valence state in the diamond (zincblende) structure. (From ref. [16].)

between states which interact to second order of perturbation theory. In Fig. 4-8 we show for the isoelectronic sequence Ge-GaAs-ZnSe-CuBr the experimental variation of some important energy gaps, as given by Greenaway and Harbecke.<sup>[16]</sup> The energy differences  $\Lambda_3 - \Lambda_1$ ,  $X_4 - X_1$ , and  $X_5 - X_1$  are only approximately proportional to  $\lambda^2$ . For  $X_1 - X_3$  the proportionality with  $\lambda$  is good. Qualitatively, Fig. 4-8 shows quite well the different symmetry origin of the splitting  $X_1 - X_3$  (first order effect in perturbation theory) from the differences  $\Lambda_3 - \Lambda_1$ ,  $X_4 - X_1$ , and  $X_5 - X_1$  (second order effects in perturbation theory).

For detailed calculations on the band structure of III-V compounds we refer the reader to refs. [4], [14] and [15].

## 4-2 Energy bands of layer type crystals

### 4-2a Symmetry properties of graphite and hexagonal BN in the two-dimensional approximation

Graphite is one of the anisotropic crystals most extensively studied because of its simple and highly symmetric structure. The graphite structure is made up of two-dimensional arrays of hexagons with carbon atoms at the vertices. The distance between nearest atoms in a given plane is much smaller than the distance between nearest atoms in different planes. Consequently the planes of carbon atoms are loosely bound between each other, whilst the atoms on the same plane are strongly bound. To a good degree of approximation one can neglect to first order the interaction between different planes and consider graphite as a layer compound.

Another strongly anisotropic crystal is hexagonal boron nitride with a structure very similar to that of graphite. Both crystals are made up of two-dimensional arrays of hexagons with almost equal lattice parameter and a very weak interaction between

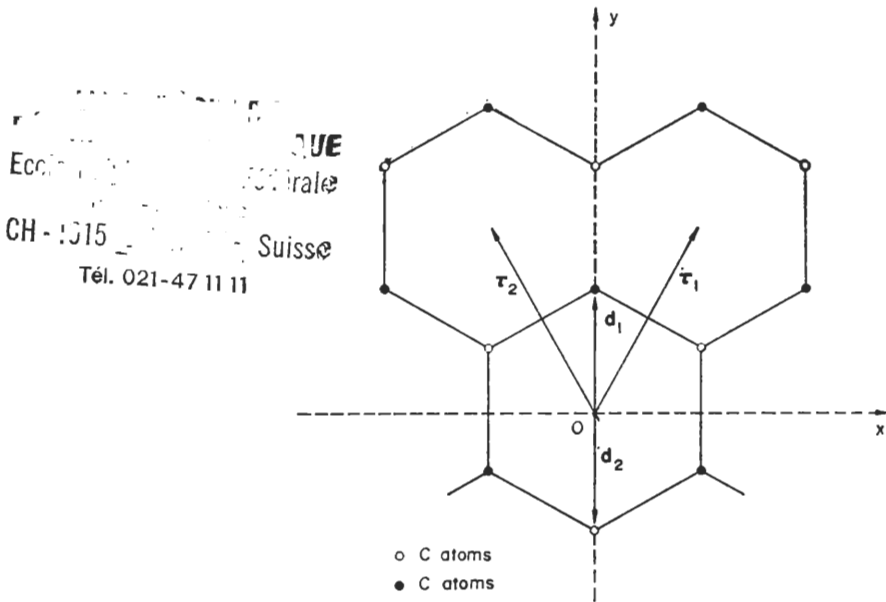


FIG. 4-9. Two-dimensional crystal structure of graphite.

different layers. In the Periodic Table boron and nitrogen atoms are adjacent to carbon; thus BN is the III-V compound corresponding to carbon and is isoelectronic with graphite. Because of this overall resemblance, a close relationship between the properties of graphite and BN is to be expected.

The two-dimensional crystal structure of graphite consists of hexagons with vertices occupied by carbon atoms (Fig. 4-9). With the choice of coordinate axis of Fig. 4-9 the primitive lattice vectors are

$$\left. \begin{aligned} \mathbf{r}_1 &= a \left( \frac{1}{2}, \frac{\sqrt{3}}{2}, 0 \right), \\ \mathbf{r}_2 &= a \left( -\frac{1}{2}, \frac{\sqrt{3}}{2}, 0 \right). \end{aligned} \right\} \quad (4-5)$$

The value of the lattice parameter  $a$  is 2.46 Å. The fundamental cell of graphite contains two atoms in the positions

$$\left. \begin{aligned} \mathbf{d}_1 &= a \left( 0, \frac{1}{2\sqrt{3}}, 0 \right), \\ \mathbf{d}_2 &= a \left( 0, -\frac{1}{2\sqrt{3}}, 0 \right). \end{aligned} \right\} \quad (4-6)$$

The primitive vectors of the reciprocal lattice are

$$\left. \begin{aligned} \mathbf{h}_1 &= \frac{2\pi}{a} \left( 1, \frac{1}{\sqrt{3}}, 0 \right), \\ \mathbf{h}_2 &= \frac{2\pi}{a} \left( -1, \frac{1}{\sqrt{3}}, 0 \right). \end{aligned} \right\} \quad (4-7)$$

The first Brillouin zone is the hexagon shown in Fig. 4-10. The symmetry points and the symmetry lines are indicated using the notations of Lomer.<sup>[17]</sup>

The point group of the graphite structure is  $D_{6h}$ . No fractional translation is associated with the operations of the point group. All the symmetry operations and their matrix representatives are given in Table 4-7. Standard crystallographic notation is

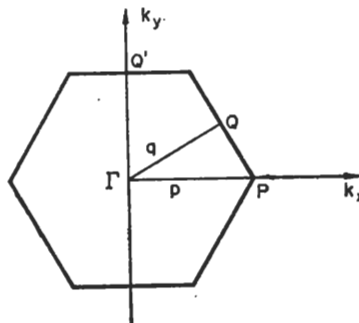


FIG. 4-10. Two-dimensional Brillouin zone for graphite (or hexagonal BN).

TABLE 4-7. Symmetry operations for the two-dimensional graphite structure. In columns 1 and 3 the symmetry operations are denoted using standard crystallographic notations. In columns 2 and 4 the corresponding coordinate transformation matrices are provided

Symmetry operations	Rotational matrix	Symmetry operations	Rotational matrix
$\{E 0\}$	$\begin{pmatrix} 1 & 0 & 0 \\ 0 & 1 & 0 \\ 0 & 0 & 1 \end{pmatrix}$	$\{I 0\}$	$\begin{pmatrix} -1 & 0 & 0 \\ 0 & -1 & 0 \\ 0 & 0 & -1 \end{pmatrix}$
$\{C_6^2 0\}$	$\begin{pmatrix} -1/2 & -\sqrt{3}/2 & 0 \\ \sqrt{3}/2 & -1/2 & 0 \\ 0 & 0 & 1 \end{pmatrix}$	$\{IC_6^2 0\}$	$\begin{pmatrix} 1/2 & \sqrt{3}/2 & 0 \\ -\sqrt{3}/2 & 1/2 & 0 \\ 0 & 0 & -1 \end{pmatrix}$
$\{C_6^4 0\}$	$\begin{pmatrix} -1/2 & \sqrt{3}/2 & 0 \\ -\sqrt{3}/2 & -1/2 & 0 \\ 0 & 0 & 1 \end{pmatrix}$	$\{IC_6^4 0\}$	$\begin{pmatrix} 1/2 & -\sqrt{3}/2 & 0 \\ \sqrt{3}/2 & 1/2 & 0 \\ 0 & 0 & -1 \end{pmatrix}$
$\{C_y 0\}$	$\begin{pmatrix} -1 & 0 & 0 \\ 0 & 1 & 0 \\ 0 & 0 & -1 \end{pmatrix}$	$\{IC_y 0\}$	$\begin{pmatrix} 1 & 0 & 0 \\ 0 & -1 & 0 \\ 0 & 0 & 1 \end{pmatrix}$
$\{C'_y 0\}$	$\begin{pmatrix} 1/2 & \sqrt{3}/2 & 0 \\ \sqrt{3}/2 & -1/2 & 0 \\ 0 & 0 & -1 \end{pmatrix}$	$\{IC'_y 0\}$	$\begin{pmatrix} -1/2 & -\sqrt{3}/2 & 0 \\ -\sqrt{3}/2 & 1/2 & 0 \\ 0 & 0 & 1 \end{pmatrix}$
$\{C''_y 0\}$	$\begin{pmatrix} 1/2 & -\sqrt{3}/2 & 0 \\ -\sqrt{3}/2 & -1/2 & 0 \\ 0 & 0 & -1 \end{pmatrix}$	$\{IC''_y 0\}$	$\begin{pmatrix} -1/2 & \sqrt{3}/2 & 0 \\ \sqrt{3}/2 & 1/2 & 0 \\ 0 & 0 & 1 \end{pmatrix}$
$\{\sigma_h 0\}$	$\begin{pmatrix} 1 & 0 & 0 \\ 0 & 1 & 0 \\ 0 & 0 & -1 \end{pmatrix}$	$\{C_6^3 0\}$ $\equiv \{I\sigma_h 0\}$	$\begin{pmatrix} -1 & 0 & 0 \\ 0 & -1 & 0 \\ 0 & 0 & 1 \end{pmatrix}$
$\{\sigma_h C_6^2 0\}$	$\begin{pmatrix} -1/2 & -\sqrt{3}/2 & 0 \\ \sqrt{3}/2 & -1/2 & 0 \\ 0 & 0 & -1 \end{pmatrix}$	$\{C_6^5 0\}$	$\begin{pmatrix} 1/2 & \sqrt{3}/2 & 0 \\ -\sqrt{3}/2 & 1/2 & 0 \\ 0 & 0 & 1 \end{pmatrix}$
$\{\sigma_h C_6^4 0\}$	$\begin{pmatrix} -1/2 & \sqrt{3}/2 & 0 \\ -\sqrt{3}/2 & -1/2 & 0 \\ 0 & 0 & -1 \end{pmatrix}$	$\{C_6 0\}$	$\begin{pmatrix} 1/2 & -\sqrt{3}/2 & 0 \\ \sqrt{3}/2 & 1/2 & 0 \\ 0 & 0 & 1 \end{pmatrix}$
$\{\sigma_h C_y 0\}$	$\begin{pmatrix} -1 & 0 & 0 \\ 0 & 1 & 0 \\ 0 & 0 & 1 \end{pmatrix}$	$\{C_x 0\}$	$\begin{pmatrix} 1 & 0 & 0 \\ 0 & -1 & 0 \\ 0 & 0 & -1 \end{pmatrix}$
$\{\sigma_h C'_y 0\}$	$\begin{pmatrix} 1/2 & \sqrt{3}/2 & 0 \\ \sqrt{3}/2 & -1/2 & 0 \\ 0 & 0 & 1 \end{pmatrix}$	$\{C'_x 0\}$	$\begin{pmatrix} -1/2 & -\sqrt{3}/2 & 0 \\ -\sqrt{3}/2 & 1/2 & 0 \\ 0 & 0 & -1 \end{pmatrix}$
$\{\sigma_h C''_y 0\}$	$\begin{pmatrix} 1/2 & -\sqrt{3}/2 & 0 \\ -\sqrt{3}/2 & -1/2 & 0 \\ 0 & 0 & 1 \end{pmatrix}$	$\{C''_x 0\}$	$\begin{pmatrix} -1/2 & \sqrt{3}/2 & 0 \\ \sqrt{3}/2 & 1/2 & 0 \\ 0 & 0 & -1 \end{pmatrix}$

## ELECTRONIC BAND STRUCTURE IN SOME CRYSTALS

used to denote symmetry operations. For instance,  $\{C_6^n|0\}$  indicates a rotation by  $2\pi n/6$  about the  $z$  axis,  $\{C_y|0\}$  indicates a rotation by  $\pi$  about the  $y$  axis,  $\{\sigma_h|0\}$  indicates the reflection in the  $(x, y)$  plane, and  $\{I|0\}$  indicates the inversion.

To classify the electronic states at a given  $\mathbf{k}$  point in the Brillouin zone we must consider the irreducible representations of the little group of  $\mathbf{k}$  whose basis functions are Bloch functions of the  $\mathbf{k}$  vector. Since the group under investigation is symmorphic, the irreducible representations of the group of  $\mathbf{k}$  at symmetry points are simply obtained from the irreducible representations of the small point group of  $\mathbf{k}$ . The irreducible representations at the symmetry points  $\Gamma$ ,  $Q$ , and  $P$  are given in Tables 4-8, 4-9, and 4-10 respectively. We have labelled the irreducible representations with  $\pm$  depending on the parity with respect to  $\{\sigma_h|0\}$ , and with  $g$  or  $u$  depending on the parity with respect to  $\{I|0\}$ . At a general point of the Brillouin zone the only symmetry operations are  $\{E|0\}$  and  $\{\sigma_h|0\}$  and the irreducible representations are given in Table 4-11.

TABLE 4-8. Irreducible representations at the point  $\Gamma$  of the Brillouin zone of two-dimensional graphite.  
Time reversal does not introduce additional degeneracies

Point $\Gamma$	$E$	$C_6^2 C_6^4$	$C_y C'_y C''_y$	$\sigma_h$	$\sigma_h C_6^2 \sigma_h C_6^4$	$\sigma_h C_y, \sigma_h C'_y, \sigma_h C''_y$	$I$	Multiply all elements by $I$
$\Gamma_{1g}^+$	1	1	1	1	1	1	1	Repeat the same characters
$\Gamma_{2g}^+$	1	1	-1	1	1	-1	1	
$\Gamma_{3g}^+$	2	-1	0	2	-1	0	2	
$\Gamma_{1g}^-$	1	1	1	-1	-1	-1	1	
$\Gamma_{2g}^-$	1	1	-1	-1	-1	1	1	
$\Gamma_{3g}^-$	2	-1	0	-2	1	0	2	
$\Gamma_{1u}^+$	1	1	1	1	1	1	-1	Multiply all characters by -1
$\Gamma_{2u}^+$	1	1	-1	1	1	-1	-1	
$\Gamma_{3u}^+$	2	-1	0	2	-1	0	-2	
$\Gamma_{1u}^-$	1	1	1	-1	-1	-1	-1	
$\Gamma_{2u}^-$	1	1	-1	-1	-1	1	-1	
$\Gamma_{3u}^-$	2	-1	0	-2	1	0	-2	

TABLE 4-9. Irreducible representations at the point  $Q$  of the Brillouin zone of two-dimensional graphite. Time reversal does not introduce additional degeneracies

Point $Q$	$E$	$C'_y$	$\sigma_h$	$\sigma_h C'_y$	$I$	Multiply all elements by $I$
$Q_{1g}^+$	1	1	1	1	1	Repeat the same characters
$Q_{2g}^+$	1	-1	1	-1	1	
$Q_{1g}^-$	1	1	-1	-1	1	
$Q_{2g}^-$	1	-1	-1	1	1	
$Q_{1u}^+$	1	1	1	1	-1	Multiply all characters by -1
$Q_{2u}^+$	1	-1	1	-1	-1	
$Q_{1u}^-$	1	1	-1	-1	-1	
$Q_{2u}^-$	1	-1	-1	1	-1	

## ELECTRONIC STATES AND OPTICAL TRANSITIONS

 TABLE 4-10. Irreducible representations at the point  $P$  of the Brillouin zone for two-dimensional graphite. Time reversal does not introduce additional degeneracies

Point $P$	$E$	$C_6^2 C_6^4$	$C_x C_x' C_x''$	$\sigma_h$	$\sigma_h C_6^2, \sigma_h C_6^4$	$IC_y IC_y' IC_y''$
$P_1^+$	1	1	1	1	1	1
$P_2^+$	1	1	-1	1	1	-1
$P_3^+$	2	-1	0	2	-1	0
$P_1^-$	1	1	1	-1	-1	-1
$P_2^-$	1	1	-1	-1	-1	1
$P_3^-$	2	-1	0	-2	1	0

INSTITUT TECHNIQUE DU  
 MATERIAU ET DE LA PHYSIQUE  
 Ecole Polytechnique Fédérale  
 de Lausanne  
 CH-1015 LAUSANNE Suisse  
 Tél. 021-47 11 11

TABLE 4-11. Irreducible representations at a general point of the Brillouin zone for two-dimensional graphite (or hexagonal BN). Time reversal does not introduce additional degeneracies

	$E$	$\sigma_h$
$I_1^+$	1	1
$I_1^-$	1	-1

 TABLE 4-12. Irreducible representations at the point  $P$  of the Brillouin zone for two-dimensional BN. For brevity  $\epsilon = e^{i2\pi/3}$ . Time reversal does not introduce additional degeneracies

Point $P$	$E$	$C_6^2$	$C_6^4$	$\sigma_h$	$\sigma_h C_6^2$	$\sigma_h C_6^4$
$P_1^+$	1	1	1	1	1	1
$P_2^+$	1	$\epsilon$	$\epsilon^2$	1	$\epsilon$	$\epsilon^2$
$P_3^+$	1	$\epsilon^2$	$\epsilon$	1	$\epsilon^2$	$\epsilon$
$P_1^-$	1	1	1	-1	-1	-1
$P_2^-$	1	$\epsilon$	$\epsilon^2$	-1	$-\epsilon$	$-\epsilon^2$
$P_3^-$	1	$\epsilon^2$	$\epsilon$	-1	$-\epsilon^2$	$-\epsilon$

The two-dimensional crystal structure of hexagonal BN consists of hexagons with vertices occupied by boron and nitrogen atoms alternatively. The structure can be obtained from Fig. 4-9 by replacing the two sublattices of carbon atoms with boron and nitrogen atoms respectively. The primitive lattice vectors are given by (4-5) with  $a = 2.504 \text{ \AA}$ . The value of the lattice parameter is very close to the value for graphite. The fundamental cell of BN contains one boron and one nitrogen atom in the positions given by (4-6). The first Brillouin zone is the hexagon shown in Fig. 4-10.

The point group of hexagonal BN is  $D_{3h}$  because of the lack of all symmetry operations which interchange the two sublattices among themselves. In particular the inversion is not a symmetry operation and the operations of the space group are those on the left hand side of Table 4-7. The irreducible representations at the symmetry points  $I$  and  $Q$  can be obtained from those for graphite (Tables 4-8 and 4-9) by dropping simply the indices  $g$  and  $u$  which are now unnecessary. The point  $P$  must be treated separately, and Table 4-12 gives the irreducible representations for this point in the case of BN.

## ELECTRONIC BAND STRUCTURE IN SOME CRYSTALS

Note that although some of the irreducible representations (Table 4-10) for the point  $P$  of graphite have degeneracy greater than one, all the irreducible representations at the point  $P$  for BN (Table 4-12) are one-dimensional, a fact which is a consequence of the lack of inversion symmetry in BN.

For completeness, we consider the selection rules for optical transitions in the dipole approximation. Because of the anisotropy of these compounds, we have different selection rules when the incident light is polarized parallel or perpendicular to the  $z$  axis. The most important selection rule applies to all the points of the Brillouin zone (Table 4-11). With the polarization vector parallel (perpendicular) to the  $z$  axis, transitions are allowed only between states of opposite (same) parity with respect to  $\{\sigma_h|0\}$ . Further restrictions can be derived at high symmetry points and are given in Table 4-13.

TABLE 4-13. Allowed optical transitions with light polarized  $\perp$  or  $\parallel$  to the  $z$  axis at the symmetry points  $\Gamma$ ,  $Q$ , and  $P$  for two-dimensional graphite and BN. At the points  $\Gamma$  and  $Q$  the selection rules for BN can be obtained from those of graphite by dropping the  $g$  and  $u$  subscripts

Point $\Gamma$ (graphite structure)	$\Gamma_{1g}^+$	$\Gamma_{2g}^+$	$\Gamma_{3g}^+$	$\Gamma_{1g}^-$	$\Gamma_{2g}^-$	$\Gamma_{3g}^-$
e $\parallel$ to $z$ axis	$\Gamma_{2u}^-$	$\Gamma_{1u}^-$	$\Gamma_{3u}^-$	$\Gamma_{2u}^+$	$\Gamma_{1u}^+$	$\Gamma_{3u}^+$
e $\perp$ to $z$ axis	$\Gamma_{3u}^+$	$\Gamma_{3u}^+$	$\Gamma_{1u}^+ \Gamma_{2u}^+ \Gamma_{3u}^+$	$\Gamma_{3u}^-$	$\Gamma_{3u}^-$	$\Gamma_{1u}^- \Gamma_{2u}^- \Gamma_{3u}^-$
Point $Q$ (graphite structure)	$Q_{1g}^+$	$Q_{2g}^+$	$Q_{1g}^-$	$Q_{2g}^-$		
e $\parallel$ to $z$ axis	$Q_{2u}^-$	$Q_{1u}^-$	$Q_{2u}^+$	$Q_{1u}^+$		
e $\perp$ to $z$ axis	$Q_{1u}^+ Q_{2u}^+$	$Q_{1u}^+ Q_{2u}^+$	$Q_{1u}^- Q_{2u}^-$	$Q_{1u}^- Q_{2u}^-$		
Point $P$ (BN structure)	$P_1^+$	$P_2^+$	$P_3^+$	$P_1^-$	$P_2^-$	$P_3^-$
e $\parallel$ to $z$ axis	$P_1^-$	$P_2^-$	$P_3^-$	$P_1^+$	$P_2^+$	$P_3^+$
e $\perp$ to $z$ axis	$P_2^+ P_3^+$	$P_1^+ P_3^+$	$P_1^+ P_2^+$	$P_2^- P_3^-$	$P_1^- P_3^-$	$P_1^- P_2^-$
Point $P$ (graphite structure)	$\mathcal{P}_1^+$	$\mathcal{P}_2^+$	$\mathcal{P}_3^+$	$\mathcal{P}_1^-$	$\mathcal{P}_2^-$	$\mathcal{P}_3^-$
e $\parallel$ to $z$ axis	$\mathcal{P}_2^-$	$\mathcal{P}_1^-$	$\mathcal{P}_3^-$	$\mathcal{P}_2^+$	$\mathcal{P}_1^+$	$\mathcal{P}_3^+$
e $\perp$ to $z$ axis	$\mathcal{P}_3^+$	$\mathcal{P}_3^+$	$\mathcal{P}_1^+ \mathcal{P}_2^+ \mathcal{P}_3^+$	$\mathcal{P}_3^-$	$\mathcal{P}_3^-$	$\mathcal{P}_1^- \mathcal{P}_2^- \mathcal{P}_3^-$

### 4-2b Electronic state calculations for graphite and BN in the two-dimensional approximation

#### Band structure calculations for graphite<sup>[17]</sup>

A preliminary analysis on the expected sequence of the energy levels in graphite can be done using the tight binding scheme. The electronic configuration of the carbon atom C is  $(1s^2, 2s^2, 2p^2)$ . As described in Section 3-2a, we consider the eight Bloch functions formed from the atomic orbitals  $2s$ ,  $2p_x$ ,  $2p_y$ ,  $2p_z$  of C in the appropriate positions of the unit cell. At a general point  $\mathbf{k}$ , the Bloch sums derived from the  $s$ ,  $p_x$ , and  $p_y$  atomic functions never mix with the Bloch functions  $p_z$  because of the symmetry operation  $\{\sigma_h|0\}$ . We can thus classify the energy states as even or odd with respect

## ELECTRONIC STATES AND OPTICAL TRANSITIONS

to  $\{\sigma_h|0\}$ ; the former give rise to the so-called  $\sigma$  bands and the latter to the so-called  $\pi$  bands. The symmetrized combinations of Bloch functions can be obtained at high symmetry points using the standard procedures described in Section 3-2c. Such combinations for the points  $\Gamma$ ,  $P$ ,  $Q'$  (equivalent to  $Q$ ) of the Brillouin zone are given in Table 4-14.

TABLE 4-14. Symmetrized combinations of Bloch functions at the symmetry points  $\Gamma$ ,  $P$ ,  $Q'$  (equivalent to  $Q$ ) for two-dimensional graphite. Subscripts  $A_1$  and  $A_2$  refer to the two carbon atoms in the unit cell

Point $P$	Point $\Gamma$	Point $Q'$
$\mathcal{P}_3^+$	$\begin{cases} s_{A_1} \\ s_{A_2} \end{cases}$	$\begin{cases} \Gamma_{1g}^+ s_{A_1} + s_{A_2} \\ \Gamma_{1u}^+ s_{A_1} - s_{A_2} \end{cases}$
	$\begin{cases} p_{xA_1} + ip_{yA_1} \\ p_{xA_1} - ip_{yA_1} \end{cases}$	$\begin{cases} \Gamma_{3g}^+ (p_{xA_1} - p_{xA_2}) \\ p_{yA_1} - p_{yA_2} \end{cases}$
	$\mathcal{P}_1^+(p_{xA_1} + ip_{yA_1}) + (p_{xA_2} - ip_{yA_2})$	$\begin{cases} \Gamma_{3u}^+ (p_{xA_1} + p_{xA_2}) \\ p_{yA_1} + p_{yA_2} \end{cases}$
	$\mathcal{P}_2^+(p_{xA_1} + ip_{yA_1}) - (p_{xA_2} - ip_{yA_2})$	$\begin{cases} \Gamma_{2u}^- p_{xA_1} + p_{xA_2} \\ \Gamma_{2g}^+ p_{xA_1} - p_{xA_2} \end{cases}$
$\mathcal{P}_3^-$	$\begin{cases} p_{zA_1} \\ p_{zA_2} \end{cases}$	$\begin{cases} \Gamma_{2u}^- p_{zA_1} + p_{zA_2} \\ \Gamma_{2g}^- p_{zA_1} - p_{zA_2} \end{cases}$
		$\begin{cases} Q_{1u}^+ s_{A_1} - s_{A_2} \\ p_{yA_1} - p_{yA_2} \end{cases}$
		$\begin{cases} Q_{1g}^+ s_{A_1} + s_{A_2} \\ p_{yA_1} - p_{yA_2} \end{cases}$
		$\begin{cases} Q_{2u}^+ p_{xA_1} + p_{xA_2} \\ Q_{2g}^+ p_{xA_1} - p_{xA_2} \end{cases}$
		$\begin{cases} Q_{2u}^- p_{zA_1} - p_{zA_2} \\ Q_{2g}^- p_{zA_1} + p_{zA_2} \end{cases}$

From Table 4-14, applying the notion of bonding and antibonding states, we can gain insight into the expected sequence of the energy levels. For  $k = 0$  we expect the low lying energy states to be formed from bonding combinations of Bloch sums of the two sublattices. We thus expect the following sequence at  $\Gamma$ :

- (i) A bonding combination of  $s$  Bloch sums which gives the state  $\Gamma_{1g}^+$ .
- (ii) A bonding combination of  $p_x$ ,  $p_y$  Bloch sums which gives the doubly degenerate state  $\Gamma_{3g}^+$ .
- (iii) A bonding combination of  $p_z$  Bloch sums which gives the state  $\Gamma_{2u}^-$ .

The above bonding combinations are then followed by antibonding states, well separated in energy. The bonding state derived from the  $s$  Bloch sums is expected to be lower in energy than the bonding states derived from the  $p$  Bloch sums. The expected order of the levels is thus

$$\Gamma_{1g}^+ \ll \Gamma_{3g}^+, \Gamma_{2u}^- \ll \Gamma_{2g}^-, \Gamma_{3u}^+, \Gamma_{1u}^+$$

with the bonding states fully occupied by the eight valence electrons per unit cell.

A similar analysis can be carried out at other symmetry points taking advantage of the compatibility relations. At the point  $Q$  the four bonding states are separated from the four antibonding states, the highest and the lowest being  $Q_{2g}^-$  and  $Q_{2u}^-$ . At the point  $P$  we expect the following sequence:

$$\mathcal{P}_3^+ < \mathcal{P}_1^+ < \mathcal{P}_3^- < \mathcal{P}_2^+, \mathcal{P}_3^+.$$

The state  $\mathcal{P}_3^-$  has degeneracy two and is only half occupied by the available electrons. Consequently at the point  $P$  the bonding states are not separated from the antibonding states, and we expect graphite to have a zero energy gap.

The above speculations of the expected sequence of the energy levels are confirmed by the detailed calculations of Bassani and Pastori Parravicini<sup>[17]</sup> using the tight binding approach in a semi-empirical way (see Section 3-2d) and are displayed in Fig. 4-11.

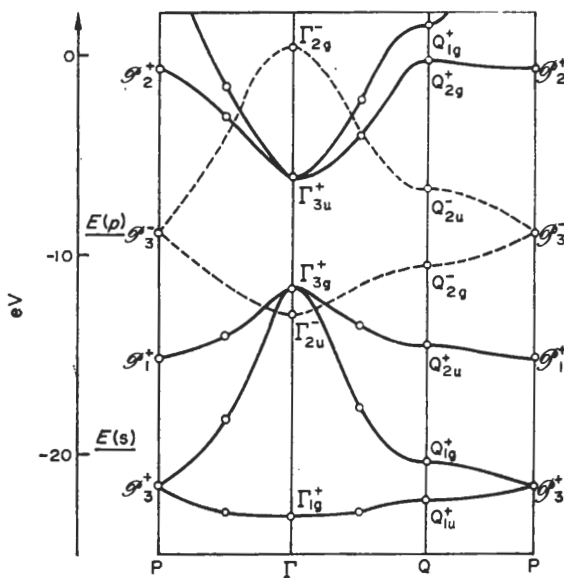


FIG. 4-11. Energy bands for two-dimensional graphite. Bands even (odd) with respect to the  $\sigma_h$  reflection are denoted by continuous (broken) lines. The energies of the valence states of carbon atom are also shown. (From Bassani and Pastori Parravicini, ref. [17].)

We see that the highest valence band and the lowest conduction band are  $\pi$  bands in the neighbourhood of  $P$  and correspond to states with an electronic density which is large in the  $z$  direction.

#### *Band structure calculations for BN<sup>[18]</sup>*

A preliminary analysis on the expected sequence of the energy levels in BN can be done similarly to the case of graphite. The electronic configuration of boron and nitrogen atoms is  $1s^2$ ,  $2s^2$ ,  $2p$  and  $1s^2$ ,  $2s^2$ ,  $2p^3$  respectively. We consider the eight Bloch functions formed by the  $2s$ ,  $2p_x$ ,  $2p_y$ ,  $2p_z$  atomic orbitals of boron and nitrogen atoms in the appropriate positions of the unit cell. At a general point  $\mathbf{k}$  we can label the crystal states as even or odd with respect to the symmetry operation  $\{\sigma_h|0\}$ . Further information can be obtained by considering the symmetrized combinations of Bloch

TABLE 4-15. Symmetrized combinations of Bloch functions at the symmetry points  $\Gamma$ ,  $P$ ,  $Q'$  for two-dimensional BN. Subscripts B and N refer to boron and nitrogen respectively

Point $P$	Point $\Gamma'$	Point $Q'$
$P_1^+ \begin{cases} s_N \\ p_{xB} + ip_{yB} \end{cases}$	$\Gamma_1^+ \begin{cases} s_N \\ s_B \end{cases}$	$Q_1^+ \begin{cases} s_N \\ s_B \\ p_{yN} \\ p_{yB} \end{cases}$
$P_2^+ \begin{cases} s_B \\ p_{xN} - ip_{yN} \end{cases}$	$\Gamma_3^+ \begin{cases} p_{xN} \\ p_{yN} \end{cases}$	$Q_2^+ \begin{cases} p_{xN} \\ p_{xB} \end{cases}$
$P_3^+ \begin{cases} p_{xN} - ip_{yN} \\ p_{xB} - ip_{yB} \end{cases}$	$\Gamma_3^- \begin{cases} p_{xB} \\ p_{yB} \end{cases}$	$Q_2^- \begin{cases} p_{zN} \\ p_{zB} \end{cases}$
$P_1^- p_{zN}$	$\Gamma_2^- p_{zN}$	$Q_2^- p_{zN}$
$P_2^- p_{zB}$	$p_{zB}$	$p_{zB}$

## ELECTRONIC STATES AND OPTICAL TRANSITIONS

functions at high high symmetry points. Such combinations for the points  $\Gamma$ ,  $P$ ,  $Q'$  (equivalent to  $Q$ ) of the Brillouin zone are given in Table 4-15.

Using the notion of bonding and antibonding state together with the information of Table 4-15, we find that the expected order of the levels at the point  $\Gamma$  is

$$\Gamma_1^+ \ll \Gamma_3^+, \Gamma_2^- \ll \Gamma_2^-, \Gamma_3^+, \Gamma_1^+$$

with the bonding states up to  $\Gamma_2^-$  fully occupied by the eight valence electrons per unit cell. At the point  $Q$  we expect that the four bonding states are well separated from the four antibonding states, the highest valence state and the lowest conduction state having symmetry  $Q_2^-$ . At the point  $P$  we expect the following sequence:

$$P_1^+ \ll P_2^+, P_3^+, P_1^- < P_2^- \text{, etc.}$$

It is possible to show that the energy expressions for the states  $P_1^-$  and  $P_2^-$  do not contain corrections from nearest neighbour atoms. Since the corrections from all the other neighbours are small, the difference in energy of the states  $P_1^-$  and  $P_2^-$  is expected to be nearly equal ( $\approx 5$  eV) to the difference of the energies of the  $p$  states in boron and

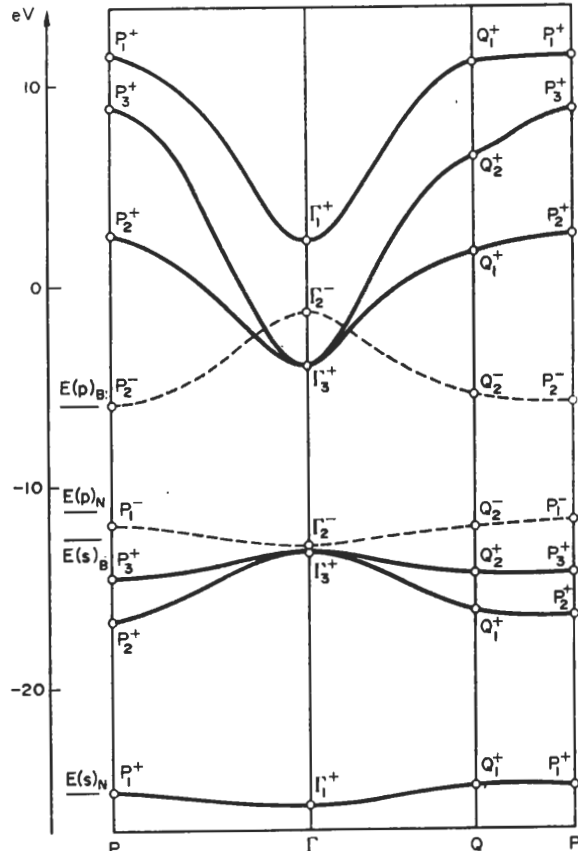


FIG. 4-12. Energy bands for two-dimensional BN. Bands even (odd) with respect to the  $\sigma_h$  reflection are denoted by continuous (broken) lines. The energies of the valence states of the boron and nitrogen atoms are also shown. (From Doni and Pastori Parravicini, ref. [18].)

nitrogen. We thus expect BN to be an insulator with energy gap of the order of several electron volts.

The above speculations are supported by detailed calculations performed by Doni and Pastori Parravicini<sup>[18]</sup> using the semi-empirical modification of the tight binding approach described in Section 3-2d. The results are shown in Fig. 4-12; it can be seen that the top of the valence bands and the bottom of the conduction bands appear at the point  $P$ , and the energy gap is approximately 5.5 eV.

### *General trends in graphite and BN energy bands*

To correlate the band structure of graphite with that of BN we can consider the perturbation scheme used in Section 4-1d. We consider qualitatively the effect on the band structure of graphite of the perturbing potential

$$V_{\text{pert}}(\mathbf{r}) = V^{(\text{BN})}(\mathbf{r}) - V^{(\text{graphite})}(\mathbf{r})$$

given by the difference between the potentials of BN and graphite crystals. We split  $V_{\text{pert}}(\mathbf{r})$  into two parts which are symmetric and antisymmetric with respect to the inversion symmetry. The symmetric potential is taken to be zero. The effect of the antisymmetric potential can be evaluated qualitatively by means of perturbation theory and symmetry considerations. The states at the symmetry points  $\Gamma$ ,  $Q$ , and  $P$  which interact via the antisymmetric potential, are given in Table 4-16.

TABLE 4-16. Pairs of states at the symmetry points  $\Gamma$ ,  $Q$ ,  $P$  of the Brillouin zone of graphite which interact via an antisymmetric potential

Point $\Gamma$	$\Gamma_{1g}^+$	$\Gamma_{2g}^+$	$\Gamma_{3g}^+$	$\Gamma_{1g}^-$	$\Gamma_{2g}^-$	$\Gamma_{3g}^-$
Point $Q$	$Q_{1g}^+$	$Q_{2g}^+$	$Q_{1u}^-$	$Q_{2u}^-$	$Q_{1u}^-$	$Q_{2u}^-$
Point $P$	$\mathcal{P}_1^+$	$\mathcal{P}_2^+$	$\mathcal{P}_3^+$	$\mathcal{P}_1^-$	$\mathcal{P}_2^-$	$\mathcal{P}_3^-$

From Table 4-16 we see that first order corrections at the symmetry points  $\Gamma$ ,  $Q$ , and  $P$  are zero except for the doubly degenerate states  $\mathcal{P}_3^+$  and  $\mathcal{P}_3^-$ . To second order, the state  $Q_{2g}^-$  interacts with the state  $Q_{2u}^-$ , and we expect an increase in the energy gap at  $Q$ . A similar but smaller effect is expected for the interaction between the states  $\Gamma_{2u}^-$  and  $\Gamma_{2g}^-$  because of the relative large energy difference. The perturbation scheme allows us to understand qualitatively the large energy gap at the point  $P$  and the relatively small shift towards higher energy for the energy gap in the  $\pi$  bands of BN at  $Q$ . These results are well supported by the detailed calculations and in agreement with experimental data. Similar considerations applied to the case of the  $\sigma$  bands lead to expected corrections on the  $\sigma$  bands of graphite which are supported by the detailed results of Fig. 4-12.

### *4-2c Electronic states of graphite and BN in the three-dimensional case*

The results of the two-dimensional approximation require modification when the interaction along the  $z$  axis is included. When the periodicity along the  $z$  direction is

considered, we have to add to the relations (4-5) and (4-7) a primitive translation vector  $\tau_3 = c(0, 0, 1)$  and a primitive reciprocal lattice vector  $\mathbf{h}_3 = (2\pi/c)(0, 0, 1)$ . The value of  $c$  is 6.71 and 6.66 Å in graphite and BN respectively. The Brillouin zone is shown in Fig. 4-13 and the crystal structures of graphite and BN are shown in Fig. 4-14(a)

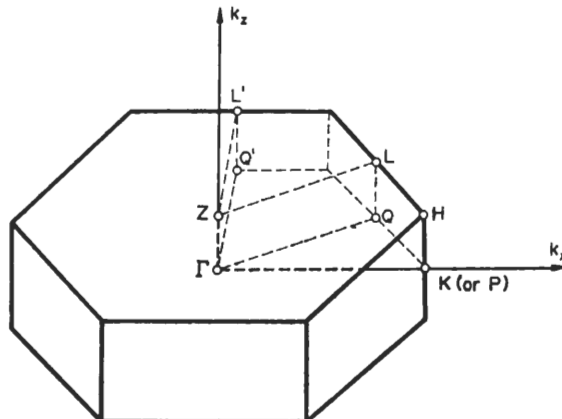


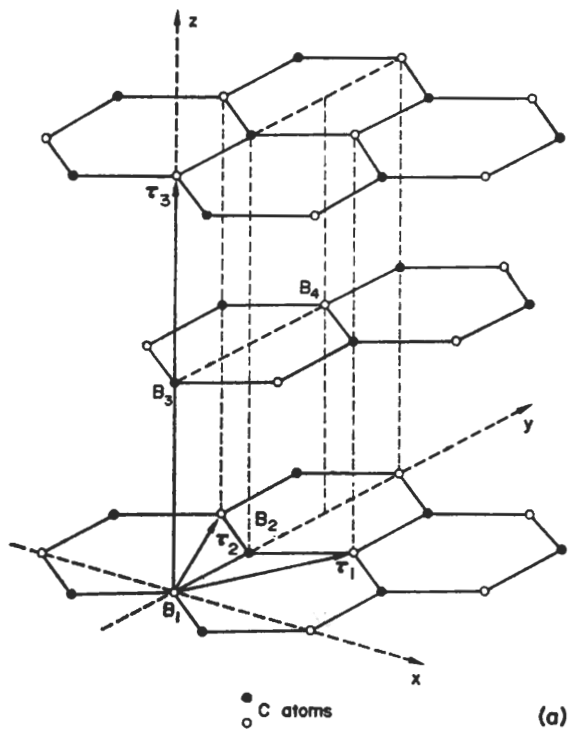
FIG. 4-13. Three-dimensional Brillouin zone for graphite (or hexagonal BN).

and (b) respectively. The unit cell of graphite, or of BN, contains four atoms—two in one plane and the remaining two in a parallel plane separated from the former by  $c/2$ . In the case of the BN structure [Fig. 4-14(b)], consecutive layers are packed directly on top of each other, whilst in the case of graphite [Fig. 4-14(a)] consecutive layers are rotated with respect to each other through  $2\pi/6$ . The point group of both three-dimensional graphite and BN is  $D_{6h}$ . The symmetry operations whose rotational part belongs to the subgroup  $D_{3h}$  do not include fractional translations; the other symmetry operations are associated with the fractional translation  $\mathbf{f} = \frac{1}{2}\tau_3$ .

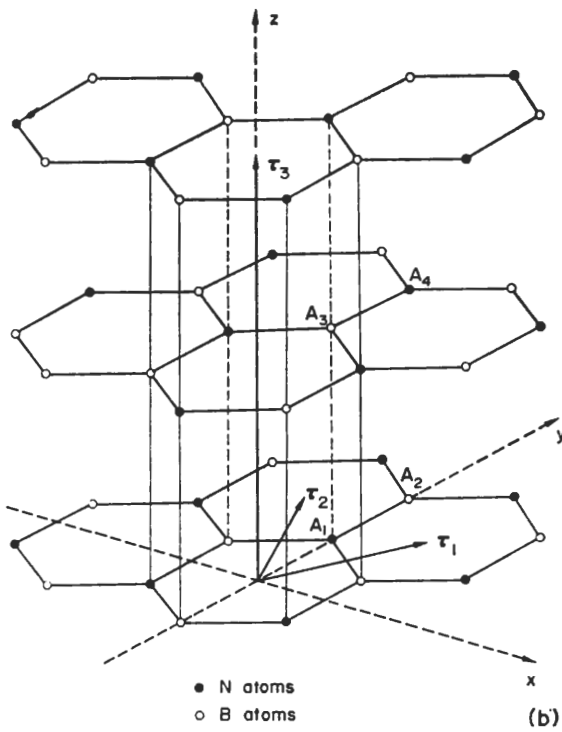
The effect of the interaction between planes can be neglected for the  $\sigma$  bands but should be considered when dealing with bands formed from  $p_z$  orbitals, since their overlap between different planes may not be negligible due to the fact that they “point” in directions perpendicular to the planes. The most important difference between the two- and three-dimensional treatments occurs in the case of graphite at the point  $P$  of the Brillouin zone, where the three-dimensional interaction removes the degeneracies and causes graphite to become a semimetal. The effect is less important at other points of the Brillouin zone for graphite, and also in the case of BN, because of the large energy gaps. Figures 4-15 and 4-16 show the band structures of three-dimensional graphite and BN as calculated by Doni and Pastori Parravicini.<sup>[18]</sup>

#### 4-2d Considerations on other layer structures

Graphite and BN are the extreme basic examples of a large class of materials which are called layer structures because they are formed by layers containing atoms strictly bound among themselves, each layer being loosely bound to the others by weak Van der Waals forces. A characteristic feature of most layer crystals is the fact that different layers may be oriented in several different ways with respect to one another; a number



(a)



(b)

FIG. 4-14. (a) Three-dimensional crystal structure of graphite. (b) Three-dimensional crystal structure of BN.

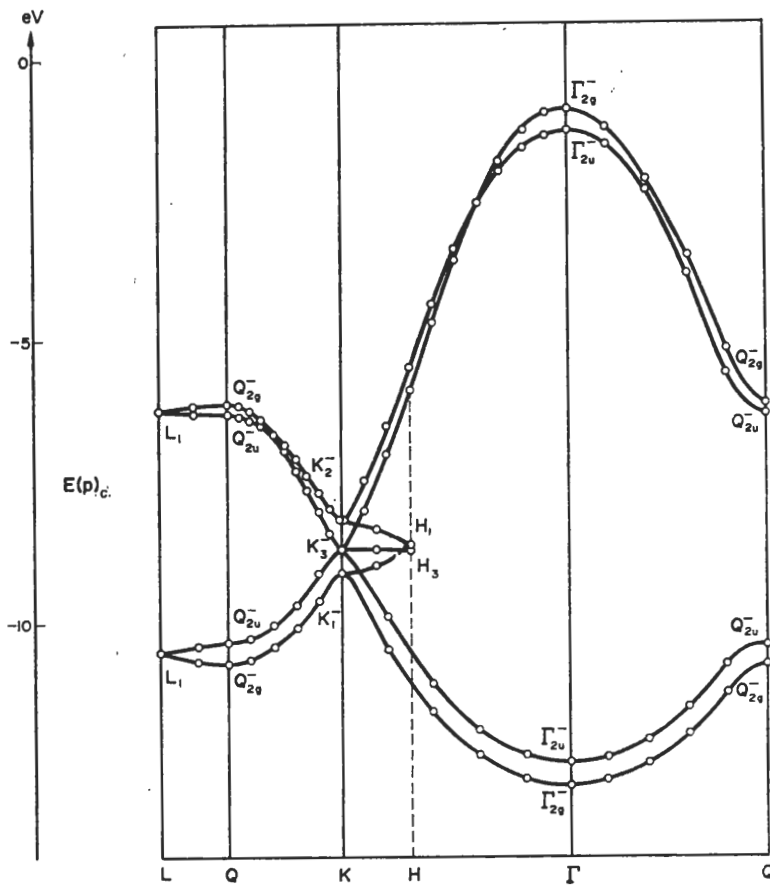


FIG. 4.15. Energy bands for three-dimensional graphite. Only bands derived from  $p_z$  atomic orbitals are considered. (From Doni and Pastori Parravicini, ref. [18].)

of polytypes results, all with the same structure of the basic layer. For the description of the structures and properties of a number of layer compounds we refer the reader to the review articles by Wilson and Yoffe<sup>[19]</sup> and Harbeck<sup>[19]</sup> and to a forthcoming series edited by Mooser.<sup>[20]</sup>

The band structure of layer materials can be interpreted<sup>[21]</sup> within the tight binding scheme by considering the symmetrized combinations of atomic orbitals and assuming that only bonding combinations are occupied by electrons. This gives a qualitative criterium for understanding the semiconductor nature of the compounds. From a quantitative point of view it is possible to perform detailed calculations with the tight binding method provided one modifies the long range tail of the atomic orbitals which are needed to construct the crystal states. Bassani and Pastori Parravicini<sup>[17]</sup> proposed this approach to take into account the fact that one should use as localized functions in the tight binding method distorted orbitals, which are appropriate to the atom in its crystal environment. For simplicity, one often adopts an empirical cutting in the long tail behaviour of the atomic orbitals to reproduce this physical effect. This approach

## ELECTRONIC BAND STRUCTURE IN SOME CRYSTALS

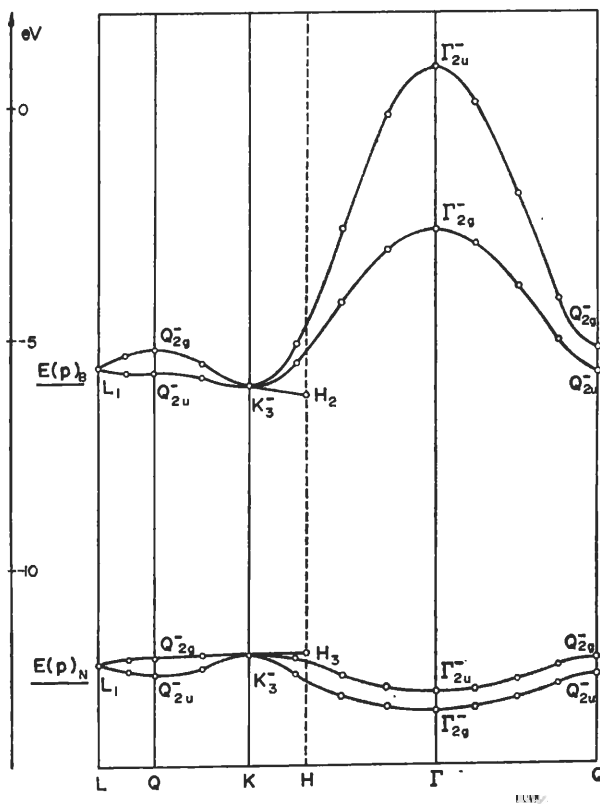


FIG. 4-16. Energy bands for three-dimensional BN. Only bands derived from  $p_z$  atomic orbitals are considered. (From Doni and Pastori Parravicini, ref. [18].)

has been used for GaS, GaSe, PbI<sub>2</sub> and some metal chalcogenides with remarkable success,<sup>[22]</sup> and is becoming quite popular for all complex semiconductors. It can be considered a variation of the interpolation scheme originally proposed by Slater and Koster<sup>[21]</sup> and discussed in Section 3-2d with the advantage that the overlap is included and one is not limited to functions which are orthogonal on different cells.

Pseudopotential calculations have also been performed for layer compounds<sup>[23]</sup> like GaSe, and are being extended to a number of complex semiconductors.<sup>[24]</sup> The valence bands obtained with the pseudopotential method are generally found to be in reasonable agreement with those obtained with the tight binding method, while some discrepancies may occur in the conduction bands; for detailed comparison we refer the reader to the original papers. It is of interest to mention that electron density maps in crystals have been computed by Schlüter<sup>[23]</sup> starting from the pseudowave functions of the occupied bands. We show in Fig. 4-17 a typical charge density map for the valence bands of GaSe. Figure 4-17 gives an interesting pictorial view of the covalent bonds Ga-Ga and Ga-Se from the pile up of charge midway between the atoms. Schlüter has also shown how this charge can be decomposed into the contributions from different bands, reconstructing bonding and non-bonding bands from their typical charge density maps in essential agreement with tight binding concepts.

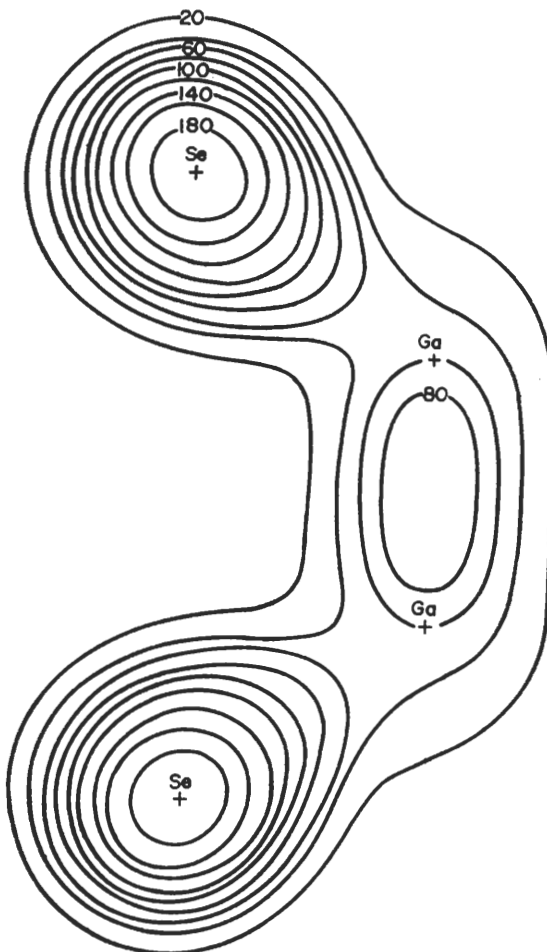


FIG. 4-17. Electron density contour map for the valence bands in GaSe. The values are plotted in units of  $e$  per unit cell. (From ref. [23].)

#### 4-3 Energy bands of linear chain type crystals: selenium and tellurium

##### 4-3a Symmetry properties of the selenium structure

Selenium and tellurium crystallize in a peculiar crystal structure made up of spiral chains with three atoms per unit cell. The selenium structure can also be described as consisting of three interlocking simple hexagonal lattices, each of them contributing one atom per unit cell (Fig. 4-18).

The primitive vectors of the translation group are:

$$\left. \begin{aligned} \tau_1 &= a \left( \frac{1}{2}, \frac{\sqrt{3}}{2}, 0 \right), \\ \tau_2 &= a \left( -\frac{1}{2}, \frac{\sqrt{3}}{2}, 0 \right), \\ \tau_3 &= c (0, 0, 1), \end{aligned} \right\} \quad (4-8)$$

BIBLIOTHÈQUE DU  
DÉPARTEMENT DE PHYSIQUE  
Ecole Polytechnique Fédérale  
PHB - Ecublens  
CH - 1015 LAUSANNE Suisse  
Tél. 021-47 11 11

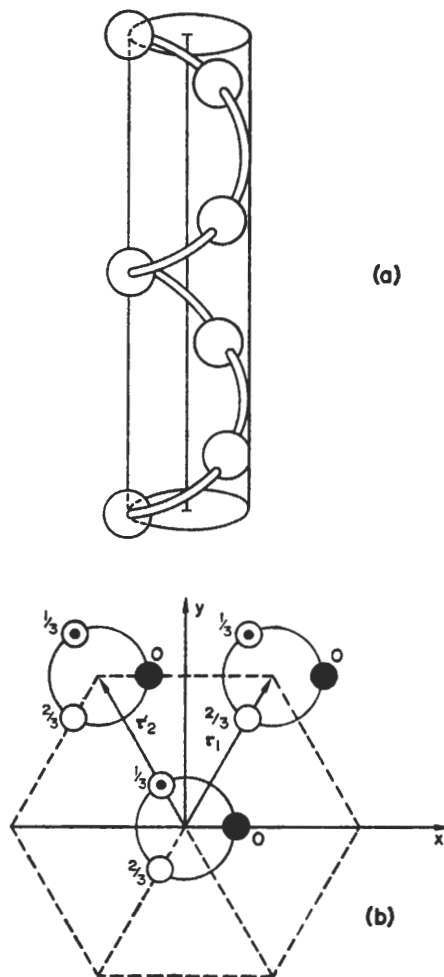


FIG. 4-18. (a) Spiral chain of selenium atoms. (b) Three-dimensional crystal structure of selenium showing the projections of the atoms on to the plane perpendicular to the  $z$  axis. The number near each atom indicates the  $z$  coordinate (in units of  $c$ ).

with  $a = 4.35 \text{ \AA}$ ,  $c = 4.95 \text{ \AA}$  for Se, and  $a = 4.44 \text{ \AA}$ ,  $c = 5.91 \text{ \AA}$  for Te. With the choice of the coordinate axes of Fig. 4-18 the positions of the atoms in the unit cell are:

$$\mathbf{d}_1 = (r, 0, 0),$$

$$\mathbf{d}_2 = \left( -\frac{r}{2}, \frac{r\sqrt{3}}{2}, \frac{c}{3} \right),$$

$$\mathbf{d}_3 = \left( -\frac{r}{2}, -\frac{r\sqrt{3}}{2}, \frac{2c}{3} \right),$$

where  $r$  indicates the radius of the spiral chain. The value of  $r$  is  $1.07 \text{ \AA}$  in Se and  $1.59 \text{ \AA}$  in Te. The angle Se-Se-Se in a chain is approximately  $105^\circ$ , and for Te-Te-Te is equal to  $102^\circ$ . The Se-Se distance along the chain is  $2.32 \text{ \AA}$  whereas the Te-Te distance

## ELECTRONIC STATES AND OPTICAL TRANSITIONS

is 2.86 Å. The ratio of the nearest distance between atoms belonging to different chains to the nearest distance between atoms of the same chain is 1.49 for Se and 1.2 for Te. Thus the interaction between atoms in the chain is expected to be larger (particularly for selenium) than the interaction between different chains, which is why some of the basic properties of these compounds can be understood by separately considering a single chain.

The fundamental vectors of the reciprocal lattice are:

$$\left. \begin{aligned} \mathbf{h}_1 &= \frac{2\pi}{a} \left( -1, \frac{1}{\sqrt{3}}, 0 \right), \\ \mathbf{h}_2 &= \frac{2\pi}{a} \left( 1, \frac{1}{\sqrt{3}}, 0 \right), \\ \mathbf{h}_3 &= \frac{2\pi}{c} (0, 0, 1). \end{aligned} \right\} \quad (4-9)$$

The Brillouin zone is similar to that of graphite shown in Fig. 4-13. In the approximation of a single chain, we need only consider the vectors  $\tau_3$  and  $\mathbf{h}_3$  in formulae (4-8) and (4-9), and the Brillouin zone of Fig. 4-13 is reduced to the line  $\Gamma - Z$ .

The symmetry analysis of selenium structure has been given by Asendorf.<sup>[25]</sup> The point group of the selenium structure is  $D_3$ . The space group is not symmorphic and some of the symmetry operations are associated with fractional translations. The space group of the selenium structure contains the threefold screw rotations

$$\{C_3 | \frac{1}{3}\tau_3\}, \quad \{C_3^2 | -\frac{1}{3}\tau_3\}$$

along the  $z$  axis and the three twofold axes

$$\{C_x | 0\}, \quad \{C'_x | \frac{1}{2}\tau_3\}, \quad \{C''_x | -\frac{1}{2}\tau_3\}$$

in the  $(x, y)$  plane. The symmetry operations are given in Table 4-17 together with coordinate transformations.

At the point  $\Gamma$  the little group of  $\mathbf{k}$  is the complete group  $D_3$ . In Table 4-18 we give the irreducible representations of the group of  $\mathbf{k}$  at the point  $\Gamma$ . At the symmetry points  $Z$ ,

TABLE 4-17. Symmetry operations for the selenium structure. In columns 1 and 3 the symmetry operations are denoted using standard crystallographic notations. Columns 2 and 4 give the rotational matrix representatives

Symmetry operations	Rotational matrix	Symmetry operations	Rotational matrix
$\{E 0\}$	$\begin{pmatrix} 1 & 0 & 0 \\ 0 & 1 & 0 \\ 0 & 0 & 1 \end{pmatrix}$	$\{C_x 0\}$	$\begin{pmatrix} 1 & 0 & 0 \\ 0 & -1 & 0 \\ 0 & 0 & -1 \end{pmatrix}$
$\{C_3 \frac{1}{3}\tau_3\}$	$\begin{pmatrix} -1/2 & -\sqrt{3}/2 & 0 \\ \sqrt{3}/2 & -1/2 & 0 \\ 0 & 0 & 1 \end{pmatrix}$	$\{C'_x \frac{1}{2}\tau_3\}$	$\begin{pmatrix} -1/2 & -\sqrt{3}/2 & 0 \\ -\sqrt{3}/2 & 1/2 & 0 \\ 0 & 0 & -1 \end{pmatrix}$
$\{C_3^2 -\frac{1}{3}\tau_3\}$	$\begin{pmatrix} -1/2 & \sqrt{3}/2 & 0 \\ -\sqrt{3}/2 & -1/2 & 0 \\ 0 & 0 & 1 \end{pmatrix}$	$\{C''_x -\frac{1}{2}\tau_3\}$	$\begin{pmatrix} -1/2 & \sqrt{3}/2 & 0 \\ \sqrt{3}/2 & 1/2 & 0 \\ 0 & 0 & -1 \end{pmatrix}$

$H$ , and  $K$  the small point group of  $\mathbf{k}$  is  $D_3$ . The irreducible representation at these points can be obtained using the appropriate procedures (see Section 2-2) for non-symmorphic groups. As in the case of  $\Gamma$  we find two one-dimensional and one two-dimensional representations, and we label these representations with subscripts 1, 2, and 3 respectively. In Table 4-19 we give the allowed optical transitions in the dipole approximation showing their dependence on the polarization direction with respect to the main axis  $z$ .

TABLE 4-18. Irreducible representations at the point  $\Gamma$  of the Brillouin zone for the selenium structure. Time reversal does not introduce additional degeneracies

Point $\Gamma$	$\{E 0\}$	$\{C_3 \frac{1}{2}\tau_3\} \{C_3^2 -\frac{1}{2}\tau_3\}$	$\{C_x 0\} \{C'_x \frac{1}{2}\tau_3\} \{C''_x -\frac{1}{2}\tau_3\}$
$\Gamma_1$	1	1	1
$\Gamma_2$	1	1	-1
$\Gamma_3$	2	-1	0

TABLE 4-19. Allowed optical transitions with light polarized  $\parallel$  or  $\perp$  to the  $z$  axis at the symmetry point  $\Gamma$  for the selenium structure

Point $\Gamma$	$\Gamma_1$	$\Gamma_2$	$\Gamma_3$
$e \parallel$ to $z$ axis	$\Gamma_2$	$\Gamma_1$	$\Gamma_3$
$e \perp$ to $z$ axis	$\Gamma_3$	$\Gamma_3$	$\Gamma_1 + \Gamma_2 + \Gamma_3$

#### 4-3b Energy bands for selenium and tellurium<sup>[26]</sup>

Selenium and tellurium are elements of the sixth column of the Periodic Table. The electronic configuration for the free atoms is  $(ns^2, np^4)$  with  $n = 4$  for Se and  $n = 5$  for Te. Inner shells are completely occupied and give crystals core states with energies nearly equal to those of the corresponding atomic states.

The band structure of selenium and tellurium has been studied by a number of authors in the one-dimensional approximation. An early simplified calculation was considered by Reitz and a more detailed calculation, based on the tight binding approach and on a semi-empirical use of the screened exchange potential, was made by Olechna and Knox. Calculations in the three-dimensional case with Green's function method have been carried out by Treusch and Sandrock, and their results are shown in Figs. 4-19 and 4-20.

We notice that both selenium and tellurium have their conduction band minima and their valence band maxima at the symmetry point  $H$ . From the correspondence between crystal states and atomic states we expect that the valence and conduction bands originate from  $p$  states and can be separated into three groups split by energy gaps. For tellurium the anisotropy of the structure is less than for selenium and the dependence of the energy bands of the components  $k_x$  and  $k_y$  in the Brillouin zone is more important. When we include relativistic effects the top valence state of tellurium is split by about 0.11 eV.

We wish to conclude these remarks by pointing out that the elements of the sixth column of the Periodic Table present all types of electronic structures:<sup>[27]</sup> oxygen and sulphur are insulators, whilst selenium and tellurium are semiconductors and polonium is a metal.

## ELECTRONIC STATES AND OPTICAL TRANSITIONS

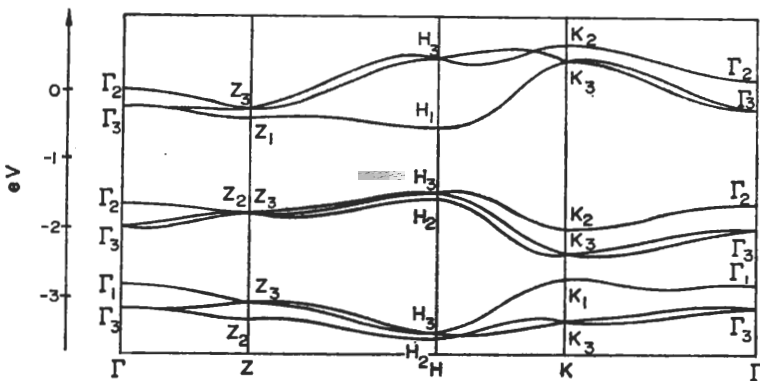


FIG. 4-19. Energy bands for selenium. (From Treusch and Sandrock, ref. [26].)

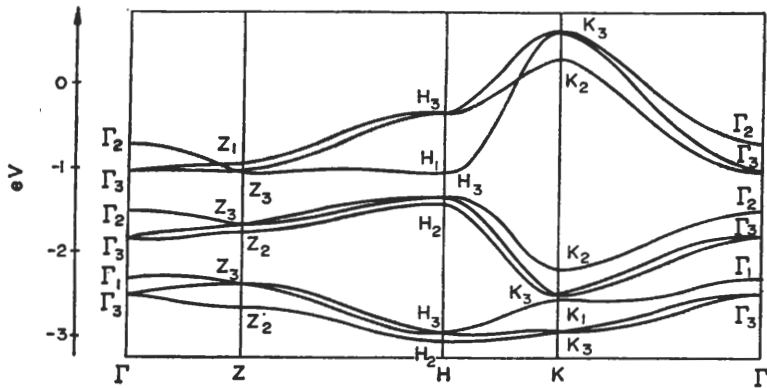


FIG. 4-20. Energy bands for tellurium. (From Treusch and Sandrock, ref. [26].)

### 4-4 Considerations on the band structure of some large gap insulators

Solid rare gases, alkali halides, silver halides are examples of a vast class of "large gap" insulators on which a lot of theoretical and experimental work has been carried out. We will not attempt to review the field, but may give some guidelines from which one can develop a feeling on how to look at the results of elaborate energy band calculations.

In order to have large gap insulators it is required that all the occupied crystal states are concentrated in the highly attractive regions of the crystal potential. In this situation, we expect that valence bands (as well as core states) of large gap insulator can be well described by the tight binding method (see Section 3-2). Let us first consider the solid rare gases<sup>[28]</sup> which crystallize in the face-centred cubic lattice with one atom per unit cell. Rare gases have the closed shell electronic configuration ( $ns^2, np^6$ ) with  $n = 2, 3, 4, 5$  for Ar, Ne, Kr, Xe, respectively. To obtain valence bands, we consider the four Bloch

sums formed from the atomic orbitals  $ns$ ,  $np_x$ ,  $np_y$ ,  $np_z$ . A classification of the symmetry properties of Bloch functions at relevant points of the Brillouin zone gives valid information on the sequence of the occupied electronic states. In Fig. 4-21 we show, as a typical example, the valence energy bands of krypton.

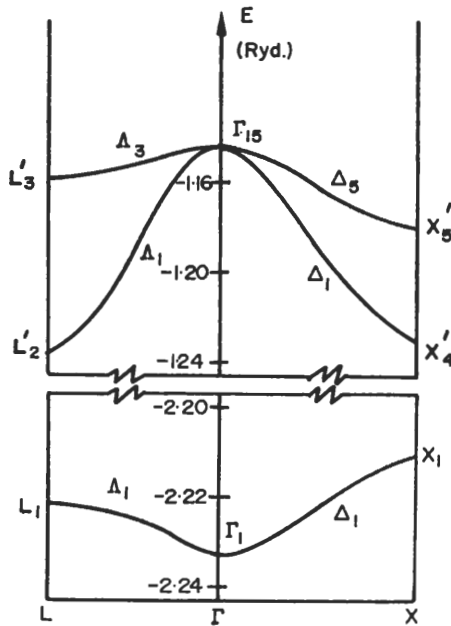


FIG. 4-21. Valence energy bands for krypton. (From Fowler, ref. [28].)

The basic features of the valence bands of solid rare gases can be understood within the tight binding scheme. At  $\mathbf{k} = 0$  the Bloch function formed with the atomic orbital  $ns$  does not interact with the Bloch functions formed with the atomic orbitals  $np_x$ ,  $np_y$ ,  $np_z$ . The  $s$ -like state  $\Gamma_1$  is thus expected to be lower in energy than the  $p$ -like state  $\Gamma_{15}$ . Away from  $\mathbf{k} = 0$ , the  $s$ -like band bends upward and the  $p$ -like bands bend downward; this occurs when the mixing between  $s$  and  $p$  Bloch functions away from  $\mathbf{k} = 0$  is negligible. In fact, considering only nearest neighbours interaction and using (3-23) we obtain the following expression for the  $s$  band in a face-centred cubic lattice

$$E_s(\mathbf{k}) = E_s + \frac{2V(ss\sigma) \left[ \cos \frac{a}{2}(k_x + k_y) + \cos \frac{a}{2}(k_y + k_z) + \cos \frac{a}{2}(k_x + k_z) \right.}{1 + 2S(ss\sigma) \left[ \cos \frac{a}{2}(k_x + k_y) + \cos \frac{a}{2}(k_y + k_z) + \cos \frac{a}{2}(k_x + k_z) \right.} \\ \left. + \cos \frac{a}{2}(k_x - k_y) + \cos \frac{a}{2}(k_y - k_z) + \cos \frac{a}{2}(k_x - k_z) \right] \quad (4-10)$$

where  $S(ss\sigma)$  and  $V(ss\sigma)$  denote the overlap and potential integral respectively. In (4-10) the crystal field integral has been neglected because rare gas atoms are neutral and their distances in the crystal are relatively large. Since  $S(ss\sigma)$  is always a positive quantity, while  $V(ss\sigma)$  is negative, expression (4-10) has its minimum at  $\mathbf{k} = 0$  and its maximum at the surface of the Brillouin zone. Similarly, for a  $p$  band, using the appropriate symmetrized combinations of Bloch sums and the reduction to independent integrals of Table 3-1,

$$E_{A_5} = E_p + \frac{V(pp\sigma) \left[ 2 + 2\cos \frac{a}{2} k_x \right] + V(pp\pi) \left[ 2 + 6\cos \frac{a}{2} k_x \right]}{1 + S(pp\sigma) \left[ 2 + 2\cos \frac{a}{2} k_x \right] + S(pp\pi) \left[ 2 + 6\cos \frac{a}{2} k_x \right]},$$

$$E_{A_1} = E_p + \frac{V(pp\sigma) 4\cos \frac{a}{2} k_x + V(pp\pi) \left[ 4 + 4\cos \frac{a}{2} k_x \right]}{1 + S(pp\sigma) 4\cos \frac{a}{2} k_x + S(pp\pi) \left[ 4 + 4\cos \frac{a}{2} k_x \right]},$$

$$E_{A_3} = E_p + \frac{V(pp\sigma) \left[ 3 + \cos \frac{a}{2} k_x \right] + V(pp\pi) \left[ 3 + 5\cos \frac{a}{2} k_x \right]}{1 + S(pp\sigma) \left[ 3 + \cos \frac{a}{2} k_x \right] + S(pp\pi) \left[ 3 + 5\cos \frac{a}{2} k_x \right]},$$

$$E_{A_1} = E_p + \frac{V(pp\sigma) 4\cos \frac{a}{2} k_x + V(pp\pi) \left[ 6 + 2\cos \frac{a}{2} k_x \right]}{1 + S(pp\sigma) 4\cos \frac{a}{2} k_x + S(pp\pi) \left[ 6 + 2\cos \frac{a}{2} k_x \right]}.$$

Since  $V(pp\sigma)$  is positive and much larger than  $V(pp\pi)$ , we have that  $A_1$  is lower than  $A_5$ ,  $A_1$  is lower than  $A_3$ , and  $p$  bands bend downward going away from  $\mathbf{k} = 0$ . Thus the basic features of the valence bands of solid rare gases can be understood in the tight binding approach.

A very similar but slightly more complicated example is that of alkali halides<sup>[29]</sup> formed by two face-centred cubic sublattices occupied by positive and negative ions respectively. This does not introduce a serious difficulty, however, since the strong ionicity of the compounds prevents mixing of the orbitals of the two different types of ions. The states of the negative ion give a valence band structure similar to that of the solid rare gases since the sublattice has the same symmetry and the negative ion configuration is also the closed shell configuration ( $ns^2, np^6$ ). The states of the positive ions are also closed shell states with atomic configuration ( $ns^2, np^6$ ). The energies of positive ion states are, nevertheless, much lower than those of the corresponding negative ions so that they can generally be treated as core states with negligible mixing. Consequently one finds the top valence band structure of alkali halides to be quite similar in shape to that of solid rare gases. Also in this case the maximum of the valence band is  $\Gamma_{15}$ . The absolute energy positions of all bands are, however, shifted with respect to those of the corresponding ionic levels by the Madelung term which is opposite

for negative and for positive ions. The Madelung shift accounts for most of the energy gap and explains why the ionic structure is strongly favoured with respect to other possibilities.

A further complication which produces a very interesting effect arises in the valence bands of the silver halides,<sup>[30]</sup> which have the same crystal structure as the alkali halides. In this case in fact we have an ion  $\text{Ag}^+$  with a filled  $5d$  electronic shell whose energy is not very far from that of the  $np$  shell of  $\text{Cl}^-$  or  $\text{Br}^-$  once account is taken of the Madelung shift. In this case we expect mixing of the  $d$  bands of silver with the  $p$  bands of the halogen ion to produce a certain amount of covalent bonding. It is mostly interesting to remark that this mixing does not take place at  $\mathbf{k} = 0$  because the  $l = 2$  atomic levels decompose into two states of symmetry  $\Gamma'_{25}$  and  $\Gamma_{12}$  as shown in Table 1-16, and these states cannot interact with the  $p$ -like  $\Gamma_{15}$  state. Mixing occurs away from  $\mathbf{k} = 0$ , with the effect of repelling levels of the same symmetry to produce relative maxima at  $L$ ,  $\Delta$ , and  $\Sigma$ , the absolute maximum of the valence band being the state  $L'_3$ . Detailed calculations, both by the tight binding method and by the APW method, confirm this analysis.<sup>[30]</sup> Figure 4-22 illustrates the valence band structure of  $\text{AgCl}$ . It may be pointed out that a valence band structure of this type, with its maximum at the surface of the Brillouin zone, is required to explain the peculiar optical properties of the silver halides.

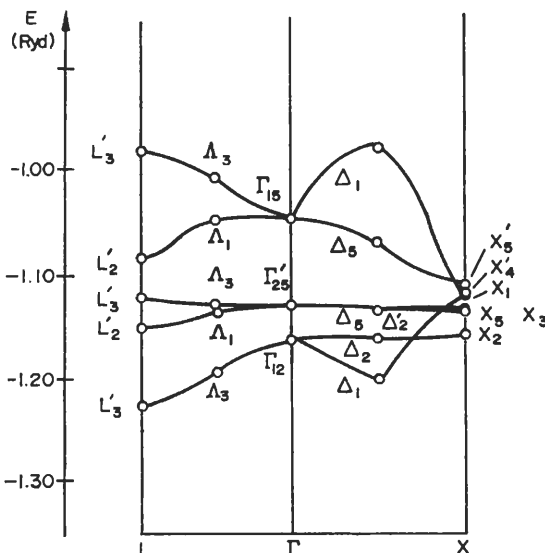


FIG. 4-22. Valence energy bands for  $\text{AgCl}$ . (From Bassani *et al.*, ref. [30].)

In the tight binding model the lowest conduction band would correspond to the first empty state of the rare gas or of the alkali atom in ionic crystals. It is immediate to observe, however, that in this case Bloch functions formed from the atomic orbitals would not be a good representation of the conduction band because such functions have a large overlap among neighbouring atoms (for instance the overlap integral  $S(ss\sigma)$  is about 0.4 between the nearest  $4s$  orbitals of argon). The conduction bands are expected to be highly delocalized and it seems natural to study them within the framework

of the OPW method (see Section 3-3) or of the pseudopotential method (see Section 3-4). This explains why the conduction states can be interpreted in terms of those of the empty lattice as modified by the effect of the orthogonalization to core and valence states as explained in Section 3-3e. As an example we give in Fig. 4-23 the conduction band structure of KCl calculated by Bassani and Giuliano<sup>[29]</sup> within the pseudopotential formalism. We may note that the minimum is  $\Gamma_1$  and there is a secondary minimum at the point  $X$  which is the state of  $d$ -like symmetry  $X_3$ . As we will show in Chapter 7, the existence of this secondary minimum may well be responsible for resonant states in the continuum in this specific case.

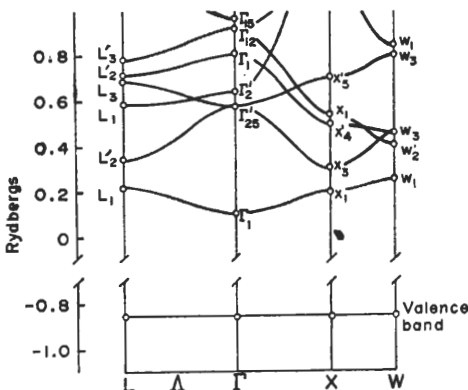


FIG. 4-23. Conduction energy bands for KCl. (From Bassani and Giuliano, ref. [29].)

#### 4-5 Considerations on the band structure of some molecular crystals

While very extensive calculations have been performed on the band structure of inorganic conductors and insulators, a comparable effort has not yet been made on the electronic structure of organic crystals. We think the reason is twofold. Firstly, the complexity of organic crystals, the difficulties in their preparation, and in the crystallographic determinations of the position of the hydrogen ions which play an essential role. Secondly, the impossibility of interpreting their optical excitation spectrum in terms of interband transitions (Chapter 5) as in the case of metals and semiconductors because of the dominant excitonic effects (Chapter 6). In the past few years the interest in organic crystals has considerably increased because the knowledge of the electronic behaviour of large macromolecules, biological molecular chains, and organic crystals, is of great importance for the understanding of the stability of the compounds, of the nature of the hydrogen bond,<sup>[31]</sup> and of other problems of biological importance.<sup>[32]</sup> Furthermore, the availability of ESCA techniques<sup>[33]</sup> and the improvements of X-ray emission techniques<sup>[34]</sup> may make it possible to investigate experimentally the band structure of organic crystals and to provide a direct comparison with theoretical calculations.

The electronic structure and Bloch functions of organic crystals can be obtained by adopting an extension of the tight binding method along ideas originally suggested by Hall, Coulson *et al.*, and Gubanov *et al.*<sup>[35]</sup> for covalent compounds. These ideas

essentially consist in providing a self-consistent field Hartree-Fock calculation for the closest atomic units and using the tight binding method for taking into account the long range interactions. They have not been particularly fruitful for inorganic crystals because in covalent bonding the atoms are the basic units and are bounded to other atoms without forming a preferred cluster.<sup>[14]</sup> However, it is to be expected that they will be applicable to the case of molecular crystals where the basic unit of the lattice is the molecule and the binding between molecules is much weaker than the binding between atoms in the same molecule. Consequently one can introduce, as a modification of the standard tight binding method, the molecular tight binding method characterized by the fact that the Bloch sums used as a basis expansion set for the crystal eigenfunctions are constructed from molecular orbitals instead of atomic orbitals. The electron-electron interaction in the same molecule is thus included self-consistently in the molecular orbitals.

A number of calculations have been recently carried out on the basic molecular crystal H<sub>2</sub>,<sup>[36]</sup> cubic ice,<sup>[37]</sup> solid HF,<sup>[38]</sup> and solid methane.<sup>[39]</sup> To give a feeling on how the molecular levels spread into energy bands in a typical molecular crystal, we report in Fig. 4-24 the valence bands of ortho-hydrogen. The translational symmetry

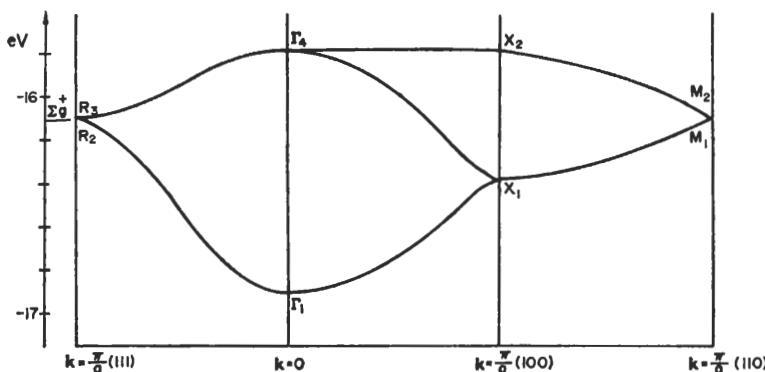


FIG. 4-24. Valence energy bands for solid ortho-hydrogen. The energy of the molecular orbital  $\Sigma_g^+$  is also shown. (From ref. [36].)

is that of a simple cubic lattice, but there are four molecules per cell so that we must consider eight valence electrons. As can be seen from Fig. 4-24, the  $\Sigma_g^+$  level of the H<sub>2</sub> molecules transforms into bands which are degenerate along the edges of the Brillouin zone cube where the energy coincides with that of the free molecule.<sup>[36]</sup> The maximum valence band width of  $\approx 1.1$  eV is at the point  $\Gamma$  due to strong splitting between the one-dimensional state  $\Gamma_1$  and the three-dimensional state  $\Gamma_4$  of the group  $T_h$ .

#### 4-6 Considerations on the band structure of simple metals

The basic difference between metals and insulators (or semiconductors) is that in metals the Fermi level  $E_F$  occurs within a band or intersects a number of bands. The surface in  $\mathbf{k}$  space corresponding to crystal states with energy  $E_F$  is called Fermi surface and relates to all electron transport phenomena in metals. It has been investigated in

## ELECTRONIC STATES AND OPTICAL TRANSITIONS

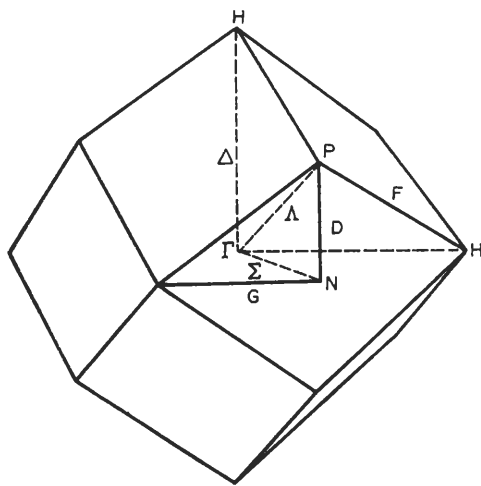


FIG. 4-25. Brillouin zone for alkali metals.

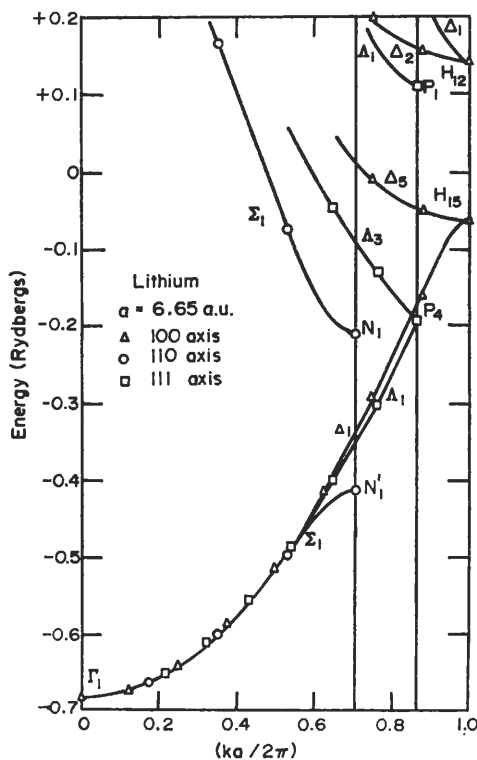


FIG. 4-26. Energy bands for lithium. (From Ham, ref. [41].)

detail both experimentally and theoretically in the past two decades by a large number of authors.<sup>[40]</sup>

In many metals the Fermi surface is only slightly distorted from the free electron like Fermi sphere, which would result for a uniform crystal potential (empty lattice), and we may classify these as simple metals. Even in simple metals the Fermi surface has peculiar shapes when the number of electrons is such that it must intersect zone boundaries where symmetry requires zero curvature for the bands and hole pockets may result. In this sense the simplest of the simple metals are the alkali metals because they have only one valence electron per unit cell and only half of the states of a band can be filled so that the Fermi surface lies quite far from the zone boundaries and deviations from sphericity are fairly small. In other cases like transition metals, noble metals, or rare earth materials, the energy bands around the Fermi level consist of the superposition of well-localized *d* bands or *f* bands and of free electron like bands and the Fermi surface is quite different from the free electron sphere.

In simple metals the nearly uniform space distribution of conduction electrons is a physical argument to justify the use of a crystal potential consisting of spherically symmetric atomic potentials inside spheres around the nuclei and constant elsewhere (muffin-tin potential). This fact explains the wide use of the cellular method, the APW method, and Green's function method for the band structure calculations in simple metals. These calculational methods have also been widely applied to non-simple metals for the reasons discussed in Section 3-6b when a muffin-tin approximation to the crystal potential is justified.

As an example we will briefly comment on alkali metals which have been extensively studied since 1933, the basic most comprehensive work being due to Ham.<sup>[41]</sup> The

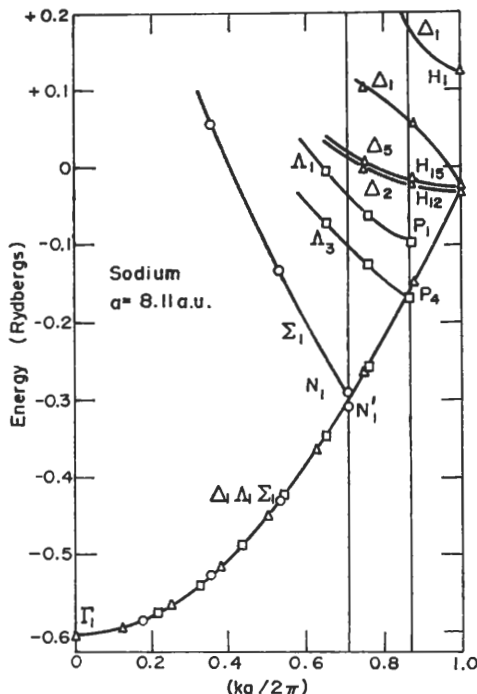


FIG. 4-27. Energy bands for sodium. (From Ham, ref. [41].)

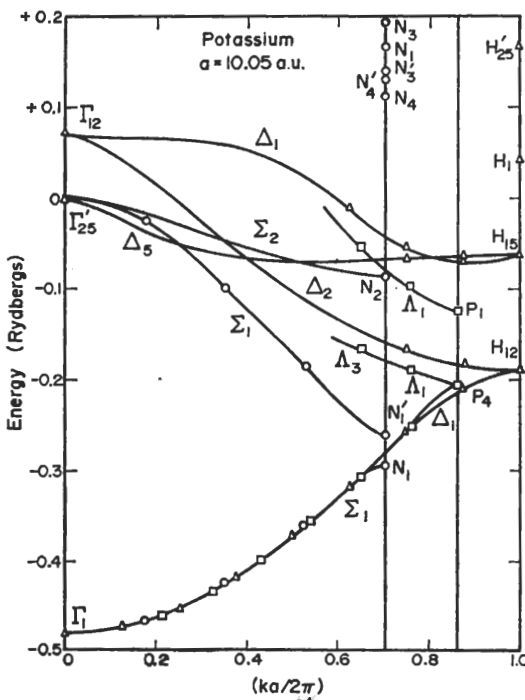


FIG. 4-28. Energy bands for potassium. (From Ham, ref. [41].)

crystal structure is body-centred cubic with one atom per unit cell. The corresponding Brillouin zone is displayed in Fig. 4-25. In Figs. 4-26, 4-27, and 4-28 we report the band structures of Li, Na, and K calculated by Ham,<sup>[41]</sup> who used Green's function method combined with the quantum defect method (see Sections 3-7 and 3-8). It can be seen that the deviations from free electron behaviour are small for any alkali metal. It can also be noticed that these deviations are larger in lithium and are minimal in sodium, which can be taken as the typical example of a simple metal.

It is very instructive to understand the trend with increasing atomic number of the states which are degenerate in the empty lattice analysis. Specifically let us consider the energy separation for the states  $N'_1$  and  $N_1$ . The state  $N_1$  has *s*-like symmetry (and also *d*-like symmetry), while the state  $N'_1$  has *p*-like symmetry. Applying the results of Section 3-3e, we expect that in lithium the state  $N_1$  is repelled from 1s core states and is pushed to higher energy than  $N'_1$ . In sodium also  $N'_1$  feels a repulsive effect from 2*p* core states; as a consequence  $N'_1$  and  $N_1$  are nearly coincident in sodium as in the empty lattice. As the atomic number increases, successive shells are filled in the core with the effect of interchanging the order of the states  $N'_1$  and  $N_1$  in K, Rb, and Cs. In Section 3-9 we interpreted with the  $\mathbf{k} \cdot \mathbf{p}$  method the trend of the effective masses in alkali metals.

### References and notes

For a comprehensive description of crystal structures see, for example R. W. G. WYCKOFF, *Crystal Structures* (Interscience, 1963). The symmetry analysis of all space groups is given in the book by C. J. BRADLEY and A. P. CRACKNELL, *The Mathematical Theory of Symmetry in Solids* (Clarendon Press, 1972).

## ELECTRONIC BAND STRUCTURE IN SOME CRYSTALS

- [1] F. HERMAN, *Phys. Rev.* **93**, 1214 (1954).
- [2] For details on the energy band calculations of diamond see the following articles: (i) Tight binding method: G. G. HALL, *Phil. Mag.* **43**, 338 (1952); **3**, 429 (1958); J. C. SLATER and G. F. KOSTER, *Phys. Rev.* **94**, 1498 (1954); A. MORITA, *J. Phys. Chem. Solids* **8**, 363 (1959); N. V. COHAN, D. PUGH, and R. H. TREDGOLD, *Proc. Phys. Soc.* **82**, 65 (1963); R. C. CHANEY, C. C. LIN, and E. E. LAFON, *Phys. Rev.* **2B**, 459 (1970); G. S. PAINTER, D. E. ELLIS, and A. R. LUBINSKY, *Phys. Rev.* **4B**, 3610 (1971). (ii) OPW and pseudopotential method: F. HERMAN, *Phys. Rev.* **88**, 1210 (1952); **93**, 1214 (1954); L. KLEINMAN and J. C. PHILLIPS, *Phys. Rev.* **116**, 880 (1959); F. BASSANI and M. YOSHIMINE, *Phys. Rev.* **130**, 20 (1963). (iii) APW method: R. KEOWN, *Phys. Rev.* **150**, 568 (1966); See also the review article by F. HERMAN, R. L. KORTUM, and C. D. KUGLIN, *Int. J. of Quantum Chem.* **1S**, 533 (1967).
- [3] F. HERMAN, *Phys. Rev.* **93**, 1214 (1954); **95**, 847 (1954); *Physica* **20**, 801 (1954); T. WOODRUFF, *Phys. Rev.* **103**, 1159 (1956); F. BASSANI, *Phys. Rev.* **108**, 263 (1957); F. BASSANI and M. YOSHIMINE, *Phys. Rev.* **130**, 20 (1963); E. O. KANE, *Phys. Rev.* **146**, 558 (1966); F. HERMAN, R. L. KORTUM, C. D. KUGLIN, and R. A. SHORT, in *Quantum Theory of Atoms, Molecules and the Solid State* (edited by P. O. LÖWDIN, Academic Press, 1966), G. DRESSELHAUS and M. S. DRESSELHAUS, *Phys. Rev.* **160**, 649 (1967).
- [4] J. C. PHILLIPS, *Phys. Rev.* **125**, 1931 (1962); F. BASSANI and V. CELLI, *J. Phys. Chem. Solids* **20**, 64 (1961); D. BRUST, J. C. PHILLIPS, and F. BASSANI, *Phys. Rev. Letters* **9**, 94 (1962); D. BRUST, *Phys. Rev.* **134A**, 1337 (1964); M. L. COHEN and T. K. BERGSTRESSER, *Phys. Rev.* **141**, 789 (1966).
- [5] M. CARDONA and F. H. POLLAK, *Phys. Rev.* **142**, 530 (1966).
- [6] W. BRINKMAN and B. GOODMAN, *Phys. Rev.* **149**, 597 (1966).
- [7] F. BASSANI and V. CELLI, *Nuovo Cimento* **11**, 805 (1959).
- [8] L. LIU, *Phys. Rev.* **126**, 1317 (1962).
- [9] F. HERMAN, *J. Electron.* **1**, 103 (1955).
- [10] F. BASSANI and L. LIU, *Phys. Rev.* **132**, 2047 (1963); S. GROVES and W. PAUL, *Phys. Rev. Letters* **11**, 194 (1963).
- [11] L. LIU and D. BRUST, *Phys. Rev.* **157**, 627 (1967); *Phys. Rev. Letters* **20**, 651 (1968); *Phys. Rev.* **173**, 777 (1968); L. LIU and E. TOSATTI, *Phys. Rev. Letters* **23**, 772 (1969); F. H. POLLAK, M. CARDONA, C. W. HIGGINBOTHAM, F. HERMAN, and J. P. VAN DYKE, *Phys. Rev.* **2B**, 352 (1970).
- [12] A. KISIEL and P. M. LEE, *J. Phys.* **2F**, 395 (1972).
- [13] J. CALLAWAY, *J. Electron.* **2**, 230 (1957).
- [14] F. BASSANI, in *Semiconductors and Semimetals* (edited by R. K. WILLARDSON and A. C. BEER, Academic Press, 1966), vol. 1, p. 21.
- [15] M. CARDONA, in *Semiconductors and Semimetals* (edited by R. K. WILLARDSON and A. C. BEER, Academic Press, 1967), vol. 1, p. 125; M. CARDONA, in *Proc. Enrico Fermi School of Physics*, course 52 on Atomic Structure and Properties of Solids, p. 514 (1972).
- [16] D. L. GREENAWAY and G. HARBEKE, *Optical Properties and Band Structure of Semiconductors* (Pergamon Press, 1968).
- [17] For electronic states in graphite, see, for example: P. R. WALLACE, *Phys. Rev.* **71**, 622 (1947); W. M. LOMER, *Proc. Roy. Soc. A*, **227**, 330 (1950); C. A. COULSON and H. TAYLOR, *Proc. Phys. Soc. London A* **65**, 815 (1952); **A** **65**, 834 (1952); F. J. CORBATO, in *Proceedings of the Third Conference on Carbon, London* (1959); F. BASSANI and G. PASTORI PARRAVICINI, *Nuovo Cimento* **50B**, 95 (1967); D. L. GREENAWAY, G. HARBEKE, F. BASSANI, and E. TOSATTI, *Phys. Rev.* **137A**, 639 (1969); A. IMATAKE and Y. UEMURA, *J. Phys. Soc. Japan* **28**, 410 (1970); G. S. PAINTER and D. E. ELLIS, *Phys. Rev.* **1B**, 4747 (1970); B. FEUERBACHER and B. FITTON, *Phys. Rev. Letters* **26**, 840 (1971); J. ZUPAN and D. KOLAR, *J. Phys.* **5C**, 3097 (1972).
- [18] E. DONI and G. PASTORI PARRAVICINI, *Nuovo Cimento* **63B**, 117 (1969); J. ZUPAN, *Phys. Rev.* **6B**, 2477 (1972).
- [19] J. A. WILSON and A. D. YOFFE, *Advan. Phys.* **18**, 193 (1969); G. HARBEKE, *Phys. Status Solidi* **27**, 9 (1968).
- [20] E. MOOSER (ed.), *The Physics of Layer Structures*, to appear.
- [21] E. MOOSER and W. B. PEARSON, *Progress in Semiconductors* **5**, 103 (1960).
- [22] E. DONI, G. GROSSO, and G. SPAVIERI, *Solid State Commun.* **11**, 493 (1972); P. G. HARPER and D. R. EDMONDSON, *Phys. Status Solidi* **44B**, 59 (1971); D. R. EDMONDSON, *Solid State Commun.* **10**, 1085 (1972); R. A. BROMLEY and R. B. MURRAY, *J. Phys.* **5C**, 738 (1972); R. A. BROMLEY, R. B. MURRAY, and A. D. YOFFE, *J. Phys.* **5C**, 746 (1972); **5C**, 759 (1972).
- [23] M. SCHLÜTER, *Nuovo Cimento* **13B**, 313 (1973).
- [24] See, for instance, I. CH. SCHLÜTER and M. SCHLÜTER, *Phys. Status Solidi* **57**, 145 (1973); *Phys. Rev.* **9B**, 1652 (1974).

## ELECTRONIC STATES AND OPTICAL TRANSITIONS

- [25] R. H. ASENDORF, *J. Chem. Phys.* **27**, 11 (1957).
- [26] For energy band calculations for selenium and tellurium see, for example: J. R. REITZ, *Phys. Rev.* **105**, 1233 (1957); D. J. OLECHNA and R. S. KNOX, *Phys. Rev.* **140**, A986 (1965); A. NUSSBAUM, *Solid State Physics* **18**, 165 (1966); J. TREUSCH and R. SANDROCK, *Phys. Status Solidi* **16**, 487 (1966); B. KRAMER and P. THOMAS, *Phys. Status Solidi* **26**, 151 (1968); T. DOI, K. NAKAO, and H. KAMIMURA, *J. Phys. Soc. Japan* **28**, 36 (1970); **28**, 822 (1970); **30**, 1400 (1971); W. DREYBRODT, K. J. BUTTON, and B. LAX, *Solid State Commun.* **8**, 1021 (1970); M. V. ORTENBERG, K. J. BUTTON, G. LANDWEHR, and D. FISCHER, *Phys. Rev.* **6B**, 2100 (1972).
- [27] A. J. VON HIPPEL, *J. Chem. Phys.* **16**, 372 (1948).
- [28] For energy band calculations of solid rare gases, see, for example: R. S. KNOX and F. BASSANI, *Phys. Rev.* **124**, 652 (1961); W. B. FOWLER, *Phys. Rev.* **132**, 1591 (1963); L. F. MATTHEISS, *Phys. Rev.* **133**, A 1399 (1964); N. O. LIPARI and W. B. FOWLER, *Phys. Rev.* **2B**, 3354 (1970).
- [29] For energy band calculations of alkali halides, see, for example: D. H. EWING and F. SEITZ, *Phys. Rev.* **50**, 760 (1936); R. C. CASELLA, *Phys. Rev.* **104**, 1260 (1956); L. P. HOWLAND, *Phys. Rev.* **109**, 1927 (1958); S. OYAMA and T. MIYAKAWA, *J. Phys. Soc. Japan* **21**, 868 (1966); Y. ONODERA, M. OKAZAKI, and T. INUI, *J. Phys. Soc. Japan* **21**, 2229 (1966); Y. ONODERA and Y. TOYOZAWA, *J. Phys. Soc. Japan* **22**, 833 (1967); P. DE CICCO, *Phys. Rev.* **153**, 931 (1967); N. O. LIPARI and A. B. KUNZ, *Phys. Rev.* **4B**, 4639 (1971); F. BASSANI and E. S. GIULIANO, *Nuovo Cimento* **8B**, 193 (1972). For experimental evidence relating to the above calculations, see, for example: T. EBY, K. J. TEEGARDEN, and D. B. DUTTON, *Phys. Rev.* **116**, 1099 (1959); K. TEEGARDEN and G. BALDINI, *Phys. Rev.* **155**, 896 (1967); D. M. ROESSLER and W. C. WALKER, *Phys. Rev.* **166**, 599 (1968); G. BALDINI and B. BOSACCHI, *Phys. Rev.* **166**, 863 (1968); F. C. BROWN, C. GÄHWILLER, H. FUJITA, A. B. KUNZ, W. SCHEIFLEY, and N. CARRERA, *Phys. Rev.* **2B**, 2126 (1970).
- [30] For energy band calculations of silver halides, see, for example: R. S. KNOX, F. BASSANI, and W. B. FOWLER, in *Photographic Sensitivity* (Maruzen & Co., Tokyo, 1963), p. 11; F. BASSANI, R. S. KNOX, and W. B. FOWLER, *Phys. Rev.* **137A**, 1217 (1965); P. M. SCOP, *Phys. Rev.* **139A**, 934 (1965). For experimental evidence relating to the above calculations, see, for example: G. ASCARELLI, *Phys. Rev. Letters* **20**, 44 (1968); S. BALLARÓ, A. BALZAROTTI, and V. GRASSO, *J. Phys.* **3C**, 2200 (1970); N. J. CARRERA and F. C. BROWN, *Phys. Rev.* **4B**, 3651 (1971); J. J. WHITE, *J. Opt. Soc. Am.* **62**, 212 (1972).
- [31] See, for instance, N. H. FLETCHER, *The Chemical Physics of Ice* (Cambridge University Press, 1970); *Rep. Progr. Phys.* **34**, 913 (1972).
- [32] See, for instance, T. M. BIRSHTEIN and O. B. PITTSYN, *Conformations of Macromolecules* (Interscience, 1966).
- [33] K. SIEGBAHN *et al.*, *ESCA Atomic, Molecular and Solid State Structure Studied by Means of Electron Spectroscopy* (edited by ABURQUIST and Wiksell, Uppsala, 1967).
- [34] For a review on this subject, see, for instance, M. COOPER, *Adv. Phys.* **20**, 453 (1971).
- [35] G. G. HALL, *Phil. Mag.* **43**, 338 (1952); **3**, 429 (1958); C. A. COULSON, L. B. RÉDEI, and D. STOCKER, *Proc. Roy. Soc. 270A*, 357 (1962); A. I. GUBANOV and A. A. NRAN'YAN, *Fizika tverd. Tela* **1**, 1044 (1959) [English transl. *Sov. Phys. Solid State* **1**, 956 (1959)].
- [36] L. A. GÓMEZ, G. PASTORI PARRAVICINI, L. RESCA, and R. RESTA, *J. Phys. C* **6**, 1926 (1973); G. PASTORI PARRAVICINI, F. PICCINI and L. RESCA, *Phys. Status Solidi*, **B 60**, 801 (1973). For the extension of the OPW method to molecular crystals see G. PASTORI PARRAVICINI and M. VITTORI, *Solid State Commun.* (1974) in press.
- [37] G. PASTORI PARRAVICINI, and L. RESCA, *J. Phys.* **4C**, L314 (1971); *Phys. Rev.* **8B**, 3009 (1973).
- [38] F. BASSANI, L. PIETRONERO, and R. RESTA, *J. Phys. C* **6**, 2133 (1973).
- [39] L. PIELA, L. PIETRONERO, and R. RESTA, *Phys. Rev.* **7B**, 5321 (1973).
- [40] See, for example: W. A. HARRISON and M. B. WEBB (eds.), *The Fermi Surface* (Wiley, 1960). See also the review article by P. B. VISSCHER and L. M. FALICOV, *Phys. Status Solidi* **54B**, 9 (1972). This article contains a comprehensive table of references on metallic elements with 566 citations.
- [41] E. WIGNER and F. SEITZ, *Phys. Rev.* **43**, 804 (1933); F. S. HAM, *Phys. Rev.* **128**, 82 (1962); **128**, 2524 (1962); See also J. CALLAWAY, *Energy Band Theory* (Academic Press, 1964), and the review article of ref. [40].

## CHAPTER 5

### INTERBAND TRANSITIONS AND OPTICAL PROPERTIES

IN THIS chapter we wish to study the relationship between the electronic band structure and the optical properties in crystals. We shall confine ourselves here to the case of interband transitions. Emphasis will be given to the discussion of that part of the structure in the optical constants which may be understood on the basis of the symmetry properties of the crystal. We shall also discuss in detail a couple of particularly effective examples. A review of the experimental situation up to 1968 for the case of semiconductors can be found in the book by Greenaway and Harbeke.<sup>[1]</sup> In the last few years new optical measurements have been accumulated for all types of solids and have been interpreted on the basis of the quantum theory of band-to-band transitions. The effect of exciton interaction on the optical spectrum will be discussed in the following chapter.

#### 5-1 General theoretical analysis of band-to-band optical transitions<sup>[2]</sup>

##### 5-1 a Basic approximations

The effect of a radiation field on the crystal electronic states can be studied using standard quantum mechanical methods. From standard classical mechanics we know that the kinetic energy of a system of  $N$  electrons

$$\sum_{i=1}^N \frac{\mathbf{p}_i^2}{2m}$$

has to be replaced, in the presence of an electromagnetic field, by the expression

$$\sum_{i=1}^N \left[ \frac{1}{2m} \left( \mathbf{p}_i + \frac{e\mathbf{A}(\mathbf{r}_i, t)}{c} \right)^2 \right],$$

where  $e$  is the absolute value of the electron charge,  $\mathbf{A}$  is the vector potential of the electromagnetic field, and the scalar potential  $V$  has been taken as zero without loss of generality because of the arbitrariness in the gauge. The Lorentz condition and the choice  $V = 0$  imply  $\nabla \cdot \mathbf{A} = 0$ . Furthermore we can now neglect non-linear effects by disregarding the term in  $\mathbf{A}^2$ . We then find that the interaction Hamiltonian of electrons in a radiation field is given by the expression

$$H_{eR} = \frac{e}{mc} \sum_{i=1}^N \mathbf{A}(\mathbf{r}_i, t) \cdot \mathbf{p}_i. \quad (5-1)$$

The effect of a radiation field on the crystal states can be studied by treating  $H_{eR}$  as a time dependent perturbation term on the electronic states of the crystal described in the previous chapters. This time dependent term will cause electrons to make transitions between occupied bands and empty bands. From the transition probability rate, the relationship between the electronic structure and the phenomenological optical constants can be derived.

We suppose that the electronic states are those computed in the adiabatic scheme and using the one-electron approximation (Section 3-1). Furthermore we make use of Koopmans' approximation (Appendix 5B), thus neglecting electron polarization effects. The above basic approximations must be taken as a starting point only in studying the optical properties of some crystals, and improvements leading to indirect transitions and exciton effects will be discussed in Section 5-4 and in Chapter 6.

### 5-1 b Quantum theory of band-to-band transitions

From elementary quantum mechanics we know that, to first order perturbation theory, the probability per unit time that a perturbation of the form  $\mathcal{L}e^{\mp i\omega t}$  (where the time dependence is completely contained in  $e^{\mp i\omega t}$ ) induces a transition from the initial state  $|i\rangle$  of energy  $E_i$  to the final state  $|f\rangle$  of energy  $E_f$  is

$$\mathcal{P}_{i \rightarrow f} = \frac{2\pi}{\hbar} |\langle f | \mathcal{L} | i \rangle|^2 \delta(E_f - E_i \mp \hbar\omega). \quad (5-2)$$

The above relation has the interpretation that a perturbation  $\mathcal{L}e^{-i\omega t}$  induces transitions with absorption of a quantum  $\hbar\omega$ , while a perturbation  $\mathcal{L}e^{i\omega t}$  gives rise to emission of a quantum  $\hbar\omega$ . Since the perturbation must be real we have the sum of both absorption and emission terms, but the choice of initial and final states in (5-2) selects out the term to be considered. If the initial state is the ground state, the emission term makes expression (5-2) vanish. Thus only the absorption term needs to be considered in discussing the optical excitation spectrum of a crystal in the ground state. The emission term in (5-2) is relevant in discussing the radiative emission due to electrons initially in excited states (luminescence, phosphorescence, and pair recombination at impurity centres). We will neglect the emission term in the present treatment, keeping in mind that it could be dealt with, when needed, just by putting the appropriate sign into the argument of the  $\delta$  function.

To second order, the transition probability rate is

$$\mathcal{P}_{i \rightarrow f} = \frac{2\pi}{\hbar} \left| \sum_{\beta} \frac{\langle f | \mathcal{L} | \beta \rangle \langle \beta | \mathcal{L} | i \rangle}{E_{\beta} - E_i \mp \hbar\omega} \right|^2 \delta(E_f - E_i \mp \hbar\omega \mp \hbar\omega), \quad (5-3)$$

where  $|\beta\rangle$  indicates all intermediate states including initial and final state. The matrix elements appearing in (5-3) can be regarded as a result of two successive processes—firstly, the system makes a transition from the state  $|i\rangle$  to the state  $|\beta\rangle$ , and, secondly, from  $|\beta\rangle$  to  $|f\rangle$ . Energy is not conserved in the intermediate transition; it is only conserved between initial and final states. Also in this case the considerations made before about absorption and emission processes apply.

In a similar way we can extend the computation of the transition probability rate to higher order as an obvious generalization of (5-2) and (5-3). We must keep in mind that the argument of the  $\delta$  function is  $E_f - E_i \mp \hbar\omega \dots \mp \hbar\omega$ , where the number of

quanta absorbed or emitted gives the order of the transition, and the matrix elements connecting the initial and the final state through different intermediate states are divided by energy differences which include an appropriate number of quanta  $\hbar\omega$ . To third order we obtain, for example,

$$\mathcal{P}_{i \rightarrow f} = \frac{2\pi}{\hbar} \left| \sum_{\alpha\beta} \frac{\langle f | \mathcal{L} | \alpha \rangle \langle \alpha | \mathcal{L} | \beta \rangle \langle \beta | \mathcal{L} | i \rangle}{(E_\alpha - E_i \mp \hbar\omega \mp \hbar\omega)(E_\beta - E_i \mp \hbar\omega)} \right|^2 \delta(E_f - E_i \mp \hbar\omega \mp \hbar\omega \mp \hbar\omega).$$

We will be mostly interested in first order transitions of type (5-2), but will also discuss effects due to higher order terms in Sections 5-3 and 5-4.

The interaction of a radiation field with the electronic states of a crystal may induce both interband and intraband transitions. In semiconductors (and insulators) the ground state of the whole crystal at zero absolute temperature, contains completely occupied or completely empty bands, and as a consequence only interband transitions need be considered. For semiconductors at finite temperatures and also for metals there is also a free carrier absorption for long wavelength radiation (in general, in the infrared region), but we will not consider the optical absorption by free carriers here although it is worth while to point out that its theory is quite similar to that of interband transitions.

We now calculate the contribution to the optical constants due to a couple of valence and conduction bands. For simplicity we make the further assumption of neglecting relativistic effects, an approximation which could easily be removed if required. The ground state of the electronic system can be written (in the adiabatic and one-electron approximation) as a Slater determinant

$$\Psi_0 = \mathcal{A}\{\psi_{v\mathbf{k}_1}(\mathbf{r}_1)\alpha(1)\psi_{v\mathbf{k}_1}(\mathbf{r}_2)\beta(2)\dots\psi_{v\mathbf{k}_Ns}(\mathbf{r}_n)\dots\psi_{v\mathbf{k}_N}(\mathbf{r}_{2N})\beta(2N)\},$$

where  $\mathcal{A}$  is the antisymmetrizing operator,  $N$  is the number of unit cells,  $v$  refers to a specific valence band,  $\alpha$  and  $\beta$  are the spin eigenfunctions, and  $s_i$  is a spin index indicating either  $\alpha$  or  $\beta$ . A trial excited state, in which the conduction wave function  $\psi_{c\mathbf{k}_f s_f}$  replaces the valence wave function  $\psi_{v\mathbf{k}_Is_I}$  can be written as

$$\Psi' = \mathcal{A}\{\psi_{v\mathbf{k}_1}(\mathbf{r}_1)\alpha(1)\Psi'_{v\mathbf{k}_1}(\mathbf{r}_2)\beta(2)\dots\psi_{c\mathbf{k}_f s_f}(\mathbf{r}_n)\dots\psi_{v\mathbf{k}_N}(\mathbf{r}_{2N})\beta(2N)\}.$$

We need the matrix elements of the operator  $H_{eR}$  [defined in (5-1)] between the ground state and the excited states. Since  $H_{eR}$  is a sum of one-particle operators, the non-vanishing matrix elements connect the ground state  $\Psi_0$  with states  $\Psi'$  having only one electron which is excited. This is shown explicitly in Appendix 5A; from formula (5A-3) we can write

$$\begin{aligned} \langle \Psi' | H_{eR} | \Psi_0 \rangle &= \frac{e}{mc} \langle \psi_{c\mathbf{k}_f s_f} | \mathbf{A} \cdot \mathbf{p} | \psi_{v\mathbf{k}_Is_I} \rangle \\ &= \frac{e}{mc} \delta_{s_i, s_f} \langle \psi_{c\mathbf{k}_f} | \mathbf{A} \cdot \mathbf{p} | \psi_{v\mathbf{k}_I} \rangle. \end{aligned}$$

For radiation of a given frequency  $\omega$  the vector potential  $\mathbf{A}$  can be written as

$$\mathbf{A}(\mathbf{r}, t) = A_0 \mathbf{e}^{i(\eta \cdot \mathbf{r} - \omega t)} + \text{c.c.}, \quad (5-4)$$

where  $\mathbf{e}$  is the polarization vector in the direction of the electric field,  $\eta$  is the wave vector of the radiation, and c.c. indicates the complex conjugate of the previous term.

## ELECTRONIC STATES AND OPTICAL TRANSITIONS

We shall only consider the effect of the first term in (5-4) which gives rise to the absorption.

The transition probability per unit time (5-2) now becomes

$$\mathcal{P}_{v_{\mathbf{k}_i s_i} \rightarrow c_{\mathbf{k}_f s_f}} = \frac{2\pi}{\hbar} \left( \frac{eA_0}{mc} \right)^2 \delta_{s_i, s_f} |\langle \psi_{c_{\mathbf{k}_f}} | e^{i\eta \cdot \mathbf{r}} \mathbf{e} \cdot \mathbf{p} | \psi_{v_{\mathbf{k}_i}} \rangle|^2 \delta(E_f - E_i - \hbar\omega), \quad (5-5)$$

which is the basic expression for computing optical constants in the frequency region of interband transitions.

Let us now consider the matrix element

$$\langle \psi_{c_{\mathbf{k}_f}} | e^{i\eta \cdot \mathbf{r}} \mathbf{e} \cdot \mathbf{p} | \psi_{v_{\mathbf{k}_i}} \rangle. \quad (5-6)$$

The function  $\psi_{c_{\mathbf{k}_f}}$  belongs to the irreducible representation of the translation group with vector  $\mathbf{k}_f$ . The function  $\psi_{v_{\mathbf{k}_i}}$ , as well as its derivative  $\mathbf{e} \cdot \mathbf{p} \psi_{v_{\mathbf{k}_i}}$ , belongs to the irreducible representation with vector  $\mathbf{k}_i$ , and  $e^{i\eta \cdot \mathbf{r}}$  belongs to the irreducible representation of vector  $\eta$ . Since the product of the irreducible representation  $\mathbf{k}_i$  by the irreducible representation  $\eta$  is the irreducible representation  $\mathbf{k}_i + \eta$ , selection rules of the type discussed in Section 2-4b result. Thus the matrix element (5-6) is zero unless

$$\mathbf{k}_f = \mathbf{k}_i + \eta + \mathbf{h}, \quad (5-7)$$

$\mathbf{h}$  being any reciprocal lattice vector. The above equation expresses the conservation of momentum in a periodic medium. We observe that for typical photon energies of the order of an electron volt, the wavelength is of the order of  $10^4$  Å and

$$|\eta| \approx 2\pi/10^4 \text{ Å}^{-1}.$$

The range of variation of  $\mathbf{k}_i$  (and  $\mathbf{k}_f$ ) is  $2\pi/a$  with  $a$  of the order of a few angstroms. The wave functions and energies in a given band are functions which depend slowly on  $\mathbf{k}$  (compared with variations of the order of  $\eta$ ), and so for all practical purposes we can neglect the radiation propagation vector  $\eta$  in eq. (5-6). Furthermore, since  $\mathbf{k}_i$  and  $\mathbf{k}_f$  are confined to the first Brillouin zone, we may write

$$\mathbf{k}_i \simeq \mathbf{k}_f. \quad (5-8)$$

We thus arrive at the result that only "vertical" transitions can be induced in an energy band diagram by the radiation field (Fig. 5-1). Equation (5-7) expresses the conservation of momentum in crystals and (5-8) is the dipole approximation. We can therefore simplify the expression for the probability per unit time given in (5-5) as

$$\mathcal{P}_{v_{\mathbf{k}s} \rightarrow c_{\mathbf{k}s}} = \frac{2\pi}{\hbar} \left( \frac{eA_0}{mc} \right)^2 |\mathbf{e} \cdot \mathbf{M}_{cv}(\mathbf{k})|^2 \delta(E_c(\mathbf{k}) - E_v(\mathbf{k}) - \hbar\omega), \quad (5-9a)$$

where

$$\begin{aligned} \mathbf{e} \cdot \mathbf{M}_{cv}(\mathbf{k}) &= \langle \psi_{c_{\mathbf{k}}} | \mathbf{e} \cdot \mathbf{p} | \psi_{v_{\mathbf{k}}} \rangle \\ &= \mathbf{e} \cdot \int_{\substack{\text{crystal} \\ \text{volume}}} \psi_c^*(\mathbf{k}, \mathbf{r}) (-i\hbar\nabla) \psi_v(\mathbf{k}, \mathbf{r}) d\mathbf{r}. \end{aligned} \quad (5-9b)$$

To obtain the number of transitions  $W(\omega)$  per unit time per unit volume induced by light of frequency  $\omega$ , we must sum (5-9a) over all possible states in the unit volume, i.e. we must sum over  $\mathbf{k}$ , the spin variable  $s$ , and over the band indices  $v$  (occupied)

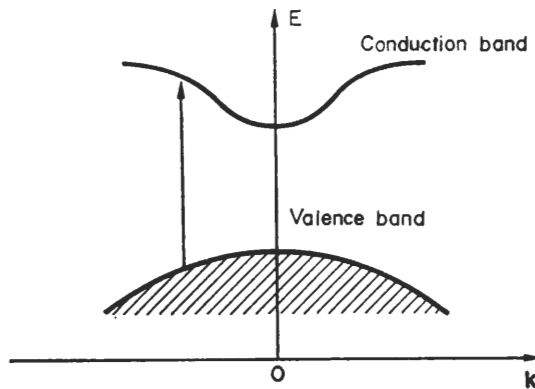


FIG. 5-1. Schematic representation in an energy band diagram of vertical transitions produced by a radiation field.

and  $c$  (empty). Since the allowed  $\mathbf{k}$  vectors are distributed in the Brillouin zone with a density  $V/(2\pi)^3$  ( $V$  being the crystal volume),

$$W(\omega) = \frac{2\pi}{\hbar} \left( \frac{eA_0}{mc} \right)^2 \sum_{v,c} \int_{BZ} \frac{2d\mathbf{k}}{(2\pi)^3} |\mathbf{e} \cdot \mathbf{M}_{cv}(\mathbf{k})|^2 \delta(E_c(\mathbf{k}) - E_v(\mathbf{k}) - \hbar\omega), \quad (5-10)$$

where the integral extends over the first Brillouin zone and the factor of 2 arises from the integration of spin variables.

### 5-1c Connection with the optical constants<sup>[1-3]</sup>

We wish now to derive the relation between expression (5-10) and the optical constants which are used phenomenologically to describe the optical properties of matter. Optical properties can be described in terms of the complex dielectric function  $\epsilon = \epsilon_1 + i\epsilon_2$  or the complex refraction index  $N = n + ik$ , where  $n$  is the ordinary refraction index and  $k$  is known as the extinction coefficient. The optical constants  $\epsilon$  and  $N$  are connected by the relation  $\epsilon = N^2$ , and the absorption coefficient  $\alpha$  depends on the above optical constants via

$$\alpha = \frac{2k\omega}{c}, \quad (5-11)$$

$$\alpha = \frac{\omega}{nc} \epsilon_2. \quad (5-12)$$

The average energy density  $u$  in a medium of a radiation field described by the vector potential (5-4) is related to the optical constants through the relation

$$u = \frac{n^2 A_0^2 \omega^2}{2\pi c^2}.$$

It is also known that the radiation in the medium propagates with velocity  $c/n$ . Using (5-10) we can now obtain microscopic expressions for the absorption coefficient and

the other optical constants. The absorption coefficient is by definition the energy absorbed in the unit time in the unit volume divided by the energy flux

$$\alpha(\omega) = \frac{\hbar\omega W(\omega)}{u(c/n)},$$

where  $\hbar\omega W(\omega)$  is the energy absorbed per unit volume and time, and the product  $u(c/n)$  of the energy density by the velocity of propagation in the medium is the energy flux. We thus obtain for the absorption coefficient

$$\alpha(\omega) = \frac{4\pi^2 e^2}{ncm^2\omega} \sum_{v,c} \int_{BZ} \frac{2d\mathbf{k}}{(2\pi)^3} |\mathbf{e} \cdot \mathbf{M}_{cv}(\mathbf{k})|^2 \delta(E_c(\mathbf{k}) - E_v(\mathbf{k}) - \hbar\omega). \quad (5-13)$$

Using (5-12)

$$\epsilon_2(\omega) = \frac{4\pi^2 e^2}{m^2\omega^2} \sum_{v,c} \int_{BZ} \frac{2 d\mathbf{k}}{(2\pi)^3} |\mathbf{e} \cdot \mathbf{M}_{cv}(\mathbf{k})|^2 \delta(E_c(\mathbf{k}) - E_v(\mathbf{k}) - \hbar\omega). \quad (5-14)$$

This is the basic expression which connects the band structure with the optical properties; it is preferred over related expressions for other optical constants because it does not depend on the refractive index.

The quantum expression for  $\epsilon_1(\omega)$  can be obtained using the dispersion relation of Kramers-Kronig<sup>[3]</sup>

$$\epsilon_1(\omega) = 1 + \frac{2}{\pi} P \int_0^\infty \omega' \epsilon_2(\omega') \frac{1}{\omega'^2 - \omega^2} d\omega', \quad (5-15)$$

where  $P$  indicates the principal part. By direct substitution of (5-14) into (5-15),

$$\epsilon_1(\omega) = 1 + \frac{8\pi e^2}{m^2} \sum_{v,c} \int_{BZ} \frac{2d\mathbf{k}}{(2\pi)^3} \frac{|\mathbf{e} \cdot \mathbf{M}_{cv}(\mathbf{k})|^2}{[E_c(\mathbf{k}) - E_v(\mathbf{k})]/\hbar} \frac{1}{[E_c(\mathbf{k}) - E_v(\mathbf{k})]^2/\hbar^2 - \omega^2}. \quad (5-16)$$

? The relations (5-14) and (5-16) allow in principle the computation of all optical constants once the band structure is known.

The optical constants satisfy some general relations which are often used to test the consistency of the approximations involved in their computation.<sup>[3,4]</sup> A very useful relation is the sum rule

$$\int_0^\infty \omega \epsilon_2(\omega) d\omega = \frac{\pi}{2} \omega_p^2, \quad (5-17a)$$

where the plasma frequency  $\omega_p$  is given by

$$\omega_p = \left( \frac{4\pi n e^2}{m} \right)^{1/2} \quad (5-17b)$$

and  $n$  denotes the density of the electrons which take part in the transition. Another useful sum rule is obtained as a particular case of the dispersion relation (5-15), taking the limit  $\omega \rightarrow 0$ .

$$\epsilon_1(0) = 1 + \frac{2}{\pi} \int_0^\infty \frac{\epsilon_2(\omega)}{\omega} d\omega. \quad (5-18)$$

Two particularly important sum rules on the index of refraction for isotropic media are

$$\int_0^\infty [n(\omega) - 1] d\omega = 0 \quad (5-19)$$

and

$$\int_0^\infty \omega k(\omega) d\omega = \frac{\pi}{4} \omega_p^2. \quad (5-20)$$

## 5-2 Structure of the optical constants at critical points

### 5-2a Theoretical discussion

The standard procedure for obtaining theoretically the optical constants of a crystal is to evaluate expression (5-14) for the imaginary part of the dielectric function. We shall now discuss in some detail specific cases and will show that a structure in the optical constants results with peaks at critical points.

The matrix elements  $|e \cdot M_{cv}(\mathbf{k})|^2$  between a given couple of valence and conduction bands are shown to be (see Section 3-9) smooth functions of  $\mathbf{k}$ , except near special  $\mathbf{k}$  vectors where  $e \cdot M_{cv}(\mathbf{k})$  vanishes because of symmetry. Neglecting such a situation and taking  $e \cdot M_{cv}(\mathbf{k})$  as a constant, we find from eq. (5-14) that the contribution to the dielectric function from a pair of bands is proportional to  $1/\omega^2$  and to the quantity

$$J_{cv}(\hbar\omega) = \int_{BZ} \frac{2d\mathbf{k}}{(2\pi)^3} \delta[E_c(\mathbf{k}) - E_v(\mathbf{k}) - \hbar\omega], \quad (5-21)$$

which is called joint density of states because it gives the density of pair of states—one occupied and the other empty—separated by an energy  $\hbar\omega$ .

The integration in (5-21) can be performed by using the properties of the  $\delta$  function. We know that

$$\int_a^b g(x) \delta[f(x)] dx = \sum_{x_0} g(x_0) \left| \frac{df}{dx} \right|_{x=x_0}^{-1}, \quad (5-22)$$

in which  $x_0$  represents a zero of the function  $f(x)$  contained in the interval  $(a, b)$ . In three dimensions

$$J_{cv}(E) = \frac{2}{(2\pi)^3} \int_{E_c(\mathbf{k}) - E_v(\mathbf{k}) = E} \frac{dS}{|\nabla_{\mathbf{k}}[E_c(\mathbf{k}) - E_v(\mathbf{k})]|}, \quad (5-23)$$

where  $dS$  represents an element of surface in  $\mathbf{k}$  space on the surface defined by the equation

$$E_c(\mathbf{k}) - E_v(\mathbf{k}) = E.$$

The joint density of states for interband transitions as a function of  $E$  shows strong variations in the neighbourhood of particular values of  $E$  which are called critical point energies. From eq. (5-23) we see that singularities in the joint density of states are expected when

$$\nabla_{\mathbf{k}} E_c(\mathbf{k}) = \nabla_{\mathbf{k}} E_v(\mathbf{k}) = 0, \quad (5-24a)$$

or more generally when

$$\nabla_{\mathbf{k}} E_c(\mathbf{k}) - \nabla_{\mathbf{k}} E_v(\mathbf{k}) = 0. \quad (5-24b)$$

Critical points of type (5-24a) occur in general at high symmetry points of the Brillouin zone, while critical points of type (5-24b) may occur at any  $\mathbf{k}$  vector. The number of critical points which may occur in the Brillouin zone has been discussed by Phillips,<sup>[5]</sup> and the types of singularity have been analysed by Van Hove.<sup>[5]</sup>

The analytic behaviour of  $J_{cv}(E)$  near a singularity may be found by expanding  $E_c(\mathbf{k}) - E_v(\mathbf{k})$  in a Taylor series about the critical point. In the expansion, linear terms do not occur because of conditions (5-24). Limiting the expansion to quadratic terms and denoting the wave vectors along the principal axes with the origin at the critical point by  $k_x, k_y, k_z$ ,

$$E_c(\mathbf{k}) - E_v(\mathbf{k}) = E_0 + \frac{\hbar^2}{2} \left( \varepsilon_x \frac{k_x^2}{m_x} + \varepsilon_y \frac{k_y^2}{m_y} + \varepsilon_z \frac{k_z^2}{m_z} \right), \quad (5-25)$$

with  $m_x, m_y, m_z$  positive quantities and  $\varepsilon_x, \varepsilon_y, \varepsilon_z$  equal to +1 or -1. We obtain four types of singularities, depending on the signs of  $\varepsilon_x, \varepsilon_y, \varepsilon_z$ . The critical points are called:

- $M_0$  when all coefficients of the quadratic expansion are positive (minimum);
- $M_1$  when two coefficients are positive and one negative (saddle point);
- $M_2$  when two coefficients are negative and one positive (saddle point);
- $M_3$  when all coefficients are negative (maximum),

where the subscripts attached to  $M$  indicate the number of negative coefficients in the expansion of the energy differences.

The analytic behaviour of the joint density of states near critical points can be obtained using (5-21) and (5-25). We report the results in Table 5-1, and we notice that there are sharp discontinuities at the critical points.

*Proof.* As an illustration of the results reported in Table 5-1, let us consider the case of the point  $M_1$ .

In the expansion (5-25) we have  $\varepsilon_x = \varepsilon_y = 1$  and  $\varepsilon_z = -1$ , and substituting in (5-21)

$$J_{cv}(E) = \int_{BZ} \frac{2d\mathbf{k}}{(2\pi)^3} \delta \left( E_0 + \frac{\hbar^2}{2} \frac{k_x^2}{m_x} + \frac{\hbar^2}{2} \frac{k_y^2}{m_y} - \frac{\hbar^2}{2} \frac{k_z^2}{m_z} - E \right).$$

We introduce the new coordinates

$$q_i = \frac{\hbar}{(2m_i)^{1/2}} k_i \quad (i = x, y, z)$$

and obtain

$$J_{cv}(E) = \frac{2}{(2\pi)^3} \frac{2^{3/2} (m_x m_y m_z)^{1/2}}{\hbar^3} \int d\mathbf{q} \delta(E_0 + q_x^2 + q_y^2 - q_z^2 - E).$$

Using cylindrical coordinates  $q, \varphi$  in the  $(q_x, q_y)$  plane, we transform the above equation into

$$J_{cv}(E) = \frac{2}{(2\pi)^3} \frac{2^{3/2} (m_x m_y m_z)^{1/2}}{\hbar^3} 2\pi \iint q dq dq_z \delta(q^2 - q_z^2 + E_0 - E).$$

TABLE 5-1. Analytic behaviour and schematic representation of the joint density of states near critical points for the three-dimensional case. For convenience  $A = \pi^{2/3} h^{-3} (m_x m_y m_z)^{1/2}$  and  $B$  indicates a constant which depends on the detailed band structure

Critical Point	Joint density of states	Schematic representation
$M_0$ Minimum	$J(E) = \begin{cases} B + O(E - E_0) & \text{when } E < E_0 \\ B + A(E - E_0)^{1/2} + O(E - E_0) & \text{when } E > E_0 \end{cases}$	
$M_1$ Saddle point	$J(E) = \begin{cases} B - A(E_0 - E)^{1/2} + O(E - E_0) & \text{when } E < E_0 \\ B + O(E - E_0) & \text{when } E > E_0 \end{cases}$	
$M_2$ Saddle Point	$J(E) = \begin{cases} B + O(E - E_0) & \text{when } E < E_0 \\ B - A(E - E_0)^{1/2} + O(E - E_0) & \text{when } E > E_0 \end{cases}$	
$M_3$ Maximum	$J(E) = \begin{cases} B + A(E_0 - E)^{1/2} + O(E - E_0) & \text{when } E < E_0 \\ B + O(E - E_0) & \text{when } E > E_0 \end{cases}$	

Using (5-22) we can integrate with respect to  $q_z$  and obtain

$$J_{cv}(E) = \frac{2}{(2\pi)^2} \frac{2^{3/2} (m_x m_y m_z)^{1/2}}{\hbar^3} \int_0^R q dq \sum_{q_{z_0}} \frac{1}{2|q_{z_0}|}, \quad (5-26)$$

with

$$q_{z_0} = \mp \sqrt{(q^2 + E_0 - E)} \quad \text{if } q^2 + E_0 - E > 0.$$

The above integration has been extended to a region surrounding the critical point; for convenience we have used a sphere of radius  $R$  in which the expansion holds. With the help of the step function

$$\eta(x) = \begin{cases} 1 & \text{for } x > 0, \\ 0 & \text{for } x < 0, \end{cases}$$

eq. (5-26) can be written as

$$J_{cv}(E) = A \int_0^R \frac{q dq}{\sqrt{(q^2 + E_0 - E)}} \eta(q^2 + E_0 - E)$$

where  $A = \pi 2^{7/2} h^{-3} (m_x m_y m_z)^{1/2}$ .

If

$$\begin{aligned} E < E_0, \quad \eta(q^2 + E_0 - E) &= 1, \\ J_{cv}(E) &= A \int_0^R \frac{q dq}{\sqrt{(q^2 + E_0 - E)}} = A(\sqrt{(E_0 - E + R^2)} - \sqrt{(E_0 - E)}) \\ &= -A\sqrt{(E_0 - E)} + O(E_0 - E), \end{aligned} \quad (5-27a)$$

where the last step is possible for an energy value  $E$  sufficiently near to the critical point energy  $E_0$  so that  $|E - E_0| \ll R^2$ . The expression  $O(E_0 - E)$  indicates a quantity that vanishes at least linearly when  $E \rightarrow E_0$ .

If  $E > E_0$ , then  $\eta(q^2 + E_0 - E) = 1$  only if  $q > \sqrt{(E - E_0)}$ . Thus

$$J_{cv}(E) = A \int_{\sqrt{(E-E_0)}}^R \frac{q dq}{\sqrt{(q^2 + E_0 - E)}} = A\sqrt{(E_0 - E + R^2)} = O(E_0 - E). \quad (5-27b)$$

Expressions (5-27a) and (5-27b) represent the contribution to the joint density of states from a region surrounding the critical point. The contribution to  $J_{cv}(E)$  from the remaining region of the Brillouin zone is a continuous quantity (provided that the other critical points are dealt with separately) which is taken into account by the smoothly energy dependent expression  $O(E - E_0)$  of Table 5-1.

To complete our discussion of the joint density of states let us consider critical points in two-dimensional and one-dimensional structures. For crystals, in which the energy depends only on two components of  $\mathbf{k}$ , say  $k_x$  and  $k_y$ , the expression (5-21) for the joint density of states becomes

$$J_{cv}(E) = \frac{2\pi}{c} \int_{BZ} \frac{2}{(2\pi)^3} dk_x dk_y \delta(E_c(k_x, k_y) - E_v(k_x, k_y) - E), \quad (5-28)$$

where  $2\pi/c$  appears because of the  $k_z$  integration, and  $BZ$  now indicates the two-dimensional Brillouin zone. Near a critical point, we can expand  $E_c(k_x, k_y) - E_v(k_x, k_y)$  in the form

$$E_c(k_x, k_y) - E_v(k_x, k_y) = E_0 + \frac{\hbar^2}{2} \left( \varepsilon_x \frac{k_x^2}{m_x} + \varepsilon_y \frac{k_y^2}{m_y} \right).$$

We have in this case three types of critical points which we denote by  $P_0$ ,  $P_1$ ,  $P_2$ , with subscripts indicating the number of coefficients which are negative. The method of calculation of the joint density of states is the same as that explained for the three-

dimensional case. At the points  $P_0$  and  $P_2$  a step function singularity occurs, while at the saddle point  $P_1$  we have a logarithmic singularity. The results are given in Table 5-2.

For crystals, in which the energy depends only on one component of  $\mathbf{k}$ , say  $k_x$ , the expression (5-21) for the joint density of states becomes

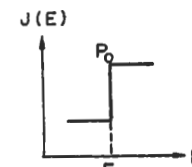
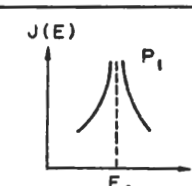
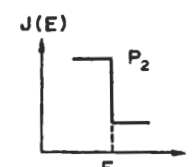
$$J_{cv}(E) = \frac{4\pi^2}{ab} \int_{BZ} \frac{2}{(2\pi)^3} dk_z \delta(E_c(k_z) - E_v(k_z) - E),$$

where  $4\pi^2/ab$  appears because of the  $k_x$ ,  $k_y$  integrations, and  $BZ$  now indicates the one-dimensional Brillouin zone. Two different critical points are obtained that we denote by  $Q_0$  and  $Q_1$ . The expression for the joint density of states can be immediately obtained using (5-22) and is given in Table 5-3.

We should like to point out at this juncture that changing the dimension of the  $\mathbf{k}$  vector has a profound effect on the nature of the singularities at the critical point. In the three-dimensional case we have basically shoulders and peak points, as can be seen from Table 5-1, while in the two-dimensional case we have a logarithmic singularity for a saddle point, and in the one-dimensional case we have sharp singularities of the type  $(E - E_0)^{-1/2}$ .

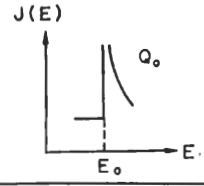
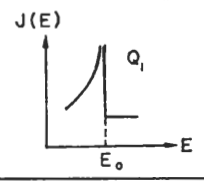
The results obtained from the theory of direct transitions can be compared with experimental results. For theoretical reasons (electron-electron, electron-lattice interaction, presence of imperfections) the singularities in the joint density of states are expected to be smoothed out in practice and to appear as peaks in the optical constants observed experimentally. We also expect the peaks in the two-dimensional case for the

TABLE 5-2. Analytic behaviour and schematic representation of the joint density of states near critical points for the two-dimensional case. For convenience  $A = (8\pi/c) h^{-2}(m_x m_y)^{1/2}$ , and  $B$  indicates a constant which depends on the detailed band structure

Critical Point	Joint density of states	Schematic representation
$P_0$ Minimum	$J(E) = \begin{cases} B + O(E - E_0) & \text{when } E < E_0 \\ B + A + O(E - E_0) & \text{when } E > E_0 \end{cases}$	
$P_1$ Saddle point	$J(E) = B - \frac{A}{\pi} \ln \left  1 - \frac{E}{E_0} \right  + O(E - E_0)$	
$P_2$ Maximum	$J(E) = \begin{cases} B + A + O(E - E_0) & \text{when } E < E_0 \\ B + O(E - E_0) & \text{when } E > E_0 \end{cases}$	

## ELECTRONIC STATES AND OPTICAL TRANSITIONS

TABLE 5-3. Analytic behavior and schematic representation of the joint density of states near critical points for the one-dimensional case. For convenience  $A = (4\pi/ab) h^{-1} m_z^{1/2}$ , and  $B$  indicates a constant which depends on the detailed band structure

Critical Point	Joint density of states	Schematic representation
$Q_0$ Minimum	$J(E) = \begin{cases} B + O(E - E_0) & \text{when } E < E_0 \\ B + A(E - E_0)^{-1/2} + O(E - E_0) & \text{when } E > E_0 \end{cases}$	
$Q_1$ Maximum	$J(E) = \begin{cases} B + A(E_0 - E)^{-1/2} + O(E - E_0) & \text{when } E < E_0 \\ B + O(E - E_0) & \text{when } E > E_0 \end{cases}$	

saddle point to be more easily detected than those in the three-dimensional case because of the sharpness of the logarithmic singularity. In the one-dimensional case they can be detected even better, as we will see in Chapter 8 in discussing the Landau levels.

We have so far considered the case of allowed transitions for which the structure in the dielectric function is basically determined by the joint density of states. The case of forbidden transitions is of no interest for  $M_1$ ,  $M_2$ , or  $M_3$  singularities because allowed transitions of equal energy occur in other regions of the Brillouin zone. In case the transition is forbidden at the edge the matrix element (5-9b) is proportional to  $(k - k_0)$ , and this dependence must be taken into account in carrying out the integration (5-14). The integral can be performed explicitly using (5-22), and one finds that the behaviour above the absorption edge is in this case  $(E - E_0)^{3/2}$  instead of  $(E - E_0)^{1/2}$  given in Table 5-1. We shall come back to this point in Chapter 6 when discussing the absorption edge including exciton effects.

### 5-2b Experimental evidence. Two examples: germanium and graphite

The basic features of the optical excitation spectra of many crystals can be explained on the basis of the analysis of Section 5-2a. The first quantitative success was obtained when the optical excitation spectrum of germanium was interpreted.<sup>[6]</sup>

The calculation was performed numerically by sampling the Brillouin zone with a large number of points and computing the energy levels of valence and conduction bands at every  $k$  point with the semi-empirical pseudopotential procedure which was discussed in Section 3-4b and whose application to the case of groups IV and III-V compounds was described in Section 4-1. Once the energy bands are computed at a large number of  $k$  values (about one thousand independent points in germanium), one can see how many times a given energy difference occurs at all possible equally spaced values

of  $\mathbf{k}$ , thus numerically computing the joint density of states (5-21) for all couples of valence and conduction bands. The accuracy of the results depends on the number of points in  $\mathbf{k}$  space, and, furthermore, an energy difference must be considered equal to another if they differ by less than a fixed energy  $\Delta E$ . The value of  $\Delta E$  can be made smaller as the number of  $\mathbf{k}$  points in the sampling increases, but one must have a large number of points within any energy difference  $\Delta E$  in order to avoid casual scattering. To obtain  $\varepsilon_2(\omega)$  the joint density of states is divided by  $\omega^2$  as indicated by (5-14) and multiplied by a constant which depends on the matrix element (5-9b) so as to satisfy the sum rule (5-17). The calculated dielectric function  $\varepsilon_2(\omega)$  so obtained is compared with the experimental curve in Fig. 5-2.

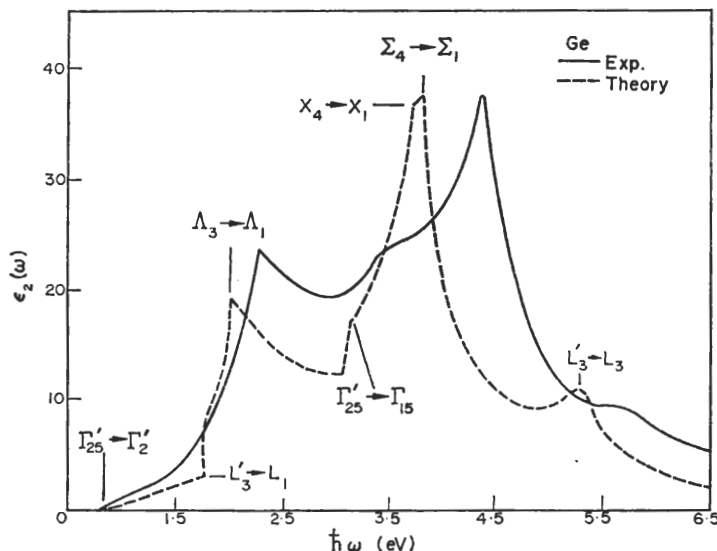


FIG. 5-2. Optical excitation spectrum of germanium shown by its  $\varepsilon_2(\omega)$  structure. The solid line gives the experimental results and the dashed line the theoretical results. The optical transitions at critical points are explicitly indicated. (From Brust *et al.*, ref. [6].)

It can be seen that the optical excitation spectrum from the direct edge at  $\approx 0.8$  eV to  $\approx 7$  eV is well interpreted by transitions from the highest valence band  $L'_3 - \Gamma'_{25} - X_4$  to the two lowest conduction bands. It can be observed that the shoulders and peaks in the density of states at critical points are clearly present in the experimental spectrum. There is a shoulder corresponding to the transition  $\Gamma'_{25} \rightarrow \Gamma'_2$  and a higher one corresponding to  $\Gamma'_{25} \rightarrow \Gamma'_{15}$ ; the shoulder at  $L'_3 \rightarrow L_1$  is followed by a peak corresponding to the transition  $A_3 \rightarrow A_1$  somewhere in the  $A$  direction; the sharp peak at about 3.5 eV is due to transitions at a number of points nearly degenerate, with a predominant contribution due to  $X_4 \rightarrow X_1$ . Further confirmation of this interpretation was obtained by the observation of the spin-orbit splittings associated to the states of the valence band  $\Gamma'_{25}$ ,  $L'_3$ , and  $A_3$  in the corresponding transitions, and by many other properties of the transitions in the presence of external perturbations which will be discussed in Chapter 8.

After the success obtained with germanium, this same analysis was carried out also for silicon, for a large number of III-V compounds and many other crystals;

we may recognize that it has now become almost a standard procedure. For a detailed critical review of the experimental determination of the optical constants in a large number of semiconductors and of their interpretation in terms of interband transitions, we refer to the book by Greenaway and Harbecke.<sup>[1]</sup>

As a second example we shall consider the optical excitation spectrum of graphite in order to show new effects due to the strong anisotropy in the optical constants. The electronic band structure of graphite has been discussed in Section 4-2, where we have shown that for this layer crystal the two-dimensional approximation to the band structure gives meaningful results, and the interlayer interaction can be treated as a small perturbation. From (5-14), neglecting the small  $k_z$  dependence of the energy,

$$\varepsilon_2(\omega) = \frac{2e^2}{cm^2\omega^2} \int_{BZ} |\mathbf{e} \cdot \mathbf{M}_{cv}(\mathbf{k})|^2 \delta(E_c(k_x, k_y) - E_v(k_x, k_y) - \hbar\omega) dk_x dk_y, \quad (5-29)$$

where  $c$  is the periodicity in the  $z$  direction, and  $BZ$  is the Brillouin zone of Fig. 4-10. From the energy band diagram of Fig. 4-11 we see that the only possible transitions with energy up to  $\approx 6$  eV occur between  $\pi$  bands, provided that  $\mathbf{e} \cdot \mathbf{M}_{cv}(\mathbf{k})$  does not vanish. When  $\mathbf{e}$  is parallel to the  $z$  axis, the matrix element  $\mathbf{e}_{\parallel} \cdot \mathbf{M}_{cv}(\mathbf{k})$  between  $\pi$  bands is zero because these bands are odd under the operation  $\{\sigma_h|0\}$ . Indicating with  $\varepsilon_{2\parallel}$  the dielectric function for light polarized parallel to the  $z$  axis, we can then write for transition between  $\pi$  bands

$$\varepsilon_{2\parallel}(\omega) = 0. \quad (5-30)$$

If the polarization vector  $\mathbf{e}$  is perpendicular to the  $z$  axis we can take  $\mathbf{e}_{\perp} \cdot \mathbf{M}_{cv}(\mathbf{k})$  as independent of  $\mathbf{k}$  and we have

$$\begin{aligned} \varepsilon_{2\perp}^{(\omega)} &= \frac{2e^2}{cm^2} \frac{1}{\omega^2} |\mathbf{e}_{\perp} \cdot \mathbf{M}_{cv}|^2 \int_{BZ} \delta(E_c(k_x, k_y) - E_v(k_x, k_y) - \hbar\omega) dk_x dk_y \\ &= \frac{4\pi^2 e^2}{m^2} \frac{1}{\omega^2} |\mathbf{e}_{\perp} \cdot \mathbf{M}_{cv}|^2 J_{cv}(\hbar\omega), \end{aligned} \quad (5-31)$$

where  $J_{cv}$  is the expression (5-28). This quantity has been computed numerically by sampling the Brillouin zone in a large number of points, calculating at each point the energy difference  $E_c(k_x, k_y) - E_v(k_x, k_y)$ , and determining the relative number of states within a suitable energy range. Because of symmetry, only the points of the restricted zone inside the first Brillouin zone have to be considered provided that a weight factor  $h/h_k$  ( $h$  order of the lattice point group,  $h_k$  order of the small point group of  $\mathbf{k}$ ) is introduced. The triangle  $\Gamma PQ$  shown in Fig. 4-10 was divided into 50,000 points, more than sufficient to give accurate values of the joint density of states. We give in Fig. 5-3 the joint density of states for  $\pi$  bands.<sup>[7]</sup> We notice that the saddle point  $Q$  is responsible for the sharp peak at  $\approx 4.5$  eV. The point  $\Gamma$  is a maximum and gives a step function. The point  $P$  is a minimum, but, because of degeneracy, linear terms in  $\mathbf{k}$  in the expansion of the energy difference do not vanish, and the density of states is continuous. In Fig. 5-3 we also give the dielectric function  $\varepsilon_{2\perp}$  and its experimental values as given by Taft and Philipp.<sup>[8]</sup> We notice the satisfactory agreement between theoretical and experimental results in the frequency range from 0 to about 6 eV, which is the region of  $\pi$  band transitions.

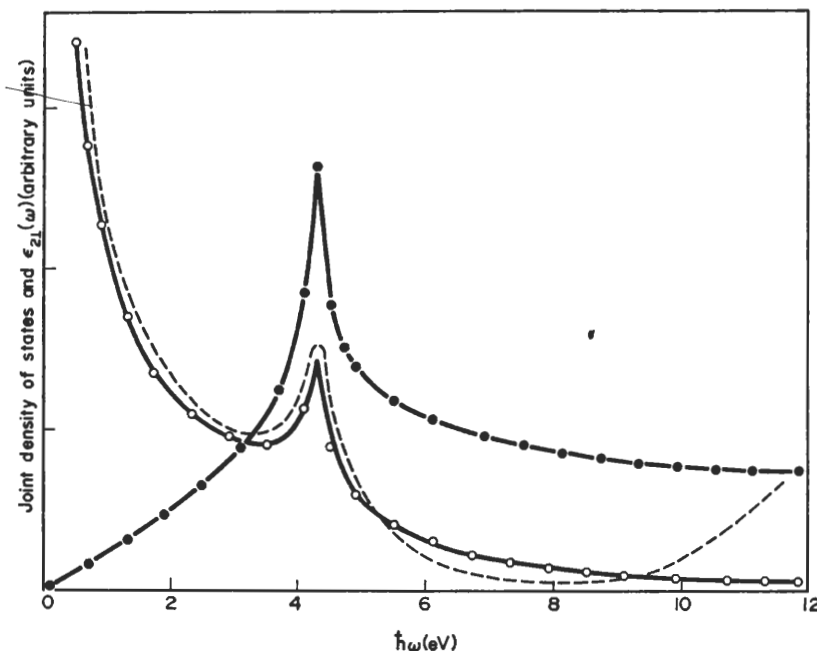


FIG. 5-3. Joint density of states (solid circles) and imaginary part of the dielectric constant (open circles) computed from the  $\pi$  bands of two-dimensional graphite. The experimental dielectric function of Taft and Philipp<sup>[8]</sup> is also given. (From Bassani and Pastori Parravicini, ref. [7].)

The contribution to the optical constants from other bands can be dealt with in a similar way.<sup>[7]</sup> In general, saddle points are responsible for sharp peaks in the frequency dependence of the imaginary part of the dielectric function as discussed in the preceding sections. It has been shown in this way that the peak at  $\approx 14$  eV is due to the saddle point at  $Q$  for the transition between  $\sigma$  bands. It has also been possible to interpret the structure in  $\epsilon_{2\parallel}$  as due to transitions between  $\pi$  bands and  $\sigma$  bands which are allowed for polarization of the electric field in the direction of the  $c$  axis.

Experimentally the dielectric function  $\epsilon_{2\perp}(\omega)$  has been obtained up to  $\approx 25$  eV by normal incidence reflectance with the polarization vector of the electric field perpendicular to the  $z$  axis.<sup>[8]</sup> Different experimental procedures have to be applied to determine  $\epsilon_{2\parallel}$  because of the impossibility of growing samples sufficiently thick in the  $z$  direction. A first procedure consists in performing reflectivity experiments as function of the angle of incidence and light polarized in the plane of incidence and using the Fresnel relations for anisotropic material.<sup>[9]</sup> Another technique consists of analysing electron energy loss data as function of momentum and energy transfer.<sup>[10]</sup> The energy loss intensity depends on the values of the dielectric functions both perpendicular and parallel to the  $c$  axis, and this allows their determination. It has been proved in this way that  $\epsilon_{2\parallel}(\omega)$  is zero for  $\hbar\omega < 6$  eV and exhibits two peaks at  $\approx 11$  and 16 eV.<sup>[10]</sup> This result indicates that the separation between  $\sigma$  and  $\pi$  bands is about 6 eV. Furthermore, the positions of the peaks correspond fairly well to the only allowed transitions  $Q_{1g}^+ \rightarrow Q_{2g}^-$  and  $Q_{1g}^+ \rightarrow Q_{2g}^+$  at the saddle point  $Q$  between  $\sigma$  and  $\pi$  bands, as can be seen from Fig. 4-11.

### 5-3 Multiphoton transitions

The experimental availability of very intense monochromatic sources has made it possible to detect processes in which two (or more) quanta are simultaneously involved in an electronic transition. The theoretical probability of two quanta processes is in practical experimental situations several orders of magnitude lower than that of single quantum processes, and consequently the detection of two-photon processes can be conveniently realized in a situation in which one-photon processes are not possible. In typical two-photon spectroscopy experiments the two light sources are, firstly, a very intense laser light with fixed frequency, and, secondly, an ordinary light whose frequency can be changed with continuity. The absorption coefficient for ordinary light as a function of frequency is measured when the laser beam is present. As lasers of variable frequency become available, more accurate experiments will be possible by using two or more laser sources, so that the field of multiphoton spectroscopy is likely to develop.

The possibility for a two-photon absorption process was first discussed theoretically by Göppert-Mayer<sup>[11]</sup> (1931), but only with the development of laser light was the effect detected experimentally.<sup>[12]</sup> Braunstein<sup>[13]</sup> calculated the two-photon absorption coefficient in a simplified model semiconductor consisting of a valence, a conduction, and a virtual band. Loudon<sup>[14]</sup> gave a more general treatment, and Inoue and Toyozawa<sup>[15]</sup> discussed the dependence of the two-photon absorption coefficient on the polarization of the beams.

We wish here to discuss the optical constants in the presence of two radiation beams of frequency  $\omega_1$  and  $\omega_2$ , with  $N_1$  and  $N_2$  photons per unit volume. In this situation the perturbation term of Section 5-1b has the form  $\mathcal{L}_1 e^{\mp i\omega_1 t} + \mathcal{L}_2 e^{\mp i\omega_2 t}$ ; to second order the transition probability rate is of type (5-3) with matrix elements containing one or the other of the two terms  $\mathcal{L}_1$  or  $\mathcal{L}_2$ , each with a corresponding argument in the  $\delta$  function. A first contribution to second order probability rate is the absorption or emission of two photons  $\hbar\omega_1$ ; another is the absorption or emission of two photons  $\hbar\omega_2$ , but the most important contribution involves one photon  $\hbar\omega_1$  and one photon  $\hbar\omega_2$ . We treat explicitly this last case, pointing out that the others could be dealt with along similar lines. We select the photon energies  $\hbar\omega_1$  and  $\hbar\omega_2$  such that each one is less, but the sum  $\hbar\omega_1 + \hbar\omega_2$  is larger than the energy gap. We can choose the vector potentials  $\mathbf{A}_1(\mathbf{r}, t)$  and  $\mathbf{A}_2(\mathbf{r}, t)$  of the radiation beams to be polarized in the fixed direction  $\mathbf{e}_1$  and  $\mathbf{e}_2$

$$\mathbf{A}_1(\mathbf{r}, t) = A_{01} \mathbf{e}_1 e^{i(\eta_1 \cdot \mathbf{r} - \omega_1 t)} + \text{c.c.}$$

and

$$\mathbf{A}_2(\mathbf{r}, t) = A_{02} \mathbf{e}_2 e^{i(\eta_2 \cdot \mathbf{r} - \omega_2 t)} + \text{c.c.}$$

We describe only absorption processes, and we shall invoke the dipole approximation by letting  $\eta_1 = \eta_2 = 0$ .

In this approximation we may still consistently disregard the term  $A^2$  in the perturbing Hamiltonian because it does not depend on space and gives no contribution to the matrix elements. The effect of this term in higher order approximations has been considered,<sup>[16]</sup> but it is much smaller than the dipole effects which we are going to calculate.

Following Braunstein's procedure,<sup>[13]</sup> we consider for simplicity a model semiconductor with a valence band  $v$ , a conduction band  $c$ , and a typical intermediate

band  $\beta$  (also called virtual band), which is supposed to give most of the contribution to the second order transition probability (5-3). Using the same analysis which leads to (5-9a) but considering two perturbation terms of the type (5-1), we find that the probability per unit time for a transition from the state  $\psi_{vks}$  to the state  $\psi_{c\bar{k}s}$ , considering as intermediate state  $\psi_{\beta\bar{k}s}$ , is

$$\begin{aligned} \mathcal{P}_{vks \rightarrow c\bar{k}s} = & \frac{2\pi}{\hbar} \left( \frac{eA_{01}}{mc} \right)^2 \left( \frac{eA_{02}}{mc} \right)^2 \left| \frac{\mathbf{e}_2 \cdot \mathbf{M}_{c\beta}(\mathbf{k}) \mathbf{e}_1 \cdot \mathbf{M}_{\beta v}(\mathbf{k})}{E_\beta(\mathbf{k}) - E_v(\mathbf{k}) - \hbar\omega_1} \right. \\ & \left. + \frac{\mathbf{e}_1 \cdot \mathbf{M}_{c\beta}(\mathbf{k}) \mathbf{e}_2 \cdot \mathbf{M}_{\beta v}(\mathbf{k})}{E_\beta(\mathbf{k}) - E_v(\mathbf{k}) - \hbar\omega_2} \right|^2 \delta(E_c(\mathbf{k}) - E_v(\mathbf{k}) - \hbar\omega_1 - \hbar\omega_2), \end{aligned} \quad (5-32)$$

where

$$\begin{aligned} \mathbf{M}_{\beta v} &= \langle \psi_\beta(\mathbf{k}, \mathbf{r}) | \mathbf{p} | \psi_v(\mathbf{k}, \mathbf{r}) \rangle, \\ \mathbf{M}_{c\beta} &= \langle \psi_c(\mathbf{k}, \mathbf{r}) | \mathbf{p} | \psi_\beta(\mathbf{k}, \mathbf{r}) \rangle. \end{aligned} \quad (5-33)$$

As shown in Section 5-1, it is a simple matter to obtain the absorption coefficient for photons of energy  $\hbar\omega_1$  in the presence of  $N_2$  photons per unit volume of energy  $\hbar\omega_2$  from the transition probability (5-32). We obtain the expression

$$\begin{aligned} \alpha(\omega_1) = & \frac{8\pi^3 \hbar e^2 N_2}{cm^4 n_1 n_2 \omega_1 \omega_2} \int_{BZ} \frac{2d^3 k}{(2\pi)^3} \left| \frac{\mathbf{e}_2 \cdot \mathbf{M}_{c\beta}(\mathbf{k}) \mathbf{e}_1 \cdot \mathbf{M}_{\beta v}(\mathbf{k})}{E_\beta(\mathbf{k}) - E_v(\mathbf{k}) - \hbar\omega_1} \right. \\ & \left. + \frac{\mathbf{e}_1 \cdot \mathbf{M}_{c\beta}(\mathbf{k}) \mathbf{e}_2 \cdot \mathbf{M}_{\beta v}(\mathbf{k})}{E_\beta(\mathbf{k}) - E_v(\mathbf{k}) - \hbar\omega_2} \right|^2 \delta(E_c(\mathbf{k}) - E_v(\mathbf{k}) - \hbar\omega_1 - \hbar\omega_2), \end{aligned} \quad (5-34)$$

where  $n_1$  and  $n_2$  are the refractive indices at the two frequencies; the other symbols have already been explained. In deriving (5-34) use has been made of the relation

$$\frac{n_2^2 A_{02}^2 \omega_2^2}{2\pi c^2} = N_2 \hbar\omega_2,$$

which connects the energy density  $(n^2 E^2)/4\pi$  of the classical electromagnetic theory with the number of photons per unit volume.

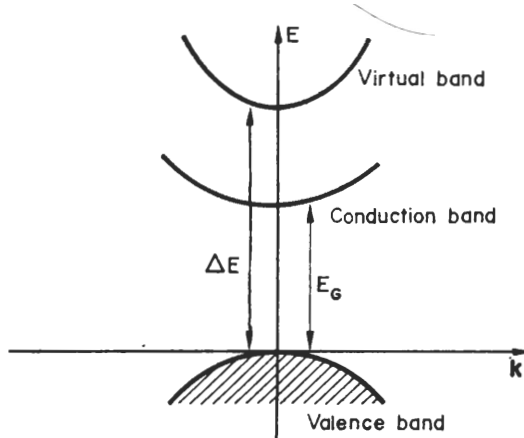


FIG. 5-4. Model semiconductor band structure to calculate two-photon absorption.

The expression (5-34) we can evaluate analytically without difficulty if we make the further approximation that the valence, conduction, and virtual bands are all spherical bands as exemplified in Fig. 5-4. In such a case we can write

$$E_v(\mathbf{k}) = -\gamma_v \frac{\hbar^2}{2m} k^2,$$

$$E_\beta(\mathbf{k}) = \gamma_\beta \frac{\hbar^2}{2m} k^2 + \Delta E,$$

$$E_c(\mathbf{k}) = \gamma_c \frac{\hbar^2}{2m} k^2 + E_G,$$

where  $\Delta E$  and  $E_G$  are shown in Fig. 5-4 and  $\gamma_i$  is a positive number which denotes the inverse of the effective mass in units of  $m$ . In the case of allowed transition (i.e. in the case when the matrix elements (5-33) do not vanish because of symmetry), we neglect in (5-34) the smooth dependence of the matrix elements from  $\mathbf{k}$ . We can then integrate expression (5-34) neglecting the mixed term and obtain the expression

$$\alpha(\omega_1) = \frac{2^{3/2}\pi e^4 |\mathbf{M}_{c\beta}|^2 |\mathbf{M}_{\beta v}|^2 N_2}{\hbar^2 c m^{3/2} (\gamma_c + \gamma_v)^{3/2} \omega_1 \omega_2} \left( \frac{1}{B} + \frac{1}{C} \right) (\hbar\omega_1 + \hbar\omega_2 - E_G)^{1/2} \quad (5-35a)$$

where

$$B = \left[ \Delta E + \frac{\gamma_\beta + \gamma_v}{\gamma_c + \gamma_v} (\hbar\omega_1 + \hbar\omega_2 - E_G) - \hbar\omega_1 \right]^2, \quad (5-35b)$$

$$C = \left[ \Delta E + \frac{\gamma_\beta + \gamma_v}{\gamma_c + \gamma_v} (\hbar\omega_1 + \hbar\omega_2 - E_G) - \hbar\omega_2 \right]^2. \quad (5-35c)$$

The value of  $\alpha(\omega_1)$  given by (5-35) is in practical experimental situations several orders of magnitude smaller than that obtained for one-photon processes at the critical point  $M_0$ , but it can exhibit a much sharper behaviour just above the energy threshold because expression  $B$  and  $C$  can become very small.

Braunstein's procedure<sup>[13]</sup> has been extended by Bassani and Hassan<sup>[17]</sup> to all the different types of critical points discussed in Section 5-2. For two-photon processes it turns out that singularities in the optical constants appear at all critical points and are sharper than those obtained for one-photon processes because of the effect of the energy denominators in the transition probability (5-32). Figure 5-5 shows a typical diagram of optical constants for a two-photon process in the vicinity of a critical point  $M_1$ .

In general, new basic information can be obtained by two-photon spectroscopy because the selection rules for such optical transitions differ from those for one-photon processes. In fact, from (5-33) we see that the allowed transitions in two-photon spectroscopy are those for which matrix elements of the appropriate components of the operator  $\mathbf{p}$  between valence virtual states and between virtual conduction states can be simultaneously different from zero. In a crystal with complete cubic symmetry, for example, the only matrix elements different from zero at  $\Gamma$  from an initial state of symmetry  $\Gamma_1$  are those to states of symmetry  $\Gamma_{15}$ , and from states  $\Gamma_{15}$  to states of symmetry  $\Gamma_1$ ,  $\Gamma_{12}$ ,  $\Gamma'_{15}$  or  $\Gamma'_{25}$  (as can be seen from Table 2-18). We therefore have

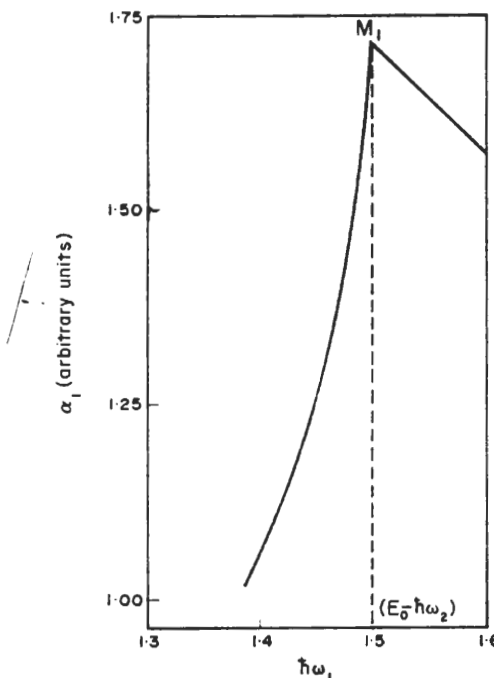


FIG. 5-5. Two-photon absorption coefficient as a function of  $\hbar\omega_1$ , near a saddle point  $M_1$ . The energy of the critical point is  $E_0$  and the fixed laser frequency is  $\omega_2$ . (From A. R. HASSAN, *Nuovo Cimento* **70B**, 21 (1970).)

the result that from a state  $\Gamma_1$  two-photon transitions are allowed only to states of symmetry  $\Gamma_1$ ,  $\Gamma_{12}$ ,  $\Gamma'_{15}$ , or  $\Gamma'_{25}$  and one-photon transitions are allowed only to states of symmetry  $\Gamma_{15}$ .

For all crystals which possess inversion symmetry, a particularly important selection rule is valid at the point  $\Gamma$  ( $\mathbf{k} = 0$ ) and at those symmetry points which contain inversion symmetry since the irreducible representations can be classified as even or odd with respect to inversion. Whilst the allowed transitions in one-photon processes are amongst states with opposite parity, the allowed transitions in two-photon processes are amongst states with the same parity since the intermediate states must have opposite parity to initial and final states. In this situation, the one-photon and two-photon absorption processes are complementary tools for the investigation of the optical properties.

Another important selection rule of general character appears at any  $\mathbf{k}$  vector in layer type crystals such as those described in Section 4-2. With light polarized perpendicular (parallel) to the  $z$  axis, one-photon transitions are allowed only amongst states of the same (opposite) parity with respect to  $\sigma_h$  as we have discussed in Section 5-2b. Two-photon transitions with both photons polarized perpendicular or parallel to the  $z$  axis are allowed only amongst states of the same parity with respect to  $\sigma_h$ . If the two beams have different polarization with respect to the  $z$  axis, the allowed transitions are only those amongst states of opposite parity.

So far the experimental results obtained in semiconductors with two-photon spectroscopy<sup>[12]</sup> have been mainly limited to cubic crystals without inversion symmetry and the power of the general selection rules described above has not been fully exploited. It is of interest to observe that two-photon spectroscopy may reveal the presence of saddle points in the electronic structure which could not be seen in the usual spectroscopy because they are forbidden to first order.

Theoretical results have been obtained in a similar way also for three-photon transitions by Bassani and Hassan,<sup>[17]</sup> and preliminary experimental evidence for three-photon transitions has been obtained in CdS by Catalano *et al.*<sup>[18]</sup> We do not wish to discuss these points any further because this field is in its infancy at present, and detailed discussions will have to be left to a later time.

#### 5-4 Indirect band-to-band transitions

##### 5-4a General remarks and electron–phonon interaction

In the previous sections we have considered the interaction of the electrons with the radiation field and we have shown that only vertical transitions may occur. As indicated in Chapter 4, there are a number of crystals, such as semiconductors silicon, germanium, etc., and insulators like AgCl whose electronic structure is characterized by the fact that the bottom of the conduction band and the top of the valence band are at different points of the Brillouin zone. Optical transitions between valence and conduction extrema would be forbidden in this case by momentum conservation (see Section 5-1). Such transitions are experimentally observed, however, albeit they are much weaker than the direct transitions.

Transitions between states which are not vertical in an energy band diagram are called indirect transitions. The possibility of indirect transitions is due to the interaction of the electrons with the vibrations of the lattice. The theory was first provided by Bardeen *et al.*<sup>[19]</sup> in order to explain the absorption tail of germanium.

It is well known that one can show by means of canonical transformations<sup>[20]</sup> that the Hamiltonian (3-9) describing the motion of the nuclei in the adiabatic approximation is equivalent to the Hamiltonian of a system of independent harmonic oscillators when the total potential energy is expanded up to second order in the nuclear displacements from the equilibrium position and normal coordinates are introduced. Corresponding to every normal mode of wave vector  $\mathbf{q}$  there is an harmonic oscillator whose energy can change by integer multiples of  $\hbar\omega_{\mathbf{q}}$ . The frequency  $\omega_{\mathbf{q}}$  as a function of momentum gives the classical vibrational dispersion spectrum, and the quanta  $\hbar\omega_{\mathbf{q}}$ , by analogy with the photons of the electromagnetic field, are called phonons. At a given  $\mathbf{q}$  vector of the Brillouin zone the phonon states can be classified according to the irreducible representations of the group of the vector  $\mathbf{q}$ , and their number is given by the number of degrees of freedom of the atoms in the unit cell.

Even in the adiabatic approximation, the presence of the phonon field produces an electron–lattice interaction.<sup>[20]</sup> In fact, during the vibrations of the lattice the atoms are displaced from their regular lattice positions, and the actual potential on any electron is consequently changed. To illustrate typical consequences of electron–lattice-interaction, we consider a simplified model in which the electron crystal potential is taken

as a sum of superimposed atomic-like potentials rigidly following the displacements of the nuclei. In the above approximation the electron-lattice perturbation Hamiltonian  $H_{eL}$  can be written as

$$H_{eL} = \sum_{\mathbf{R}_a} [V(\mathbf{r} - \mathbf{R}_a - \delta\mathbf{R}_a) - V(\mathbf{r} - \mathbf{R}_a)], \quad (5-36)$$

where the sum runs on all the equilibrium atomic positions  $\mathbf{R}_a$  in the crystal,  $\delta\mathbf{R}_a$  represents the vibrational displacement, and  $V(\mathbf{r} - \mathbf{R}_a)$  is the atomic-like potential corresponding to the atom based at  $\mathbf{R}_a$ . We expand (5-36) in terms of  $\delta\mathbf{R}_a$  and retain the first order term

$$H_{eL} = - \sum_{\mathbf{R}_a} \delta\mathbf{R}_a \cdot \nabla_{\mathbf{r}} V(\mathbf{r} - \mathbf{R}_a). \quad (5-37)$$

It is convenient to expand  $\delta\mathbf{R}_a$  in normal coordinates, which is always possible because of the translational symmetry of the lattice. The electron-lattice interaction (5-37) can therefore be separated into a sum of terms, each appropriate to a given phonon of a given branch, of the type

$$H_{ep} = \left( \frac{\hbar}{2M\omega_q} \right)^{1/2} \left[ A(\mathbf{q}) \sum_{\mathbf{R}_a} \mathbf{e}_a e^{i(\mathbf{q} \cdot \mathbf{R}_a - \omega_q t)} \cdot \nabla_{\mathbf{r}} V(\mathbf{r} - \mathbf{R}_a) + \text{c.c.} \right], \quad (5-38)$$

where  $\mathbf{e}_a$  is an appropriate polarization vector corresponding to a phonon of momentum  $\mathbf{q}$  and frequency  $\omega$ ,  $M$  indicates the total mass of the crystal, and  $A(\mathbf{q})$  and  $A^*(\mathbf{q})$  are the annihilation and creation operators respectively. The normalization factor  $(\hbar/2M\omega)^{1/2}$  has been introduced so that the matrix elements of  $A(\mathbf{q})$  and  $A^*(\mathbf{q})$  between multiphonon wave functions satisfy the condition<sup>[20]</sup>

$$\left. \begin{aligned} \langle n - 1 | A(\mathbf{q}) | n \rangle &= \sqrt{n}, \\ \langle n + 1 | A^*(\mathbf{q}) | n \rangle &= \sqrt{(n + 1)}, \end{aligned} \right\} \quad (5-39)$$

where  $|n\rangle$  indicates a state with phonon occupation number  $n$ . The electron-phonon interaction term (5-38) can be rewritten as

$$H_{ep} = A(\mathbf{q}) e^{-i\omega_q t} V_p(\mathbf{q}, \mathbf{r}) + \text{c.c.} \quad (5-40a)$$

with

$$V_p(\mathbf{q}, \mathbf{r}) = \left( \frac{\hbar}{2M\omega_q} \right)^{1/2} \sum_{\mathbf{R}_a} e^{i\mathbf{q} \cdot \mathbf{R}_a} \mathbf{e}_a \cdot \nabla_{\mathbf{r}} V(\mathbf{r} - \mathbf{R}_a). \quad (5-40b)$$

We notice that (5-40b) is a Bloch function of vector  $\mathbf{q}$ . When crystal symmetry is fully exploited,  $V_p(\mathbf{q}, \mathbf{r})$  belongs to an appropriate irreducible representation of the vector  $\mathbf{q}$  as explained in the footnote of Section 3-2c. The first term in (5-40a) produces absorption of a phonon, and the second produces emission of the same phonon.

The theory of indirect optical transitions can now be developed by considering the perturbation Hamiltonian

$$H' = H_{eR} + H_{ep} \quad (5-41)$$

and using the results of second order time dependent perturbation theory summarized by formula (5-3). We obtain all possible expressions of the type (5-3), where one of the matrix elements relates to the electron-radiation interaction and the other to the electron-phonon interaction of the perturbation (5-41). This is because the matrix element of  $H_{eR}$  conserves momentum, while the matrix element of  $H_{ep}$  transfers a specific momentum  $\mathbf{q}$ .

## ELECTRONIC STATES AND OPTICAL TRANSITIONS

### 5-4b Properties of indirect transitions

We wish now to discuss further the absorption coefficient in a model semiconductor with energy bands exemplified by Fig. 5-6. The transition probability per unit time of a process in which the valence electron  $\psi_{v\mathbf{k}_1s}$  is scattered to the conduction state  $\psi_{c\mathbf{k}_2s}$  and a photon of energy  $\hbar\omega$  and a phonon of momentum  $\mathbf{q} = \mathbf{k}_2 - \mathbf{k}_1$  (and energy  $\hbar\omega_q$ ) are both absorbed can be obtained from eq. (5-3) as

$$\begin{aligned}\mathcal{P}_{v\mathbf{k}_1s \rightarrow c\mathbf{k}_2s} &= \frac{2\pi}{\hbar} \left( \frac{eA_0}{mc} \right)^2 \left| \frac{\langle \psi_{c\mathbf{k}_2} | V_p(\mathbf{q}, \mathbf{r}) | \psi_{\beta\mathbf{k}_1} \rangle n_q^{1/2} \langle \psi_{\beta\mathbf{k}_1} | \mathbf{e} \cdot \mathbf{p} | \psi_{v\mathbf{k}_1} \rangle}{E_\beta(\mathbf{k}_1) - E_v(\mathbf{k}_1) - \hbar\omega} \right|^2 \\ &\times \delta(E_c(\mathbf{k}_2) - E_v(\mathbf{k}_1) - \hbar\omega + \hbar\omega_q).\end{aligned}\quad (5-42)$$

INSTITUT SUISSÉ  
DE PHYSIQUE  
ÉCONOMIQUE  
Fédérale  
lens  
CH-1015 Suisse  
Tél. 021-47 11 11.

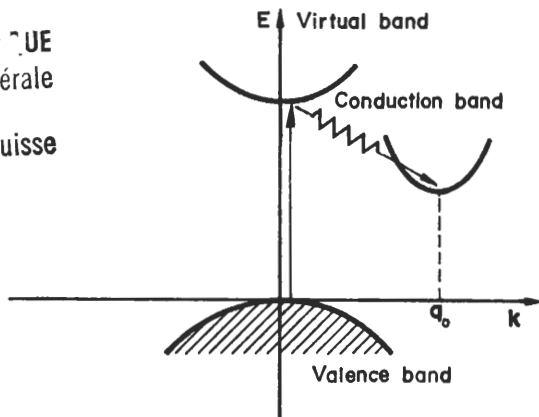


FIG. 5-6. Model semiconductor band structure to calculate the absorption coefficient due to indirect transitions.

In this model we have considered only one virtual band, but it would be easy to add other similar terms associated with other virtual states. In (5-42)  $n_q$  denotes the phonon occupation number, which in thermal equilibrium is given by the Bose-Einstein expression

$$n_q = \frac{1}{e^{(\hbar\omega_q/kT)} - 1}.$$

Using the standard procedures of Section 5-1 we obtain the following expression for the absorption coefficient:

$$\begin{aligned}\alpha_{\text{phonon abs}}(\omega) &= \frac{4\pi^2 e^2}{ncm^2\omega} \int_{\text{BZ}} \int_{\text{BZ}} \frac{2}{(2\pi)^3 (2\pi)^3} d\mathbf{k}_1 d\mathbf{k}_2 \\ &\times \left| \frac{\langle \psi_{c\mathbf{k}_2} | V_p(\mathbf{q}, \mathbf{r}) | \psi_{\beta\mathbf{k}_1} \rangle n_q^{1/2} \langle \psi_{\beta\mathbf{k}_1} | \mathbf{e} \cdot \mathbf{p} | \psi_{v\mathbf{k}_1} \rangle}{E_\beta(\mathbf{k}_1) - E_v(\mathbf{k}_1) - \hbar\omega} \right|^2 \delta(E_c(\mathbf{k}_2) - E_v(\mathbf{k}_1) - \hbar\omega + \hbar\omega_q).\end{aligned}\quad (5-43)$$

As an example of the application of (5-43) we consider the case of indirect optical transitions between spherical bands. Furthermore, we suppose that the quantity

$$C = \left| \frac{\langle \psi_{c\mathbf{k}_2} | V_p(\mathbf{q}, \mathbf{r}) | \psi_{\beta\mathbf{k}_1} \rangle \langle \psi_{\beta\mathbf{k}_1} | \mathbf{e} \cdot \mathbf{p} | \psi_{v\mathbf{k}_1} \rangle}{E_p(\mathbf{k}_1) - E_v(\mathbf{k}_1) - \hbar\omega} \right|^2$$

to a good degree of approximation can be regarded as independent of the wave vectors  $\mathbf{k}_1$  and  $\mathbf{k}_2$  in the vicinity of the extrema; this is a good approximation for allowed transitions when the energy denominator in (5-43) is not too small. The absorption of light begins at  $\hbar\omega = E_G - k\theta$ , where  $E_G$  is the energy gap and  $k\theta$  is the energy of the phonon with vector  $\mathbf{q}_0$  equal to the vector which connects band extrema in the Brillouin zone. For phonon energies  $\hbar\omega$  a little larger than  $E_G - k\theta$ , transitions involve pairs of valence and conduction states separated in momentum space by vectors very near to  $\mathbf{q}_0$  so that it is a good approximation to take the energy of the phonon involved as a constant equal to  $k\theta$  and to maintain the phonon occupation number  $n_{\mathbf{q}}$  independent of  $\mathbf{k}_1$  and  $\mathbf{k}_2$ . The expression (5-43) then becomes

$$\alpha_{\text{phonon abs}}(\omega) = \frac{4\pi^2 e^2 C n_{\mathbf{q}_0}}{ncm^2 \omega} \int_{\text{BZ}} \int_{\text{BZ}} \frac{2}{(2\pi)^3 (2\pi)^3} d\mathbf{k}_1 d\mathbf{k}_2 \delta(E_c(\mathbf{k}_2) - E_v(\mathbf{k}_1) - \hbar\omega + k\theta). \quad (5-44)$$

In the case of the parabolic bands, we can write

$$E_c(\mathbf{k}_2) = \frac{\hbar^2 \mathbf{k}_2^2}{2m_c^*} + E_G \quad \text{and} \quad E_v(\mathbf{k}_1) = -\frac{\hbar^2 \mathbf{k}_1^2}{2m_v^*},$$

where  $\mathbf{k}_1$  and  $\mathbf{k}_2$  are referred to their respective extrema. If we introduce the above expression into (5-44), use polar coordinates, and perform the integrations by means of property (5-22), we obtain

$$\begin{aligned} & \int_{\text{BZ}} \int_{\text{BZ}} \frac{2}{(2\pi)^3 (2\pi)^3} d\mathbf{k}_1 d\mathbf{k}_2 \delta\left(\frac{\hbar^2 \mathbf{k}_2^2}{2m_c^*} + \frac{\hbar^2 \mathbf{k}_1^2}{2m_v^*} + E_G - \hbar\omega + k\theta\right) \\ &= \begin{cases} 0 & \text{for } \hbar\omega < E_G - k\theta \\ \frac{1}{8(2\pi)^3} \left(\frac{2m_v^*}{\hbar^2}\right)^{3/2} \left(\frac{2m_c^*}{\hbar^2}\right)^{3/2} (\hbar\omega - E_G + k\theta)^2 & \text{for } \hbar\omega > E_G - k\theta. \end{cases} \end{aligned}$$

Substituting the above expression into (5-44) we find that the contribution to the absorption coefficient due to the absorption of a phonon is given by

$$\alpha_{\text{phonon abs}}(\omega) = \begin{cases} 0 & \text{for } \hbar\omega < E_G - k\theta, \\ C_1(\hbar\omega - E_G + k\theta)^2 n_{\mathbf{q}_0} & \text{for } \hbar\omega > E_G - k\theta, \end{cases} \quad (5-45a)$$

where

$$C_1 = \frac{C}{\omega} \frac{4\pi^2 e^2}{ncm^2} \frac{1}{8(2\pi)^3} \left(\frac{2m_v^*}{\hbar^2}\right)^{3/2} \left(\frac{2m_c^*}{\hbar^2}\right)^{3/2}. \quad (5-45b)$$

Another contribution to the absorption coefficient is due to the emission of a phonon and can be obtained using the same procedure, the only differences from the previous case being the sign of the phonon energy and the normalization (5-39). We obtain

$$\alpha_{\text{phonon emiss}}(\omega) = \begin{cases} 0 & \text{for } \hbar\omega < E_G + k\theta, \\ C_1(\hbar\omega - E_G - k\theta)^2 (n_{\mathbf{q}_0} + 1) & \text{for } \hbar\omega > E_G + k\theta, \end{cases} \quad (5-46)$$

as the contribution to indirect transitions due to creation of a phonon of momentum  $\mathbf{q}_0$ .

## ELECTRONIC STATES AND OPTICAL TRANSITIONS

The total absorption coefficient is then

$$\alpha_{\text{tot}}(\omega) = \alpha_{\text{phonon abs}}(\omega) + \alpha_{\text{phonon emiss}}(\omega), \quad (5-47)$$

which depends quadratically on energy and exhibits two steps—one for  $\hbar\omega = E_G - k\theta$  and one for  $\hbar\omega = E_G + k\theta$ , the difference between the two steps being equal to  $2k\theta$ . We should like to point out that indirect transitions have a strong temperature dependence because of  $n_{q_0}$ ; at very low temperature only the contribution  $\alpha_{\text{phonon emiss}}$  can be observed but, increasing the temperature, the contribution  $\alpha_{\text{phonon abs}}$  comes in with relative intensity given by the Boltzman factor. One should note that at a given  $q_0$  more phonons can participate in optical transitions, each of them giving a contribution to the absorption coefficient in accordance with (5-45) and (5-46).

Selection rules play a role in determining which phonon contribute to indirect transitions. The allowed transitions are those for which the matrix elements of the appropriate component of the operator  $p$ , and the matrix element of the operator  $V_p(q, r)$  with the symmetry of the phonon in consideration between virtual states and initial or final states can be simultaneously different from zero. Using the results of Section 2-4, selection rules for indirect transitions can easily be established. They have been used by Lax and Hopfield<sup>[21]</sup> to locate the type of phonon which participate in the absorption edge of germanium and silicon and by a number of authors for other compounds.<sup>[22]</sup>

In conclusion it is worth-while to mention that the theory of indirect transitions has been extended to third order to include the cases of two-phonon one-photon transitions and two-photon phonon-assisted transitions.<sup>[23]</sup> In particular, Bassani and Hassan<sup>[23]</sup> have shown that the probability of two-photon one-phonon transitions is much higher than the probability of three-photon transitions with the intensity of the light sources presently available. In a similar way, one-photon one-phonon transitions are much more probable than two-photon transitions, and for this reason we have attributed the absorption of a typical semiconductor sketched in Fig. 5-6 to one-photon phonon-assisted transitions.

## APPENDIX 5A

### Matrix elements of one-electron and two-electron operators between determinantal states

In this and the following chapter we need matrix elements of one-electron and two-electron operators between Slater determinantal states.<sup>[24]</sup> We summarize here some results which are useful in their calculation.

Let  $|A\rangle$  be the determinantal state

$$|A\rangle = \mathcal{A}\{a_1(1) a_2(2) \dots a_N(N)\}$$

for a  $N$  particle system,  $a_i$  being a set of orthonormal one-electron function and  $\mathcal{A}$  the operator of antisymmetrization with the appropriate normalization factor  $(N!)^{-1/2}$ . Let

$$G_1 = \sum_{i=1}^N g_1(i)$$

be an operator sum of one particle operators and

$$G_2 = \frac{1}{2} \sum_{i \neq j} g_2(i, j)$$

be an operator sum of two-particle operators.

The expectation values of the operators  $G_1$  and  $G_2$  on the state  $|A\rangle$  are, respectively,

$$\langle A | G_1 | A \rangle = \sum_i \langle a_i | g_1 | a_i \rangle \quad (5A-1)$$

and

$$\langle A | G_2 | A \rangle = \frac{1}{2} \sum_{ij} [\langle a_i a_j | g_2 | a_i a_j \rangle - \langle a_i a_j | g_2 | a_j a_i \rangle], \quad (5A-2)$$

where the usual abbreviation for two-electron integrals has been used, i.e.

$$\langle a_1 a_2 | g_2 | a_3 a_4 \rangle = \int \int a_1^*(\mathbf{r}_1) a_2^*(\mathbf{r}_2) g_2(\mathbf{r}_1, \mathbf{r}_2) a_3(\mathbf{r}_1) a_4(\mathbf{r}_2) d\mathbf{r}_1 d\mathbf{r}_2.$$

The matrix elements of the operators  $G_1$  and  $G_2$  between the states:

$$|A\rangle = \mathcal{A}\{a_1(1) a_2(2) \dots \underline{a_k(k)} \dots a_N(N)\}$$

and

$$|B\rangle = \mathcal{A}\{a_1(1) a_2(2) \dots \underline{b_k(k)} \dots a_N(N)\},$$

which differ by only one of the one-particle functions, are, respectively,

$$\langle A | G_1 | B \rangle = \langle a_k | g_1 | b_k \rangle \quad (5A-3)$$

and

$$\langle A | G_2 | B \rangle = \sum_j [\langle a_k a_j | g_2 | b_k a_j \rangle - \langle a_k a_j | g_2 | a_j b_k \rangle]. \quad (5A-4)$$

From (5A-1) it follows that

$$\langle B | G_1 | B \rangle - \langle A | G_1 | A \rangle = \langle b_k | g_1 | b_k \rangle - \langle a_k | g_1 | a_k \rangle. \quad (5A-5)$$

From (5A-2) we easily obtain

$$\begin{aligned} & \langle B | G_2 | B \rangle - \langle A | G_2 | A \rangle \\ &= \sum_j [\langle b_k a_j | g_2 | b_k a_j \rangle - \langle b_k a_j | g_2 | a_j b_k \rangle] \\ &\quad - [\langle b_k a_k | g_2 | b_k a_k \rangle - \langle b_k a_k | g_2 | a_k b_k \rangle] \\ &\quad - \sum_j [\langle a_k a_j | g_2 | a_k a_j \rangle - \langle a_k a_j | g_2 | a_j a_k \rangle]. \end{aligned} \quad (5A-6)$$

The matrix elements of the operators  $G_1$  and  $G_2$  between the states

$$|A\rangle = \mathcal{A}\{a_1(1) a_2(2) \dots \underline{a_k(k)} \dots \underline{a_l(l)} \dots a_N(N)\}$$

and

$$|C\rangle = \mathcal{A}\{a_1(1) a_2(2) \dots \underline{c_k(k)} \dots \underline{c_l(l)} \dots a_N(N)\}$$

which differ in two one-electron functions, are

$$\langle A | G_1 | C \rangle = 0 \quad (5A-7)$$

and

$$\langle A | G_2 | C \rangle = \langle a_k a_l | g_2 | c_k c_l \rangle - \langle a_k a_l | g_2 | c_l c_k \rangle. \quad (5A-8)$$

The matrix elements of the operators  $G_1$  and  $G_2$  between states which differ by more than two pairs of functions are zero.

## APPENDIX 5B

## Koopmans' approximation

From Section 3-1 we consider the Hamiltonian for the many-electron system of the form

$$H_e(\mathbf{r}_1, \mathbf{r}_2, \dots, \mathbf{r}_N) = \sum_{i=1}^N H_i + \frac{1}{2} \sum_{i \neq j} \frac{e^2}{r_{ij}} \quad (5B-1)$$

with

$$H_i = -\frac{\hbar^2}{2m} \nabla_i^2 - \sum_j \frac{z_j e^2}{|\mathbf{R}_j - \mathbf{r}_i|}.$$

We write the ground state of the system in the form

$$\Psi_0 = \mathcal{A}\{\psi_1(1), \psi_2(2), \dots, \psi_N(N)\},$$

where the  $\psi_i$  satisfy Hartree-Fock equations

$$H_{HF}\psi_i = E_i\psi_i, \quad (5B-2)$$

where

$$H_{HF} = H(1) + V_{coul}(1) + V_{exch}(1) \quad (5B-3)$$

with

$$V_{coul}\psi_i(1) = \sum_j \psi_i(1) \int \psi_j^*(2) \frac{e^2}{r_{12}} \psi_j(2) d\tau_2 \quad (5B-4)$$

and

$$V_{exch}\psi_i = - \sum_j \psi_j(1) \int \psi_j^*(2) \frac{e^2}{r_{12}} \psi_i(2) d\tau_2. \quad (5B-5)$$

In (5B-4) and (5B-5) integration involves also summation over spin coordinates. Multiplying (5B-2) by  $\langle \psi_i |$  we have in general for any Hartree-Fock state:

$$E_i = \langle \psi_i | H_i | \psi_i \rangle + \sum_j \left[ \langle \psi_i \psi_j | \frac{e^2}{r_{12}} | \psi_i \psi_j \rangle - \langle \psi_i \psi_j | \frac{e^2}{r_{12}} | \psi_j \psi_i \rangle \right]. \quad (5B-6)$$

Consider a trial excited state  $\Phi_{\varphi_i, \psi_i}$  obtained by replacing in  $\Psi_0$  one of the function  $\psi_i$  with an excited function  $\varphi_i$ , with all other functions unchanged. This corresponds to neglecting dynamical polarization effects. We may thus write

$$\Phi_{\varphi_i, \psi_i} = \mathcal{A}\{\psi_1(1), \psi_2(2), \dots, \varphi_i(i), \dots, \psi_N(N)\}.$$

By using expression (5A-5) and (5A-6),

$$\begin{aligned} & \langle \Phi_{\varphi_i, \psi_i} | H_e | \Phi_{\varphi_i, \psi_i} \rangle - \langle \Psi_0 | H_e | \Psi_0 \rangle \\ &= \langle \varphi_i | H_i | \varphi_i \rangle - \langle \psi_i | H_i | \psi_i \rangle \\ &+ \sum_j \left[ \langle \varphi_i \psi_j | \frac{e^2}{r_{12}} | \varphi_i \psi_j \rangle - \langle \varphi_i \psi_j | \frac{e^2}{r_{12}} | \psi_j \varphi_i \rangle \right] \\ &- \left[ \langle \varphi_i \psi_i | \frac{e^2}{r_{12}} | \varphi_i \psi_i \rangle - \langle \varphi_i \psi_i | \frac{e^2}{r_{12}} | \psi_i \varphi_i \rangle \right] \\ &- \sum_j \left[ \langle \psi_i \psi_j | \frac{e^2}{r_{12}} | \psi_i \psi_j \rangle - \langle \psi_i \psi_j | \frac{e^2}{r_{12}} | \psi_j \psi_i \rangle \right]. \end{aligned} \quad (5B-7)$$

When the excited function  $\varphi_i$  satisfies the Hartree-Fock equation (5B-2) with  $V_{\text{coul}}$  and  $V_{\text{exch}}$  defined by (5B-4) and (5B-5), (5B-7) takes the more effective form

$$\begin{aligned} \langle \Phi_{\varphi_i, \psi_i} | H_e | \Phi_{\varphi_i, \psi_i} \rangle - \langle \Psi_0 | H_e | \Psi_0 \rangle \\ = E'_i - E_i - \left[ \langle \varphi_i \psi_i | \frac{e^2}{r_{12}} | \varphi_i \psi_i \rangle - \langle \varphi_i \psi_i | \frac{e^2}{r_{12}} | \psi_i \varphi_i \rangle \right], \end{aligned} \quad (5B-8)$$

where use has been made of (5B-6) and of a similar expression for the eigenvalue  $E'_i$  of  $\varphi_i$ . In most practical situations in crystals, the electron-hole interaction

$$\left[ \langle \varphi_i \psi_i | \frac{e^2}{r_{12}} | \varphi_i \psi_i \rangle - \langle \varphi_i \psi_i | \frac{e^2}{r_{12}} | \psi_i \varphi_i \rangle \right]$$

is negligible compared with the difference  $E'_i - E_i$  because the wave functions extend over the entire lattice. In this case we have

$$\langle \Phi_{\varphi_i, \psi_i} | H_e | \Phi_{\varphi_i, \psi_i} \rangle - \langle \Psi_0 | H_e | \Psi_0 \rangle \approx E'_i - E_i, \quad (5B-9)$$

i.e. the difference of the expectation values of the many-body Hamiltonian  $H_e$  on two determinantal states which differ by only one of the one-particle functions equals the difference of the corresponding Hartree-Fock eigenvalues (Koopmans' approximation).

With a similar procedure it would be easy to show that the Hartree-Fock energy of each one-electron state coincides with the energy required to remove that electron from the system (Koopmans' theorem), provided that one neglects dynamical polarization effects.

When the Hamiltonian (5B-1) does not contain spin dependent terms and the ground state  $\Psi_0$  has total spin equal zero, it is convenient to take trial excited states of a definite spin multiplicity. For triplet states (total spin = 1) we have:

$$\left. \begin{array}{l} \Phi_{\varphi_i, \frac{1}{2}, \psi_i, \frac{1}{2}}, \\ \frac{1}{\sqrt{2}} (\Phi_{\varphi_i, \frac{1}{2}, \psi_i, \frac{1}{2}} - \Phi_{\varphi_i, \frac{1}{2}, \psi_i, \frac{1}{2}}), \\ \Phi_{\varphi_i, \frac{1}{2}, \psi_i, \frac{1}{2}}, \end{array} \right\} \quad (5B-10)$$

and for singlet states (total spin = 0)

$$\frac{1}{\sqrt{2}} (\Phi_{\varphi_i, \frac{1}{2}, \psi_i, \frac{1}{2}} + \Phi_{\varphi_i, \frac{1}{2}, \psi_i, \frac{1}{2}}), \quad (5B-11)$$

where  $\varphi_{i\downarrow}$ ,  $\varphi_{i\uparrow}$  indicates the product  $\varphi_i(\mathbf{r})\alpha$ ,  $\varphi_i(\mathbf{r})\beta$  respectively.

We indicate trial excited states of type (5B-10) and (5B-11) of a given spin multiplicity with  $\Phi_{\varphi_i, \psi_i}^{(M)}$ , where  $M = 1$  for triplet states and  $M = 0$  for singlet states. With procedures similar to those applied to derive (5B-8),

$$\begin{aligned} \langle \Phi_{\varphi_i, \psi_i}^{(M)} | H_e | \Phi_{\varphi_i, \psi_i}^{(M)} \rangle - \langle \Psi_0 | H_e | \Psi_0 \rangle \\ = E'_i - E_i - \left[ \langle \varphi_i \psi_i | \frac{e^2}{r_{12}} | \varphi_i \psi_i \rangle - 2\delta_M \langle \varphi_i \psi_i | \frac{e^2}{r_{12}} | \psi_i \varphi_i \rangle \right], \end{aligned} \quad (5B-12)$$

where  $\delta_M = 1$  for singlet states and  $\delta_M = 0$  for triplet states, and integration involves only space coordinates. We will use this result in the next chapter in discussing singlet and triplet excitons. In the Koopmans' approximation (5B-12) is replaced by (5B-9).

## References and notes

- [1] D. L. GREENAWAY and G. HARBEKE, *Optical Properties and Band Structure of Semiconductors* (Pergamon Press, 1968).
- [2] See, for example, F. BASSANI, in *Proceedings of the International School of Physics "Enrico Fermi"* (Academic Press, 1966), vol. 34, p. 33. For additional information to various problems related to optical transitions, we recommend F. ABELÈS (ed.), *Optical Properties of Solids* (North-Holland, 1972).
- [3] F. STERN, *Solid State Physics* **15**, 300 (1963); J. TAUC, in *Proceedings of the International School of Physics "Enrico Fermi"* (Academic Press, 1966), vol. 34, p. 63.
- [4] For a general analysis of sum rules see M. ALTARELLI, D. L. DEXTER, H. M. NUSSENZVEIG, and D. Y. SMITH, *Phys. Rev. B* **6**, 4502 (1972); M. ALTARELLI and D. Y. SMITH, *Phys. Rev. B* **9**, 1290 (1974).
- [5] J. C. PHILLIPS, *Phys. Rev.* **104**, 1263 (1956); L. VAN HOVE, *Phys. Rev.* **89**, 1189 (1953).
- [6] D. BRUST, J. C. PHILLIPS, and F. BASSANI, *Phys. Rev. Letters* **9**, 94 (1962); D. BRUST, *Phys. Rev.* **134**, A 1337 (1964). See also the review article by J. C. PHILLIPS, *Solid State Physics* **18**, 56 (1966).
- [7] F. BASSANI and G. PASTORI PARRAVICINI, *Nuovo Cimento* **50B**, 95 (1967).
- [8] E. A. TAFT and H. R. PHILIPP, *Phys. Rev.* **138**, A 197 (1965).
- [9] D. L. GREENAWAY, G. HARBEKE, F. BASSANI, and E. TOSATTI, *Phys. Rev.* **178**, 1340 (1969).
- [10] K. ZEPPENFELD, *Phys. Letters* **25A**, 335 (1967); E. TOSATTI, *Nuovo Cimento* **63B**, 54 (1969); E. TOSATTI and F. BASSANI, *Nuovo Cimento* **65B**, 161 (1970).
- [11] M. GöPPERT-MAYER, *Ann. Phys.* **9**, 273 (1931).
- [12] See, for example: W. KAISER and C. G. B. GARRETT, *Phys. Rev. Letters* **7**, 229 (1961); J. A. GIORDMAINE and J. A. HOWE, *Phys. Rev. Letters* **11**, 207 (1963); I. D. ABELLA, *Phys. Rev. Letters* **9**, 453 (1962); J. J. HOPFIELD, J. M. WORLOCH, and K. PARK, *Phys. Rev. Letters* **11**, 414 (1963); J. J. HOPFIELD and J. M. WORLOCH, *Phys. Rev.* **137**, A 1455 (1965); N. G. BASOV, A. Z. GRASYUK, I. G. ZUBAREV, and V. A. KATULIN, *JETP Letters* **1**, 118 (1965); C. K. N. PATEL, P. A. FLEURY, R. E. SLUSHER and H. L. FRISCH, *Phys. Rev. Letters* **16**, 971 (1966); P. J. REGENSBURGER and E. PANIZZA, *Phys. Rev. Letters* **18**, 113 (1967); E. PANIZZA, *Appl. Phys. Letters* **10**, 265 (1967).
- [13] R. BRAUNSTEIN, *Phys. Rev.* **125**, 475 (1962). See also R. BRAUNSTEIN and M. OCKMAN, *Phys. Rev.* **134A**, 499 (1964).
- [14] R. LOUDON, *Proc. Phys. Soc.* **80**, 952 (1962).
- [15] M. INOUE and Y. TOYOZAWA, *J. Phys. Soc. Japan* **20**, 363 (1965). See also D. FRÖHLICH, B. STAGNINUS, and S. THURM, *Phys. Status Solidi* **40**, 287 (1970).
- [16] M. IANNUZZI and E. POLACCO, *Phys. Rev. Letters* **13**, 371 (1964); M. IANNUZZI and E. POLACCO, *Phys. Rev.* **138**, A 806 (1965); G. FORNACA, M. IANNUZZI, and E. POLACCO, *Nuovo Cimento* **36**, 1230 (1965); A. GOLD and J. P. HERNANDEZ, *Phys. Rev.* **139**, A 2002 (1965).
- [17] F. BASSANI and A. R. HASSAN, *Opt. Commun.* **1**, 371 (1970); A. R. HASSAN, *Nuovo Cimento* **70B**, 21 (1970); F. BASSANI and A. R. HASSAN, *Nuovo Cimento* **7B**, 313 (1972).
- [18] I. M. CATALANO, A. CINGOLANI, and A. MINAFRA, *Phys. Rev.* **5B**, 1629 (1972); *Optics Commun.* **5**, 212 (1972).
- [19] J. BARdeen, F. J. BLATT, and L. J. HALL, in *Photoconductivity Conference* (R. G. BRECKENRIDGE et al., eds.) (Wiley, 1957), p. 146.
- [20] J. M. ZIMAN, *The Principles of the Theory of Solids* (Cambridge University Press, 1972); R. E. PEIERLS, *Quantum Theory of Solids* (Clarendon Press, 1955).
- [21] M. LAX and J. J. HOPFIELD, *Phys. Rev.* **124**, 115 (1961).
- [22] See, for example: F. BASSANI, R. S. KNOX, and W. BEAL FOWLER, *Phys. Rev.* **137**, A 1217 (1965); N. O. FOLLAND and F. BASSANI, *J. Phys. Chem. Solids* **29**, 281 (1968).
- [23] V. A. KOVARSKII and E. V. VITIU, *Soviet Physics Semiconductors* **3**, 354 (1969); B. M. ASHKINADZE, A. I. BODRYSHIVA, E. V. VITIU, V. A. KOVARSKY, A. V. LELYAKOV, S. A. MOSHALENKO, S. L. PYSHKIN, and S. I. RADAUTSAN, in *Proceedings of the IXth International Conference on the Physics of Semiconductors* (Moscow, 1968), p. 189; B. M. ASHKINADZE, S. M. RYVKIN, and I. D. YAROSHETSKII, *Soviet Physics Semiconductors* **2**, 1285 (1969); N. O. FOLLAND, *Phys. Rev.* **1B**, 1648 (1970); F. BASSANI and A. R. HASSAN, *Nuovo Cimento* **7B**, 313 (1972).
- [24] J. C. SLATER, *Phys. Rev.* **34**, 1293 (1929), **38**, 1109 (1931). See also M. TINKHAM, *Group Theory and Quantum Mechanics* (McGraw-Hill, 1964).
- [25] T. KOOPMANS, *Physica* **1**, 104 (1934); F. SEITZ, *The Modern Theory of Solids* (McGraw-Hill, 1940).

## CHAPTER 6

TOULOUSE  
DU  
Institut Universitaire de France  
Ecole Polytechnique Fédérale de Lausanne  
CH-1015 Lausanne Suisse  
Tél. 021-471111

### EXCITONS IN CRYSTALS

#### 6-1 General considerations

THE absorption of light at the fundamental edge in pure semiconductors reveals two different kinds of electronic transitions. At photon energies greater than the energy gap the absorption of light corresponds to processes in which an electron is transferred to the conduction band and a hole is left in the valence band. At energies lower than the energy gap there are absorption peaks which correspond to processes in which the conduction electron and the valence hole are bound to one another in states within the forbidden energy gap. The possibility that electrons can exist in insulators in excited bound states, or excitons, was first suggested by Frenkel and Peierls.<sup>[1]</sup>

The theory of excitons in crystals has been developed on the basis of approximations similar to those applied in the description of the motion of electrons in the band formalism. There are two basically distinct and extreme points of view of dealing with electrons in crystals: in the tight binding approximation one visualizes an electron as "localized" on a given atom (or molecule), the effect of the other atoms giving a small perturbation; in the nearly free electron approximation one visualizes an electron as spread out over the whole crystal and moving in a weak periodic potential. These basic approximations have also been considered for excitons, and give tightly bound and weakly bound excitons respectively. In many cases, excitons cannot be interpreted in either of these two ways because the situations are rather intermediate between. There are classes of crystals, however, whose exciton spectra can be explained by one or other of these two basic and extreme approximations.

The tight binding approach to the problem of excitons has been widely and successfully used to study those crystals which can be considered as an ensemble of weakly interacting atoms or molecules. Many molecular crystals<sup>[2]</sup> belong to such a class. In the tight binding scheme an exciton is described as an atomic or molecular excitation, travelling through the crystal because of the interaction with the other atoms or molecules of the lattice. The above picture has been generalized<sup>[3]</sup> by extending the region of excitation to several unit cells whilst still maintaining localization.

The weak binding approach to the problem of excitons is particularly convenient for dealing with crystals in which the excitation region is spread over a large number of lattice cells. This alternative treatment originally formulated by Wannier and Mott<sup>[4]</sup> can be visualized as a correction to the electronic transition energy between valence and conduction band due to the interaction potential between the extra electron in the conduction band and the hole in the valence band. This description is expected to be particularly convenient for crystals with a high dielectric constant and consequently weak electron-hole interaction.

Attempts have also been made to develop an approach valid for intermediate binding by making use of the crystal band structure and of the corresponding localized Wannier functions. The problem in this case becomes more complicated and requires a great deal of numerical computation. The applicability of the intermediate binding approach to practical problems has been recently tested.<sup>[5]</sup>

The basic techniques to deal with electrons in crystals have been described in Section 3-1, and it has been shown that in order to arrive at a manageable scheme one has to accept the adiabatic, the one-electron, and the average potential approximations. The problem of excitons in crystals arises from the inaccuracy of those approximations in computing the true states, which we now call exciton states, of the entire electron Hamiltonian. We shall now discuss the foundations of the theory of excitons with specific applications to large gap insulators or organic crystals and to small gap semiconductors. For a review of the extensive literature we refer the reader, for example, to the article by Nikitine,<sup>[6]</sup> to the book of Greenaway and Harbecke,<sup>[7]</sup> and to the classical textbooks on excitons by Davydov<sup>[2]</sup> and by Knox.<sup>[8]</sup> Before considering some typical effects we wish to display the symmetry properties of the electron Hamiltonian

$$H_e = \sum_i H_i + \frac{1}{2} \sum_{i \neq j} \frac{e^2}{|\mathbf{r}_i - \mathbf{r}_j|} \quad (6-1a)$$

with

$$H_i = -\frac{\hbar^2}{2m} \nabla_i^2 - \sum_l \frac{z_l e^2}{|\mathbf{R}_l - \mathbf{r}_i|}, \quad (6-1b)$$

all symbols already explained in Section 3-1. We see that  $H_e$  is invariant under application of the space group symmetry operations to all electron coordinates. The translational symmetry of the crystal implies that the eigenfunctions  $\Psi(\mathbf{r}_1, \mathbf{r}_2, \dots, \mathbf{r}_m, \dots)$  of  $H_e$  satisfy the Bloch theorem

$$\Psi(\mathbf{r}_1 + \boldsymbol{\tau}_n, \mathbf{r}_2 + \boldsymbol{\tau}_n, \dots, \mathbf{r}_m + \boldsymbol{\tau}_n, \dots) = e^{i\mathbf{k}_{ex} \cdot \boldsymbol{\tau}_n} \Psi(\mathbf{r}_1, \mathbf{r}_2, \dots, \mathbf{r}_m \dots),$$

with the wave vector  $\mathbf{k}_{ex}$ \* defined in the first Brillouin zone. The remaining symmetry operations of the crystal imply degeneracies which can be analysed using the standard procedures described in Chapter 2. In particular, exciton wave functions with a given wave vector  $\mathbf{k}_{ex}$  are classified according to the irreducible representations of the group of  $\mathbf{k}_{ex}$ , and in a given exciton band the exciton energies corresponding to  $\mathbf{k}_{ex}$  and to all the points of the star of  $\mathbf{k}_{ex}$  are the same.

## 6-2 Tight binding excitons

### 6-2a Tight binding excitons in a two-band model

To obtain the main features of the tight binding approach to the exciton problem we consider a two-band model and we analyse how exciton effects modify the results of the one-electron approximation.

\* For convenience we use the notation  $\mathbf{k}_{ex}$  to indicate wave vectors of the eigenstates of the many-body Hamiltonian and  $\mathbf{k}$  to indicate wave vectors of the states in the one-electron approximation.

In the one-electron approximation, the ground state of the system in our idealized model is described by a Slater determinant

$$\Psi_0 = \mathcal{A}\{\psi_{v\mathbf{k}_1}(\mathbf{r}_1) \alpha(1), \psi_{v\mathbf{k}_1}(\mathbf{r}_2) \beta(2), \dots, \psi_{v\mathbf{k}_N}(\mathbf{r}_{2N}) \beta(2N)\}, \quad (6-2)$$

where  $\mathcal{A}$  indicates the operator which antisymmetrizes the product functions for exchange of identical particles,  $\psi_{v\mathbf{k}}$  are the one-electron wave functions of the valence band, and  $\alpha$  and  $\beta$  indicate the two spin eigenfunctions  $\begin{pmatrix} 1 \\ 0 \end{pmatrix}$  and  $\begin{pmatrix} 0 \\ 1 \end{pmatrix}$ . It is often convenient to express the valence Bloch functions in terms of the Wannier functions of the valence band, defined in Section 3-2a; in special cases as shown there the Wannier functions reduce to atomic or molecular functions. Taking advantage of the orthogonality of the Wannier functions centred on different cells, using the determinant product rules and remembering that the matrix  $A_{nm} = \frac{1}{\sqrt{N}} e^{i\mathbf{k}_n \cdot \tau_m}$  is unitary, we obtain for the ground state  $\Psi_0$  the expression

$$\Psi_0 = \mathcal{A}\{a_{v\tau_1}(\mathbf{r}_1) \alpha(1), a_{v\tau_1}(\mathbf{r}_2) \beta(2), \dots, a_{v\tau_N}(\mathbf{r}_{2N}) \beta(2N)\}, \quad (6-3)$$

where  $a_{v\tau}$  is the valence Wannier function centred on the cell  $\tau$  of the crystal.

As trial excited states of the crystal, in the one-electron approximation, we can take the Slater determinant

$$\Phi_{c\tau_e s_e, v\tau_h s_h} = \mathcal{A}\{a_{v\tau_1}(\mathbf{r}_1) \alpha(1), a_{v\tau_1}(\mathbf{r}_2) \beta(2), \dots, a_{c\tau_e s_e}(\mathbf{r}_m) \alpha(s_e), \dots, a_{v\tau_N}(\mathbf{r}_{2N}) \beta(2N)\} \quad (6-4)$$

in which the conduction Wannier function  $a_{c\tau_e s_e}$  ( $= a_{c\tau_e} \alpha$  or  $a_{c\tau_e} \beta$  when  $s_e = \frac{1}{2}$  or  $-\frac{1}{2}$ ) replaces the function  $a_{v\tau_h s_h}$  ( $= a_{v\tau_h} \alpha$  or  $a_{v\tau_h} \beta$  when  $s_h = \frac{1}{2}$  or  $-\frac{1}{2}$ ). We can visualize the state  $\Phi_{c\tau_e s_e, v\tau_h s_h}$  as containing an extra electron in the cell  $\tau_e$  and a hole in the cell  $\tau_h$ , as indicated in Fig. 6-1.

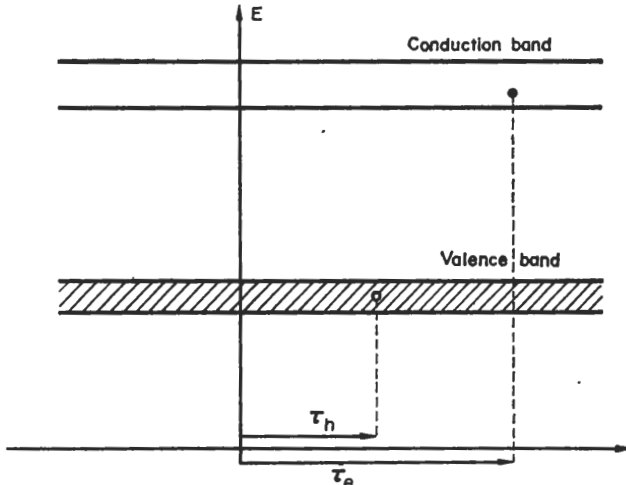


FIG. 6-1. Schematic picture of an exciton in the Wannier representation. A trial excited state  $\Phi_{c\tau_e s_e, v\tau_h s_h}$  represents an extra electron in the cell  $\tau_e$  and a hole in the cell  $\tau_h$ .

## ELECTRONIC STATES AND OPTICAL TRANSITIONS

The state  $\Phi_{c\tau_e s_e, v\tau_h s_h}$  is an eigenfunction of the component of the total spin in the direction of the axis of quantization with eigenvalue  $(s_e - s_h) \hbar$ . Since the Hamiltonian (6-1) does not contain spin dependent terms it is convenient to take linear combinations of the states

$$\Phi_{c\tau_e \frac{1}{2}, v\tau_h \frac{1}{2}}, \Phi_{c\tau_e \frac{1}{2}, v\tau_h \frac{-1}{2}}, \Phi_{c\tau_e \frac{-1}{2}, v\tau_h \frac{1}{2}}, \Phi_{c\tau_e \frac{-1}{2}, v\tau_h \frac{-1}{2}}$$

to obtain eigenfunctions of a definite spin multiplicity. For triplet states (total spin = 1),

$$\left. \begin{aligned} & \Phi_{c\tau_e \frac{1}{2}, v\tau_h \frac{1}{2}}, \\ & \frac{1}{\sqrt{2}} (\Phi_{c\tau_e \frac{1}{2}, v\tau_h \frac{1}{2}} - \Phi_{c\tau_e \frac{-1}{2}, v\tau_h \frac{1}{2}}), \\ & \Phi_{c\tau_e \frac{-1}{2}, v\tau_h \frac{1}{2}} \end{aligned} \right\} \quad (6-5a)$$

and for singlet states (total spin = 0)

$$\frac{1}{\sqrt{2}} (\Phi_{c\tau_e \frac{1}{2}, v\tau_h \frac{1}{2}} + \Phi_{c\tau_e \frac{-1}{2}, v\tau_h \frac{-1}{2}}). \quad (6-5b)$$

We indicate wave functions of a given spin multiplicity by  $\Phi_{c\tau_e, v\tau_h}^{(M)}$ , where  $M = 1$  for triplet states and  $M = 0$  for singlet states, and in the following we shall use consistently only one of the components (6-5a) for triplet states.

We now use the states (6-5a) and (6-5b) as a basis set to expand triplet and singlet exciton states respectively. An exciton state of multiplicity  $M$  and wave vector  $\mathbf{k}_{ex}$  can be expanded in the form

$$\Psi_{\mathbf{k}_{ex}}^{(M)} = \sum_{\tau_\beta} F(\tau_\beta) \frac{1}{\sqrt{N}} \sum_{\tau_n} e^{i\mathbf{k}_{ex} \cdot \tau_n} \Phi_{c\tau_n, v\tau_n + \tau_\beta}^{(M)}, \quad (6-6)$$

where

$$\frac{1}{\sqrt{N}} \sum_{\tau_n} e^{i\mathbf{k}_{ex} \cdot \tau_n} \Phi_{c\tau_n, v\tau_n + \tau_\beta}^{(M)}$$

describes an electron in a lattice site, a hole in a lattice site distant  $\tau_\beta$  from the first, the electron-hole pair travelling with wave vector  $\mathbf{k}_{ex}$ , and with the requirement that  $F(\tau_\beta)$  be determined by detailed calculations.

In the limit of strongly localized excitons, no transfer of the excited electron to different cells occurs, and we can take  $F(\tau_\beta) = \delta_{\tau_\beta, 0}$  in (6-6). In the strong binding limit we can thus write

$$\Psi_{\mathbf{k}_{ex}}^{(M)} = \frac{1}{\sqrt{N}} \sum_{\tau_n} e^{i\mathbf{k}_{ex} \cdot \tau_n} \Phi_{c\tau_n, v\tau_n}^{(M)}, \quad (6-7)$$

and the energies of the exciton states become

$$\begin{aligned} E^{(M)}(\mathbf{k}_{ex}) &= \langle \Psi_{\mathbf{k}_{ex}}^{(M)} | H_e | \Psi_{\mathbf{k}_{ex}}^{(M)} \rangle \\ &= E_{nn}^{(M)} + \sum_{\substack{\tau_m \\ (\tau_m \neq \tau_n)}} e^{i\mathbf{k}_{ex} \cdot (\tau_m - \tau_n)} E_{nm}^{(M)}, \end{aligned} \quad (6-8)$$

where

$$E_{nn}^{(M)} = \langle \Phi_{c\tau_n, v\tau_n}^{(M)} | H_e | \Phi_{c\tau_n, v\tau_n}^{(M)} \rangle. \quad (6-9)$$

The explicit expression for the matrix elements (6-9) is derived in Appendix 6A. The diagonal matrix elements  $E_{nn}^{(M)}$  are given by (6A-3) and (6A-4) (dropping the unnecessary subscript  $\tau_n$ ):

$$\begin{aligned}
 E_{nn}^{(M)} = & \langle \Psi_0 | H_e | \Psi_0 \rangle + \langle a_c | H_1 | a_c \rangle - \langle a_v | H_1 | a_v \rangle \\
 & + \sum_j \left[ 2\langle a_c a_{v\tau_j} | \frac{e^2}{r_{12}} | a_c a_{v\tau_j} \rangle - \langle a_c a_{v\tau_j} | \frac{e^2}{r_{12}} | a_{v\tau_j} a_c \rangle \right] \\
 & - \sum_j \left[ 2\langle a_v a_{v\tau_j} | \frac{e^2}{r_{12}} | a_v a_{v\tau_j} \rangle - \langle a_v a_{v\tau_j} | \frac{e^2}{r_{12}} | a_{v\tau_j} a_v \rangle \right] \\
 & - \left[ \langle a_c a_v | \frac{e^2}{r_{12}} | a_c a_v \rangle - 2\delta_M \langle a_c a_v | \frac{e^2}{r_{12}} | a_v a_c \rangle \right]. \quad (6-10)
 \end{aligned}$$

In the strong binding limit, the terms appearing in (6-10) have a simple physical meaning. In this case, the Wannier functions  $a_c(\mathbf{r})$  and  $a_v(\mathbf{r})$  coincide with excited and ground state atomic orbitals respectively, and the expectation value of the electron Hamiltonian in a trial excited state then differs from the expectation value in the ground state by the following quantities:

- (i) The atomic excitations energy, given by the second and third terms on the right hand side of expression (6-10).
- (ii) The contributions of Coulomb and exchange interaction between electrons on different atoms and the electron under consideration in the states  $a_c(\mathbf{r})$  and  $a_v(\mathbf{r})$  given by the other two terms of the right hand side of expression (6-10).
- (iii) The Coulomb and exchange interaction of the electron in the state  $a_c(\mathbf{r})$  with the hole left in the state  $a_v(\mathbf{r})$ .

For the non-diagonal matrix elements of the operator  $H_e$  we have from (6A-8)

$$E_{nm}^{(M)} = 2\delta_M \langle a_{v\tau_m} a_{c\tau_n} | \frac{e^2}{r_{12}} | a_{c\tau_m} a_{v\tau_n} \rangle - \langle a_{v\tau_m} a_{c\tau_n} | \frac{e^2}{r_{12}} | a_{v\tau_n} a_{c\tau_m} \rangle. \quad (6-11)$$

The quantity  $E_{nm}^{(M)}$  is related to the probability that an electron in the  $n$ th cell jumps to the fundamental state, while an electron in the  $m$ th cell makes a transition from the fundamental state to the excited state.

Equation (6-8) then gives a physical description of an exciton as an excitation region in the crystal having a formation energy  $E_{nn}^{(M)}$  nearly equal to the atomic excitation energy and an additional term which depends on  $k_{ex}$  and is responsible for the propagation of the exciton through the crystal.

Before passing on we should like to add a few remarks on the matrix elements appearing in (6-11). In the limiting case of negligible overlap between  $a_{c\tau_m}$  and  $a_{c\tau_n}$ , or  $a_{v\tau_m}$  and  $a_{v\tau_n}$ , the term

$$-\langle a_{v\tau_m} a_{c\tau_n} | \frac{e^2}{r_{12}} | a_{v\tau_n} a_{c\tau_m} \rangle \quad (6-12a)$$

vanishes, but the term

$$2\delta_M \langle a_{v\tau_m} a_{c\tau_n} | \frac{e^2}{r_{12}} | a_{c\tau_m} a_{v\tau_n} \rangle, \quad (6-12b)$$

which represents the Coulomb interaction between the two charge clouds  $a_v^*(\mathbf{r} - \tau_m) \times a_c(\mathbf{r} - \tau_m)$  and  $a_c^*(\mathbf{r} - \tau_n) a_v(\mathbf{r} - \tau_n)$ , is still different from zero for singlet excitons. This term is often referred to as "excitation transfer interaction". From electrostatics we know that the Coulomb interaction between two neutral cloud charges can be approximated by the dipole-dipole coupling term

$$\langle a_{v\tau_m} a_{c\tau_n} | \frac{e^2}{r_{12}} | a_{c\tau_m} a_{v\tau_n} \rangle = \frac{\mu_{vc} \cdot \mu_{cv} R^2 - 3(\mu_{vc} \cdot \mathbf{R})(\mu_{cv} \cdot \mathbf{R})}{R^5} \quad (6-13a)$$

with

$$\mu_{vc} = e \int a_v^*(\mathbf{r}) \mathbf{r} a_c(\mathbf{r}) d\mathbf{r} \quad (6-13b)$$

and

$$\mathbf{R} = \tau_m - \tau_n. \quad (6-13c)$$

Because the matrix elements involving Coulomb interaction between two cloud charges are slowly varying with distance, the sum appearing in (6-8) has to be evaluated using appropriate techniques as described by a number of authors.<sup>[9]</sup>

### 6-2b Relevant aspects of the tight binding exciton theory

The simplified model described above can be used, with some caution, to understand qualitatively some features of tight binding excitons. For a quantitative interpretation the model must be appropriately extended. Any extension of the model generally involves remarkable complications in the diagonalization problem. Furthermore, some basic effects such as the breakdown of the rigid lattice approximation and the inclusion of electron and lattice polarization effects, present formidable theoretical problems,<sup>[10]</sup> and in practice hardly more than a qualitative agreement with experimental data can be obtained. We shall now sketch briefly some of the most relevant aspects appearing in tight binding exciton theory.

We first of all consider an important aspect of singlet excitons arising when the valence or the conduction bands are degenerate. For simplicity we discuss a case which has been solved exactly, namely that of cubic crystals with Wannier functions  $a_v(\mathbf{r})$  and  $a_c(\mathbf{r})$ ,  $s$ -like and  $p$ -like respectively. When the conduction band indices  $c$  and  $c'$  are different, the excitation transfer interaction (6-13a) becomes

$$\langle a_{v\tau_m} a_{c\tau_n} | \frac{e^2}{r_{12}} | a_{c'\tau_m} a_{v\tau_n} \rangle = \frac{\mu_{vc'} \cdot \mu_{cv} R^2 - 3(\mu_{vc'} \cdot \mathbf{R})(\mu_{cv} \cdot \mathbf{R})}{R^5}. \quad (6-14)$$

For singlet state we can approximate  $E_{nm}^{(M=0)}$  given by (6-11) using (6-14); (6-8) then becomes

$$E^{(M=0)}(\mathbf{k}_{ex}) = E_{nn}^{(M=0)} + 2 \sum_{\mathbf{R} \neq 0} e^{i\mathbf{k}_{ex} \cdot \mathbf{R}} [\mu_{vc'} \cdot \mu_{cv} R^2 - 3(\mu_{vc'} \cdot \mathbf{R})(\mu_{cv} \cdot \mathbf{R})] R^{-5}.$$

For cubic crystals the sum on the lattice sites has been evaluated by Cohen and Keffer,<sup>[9]</sup> and using this we find that

$$E^{(M=0)}(\mathbf{k}_{ex}) = E_{nn}^{(M=0)} - 2 \frac{4\pi}{3} \frac{1}{\Omega} [\mu_{vc'} \cdot \mu_{cv} k_{ex}^2 \delta_{cc'} - 3(\mu_{vc'} \cdot \mathbf{k}_{ex})(\mu_{cv} \cdot \mathbf{k}_{ex})] k_{ex}^{-2} + O(k_{ex}), \quad (6-15)$$

where  $\Omega$  is the volume of the unit cell. This expression has a pathological behaviour for  $\mathbf{k}_{ex} = 0$ . In fact, for a given  $\mathbf{k}_{ex}$  vector, (6-15) leads to two different results depending on the relative orientations of  $\mathbf{k}_{ex}$ ,  $\mu_{cv}$  and  $\mu_{vc'}$ . In general we can choose the reference so that  $c = c'$ , and we then find that

$$E^{(M=0)}(\mathbf{k}_{ex}) = E_{nn}^{(M=0)} + 2 \frac{8\pi}{3} |\mu_{vc}|^2 \frac{1}{\Omega} + O(k_{ex}) \quad \text{when } \mu \parallel \mathbf{k}_{ex} \quad (6-16a)$$

(longitudinal excitons),

and

$$E^{(M=0)}(\mathbf{k}_{ex}) = E_{nn}^{(M=0)} - 2 \frac{4\pi}{3} |\mu_{vc}|^2 \frac{1}{\Omega} + O(k_{ex}) \quad \text{when } \mu \perp \mathbf{k}_{ex} \quad (6-16b)$$

(transverse excitons).

This longitudinal transverse splitting was first discovered by Heller and Marcus;<sup>[9]</sup> it is important in any dipole allowed optical transition and is connected with the break in cubic symmetry due to the induced dipoles at lattice points.

Another generalization is obtained when the restriction  $F(\tau_\beta) = \delta_{\tau_\beta, 0}$  in (6-6) is relaxed and the desired order of neighbours of electron-hole separation is included in the theory. This is useful for describing excitons in crystals when hole states are explicitly associated with one sublattice and the electrons with another sublattice. This generalization includes the so-called transfer model<sup>[11]</sup> of excitons which has been used, for example, for alkali halide crystals, where the excitons exist as a result of the electron of the halogen ion being transferred to the alkali ion to form a neutral atomic pair. We should also point out that in molecular crystals with more than one molecule per unit cell, the electron-hole interaction between neighbouring molecules produces a splitting of the molecular electronic states, which is called Davydov splitting.<sup>[2]</sup>

Of course, in the simplified model described above, spin-orbit interaction and other relativistic effects have been neglected. The most satisfactory way of including relativistic effects is to consider the same formalism with relativistic Wannier (or atomic) functions replacing the non-relativistic ones. In practice it is convenient to consider approximate treatments and to include spin-orbit interaction only in the one-particle operator (6-1b). The qualitative effect of this extension can be understood in the strong binding limit by pointing out that the exciton formation energy given by (6-10) is nearly equal to the atomic excitation energy including spin-orbit energy. Another effect of spin-orbit interaction is to produce a mixing between singlet and triplet states, so that the states are better classified by the irreducible representation of the crystal symmetry group as will be shown later.

### 6-2c Optical transitions with exciton effects

We shall now discuss how the optical constants of a crystal can be computed, at least in principle, when exciton states are known. The effect of a radiation field is provided by the introduction of the perturbation term

$$H_{eR} = \frac{e}{mc} \sum_i \mathbf{A}(\mathbf{r}_i, t) \cdot \mathbf{p}_i,$$

as discussed in Section 5-1. The transition probability from the ground state of the system to an exciton state induced by  $H_{eR}$  can be derived by means of standard time dependent perturbation theory.

Let us first consider the simplified model of Section 6-2a. The probability per unit time of a transition from the fundamental state  $\Psi_0$  (defined by eq. (6-3)) to the exciton state  $\Psi_{k_{ex}}^{(M)}$  (defined by eq. (6-7)) is given by

$$\Phi_{\Psi_0 \rightarrow \Psi_{k_{ex}}^{(M)}} = \frac{2\pi}{\hbar} \left( \frac{eA_0}{mc} \right)^2 \delta_{k_{ex}} \delta_M |\mathbf{e} \cdot \mathbf{M}_{cv}|^2 \delta(E_{ex} - E_0 - \hbar\omega), \quad (6-17a)$$

where

$$|\mathbf{e} \cdot \mathbf{M}_{cv}|^2 = \mathbf{e} \cdot \int \mathbf{a}_c^*(\mathbf{r}) \mathbf{p} \mathbf{a}_v(\mathbf{r}) d\mathbf{r} \quad (6-17b)$$

and  $\mathbf{e}$  indicates the polarization direction of the electric field. Equations (6-17) have been obtained in the dipole approximation with a procedure completely analogous to that described in Chapter 5 in obtaining eq. (5-9). Apart from the conservation of energy, there are two  $\delta$  functions which indicate total spin conservation and momentum conservation; they can be easily understood from symmetry considerations. In fact, in a semiconductor the ground state  $\Psi_0$  is non-degenerate and belongs to the identity representation of the space group. Since the total spin of  $\Psi_0$  is equal to zero and  $H_{ex}$  does not depend on spin, only singlet transverse excitons can be induced by the radiation field. Furthermore,  $\Psi_0$  is invariant under lattice translations; therefore only singlet excitons with  $k_{ex} = \eta$  can be excited by a radiation field of wave number  $|\eta| = 2\pi/\lambda$ , which can be neglected in comparison with the size of the Brillouin zone. In general, for tightly bound excitons, one expects absorption of light to occur at energies closely related to the excitation energies of the atoms, the matrix elements being not too different from those of isolated atoms.

Expressions more complicated than (6-17) are obtained when the restrictions of the simplified model are relaxed. However, only singlet transverse excitons with  $k_{ex} \approx 0$  can be produced in the dipole approximation. In this case a photon represents a perturbation with the symmetry of  $\mathbf{e} \cdot \mathbf{r}$ ; since the fundamental state of the crystal belongs to the identity representation, the allowed transitions are those to exciton states with the same symmetry of the photon perturbation.

### 6-3 Weak binding excitons

#### 6-3a Weak binding excitons in a two-band model<sup>[4,12]</sup>

We wish now to consider an alternative treatment of excitons which is particularly convenient in the weak binding limit. This treatment has been proved useful in understanding, at least qualitatively, a number of features of the absorption spectrum of most inorganic crystals, particularly of small gap semiconductors.

We shall consider first of all a two-band model semiconductor. As in the previous section, we write the fundamental state in the form

$$\Psi_0 = \mathcal{A}\{\psi_{v\mathbf{k}_1}(\mathbf{r}_1)\alpha(1), \psi_{v\mathbf{k}_1}(\mathbf{r}_2)\beta(2), \dots, \psi_{v\mathbf{k}_N}(\mathbf{r}_{2N})\beta(2N)\}, \quad (6-18)$$

but we now remain in the Bloch representation because the Wannier functions in this case would extend to a large number of lattice cells. As trial functions for the excited states we take

$$\Phi_{c\mathbf{k}_es_e, v\mathbf{k}_hs_h} = \mathcal{A}\{\psi_{v\mathbf{k}_1}(\mathbf{r}_1)\alpha(1), \psi_{v\mathbf{k}_1}(\mathbf{r}_2)\beta(2), \dots, \psi_{c\mathbf{k}_es_e}(\mathbf{r}_m), \dots, \psi_{v\mathbf{k}_N}(\mathbf{r}_{2N})\beta(2N)\}, \quad (6-19a)$$

in which the conduction wave function  $\psi_{ck_e s_e}$  ( $= \psi_{ck_e} \alpha$  or  $\psi_{ck_e} \beta$  when  $s_e = \frac{1}{2}$  or  $\frac{3}{2}$  respectively) replaces the valence wave function  $\psi_{vk_h s_h}$  ( $= \psi_{vk_h} \alpha$  or  $\psi_{vk_h} \beta$  when  $s_h = \frac{1}{2}$  or  $\frac{3}{2}$  respectively). We can think of the state  $\Phi_{ck_e s_e, vk_h s_h}$  as containing an electron  $\psi_{ck_e s_e}$  in the conduction band and a hole  $\psi_{vk_h s_h}$  in the valence band, as shown in Fig. 6-2.

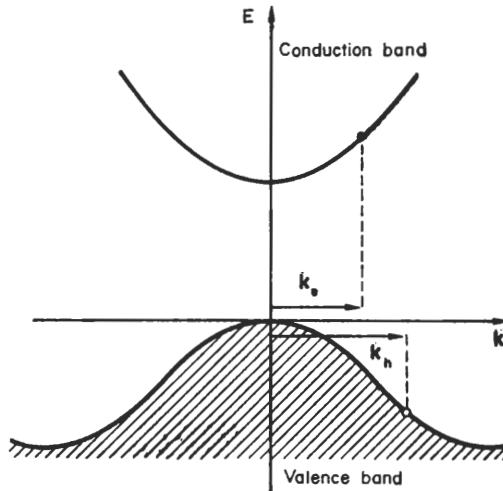


FIG. 6-2. Schematic picture of an exciton in the Bloch representation. The state  $\Phi_{ck_e s_e, vk_h s_h}$  represents an extra electron of wave vector  $k_e$  in the conduction band and a hole of wave vector  $k_h$  in the valence band.

Since we have taken the Hamiltonian (6-1) to be spin independent it is convenient to consider trial states of a definite spin multiplicity, keeping in mind that this will not be possible when spin-orbit effects are important, in which case simple Slater determinants (6-19a) will be considered. We obtain for triplet states (total spin = 1):

$$\left. \begin{aligned} &\Phi_{ck_e \frac{1}{2}, vk_h \frac{1}{2}}, \\ &\frac{1}{\sqrt{2}} (\Phi_{ck_e \frac{1}{2}, vk_h \frac{1}{2}} - \Phi_{ck_e \frac{3}{2}, vk_h \frac{1}{2}}), \\ &\Phi_{ck_e \frac{3}{2}, vk_h \frac{1}{2}}, \end{aligned} \right\} \quad (6-19b)$$

and for singlet states (total spin = 0)

$$\frac{1}{\sqrt{2}} (\Phi_{ck_e \frac{1}{2}, vk_h \frac{1}{2}} + \Phi_{ck_e \frac{3}{2}, vk_h \frac{1}{2}}). \quad (6-19c)$$

We indicate trial excited states of a given multiplicity with  $\Phi_{ck_e, vk_h}^{(M)}$ , where  $M = 1$  or  $0$  for triplet states and singlet states respectively.

The representation based on the functions  $\Phi_{ck_e, vk_h}^{(M)}$  is completely equivalent from a mathematical point of view to the representation based on the functions  $\Phi_{ck_e, vk_h}^{(M)}$  of the previous section, but it is more convenient to use the form (6-19) for weakly bound excitons. We should point out that the trial excited states  $\Phi_{ck_e, vk_h}^{(M)}$  are characterized by the wave vector  $k_e - k_h$ . Since the electron Hamiltonian  $H_e$  is invariant under lattice vector translations, it follows that a state  $\Phi_{ck_e, vk_h}^{(M)}$  can interact only with states

$\Phi_{c\mathbf{k}', v\mathbf{k}'}^{(M')}$  of the same translational symmetry, i.e.  $\mathbf{k}_e - \mathbf{k}_h = \mathbf{k}'_e - \mathbf{k}'_h$ , and of the same spin multiplicity, i.e.  $M = M'$ . An exciton state of multiplicity  $M$  and wave vector  $\mathbf{k}_{ex}$  can then be expanded in the form

$$\Psi_{ex}^{(M)} = \sum_{\mathbf{k}} A(\mathbf{k}) \Phi_{c\mathbf{k} + \frac{1}{2}\mathbf{k}_{ex}, v\mathbf{k} - \frac{1}{2}\mathbf{k}_{ex}}^{(M)}, \quad (6-20)$$

in which only trial states of total vector  $\mathbf{k}_{ex}$  appear. In the weak binding limit it can be shown (see Appendix 6B) that the Fourier transform  $F(\mathbf{r})$  of  $A(\mathbf{k})$

$$F(\mathbf{r}) = \sum_{\mathbf{k}} A(\mathbf{k}) e^{i\mathbf{k} \cdot \mathbf{r}} \quad (6-21)$$

satisfies the "effective mass equation"

$$\left[ E_{cv}(-i\nabla, \mathbf{k}_{ex}) - \frac{e^2}{er} + J_{cv}(\mathbf{k}_{ex}) \delta_M \delta(\mathbf{r}) \right] F(\mathbf{r}) = E_{ex} F(\mathbf{r}), \quad (6-22)$$

where  $E_{cv}(-i\nabla, \mathbf{k}_{ex})$  denotes the differential operator obtained by expanding the function  $E_c(\mathbf{k} + \frac{1}{2}\mathbf{k}_{ex}) - E_v(\mathbf{k} - \frac{1}{2}\mathbf{k}_{ex})$  in powers of  $\mathbf{k}$  and replacing  $\mathbf{k}$  by the operator  $-i\nabla$ , the quantity  $-e^2/er$  indicates the Coulomb-like electron-hole interaction, the term  $J_{cv}(\mathbf{k}_{ex})$  is defined by (6B-8) and was introduced by Onodera and Toyozawa<sup>[13]</sup> to describe the short range electron-hole exchange interaction, and  $E_{ex}$  is the exciton energy measured from the ground energy. All screening effects due to the electron polarization or to the lattice displacement polarization are taken into account through the dielectric function  $\epsilon$ . In general  $\epsilon$  is a rather complicated function of the electron-hole distance,<sup>[10]</sup> but in the case of weakly bound excitons it is possible to approximate  $\epsilon$  with the static dielectric constant (see also Section 6-4c). Furthermore, eq. (6-22) is valid only when the function  $A(\mathbf{k})$  is peaked in  $\mathbf{k}$  space (see Appendix 6B), which corresponds to a function  $F(\mathbf{r})$  very extended in real space.

Because of the way in which it was obtained (see Appendix 6B), eq. (6-22) is still valid if we change the origin of  $\mathbf{k}$  space referring the  $\mathbf{k}$  vector to the value  $\mathbf{k}_0$  which is a critical point for the energy band difference  $E_c(\mathbf{k} + \frac{1}{2}\mathbf{k}_{ex}) - E_v(\mathbf{k} - \frac{1}{2}\mathbf{k}_{ex})$ , as discussed in Section 5-2 in the limit  $\mathbf{k}_{ex} = 0$ . Since  $A(\mathbf{k} - \mathbf{k}_0)$  is peaked at the origin, we can retain only quadratic terms in the expansion of  $E_c(\mathbf{k} + \frac{1}{2}\mathbf{k}_{ex}) - E_v(\mathbf{k} - \frac{1}{2}\mathbf{k}_{ex})$  about the critical point  $\mathbf{k}_0$ , and we have

$$E_{cv}(-i\nabla, \mathbf{k}_{ex}) = E_0 - \frac{\hbar^2}{2\mu_x} \frac{\partial^2}{\partial^2 x^2} - \frac{\hbar^2}{2\mu_y} \frac{\partial^2}{\partial^2 y^2} - \frac{\hbar^2}{2\mu_z} \frac{\partial^2}{\partial^2 z^2}, \quad (6-23)$$

where  $E_0$  is the energy gap at the critical point and  $\mu_i$  ( $i = x, y, z$ ) are the components of the reduced effective mass in one of its principal directions.

It is instructive to give an intuitive picture of the exciton functions, which is useful particularly for symmetry considerations. Equation (6-20) can be written formally in the limit  $\mathbf{k}_{ex} = 0$ , and neglecting the restriction of definite spin multiplicity

$$\Psi_{ex} = \sum_{\mathbf{k}} A(\mathbf{k}) \psi_{cks_e}(\mathbf{r}_e) T_{vks_h}(\mathbf{r}_h), \quad (6-24)$$

where we have replaced the Slater determinant  $\Phi_{cks_e, vks_h}$  with the two-particle wave function  $\psi_{cks_e}(\mathbf{r}_e) T_{vks_h}(\mathbf{r}_h)$  that describes one electron in the state  $\psi_{cks_e}(\mathbf{r}_e)$  and the missing valence electron  $\psi_{vks_h}(\mathbf{r}_h)$ . Because of the localization of  $A(\mathbf{k})$  near a critical point  $\mathbf{k}_0$ ,

we can write

$$\begin{aligned}\Psi_{ex} &= \sum_{\mathbf{k}} A(\mathbf{k} - \mathbf{k}_0) e^{i(\mathbf{k}-\mathbf{k}_0) \cdot (\mathbf{r}_e - \mathbf{r}_h)} \psi_{c_{\mathbf{k}_0 s_e}}(\mathbf{r}_e) T \psi_{v_{\mathbf{k}_0 s_h}}(\mathbf{r}_h) \\ &= F(\mathbf{r}_e - \mathbf{r}_h) \psi_{c_{\mathbf{k}_0 s_e}}(\mathbf{r}_e) T \psi_{v_{\mathbf{k}_0 s_h}}(\mathbf{r}_h)\end{aligned}\quad (6-25)$$

with  $T$  defined in Section 1-6. An exciton state can be regarded as the product of an envelope function  $F(\mathbf{r}_e - \mathbf{r}_h)$  that describes the relative motion of the electron and hole, modulated on atomic scale by the Bloch functions of the valence and the conduction band at the critical point.

### 6-3b Examples of solution of the effective mass equation

#### Isotropic band model

We discuss here the exciton effects in the case of isotropic valence and conduction bands, such as occur at the edge of cubic crystals, with the extrema at  $\mathbf{k}_0 = 0$ , as sketched in Fig. 6-3. We expand conduction and valence band energies near the extrema and consider only quadratic terms, so that (6-22) becomes

$$\left[ -\frac{\hbar^2}{2\mu} \nabla^2 - \frac{e^2}{\epsilon r} + J_{cv}(\mathbf{k}_{ex} = 0) \delta_M \delta(\mathbf{r}) \right] F(\mathbf{r}) = (E_{ex} - E_G) F(\mathbf{r}). \quad (6-26)$$

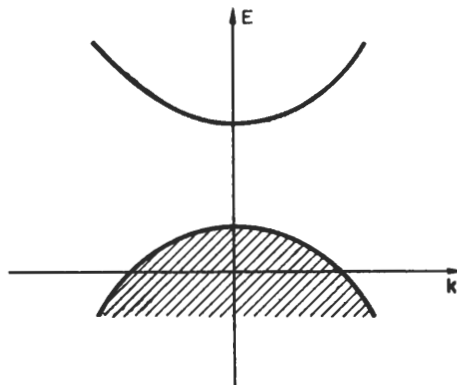


FIG. 6-3. Isotropic two-band model semiconductor with the top of the valence band and the bottom of the conduction band at  $\mathbf{k} = 0$ .

In the weak binding limit,  $\epsilon$  is a constant and the short range exchange term can be neglected. The above equation then reduces to the Schrödinger equation for a hydrogen-like system. The solutions for bound states are the hydrogen-like functions  $F_{nlm}(r)$ , corresponding to the eigenvalues

$$E_{ex} = E_G - \frac{R}{n^2}, \quad (6-27)$$

where  $R = (\mu e^4)/(2\hbar^2 \epsilon^2)$  indicates an effective Rydberg. For non-bound states the eigenfunctions are  $F_{slm}(r)$ , where  $s$  is a continuous index describing the ionized states of the hydrogen-like system, the radial part being<sup>[14]</sup>

$$R_{sl}(r) = \frac{e^{i\pi\alpha} |I(l+1-i\alpha)|}{(2l+1)!} (2sr)^l e^{isr} F(-i\alpha + l + 1; 2l + 2; -2isr),$$

where

$$\alpha = (R/E)^{1/2}, \quad E = (E_{ex} - E_G) > 0, \quad s = (2\mu E/\hbar^2)^{1/2}$$

and  $F(-i\alpha + l + 1; 2l + 2; -2isr)$  is the confluent hypergeometric function. When  $E \gg R$  the hydrogen solutions are with good approximation plane waves, the Fourier transform  $A(\mathbf{k})$  is a  $\delta$  function, and consequently only an electron-hole couple constitute the exciton state.

Using the above results, we can obtain some insight into the consistency of the effective mass approximation following a method suggested by Luttinger and Kohn<sup>[15]</sup> for shallow impurity states. The radius of the first orbit of an hydrogen-like system is  $a_{ex} = a_B e(m/\mu)$  (with  $a_B$  = Bohr radius = 0.529 Å). The wave function  $F_{100}$  of the fundamental state is

$$F_{100}(\mathbf{r}) = \frac{1}{\sqrt{(\pi a_{ex}^3)}} e^{-r/a_{ex}},$$

and its Fourier transform is

$$A(k) = \frac{2\pi a_{ex}^2}{\sqrt{(\pi a_{ex}^3)}} \frac{1}{[1 + (ka_{ex})^2]^2}.$$

Let  $k_s$  denote the radius of the sphere with volume equal to the first Brillouin zone. The ratio between the values of  $A(k)$  for  $k = k_s$  and  $k = 0$  is

$$\frac{A(k_s)}{A(0)} = \frac{1}{[1 + (k_s a_{ex})^2]^2}. \quad (6-28)$$

The validity of the effective mass approximation (see Appendix 6B) requires that  $A(k)$  be strongly peaked in  $\mathbf{k}$  space; in particular it is required that the ratio (6-28) between the value of  $A(k)$  at the boundary of the Brillouin zone and its maximum value be a small number. To represent the case of a typical valence semiconductor we choose

$$\epsilon \approx 10, \mu \approx 0.5 \text{ m}, a_{ex} \approx 10 \text{ Å}, k_s \approx 1 \text{ Å}^{-1}.$$

The ratio  $A(k_s)/A(0)$  from (6-28) is of the order of  $10^{-4}$ , and its smallness justifies the effective mass approximation for the lowest exciton state. The other states are more widely spread in coordinate space so that their Fourier transforms are more peaked in  $\mathbf{k}$  space and the effective mass approximation is even better justified.

We should like to add a few considerations on the electron-hole exchange interaction<sup>[13]</sup> of formula (6-22). Since an exciton in a  $s$  state of the relative motion has a non-vanishing value of the envelope function at  $\mathbf{r} = 0$ , we see that corrections due to electron-hole exchange interaction are important mainly on  $1s$  excitons. Furthermore, if excitons tend to be localized, exchange corrections are expected to be very important.

#### Anisotropic band model<sup>[16]</sup>

We wish now to consider the exciton effects in crystals which are anisotropic along a crystal axis ( $z$  axis). We denote by  $\mu_{||}$  and  $\mu_{\perp}$  the reduced masses parallel and perpendicular to the direction of the  $z$  axis and  $\epsilon_{||}$  and  $\epsilon_{\perp}$  the corresponding effective dielectric constants. The effective electron-hole interaction in the anisotropic case can be obtained as the solution of Poisson's equation

$$\operatorname{div} \mathbf{D} = \operatorname{div} (\epsilon \cdot \nabla V) = 4\pi e^2 \delta(\mathbf{r}).$$

The result is

$$V = -\frac{e^2}{[\epsilon_{\perp}\epsilon_{||}(x^2 + y^2 + \epsilon_{\perp}/\epsilon_{||}z^2)]^{1/2}}.$$

The effective mass equation for excitons in an anisotropic crystal is thus

$$\left[ -\frac{\hbar^2}{2\mu_{||}} \frac{\partial^2}{\partial z^2} - \frac{\hbar^2}{2\mu_{\perp}} \left( \frac{\partial^2}{\partial x^2} + \frac{\partial^2}{\partial y^2} \right) - \frac{e^2}{[\epsilon_{\perp}\epsilon_{||}(x^2 + y^2 + \epsilon_{\perp}/\epsilon_{||}z^2)]^{1/2}} \right] F(\mathbf{r}) = (E_{ex} - E_G) F(\mathbf{r}). \quad (6-29)$$

Making the substitution

$$x' = x, \quad y' = y, \quad z' = \left( \frac{\mu_{||}}{\mu_{\perp}} \right)^{1/2} z,$$

eq. (6-29) becomes

$$\left[ -\frac{\hbar^2}{2\mu_{\perp}} \nabla_{r'}^2 - \frac{e^2}{[\epsilon_{||}\epsilon_{\perp}(x'^2 + y'^2 + \gamma z'^2)]^{1/2}} \right] F(\mathbf{r}') = (E_{ex} - E_G) F(\mathbf{r}'), \quad (6-30)$$

where

$$\gamma = \frac{\epsilon_{\perp}}{\epsilon_{||}} \frac{\mu_{\perp}}{\mu_{||}}$$

is the anisotropy parameter. Equation (6-30) shows that the anisotropy of the dielectric constant tend to counterbalance that of the effective mass.

For  $\gamma = 1$  (isotropic case) we recover the standard hydrogen problem. In the complete anisotropy limit  $\gamma = 0$  we are left with a two-dimensional problem which has been solved exactly, and gives for bound states

$$E_{ex} = E_G - \frac{R}{(n + \frac{1}{2})^2}$$

with  $n = 0, 1, 2$ .

For a general value of  $\gamma$ , eq. (6-30) can be solved using variational methods or perturbation theory.<sup>[16]</sup> In particular, Baldereschi and Diaz<sup>[16]</sup> have shown that the energies vary slowly from those of the isotropic case as  $\gamma$  decreases, so that the two-dimensional

TABLE 6-1. Comparison between experimental and theoretical exciton eigenvalues in the anisotropic crystals GaSe, and MoS<sub>2</sub>. (From Baldereschi and Diaz, ref. [16].) Energies are in electron volts

	GaSe		MoS <sub>2</sub>			
	Exp. <sup>(a)</sup>	Theor.	Series A		Series B	
			Exp. <sup>(b)</sup>	Theor.	Exp. <sup>(b)</sup>	Theor.
$\Sigma_g^+(1)$	2.1099	2.1099	1.9356	1.9356	2.1328	2.1328
$\Sigma_g^+(2)$	2.1246	2.1246	1.9680	1.9680	2.2323	2.2323
$\Sigma_g^+(3)$	...	2.1271	...	1.9729	...	2.2466
$\Sigma_g^+(4)$	2.1273	2.1273	1.9744	1.9742	2.2515	2.2515
$\Sigma_g^+(5)$	...	2.1281	...	1.9756	...	2.2553
$\Sigma_g^+(6)$	2.1283	2.1283	1.9763	1.9763	2.2581	2.2582

(a) See J. E. BREBNER and E. MOOSER, *Phys. Letters* **24A**, 274 (1967).

(b) See B. L. EVANS and P. A. YOUNG, *Phys. Status Solidi* **25**, 417 (1968).

model is always unrealistic. The states of (6-30) are classified in accordance with the different irreducible representations of the cylindrical group  $D_{\infty h}$ . The energies and wave functions of the totally symmetric representation  $\Sigma_g^+$  of the cylindrical group are directly related to the energy positions and oscillator strengths of exciton spectra, as will become apparent from the results of the next section. In Table 6-1 we give some low lying energy states  $\Sigma_g^+$  for the layer compounds GaSe, and MoS<sub>2</sub> as computed by Baldereschi and Diaz;<sup>[16]</sup> for comparison purpose the experimental exciton energies are also given. The satisfactory agreement between theoretical and experimental results seems to indicate the validity of eq. (6-30) for the interpretation of exciton spectra in anisotropic crystals.

### 6-3c Optical properties with exciton effects in a two-band model semiconductor

In the case of a two-band model semiconductor, the imaginary part the dielectric function when exciton effects are neglected is given by (5-14) as

$$\varepsilon_{2F}(\omega) = \frac{4\pi^2 e^2}{m^2 \omega^2} \int_{BZ} \frac{2d\mathbf{k}}{(2\pi)^3} |\mathbf{e} \cdot \mathbf{M}_{cv}(\mathbf{k})|^2 \delta(E_c(\mathbf{k}) - E_v(\mathbf{k}) - \hbar\omega),$$

where we have used the subscript  $F$  to indicate explicitly that free electron–hole pairs are considered.

When the transition is allowed, the matrix elements  $\mathbf{e} \cdot \mathbf{M}_{cv}(\mathbf{k})$  can be taken as a constant in the vicinity of the critical point (first class transitions); when the transition is dipole forbidden  $\mathbf{e} \cdot \mathbf{M}_{cv}(\mathbf{k})$  vanishes at the critical point and can be taken as proportional to  $\mathbf{k}$  (second class transitions). For first class transitions we put  $\mathbf{e} \cdot \mathbf{M}_{cv}(\mathbf{k}) = \mathbf{e} \cdot \mathbf{M}_{cv}(0)$ , and integrate over the Brillouin zone volume. We thus obtain for the two-band model sketched in Fig. 6-3

$$\left. \begin{aligned} \varepsilon_{2F}(\omega) &= 0 && \text{for } \hbar\omega < E_G, \\ \varepsilon_{2F}(\omega) &= \frac{4\pi^2 e^2}{m^2 \omega^2} |\mathbf{e} \cdot \mathbf{M}_{cv}(0)|^2 \frac{1}{2\pi} \left( \frac{2\mu}{\hbar^2} \right)^{3/2} (\hbar\omega - E_G)^{1/2} && \text{for } \hbar\omega > E_G. \end{aligned} \right\} \quad (6-31)$$

For second class transitions we put  $\mathbf{M}_{cv}(\mathbf{k}) = C\mathbf{k}$  and similarly obtain

$$\left. \begin{aligned} \varepsilon_{2F}(\omega) &= 0 && \text{for } \hbar\omega < E_G, \\ \varepsilon_{2F}(\omega) &= \frac{4\pi^2 e^2}{m^2 \omega^2} |C|^2 \frac{1}{2\pi} \left( \frac{2\mu}{\hbar^2} \right)^{5/2} (\hbar\omega - E_G)^{3/2} && \text{for } \hbar\omega > E_G. \end{aligned} \right\} \quad (6-32)$$

The above results of course coincide with those derived in Chapter 5 for interband transitions.

Following Elliott<sup>[12]</sup> we now study how the above expressions are modified when exciton effects are included in the theory. We apply the same general procedure as was used in Section 5-1 to deal with the electron radiation interaction Hamiltonian

$$H_{eR} = \frac{e}{mc} \sum_i \mathbf{A}(\mathbf{r}_i, t) \cdot \mathbf{p}_i$$

and we obtain, in the dipole approximation, the probability per unit time of a transition from the ground state  $\Psi_0$  [defined by eq. (6-18)] to the exciton state  $\Psi_{k_{ex}}^{(M)}$  [defined by eq. (6-20)]:

$$\mathcal{P}_{\Psi_0 \rightarrow \Psi_{k_{ex}}^{(M)}} = \frac{2\pi}{\hbar} \left( \frac{eA_0}{mc} \right)^2 \delta_{k_{ex}} \delta_M \left| \sum_{\mathbf{k}} A(\mathbf{k}) \mathbf{e} \cdot \mathbf{M}_{cv}(\mathbf{k}) \right|^2 \delta(E_{ex} - E_0 - \hbar\omega), \quad (6-33a)$$

$$|\langle \Psi_{ex}^{(M)} | H_{eR} | \Psi_0 \rangle|^2$$

where

$$\mathbf{e} \cdot \mathbf{M}_{cv}(\mathbf{k}) = \mathbf{e} \cdot \int_{\text{crystal volume}} \psi_c^*(\mathbf{k}, \mathbf{r}) \mathbf{p} \psi_v(\mathbf{k}, \mathbf{r}) d\mathbf{r}, \quad (6-33b)$$

and  $A(\mathbf{k})$  is the Fourier transform of the envelope function.

We now consider first class transitions for which we can take  $\mathbf{e} \cdot \mathbf{M}_{cv}(\mathbf{k})$  as a constant and (6-33a) becomes

$$\mathcal{D}_{\psi_0 \rightarrow \psi_{k_{ex}}^{(M)}} = \frac{2\pi}{\hbar} \left( \frac{eA_0}{mc} \right)^2 \delta_{k_{ex}} \delta_M |\mathbf{e} \cdot \mathbf{M}_{cv}(0)|^2 |F(0)|^2 \delta(E_{ex} - E_0 - \hbar\omega), \quad (6-33c)$$

where we have made use of the relation  $\sum_{\mathbf{k}} A(\mathbf{k}) = F(0)$  implied by the definition (6-21).

For bound states  $F(0)$  is different from zero only for  $s$  states of the relative motion, and in such cases we have  $F_{nlm}(0) = 1/\sqrt{\pi a_{ex}^3 n^3}$ . The absorption spectrum for energies below the energy gap consists of a series of lines at energy values

$$E = E_G - \frac{R}{n^2} \quad (n = 1, 2, 3, \dots) \quad (6-34)$$

with intensities decreasing as  $1/n^3$ . The line with  $n = 2$  is consequently eight times weaker than the line with  $n = 1$ , and the line with  $n = 3$  is 27 times weaker. For high values of the quantum number  $n$  (i.e. for energies just below the energy gap), the density of exciton states per unit energy is

$$D(E) = 2 \frac{\partial n}{\partial E} = \frac{2n^3}{R}$$

and, since the intensity decreases as  $1/n^3$ , we obtain a finite limit in the absorption coefficient for energies near  $E_G$ .

We thus expect the absorption below the energy gap to consist of a strong line and a few weaker lines, leading to a constant value of the absorption coefficient at the ionization limit.

Above the ionization limit the effect of the Coulomb interaction is simply to introduce the factor

$$|F_{s00}(0)|^2 = \frac{\pi x e^{ix}}{\sinh \pi x}, \quad x = [R/(\hbar\omega - E_G)]^{1/2},$$

in the results appropriate to the interband transitions discussed in Chapter 5. We obtain

$$\varepsilon_2(\omega) = \varepsilon_{2F}(\omega) \frac{\pi x e^{ix}}{\sinh \pi x}, \quad (6-35)$$

where  $\varepsilon_{2F}$  indicates the dielectric function in the case of free electron-holes as given by expression (6-31). We see that for  $x \ll 1$ , i.e.  $(\hbar\omega - E_G) \gg R$ , we simply obtain  $\varepsilon_2(\omega) = \varepsilon_{2F}(\omega)$ ; similarly for  $x \gg 1$ , i.e.  $(\hbar\omega - E_G) \ll R$ , we obtain  $\varepsilon_2(\omega) = 2\pi x \varepsilon_{2F}(\omega)$ , and thus we have a finite limit in the absorption coefficient at energies near the energy gap. A schematic picture of the absorption coefficient obtained by including exciton effects is given in Fig. 6-4.

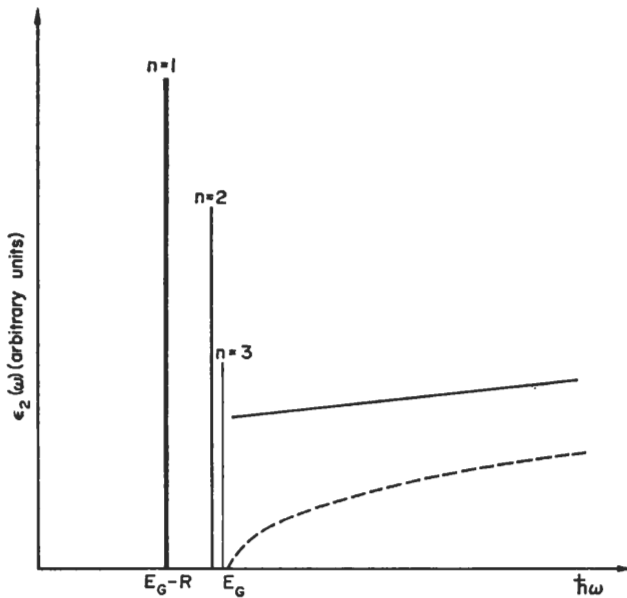


FIG. 6-4. Schematic diagram of the dielectric function for first class optical transitions with inclusion of exciton effects. The dashed line indicates the dielectric function neglecting exciton effects.

We now consider second class optical transitions. In this case we can take  $\mathbf{M}_{cv}(\mathbf{k}) = C\mathbf{k}$ , and (6-33a) becomes

$$\mathcal{P}_{\psi_0 \rightarrow \psi_{k_{ex}}^{(M)}} = \frac{2\pi}{\hbar} \left( \frac{eA_0}{mc} \right)^2 \delta_{k_{ex}} \delta_M |C|^2 \left[ \left[ \mathbf{e} \cdot \frac{\partial}{\partial \mathbf{r}} F(\mathbf{r}) \right]_{\mathbf{r}=0} \right]^2 \delta(E_{ex} - E_0 - \hbar\omega),$$

where we have made use of the relation  $\sum_{\mathbf{k}} \mathbf{k} A(\mathbf{k}) = [\partial F(\mathbf{r})/\partial \mathbf{r}]_{\mathbf{r}=0}$  implied by the definition (6-21).

For bound states  $[\partial/\partial \mathbf{r} F_{nlm}(\mathbf{r})]_{\mathbf{r}=0}$  is different from zero only for  $p$  states of the envelope function, and in such cases we have

$$\left[ \frac{\partial}{\partial \mathbf{r}} F_{nlm}(\mathbf{r}) \right]_{\mathbf{r}=0} = \left( \frac{n^2 - 1}{\pi a_{ex}^5 n^5} \right)^{1/2}.$$

Thus we do not have the line with  $n = 1$  but only absorption at energy values given by

$$E = E_G - \frac{R}{n^2} \quad (n = 2, 3, 4, \dots) \quad (6-36)$$

with intensities proportional to  $(n^2 - 1)/n^5$ .

For energies larger than the energy gap

$$\varepsilon_2(\omega) = \varepsilon_{2F}(\omega) \frac{\pi x(1 + x^2)e^{\pi x}}{\sinh \pi x}, \quad (6-37)$$

where  $x = [R/(\hbar\omega - E_G)]^{1/2}$  and  $\varepsilon_{2F}$  denote the free pair expression (6-32). In Fig. 6-5 we give a schematic picture of the absorption coefficient obtained by including exciton effects in the case of second class transitions.

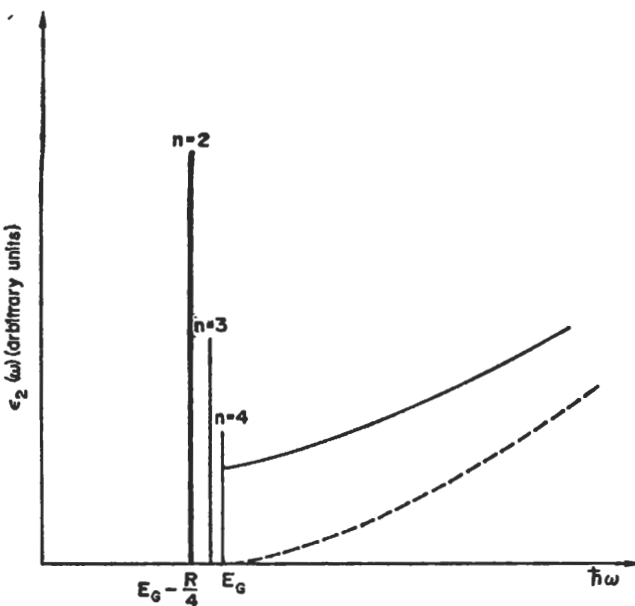


FIG. 6-5. Schematic diagram of the dielectric function for second class optical transitions with inclusion of exciton effects. The dashed line indicates the dielectric function neglecting exciton effects.

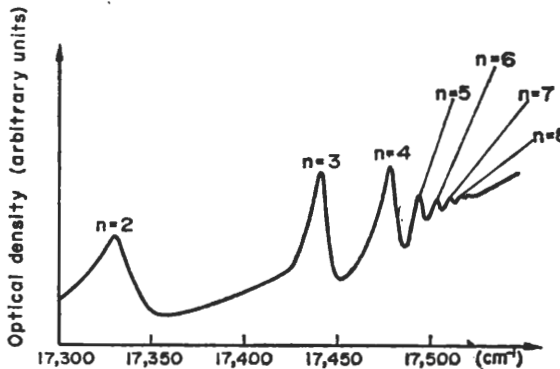


FIG. 6-6. Optical density for the yellow exciton series of  $\text{Cu}_2\text{O}$  at 4.2K.  
(After Nikitine, ref. [17].)

The results obtained in the case of parabolic bands and within the effective mass approximation are summarized in Table 6-2.

As an example of second class transitions we consider the case of cuprous oxide.<sup>[17]</sup> At low temperatures a hydrogen-like yellow series has been observed with lines going from  $n = 2$  to  $n = 9$ ; Fig. 6-6 shows the position of the exciton lines. This series has been interpreted as due to second class exciton transitions, and the series is well described by the formula

$$\nu_n = 17250 - \frac{786}{n^2} \text{ cm}^{-1} \quad (n = 2, 3, 4, \dots).$$

## ELECTRONIC STATES AND OPTICAL TRANSITIONS

TABLE 6-2. Frequency dependence of the absorption coefficient in the case of transitions between spherical parabolic bands with and without exciton effects

First class transitions (dipole allowed)	
Exciton effects neglected	Exciton effects included
$\varepsilon_{2F}(\hbar\omega) = 0 \text{ for } \hbar\omega < E_G$	lines at $\hbar\omega = E_G - \frac{R}{n^2}$ $n = 1, 2, 3, \dots$ with oscillator strength $f_n \sim \frac{1}{n^3}$
Second class transitions (dipole forbidden)	
Exciton effects neglected	Exciton effects included
$\varepsilon_{2F}(\hbar\omega) = C \frac{1}{\omega^2} (\hbar\omega - E_G)^{1/2} \text{ for } \hbar\omega > E_G$	lines at $\hbar\omega = E_G - \frac{R}{n^2}$ $n = 2, 3, 4, \dots$ with oscillator strength $f_n \sim \frac{n^2 - 1}{n^3}$
$\varepsilon_{2F}(\hbar\omega) = C \frac{1}{\omega^2} (\hbar\omega - E_G)^{3/2} \text{ for } \hbar\omega > E_G$	$\varepsilon_2(\hbar\omega) = \varepsilon_{2F}(\hbar\omega) \frac{\pi x e^{\pi x}}{\sinh \pi x}$ $x = \left( \frac{R}{\hbar\omega - E_G} \right)^{1/2}$

We should like to conclude this section by considering exciton effects at other critical points. First of all we recall that the effective mass formalism, as derived in Appendix 6B, is not limited to critical points of type  $M_0$  but can be valid also in the vicinity of the other critical points. In fact the condition that the envelope function  $F(\mathbf{r})$  is extended in real space and is peaked in  $\mathbf{k}$  space is generally true at all critical points in crystals with a large dielectric constant.

At the critical point  $M_3$ , the effective mass equation is easily solved, as shown by Velický and Sak.<sup>[18]</sup> The free electron-hole contribution

$$\varepsilon_{2F}(\omega) = \frac{4\pi^2 e^2}{m^2 w^2} |\mathbf{e} \cdot \mathbf{M}_{cv}(\mathbf{k}_0)|^2 \frac{1}{2\pi} \left( \frac{2\mu}{\hbar^2} \right)^{3/2} (E_0 - \hbar\omega)^{1/2} \text{ for } \hbar\omega < E_0$$

is modified to

$$\varepsilon_2(\omega) = \varepsilon_{2F}(\omega) \frac{\pi x' e^{\pi x'}}{\sinh \pi x'},$$

where  $x' = [R/(E_0 - \hbar\omega)]^{1/2}$ . This expression is very similar to (6-35), but in this case no discrete levels exist for  $\hbar\omega > E_0$ . The shape of the imaginary part of the dielectric function is shown in Fig. 6-7, and we see that the  $M_3$  singularity is weakened by the electron-hole interaction.

The problem of exciton effects at saddle points is much more complicated because of the difficulty of solving exactly the Schrödinger equation when one or two of the masses have different signs. Considerations for saddle points  $M_1$  and  $M_2$  have been

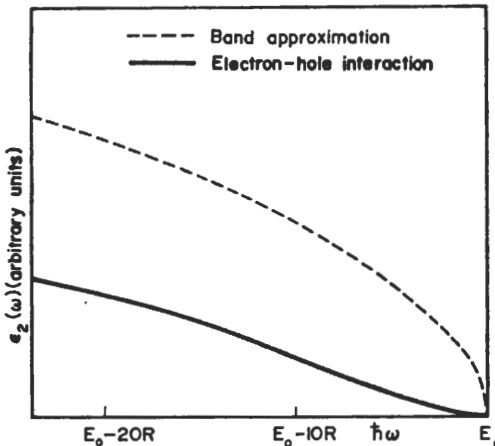


FIG. 6-7. Change in  $\epsilon_2(\omega)$  at the critical point  $M_3$  due to electron-hole interaction (After Velický and Sak, ref. [18].).

made by Velický and Sak;<sup>[18]</sup> they approximated the electron-hole coulomb interaction by a delta function potential as suggested by Koster and Slater.<sup>[19]</sup> This procedure has the advantage that it leads to exact solutions and meaningful qualitative inferences can therefore be drawn. It is shown<sup>[18]</sup> that the point  $M_1$  is enhanced and sharpened by the electron-hole interaction (as we know to be the case for  $M_0$ ), while the point  $M_2$  is weakened (as we know to be the case for  $M_3$ ).

When the actual electron-hole interaction  $-e^2/\epsilon r$  is considered it has been suggested by Phillips,<sup>[20]</sup> using semiclassical arguments, that resonant exciton states may exist below critical points of type  $M_1$ . The effective mass equation at a critical point  $M_1$  with negative reduced mass in the  $z$  direction can be written as

$$\left[ -\frac{\hbar^2}{2\mu_x} \frac{\partial^2}{\partial x^2} - \frac{\hbar^2}{2\mu_y} \frac{\partial^2}{\partial y^2} + \frac{\hbar^2}{2\mu_z} \frac{\partial^2}{\partial z^2} - \frac{e^2}{\epsilon r} \right] F(r) = (E - E_0) F(r). \quad (6-38)$$

Since one of the effective masses is negative, we do not have the possibility of localized exciton states in a strict sense. In general, the envelope function  $F(r)$  of (6-38) consists of a part which is localized and goes to zero as the electron-hole separation increases and a part which is a running wave and represents the asymptotic behaviour. Corresponding to a resonant state the localized part of the envelope function is large with respect to the scattering part, and this gives a sharp increase in the modulating factor  $|F(0)|^2$  of (6-33c). Inclusion of the electron-hole interaction thus provides the possibility for an energy dependent modulating factor which may produce additional peaks in the absorption coefficient. Equation (6-38) has never been solved exactly since it is not separable, but Kane<sup>[21]</sup> has obtained numerical solutions for the cylindrical case  $\mu_x = \mu$ , in the adiabatic approximation. This consists of writing  $F(r)$  as the product of two functions, one of which depends only on the variable  $z$  while the other depends principally on  $\varrho = \sqrt{(x^2 + y^2)}$ , and separating (6-38) into two coupled equations which can be solved by numerical integration. When the ratio  $\mu_z/\mu_x$  is very large ( $> 40$ ), Kane finds a resonant state with a peak below the  $M_1$  point by an energy not too far from that of the two-dimensional bound state  $-\frac{2\mu_x e^4}{\hbar^2 \epsilon^2}$ . As the ratio  $\mu_z/\mu_x$  decreases,

the resonance broadens and the energy has a small shift toward its value at the critical point; however, since the adiabatic approximation loses its validity as  $\mu_z/\mu_x$  decreases, one cannot use this result as a criterion for the existence of excitons at saddle points. The above discussion indicates that this problem is still rather unsettled, but experimental evidence is mounting in favour of saddle point excitons at the  $A_3 \rightarrow A_1$  transition of cubic semiconductors.<sup>[22]</sup>

Finally, we should like to point out that Kamimura and Nakao,<sup>[23]</sup> using the Koster-Slater model<sup>[19]</sup> in the two-dimensional approximation to study exciton effects in highly anisotropic crystals, have shown the appearance of a bound state below the critical point  $P_0$ , while the critical point  $P_2$  is smeared out. The saddle point  $P_1$  is only slightly modified, the logarithmic singularity being changed into a very sharp absorption peak.

### 6-3d Excitons at the edge of degenerate bands. Two examples

We should like to consider the problem of weakly bound excitons in the case when the valence or the conduction bands are degenerate at a given point of the Brillouin zone, say  $\mathbf{k} = 0$ . Let us suppose that the valence and conduction band energies near  $\mathbf{k} = 0$  are obtained by the solution of the secular problems

$$|E_{vv'}(\mathbf{k}) - E\delta_{vv'}| = 0,$$

$$|E_{cc'}(\mathbf{k}) - E\delta_{cc'}| = 0,$$

respectively, where  $E_{vv'}(\mathbf{k})$  and  $E_{cc'}(\mathbf{k})$  are quadratic in  $\mathbf{k}$ . We define the operator  $E_{cv;c'v'}(-i\nabla, \mathbf{k}_{ex}) = \delta_{vv'}E_{cc'}(-i\nabla + \frac{1}{2}\mathbf{k}_{ex}) - \delta_{cc'}E_{vv'}(-i\nabla - \frac{1}{2}\mathbf{k}_{ex}) + \delta(\mathbf{r})\delta_M J_{cv;c'v'}(\mathbf{k}_{ex})$ , where

(6-39a)

$$J_{cv;c'v'}(\mathbf{k}_{ex}) = 2 \int \int a_c^*(\mathbf{r}_1) a_v^*(\mathbf{r}_2) \frac{e^2}{|\mathbf{r}_1 - \mathbf{r}_2|} a_v(\mathbf{r}_1) a_{c'}(\mathbf{r}_2) d\mathbf{r}_1 d\mathbf{r}_2$$

$$+ 2 \frac{4\pi}{3} \frac{1}{Q} \frac{3(\mu_{cv} \cdot \mathbf{k}_{ex})(\mu_{v'c'} \cdot \mathbf{k}_{ex}) - (\mu_{cv} \cdot \mu_{v'c'}) k_{ex}^2}{k_{ex}^2} + O(k_{ex}^2), \quad (6-39b)$$

$a_c$  and  $a_v$  are the Wannier functions of the conduction and valence band, and  $\mu_{vc}$  is the dipole moment  $\int a_v^*(\mathbf{r}) e a_c(\mathbf{r}) d\mathbf{r}$ . The effective mass equation (6-22) is now generalized<sup>[13]</sup> to give the matrix equation

$$\sum_{c'v'} \left[ E_{cv;c'v'}(-i\nabla, \mathbf{k}_{ex}) - \frac{e^2}{er} \delta_{vv'} \delta_{cc'} + J_{cv;c'v'}(\mathbf{k}_{ex}) \delta_M \delta(\mathbf{r}) \right] F_{c'v'}(\mathbf{r}) = E_{ex} F_{cv}(\mathbf{r}), \quad (6-40)$$

which shows that when valence or conduction bands are degenerate, an exciton does not include a unique pair of valence and conduction bands but consists of a mixture of degenerate or nearly degenerate bands.

Equation (6-25) is extended to give

$$\Psi_{ex} = \sum_{cv} F_{cv}(\mathbf{r}_e - \mathbf{r}_h) \psi_{ckos_n}(\mathbf{r}_e) T \psi_{vkosh_n}(\mathbf{r}_h). \quad (6-41)$$

From (6-41) we can obtain in a very simple way a group theoretical analysis of exciton states.<sup>[24]</sup> Let  $\Gamma_c$  and  $\Gamma_v$  denote the irreducible representations of the conduction and of

the valence wave functions at  $\mathbf{k}_0$ , and let  $\Gamma_{\text{env}}$  represent the symmetry of the set of envelope functions  $\{F_{cv}(\mathbf{r})\}$ . The triple product functions (6-41) constitute a basis for the product representation

$$\Gamma_c \times \Gamma_v^* \times \Gamma_{\text{env}}$$

of the little group of  $\mathbf{k}_0$ . In order to obtain the degeneracies and the symmetry of the excitons, we must decompose the product representation into irreducible representations of the group of  $\mathbf{k}_0$ , and we have

$$\Gamma_c \times \Gamma_v^* \times \Gamma_{\text{env}} = \sum_{\alpha} \Gamma_{\text{ex}}^{(\alpha)}. \quad (6-42)$$

Note that double group representations are used for the electron and hole wave functions and simple group representations for the exciton states because electron and holes have half-spin and the excitons have integer spin.

In order to study the transitions involving degenerate bands we need to consider the problem of selection rules for optical transitions in the dipole approximation. Since the ground crystal state is characterized by the wave vector  $\mathbf{k}_{\text{ex}} = 0$  and symmetry  $\Gamma_1$ , we must consider only excitons with wave vector  $\mathbf{k}_{\text{ex}} = 0$  and symmetry equal to that of the function  $\mathbf{e} \cdot \mathbf{r}$ . Further restrictions can be obtained by noting that the transition probability from the ground state  $\Psi_0$  to the exciton state  $\Psi_{\text{ex}}$  is proportional in the weak binding limit to

$$\left| \sum_{cv} F_{cv}(0) \mathbf{e} \cdot \mathbf{M}_{cv}(\mathbf{k}_0) \right|^2.$$

In order to have allowed exciton transitions, it is necessary that the matrix element  $\mathbf{e} \cdot \mathbf{M}_{cv}(\mathbf{k}_0)$  between the band states be non-zero. It is also necessary that  $F_{cv}(0)$  be non-zero. To determine when  $F_{cv}(0)$  may be different from zero, let us substitute the point group of the crystal by the full rotational group symmetry. The envelope functions become  $s, p, d, \dots$  type, and we know that only  $s$  functions can be different from zero at the origin. On the other hand, the representation  $D^{(0)}$  (with  $s$  basis functions) of the rotational group is compatible only with the representation  $\Gamma_1$  of the point group of the crystal. We thus have  $F_{cv}(0) \neq 0$  only if  $\Gamma_{\text{env}} = \Gamma_1$ .

In conclusion the selection rules for optical transitions in the dipole approximation may be summarized as follows:

- (i) Only excitons with wave vectors equal to zero can be excited.
- (ii) The dipole matrix of band theory must be different from zero.
- (iii) The larger probability is given by an envelope function  $\Gamma_1$ .
- (iv) Transitions are possible only to exciton states belonging to the same irreducible representation as the perturbation  $\mathbf{e} \cdot \mathbf{r}$ .

#### *An illustrative example: exciton effects at the fundamental absorption edge of CsI*

We think it instructive to discuss now in some detail a specific crystal, such as CsI, in which excitons are associated with degenerate bands and the electron-hole interaction is very strong. Although it is possible to solve the effective mass equation for degenerate bands quantitatively,<sup>[25]</sup> it always presents a difficult task and it is therefore a great help to be able to understand a number of features of the optical absorption curves on the basis of symmetry properties and of qualitative considerations.

Let us first consider the symmetry properties of CsI crystal. Caesium iodide crystallizes in a simple cubic lattice with two ions per unit cell:  $\text{I}^-$  in the position  $(0, 0, 0)$  and  $\text{Cs}^+$

## L ELECTRONIC STATES AND OPTICAL TRANSITIONS

in the position  $(a/2, a/2, a/2)$ . The reciprocal lattice is also cubic, and the first Brillouin zone is shown in Fig. 6-8 with standard notations used for symmetry points and symmetry lines. The point group of CsI is  $O_h$ , and no fractional translation is associated with rotational symmetry operations. At the points  $\Gamma$ ,  $R$ ,  $X$ , and  $M$  the irreducible representations of the group of  $\mathbf{k}$  can be obtained from those of the points  $\Gamma$  and  $X$  of the zincblende structure (Tables 4-4 and 4-5) by adding inversion symmetry.

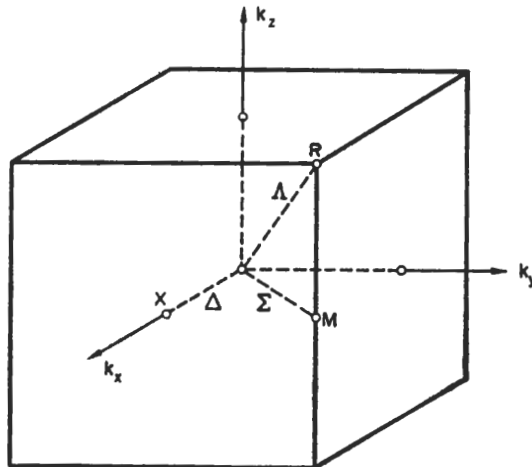


FIG. 6-8. Brillouin zone for CsI crystal.

The band structure calculations of CsI require a relativistic treatment because of the high atomic numbers of caesium and iodine. In Fig. 6-9 we report the results obtained by Onodera<sup>[26]</sup> using the relativistic Green's function method (with slight modifications of the computed energy levels to reproduce some basic experimental properties of CsI, such as the energy gap). The top of the valence band occurs at  $\Gamma$  with the states  $\Gamma_8^-$  and  $\Gamma_6^-$  (split by spin-orbit interaction). The lowest conduction states at  $\Gamma$  are  $\Gamma_6^+$  and  $\Gamma_8^+$ .

The band structure of Fig. 6-9 and the effective mass exciton formalism for degenerate bands can be used to interpret the experimental absorption spectrum of CsI. For convenience the absorption spectrum<sup>[27]</sup> of thin CsI films is shown in Fig. 6-10, with the interpretation of the first exciton peaks as given by Onodera.<sup>[26]</sup>

To determine the symmetry of the excitons associated with the four  $M_0$  band edges  $(\Gamma_8^-, \Gamma_6^+)$ ,  $(\Gamma_6^-, \Gamma_6^+)$ ,  $(\Gamma_8^-, \Gamma_8^+)$ , and  $(\Gamma_6^-, \Gamma_8^+)$ , we apply relation (6-42) with  $\Gamma_{\text{env}}$  equal to the identity representation. Using Tables 2-11 and 2-4 for the characters, we obtain

$$\Gamma_8^- \times \Gamma_6^+ = \Gamma'_{12} + \Gamma_{25} + \underline{\Gamma_{15}},$$

$$\Gamma_6^- \times \Gamma_6^+ = \Gamma'_1 + \underline{\Gamma_{15}},$$

$$\Gamma_8^- \times \Gamma_8^+ = \Gamma'_1 + \Gamma'_2 + \Gamma'_{12} + 2\Gamma_{25} + 2\underline{\Gamma_{15}},$$

$$\Gamma_6^- \times \Gamma_8^+ = \Gamma'_{12} + \Gamma_{25} + \underline{\Gamma_{15}}.$$

We have underlined the excitons of symmetry  $\Gamma_{15}$  because these are the only excitons which can be excited in the dipole approximation. The first peak at 5.81 eV in Fig. 6-10

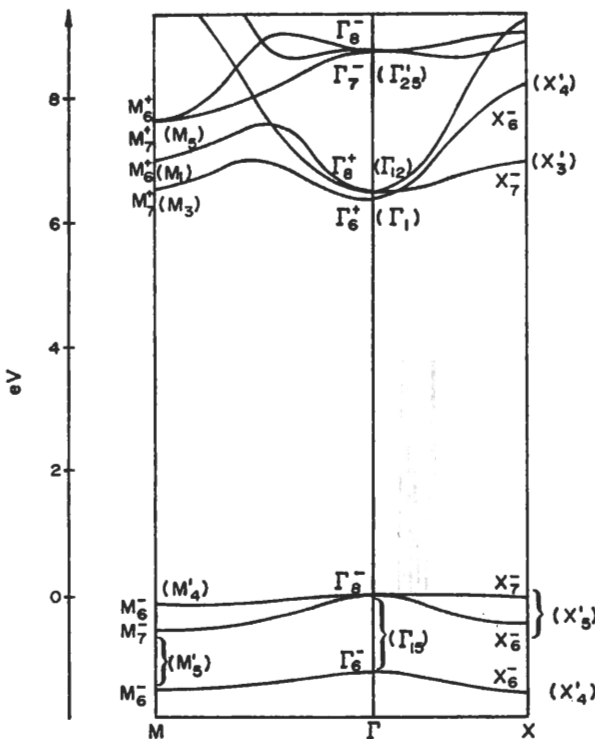


FIG. 6-9. Energy bands for CsI. (After Onodera, ref. [26].) The notations appropriate to double group representations are used. The notations appropriate to simple group representations are given in parentheses.

is attributed to the  $(\Gamma_8^-, \Gamma_6^+)$  exciton; the peak at 6.9 eV with energy separation nearly equal to the splitting  $E(\Gamma_8^-) - E(\Gamma_6^+)$  is attributed to the spin-orbit partner  $(\Gamma_6^-, \Gamma_6^+)$ . The doublet of lines at 5.92 and 6.00 eV is attributed to the two  $\Gamma_{15}$  excitons associated with the  $(\Gamma_8^-, \Gamma_8^+)$  edge. The low intensity of the peak at 5.92 eV respect to that at 6.00 eV has been explained by Onodera.<sup>[26]</sup> The spin-orbit partner of this doublet is due to the edge  $(\Gamma_6^-, \Gamma_8^+)$  and appears at 6.9 eV. The peaks at 6.23 and 6.33 eV can be interpreted as  $2s$  Wannier excitons. The exciton at 6.23 eV is the  $n = 2$  correspondent of the  $(\Gamma_8^-, \Gamma_6^+)$  exciton. The exciton at 6.33 eV corresponds to the doublet  $(\Gamma_8^-, \Gamma_8^+)$ ; because of the larger envelope function, exchange effects determining the doublet splitting are less important and the doublet is not resolved. The difference in energy of 0.10 eV corresponds to the energy separation of  $\Gamma_6^+$  and  $\Gamma_8^+$  states.

Strong support of the above assignments is provided by the temperature dependence of the exciton peaks: in fact the temperature dependent shift of the exciton peaks associated with the band edge  $\Gamma_8^+$  is quite different from the shift of the excitons involving the band edge  $\Gamma_6^+$ . This different shift is ascribed<sup>[26]</sup> to the different sensitivity of the states  $\Gamma_6^+$  ( $\Gamma_1$  in simple group notations) and  $\Gamma_8^+$  ( $\Gamma_{12}$  in simple group notations) to change in potential brought about by a modification of the lattice constant.

At higher energies other structures appear in the optical constants, but their interpretation is not clearly understood, and only a few qualitative speculations have been made.

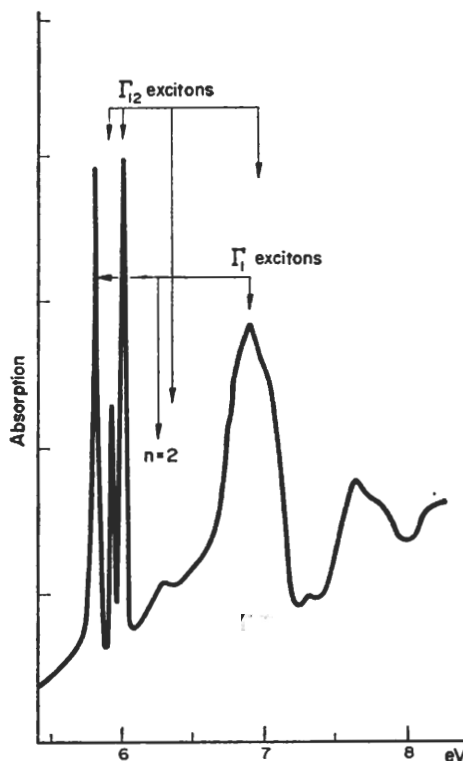


FIG. 6-10. Absorption spectrum at 10K of thin CsI film. (After Tee-garden and Baldini, ref. [27].) The interpretation of exciton peaks is due to Onodera<sup>[26]</sup>.

*A second illustrative example: the structure of the  $n = 1$  exciton line in GaSe*

As discussed in Section 4-2, GaSe is a layer semiconductor characterized by a strong anisotropy. Excitons in GaSe have been investigated experimentally by a number of authors.<sup>[28]</sup> It has been shown in Section 6-3 b that a two-band model with anisotropic values for the effective masses and for the dielectric constants can account for the observed exciton lines.

We wish to show that full account of the lattice symmetry predicts a splitting of the  $n = 1$  line. The symmetry properties of GaSe structure are the same as those of BN (Section 4-2a); for convenience, in Table 6-3 we report both the irreducible representations of the point group  $D_{3h}$  and the additional irreducible representations of the double group  $D'_{3h}$ . The band structure of GaSe computed by Schlüter<sup>[29]</sup> shows that the top of the valence band is the state  $\Gamma_4$  and the bottom of the conduction band is the state  $\Gamma_5$  when spin-orbit interaction is considered. To determine the symmetry of the excitons associated with the  $M_0$  band edge ( $\Gamma_4, \Gamma_5$ ) we apply (6-42) with  $\Gamma_{\text{env}}$  equal to the identity representation and we obtain three exciton states

$$\Gamma_4 \times \Gamma_5 = \Gamma_3^+ + \Gamma_2^- + \Gamma_1^-$$

as can be immediately seen from Table 6-3. Of the above states  $\Gamma_3^+$  is allowed for transitions with light polarized perpendicular to the  $c$  axis,  $\Gamma_2^-$  is allowed for light polarized

TABLE 6-3. Irreducible representations of the simple group  $D_{3h}$  and of the double group  $D'_{3h}$  of GaSe. The notations for the symmetry operations are the same as in Table 4-8.  $\Gamma_1^\pm, \Gamma_2^\pm, \Gamma_3^\pm$  are the irreducible representations of the simple group;  $\Gamma_4, \Gamma_5, \Gamma_6$  are the additional irreducible representations. No additional degeneracy is introduced by time reversal symmetry

Point $\Gamma$	$E$	$E$	$C_6^2$ $C_6^4$	$\overline{C_6^2}$ $\overline{C_6^4}$	$C_y$ $\overline{C_y}$	$C'_y$ $\overline{C'_y}$	$C''_y$ $\overline{C''_y}$	$\sigma_h$ $\overline{\sigma_h}$	$\sigma_h C_6^2$ $\sigma_h C_6^4$	$\overline{\sigma_h C_6^2}$ $\overline{\sigma_h C_6^4}$	$\sigma_h C_y$ $\overline{\sigma_h C_y}$	$\sigma_h C'_y$ $\overline{\sigma_h C'_y}$	$\sigma_h C''_y$ $\overline{\sigma_h C''_y}$	
$\Gamma_1^+$	1	1	1	1		1		1	1	1		1		1
$\Gamma_2^+$	1	1	1	1		-1		1	1	1		-1		
$\Gamma_3^+$	2	2	-1	-1		0		2	-1	-1		0		
$\Gamma_1^-$	1	1	1	1		1		-1	-1	-1		-1		
$\Gamma_2^-$	1	1	1	1		-1		-1	-1	-1		1		
$\Gamma_3^-$	2	2	-1	-1		0		-2	1	1		0		
$\Gamma_4$	2	-2	1	-1		0		0	$\sqrt{3}$	$-\sqrt{3}$		0		
$\Gamma_5$	2	-2	1	-1		0		0	$-\sqrt{3}$	$\sqrt{3}$		0		
$\Gamma_6$	2	-2	2	-2		0		0	0	0		0		

parallel to the  $c$  axis, and the state  $\Gamma_1^-$  is forbidden (see Table 4-13). As a consequence the  $n = 1$  excitons in GaSe split into two lines, one of which ( $\Gamma_2^-$ ) increases in intensity when the angle between the  $c$  axis and the direction of propagation of a beam polarized in the plane of incidence increases, as first observed by Brebner *et al.*<sup>[28]</sup> It can also be shown, by neglecting spin-orbit interaction and considering the products of the representations of the separate spin functions  $D^{(0)}$  and  $D^{(1)}$  by the representations of the simple group, that in lowest order  $\Gamma_3^+$  is a triplet and  $\Gamma_2^-$  a singlet state, so that the stronger transition will be the  $\Gamma_2^-$  in agreement with experiments by Brebner *et al.*<sup>[28]</sup>

Similar results are obtained for the  $n = 1$  exciton line of PbI<sub>2</sub>, but in this case the symmetry group is  $D_{3d}$ , and a similar analysis shows that, even in lowest order, the singlet and triplet states are always mixed.<sup>[29]</sup>

#### 6-4 Intermediately bound excitons<sup>[5]</sup>

##### 6-4a Theory and general considerations

As shown in Sections 6-2 and 6-3, the Frenkel-Peierls model for the excitons applies when the wave functions of the excited states are well localized within the unit cell of the lattice and the Wannier-Mott effective mass model when the wave functions of the excited states extend over a very large number of unit cells. In a number of situations, however, the observed excitons do not belong to the above cases. This happens even for the lowest exciton states in semiconductors, but is typical for large gap insulators and for excitons due to transitions from core states. For this reason approaches have been attempted to deal with intermediate binding. We will briefly describe an approach which includes explicitly the band structure of the crystal and also takes advantage of the localization of the Wannier functions, and we refer the reader to references [5] for related methods and pseudopotential corrections.

We make use of expansion (6-20), dropping the inessential total spin index because we wish to consider also the case with spin-orbit interaction.

## ELECTRONIC STATES AND OPTICAL TRANSITIONS

Substituting into the many particle Schrödinger equation with Hamiltonian (6-1), and making use of (6B-1) and (6B-2), we obtain a general equation which we write, in the limit  $\mathbf{k}_{\text{ex}} = 0$ ,

$$[E_c(\mathbf{k}) - E_v(\mathbf{k}) - E] A_{cv}(\mathbf{k}) + \sum_{c'v'} \sum_{\mathbf{k}'} A_{c'v'}(\mathbf{k}') U_{cv;c'v'}(\mathbf{k}, \mathbf{k}') = 0 \quad (6-43)$$

with

$$\begin{aligned} U_{cv;c'v'}(\mathbf{k}, \mathbf{k}') &= - \int \psi_c^*(\mathbf{k}, \mathbf{r}_1) \psi_{v'}^*(\mathbf{k}', \mathbf{r}_2) \frac{e^2}{|\mathbf{r}_1 - \mathbf{r}_2|} \psi_{c'}(\mathbf{k}', \mathbf{r}_1) \psi_v(\mathbf{k}, \mathbf{r}_2) d\mathbf{r}_1 d\mathbf{r}_2 \\ &\quad + \int \psi_c^*(\mathbf{k}, \mathbf{r}_1) \psi_{v'}^*(\mathbf{k}', \mathbf{r}_1) \frac{e^2}{|\mathbf{r}_1 - \mathbf{r}_2|} \psi_v(\mathbf{k}, \mathbf{r}_2) \psi_{c'}(\mathbf{k}', \mathbf{r}_2) d\mathbf{r}_1 d\mathbf{r}_2, \end{aligned} \quad (6-44)$$

and the integration also includes summation on spin variables. Equation (6-43) is a system of integral equations which contains all couple of bands. The kernel  $U_{cv;c'v'}(\mathbf{k}, \mathbf{k}')$  is non-separable in general so that a direct solution is impossible. We have seen in Appendix 6B when this kernel can be simplified to a local kernel  $U(\mathbf{k} - \mathbf{k}')$  (see eq. 6B-11). We can now show that it can be expressed as a sum of separable factors in  $\mathbf{k}$  and  $\mathbf{k}'$  by expressing the Bloch functions appearing in (6-44) in terms of Wannier functions and retaining only the most important contributions.

By dividing (6-43) by  $E_c(\mathbf{k}) - E_v(\mathbf{k}) - E$ , multiplying by  $e^{i\mathbf{k} \cdot \tau_0}$ , and summing over  $\mathbf{k}$ , we obtain a set of linear homogeneous equations in the Fourier transforms  $A_{cv}(\tau)$ . The system of linear equations is

$$\begin{aligned} A_{cv}(\tau_0) + \sum_{c'v'} A_{c'v'}(0) J_{cv;c'v'}^{(1)}(\mathbf{k}_{\text{ex}} = 0) \frac{1}{N} \sum_{\mathbf{k}} \frac{e^{i\mathbf{k} \cdot \tau_0}}{E_c(\mathbf{k}) - E_v(\mathbf{k}) - E} \\ + \sum_{c'v'} \sum_{\tau} A_{c'v'}(\tau) [J_{cv;c'v'}^{(2)}(\tau) - Q_{cv;c'v'}(\tau)] \frac{1}{N} \sum_{\mathbf{k}} \frac{e^{i\mathbf{k} \cdot (\tau_0 - \tau)}}{E_c(\mathbf{k}) - E_v(\mathbf{k}) - E} = 0, \end{aligned} \quad (6-45a)$$

where

$$A_{cv}(\tau) = \sum_{\mathbf{k}} e^{i\mathbf{k} \cdot \tau} A_{cv}(\mathbf{k}),$$

$J_{cv;c'v'}^{(1)}(\mathbf{k}_{\text{ex}})$  is the long range polarization term, which in cubic crystals is

$$J_{cv;c'v'}^{(1)}(\mathbf{k}_{\text{ex}}) = \frac{4}{3} \pi \frac{1}{Q} \frac{3(\mu_{cv} \cdot \mathbf{k}_{\text{ex}})(\mu_{v'c'} \cdot \mathbf{k}_{\text{ex}}) - (\mu_{cv} \cdot \mu_{v'c'}) k_{\text{ex}}^2}{k_{\text{ex}}^2} + O(k_{\text{ex}}^2) \quad (6-45b)$$

as already discussed in Section 6-2,

$$Q_{cv;c'v'}(\tau) = \int a_c^*(\mathbf{r}_1 - \tau) a_{v'}^*(\mathbf{r}_2) \frac{e^2}{|\mathbf{r}_1 - \mathbf{r}_2|} a_{c'}(\mathbf{r}_1 - \tau) a_v(\mathbf{r}_2) d\mathbf{r}_1 d\mathbf{r}_2 \quad (6-45c)$$

is a Coulomb term between valence and conduction states, and

$$J_{cv;c'v'}^{(2)}(\tau) = \int a_c^*(\mathbf{r}_1 - \tau) a_{v'}^*(\mathbf{r}_2) \frac{e^2}{|\mathbf{r}_1 - \mathbf{r}_2|} a_v(\mathbf{r}_1) a_{c'}(\mathbf{r}_2 - \tau) d\mathbf{r}_1 d\mathbf{r}_2 \quad (6-45d)$$

is a corresponding exchange term.

The polarization term is responsible for the longitudinal transverse splitting because its value depends on whether the dipole moment  $\mu$  is parallel or perpendicular to the exciton momentum  $\mathbf{k}_{\text{ex}}$  even in the limit of zero momentum. In this formulation triplet

and singlet states are mixed because spin-orbit splitting are included in the band energy.

The consistency conditions for the coefficients  $A_{cv}(\tau)$  gives the Fredholm determinant equation which allows a calculation of the eigenvalues  $E$  and of the coefficients themselves. The difference with the previous approaches is that now the all band structure appears in the computation of the term

$$\frac{1}{N} \sum_{\mathbf{k}} \frac{e^{i\mathbf{k} \cdot \tau}}{E_c(\mathbf{k}) - E_v(\mathbf{k}) - E}$$

and the localization of the Wannier functions proves useful in the calculation of (6-45b), (6-45c), and (6-45d). The advantage of the method is when one can consider only a few values of  $\tau$ , so that the set of linear equations is very small. This means that the exciton wave functions extend over a few cells of the lattice, which may be the case for the low exciton states. In some cases one can consider only the case  $\tau = 0$  (one site approximation) neglecting all other terms in (6-45) and still obtain a good approximation.

It may be interesting to observe that from equation (6-45) one can obtain back the Peierls-Frenkel model of Section 6-2 by neglecting the  $\mathbf{k}$  dependence of the energy bands  $E(\mathbf{k})$  and the Mott-Wannier weak binding model by considering those states where  $A_{cv}(\tau)$  extends over a large number of cells so that only large values of  $\tau$  are important, and  $\tau$  can be treated as a continuous variable.

We finally notice that when spin-orbit splitting is negligible the terms  $J^{(2)}(\tau)$  and  $J^{(1)}(\mathbf{k}_{ex})$  will be present with factor 2 only for singlet states as shown in the previous cases discussed in Sections 6-2 and 6-3, so that one can estimate immediately the singlet-triplet splitting and the longitudinal-transverse separation for the singlet state.

#### 6-4b An example: solid argon

As an example we can apply the above procedure to compute the lowest exciton states of solid argon in the one-site approximation. A schematic band structure is shown for convenience in Fig. 6-11, with an indication of the bands involved near  $\mathbf{k} = 0$ . We observe that

$$\Gamma_8^- \times \Gamma_6^+ = \Gamma_{25} + \Gamma'_{12} + \underline{\Gamma_{15}}$$

$$\Gamma_6^- \times \Gamma_6^+ = \Gamma'_1 + \underline{\Gamma_{15}},$$

so that, by choosing symmetry adapted combinations of Wannier functions of the different bands which produce excitons of symmetry  $\Gamma_{15}$ , allowed for optical transitions, one is left with only a two by two set of homogeneous equations for transverse excitons and a similar system for longitudinal excitons. The results obtained for solid argon are

TABLE 6-4. Lowest exciton binding energies in argon. For comparison the experimental values are given in parenthesis. Energies are in electron volts. (From Altarelli and Bassani, ref. [5].)

	$E_1$	$E_2$	$\Delta E$
Transversal	1.92 (2.16)	1.63 (1.86)	0.29 (0.30)
Longitudinal	1.90	1.24	0.66
$\Delta_{L-T}$	0.02	0.39	

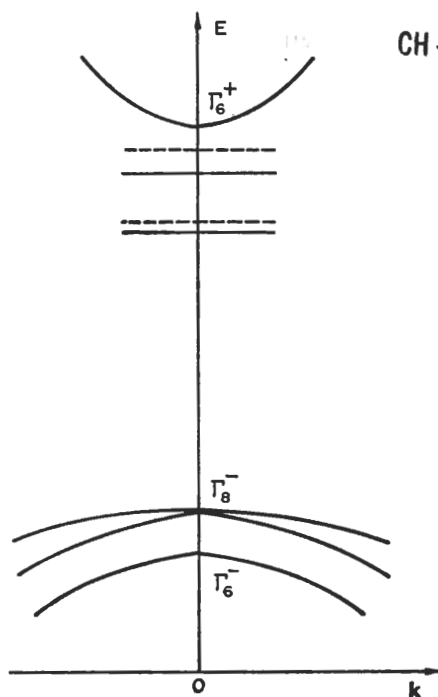


FIG. 6-11. Schematic band structure of solid argon near  $k = 0$  with indication of the spin-orbit separation in the valence band. The positions of the  $n = 1$  transversal (longitudinal) excitons are indicated with a solid (broken) line.

reported in Table 6-4, where for comparison the experimental values are given in parentheses. It can be observed that the agreement is encouraging already in the one-site approximation. In particular the separation of the exciton peaks is larger than the spin-orbit separation of the bands, which is about the same as the atomic value (0.18 eV).

#### 6-4c *Comments on polarization screening*

The reader may have noticed that for the weak binding case of Section 6-3 we have screened the electron-hole interaction in eq. (6-22) by the dielectric constant, while in the case of tightly bound excitons of Section 6-2 and in the present analysis, summarized in eq. (6-45), we have not considered polarization screening. This decision can really be justified in the extreme cases that the excited wave function has a Bohr radius at least one order of magnitude larger than the lattice parameter or is confined within the unit cell. The choice of the screening function to be used in the intermediate range is still not completely settled, though a lot of progress has been made in the general understanding of the problem.<sup>[30]</sup>

Considering the interaction as instantaneous in time we can neglect the phonon contribution to screening which is present in ionic crystals,<sup>[10]</sup> and we may just consider the electronic part. This can be seen as due to a self-consistency requirement by which the creation of the excited state modifies the Bloch functions of the remaining electrons and therefore the electron density, thus producing a screening of the interac-

<sup>t</sup>ion. We do not attempt here a complete derivation of these effects, but only recall the important result that the Fourier transforms of the bare electron-hole interaction are screened in the crystal by the dielectric function  $\epsilon_1(\mathbf{q}, \omega)$  so that the effective electron-hole interaction to be considered is

$$V_{\text{eff}}(\mathbf{q}, \omega) = \frac{V(\mathbf{q})}{\epsilon_1(\mathbf{q}, \omega)} = - \frac{4\pi e^2}{q^2 \epsilon_1(\mathbf{q}, \omega)}. \quad (6-46)$$

In (6-46)  $\epsilon_1(\mathbf{q}, \omega)$  is often replaced with its static limit  $\epsilon_1(\mathbf{q}, 0)$  because  $\omega$  can be considered negligible compared to the frequencies of the virtual transitions involved  $(E_c - E_v)/\hbar$ .

Expressions for the dielectric function are given in the literature to various degrees of sophistication.<sup>[30]</sup> In the random phase approximation we have

$$\epsilon(\mathbf{q}, \omega) = 1 + \frac{4\pi e^2}{q^2} \sum_{vck} \frac{|\langle \psi_{ck} | e^{-i\mathbf{q} \cdot \mathbf{r}} | \psi_{vk+q} \rangle|^2}{E_c(\mathbf{k}) - E_v(\mathbf{k} + \mathbf{q}) - \hbar\omega - i\hbar\theta}. \quad (6-47)$$

In the case  $\mathbf{q} = 0$  it is easily proved that (6-47) reduces to the familiar expressions (5-14) and (5-16). It can also be proved that in semiconductors and insulators  $\epsilon_1(\mathbf{q}, 0)$  tends to a finite value  $\epsilon(0)$  for small values of  $\mathbf{q}$  while for values of  $\mathbf{q}$  larger than a few reciprocal lattice vectors it drops rapidly to 1.

Since the effective mass approximation is valid when electron and hole are separated by many lattice cells, small values of  $\mathbf{q}$  give the main contribution to the Fourier transform of the interaction so that the value  $\epsilon(0)$  can be used as we have done in Section 6-3. In the tight binding case, electron and hole are in the same cell, so that very large values of  $\mathbf{q}$  appear in the Fourier transform of the interaction, and one can choose the screening constant to be 1. In the intermediate case discussed in Section 6-4a the Fourier transform (6-46) with expression (6-47) should be used to obtain the interaction; however, when electron and hole are confined to the same cell or to the few nearest cells,  $\epsilon_1(\mathbf{q}, 0) \approx 1$  can still be used and no screening is necessary.

## 6-5 Two-photon exciton transitions

The theory of two-photon exciton transitions can be developed using a formalism similar to that considered in Section 5-3 and furnishes a powerful additional tool for the investigation of excitons. Loudon<sup>[31]</sup> treated the problem of two-photon exciton transitions considering as intermediate states the exciton states associated with virtual bands different from the final conduction band; Mahan<sup>[31]</sup> considered as intermediate states the excitons associated with the final conduction band which differ by the envelope function. Both processes are present, but Mahan's mechanism seems to be favoured in crystals with strong electron-hole interaction.

In Section 5-3 we discussed a number of situations in which transitions forbidden in one-photon spectroscopy are allowed in two-photon spectroscopy and vice versa.

A similar situation may occur for exciton transitions both in the Loudon model and in the Mahan model, because we must consider products of matrix element of the type

$$\frac{\langle \Psi_{fex} | H_{eR} | \Psi_{\beta ex} \rangle \langle \Psi_{\beta ex} | H_{eR} | \Psi_0 \rangle}{E_{\beta ex} - E_0 - \hbar\omega},$$

where  $H_{eR}$  is the usual electron-radiation interaction,  $\Psi_{\beta ex}$  is an intermediate exciton state, and  $\Psi_{fex}$  is the final exciton reached by the two-photon transition. To every

matrix element we can apply the selection rules discussed in Section 6-3d and obtain the final exciton states which are allowed by two-photon transitions. In the Mahan model, where the exciton functions only differ by their envelope functions, we can see immediately that if  $s$  excitons are allowed in one-photon transitions,  $p$  excitons will be allowed in two-photon processes and vice versa.

A particular case where this situation occurs is in Cu<sub>2</sub>O, for which one photon  $p$  excitons had been shown in Fig. 6-6. Evidence for two-photon  $s$  excitons has been found by Pradère *et al.*<sup>[31]</sup> The above authors also found evidence for two-photon transitions to  $p$  excitons in CdS, while other evidence for two-photon transitions to  $p$  excitons was found by Fröhlich *et al.*<sup>[31]</sup> in the case of ionic crystals.

We could here repeat the considerations made in the previous chapter about the promising hopes modern laser techniques raise in this field.

## 6-6 Indirect exciton transitions

In the previous sections we have considered excitons in the rigid lattice approximation. The relaxation of the rigid lattice approximation poses very difficult theoretical problems. We should take account of the following:

- (i) The electron-hole interaction has to be screened by an appropriate  $r$ -dependent dielectric function which must also include lattice polarization effects.<sup>[10]</sup>
- (ii) When an exciton is formed the electron charge density distribution changes and a polarization of the lattice follows the exciton in its motion through the lattice. The interaction of the lattice vibrations with the exciton produces a half width of the exciton line spectrum which can be of the order of 0.1 eV in ionic crystals because of the strong electron-phonon interaction.<sup>[32]</sup>
- (iii) There is the possibility of indirect exciton transitions induced by light to excitons with  $\mathbf{k}_{ex} \neq 0$  when a phonon of the same momentum  $\mathbf{k}_{ex}$  is absorbed or emitted.

We shall now consider (iii) briefly within the theory of weak binding discussed in Section 6-3. We consider the case of parabolic non-degenerate energy bands with a maximum of the valence band at  $\mathbf{k} = 0$  and a minimum of the conduction band at  $\mathbf{k} = \mathbf{q}_0$  [see Fig. 6-12(a)]:

$$E_c(\mathbf{k}_e) = \frac{\hbar^2(\mathbf{k}_e - \mathbf{q}_0)^2}{2m_c^*} + E_G,$$

$$E_v(\mathbf{k}_h) = -\frac{\hbar^2 \mathbf{k}_h^2}{2m_v^*}.$$

We shall compare the results obtained by including exciton effects with the results of Section 5-4 relative to indirect interband transitions.

The exciton states with wave vector  $\mathbf{k}_{ex}$  are obtained by solving the effective mass equation (6-22). In our model semiconductor we have

$$\begin{aligned} E_{cv}(\mathbf{k}, \mathbf{k}_{ex}) &= E_G + \frac{\hbar^2}{2m_c^*} \left( \mathbf{k} + \frac{1}{2} \mathbf{k}_{ex} - \mathbf{q}_0 \right)^2 + \frac{\hbar^2}{2m_c^*} \left( \mathbf{k} - \frac{1}{2} \mathbf{k}_{ex} \right)^2 \\ &= E_G + \frac{\hbar^2}{2(m_c^* + m_v^*)} (\mathbf{k}_{ex} - \mathbf{q}_0)^2 + \frac{\hbar^2}{2\mu} \left[ \mathbf{k} - \frac{1}{2} \frac{m_c^* - m_v^*}{m_c^* + m_v^*} (\mathbf{k}_{ex} - \mathbf{q}_0) \right]^2, \end{aligned}$$

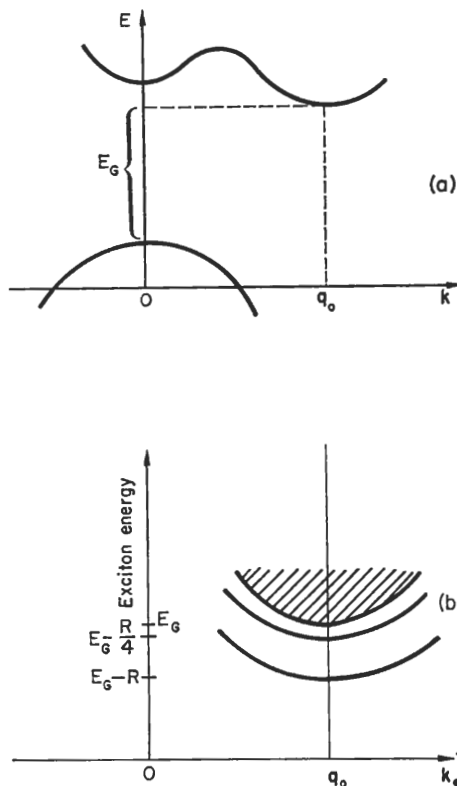


FIG. 6-12. (a) Schematic energy band representation. (b) Exciton bands in the vicinity of the wave vector  $q_0$ .

where  $\mu$  indicates the reduced mass. For  $\mathbf{k}_{\text{ex}} = \mathbf{q}_0$  the effective mass equation (6-22) becomes (neglecting short range terms):

$$\left[ -\frac{\hbar^2}{2\mu} \nabla^2 - \frac{e^2}{er} \right] F(\mathbf{r}) = (E_{\text{ex}} - E_G) F(\mathbf{r}). \quad (6-48)$$

The possible exciton energies  $E_{\text{ex}}(\mathbf{q}_0)$  are

$$E_{\text{ex}}(\mathbf{q}_0) = E_G - \frac{R}{n^2}$$

for states below the gap and a continuum for states above the indirect gap. The possible exciton energies  $E_{\text{ex}}(\mathbf{q}_0)$  corresponding to  $\mathbf{q}_0$  are shown in Fig. 6-12(b). For excitons with  $\mathbf{k}_{\text{ex}} \neq \mathbf{q}_0$ , the expression  $E_{\text{ex}}(\mathbf{k}, \mathbf{k}_{\text{ex}})$  presents a minimum equal to  $E_G + \frac{\hbar^2}{2(m_c^* + m_v^*)} \times (\mathbf{k}_{\text{ex}} - \mathbf{q}_0)^2$  and has isotropic quadratic form near the minimum with reduced mass  $\mu$ . The effective mass equation is similar to (6-48) except for the replacement of  $E_G$  by the quantity  $E_G + \frac{\hbar^2}{2(m_c^* + m_v^*)} (\mathbf{k}_{\text{ex}} - \mathbf{q}_0)^2$ . The energies of the excitons with  $\mathbf{k}_{\text{ex}} \neq \mathbf{q}_0$  are therefore obtained simply by adding the "total kinetic energy"  $\frac{\hbar^2}{2(m_c^* + m_v^*)} (\mathbf{k}_{\text{ex}} - \mathbf{q}_0)^2$ "

## ELECTRONIC STATES AND OPTICAL TRANSITIONS

to the excitons with wave vector  $\mathbf{q}_0$ . The resulting exciton bands are schematically represented in Fig. 6-12(b), where we have indicated the energy of the ground state at the origin.

We can now calculate optical constants due to indirect exciton transitions using standard second order perturbation theory with the interactions between the electron and the electromagnetic field and between the electron and the phonon field as time dependent perturbations, as discussed in detail in Section 5-4. With assumptions and procedures similar to those leading to expression (5-44), one finds that the contribution to the absorption coefficient in a process in which a photon and a phonon are simultaneously absorbed is given by

$$\alpha_{\text{phonon abs}}(\omega) = \frac{4\pi^2 e^2 C n_{\mathbf{q}_0} |F(0)|^2}{ncm^2 \omega} \int_{\text{BZ}} \frac{2}{(2\pi)^3} d\mathbf{k}_{\text{ex}} \delta(E(\mathbf{k}_{\text{ex}}) - E_0 - \hbar\omega + K\theta), \quad (6-49)$$

where the notations used are the same as those of Section 5-4, and  $|F(0)|^2$  now appears because as we have seen in Section 6-3, the probability of a transition is proportional to the probability that the electron and the hole are at the same point. Using exciton energies determined by (6-48) in carrying out the integration (6-49) we obtain for the first exciton band

$$\alpha_{\text{phonon abs}}(\omega) = \begin{cases} 0 & \text{for } \hbar\omega < (E_G - R - K\theta), \\ C_2(\hbar\omega - E_G + R + K\theta)^{1/2} n_{\mathbf{q}_0} |F(0)|^2 & \text{for } \hbar\omega > (E_G - R - K\theta), \end{cases} \quad (6-50)$$

where

$$C_2 = \frac{C}{\omega} \frac{4\pi^2 e^2}{ncm^2} \frac{2}{(2\pi)^3} \left( \frac{m_c^* + m_v^*}{\hbar^2} \right)^{3/2}.$$

To include all the exciton bands we must sum expressions of type (6-50). The absorption coefficient for energies above the gap is quite a complicated function, but for  $\hbar\omega \gg (E_G - K\theta)$  the dependence coincides with that of expression (5-45a).

For the contribution to the absorption coefficient due to the emission of a phonon corresponding to the first exciton band we obtain in a similar way

$$\alpha_{\text{phonon emiss}}(\omega) = \begin{cases} 0 & \text{for } \hbar\omega < (E_G - R + K\theta), \\ C_2(\hbar\omega - E_G + R - K\theta)^{1/2} (n_{\mathbf{q}_0} + 1) |F(0)|^2 & \text{for } \hbar\omega > (E_G - R + K\theta). \end{cases} \quad (6-51)$$

From (6-50) and (6-51) we can see that the total absorption coefficient

$$\alpha_{\text{tot}}(\omega) = \alpha_{\text{phonon abs}}(\omega) + \alpha_{\text{phonon emiss}}(\omega) \quad (6-52)$$

has two steps—one for  $\hbar\omega = (E_G - K\theta - R)$  and one for  $\hbar\omega = (E_G + K\theta - R)$ , the difference between the two steps being equal to  $2K\theta$ . When more phonons of given  $\mathbf{q}_0$  can participate in optical transitions, each of them gives its own contribution to the absorption coefficient.

The temperature dependence is contained in the term  $n_{q_0}$  which gives the number of phonons in thermodynamic equilibrium according to Bose-Einstein statistics. The indirect exciton transitions as a consequence are strongly temperature dependent, and in particular the contribution  $\alpha_{\text{phonon abs}}(\omega)$  in (6-52) disappears at sufficiently low temperatures.

As an example of the application of the theory of indirect exciton transitions we consider the case of the absorption edge of Cu<sub>2</sub>O crystals.<sup>[17]</sup> In Fig. 6-13 the absorp-

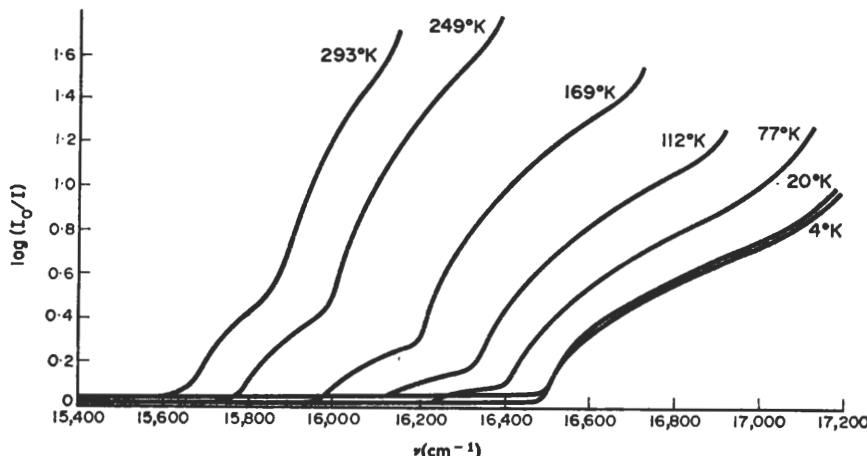


FIG. 6-13. Absorption edge of Cu<sub>2</sub>O at different temperatures. (After Nikitine, ref. [17].)

tion spectrum of Cu<sub>2</sub>O at different temperatures is reported. At any given temperature the absorption spectrum exhibits two steps corresponding to the thresholds of indirect exciton transitions with absorption or emission of one phonon. The energy difference of the two thresholds gives twice the energy of the phonon involved in the process (this difference, of course, does not depend on the temperature, while the energy gap does, and this explains the shift of the thresholds to higher energies as the temperature decreases). According to the theory previously discussed, we can decompose  $\alpha(\omega)$  into two parts:

$$\alpha(\omega) = \alpha_{\text{phonon abs}}(\omega) + \alpha_{\text{phonon emiss}}(\omega)$$

with

$$\alpha_{\text{phonon abs}}(\omega) = a(\hbar\omega - E_G(T) + K\theta)^{1/2} n_{q_0}$$

and

$$\alpha_{\text{phonon emiss}}(\omega) = a(\hbar\omega - E_G(T) - K\theta)^{1/2} (n_{q_0} + 1),$$

with appropriate values for  $a$  and  $E_G(T)$ .

The frequency dependence of  $\alpha^2_{\text{phonon abs}}$  and  $\alpha^2_{\text{phonon emiss}}$  are respectively displayed in Fig. 6-14. Straight lines are obtained in agreement with the above relations. The slope of the lines is strongly temperature dependent; in fact the slope is proportional to  $n_{q_0}^2$  for phonon absorption and to  $(n_{q_0} + 1)^2$  for phonon emission, and from Bose-Einstein statistics we have

$$n_{q_0} = \frac{1}{e^{\hbar\omega q_0 / KT} - 1}.$$

## ELECTRONIC STATES AND OPTICAL TRANSITIONS

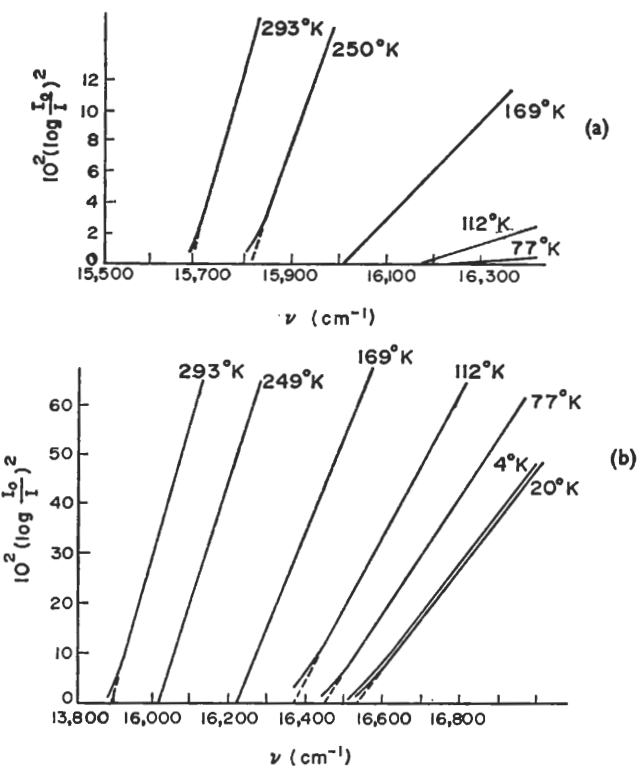


FIG. 6-14. (a) Plot of  $\alpha_{\text{phonon abs}}^2$  versus  $\nu$  for  $\text{Cu}_2\text{O}$  at different temperatures. (b) Plot of  $\alpha_{\text{phonon emiss}}^2$  versus  $\nu$  for  $\text{Cu}_2\text{O}$  at different temperatures. (After Nikitine ref. [17].)

The model described above is particularly simple because no allowance is made either for the anisotropy of the effective masses or for the possible degeneracy of the top of the valence band or of the bottom of the conduction band. Extensions can be made in a way similar to that outlined in Section 6-3d. Baldereschi and Lipari<sup>[25]</sup> have succeeded in computing the indirect exciton energies and wave functions in silicon, germanium, and in a number of III-V semiconductors.

Experimental evidence for the existence of indirect excitons is available in many semiconductors.<sup>[34]</sup> Third order processes for excitonic transitions involving one photon and two phonons or two photons and one phonon have been theoretically studied.<sup>[35]</sup> The available experimental evidence shows clearly the first type of process, while experimental evidence of indirect two-photon excitons is still lacking.

### 6-7 Interband mixing and high energy excitons

In concluding this chapter we should like to mention an interesting extension of the exciton theory described in Sections 6-2, 6-3, and 6-4, which may be obtained by considering the fact that the expansion of the excitons in Slater determinants should be made on all couples of valence and conduction bands, as shown for instance in (6-45). The system of eqs. (6-45) for the expansion coefficients include, then, the electron-electron interaction between different bands. Since this approach can include some

correlation effects, it is usually developed in the literature [5] using the second quantization formalism of many-body theory.

In all the preceding sections we have only considered the case of coupling of nearly degenerate bands, since the other couples of bands were supposed to give negligible mixing because very far in energy. This condition is no longer valid for excitons of higher energy which may originate from core states or from valence bands to higher conduction bands, and which we may generally call resonant excitons. In that case eq. (6-45) should be solved by including interaction between all bands and extending  $E$  into the complex plane because it is always degenerate with some energy difference  $E_c(\mathbf{k}) - E_v(\mathbf{k})$ . One will obtain complex solutions  $E = E_r - i\Gamma$  of the compatibility equation (6-45), which will give resonant states when  $\Gamma \ll E_r$ . In the case of core excitons, since they begin to appear at energies so high that the oscillator strength of interband transitions has already almost saturated the sum rules, it is certain that the condition  $\Gamma \ll E_r$  is verified. In the case of resonant excitons just above the edge, like those originating from secondary minima of the conduction band or from saddle points in the joint density of states, the resonance condition must be explicitly shown.

We may mention that experimental evidence for high energy excitons due to electronic transitions from core states has been obtained in all type of materials by extensive use of synchrotron radiation as a light source.<sup>[36]</sup> Resonant excitons not far from the absorption edge have been observed in many alkali halides and rare gas solids, though their interpretation<sup>[37]</sup> in this case is complicated by strong interband transitions at the same frequency.

## APPENDIX 6A

### Evaluation of matrix elements appearing in the tight binding exciton theory

Using the results of Appendix 5A and 5B we calculate here explicit expression for the matrix elements occurring in the treatment of tight binding excitons.

We first consider the diagonal matrix elements

$$E_{nn}^{(M)} = \langle \Phi_{c_{\pi_n}, v_{\pi_n}}^{(M)} | H_e | \Phi_{c_{\pi_n}, v_{\pi_n}}^{(M)} \rangle, \quad (6A-1)$$

where  $\Phi_{c_{\pi_n}, v_{\pi_n}}^{(M)}$  indicates an appropriate state of type (6-5a) or (6-5b). For a triplet state, let us consider, for instance, the matrix element

$$\langle \Phi_{c_{\pi_n \frac{1}{2}}, v_{\pi_n \frac{1}{2}}} | H_e | \Phi_{c_{\pi_n \frac{1}{2}}, v_{\pi_n \frac{1}{2}}} \rangle.$$

By applying (5B-7),

$$\begin{aligned} \langle \Phi_{c_{\pi_n \frac{1}{2}}, v_{\pi_n \frac{1}{2}}} | H_e | \Phi_{c_{\pi_n \frac{1}{2}}, v_{\pi_n \frac{1}{2}}} \rangle &= \langle \Psi_0 | H_e | \Psi_0 \rangle \\ &+ \langle a_{c_{\pi_n \frac{1}{2}}} | H_1 | a_{c_{\pi_n \frac{1}{2}}} \rangle - \langle a_{v_{\pi_n \frac{1}{2}}} | H_1 | a_{v_{\pi_n \frac{1}{2}}} \rangle \\ &+ \sum_{js} \left[ \langle a_{c_{\pi_n \frac{1}{2}}} a_{v_{\pi_n \frac{1}{2}}} | \frac{e^2}{r_{12}} | a_{c_{\pi_n \frac{1}{2}}} a_{v_{\pi_n \frac{1}{2}}} \rangle - \langle a_{c_{\pi_n \frac{1}{2}}} a_{v_{\pi_n \frac{1}{2}}} | \frac{e^2}{r_{12}} | a_{v_{\pi_n \frac{1}{2}}} a_{c_{\pi_n \frac{1}{2}}} \rangle \right] \\ &- \left[ \langle a_{c_{\pi_n \frac{1}{2}}} a_{v_{\pi_n \frac{1}{2}}} | \frac{e^2}{r_{12}} | a_{c_{\pi_n \frac{1}{2}}} a_{v_{\pi_n \frac{1}{2}}} \rangle - \langle a_{c_{\pi_n \frac{1}{2}}} a_{v_{\pi_n \frac{1}{2}}} | \frac{e^2}{r_{12}} | a_{v_{\pi_n \frac{1}{2}}} a_{c_{\pi_n \frac{1}{2}}} \rangle \right] \\ &- \sum_{js} \left[ \langle a_{v_{\pi_n \frac{1}{2}}} a_{v_{\pi_n \frac{1}{2}}} | \frac{e^2}{r_{12}} | a_{v_{\pi_n \frac{1}{2}}} a_{v_{\pi_n \frac{1}{2}}} \rangle - \langle a_{v_{\pi_n \frac{1}{2}}} a_{v_{\pi_n \frac{1}{2}}} | \frac{e^2}{r_{12}} | a_{v_{\pi_n \frac{1}{2}}} a_{v_{\pi_n \frac{1}{2}}} \rangle \right] \end{aligned} \quad (6A-2)$$

## ELECTRONIC STATES AND OPTICAL TRANSITIONS

with  $j = 1, 2, \dots, N$  and  $s = \frac{1}{2}, \frac{1}{2}$ . Performing the integral on spin variables, we obtain

$$\begin{aligned} \langle \Phi_{c\tau_{n\frac{1}{2}}, v\tau_{n\frac{1}{2}}} | H_e | \Phi_{c\tau_{n\frac{1}{2}}, v\tau_{n\frac{1}{2}}} \rangle &= \langle \Psi_0 | H_e | \Psi_0 \rangle \\ &+ \langle a_{c\tau_n} | H_1 | a_{c\tau_n} \rangle - \langle a_{v\tau_n} | H_1 | a_{v\tau_n} \rangle \\ &+ \sum_j \left[ 2 \langle a_{c\tau_n} a_{v\tau_j} | \frac{e^2}{r_{12}} | a_{c\tau_n} a_{v\tau_j} \rangle - \langle a_{c\tau_n} a_{v\tau_j} | \frac{e^2}{r_{12}} | a_{v\tau_j} a_{c\tau_n} \rangle \right] \\ &- \sum_j \left[ 2 \langle a_{v\tau_n} a_{v\tau_j} | \frac{e^2}{r_{12}} | a_{v\tau_n} a_{v\tau_j} \rangle - \langle a_{v\tau_n} a_{v\tau_j} | \frac{e^2}{r_{12}} | a_{v\tau_j} a_{v\tau_n} \rangle \right] \\ &- \left[ \langle a_{c\tau_n} a_{v\tau_n} | \frac{e^2}{r_{12}} | a_{c\tau_n} a_{v\tau_n} \rangle \right]. \end{aligned} \quad (6A-3)$$

For the singlet state (6-5b) it can be easily verified that the last bracket in (6A-3) is replaced by

$$- \left[ \langle a_{c\tau_n} a_{v\tau_n} | \frac{e^2}{r_{12}} | a_{c\tau_n} a_{v\tau_n} \rangle - 2 \langle a_{c\tau_n} a_{v\tau_n} | \frac{e^2}{r_{12}} | a_{v\tau_n} a_{c\tau_n} \rangle \right]. \quad (6A-4)$$

Let us now consider the non-diagonal matrix elements

$$E_{nm}^{(M)} = \langle \Phi_{c\tau_n, v\tau_n}^{(M)} | H_e | \Phi_{c\tau_m, v\tau_m}^{(M)} \rangle. \quad (6A-5)$$

For a triplet state we have, using (5A-8), the following expression for the matrix element:

$$\begin{aligned} \langle \Phi_{c\tau_{n\frac{1}{2}}, v\tau_{n\frac{1}{2}}} | H_e | \Phi_{c\tau_{m\frac{1}{2}}, v\tau_{m\frac{1}{2}}} \rangle &= \langle a_{v\tau_{m\frac{1}{2}}} a_{c\tau_{n\frac{1}{2}}} | \frac{e^2}{r_{12}} | a_{c\tau_{m\frac{1}{2}}} a_{v\tau_{n\frac{1}{2}}} \rangle - \langle a_{v\tau_{m\frac{1}{2}}} a_{c\tau_{n\frac{1}{2}}} | \frac{e^2}{r_{12}} | a_{v\tau_{n\frac{1}{2}}} a_{c\tau_{m\frac{1}{2}}} \rangle \\ &= - \langle a_{v\tau_m} a_{c\tau_n} | \frac{e^2}{r_{12}} | a_{v\tau_n} a_{c\tau_m} \rangle, \end{aligned} \quad (6A-6)$$

where the final result has been obtained by integrating over the spin variables explicitly. For singlet states we obtain

$$\begin{aligned} &\left\langle \frac{1}{\sqrt{2}} (\Phi_{c\tau_{n\frac{1}{2}}, v\tau_{n\frac{1}{2}}} + \Phi_{c\tau_{n\frac{1}{2}}, v\tau_{n\frac{1}{2}}}) | H_e | \frac{1}{\sqrt{2}} (\Phi_{c\tau_{m\frac{1}{2}}, v\tau_{m\frac{1}{2}}} + \Phi_{c\tau_{m\frac{1}{2}}, v\tau_{m\frac{1}{2}}}) \right\rangle \\ &= \frac{1}{2} \{ \langle \Phi_{c\tau_{n\frac{1}{2}}, v\tau_{n\frac{1}{2}}} | H_e | \Phi_{c\tau_{m\frac{1}{2}}, v\tau_{m\frac{1}{2}}} \rangle + \langle \Phi_{c\tau_{n\frac{1}{2}}, v\tau_{n\frac{1}{2}}} | H_e | \Phi_{c\tau_{m\frac{1}{2}}, v\tau_{m\frac{1}{2}}} \rangle \\ &\quad + \langle \Phi_{c\tau_{n\frac{1}{2}}, v\tau_{n\frac{1}{2}}} | H_e | \Phi_{c\tau_{m\frac{1}{2}}, v\tau_{m\frac{1}{2}}} \rangle + \langle \Phi_{c\tau_{n\frac{1}{2}}, v\tau_{n\frac{1}{2}}} | H_e | \Phi_{c\tau_{m\frac{1}{2}}, v\tau_{m\frac{1}{2}}} \rangle \} \\ &= 2 \langle a_{v\tau_m} a_{c\tau_n} | \frac{e^2}{r_{12}} | a_{v\tau_n} a_{v\tau_m} \rangle - \langle a_{v\tau_m} a_{c\tau_n} | \frac{e^2}{r_{12}} | a_{v\tau_n} a_{c\tau_m} \rangle, \end{aligned} \quad (6A-7)$$

where again the final result has been obtained using (5A-8) and by integrating over the spin variables. We can thus write

$$\begin{aligned} E_{nm}^{(M)} &= \langle \Phi_{c\tau_n, v\tau_n}^{(M)} | H_e | \Phi_{c\tau_m, v\tau_m}^{(M)} \rangle \\ &= 2\delta_M \langle a_{v\tau_m} a_{c\tau_n} | \frac{e^2}{r_{12}} | a_{c\tau_m} a_{v\tau_n} \rangle - \langle a_{v\tau_m} a_{c\tau_n} | \frac{e^2}{r_{12}} | a_{v\tau_n} a_{c\tau_m} \rangle. \end{aligned} \quad (6A-8)$$

## APPENDIX 6B

## Effective mass equation for weakly bound excitons

In the Hartree-Fock approximation the fundamental state  $\Psi_0$  and the trial excited states of definite multiplicity  $\Phi_{c\mathbf{k}_e, v\mathbf{k}_h}^{(M)}$  are given by eqs. (6-18) and (6-19) respectively. We need the matrix elements between trial excited states of the electron system Hamiltonian  $H_e$  defined by (6-1).

The diagonal matrix elements of  $H_e$  are given by (5B-12) with  $\varphi_i \equiv \psi_{c\mathbf{k}_e}$  and  $\psi_i \equiv \psi_{v\mathbf{k}_h}$ . If we take as zero of energy the energy  $\langle \Psi_0 | H_e | \Psi_0 \rangle$  and use the Koopmans' approximation (5B-9), we have

$$\langle \Phi_{c\mathbf{k}_e, v\mathbf{k}_h}^{(M)} | H_e | \Phi_{c\mathbf{k}_e, v\mathbf{k}_h}^{(M)} \rangle = E_c(\mathbf{k}_e) - E_v(\mathbf{k}_h). \quad (6B-1)$$

Because of the translational symmetry of  $H_e$ , the non-diagonal matrix elements of  $H_e$  are only non-zero amongst electron-hole pairs with the same total wave vector  $\mathbf{k}_e - \mathbf{k}_h = \text{constant} = \mathbf{k}_{ex}$ . Using (5A-8), we obtain

$$\langle \Phi_{c\mathbf{k}_e, v\mathbf{k}_h}^{(M)} | H_e | \Phi_{c\mathbf{k}'_e, v\mathbf{k}'_h}^{(M)} \rangle = 2\delta_M \langle \psi_{c\mathbf{k}_e} \psi_{v\mathbf{k}_h} | \frac{e^2}{r_{12}} | \psi_{v\mathbf{k}_h} \psi_{c\mathbf{k}'_e} \rangle - \langle \psi_{c\mathbf{k}_e} \psi_{v\mathbf{k}'_h} | \frac{e^2}{r_{12}} | \psi_{c\mathbf{k}'_e} \psi_{v\mathbf{k}_h} \rangle. \quad (6B-2)$$

Let us first examine the second term in the right hand side of eq. (6B-2), appearing both in triplet and singlet excitons. We have

$$\begin{aligned} & \langle \psi_{c\mathbf{k}_e} \psi_{v\mathbf{k}_h} | \frac{e^2}{r_{12}} | \psi_{c\mathbf{k}'_e} \psi_{v\mathbf{k}'_h} \rangle \\ &= \iint d\mathbf{r}_1 d\mathbf{r}_2 \frac{e^2}{r_{12}} e^{-i(\mathbf{k}_e - \mathbf{k}'_e) \cdot \mathbf{r}_1} e^{-i(\mathbf{k}_h - \mathbf{k}'_h) \cdot \mathbf{r}_2} u_{c\mathbf{k}_e}^*(\mathbf{r}_1) u_{c\mathbf{k}'_e}(\mathbf{r}_1) u_{v\mathbf{k}_h}^*(\mathbf{r}_2) u_{v\mathbf{k}'_h}(\mathbf{r}_2). \end{aligned} \quad (6B-3)$$

Following Kohn,<sup>[15]</sup> we expand the periodic functions  $u_{c\mathbf{k}_e}^*(\mathbf{r}_1) u_{c\mathbf{k}'_e}(\mathbf{r}_1)$  and  $u_{v\mathbf{k}_h}^*(\mathbf{r}_2) u_{v\mathbf{k}'_h}(\mathbf{r}_2)$  in plane waves with vectors equal to reciprocal lattice vectors

$$u_{c\mathbf{k}_e}^*(\mathbf{r}_1) u_{c\mathbf{k}'_e}(\mathbf{r}_1) u_{v\mathbf{k}_h}^*(\mathbf{r}_2) u_{v\mathbf{k}'_h}(\mathbf{r}_2) = \sum_{mn} a_{mn} e^{i\mathbf{h}_m \cdot \mathbf{r}_1} e^{i\mathbf{h}_n \cdot \mathbf{r}_2} \quad (6B-4)$$

with

$$a_{mn} = \iint d\mathbf{r}_1 d\mathbf{r}_2 e^{-i\mathbf{h}_m \cdot \mathbf{r}_1} e^{-i\mathbf{h}_n \cdot \mathbf{r}_2} u_{c\mathbf{k}_e}^*(\mathbf{r}_1) u_{c\mathbf{k}'_e}(\mathbf{r}_1) u_{v\mathbf{k}_h}^*(\mathbf{r}_2) u_{v\mathbf{k}'_h}(\mathbf{r}_2). \quad (6B-5)$$

In particular we have

$$a_{00} \approx 1 \quad (6B-6)$$

if we neglect the small variation of  $u_{ck}$  and  $u_{vk}$  with  $\mathbf{k}$ . Furthermore  $a_{mn}$  with  $m$  or  $n \neq 0$  are surely less than  $a_{00}$  as can be established from the mathematical form of (6B-5). The range of variation within the Brillouin zone of the states  $\Phi_{c\mathbf{k}_e, v\mathbf{k}_h}^{(M)}$  which have appreciable coefficients in the expansion of an exciton state is assumed to be small enough to justify the approximation (6B-6) and others which we shall also make. These approximations are accurate for excitons whose wave functions extend over a large number of unit cells.

## ELECTRONIC STATES AND OPTICAL TRANSITIONS

If we substitute (6B-4) in (6B-3), and we remember that the Fourier transform of  $1/r$  is  $4\pi/k^2$ , we immediately have that the term  $a_{00}$  is dominant in the weak binding limit and we thus obtain

$$\begin{aligned} \langle \psi_{c_{k_e}} \psi_{v_{k_h}} | \frac{e^2}{r_{12}} | \psi_{c_{k_e'}} \psi_{v_{k_h'}} \rangle &\simeq \iint d\mathbf{r}_1 d\mathbf{r}_2 \frac{e^2}{r_{12}} e^{-i(\mathbf{k}_e - \mathbf{k}_e') \cdot (\mathbf{r}_1 - \mathbf{r}_2)} \\ &= \int d\mathbf{r} \frac{e^2}{r} e^{-i(\mathbf{k}_e - \mathbf{k}_e') \cdot \mathbf{r}}. \end{aligned} \quad (6B-7)$$

A similar procedure, applied in calculating the first term of the right hand side of (6B-2), would give zero because of the orthogonality of the functions  $u_{ck}$  and  $u_{vk}$ . However, Onodera and Toyazawa<sup>[13]</sup> pointed out in this case that the condition (6B-6) is not valid; we would rather have  $a_{00} \simeq 0$  and consequently the other terms of the expansion (6B-4) cannot be neglected. They show by expanding the functions  $\psi_{ck}$ ,  $\psi_{vk_h}$ ,  $\psi_{vk_h'}$ , and  $\psi_{ck_e'}$  in Wannier functions and considering only one- and two-centre integrals with a sum procedure discussed by Knox<sup>[8]</sup> that one obtains

$$\begin{aligned} J_{cv}(\mathbf{k}_{ex}) &= 2 \langle \psi_{c_{k_e}} \psi_{v_{k_h}} | \frac{e^2}{r_{12}} | \psi_{v_{k_h}} \psi_{c_{k_e'}} \rangle \\ &= 2 \iint a_c^*(\mathbf{r}_1) a_v^*(\mathbf{r}_2) \frac{e^2}{r_{12}} a_v(\mathbf{r}_1) a_c(\mathbf{r}_2) d\mathbf{r}_1 d\mathbf{r}_2 \\ &\quad + 2 \frac{4\pi}{3} \frac{1}{\Omega} \frac{3(\mu_{cv} \cdot \mathbf{k}_{ex})(\mu_{vc} \cdot \mathbf{k}_{ex}) - (\mu_{cv} \cdot \mu_{vc}) \mathbf{k}_{ex}^2}{k_{ex}^2} + O(k_{ex}^2), \end{aligned} \quad (6B-8)$$

where

$$\mu_{vc} = e \int a_v^*(\mathbf{r}) \mathbf{r} a_c(\mathbf{r}) d\mathbf{r}.$$

We can thus write the non-diagonal matrix elements (6B-2) in the form

$$\langle \Phi_{c_{k_e}, v_{k_h}}^{(M)} | H_e | \Phi_{c_{k_e'}, v_{k_h'}}^{(M)} \rangle \simeq - \int d\mathbf{r} \frac{e^2}{r} e^{-i(\mathbf{k}_e - \mathbf{k}_e') \cdot \mathbf{r}} + J_{cv}(\mathbf{k}_{ex}) \delta_M. \quad (6B-9)$$

An exciton state  $\Psi_{\mathbf{k}_{ex}}^{(M)}$  of wave vector  $\mathbf{k}_{ex}$  can always be expanded in the form

$$\Psi_{\mathbf{k}_{ex}}^{(M)} = \sum_{\mathbf{k}} A(\mathbf{k}) \Phi_{c_{\mathbf{k}} + \frac{1}{2}\mathbf{k}_{ex}, v_{\mathbf{k}} - \frac{1}{2}\mathbf{k}_{ex}}^{(M)}, \quad (6B-10)$$

where  $A(\mathbf{k})$  are the expansion coefficients and  $\Phi_{c_{\mathbf{k}} + \frac{1}{2}\mathbf{k}_{ex}, v_{\mathbf{k}} - \frac{1}{2}\mathbf{k}_{ex}}^{(M)}$  denotes the most general electron-hole pair with total wave vector  $\mathbf{k}_{ex}$ . Substituting (6B-10) into the equation

$$H_e \Psi_{\mathbf{k}_{ex}}^{(M)} = E_{ex} \Psi_{\mathbf{k}_{ex}}^{(M)}$$

and multiplying by  $\langle \Phi_{c_{k_e'}, v_{k_h'}}^{(M)} |$  using (6B-1) and (6B-9), we obtain the following equations for the coefficients  $A(\mathbf{k})$ :

$$\begin{aligned} &[E_c(\mathbf{k} + \frac{1}{2}\mathbf{k}_{ex}) - E_v(\mathbf{k} - \frac{1}{2}\mathbf{k}_{ex}) - E_{ex}] A(\mathbf{k}) \\ &+ \sum_{\mathbf{k}'} \left[ - \int d\mathbf{r} \frac{e^2}{r} e^{-i(\mathbf{k} - \mathbf{k}') \cdot \mathbf{r}} + J_{cv}(\mathbf{k}_{ex}) \delta_M \right] A(\mathbf{k}') = 0. \end{aligned} \quad (6B-11)$$

The set of linear equations (6B-11) gives compatibility relations from which in principle the exciton problem can be solved. However, the order of the secular determinant is

so large that in practice it is better to approximate eqs. (6B-11) with a differential equation of the Fourier transform of  $A(\mathbf{k})$

$$F(\mathbf{r}) = \sum_{\mathbf{k}} A(\mathbf{k}) e^{i\mathbf{k} \cdot \mathbf{r}}. \quad (6B-12)$$

Letting  $E_{cv}(\mathbf{k}, \mathbf{k}_{ex})$  denote the expression

$$E_c(\mathbf{k} + \frac{1}{2}\mathbf{k}_{ex}) - E_v(\mathbf{k} - \frac{1}{2}\mathbf{k}_{ex})$$

and noting that

$$F(0) = \sum_{\mathbf{k}} A(\mathbf{k}),$$

we transform (6B-11) into

$$[E_{cv}(\mathbf{k}, \mathbf{k}_{ex}) - E_{ex}] A(\mathbf{k}) + \left[ - \int d\mathbf{r} \frac{e^2}{r} F(\mathbf{r}) e^{-i\mathbf{k} \cdot \mathbf{r}} + J_{cv}(\mathbf{k}_{ex}) \delta_M F(0) \right] = 0. \quad (6B-13)$$

We notice that

$$(-i\nabla) F(\mathbf{r}) = \sum_{\mathbf{k}} \mathbf{k} A(\mathbf{k}) e^{i\mathbf{k} \cdot \mathbf{r}},$$

and thus

$$f(-i\nabla) F(\mathbf{r}) = \sum_{\mathbf{k}} f(\mathbf{k}) A(\mathbf{k}) e^{i\mathbf{k} \cdot \mathbf{r}},$$

where  $f(\mathbf{k})$  denotes an arbitrary function of  $\mathbf{k}$  and  $f(-i\nabla)$  is the operator obtained by expanding  $f(\mathbf{k})$  in powers of  $\mathbf{k}$  and replacing  $\mathbf{k}$  by the operator  $(-i\nabla)$ . In particular we have

$$[E_{cv}(-i\nabla, \mathbf{k}_{ex}) - E_{ex}] F(\mathbf{r}) = \sum_{\mathbf{k}} [E_{cv}(\mathbf{k}, \mathbf{k}_{ex}) - E_{ex}] A(\mathbf{k}) e^{i\mathbf{k} \cdot \mathbf{r}}. \quad (6B-14)$$

From (6B-13) and (6B-14), we immediately obtain the result that the Fourier transforms of the function

$$[E_{cv}(-i\nabla, \mathbf{k}_{ex}) - E_{ex}] F(\mathbf{r}) - \frac{e^2}{r} F(\mathbf{r}) + J_{cv}(\mathbf{k}_{ex}) \delta_M F(\mathbf{r}) \delta(\mathbf{r})$$

are zero, and hence the function itself must be zero. We thus obtain

$$\left[ E_{cv}(-i\nabla, \mathbf{k}_{ex}) - \frac{e^2}{r} + J_{cv}(\mathbf{k}_{ex}) \delta_M \delta(\mathbf{r}) \right] F(\mathbf{r}) = E_{ex} F(\mathbf{r}). \quad (6B-15)$$

Equation (6B-15) is the effective mass equation in the Hartree-Fock approximation. However, as mentioned in the text, inclusion of correlation effects, which can be represented as the contribution of different configurations from all electron bands, results in a screening of the electron-hole interaction by a dielectric function  $\epsilon(r)$ . The effective mass equation for the exciton envelope function  $F(\mathbf{r})$  then becomes

$$\left[ E_{cv}(-i\nabla, \mathbf{k}_{ex}) - \frac{e^2}{\epsilon r} + J_{cv}(\mathbf{k}_{ex}) \delta_M \delta(\mathbf{r}) \right] F(\mathbf{r}) = E_{ex} F(\mathbf{r}). \quad (6B-16)$$

Equation (6B-16) is remarkably simplified in the limiting case of weak binding excitons; in this case  $\epsilon(r)$  can be replaced by a dielectric constant independent of  $r$ , the short range interaction can be neglected, and the equation becomes the same for singlet and triplet excitons.

## ELECTRONIC STATES AND OPTICAL TRANSITIONS

### References and notes

- [1] J. FRENKEL, *Phys. Rev.* **37**, 17 (1931); **37**, 1276 (1931); R. E. PEIERLS, *Annln. Physik* **13**, 905 (1932).
- [2] A. S. DAVYDOV, *Theory of Molecular Excitons* (McGraw-Hill, 1962).
- [3] See, for example: A. W. OVERHAUSER, *Phys. Rev.* **101**, 1702 (1956); D. L. DEXTER, *Phys. Rev.* **108**, 707 (1957); T. MUTO, *Progr. Theor. Phys. Suppl.* **12**, 3 (1959); see also the other articles contained in the same volume.
- [4] G. H. WANNIER, *Phys. Rev.* **52**, 191 (1937); N. F. MOTT, *Trans. Faraday Soc.* **34**, 500 (1938).
- [5] See, for example: Y. TAKEUTI, *Progr. Theor. Phys.* **18**, 421 (1957); *Progr. Theor. Phys. Suppl.* **12**, 74 (1959); C. HORIE, *Progr. Theor. Phys.* **21**, 113 (1959); J. HERMANSON and J. C. PHILLIPS, *Phys. Rev.* **150**, 652 (1966); J. HERMANSON, *Phys. Rev.* **150**, 660 (1966); Y. ONODERA and Y. TOYOZAWA, *J. Phys. Soc. Japan* **22**, 833 (1967); T. MIYAKAWA, *J. Phys. Soc. Japan* **24**, 768 (1968); M. ALTARELLI and F. BASSANI, *J. Phys.* **C4**, L328 (1971); M. ALTARELLI and F. BASSANI, in *Proceedings of the XIth International Conference on the Physics of Semiconductors, Warsaw*, 1972.
- [6] S. NIKITINE, *Progress in Semiconductors* **6**, 233 (1962).
- [7] D. L. GREENAWAY and G. HARBEKE, *Optical Properties and Band Structure of Semiconductors* (Pergamon Press, 1968).
- [8] R. S. KNOX, *Theory of Excitons, Solid State Physics*, (Academic Press, 1963), Suppl. 5.
- [9] M. BORN and M. BRADBURN, *Proc. Cambridge Phil. Soc.* **39**, 104 (1943); W. R. HELLER and A. MARCUS, *Phys. Rev.* **84**, 809 (1951); M. H. COHEN and F. KEFFER, *Phys. Rev.* **99**, 1128 (1955). For further details see also ref. [8], p. 24.
- [10] For the derivation of an effective electron-hole interaction including phonons, see, for example: H. HAKEN, in *Polarons and Excitons* (edited by C. G. KUPER and G. D. WHITFIELD, Plenum Press, 1963), p. 295.
- [11] See, for example: N. F. MOTT and R. W. GURNEY, *Electronic Processes in Ionic Crystals* (Oxford University Press, 1940); F. SEITZ, *The Modern Theory of Solids* (McGraw-Hill, 1940).
- [12] G. DRESSELHAUS, *J. Phys. Chem. Solids* **1**, 14 (1956); R. J. ELLIOTT, *Phys. Rev.* **108**, 1384 (1957); R. J. ELLIOTT, in *Polarons and Excitons* (edited by C. G. KUPER and G. D. WHITFIELD, Plenum Press 1963) p. 269. J. O. DIMMOCK, in *Semiconductors and Semimetals* **3** (edited by R. K. WILLARDSON and A. C. BEER, Academic Press, 1967), p. 259. See also ref. [8].
- [13] Y. ONODERA and Y. TOYOZAWA, *J. Phys. Soc. Japan*, **22**, 833 (1967).
- [14] See, for example: N. F. MOTT and H. S. W. MASSEY, *Theory of Atomic Collisions* (Clarendon Press, Oxford 1940).
- [15] J. M. LUTTINGER and W. KOHN, *Phys. Rev.* **97**, 869 (1955); **98**, 915 (1955); W. KOHN, *Solid State Physics* **5**, 257 (1957).
- [16] S. NIKITINE, *Compt. Rend.* **240**, 1415 (1955); J. BARRIOL, S. NIKITINE, and M. SIESKIND, *Compt. Rend.* **242**, 790 (1956); J. L. BREBNER, R. FIVAZ, and E. MOOSER, *Nature* **210**, 931 (1966); M. SHINADA and S. SUGANO, *J. Phys. Soc. Japan* **20**, 1274 (1965); **21**, 1936 (1966); P. G. HARPER and J. A. HILDER, *Phys. Status Solidi* **26**, 69 (1968); J. A. DÉVERIN, *Nuovo Cimento* **63B**, 1 (1969); A. BALDERESCHI and M. G. DIAZ, *Nuovo Cimento* **68B**, 217 (1970).
- [17] S. NIKITINE, in *Optical Properties of Solids* (edited by S. NUDELMAN and S. S. MITRA, Plenum Press 1969), p. 197.
- [18] B. VELICKÝ and J. SAK, *Phys. Status Solidi* **16**, 147 (1966).
- [19] G. F. KOSTER and J. C. SLATER, *Phys. Rev.* **96**, 1208 (1954).
- [20] J. C. PHILLIPS, *Solid State Physics* **18**, 56 (1966).
- [21] E. O. KANE, *Phys. Rev.* **180**, 852 (1969).
- [22] M. CARDONA and G. HARBEKE, *J. Appl. Phys.* **34**, 813 (1963); J. E. ROWE, F. H. POLLAK, and M. CARDONA, *Phys. Rev. Letters* **22**, 933 (1969); S. ANTOCI, E. REGUZZONI, and G. SAMOGGIA, *Phys. Rev. Letters* **24**, 1304 (1970).
- [23] H. KAMIMURA and K. NAKAO, *J. Phys. Soc. Japan* **24**, 1313 (1968).
- [24] J. J. HOPFIELD, *J. Phys. Chem. Solids* **15**, 97 (1960); J. J. HOPFIELD and D. G. THOMAS, *Phys. Rev.* **122**, 35 (1961); M. BALKANSKI and J. DES CLOIZEAUX, *J. Phys. Radium* **22**, 41 (1961).
- [25] A. BALDERESCHI and N. O. LIPARI, *Phys. Rev. B* **3**, 439 (1971); **B** **3**, 2497 (1971); **B** **6**, 3764 (1972).
- [26] Y. ONODERA, *J. Phys. Soc. Japan* **25**, 469 (1968).
- [27] K. TEEGARDEN and G. BALDINI, *Phys. Rev.* **155**, 896 (1967).
- [28] See, for example: F. BASSANI, D. L. GREENAWAY, and G. FISHER, in *Proceedings International Conference on the Physics of Semiconductors, Paris*, 1964; J. L. BREBNER, J. HALPERN, and E. MOOSER,

*Helv. Phys. Acta* **40**, 382 (1967); J. L. BREBNER and E. MOOSER, *Phys. Letters* **24A**, 274 (1967); A. BALZAROTTI and M. PIACENTINI, *Solid State Commun.* **10**, 421 (1972).

[29] CH. SCHLÜTER and M. SCHLÜTER, *Phys. Rev. B* **9**, 1652 (1974).

[30] For theoretical aspects of the dielectric function in crystals, see, for example: W. KOHN, *Phys. Rev.* **110**, 857 (1958); J. HUBBARD, *Proc. Royal Soc. A* **240**, 539 (1957); **A** **244**, 199 (1958); H. EHRENRICH and M. H. COHEN, *Phys. Rev.* **115**, 786 (1959); A. MORITA, M. AZUMA, and H. NARA, *J. Phys. Soc. Japan* **17**, 1570 (1962); Y. ABE, Y. OSAKA, and A. MORITA, *J. Phys. Soc. Japan* **17**, 1576 (1962); H. NARA, *J. Phys. Soc. Japan* **20**, 778 (1965); V. L. BONCH-BRUEVICH, in *Proceedings of the International School of Physics "Enrico Fermi"* (Academic Press, 1966), vol. 34, p. 337. See also ref. [10]. For simple model semiconductors dielectric functions, see: D. R. PENN, *Phys. Rev.* **128**, 2093 (1962); E. TOSATTI and G. PASTORI PARRAVICINI, *J. Phys. Chem. Solids* **32**, 623 (1971). For detailed calculations of  $\epsilon(q, \omega)$  in silicon and germanium, see: J. P. WALTER and M. L. COHEN, *Phys. Rev. B* **5**, 3101 (1972); S. J. SRAMEK and M. L. COHEN, *Phys. Rev. B* **6**, 3800 (1972).

[31] R. LOUDON, *Proc. Phys. Soc.* **80**, 952 (1962); G. D. MAHAN, *Phys. Rev. Letters* **20**, 332 (1968); *Phys. Rev.* **170**, 825 (1968). For other aspects see, for example: D. FRÖHLICH, B. STAGINNUS, and F. SCHÖNHERR, *Phys. Rev. Letters* **19**, 1032 (1967); D. FRÖHLICH and B. STAGINNUS, *Phys. Rev. Letters* **19**, 496 (1967); F. PRADÈRE, B. SACKS, and A. MYSYROWICZ, *Opt. Commun.* **1**, 234 (1969); D. FRÖHLICH, B. STAGINNUS, and Y. ONODERA, *Phys. Status Solidi* **40**, 547 (1970); F. PRADÈRE and A. MYSYROWICZ, in *Proceedings of the Xth International Conference on the Physics of Semiconductors Boston*, 1970, p. 101; A. BIVAS, C. MARANGE, J. B. GRUN and B. SCHWAB, *Optics Commun.* **6**, 142 (1972); T. R. BADER and A. GOLD, *Phys. Rev.* **171**, 997 (1968); M. M. DENISOV and V. P. MAKAROV, *Phys. Status Solidi B* **56**, 9 (1973); E. DONI, R. GIRLANDA and G. PASTORI PARRAVICINI, *Solid State Commun.* **14**, 873 (1974) and *Phys. Status Solidi B* (1974) to appear. For bi-exciton levels and related optical transitions see, for instance, R. LEVI and J. B. GRUN, *Phys. Status Solidi A* **22**, 11 (1974); F. BASSANI, J. J. FORNEY and A. QUATTROPANI, *Phys. Status Solidi B* (1974) to appear and *Nuovo Cimento B* (1974) to appear.

[32] Y. TOYOZAWA, *J. Phys. Chem. Solids* **25**, 59 (1964).

[33] For the theory of two-dimensional indirect excitons in anisotropic crystals, see K. NAKAO, H. KAMIMURA, and Y. NISHINA, *Nuovo Cimento* **63B**, 45 (1969).

[34] W. P. DUMKE, *Phys. Rev.* **118**, 938 (1960); P. J. DEAN, J. R. HAYNES and W. F. FLOOD, *Phys. Rev.* **161**, 711 (1967); F. EVANGELISTI, A. FROVA, MARGHERITA ZANINI, and E. O. KANE, *Solid State Commun.* **11**, 611 (1972).

[35] N. O. FOLLAND, *Phys. Rev. B* **1**, 1648 (1970); F. BASSANI and A. R. HASSAN, *Nuovo Cimento* **7B**, 313 (1972).

[36] See, for example: R. P. GODWIN, *Springer Tracts in Modern Physics* **51**, 1 (Springer-Verlag, Berlin 1969); F. C. BROWN, C. GÄHWILLER, H. FUJITA, A. B. KUNZ, W. SCHEIFLEY, and N. CARRERA, *Phys. Rev. B* **2**, 2126 (1970); R. HAENSEL, G. KEITEL, P. SCHREIBER, and C. KUNZ, *Phys. Rev.* **188**, 1375 (1969); S. SATO, M. WATANABE, Y. IGUCHI, S. NAKAI, Y. NAKAMURA, and T. SAGAWA, *J. Phys. Soc. Japan* **33**, 1638 (1972).

[37] J. C. PHILLIPS, in *Proceedings of the International School of Physics "Enrico Fermi"* (Academic Press, 1966), vol. 34, p. 155, and quoted references; G. BALDINI and B. BOSACCHI, *Phys. Status Solidi* **38**, 325 (1970).

BIBLIOTHÈQUE  
 DÉPARTEMENT DE Phys.  
 Ecole Polytechnique Fédérale  
 PHB - Ecublens  
 CH - 1015 LAUSANNE Suisse  
 Tél. 021-71111

## CHAPTER 7

# IMPURITY STATES IN INSULATORS AND SEMICONDUCTORS

### 7-1 Introduction

The general term "impurity states" is used to indicate localized electronic states of the crystal which are due to a number of possible causes.

- (i) A foreign atom different from the other atoms of the lattice (substitutional or interstitial impurity).
- (ii) The absence of one or more atoms from the lattice (vacancy).
- (iii) The displacement of one or more atoms from regular equilibrium positions in the lattice (interstitials, dislocations).
- (iv) The termination of the crystal at its physical boundary (surfaces).

In all cases there is a break in the translational periodicity of the lattice, with an additional potential which tends to zero at positions far removed from the disturbance (a point in the case of impurities or vacancies, a line in the case of dislocations, a surface at the boundary of the lattice). In general we can write the Schrödinger equation in the one-electron approximation as follows:

$$-\frac{\hbar^2}{2m} \nabla^2 \Phi + [V_c + U] \Phi = E \Phi, \quad (7-1)$$

where  $V_c$  denotes the potential of the perfect lattice and  $U$  the additional potential due to the disturbance.

We shall concentrate primarily on point defects (due to impurities or to vacancies) where the potential  $U$  is nearly spherically symmetric about a fixed point. We shall discuss the electronic states from different points of view depending on the relative importance of the lattice potential  $V_c$  and of the impurity potential  $U$  in the determination of the eigenstates of (7-1). Firstly, for a given impurity potential  $U$ , the crystal potential  $V_c$  may act as a small perturbation on those states whose electronic wave functions do not extend appreciably over the lattice and are localized in the region where  $U$  is large. The states which satisfy the above conditions are called tightly bound states. On the other hand, the opposite situation may occur for other states whose electronic wave function is spread out in the region where the lattice potential  $V_c$  is dominant; in this case  $U$  can be regarded as a perturbation. These are called shallow impurity states. Finally, we also have to deal in some cases with the most general situation

where the impurity potential  $U$  and the lattice potential  $V_c$  are of comparable importance. The problem in this case has not yet found a definite solution from the standpoint of performing detailed calculations and comparing with experiment, but qualitative remarks can be made and model calculations can be carried out.

In the following sections we shall discuss separately the various types of electronic impurity states described above and we shall illustrate the approximate procedures to be used in each case. We shall make extensive use of arguments based on symmetry, since they provide results of immediate physical significance and greatly simplify the numerical calculations.

Since the field of impurity states is very extensive, we cannot attempt to refer to all the relevant papers and do justice to all the important contributions. The purpose of this chapter is just to illustrate some concepts which are relevant to impurity states.

## 7-2 Tightly bound impurity states

### 7-2a General remarks and classification of the states

In the case of a substitutional impurity we can choose the origin at the lattice site occupied by the impurity, and  $U(\mathbf{r})$  can include the full atomic potential of the impurity. This corresponds to subtracting the contribution from the atom which has been replaced by the impurity from the potential  $V_c(\mathbf{r})$  of eq. (7-1) so that in this case

$$V_c(\mathbf{r}) = \sum' V_a(\mathbf{r} - \mathbf{R}_n), \quad (7-2)$$

where the prime indicates that the lattice site at  $\mathbf{R}_n = 0$  is not considered and the translational symmetry is lost. If the impurity is at an interstitial position,  $V_c(\mathbf{r})$  remains the total lattice potential and  $U(\mathbf{r})$  is the potential of the impurity, the origin being chosen at the interstitial position.

The basic approximation to be used for strongly localized states is to treat (7-2) as a perturbation. The unperturbed states are the solutions of the impurity problem

$$-\frac{\hbar^2}{2m} \nabla^2 \psi_{nlm}(\mathbf{r}) + U(\mathbf{r}) \psi_{nlm}(\mathbf{r}) = E_{nl} \psi_{nlm}(\mathbf{r}). \quad (7-3)$$

The atomic wave functions are classified in order of increasing energy by the total quantic number  $n$ , and according to the irreducible representations of the rotation inversion group by the value of  $l$  as discussed in Section 1-4. The atomic eigenvalues and eigenfunctions can be computed in the Hartree-Fock approximation and are to be considered as the starting point in studying eq. (7-1).

As shown in detail in Chapter 1, the eigenstates of eq. (7-1) must be classified according to the symmetry group of the total Hamiltonian. This coincides with the point group of the lattice or is a subgroup of it, depending on the position of the impurity and on the lattice structure. A substitutional impurity in alkali-halides, for instance, maintains the full  $O_h$  point symmetry to the total Hamiltonian, but a substitutional impurity in germanium or silicon reduces the point symmetry from  $O_h$  to the subgroup  $T_d$ , because all symmetry operations which interchange the atoms in the unit cell are not allowed any more. A large number of symmetry examples are given in Chapters 1 and 2;

## ELECTRONIC STATES AND OPTICAL TRANSITIONS

as a further reference to the irreducible representations of all existing point groups we may give some of the books on group theory quoted in the earlier chapters.<sup>[1]</sup>

The problem of interest here is to establish how the states of the free atom, or the free ion, are split by the surrounding lattice. This is done by deciding how the irreducible representations of the full rotation-inversion group decompose into the irreducible representations of the symmetry group of the Hamiltonian. We can apply the general rules of group theory as described in Section 1-4. We have to compute the characters of the state of the free atom for those symmetry operations which belong to the symmetry group of the Hamiltonian and see how they decompose into the characters of the irreducible representations of the symmetry group of the Hamiltonian. We can write

$$\chi^{(l)}(R) = \sum_{\alpha} a_{\alpha}^{(l)} \chi^{\alpha}(R). \quad (7-4)$$

On the left hand side of (7-4) we have the character of the representation  $D^{(l)}$  of the rotation group, which is given, for a rotation of an angle  $\varphi$ , by

$$\chi^{(l)}(R_{\varphi}) = \frac{\sin(2l+1)\varphi/2}{\sin\varphi/2}, \quad (7-5)$$

as shown in Section 1-4. The integer coefficients  $a_{\alpha}^{(l)}$  of (7-4) indicate how many times the irreducible representation  $D^{(\alpha)}$  of the crystal point group (defined by its characters  $\chi^{(\alpha)}(R)$ ) is contained into the representation  $D^{(l)}$  of the rotation group. The decomposition indicated by (7-4) can be seen by inspection for all symmetry operations  $R$ ; but we can also use the standard expression obtained at the end of Section 1-2a:

$$a_{\alpha}^{(l)} = \frac{1}{h} \sum_{R} \chi^{(\alpha)}(R)^* \chi^{(l)}(R), \quad (7-6)$$

where  $h$  is the number of symmetry operations of the point group.

We can also include spin-orbit interaction in the present scheme by classifying the crystal states and the atomic states using the irreducible representations of the double group introduced by Bethe<sup>[2]</sup> and Opechowski.<sup>[3]</sup> As demonstrated in Chapter 1, the double group is formed by adding the rotation by  $2\pi$  to the symmetry operations, thereby changing the signs of the spin functions, and by constructing a new multiplication table and a new separation into classes based on the fact that all rotations are now measured in modules of  $4\pi$ . In the rotational-inversion group of the atom, this amounts to letting  $j$  be semi-integer. Equation (7-5) still holds except that  $l$  is replaced by  $j$ , and the parity under inversion is the same as that of the  $l$  state from which the  $j$  state is obtained. In the crystal group, the irreducible representations of the new double group, which are of interest for semi-integer spin, must have the property that the character of the  $2\pi$  rotation (called  $E$ ) is opposite to  $E$ , since spinor functions change their sign under  $E$ .

## EXAMPLES

### *Trigonal and cubic symmetries*

As a first example let us consider uniaxial crystals which have trigonal symmetry such as GaS, GaSe, CrCl<sub>3</sub>, MoS<sub>2</sub>, PbI<sub>2</sub>, etc., mentioned in previous chapters. The lattice point group is of the type  $D_3$  or  $D_{3h} = D_3 \times \{E, \sigma_h\}$ , or  $D_{3d} = D_3 \times \{E, I\}$ ,

where  $D_3$  indicates the six operations of symmetry which preserve an equilateral triangle,  $\sigma_h$  indicates the reflection with respect to the plane perpendicular to the optical axis, and  $I$  indicates the inversion. We already considered the group  $D_{3h}$  in the second example of Section 6-3d. Let us now consider the group  $D_{3d}$  with character table given in Table 7-1. The traces of the matrices which represent this group  $D_{3d}$  when the basis functions are spherical harmonics (basic functions of the irreducible representations of the rotation-inversion group) are given in Table 7-2. They are obtained by applying expression (7-5) and taking into account the parity of spherical harmonics.

 TABLE 7-1. Character table of the group  $D'_{3d}$ 

NB—The operations  $C_3, C'_2, \bar{C}_3, \bar{C}'_2$  indicate respectively rotation by  $2\pi/3$  about the  $c$  axis, rotation by  $\pi$  about axes perpendicular to it, and their products by  $E$  (rotation by  $2\pi$ ). The other operations are the products of the above operations by the inversion. We observe that the simple group is isomorphous to that of Table 1-6. The irreducible representations of the double group are also given, with subscripts  $g$  and  $u$  to denote parity.  $\Gamma_4$  and  $\Gamma_5$  are degenerate by time reversal symmetry. Notice the difference between the additional irreducible representations of the present group and those of  $D_{3h}$  (Table 6-3)

Irreducible representations	Operations											
	$E$	$E$	$2C_3$	$2\bar{C}_3$	$3C'_2$	$3\bar{C}'_2$	$I$	$\bar{I}$	$2C_3I$	$2\bar{C}_3I$	$3C'_2I$	$3\bar{C}'_2I$
$\Gamma_{1g}$ , or $\Gamma_{1u}$	1	1	1	1	1	1	$\pm 1$	$\pm 1$	$\pm 1$	$\pm 1$	$\pm 1$	$\pm 1$
$\Gamma_{2g}$ , or $\Gamma_{2u}$	1	1	1	1	-1	-1	$\pm 1$	$\pm 1$	$\pm 1$	$\pm 1$	$\mp 1$	$\mp 1$
$\Gamma_{3g}$ , or $\Gamma_{3u}$	2	2	-1	-1	0	0	$\pm 2$	$\pm 2$	$\mp 1$	$\mp 1$	0	0
$\Gamma_{4g}$ , or $\Gamma_{4u}$	1	-1	-1	1	$i$	$-i$	$\pm 1$	$\mp 1$	$\mp 1$	$\pm 1$	$\pm i$	$\mp i$
$\Gamma_{5g}$ , or $\Gamma_{5u}$	1	-1	-1	1	$-i$	$i$	$\pm 1$	$\mp 1$	$\mp 1$	$\pm 1$	$\mp i$	$\pm i$
$\Gamma_{6g}$ , or $\Gamma_{6u}$	2	-2	1	-1	0	0	$\pm 2$	$\mp 2$	$\pm 1$	$\mp 1$	0	0

The following decomposition results from applying eq. (7-4) or (7-6):

$$\text{State } s (l=0) = \Gamma_{1g},$$

$$\text{State } p (l=1) = \Gamma_{3u} + \Gamma_{2u},$$

$$\text{State } d (l=2) = \Gamma_{3g} + \Gamma_{3g} + \Gamma_{1g} = 2\Gamma_{3g} + \Gamma_{1g},$$

$$\text{State } f (l=3) = 2\Gamma_{3u} + 2\Gamma_{2u} + \Gamma_{1u}.$$

Including the spin-orbit interaction, the atomic states are classified by their semi-integer  $j$  values, and one similarly obtains from Tables 7-1 and 7-2:

$$1/2 \text{ state} = \Gamma_{6g}, \text{ or } \Gamma_{6u},$$

$$3/2 \text{ state} = \Gamma_{6g} + \Gamma_{4g} + \Gamma_{5g}, \text{ or } \Gamma_{6u} + \Gamma_{4u} + \Gamma_{5u},$$

$$5/2 \text{ state} = 2\Gamma_{6g} + \Gamma_{4g} + \Gamma_{5g}, \text{ or } 2\Gamma_{6u} + \Gamma_{4u} + \Gamma_{5u},$$

$$7/2 \text{ state} = 3\Gamma_{6g} + \Gamma_{4g} + \Gamma_{5g}, \text{ or } 3\Gamma_{6u} + \Gamma_{4u} + \Gamma_{5u},$$

where the parity depends on the space part of the function given by  $l$  (for instance a  $p_{1/2}$  state gives  $\Gamma_{6u}$  while a  $s_{1/2}$  state gives  $\Gamma_{6g}$ ). The above results indicate how all atomic levels split when the atom is placed in a trigonal crystal (notice that the  $p$  level splits in this case while it does not split in cubic symmetry).

## ELECTRONIC STATES AND OPTICAL TRANSITIONS

TABLE 7-2. Traces of the representations  $D^{(l)}$  and  $D^{(j)}$  for the operations of the group  $D_{3d}^l$ . Only values of  $l$  up to  $l = 3$  and values of  $j$  up to  $7/2$  are considered. NB—For the semi-integer representations  $j$ , we could also write odd representations, obtained by choosing negative characters for the inversion  $I$

$\chi^{(l)}(R)$	(R)											
	$E$	$E$	$2C_3$	$2\bar{C}_3$	$3C'_2$	$3\bar{C}'_2$	$I$	$I$	$2C_3I$	$2\bar{C}_3I$	$3C'_2I$	$3\bar{C}'_2I$
$l = 0$	1	1	1	1	1	1	1	1	1	1	1	1
$l = 1$	3	3	0	0	-1	-1	-3	-3	0	0	1	1
$l = 2$	5	5	-1	-1	1	1	5	5	-1	-1	1	1
$l = 3$	7	7	1	1	-1	-1	-7	-7	-1	-1	1	1
$j = 1/2$	2	-2	1	-1	0	0	2	-2	1	-1	0	0
$j = 3/2$	4	-4	-1	1	0	0	4	-4	-1	1	0	0
$j = 5/2$	6	-6	0	0	0	0	6	-6	0	0	0	0
$j = 7/2$	8	-8	1	-1	0	0	8	-8	1	-1	0	0

TABLE 7-3. Different notations used in the literature to indicate the irreducible representations of  $O_h$  (for the corresponding characters see Table 1-4)

Bethe	$\Gamma_1$	$\Gamma_2$	$\Gamma_3$	$\Gamma_4$	$\Gamma_5$	$\Gamma'_1$	$\Gamma'_2$	$\Gamma'_3$	$\Gamma'_4$	$\Gamma'_5$
BSW	$\Gamma_1$	$\Gamma_2$	$\Gamma_{12}$	$\Gamma'_{15}$	$\Gamma'_{25}$	$\Gamma'_1$	$\Gamma'_2$	$\Gamma'_{12}$	$\Gamma_{15}$	$\Gamma_{25}$
Chemists	$A_{1g}$	$A_{2g}$	$E_g$	$T_{1g}$	$T_{2g}$	$A_{1u}$	$A_{2u}$	$E_u$	$T_{1u}$	$T_{2u}$

As a second example, which we shall use very frequently in the following discussions, and which is relevant to most experiments performed up to now, let us consider the group  $O_h$  relative to a cubic lattice. The character table of  $O_h$  is given in Chapter 1 (Table 1-4), and since the representations of the group  $O_h$  are often used in the literature with different symbols, we give in Table 7-3 the correspondence between the different notations.

In order to decide how the states of the free atom or free ion are split by the crystal field, we must construct the character table for the states of the free atom considering the same symmetry operations as given in Table 1-4. This has been done in Table 1-14 for integer spin states. Using eq. (7-6), or by inspection, we can decide how the states of the atom split into the states of the symmetry group  $O_h$  of the total Hamiltonian. We obtain:

- State  $s$  ( $l = 0$ ) =  $\Gamma_1(A_{1g})$ ,
- State  $p$  ( $l = 1$ ) =  $\Gamma_{15}(T_{1u})$ ,
- State  $d$  ( $l = 2$ ) =  $\Gamma'_{25}(T_{2g}) + \Gamma_{12}(E_g)$ ,
- State  $f$  ( $l = 3$ ) =  $\Gamma_{15} + \Gamma_{25}(T_{2u}) + \Gamma'_2(A_{2u})$ ,
- State  $g$  ( $l = 4$ ) =  $\Gamma'_{25} + \Gamma'_{15} + \Gamma_{12} + \Gamma_1$ ,
- State  $h$  ( $l = 5$ ) =  $\Gamma_{25} + 2\Gamma_{15} + \Gamma'_{12}(E_u)$ ,
- State  $i$  ( $l = 6$ ) =  $2\Gamma'_{25} + \Gamma'_{15} + \Gamma_{12} + \Gamma_2(A_{2g}) + \Gamma_1$ ,

where in parentheses we have also reported the notations more commonly used in the literature. The additional irreducible representations of the double group appropriate to semi-integer spin functions for the cubic point group  $O_h'$ , are given in Table 2-11. Also in this case we can decompose the atomic states, classified according to semi-integer values of  $j$  with characters given by (7-5) and reported in Table 1-21, into the states of the double group  $O_h'$ . We obtain:

$$\begin{aligned} 1/2 \text{ state} &= \Gamma_6^+, & \text{or } \Gamma_6^-, \\ 3/2 \text{ state} &= \Gamma_8^+, & \text{or } \Gamma_8^-, \\ 5/2 \text{ state} &= \Gamma_8^+ + \Gamma_7^+, & \text{or } \Gamma_8^- + \Gamma_7^-, \\ 7/2 \text{ state} &= \Gamma_8^+ + \Gamma_7^+ + \Gamma_6^+, & \text{or } \Gamma_8^- + \Gamma_7^- + \Gamma_6^-, \end{aligned}$$

where even or odd irreducible representations are obtained depending on the parity of  $l$  from which the  $j$  state originates (for instance a  $p_{3/2}$  state corresponds to the odd  $\Gamma_8^-$  while a  $d_{3/2}$  state corresponds to the even  $\Gamma_8^+$ ).

### 7-2b Many-electron states

If we have more than one electron to consider, we must first construct the possible atomic spectroscopic states by giving the total angular momentum  $L$ , which is an appropriate combination of the angular momenta  $l$ , taking account of the exclusion principle when necessary. Each atomic spectroscopic state, defined by the total angular momentum, will transform as indicated above and will split into states of the point group as explained previously. Let us consider, for instance, the case of two electrons in a  $d$  shell of a transition metal ion. Then, by combining the angular momenta of the two electrons using the methods of atomic spectroscopy and taking into account the fact that the total spin can be 0 or 1, we obtain the states  $^1S$ ,  $^3P$ ,  $^1D$ ,  $^3F$ ,  $^1G$ . They are split by the crystal field with the symmetry group  $O_h$  in the way previously indicated. The connection between the atomic and the impurity states for this case, based on a weak cubic field, is shown in Fig. 7-1.

When the crystal field in the atom is strong compared with the effect of the electron-electron interaction, which is responsible for splitting states of the same shell and different total angular momentum  $L$ , we should first classify the states  $l$  of the individual electrons according to the crystal symmetry as explained in Section 7-2a. Then we should combine them by taking into account electron-electron interaction and using the exclusion principle. The final states which will emerge will be the same, but their expected energy sequence will be different. More details on this point can be found in the book by Knox and Gold.<sup>[11]</sup>

Also in this case we are able to obtain the final impurity states, including spin-orbit interaction, by splitting the states for particles without spin into the states of the double group appropriate to semi-integer spin. The problem can be approached from two standpoints depending on whether the spin-orbit splitting is smaller than the crystal field splitting or vice versa. In the first case we start with the atomic states classified according to their  $L$  value, then we turn on the crystal field and split those states into the states of the simple point group of the lattice around the impurity, and finally we turn on the spin-orbit interaction and split the states of the simple group into the states of the double group (for the cubic group see Table 1-16 at  $\Gamma$ ). In the second case

## ELECTRONIC STATES AND OPTICAL TRANSITIONS

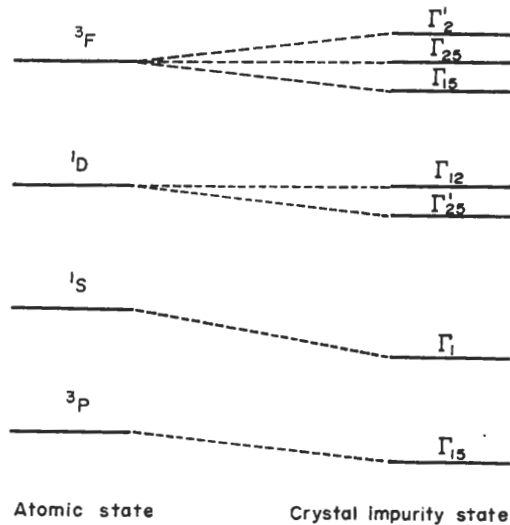


FIG. 7-1. Splittings of atomic states in a weak cubic field.

**L'INSTITUÉQUE DU  
DÉPARTEMENT DE PHYSIQUE  
Ecole Polytechnique Fédérale  
de Lausanne  
CH-1015 LAUSANNE Suisse  
TEL. 021 71 11 11**

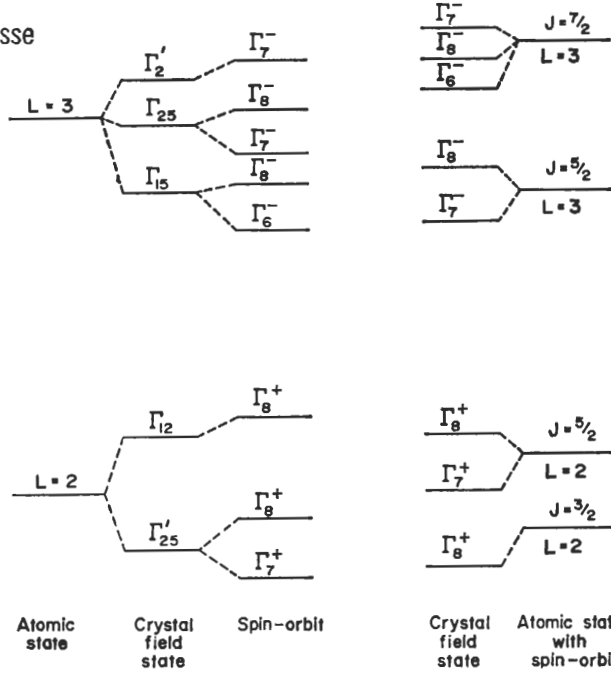


FIG. 7-2. Crystal field and spin-orbit splitting of atomic degenerate states. Both cases of strong crystal field and of strong spin-orbit interaction are considered.

we first consider the spin-orbit interaction in the classification of the atomic states and obtain atomic states defined by their total  $J$  value and their parity, then we split the  $J$  states as previously explained. The qualitative result is the same, but the two approaches will give a different sequence of states.

As an example of the combined effect of crystal field and spin-orbit interaction, we have shown in Fig. 7-2 the splitting of one electron in a  $d$  state and of one electron in an  $f$  state due to the crystal cubic field and to the spin-orbit interaction. We can see at once that the sequence of levels is different, dependent on whether the crystal field or the spin-orbit interaction is predominant. The extension to many electron systems is straightforward. The above analysis applies to transition metals or rare earth impurities in cubic lattices. It can often be applied also to the  $d$  and  $f$  bands of crystals containing transition or rare earth elements if such bands are sufficiently narrow that their  $\mathbf{k}$  dependence can be neglected in the tight binding approximation of Section 3-2.

### 7-2c Computation of the splittings

#### General remarks

The effect of the crystal field on the atomic levels can be computed using the techniques of perturbation theory and taking advantage of symmetry. We must estimate the effect of the perturbing potential on the energy states by evaluating the integral

$$I^{(\alpha)} = \int d\mathbf{r} \psi_0^{(\alpha)l} V_c \psi_0^{(\alpha)l}, \quad (7-7)$$

where  $V_c$  is given by (7-2) and the wave functions  $\psi_0^{(\alpha)l}$  are chosen to be the partner functions belonging to the same row  $i$  of the same irreducible representation  $(\alpha)$  of the symmetry group of the total Hamiltonian. Such functions are linear combinations of the zero order functions  $\psi_0^{nlm}$  which are solutions of (7-3). We can write

$$\psi_0^{(\alpha)l} = \sum_m \psi_0^{nlm} a_m^{(\alpha)l}, \quad (7-8)$$

where the coefficients are all determined by symmetry if the representation  $(\alpha)$  is contained only once in the atomic state  $nl$ . In this way for every atomic function we obtain the corresponding symmetrized zero order wave functions appropriate to the reduced symmetry, as indicated in the examples of the previous section, and substitute them into (7-7). In this case the energy correction is just  $\Delta E^{(\alpha)} = I^{(\alpha)}$ . If the representation  $\alpha$  is contained more than once in the atomic state  $l$  we can obtain more independent functions of the correct symmetry and we must then consider the matrix  $I_{ij}^{(\alpha)}$  between states of the same symmetry, and finally solve the determinant provided by degenerate perturbation theory

$$|(E_{ni} - E^{(\alpha)}) \delta_{ij} + I_{ij}^{(\alpha)}| = 0, \quad (7-9)$$

where  $i$  and  $j$  run over the independent functions belonging to the same row of the irreducible representation  $(\alpha)$ . We have given examples in Section 7-2a; it can be seen that in the case of the cubic field we need only to consider one function for the atomic states with  $l < 4$ , so that to first order  $\Delta E^{(\alpha)} = I^{(\alpha)}$ .

The crystal potential  $V_c(\mathbf{r})$  can be expanded about the origin in terms of spherical harmonics. In general we can write the crystal potential in the form

$$V_c(\mathbf{r}) = \sum_{l,m} A_l a_l^m Y_l^m(\theta, \varphi) \frac{r^l e^2}{r_0^{l+1}}, \quad (7-10a)$$

where  $r_0$  is the lattice distance, the coefficients  $a_l^m$  can be determined by symmetry, and the coefficients  $A_l$  can be computed when the electronic distribution in the lattice is known. Quite often in the calculation of the crystal field splittings, the factors  $A_l$  are taken as disposable parameters, since the electron density around the impurity is not known with sufficient precision.<sup>[4]</sup> In the case of an ionic crystal, assuming the lattice not to be modified by the impurity and no overlap between electrons of surrounding ions and electrons at the impurity, the computation of  $A_l$  reduces to that of lattice sums for which analytic expressions have been given by De Wette and Nijboer.<sup>[5]</sup> The results of numerical computations which give the coefficients  $A_l$  are also available in the literature.<sup>[6]</sup> A considerable simplification occurs in the expressions appearing in (7-10a) because the crystal potential  $V_c(r)$  has the full symmetry of the lattice around the imperfection; as a consequence, only combinations of spherical harmonics which belong to the fully symmetric representations  $\Gamma_1$  will appear. In general we can rewrite (7-10a) in the form

$$V_c = \sum_l \frac{A_l}{r_0^{l+1}} S_l^{\Gamma_1}(\vartheta, \varphi) r^l, \quad (7-10b)$$

where  $S_l^{\Gamma_1}$  indicates the combination of spherical harmonics of a given  $l$  which belongs to  $\Gamma_1$ . The symmetry of the lattice greatly reduces the number of spherical harmonics needed in the expansion (7-10). If we have inversion symmetry for instance, only even values of  $l$  will contribute. In the case of a cubic material the results obtained in Section 7-23 indicate that terms only with  $l = 0$ ,  $l = 4$ , and  $l = 6$  will contribute if we limit the expansion to  $l \leq 7$ .

The spherically symmetric term of expansion (7-10b) ( $l = 0$ ) produces a shift in all the atomic states, and this shift is nearly constant for all the deep impurity states; this is because the term with  $l = 0$  does not depend on  $r$  when the charges do not overlap. The other terms of expansion (7-10b), are responsible for the splitting because when inserted into (7-7) they give a contribution which is different for states belonging to different irreducible representations of the point group of the lattice around the impurity. When we have expansion (7-10b) and expansions (7-8) for all the states of interest, we can compute all the energy corrections as functions of the parameters  $A_l$  arising in the lattice potential and as functions of the expectation values of  $r^l$  with the atomic radial function of the unperturbed problem  $\langle \psi_0^{lm} | r^l | \psi_0^{lm} \rangle$ . The angular integrations appearing in (7-7) can always be performed because they reduce to integrals of products of three spherical harmonics. They can be performed by expanding the product of two spherical harmonics into a sum of spherical harmonics, with  $l$  ranging between the modulus of the difference and the sum of the  $l$  values of the two factors, and then using the orthonormality of spherical harmonics. The general expression which results is

$$\int \delta\Omega Y_{l_1}^{*m_1} Y_{l_2}^{m_2} Y_{l_3}^{m_3} = \left[ \frac{(2l_1 + 1)(2l_2 + 1)(2l_3 + 1)}{4\pi} \right]^{1/2} \begin{pmatrix} l_1 & l_2 & l_3 \\ 0 & 0 & 0 \end{pmatrix} \begin{pmatrix} l_1 & l_2 & l_3 \\ m_1 & m_2 & m_3 \end{pmatrix}, \quad (7-11)$$

where the  $3j$  symbols  $\begin{pmatrix} j_1 & j_2 & j_3 \\ m_1 & m_2 & m_3 \end{pmatrix}$  are numerical factors related to the Clebsh-Gordon coefficients and tabulated in spectroscopy books.<sup>[7]</sup> We can see immediately that if we consider  $d$  shell electrons,  $l_1$  and  $l_3$  will be equal to 2 and no contribution will be obtained with  $l_2 > 4$ ; if we consider  $f$  shell electrons,  $l_1 = l_3 = 3$  and no contribution will result with  $l_2 > 6$ . Considering transition metals or rare earth elements as our basic impurities, therefore, we need only expand the potential in (7-10) as far as  $l = 4$

and  $l = 6$  respectively. For this reason, the only parameters to be computed for example for any impurity we consider, will be  $\langle \psi_d | r^4 | \psi_d \rangle$  for  $d$  shell electrons and  $\langle \psi_f | r^4 | \psi_f \rangle$ , and  $\langle \psi_f | r^6 | \psi_f \rangle$  for  $f$  shell electrons.

### One-electron impurity in a cubic lattice

Let us now consider a cubic lattice of point ions with the NaCl structure or the CaF<sub>2</sub> structure and a substitutional impurity with one electron in the  $d$  or the  $f$  shell. To compute the crystal field splitting we should first express the crystal potential as a function of the cubic harmonics of symmetry  $\Gamma_1$  (the  $S_l^{\Gamma_1}$  of (7-10b)) by computing the parameters  $A_0$ ,  $A_4$ , and  $A_6$ . The cubic harmonics  $S_l^{\Gamma_1}$  for all values of  $l$  can be easily obtained as explained in Section 1-4 and are given in the literature.<sup>[11]</sup> The coefficients  $A_4$  and  $A_6$  have been computed by De Wette and Nijboer<sup>[5]</sup> and  $A_0$  is the Madelung constant which is not relevant to our calculation. For the NaCl structure we have

$$\left. \begin{aligned} S_0^{\Gamma_1} &= Y_0^0, \quad A_0 = \text{Madelung constant;} \\ S_4^{\Gamma_1} &= \sqrt{\left(\frac{4\pi}{9}\right)} \left\{ Y_4^0 + \sqrt{\left(\frac{5}{14}\right)} [Y_4^4 + Y_4^{-4}] \right\}, \quad A_4 = -3.58; \\ S_6^{\Gamma_1} &= \sqrt{\left(\frac{4\pi}{13}\right)} \left\{ Y_6^0 + \sqrt{\left(\frac{7}{2}\right)} [Y_6^4 + Y_6^{-4}] \right\}, \quad A_6 = -0.99. \end{aligned} \right\} \quad (7-12)$$

For the CaF<sub>2</sub> lattice the cubic harmonics of the above formula are the same, but the lattice sums are different. They have been computed by Vettori and Bassani<sup>[8]</sup> using the method of De Wette and Nijboer; they find  $A_4 = 2.715$  and  $A_6 = -1.94$ . The reason for the change of sign of the lattice sum  $A_4$  in going from the NaCl to the CaF<sub>2</sub> lattice is discussed by McClure<sup>[9]</sup> in terms of the position of the nearest ions. In comparing the above results with those obtained by considering only nearest ions,<sup>[10]</sup> it can be seen that more than 80 per cent of the contribution to the coefficients  $A_4$  and  $A_6$  is provided by the nearest ions. This explains why calculations performed initially in the simpler way gave reasonable agreement with experiment.<sup>[11]</sup>

We must next construct the functions  $\psi_0^{(\alpha)i}(\mathbf{r})$  of (7-8) as appropriate combinations of the atomic wave functions with  $l = 2$  or  $l = 3$ . The technique for obtaining this result has been described in Chapter 1 and can be summarized in the formula

$$\psi_0^{(\alpha)i}(\mathbf{r}) = \frac{1}{h} \sum_{\mathbf{R}} D_{ii}^{(\alpha)}(R) O_{\mathbf{R}} \psi_0^{nlm}(\mathbf{r}), \quad (7-13)$$

where  $D_{ii}^{(\alpha)}(R)$  indicates a matrix element corresponding to the operation  $R$  in the irreducible representation  $(\alpha)$ . For simplicity we can sum over  $i$

$$\psi_0^{(\alpha)} = \frac{1}{h} \sum_{\mathbf{R}} \chi^{(\alpha)}(R) O_{\mathbf{R}} \psi_0^{nlm}(\mathbf{r}) \quad (7-14)$$

and then use characters which are given in the tables.

In this last case, however, the function belongs to the irreducible representation  $(\alpha)$  but not to a particular row. We should thus obtain all functions and then choose those linear combinations which are mutually orthogonal as the basic set for the construction of the  $D_{ij}^{(\alpha)}$ . Once this is done, formula (7-13) can be applied. We derived cubic harmonics for  $l = 1$ ,  $l = 2$ , and  $l = 3$  in Table 1-16. Complete tables of cubic harmonics and of

all symmetrized combinations of spherical harmonics can be found in the literature.<sup>[12]</sup> The cubic harmonic expressions can be inserted into formula (7-7) after multiplication by the radial wave functions. On substituting expression (7-12) into expression (7-10b) for the crystal potential, we can perform all the angular integrals using formula (7-11).

For a  $d$  electron in a cubic field we finally obtain a result which, expressed in the usual notations, is

$$\left. \begin{aligned} I^{F_{2s'}} &= -4Dq, & q &= \frac{e}{105} \langle r^4 \rangle; \\ && \text{with} & \\ I^{F_{12}} &= 6Dq, & D &= -\frac{e}{r_0^5} A_4. \end{aligned} \right\} \quad (7-15)$$

The cubic field splitting of  $d$  states is equal to  $10Dq$ ,  $D$  being the term which depends on the particular lattice through  $r_0$  and  $q$  being the term which depends on the impurity through  $\langle r^4 \rangle$ .

A similar analysis could be performed for an  $f$  electron without difficulty. However, we observe that  $\langle r^4 \rangle$  and  $\langle r^6 \rangle$  for  $f$  electrons are very small since the  $f$  wave function is strongly localized near the nucleus. For the same reason the spin-orbit interaction is large for  $f$  electrons whereas it is small for  $d$  electrons. It follows therefore in the case of  $f$  electrons that we must work in the  $j$  scheme by first applying the spin-orbit interaction and then the crystal field (see Section 7-2b).

#### *Field splitting for the many electron case. An example: $\text{Sm}^{++}$ in $\text{SrF}_2$*

In most experimental situations we have more than one electron in the  $f$  or in the  $d$  shell. In these cases we follow the same procedure as described above, but starting from the appropriate many-electron atomic states and using many-electron wave functions. The crystal potential is the sum of one electron potentials

$$V_c(\mathbf{r}_1, \mathbf{r}_2, \dots, \mathbf{r}_n) = \sum_i V_c(\mathbf{r}_i), \quad (7-16)$$

where  $V_c(\mathbf{r}_i)$  is given by (7-10). The wave functions can be expressed as combinations of Slater determinants and the integrals  $I^{(\alpha)}$  of (7-7) can be computed to give the splittings. In the case of cubic symmetry, all splittings of  $f$  levels can be expressed as functions of  $A_4$ ,  $A_6$  and of  $\langle f | r^4 | f \rangle$  and  $\langle f | r^6 | f \rangle$ , and all splittings of  $d$  levels can be expressed in terms of  $A_4$  and  $\langle d | r^4 | d \rangle$ .

To give an example where it is necessary both to include spin-orbit splitting and to consider many electrons, we will describe briefly the problem of  $\text{Sm}^{++}$  in the crystal  $\text{SrF}_2$  which has been studied by Vetri and Bassani.<sup>[8]</sup> The impurity we consider has the configuration  $f^6$  and we shall concentrate on the state  ${}^7F$ . This state has been experimentally investigated<sup>[13]</sup> by observing emission from the higher state  ${}^5D_0$ . For the  ${}^7F$  state,  $L = 3$  and  $S = 3$ , so that we have a multiplet of states with  $J = 0, 1, 2, \dots, 6$ . The separation between states with different  $J$  is produced by the spin-orbit interaction and increases with  $J$  from about  $300 \text{ cm}^{-1}$  to about  $1000 \text{ cm}^{-1}$ . The crystal field will split every term of the multiplet into crystal states of the cubic symmetry according to the results discussed in Section 7-2a.

To compute the splittings we proceed as follows:

- Express the crystal states of the desired symmetry as linear combinations of eigenfunctions of  $L$ ,  $S$ ,  $J$ ,  $J_z$ . Since the rotational properties of the functions do not depend on the number of electrons, the combinations will be the same as those given in Table 1-16 for  $l = 2$  and  $l = 3$  and can be similarly obtained for the other values of  $J$ .
- Expand the eigenfunctions  $|LSJJ_z\rangle$  in terms of eigenfunctions  $|LL_zSS_z\rangle$  using

$$|LSJJ_z\rangle = \sum_{L_z S_z} (LL_zSS_z|JJ_z) |LL_zSS_z\rangle, \quad (7-17)$$

- where  $(LL_zSS_z|JJ_z)$  are the Clebsch-Gordon coefficients and the sum is over the terms  $S_z$  and  $L_z$  such that  $S_z + L_z = J_z$ .
- Express the many electron states  $|33L_zS_z\rangle$  as combinations of Slater determinants formed from one electron functions, each one specified by  $l = 3$  and  $-3 \leq m \leq 3$ .

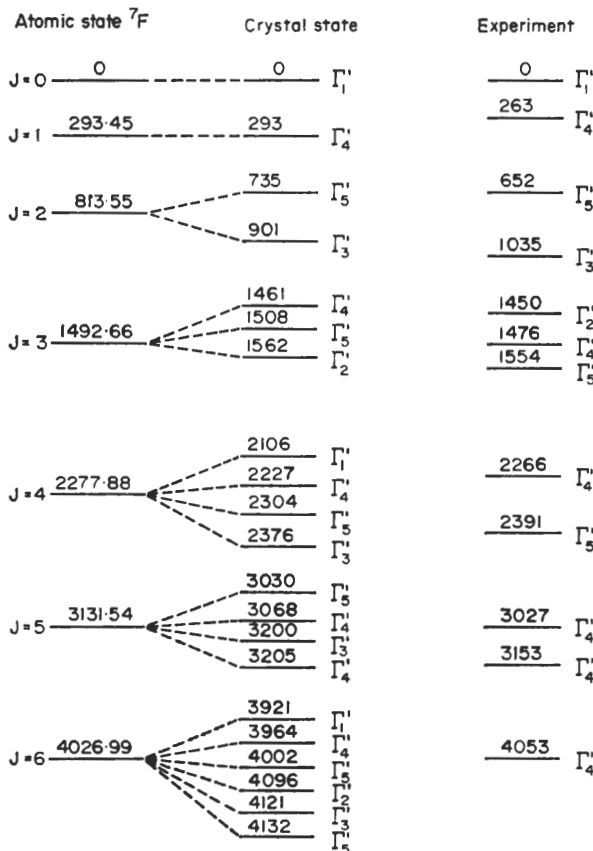


FIG. 7-3. Crystal field splittings of the  $J$  states  $^7F$  of  $\text{Sm}^{++}$  in  $\text{SrF}_2$  ( $\text{in cm}^{-1}$ ). The theoretical values are taken from ref. [8] and the experimental values from ref. [13]. The notations of Bethe have been used in this case (see Table 7-3).

(iv) Finally, compute the matrix elements

$$I^{(\alpha)} = \langle \psi_{0j}^{(\alpha)\dagger} | \sum_i V_c(\mathbf{r}_i) | \psi_{0j}^{(\alpha)\dagger} \rangle, \quad (7-18)$$

which can be expressed as combinations of integrals whose angular parts are of the type (7-11); these can be integrated out to give the final results in term of  $A_4$ ,  $A_6$ ,  $\langle r^4 \rangle$ , and  $\langle r^6 \rangle$ ,

These parameters have been computed, and the final results which have been obtained for the  $\Delta E^{(\alpha)}$  splittings are in fair agreement with the available experimental data.<sup>[13]</sup> We may also add that, although the crystal field splittings are smaller than the multiplet separations, in some cases one should consider the  $J - J$  interaction by taking into account the mixing of different  $J$  values having states of the same crystal symmetry. To illustrate the discussion we sketch in Fig. 7-3 the results obtained in ref. [8].

#### 7-2d Selection rules for optical transitions—Ligand field mixing

Just a few remarks can be made concerning allowed and forbidden transitions between impurity states in crystals. To zero order the selection rules are the same as in the free impurity ions. They are not modified when we introduce the crystal field to first order because a mixing of wave functions from atomic shells is not produced. In this case all transitions between states of a shell split by the field would be forbidden. If we include the interaction between different shells, however, some transitions which are dipole forbidden in the free atom become dipole allowed in the crystal. This can be understood by noting that a number of crystal representations are contained in a state of a given angular momentum and some of them will be allowed and some forbidden from a given initial state ( $\alpha$ ). To illustrate the point, we see that in a cubic crystal, for example, transitions between the state  $\Gamma_1$  of  $l = 0$  and the state  $\Gamma_{15}$  of  $l = 3$  are dipole allowed, while the corresponding transitions of the free ion are dipole forbidden. Similar considerations can be applied to the magnetic dipole and electric quadrupole transitions, although they are orders of magnitude smaller than the electric dipole transitions. It may also be observed that weak transitions are seen even when they would be forbidden by the selection rules of the crystal point group. This is the case for transitions amongst the states  $\Gamma'_{25}$  and  $\Gamma_{12}$  which split from the  $d$  shell, and is due to a relaxation of the symmetry produced by imperfections or by the lattice vibrations. These disturbances have a very small effect on the energies and on the wave functions of the impurity states but are sufficient to make the transition possible. The reader should consult the article by McClure<sup>[9]</sup> for references to the extensive literature on these problems.

We also wish to point out that the present theory must be improved in many ways when there is overlap between the wave functions of the impurity states and the wave functions of the neighbouring atoms. This implies a mixing between the impurity orbitals and the atomic orbitals of the nearest ions of the lattice; such a mixing has been observed in the hyperfine interaction. The mixed orbitals are called ligands. To use them properly in the calculations of the crystal field splittings, attention must be given to the self-consistency of the potential of the mixed orbitals and to the requirements of orthogonality to the other electronic states. Ligand field theory has been investigated by a number of authors. We refer to the article by McClure<sup>[9]</sup> and to the book by Ballhausen<sup>[14]</sup> for a detailed account; also refer the reader to the McClure for an extensive review of the experimental situation.

### 7-3 Shallow impurity states

#### 7-3a Introduction

It is a very common situation in semiconductors and metals to deal with electronic states which are very slightly bound to the impurity so that their wave functions extend over a large portion of the lattice. The eigenvalues and the eigenfunctions of these states are dominated by the periodic potential  $V_c$  of (7-1), and in this case it is the impurity potential  $U(r)$  which plays the role of a small perturbation. This is the case, for instance, of donor impurities like phosphorus, arsenic, antimony, or of acceptor impurities like aluminium, gallium, indium in germanium and silicon crystals. The electrical conductivity of the semiconductor is dominated by the properties of the impurity states because the electron or hole bound to the impurity can be thermally ionized near room temperature. The optical absorption in the infrared measured as function of temperature gives evidence for a number of discrete electronic states bound to the impurity. The scattering cross-section of electrons due to the ionized impurities dominates the electrical resistivity at low temperatures and shows effects due to resonances in the conduction band.

A very good review of shallow impurity states in elementary semiconductors is given in the article by Kohn.<sup>[15]</sup> More recent experimental data on the spectroscopy of impurity states can't be found in a number of excellent articles, some of which are given in ref. [16] for donor states and in ref. [17] for acceptor states. In recent years experimental evidence has also been produced for the existence of resonant states. We mention some papers concerning resonant states due to acceptor impurities in ref. [18] and to donor impurities in ref. [19].

The theory of shallow impurity states has been based on the effective mass approximation which was first introduced by Peierls,<sup>[20]</sup> Wannier,<sup>[21]</sup> and Adams,<sup>[22]</sup> and was clarified and used with great effectiveness by Kittel and Mitchell<sup>[23]</sup> and Luttinger and Kohn.<sup>[24]</sup> An extension of the theory to allow for resonant states has been first given by Peterson.<sup>[25]</sup>

To understand the significance and the true domain of validity of the effective mass approximation is a difficult problem; for this reason alternative approaches have been used, based on different representations of (7-1). We shall consider the crystal momentum representation of Luttinger and Kohn<sup>[24]</sup> and we shall also use the extended zone scheme in common with Iadonisi and Preziosi<sup>[26]</sup> who showed that most physical results obtained using the effective mass approximation retain their validity under less restrictive conditions. We shall also briefly describe the Wannier representation introduced by Koster and Slater<sup>[27]</sup> and used quite extensively for impurity problems when the effective mass approximation is expected to break down. We should also like to mention a general study of scattering states through a consideration of resonant states given by Callaway<sup>[29]</sup> in the Wannier representation.

A problem of great interest is to extend the effective mass approximation so as to take into account the details of the energy band structure and to derive all resonant states, in a natural way. An attempt in this direction has been made by Bassani *et al.*,<sup>[30]</sup> and detailed calculations have been performed on bound and resonant states in a number of cubic semiconductors.<sup>[31]</sup> We will give here the basic principles and refer the reader to a forthcoming review article for more details and for a more extensive review of the recent literature.<sup>[32]</sup>

## 7-3b General formulation of the impurity problem

We can soon convince ourselves that it would be impossible to use ordinary perturbation theory in order to solve eq. (7-1) in a situation when the impurity potential  $U$  is the perturbation. In such a case, in fact, the unperturbed states are the eigenfunctions of the equation

$$H_0\psi = \left( \frac{p^2}{2m} + V_c \right) \psi(\mathbf{k}, \mathbf{r}) = E(\mathbf{k}) \psi(\mathbf{k}, \mathbf{r}), \quad (7-19)$$

which are Bloch waves extending over the entire lattice. The eigenvalues  $E(\mathbf{k})$  give energy bands which depend continuously on the wave vector  $\mathbf{k}$  and may be separated by energy gaps at the boundaries of the Brillouin zones. We can consider all values of  $\mathbf{k}$ , in which cases we adopt the "extended zone scheme" for which every Brillouin zone corresponds to a band; or we can consider only those values which differ by less than a reciprocal lattice vector, the "reduced zone scheme" for which subscripts are needed to specify the different bands. The nature of such states has been extensively discussed in Chapters 2 and 3, and exemplified in Chapter 4. The matrix elements of the perturbing impurity potential are all negligibly small for an infinite lattice, but they give a finite contribution due to the fact that there is an infinite number of them; furthermore, the difference between the unperturbed levels tends to zero. For these reasons one cannot use Bloch functions as zero order functions in a perturbation expansion, but one must adopt a more suitable approach, which resembles in many ways that used for exciton states in Chapter 6.

A way to proceed is to consider the Bloch functions of (7-19) as the basic expansion set with which to represent the Schrödinger equation (7-1). This is the "crystal momentum representation" which we now discuss in the extended zone scheme. We can write any wave function of (7-1) as

$$\Phi(\mathbf{r}) = \int \varphi(\mathbf{k}) \psi(\mathbf{k}, \mathbf{r}) d\mathbf{k}. \quad (7-20)$$

Substituting (7-20) into (7-1),

$$[H_0 + U(\mathbf{r})] \int \varphi(\mathbf{k}') \psi(\mathbf{k}', \mathbf{r}) d\mathbf{k}' = E \int \varphi(\mathbf{k}') \psi(\mathbf{k}', \mathbf{r}) d\mathbf{k}' \quad (7-21)$$

which, because of (7-19), can also be written

$$\int \varphi(\mathbf{k}') E(\mathbf{k}') \psi(\mathbf{k}', \mathbf{r}) d\mathbf{k}' + U(\mathbf{r}) \int \varphi(\mathbf{k}') \psi(\mathbf{k}', \mathbf{r}) d\mathbf{k}' = E \int \varphi(\mathbf{k}') \psi(\mathbf{k}', \mathbf{r}) d\mathbf{k}'. \quad (7-22)$$

Premultiplying by  $\psi^*(\mathbf{k}, \mathbf{r})$ , integrating over  $\mathbf{r}$ , and making use of the following orthogonality of the Bloch functions,

$$\int \psi^*(\mathbf{k}, \mathbf{r}) \psi(\mathbf{k}', \mathbf{r}) d\mathbf{r} = \delta(\mathbf{k} - \mathbf{k}'), \quad (7-23)$$

we finally obtain

$$[E(\mathbf{k}) - E] \varphi(\mathbf{k}) + \int d\mathbf{k}' U(\mathbf{k}, \mathbf{k}') \varphi(\mathbf{k}') = 0, \quad (7-24a)$$

where we have set

$$U(\mathbf{k}, \mathbf{k}') = \int d\mathbf{r} \psi^*(\mathbf{k}, \mathbf{r}) U(\mathbf{r}) \psi(\mathbf{k}', \mathbf{r}). \quad (7-24b)$$

Equation (7-24) corresponds to (7-1) in the extended crystal momentum representation. The integrals in (7-24a) extend over all  $\mathbf{k}$  space and include all the electronic bands of the lattice. We could equally well have worked in the reduced zone scheme but then

a sum over all energy bands would have to be included as required by the completeness of the expansion set. In general the correspondence between the extended zone scheme and the reduced zone scheme can be established using the correspondence

$$\psi(\mathbf{k} + \mathbf{h}_n, \mathbf{r}) \equiv \psi_n(\mathbf{k}, \mathbf{r}), \quad E(\mathbf{k} + \mathbf{h}_n) \equiv E_n(\mathbf{k}). \quad (7-25a)$$

For every function  $f(\mathbf{k})$ , which depends on  $\mathbf{k}$ , we can write

$$\int f(\mathbf{k}) d\mathbf{k} = \sum_n \int_{BZ} f_n(\mathbf{k}) d\mathbf{k}, \quad (7-25b)$$

where the integral on the left hand side is over all  $\mathbf{k}$  space. Using relations (7-25) one can immediately verify that (7-24) coincides with that derived by Luttinger and Kohn.<sup>[24]</sup>

We can also write (7-24) in a different form:

$$\varphi(\mathbf{k}) = \delta(\mathbf{k} - \mathbf{k}_0) - \frac{\int U(\mathbf{k}, \mathbf{k}') \varphi(\mathbf{k}') d\mathbf{k}'}{E(\mathbf{k}) - E - i\varepsilon}, \quad (7-26)$$

where  $\mathbf{k}_0$  is a value of  $\mathbf{k}$  on the surface  $E(\mathbf{k}) = E$  and  $\varepsilon$  indicates an infinitesimal quantity which is positive for electrons as required by the condition that the wave function  $\Phi(\mathbf{r})$  sufficiently far from the impurity should consist of an incoming Bloch function and of outgoing scattering waves<sup>[33]</sup> (causality condition). Equation (7-26) is of great use in scattering theory because it includes those values of  $E$  for which there is a surface in  $\mathbf{k}$  space where  $E = E(\mathbf{k})$ . Substituting eq. (7-26) into expansion (7-20) and using the definition of  $U(\mathbf{k}, \mathbf{k}')$ , we can obtain the solution in a more familiar form:

$$\Phi(\mathbf{r}) = \psi(\mathbf{k}_0, \mathbf{r}) - \int G(\mathbf{r}', \mathbf{r}) U(\mathbf{r}') \Phi(\mathbf{r}') d\mathbf{r}', \quad (7-27a)$$

with

$$G(\mathbf{r}', \mathbf{r}) = \int d\mathbf{k} \frac{\psi^*(\mathbf{k}, \mathbf{r}') \psi(\mathbf{k}, \mathbf{r})}{E(\mathbf{k}) - E - i\varepsilon}. \quad (7-27b)$$

Equation (7-27) is the extension of the Lippmann–Schwinger equation of the formal theory of scattering to crystals.<sup>[33]</sup> When  $E \neq E(\mathbf{k})$ , the equation retains its validity, but the incoming wave  $\psi(\mathbf{k}_0, \mathbf{r})$  is not present and the extension into the complex plane with the infinitesimal immaginary part  $i\varepsilon$  is not necessary.

Equation (7-24) can also be written in real space by considering the Fourier transform of the expansion function  $\varphi(\mathbf{k})$  defined by (7-20),

$$\varphi(\mathbf{r}) = \int \varphi(\mathbf{k}) e^{i\mathbf{k} \cdot \mathbf{r}} d\mathbf{k}. \quad (7-28a)$$

Multiplying (7-24) by  $e^{i\mathbf{k} \cdot \mathbf{r}}$  and integrating over  $\mathbf{k}$  using (7-28a) and the general expression

$$\int d\mathbf{k} E(\mathbf{k}) \varphi(\mathbf{k}) e^{i\mathbf{k} \cdot \mathbf{r}} = E(-i\nabla) \varphi(\mathbf{r}), \quad (7-28b)$$

we obtain

$$[E(-i\nabla) - E] \varphi(\mathbf{r}) + \int U(\mathbf{r}', \mathbf{r}) \varphi(\mathbf{r}') d\mathbf{r}' = 0 \quad (7-29a)$$

with

$$U(\mathbf{r}', \mathbf{r}) = \iiint d\mathbf{k}' d\mathbf{k} e^{-i\mathbf{k}' \cdot \mathbf{r}'} \psi^*(\mathbf{k}', \mathbf{r}') U(\mathbf{r}'') \psi(\mathbf{k}, \mathbf{r}'') e^{i\mathbf{k} \cdot \mathbf{r}} d\mathbf{r}''. \quad (7-29b)$$

Equation (7-29) has been studied by Iadonisi and Preziosi<sup>[26]</sup> who have shown that the properties of  $U(r', r)$  are very similar to those of  $U(r)$  (boundedness, smoothness, etc.), so that a number of results derived within the local approximation  $U(r, r') \approx U(r) \delta(r - r')$  will also be appropriate to the non-local problem in the exact formulation expressed in (7-29).

Another representation, essentially equivalent to the previous ones, can be obtained in terms of the Wannier function described in Section 3-2a. Such a formulation was proposed by Koster and Slater<sup>[27]</sup> and can easily be obtained by expanding the solution of (7-1) in the complete set of Wannier functions

$$a_n(r - \tau_i) = \frac{\Omega^{1/2}}{(2\pi)^{3/2}} \int_{BZ} dk \psi_n(k, r) e^{ik \cdot \tau_i}, \quad (7-30)$$

$\Omega$  being the volume of the unit cell. We then have

$$\Phi(r) = \sum_{ni} B_n(\tau_i) a_n(r - \tau_i). \quad (7-31)$$

In the same manner as previously shown for the Bloch representation, it can be shown by substituting into eq. (7-1) that the coefficients  $B_n(\tau_i)$  satisfy the equations

$$\sum_j \langle ni | H_0 - E | nj \rangle B_n(\tau_j) + \sum_{jm} \langle ni | U | mj \rangle B_m(\tau_j) = 0, \quad (7-32)$$

where the matrix elements are defined in the usual way between Wannier functions of the type (7-30) labelled by the band index and the lattice vector. The secular determinant of the system of homogeneous linear equations (7-32) gives in principle the eigenvalues of our problem. If the impurity potential extends over one lattice site only, and if we can neglect the matrix elements between different bands, (7-32) assumes a simple form which can be solved and discussed more easily.<sup>[27, 29]</sup> In general both conditions are not satisfied, and (7-32) is very difficult to solve for real physical problems.

As is the case for the Bloch representation, we can extend the present formulation to include scattering states for which  $E = E(k)$ . This is easily accomplished through the introduction of the Green's function for outgoing waves

$$\mathcal{G}_n(\tau_i - \tau_j) = \langle ni | (E - H_0)^{-1} | nj \rangle, \quad (7-33)$$

where  $E$  is defined in the usual way by adding a small positive imaginary part, set equal to zero after the integration is performed. Equation (7-32) can be written as

$$B_n(\tau_i) = B_n^{(0)}(\tau_i) + \sum_{ktj} \mathcal{G}_n(\tau_i - \tau_j) \langle nj | U | tk \rangle B_t(\tau_k), \quad (7-34)$$

where  $B_n^{(0)}(\tau_i)$  is the solution of the homogeneous equation obtained from (7-32) by putting  $U = 0$ . In that case, expansion (7-31) must reduce to a Bloch function, and consequently

$$B_n^{(0)}(\tau_i) = \frac{\Omega^{1/2}}{(2\pi)^{3/2}} e^{-ik_0 \cdot \tau_i}, \quad (7-35)$$

where  $k_0$  gives the direction of the incoming wave of energy  $E(k_0)$ . Equation (7-34) in the Wannier representation corresponds to eq. (7-26) in the Bloch representation; by substitution into the expansion (7-31) we can also obtain the expression corre-

sponding to (7-27), which seems superfluous to write down explicitly. This result is the analogue of the Lippmann-Schwinger equation of formal-scattering theory.<sup>[33]</sup> Callaway<sup>[29]</sup> has shown that all concepts of scattering theory, and in particular the existence of resonant states, can be derived in this formalism. The formulation has been adopted for the case of impurity states in grey tin by Liu and Brust.<sup>[28]</sup>

It is also very instructive to obtain localized impurity states, resonant states, and scattering states in the Bloch representation from a formal analysis of the Fredholm determinant obtained from the integral equation (7-24) as done by Bassani *et al.*<sup>[30]</sup> For completeness, we should just like to mention the results. The values of  $E$  can be obtained from the solutions of the determinant equation<sup>[30]</sup>

$$\left| \delta_{nn'} + \int d\mathbf{k}' \frac{f_n(\mathbf{k}') f_{n'}^*(\mathbf{k}')}{E - E(\mathbf{k}')} \right| = 0, \quad (7-36)$$

with

$$f_n(\mathbf{k}) = \int d\mathbf{r} \psi(\mathbf{k}, \mathbf{r}) \sqrt{(-U(\mathbf{r}))} g_n(\mathbf{r}), \quad (7-37)$$

$g_n(\mathbf{r})$  being the function of an arbitrary complete set which can be chosen so as to improve convergence. Real values of  $E$  occur in the energy gaps where  $E \neq E(\mathbf{k})$  and correspond to bound states. The determinant eq. (7-36) has also complex solutions for energies inside the energy bands when it is properly extended into the complex plane. The solutions in the lower half of the complex plane with the imaginary part much smaller than the real part are resonant states since it can be proved that they have abnormally large scattering amplitudes (or abnormally large localized functions).<sup>[30]</sup>

In principle it does not matter for the impurity problem which one of the above three formulations, as indicated by eq. (7-24), (7-29), or (7-32) we use; they are all equivalent and must lead to the same results. In practice, approximations must always be made, and a particular formulation may be preferred. For deep impurity states, which originate from sharp potentials, the Wannier function representation may be more suitable, but for shallow states, produced by long range potentials, the Bloch function representation is to be adopted. In the following we shall mostly concentrate on the latter representation.

### 7-3c Effective mass approximation and applications

We consider the case when the potential  $U(\mathbf{r})$  is weak and slowly varying. From (7-24) or (7-29) one can easily derive an approximate equation which is very easy to solve and has proved to be very useful for dealing with shallow impurity states. This consists of a Schrödinger-like equation for the envelope function  $\varphi(\mathbf{r})$  defined in (7-28a) and closely resembles the corresponding equation obtained in Chapter 6 for weakly bound excitons. Such effective mass equation is

$$\left( -\frac{\hbar^2}{2m_x^*} \frac{\partial^2}{\partial x^2} - \frac{\hbar^2}{2m_y^*} \frac{\partial^2}{\partial y^2} - \frac{\hbar^2}{2m_z^*} \frac{\partial^2}{\partial z^2} \right) \varphi(\mathbf{r}) + U(\mathbf{r}) \varphi(\mathbf{r}) = E \varphi(\mathbf{r}), \quad (7-38)$$

where the effective masses in their principal directions are given by  $\frac{1}{m_i^*} = \frac{1}{\hbar^2} \frac{\partial^2 E(\mathbf{k})}{\partial k_i^2}$ ,

and  $E$  is referred to a critical point energy. The above equation can be obtained immediately from (7-29) by expanding  $E(\mathbf{k})$  in powers of  $\mathbf{k}$  near a critical point in the

band structure ( $\nabla_{\mathbf{k}} E(\mathbf{k}) = 0$ ) neglecting higher than second order powers and making the approximation

$$U(\mathbf{r}', \mathbf{r}) \simeq U(\mathbf{r}) \delta(\mathbf{r} - \mathbf{r}'), \quad (7-39)$$

which is valid for a smooth potential.<sup>[26]</sup>

To see more clearly the approximations involved, and to open up the possibility for further extensions, we shall discuss the effective mass approximation, from the point of view of (7-24) as done by Luttinger and Kohn.<sup>[24]</sup> Let us examine in detail the expression (7-24b), which can also be written in the reduced zone scheme

$$U_{nn'}(\mathbf{k}, \mathbf{k}') = \int d\mathbf{r} \psi_n^*(\mathbf{k}, \mathbf{r}) U(\mathbf{r}) \psi_{n'}(\mathbf{k}', \mathbf{r}) = \int d\mathbf{r} U(\mathbf{r}) e^{i(\mathbf{k}' - \mathbf{k}) \cdot \mathbf{r}} u_n^*(\mathbf{k}, \mathbf{r}) u_{n'}(\mathbf{k}', \mathbf{r}), \quad (7-40)$$

where  $u_n(\mathbf{k}, \mathbf{r})$  denotes the periodic part of the Bloch function  $\psi_n(\mathbf{k}, \mathbf{r})$ . We follow the same reasoning as in Appendix 6B. Let us suppose that the main contributions to expansion (7-20) come from  $\mathbf{k}$  values near the extremum of the band, which we may suppose to be at  $\mathbf{k} = 0$  for simplicity. Then the periodic part of the Bloch functions  $u_n(\mathbf{k}, \mathbf{r})$  can be expanded with respect to  $\mathbf{k}$  and only the first term in the expansion need be retained. The periodic part of the integrand in (7-40) then becomes independent of  $\mathbf{k}$  and can be expanded in a Fourier series in terms of the reciprocal lattice vectors  $\mathbf{h}$  to obtain

$$U_{nn'}(\mathbf{k}, \mathbf{k}') = \sum_{\mathbf{h}} A_{nn'}^{(\mathbf{h})} U(\mathbf{k}' - \mathbf{k} + \mathbf{h}). \quad (7-41)$$

Consistent with the approximation that the only  $\mathbf{k}$  values of importance are those near the minimum of the band, we can neglect all the terms with  $\mathbf{h} \neq 0$  in (7-41). This is valid for a smooth potential because of the well known properties of Fourier transforms. Furthermore the orthogonality condition between Bloch functions requires  $A_{nn'}^{(0)} = \delta_{nn'}$ , so that in the approximation of a smooth potential any mixing between different bands is removed. Expression (7-40) then becomes

$$U_{nn'}(\mathbf{k}, \mathbf{k}') \simeq U(\mathbf{k} - \mathbf{k}') \delta_{nn'}, \quad (7-42)$$

and (7-24) becomes

$$[E_n(\mathbf{k}) - E] \varphi_n(\mathbf{k}) + \int U(\mathbf{k} - \mathbf{k}') \varphi_n(\mathbf{k}') d\mathbf{k}' = 0. \quad (7-43)$$

The above equation in momentum space can be transformed into an equivalent equation in real space by multiplying by  $e^{i\mathbf{k} \cdot \mathbf{r}}$ , formally extending the  $\mathbf{k}$  space to infinity, which is consistent with our basic assumption, and integrating over  $\mathbf{k}$ . If we also expand  $E_n(\mathbf{k})$  about the extremum, retaining the lowest  $\mathbf{k}$  dependent term in the expansion, we obtain eq. (7-38), which is the usual form of the effective mass approximation. It also holds in the cases where the extrema are at  $\mathbf{k}_c \neq 0$ , but in those cases the Fourier space of  $\varphi(\mathbf{r})$  is referred to  $\mathbf{k} - \mathbf{k}_c$ .<sup>[30]</sup> In this approximation we may also recall that the expansion of the impurity wave function (7-20) becomes

$$\Phi(\mathbf{r}) \simeq \varphi(\mathbf{r}) \psi(\mathbf{k}_c, \mathbf{r}), \quad (7-44)$$

as can immediately be obtained from (7-20) which is to first order

$$\Phi(\mathbf{r}) \simeq \int \varphi(\mathbf{k} - \mathbf{k}_c) e^{i(\mathbf{k} - \mathbf{k}_c) \cdot \mathbf{r}} e^{i\mathbf{k}_c \cdot \mathbf{r}} u_n(\mathbf{k}_c, \mathbf{r}) d\mathbf{k}. \quad (7-45)$$

The effective mass eq. (7-38) with wave function (7-44) has been used extensively to interpret impurity states in semiconductors in a manner very similar to that used

for loosely bound excitons in the previous chapter. In general it is not a very good approximation for the ground state, whose wave function is restricted to a small distance from the impurity where the potential is not slowly varying and depends strongly on the specific impurity. In fact for different impurities the energy position of the ground state is quite different (chemical shift), and this can be explained only in terms of the short range impurity dependent part of the potential.<sup>[34]</sup> If the minimum of the conduction band is at  $\mathbf{k}_c \neq 0$  there is also an interaction between equivalent minima which produces a shift and splitting of the ground state. We will expand this last point in the next section when we consider an extension of the effective mass approximation.

For excited states the effective mass approximation (7-38) is usually appropriate since their wave functions extend quite far from the impurity and the approximations described above are justified. The case of cubic semiconductors with the minimum of the conduction band at  $\mathbf{k} = 0$ , such as GaAs, and a number of II-VI compounds, is very simple to study. The effective mass tensor is in these cases isotropic, and one obtains hydrogen like solutions with

$$E_n = -\frac{m^* e^4}{2\hbar^2 \epsilon^2 n^2}, \quad (7-46)$$

$\epsilon$  being the value of the dielectric constant at the appropriate frequency. For many semiconductors of interest, however, such as the elementary cubic semiconductors germanium and silicon discussed in Chapter 4, the minimum of the conduction band is at  $\mathbf{k}_c \neq 0$ . In germanium it occurs at the point  $L(\mathbf{k} = (2\pi/a)(\frac{1}{2}, \frac{1}{2}, \frac{1}{2}))$ , and in silicon along the line  $A(\mathbf{k} = (2\pi/a)(0.8, 0, 0))$ ; the effective mass tensor is anisotropic, and symmetry allows a longitudinal effective mass  $m_l^*$  in the direction of  $\mathbf{k}_c$  and a transversal effective mass  $m_t^*$  perpendicular to it. The effective mass equation (7-38) in this case becomes

$$\left[ -\frac{\hbar^2}{2m_l^*} \left( \frac{\partial^2}{\partial x^2} + \frac{\partial^2}{\partial y^2} \right) - \frac{\hbar^2}{2m_t^*} \frac{\partial^2}{\partial z^2} \right] \varphi(\mathbf{r}) - \frac{e^2}{\epsilon r} \varphi(\mathbf{r}) = E\varphi(\mathbf{r}). \quad (7-47)$$

The solutions of (7-47) can be obtained only by variational procedures. Luttinger and Kohn<sup>[24]</sup> computed the ground state, Faulkner<sup>[35]</sup> the excited states, and Baldereschi and Diaz<sup>[36]</sup> obtained also the transition probabilities as functions of the anisotropy parameter  $\gamma = m_l^*/m_t^*$  for both germanium and silicon. We show in Fig. 7-4 how the energy levels depend on  $\gamma^{1/3}$  and how the states  $nl$  of the rotation group split into states with quantum numbers  $n|l_z|$ , as expected from the cylindrical symmetry. The results obtained for the excited states are in good agreement with the experimental data on silicon and germanium as shown in Table 7-4.

For non-cubic semiconductors, not only is the effective mass tensor always anisotropic, but so is the effective dielectric function. For uniaxial crystals with band extrema at  $\mathbf{k}_c = 0$  we have  $m_x^* = m_y^* \neq m_z^*$  and  $\epsilon_x = \epsilon_y \neq \epsilon_z$ . This gives an equation similar to (7-47) except for the anisotropy of the impurity potential

$$\left[ -\frac{\hbar^2}{2m_\perp} \left( \frac{\partial^2}{\partial x^2} + \frac{\partial^2}{\partial y^2} \right) - \frac{\hbar^2}{2m_\parallel} \frac{\partial^2}{\partial z^2} \right] \varphi(\mathbf{r}) - \frac{e^2}{\sqrt{(\epsilon_\parallel \epsilon_\perp)} \sqrt{\left( x^2 + y^2 + \frac{\epsilon_\perp}{\epsilon_\parallel} z^2 \right)}} \varphi(\mathbf{r}) = E\varphi(\mathbf{r}). \quad (7-48)$$

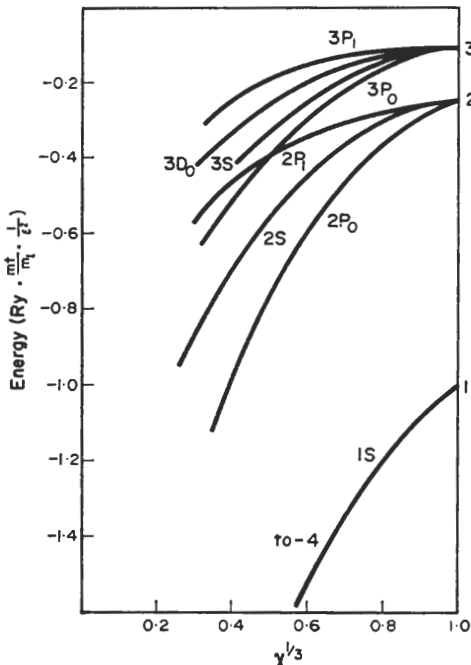


FIG. 7-4. Energy levels of donors in anisotropic systems (in effective Rydbergs), as functions of the anisotropy parameter  $\gamma$ . (From ref. [35] and [36].)

TABLE 7-4. Theoretical binding energy levels of donor impurities, with Coulomb-like potentials, in silicon and germanium (in meV). Values of the ground state splittings are also given. Experimental values are given for three typical impurities. (The theoretical values are from ref. [35], [36] and [38]; the experimental values from ref. [15] and [16].)

Substance	State							
	1S	2P₀	2S	2P₁	3P₀	3S	3P₁	4P₀
Si (theory)	31.27 (10.6–1.1)	11.51	8.83	6.40	5.48	4.75	3.12	3.33
Si(P)	45.5–33.9–32.6	11.45		6.39	5.46		3.12	3.38
Si (As)	53.7–32.6–31.2	11.49		6.37	5.51		3.12	
Si (Sb)	42.7–32.9–30.6	11.52		6.46	5.51		3.12	
Ge (theory)	9.81 (0.6)	4.74	3.52	1.73	2.56	2.01	1.03	1.67
Ge (P)	12.89–9.88	4.75		1.73	2.56		1.05	
Ge (As)	14.17–9.96	4.75		1.73	2.56		1.04	
Ge (Sb)	10.32–10.01	4.74		1.73	2.57		1.04	

Measuring energy in effective Rydbergs  $\frac{m_\perp^* e^4}{2\hbar e_\perp \epsilon_{||}}$ , the length in units of the Bohr radius  $a_0^* = \frac{\hbar^2 (\epsilon_\perp \epsilon_{||})^{1/2}}{m_\perp^* e^2}$ , and performing a change of variables, we obtain the equation

$$-\nabla^2 \varphi - \frac{2}{\sqrt{(x_1^2 + y_1^2 + \gamma z_1^2)}} \varphi = E \varphi, \quad (7-49a)$$

or, equivalently,

$$-\left(\frac{\partial^2}{\partial x^2} + \frac{\partial^2}{\partial y^2}\right)\varphi - \gamma \frac{\partial^2\varphi}{\partial z^2} - \frac{2}{r}\varphi = E\varphi, \quad (7-49 \text{ b})$$

where

$$\gamma = \frac{m_{\perp}}{m_{\parallel}} \frac{\epsilon_{\perp}}{\epsilon_{\parallel}}.$$

is the anisotropy parameter.

The results of Fig. 7-4 show that the energy values of all levels decrease with decreasing  $\gamma$ , but only for very large anisotropies does one approach the two-dimensional limit. It is also interesting to observe that the anisotropy of the dielectric constant tends to compensate for the effective mass anisotropy in giving the value of  $\gamma$ . This all indicates that the anisotropy effect on the energy levels of excited impurity states will be small even in layer compounds.

Throughout the present section we have considered the impurity potential  $U(r)$  to be Coulomb-like, with a screening given by the static dielectric constant. This is a valid approximation only for the long-range behaviour of the potential when the impurity in the insulator or in the semiconductor introduces an extra charge as may be the case for interstitial monovalent elements (lithium in germanium for instance), for substitutional impurities with an extra-valence electron (arsenic in germanium for instance), or for substitutional impurities with an electron missing (extra hole) (gallium in germanium for instance). In these cases in fact the long range impurity potential is that of a charge in the dielectric medium, and the screening of this charge is the static dielectric constant because of the same reasoning applied to justify the electron-hole interaction in Section 6-4. We do not wish to repeat the argument again, but may recall that it is based on the fact that the long range potential involves the Fourier transforms with small momentum  $4\pi e^2/q^2$  and the screening function  $\epsilon(q)$  is nearly a constant for values of  $q$  small compared to a reciprocal lattice vector.

More generally, the true potential  $U(r)$  can be written as

$$U(r) = \frac{1}{(2\pi)^3} \int d\mathbf{q} \frac{V(\mathbf{q})}{\epsilon(\mathbf{q})} e^{i\mathbf{q} \cdot \mathbf{r}}, \quad (7-50)$$

where  $V(\mathbf{q})$  is the Fourier transform of the bare impurity potential, which only for small values of  $q$  reduces to  $\mp 4\pi e^2/q^2$ . For intermediate and large values of  $q$  the expression of the bare potential is very complicated and depends on the type of impurity (it is the difference between the potential of the impurity and the substituted atom in the case of substitutional impurities). The expression for the dielectric function is also more complicated because it includes large values of  $q$  where  $\epsilon(\mathbf{q})$  drops from its static value  $\epsilon(0)$  to 1. Expressions for (7-50) have been investigated by Morita and Nara<sup>[37]</sup> and we refer to them for further details. We only wish to mention that for small values of  $r$  the potential (7-50) deviates from Coulomb-like behaviour by a function which is called "central cell correction". To compute the "central cell correction" is a difficult problem, and a considerable simplification can be achieved by extending to the impurity problem the pseudopotential approach which we discussed in Chapter 3. This was done by Hermanson and Phillips,<sup>[34]</sup> who transformed the impurity equation (7-1) into a pseudopotential equation, and could then define an impurity pseudopotential, eventually constructed as the difference of atomic pseudopotentials at the lattice sites. We

refer the reader to ref. [34] for further discussion of this point and for qualitative arguments to understand the chemical shifts. We may perhaps emphasize that this problem is still at a rather qualitative stage. In the following of this section we will not consider explicitly “central cell corrections”, though we shall have to take into account the  $\mathbf{q}$  dependence of  $\epsilon(\mathbf{q})$  when considering interaction between extrema of the Brillouin zone at different points of  $\mathbf{k}$  space.

### 7-3d Intervalley mixing and degenerate bands

#### Intervalley mixing

From the experimental results of Table 7-4 we can see that the ground state is a multiplet with considerable separation between the composing states (singlet  $A$ , doublet  $E$ , and triplet  $T_1$  in silicon). The ground state of (7-38) is degenerate when the minimum of the band is at  $\mathbf{k}_c$  away from the centre of the Brillouin zone because there are a number of equivalent minima at all points of the star  $R\mathbf{k}_c$ ,  $R$  being a symmetry operation, and correspondingly a number of different functions of type (7-44). In germanium for instance, the minimum of the conduction band is  $L_1$ , and there are four equivalent minima at

$$\mathbf{k}_{c_1} = \frac{2\pi}{a} \left( \frac{1}{2}, \frac{1}{2}, \frac{1}{2} \right), \quad \mathbf{k}_{c_2} = \frac{2\pi}{a} \left( \frac{1}{2}, \frac{1}{2}, \frac{1}{2} \right), \quad \mathbf{k}_{c_3} = \frac{2\pi}{a} \left( \frac{1}{2}, \frac{1}{2}, \frac{1}{2} \right),$$

and  $\mathbf{k}_{c_4} = \frac{2\pi}{a} \left( \frac{1}{2}, \frac{1}{2}, \frac{1}{2} \right);$

the negative points  $-\mathbf{k}_c$  are not to be counted separately because they are indistinguishable from the previous ones since they differ by a reciprocal lattice vector. Actually both points  $\mathbf{k}_c$  and  $-\mathbf{k}_c$  in this case are needed to construct the  $\mathbf{k}$  region in which to use the effective mass approximation.<sup>[30]</sup> In the case of silicon, the minimum of the conduction band is in the direction  $A$ , and we have six equivalent minima

$$\frac{2\pi}{a} (\pm\alpha, 0, 0), \quad \frac{2\pi}{a} (0, \pm\alpha, 0), \quad \frac{2\pi}{a} (0, 0, \pm\alpha).$$

The ground state  $\Phi_{\mathbf{k}_c}(\mathbf{r})$  given in (7-44) is six times degenerate in silicon and four times degenerate in germanium.

The above degeneracies are not allowed by the symmetry of the lattice, and these states must split into states which belong to the irreducible representations of the symmetry group. For instance we can see that the four functions of type (7-44) in germanium can be combined to give partner functions of the two irreducible representations  $A_1$  and  $T_1$ , and the six functions of type (7-44) in silicon can be combined to give partner functions for the irreducible representations  $A_1$ ,  $E$ , and  $T_1$  of Table 7-3. We can leave it as an exercise for the reader to derive the appropriate combinations of wave functions using the projection operator technique of Chapter 1 [see also formula (7-13)]. They are given for convenience in Table 7-5. To remove the degeneracy we have to go beyond the effective mass approximation described in Section 7-3c. To first order this is done in the usual way by considering the matrix elements of the impurity potential between different equivalent minima and by solving the resulting secular determinant. The symmetry analysis reduces the size of the secular determinant. In germanium and silicon all the coefficients of the resulting wave functions are given

TABLE 7-5. Linear combinations of impurity wave functions which are partner functions of the irreducible representations of the group  $T_d$ . The functions are labelled by the value of  $k_c$  and the coefficients of the linear combinations are given in appropriate columns.  
NB—Each coefficient will have to be multiplied by its appropriate normalization factor

$\Phi_{k_c t}(\mathbf{r})$	$A_1$	$E$	$T_1$	
$(2\pi/a)(\alpha, 0, 0)$	1	1 1	1 0 0	
$(2\pi/a)(0, \alpha, 0)$	1	0 -2	0 1 0	
$(2\pi/a)(0, 0, \alpha)$	1	-1 1	0 0 1	
$(2\pi/a)(\bar{\alpha}, 0, 0)$	1	1 1	-1 0 0	
$(2\pi/a)(0, \bar{\alpha}, 0)$	1	0 -2	0 -1 0	
$(2\pi/a)(0, 0, \bar{\alpha})$	1	-1 1	0 0 -1	
$(2\pi/a)(\frac{1}{2}, \frac{1}{2}, \frac{1}{2})$	1		1 1 1	
$(2\pi/a)(\frac{1}{2}, \frac{1}{2}, \frac{1}{2})$	1		1 -1 -1	
$(2\pi/a)(\frac{1}{2}, \frac{1}{2}, \frac{1}{2})$	1		-1 1 -1	
$(2\pi/a)(\frac{1}{2}, \frac{1}{2}, \frac{1}{2})$	1		-1 -1 1	

by symmetry, as in Table 7-5, and one can compute immediately the expectation value of the Hamiltonian, which includes the splitting between states due to the interactions between equivalent minima. From the combinations given in Table 7-5 one can immediately obtain in the case of silicon

$$E_{A_1} = E_0 - \lambda - 4\mu,$$

$$E_E = E_0 - \lambda + 2\mu,$$

$$E_{T_1} = E_0 + \lambda,$$

where

$$\lambda = - \langle \varphi_{sk_c}(\mathbf{r}) \psi(\mathbf{k}_0, \mathbf{r}) | U(\mathbf{r}) | \varphi_{sk_c}(\mathbf{r}) \psi(-\mathbf{k}_0, \mathbf{r}) \rangle$$

and

$$\mu = - \langle \varphi_{sk_c}(\mathbf{r}) \psi(\mathbf{k}_0, \mathbf{r}) | U(\mathbf{r}) | \varphi_{sk_c}(\mathbf{r}) \psi(\mathbf{k}'_0, \mathbf{r}) \rangle,$$

are the only two independent integrals. In the case of germanium we obtain

$$E_{A_1} = E_0 - 3\mu, \quad E_{T_1} = E_0 + \mu,$$

$\mu$  being in this case the only independent integral between two  $k_c$  values of Table 7-5. Calculations of the above parameters for silicon and germanium have been performed by Baldereschi<sup>[38]</sup> who took into account the  $q$  dependence of the dielectric function in the coulomb approximation as mentioned at the end of the preceding paragraph 7-3c. The theoretical splittings have been reported in Table 7-4 together with the experimental data. It can be observed that the splittings of the ground state degeneracies are in reasonable agreement with experiment, while the absolute positions are not because of the chemical shifts discussed at the end of the preceding section.

We may also mention at this point that, in addition to mixing from equivalent minima, one can have contributions of secondary minima to the wave function of the ground state. This has been proved by Castner<sup>[38]</sup> with a detailed analysis of experimental paramagnetic resonance data on donor impurities. We will discuss this point in a more general way in connection with resonant states in the next section.

Another thing to be kept in mind when considering intervalley interaction is that it must also exist for higher energy states, where similar splittings in principle should occur. In reality, for excited states in most semiconductors, the envelope wave function  $F_{ni}(r)$  is so extended and smooth, that the effective mass assumptions of the previous sections are better verified and the splitting is totally negligible. This result will also follow naturally from the analysis of Section 7-3e.

### Degenerate bands

A similar problem of band mixing arises when the energy band extremum near the impurity levels is degenerate, but in this case the mixing cannot be considered by perturbation theory. Such is the case for acceptor states in group IV semiconductors, where the top of the valence band is  $\Gamma'_{2s}$  and is split by spin-orbit interaction into  $\Gamma_8^+$  and  $\Gamma_7^+$ . Even if we regard the interaction between states  $\Gamma_8^+$  and  $\Gamma_7^+$  as being very small, we still have a degenerate problem and must include the interaction between the two bands which go into  $\Gamma_8^+$  at  $\mathbf{k} = 0$ . This situation is schematically sketched in Fig. 7-5 and it is common to most cubic materials. The problem is to extend the

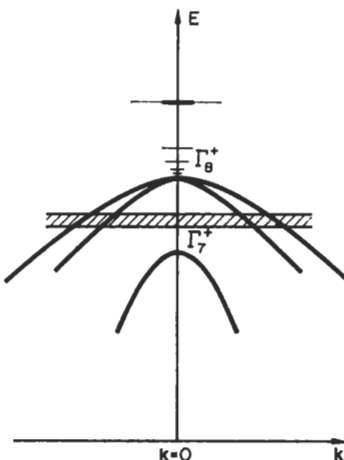


FIG. 7-5. Schematic band structure near the top of the valence band in typical cubic semiconductors with degeneracies of the levels and spin-orbit splittings. The acceptor bound and resonant states are indicated by lines and by stripes respectively.

effective mass equation, since in this case we cannot expand  $E(\mathbf{k})$  independently for each of the valence bands. It has been shown<sup>[39]</sup> using the  $\mathbf{k} \cdot \mathbf{p}$  perturbation method that the values of  $E(\mathbf{k})$  near  $\mathbf{k} = 0$  are given by the roots of the determinantal equation

$$\left| \sum_{\alpha\beta} D_{ij}^{\alpha\beta} k_\alpha k_\beta - \lambda \epsilon_i \delta_{ij} - E \delta_{ij} \right| = 0, \quad (7-51)$$

where  $\alpha$  and  $\beta$  indicate  $x, y, z$ ;  $i$  and  $j$  are indices which refer to the degenerate functions ( $1 \dots 6$ );  $\epsilon_i$  is zero for  $i = 1, 2, 3, 4$  and unity for  $i = 5, 6$ , so that the second term in (7-51) accounts for the spin-orbit splitting ( $\lambda$  at  $\mathbf{k} = 0$ ). The quantities  $D_{ij}$  are parameters related to matrix elements of the momentum which correspond to the inverse of the effective mass tensor in the case of no coupling between bands (off-diagonal

terms equal to zero). In germanium  $\lambda$  is sufficiently large to neglect mixing between the states separated by the spin-orbit interaction and the determinant (7-51) splits into two determinants, one 4 by 4 which gives  $\Gamma_8^+$  in the limit  $\mathbf{k} = 0$ , and the other 2 by 2 which gives  $\Gamma_7^+$  in the limit  $\mathbf{k} = 0$ . The form of the matrix (7-51) depends on the choice of the unperturbed functions at  $\mathbf{k} = 0$ , and a number of equivalent expressions can be obtained in terms of only three independent parameters, as first shown by Dresselhaus *et al.*<sup>[40]</sup> A particularly convenient expression has been suggested by Luttinger,<sup>[40]</sup> when one considers only the 4 by 4 matrix, by introducing the 4 by 4 matrices  $J_x$ ,  $J_y$ , and  $J_z$  which satisfy the angular momentum commutation rules. Then the matrix Hamiltonian takes the form

$$H = \frac{\hbar^2}{m} \left\{ \left( \gamma_1 + \frac{5}{2} \gamma_2 \right) \frac{\mathbf{k}^2}{2} - \gamma_2 (k_x^2 J_x^2 + k_y^2 J_y^2 + k_z^2 J_z^2) \right. \\ \left. - 2\gamma_3 [\{k_x, k_y\} \{J_x, J_y\} + \{k_y, k_z\} \{J_y, J_z\} + \{k_z, k_x\} \{J_z, J_x\}] \right\}, \quad (7-52)$$

where  $\{a, b\} = \frac{1}{2}(ab + ba)$ , and  $\gamma_1$ ,  $\gamma_2$ ,  $\gamma_3$  are dimensionless parameters which can be related to sums of momentum matrix elements, but are usually fitted to experiments. The quartic equation near  $\Gamma_8^+$  can be solved for small  $\mathbf{k}$  to give an expression of the form

$$E(\mathbf{k}) = Ak^2 \pm [Bk^4 + C(k_x^2 k_y^2 + k_y^2 k_z^2 + k_z^2 k_x^2)]^{1/2},$$

$A$ ,  $B$ , and  $C$  being parameters related to  $\gamma_i$ , which can be measured experimentally by fitting cyclotron resonance data.<sup>[40]</sup>

To extend the effective mass equation (7-38), we must consider (7-51) as a matrix operator representing the effective Hamiltonian and add the term  $U(\mathbf{r})$  to the diagonal elements. The Hamiltonian operator has matrix elements

$$H_{ij} = \sum_{\alpha} D_{ij}^{\alpha\beta} \left( -i \frac{\partial}{\partial x_{\alpha}} \right) \left( -i \frac{\partial}{\partial x_{\beta}} \right) - \lambda \epsilon_i \delta_{ij} + U \delta_{ij}, \quad (7-53)$$

and the envelope wave function is a vector  $\varphi_j$  which gives for the impurity function

$$\Phi \simeq \sum_j \varphi_j(\mathbf{r}) \psi_j(0, \mathbf{r}). \quad (7-54)$$

The problem is to solve the set of six (four if we neglect the spin-orbit split-off band) coupled differential equations

$$\sum_j \sum_{\alpha\beta} D_{ij}^{\alpha\beta} \left( -i \frac{\partial}{\partial x_{\alpha}} \right) \left( -i \frac{\partial}{\partial x_{\beta}} \right) \varphi_j - \lambda \epsilon_i \varphi_i + U(\mathbf{r}) \varphi_i = E \varphi_i. \quad (7-55)$$

Approximate solutions have been obtained using  $U(\mathbf{r}) = -e^2/\epsilon r$ , expanding  $\varphi_j$  in spherical harmonics with  $l \leq 2$  and using a functional form for the radial parts with coefficients to be determined by the variational principle.<sup>[41]</sup> The theoretical values which have been found for the ionization energy of the hole ground state are  $\sim 9$  meV in germanium and 34 meV in silicon, to be compared with the experimental values of  $\sim 11$  meV and 45–71 meV respectively, the range of values accounting for the observed chemical shifts. In silicon the discrepancy is considerable and is probably due to the neglect of central cell corrections. The excited states of silicon show better agreement with experiment but not such good agreement as in the case of donor states. Recently, Baldereschi and Lipari<sup>[41]</sup> used a more convenient method of solution by transforming

## ELECTRONIC STATES AND OPTICAL TRANSITIONS

(7-52) and correspondingly (7-55) into a spherically symmetric part and a much smaller cubic correction term proportional to  $\gamma_3 - \gamma_2$ , which can be treated by perturbation theory. Because of their predominantly spherical symmetric contribution, the acceptor states can be classified by their angular momentum and their envelope functions; they have been classified and computed in this way by Baldereschi and Lipari.<sup>[41]</sup> We report some of their results in Table 7-6.

TABLE 7-6. Ionization energies (meV) of acceptor impurities in the Coulomb-like approximation computed for some typical semiconductors. (From Baldereschi and Lipari<sup>[41]</sup>.) The values of the dielectric constants and of the band parameters are also given (from refs. [40] and [41]). Some experimental values are also given (from ref. [17]).

Crystal	$\epsilon_0$	$\gamma_1$	$\gamma_2$	$\gamma_3$	$E_{\text{ion}}(1S_{3/2})$	$E_{\text{ion}}(\text{exp})$
Si	11.4	4.22	0.39	1.44	31.6	6.89 (Al)
Ge	15.36	13.35	4.25	5.69	9.7	11.8 (Ga)
AlSb	12	4.15	1.01	1.75	42.4	
GaP	10.75	4.20	0.98	1.66	47.4	
GaAs	12.56	7.65	2.41	3.28	25.7	
InSb	17.9	35.08	15.64	16.91	8.6	
ZnS	8.1	2.54	0.75	1.09	175.6	

### 7-3e Band mixing and resonant states

Let us now consider a more general case where one must take into account a number of minima (maxima for a repulsive potential) in the band structure. The extrema can belong to different bands and have quite different energies or may be due to equivalent points when  $\mathbf{k}_c \neq 0$ . It has been shown that more than one minimum may be required to construct the bound state wave functions.<sup>[30]</sup> It has also been proved that the nature of the band structure may produce resonances in the continuum, which are quite different in origin from those predicted in ordinary scattering theory.<sup>[29,30]</sup>

We start from the integral formulation of (7-24), written in such a way as to automatically include the boundary conditions and the scattering states. The equation is

$$\varphi(\mathbf{k}) = \delta(\mathbf{k} - \mathbf{k}_0) - \int \frac{d\mathbf{k}' U(\mathbf{k}, \mathbf{k}') \varphi(\mathbf{k}')}{E(\mathbf{k}) - E - ie}, \quad (7-56)$$

where  $e$  is a positive infinitesimal quantity which goes to zero after the integration is performed, and  $U(\mathbf{k}, \mathbf{k}')$  is the Bloch transform of the impurity potential described in Section 7-3b. Following Bassani *et al*<sup>[30]</sup> we separate the domain of definition of the function  $\varphi(\mathbf{k})$  into a number of subzones each containing a minimum at a point  $\mathbf{k}_{ct}$ . Some (but not all) of these points will be points of the same star, the others will provide a contribution from different bands. The separations can be made so that all reciprocal space is covered and (7-56) will be reduced to a system of  $n$  coupled integral equations where  $n$  is the number of subzones.

For bound states the system becomes

$$\begin{aligned} [E(\mathbf{k}) - E] \varphi_i(\mathbf{k}) &= - \int_{\Omega_1} U_{i1}(\mathbf{k}, \mathbf{k}') \varphi_1(\mathbf{k}') d\mathbf{k}' \dots \\ &\quad - \int_{\Omega_i} U_{ii}(\mathbf{k}, \mathbf{k}') \varphi_i(\mathbf{k}') d\mathbf{k}' - \dots \int_{\Omega_n} U_{in}(\mathbf{k}, \mathbf{k}') \varphi_n(\mathbf{k}') d\mathbf{k}', \end{aligned} \quad (7-57)$$

where  $\varphi(\mathbf{k}) = \varphi_1(\mathbf{k})$  in  $\Omega_1$ ,  $\varphi(\mathbf{k}) = \varphi_i(\mathbf{k})$  in  $\Omega_i$ , and so on; and the matrix element  $U_{rs}(\mathbf{k}, \mathbf{k}')$  is defined for  $\mathbf{k}$  in the subzone  $\Omega_r$  and  $\mathbf{k}'$  in the subzone  $\Omega_s$ .

For a slowly varying potential, we can suppose that  $U_{rs}(\mathbf{k}, \mathbf{k}')$  is much smaller for  $r \neq s$  than for  $r = s$ . Consequently, to first order we can uncouple eq. (7-57) and obtain a set of independent homogenous equations

$$[E(\mathbf{k}) - E] \varphi_i^{(0)}(\mathbf{k}) = - \int_{\Omega_i} d\mathbf{k}' U_{ii}(\mathbf{k}, \mathbf{k}') \varphi_i^{(0)}(\mathbf{k}'), \quad (7-58)$$

each giving a set of eigenvalues  $E_{in}^{(0)}$  and a set of eigenfunctions  $\varphi_{in}^{(0)}(\mathbf{k})$ . Each eq. (7-58) can be transformed into the corresponding differential equation, and solved in the effective mass approximation (7-38) described in Section 7-3c.

These are the zero order solutions and can be used as a basis on which to expand the exact function  $\varphi(\mathbf{k})$ . We then have

$$\varphi(\mathbf{k}) = \sum_{i'n'} c_{i'n'} \varphi_{i'n'}^{(0)}(\mathbf{k}), \quad (7-59)$$

which can be substituted into (7-57). Multiplying the result by any of the states  $\varphi_{in}^{(0)*}(\mathbf{k})$ , integrating over  $\mathbf{k}$ , and taking into account the result at zero order and the orthogonality of the functions in  $\mathbf{k}$  space, we obtain for the coefficients  $c_{in}$  the secular system of equations

$$(E_{in}^{(0)} - E) c_{in} + \sum_{i' \neq i, n'} c_{i'n'} U_{in, i'n'} = 0, \quad (7-60 \text{ a})$$

where the terms

$$U_{in, i'n'} = \int d\mathbf{k} d\mathbf{k}' \varphi_{in}^{(0)*}(\mathbf{k}) U_{ii'}(\mathbf{k}, \mathbf{k}') \varphi_{i'n'}^{(0)}(\mathbf{k}') \quad (7-60 \text{ b})$$

give the contributions of the mixing of different subzones via the impurity potential. The eigenvalues are obtained as solutions of the secular determinant

$$|(E_{in}^{(0)} - E) \delta_{in, i'n'} + U_{in, i'n'} (1 - \delta_{ii'})| = 0. \quad (7-61)$$

The indices  $n$  and  $n'$  can be extended to the states of the continuum of every subzone so that we can include interactions between states of the continuum of one band and discrete states from a different minimum in the interaction (7-60b) between the two subzones.

Equation (7-61) is the basis for taking into account the contributions of all different minima to the energy states of an impurity. If the matrix elements  $U_{in, i'n'}$  of (7-60b) between different bands are non-negligible, we must consider interband mixing and the function  $\varphi(\mathbf{k})$  of eq. (7-59); consequently the impurity wave function (7-44) will then contain relevant contributions from minima of different bands.

The same type of reasoning can be extended to the case of scattering states. It has been proved<sup>[30]</sup> that an eigenvalue equation can still be written in the form of (7-61) even when  $E$  is degenerate with the continuum of a band  $E_{in}^{(0)} = E_i(\mathbf{k})$ , but in that case  $E$  has to be extended into the complex plane and the solutions of (7-61) will be complex. If we obtain solutions of the type  $E_0 - i\Gamma_0$ , with  $\Gamma_0 \ll E_0$ , the energy being measured from the band extremum, these solutions are resonances and correspond to large values of the scattering amplitude. The zero order solutions suggest that resonances are associated with secondary minima in the conduction band at energies higher than the absolute minimum. The bound states associated with secondary minima will be shifted and broadened when the interaction with the continuum of the lower band is

turned on; they will appear as resonant states unless the interaction with the states of the continuum is so strong that the broadening will make them merge into ordinary scattering states. The basic difference between this type of resonance and the type described in ordinary scattering theory<sup>[33]</sup> is that here it is due to secondary minima in the band structure, and the shape of the potential is of minor importance. A Coulomb potential, for instance, will have no resonances in ordinary scattering theory but may well have a resonance in crystals.

The amount of mixing of Bloch functions at different minima and the strength of the resonances are determined in each case by the separation between the absolute and the secondary minima and by the behaviour of  $E(\mathbf{k})$  near such minima (values of the effective masses if we expand to second order). To exemplify the discussion given above let us consider a hypothetical case of a band structure with two minima, one at  $\mathbf{k} = 0$  and the other at  $\mathbf{k} = \mathbf{k}_c$ , as shown in Fig. 7-6. Let us suppose that we have

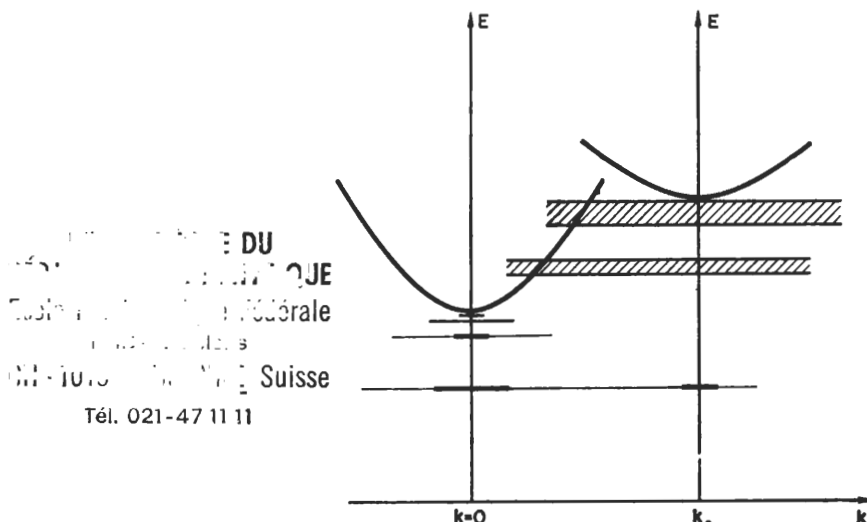


FIG. 7-6. Schematic model of a band structure with two minima at different values of  $k$  (conduction band structures of typical semiconductors and alkali-halide crystals). The bound and resonant states are indicated by lines and stripes respectively. Note: The bound states are indicated with horizontal lines whose length indicates the extent of  $k$  space covered by the envelope function  $\varphi(k)$ . The width of the stripes visualizes the effect of lifetime broadening.

solved the first order equation (7-58) for the bound states in the approximation of Section 7-3c for instance. We now wish to investigate what happens to the ground state of the secondary minimum  $E_{21}^{(0)}$  to first order when we turn on the interaction with the continuum of states  $E_{1k}^{(0)}$  only. Equation (7-61) becomes, in this case,

$$E_{21}^{(0)} - E = \int dk \frac{|U_{21}(\mathbf{k})|^2}{E(\mathbf{k}) - E}, \quad (7-62 \text{ a})$$

with

$$U_{21}(\mathbf{k}) = \int d\mathbf{k}' d\mathbf{k}'' \varphi_2^{(0)*}(\mathbf{k}') U_{21}(\mathbf{k}', \mathbf{k}'') \varphi_1^{(0)}(\mathbf{k}''). \quad (7-62 \text{ b})$$

The above equation admits complex solutions for  $E$  in the lower half of the complex plane and, if the interaction (7-62 b) is not too strong or the density of states of the band at  $E(\mathbf{k}) = E$  is not too large, the solution corresponds to a resonance with a width determined by the imaginary part. A more detailed analysis of the connection between scattering states and resonant states is given in ref. [32]. It may be a good exercise to see how the above concepts are visually displayed in Fig. 7-6.

The above illustration is still quite far from reality for two reasons. Firstly, because we must include interaction between the bound states of the absolute minimum and the states of the secondary minima. Secondly, because if the secondary minimum is away from the centre of the Brillouin zone, we must include the intervalley interaction described in the preceding section. Since the intervalley interaction gives the splitting of a degeneracy, its effect on the energy is usually larger unless the energy separation between the minima is very small. As a result of intervalley interaction, resonant states as well as bound states will classify according to the symmetry of the lattice. Detailed

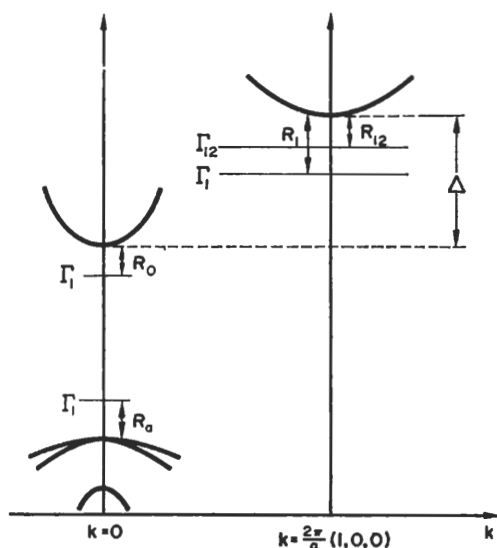


FIG. 7-7. Schematic indication of lowest impurity states for donors and acceptors in a typical III-V compound (GaAs) (from ref. [31] and [41]). The important states are also indicated. Note: The diagram is not to scale, but the relevant energy separations are  $\Delta = 0.36$  eV,  $R_0 = 5.5$  meV,  $R_1 = 67.3$  meV,  $R_{12} = 66.85$  meV,  $R_a = 9.9$  meV.

calculations with the above procedure have been performed on the ground states and resonant states of donors in gallium, arsenide, and germanium and also on the  $F$  centres in alkali-halide crystals.<sup>[31]</sup> The results obtained indicate a mixing between bands which depends on the separation between the absolute and the secondary minima. To illustrate the concepts above, we give in Fig. 7-7 a schematic diagram of the band structure of GaAs and indicate the position and symmetry of acceptor and donor ground states and of the lowest donor resonant states. We provide also the numerical values of the

computed states though they are not sufficiently accurate to afford a good comparison with experiment. Although the general line to follow is laid down, the computation of impurity states taking into account interband mixing and deviation from Coulomb-like behaviour of the potential is still a problem for future research.

We may mention that recent experiments quoted in ref. [19] give evidence of electron transitions from the principal minimum of the conduction band to resonant impurity states below  $X_1$  in InP, just as expected from the situation schematically shown in Fig. 7-7. In zincblende type compounds we may recall from Section 4-1 that we have another minimum  $X_3$  above the secondary minimum  $X_1$  at the point  $X$  of the Brillouin zone and consequently we expect two sets of impurity levels—one for each minimum. This has been observed by Onton<sup>[19]</sup> and is due to interband mixing at the same point of the reduced zone; the nature of this resonance is more similar to the acceptor resonant state schematically shown in Fig. 7-5, and experimentally observed (ref. [18]).

#### 7-4 Intermediately bound impurity states. Isoelectronic impurities

We here wish to mention the case when the impurity wave function (7-20) is considerably localized in real space so that the type of approach used in the last section can hardly be justified. This occurs for deep impurity levels in semiconductors and in the case of isoelectronic substitutional impurities (like N substituting P in GaP). It is also the case for colour centres in ionic crystals, due to impurities like silver or to a cation vacancy (*F* centre).

In such cases the expansion in Wannier function (7-31) is a better representation to use, and attempts have been made to compute the energy levels by the Koster and Slater method in the one-band one-site approximation. The treatment develops along lines similar to the intermediate binding exciton case of Section 6-4, but is much simpler here because of the one-particle nature of the potential.

In the case of isoelectronic impurities one may or may not obtain bound states depending on the strength of the potential and on the width of band. When no bound states are obtained, the only effect of the impurities is to modify slightly the band structure, an effect which is felt only at high concentrations when we have mixed crystals and approach the situation of disordered materials. We do not consider such problems for which we refer the reader to more specific books and articles.<sup>[42]</sup> We are only interested in the states associated to individual impurities, and to find them when the potential is localized we go back to expression (7-24) and expand the Bloch functions in terms of Wannier functions only in the kernel (7-24b). If we retain only one term in the sum over lattice points (one site approximation) and considering only one band, the matrix element  $U_{cc'}(\mathbf{k}, \mathbf{k}')$  reduces to

$$U_{cc'}(0) \simeq \delta_{cc'} \int a_c^*(\mathbf{r}) U(\mathbf{r}) a_c(\mathbf{r}) d\mathbf{r} \simeq J \frac{\Omega}{(2\pi)^3}, \quad (7-63)$$

so that (7-24) becomes

$$(E - E_c(\mathbf{k})) \varphi(\mathbf{k}) \simeq J \frac{\Omega}{(2\pi)^3} \int_{BZ} \varphi(\mathbf{k}') d\mathbf{k}', \quad (7-64)$$

where the limitation to one band and to one site is rather drastic but could eventually be relaxed. From (7-64) we obtain, as a consistency condition for the term  $\int_{BZ} \varphi(\mathbf{k}') d\mathbf{k}'$ , the eigenvalue equation

$$1 = J \frac{\Omega}{(2\pi)^3} \int_{BZ} \frac{d\mathbf{k}}{E - E_c(\mathbf{k})}. \quad (7-65)$$

The analysis of the above equation can be performed as indicated by Faulkner,<sup>[43]</sup> and it is found that, in order to obtain a bound state solution of (7-65), the following relation must hold:

$$|J| > 1 \left/ \left( \frac{1}{E} \right) \right., \quad (7-66a)$$

where  $J$  measures the strength of the localized potential averaged on the Wannier function as in (7-63) and

$$\left( \frac{1}{E} \right) = \frac{\Omega}{(2\pi)^3} \int_{BZ} \frac{d\mathbf{k}}{E_c(\mathbf{k})} \quad (7-66b)$$

gives a measure of the averaged band energy. It appears that if a band is narrow a much smaller potential is needed to produce a bound state than if the band is wide. Here again the two combined effects of the band structure and the potential  $U(\mathbf{r})$  come into play, but the whole band is important, rather than a small region about the critical point. Detailed calculations in this framework have been recently carried out by Baldereschi and Hopfield,<sup>[43]</sup> who computed the value of  $J$  using a pseudopotential impurity potential  $U(\mathbf{r})$ , screened by a dielectric function which allows for local distortions. We report in Table 7-7 a comparison of the theoretical predictions and experimental

TABLE 7-7. Existence of bound states for a number of isoelectronic impurities in some semiconductors (from ref. [43])

Bound state	Material						
	Si:Ge	Si:Sn	GaP:As	GaP:Sb	GaP:Bi	ZnS:Tl	ZnS:Se
Theory	no	no	no	yes	yes	yes	no
Experimental	no		no	no	yes	yes	no

findings concerning the existence of bound states for some isoelectronic acceptor type impurities. These are, of course, preliminary results, and a lot of progress is expected in this field. For a more general and detailed analysis of the present situation concerning isoelectronic impurities we refer the reader to the excellent review by Gzaja,<sup>[44]</sup> where reference to other articles can be found.

At this point we should consider deep levels such as those which arise from impurities and vacancies in alkali-halide crystals or more generally in large gap insulators. These traps have taken the name of colour centres because transitions between their

levels occur in the visible region of the spectrum and give a colour to the otherwise transparent insulator. The theoretical study of those levels is still in general at a rather primitive stage. The reason is that they rarely are so tightly bound that the approach of Section 7-2 can be used (thallium activated samples may be such an example) and, on the other hand, the dielectric constants of these materials are small, so that the impurity potential is strong and the approach of Section 7-3 is unreliable. In addition the ionic polarization effects produce very strong central cell corrections which also depend on the distortion of the ions around the impurities and are difficult to take into account properly. The experimental amount of information is, however, enormous, but it must usually be interpreted on rather qualitative bases. It must be pointed out, nevertheless, that all the effects discussed in this chapter take place in colour centres as well, so that a common knowledge exists in the fields of colour centres and semiconductor impurities. Effects such as the resonances in the continuum and interband mixings have been first observed in colour centres<sup>[45]</sup> and were later extended to semiconductors. We will not dwell into this field any further, but may refer the reader to a couple of very good specialized books.<sup>[46]</sup>

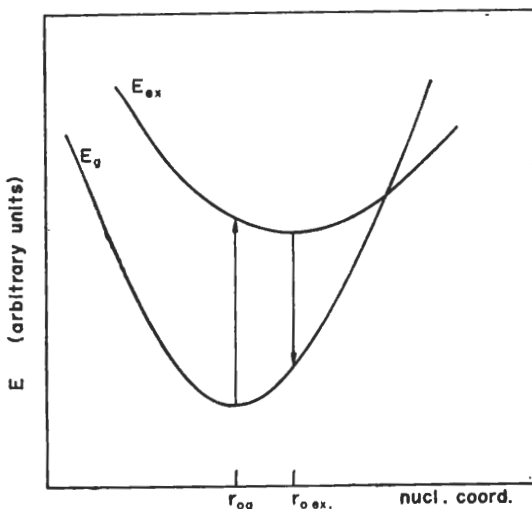


FIG. 7-8. Schematic Seitz plot of the electronic energy of a ground and of an excited impurity state versus the positions of the ions neighbouring the impurity. Observe that the non-crossing rule is expected to hold when vibrations are considered.

We wish at least to point out, however, that in ionic crystals the distortion of the lattice is strictly connected to the electronic level of the deep impurity, the equilibrium configuration being quite different for a ground state and for an excited state. This is a general situation which occurs every time the wave function is localized so that its corresponding energy is sensitive to small displacements of the neighbouring ions. It is visually well represented by the Seitz diagram which we show in Fig. 7-8 as an exemplification. For further details on this effect, which is also typical of excitons in ionic crystals, we refer the reader to a review article by Dexter.<sup>[47]</sup>

### 7-5 Considerations on optical transition processes involving impurities

We specifically mentioned in Section 7-2d the problem of electronic transitions between tightly bound impurity levels because we needed to consider the effect of the crystal field, but also that of the vibrations of the lattice to explain why forbidden transitions are observed.

In the effective mass approximation of Section 7-3b the transition probabilities between impurity states can be computed to first order by considering the matrix elements of the electron-photon interaction  $H_{eR} = (e/mc) \mathbf{A} \cdot \mathbf{p}$  between wave functions of type (7-44). Since the Bloch function is always the same, the contribution to the matrix elements comes from the envelope functions so that one can compute intensity ratios and selection rules from the envelope functions alone. In fact, as shown in the two previous chapters, the probability amplitude will be proportional to

$$a_{if} \simeq \int \varphi_i^*(\mathbf{r}) \psi^*(\mathbf{k}_0, \mathbf{r}) \mathbf{p} \varphi_f(\mathbf{r}) \psi(\mathbf{k}_0, \mathbf{r}) d\mathbf{r}, \quad (7-67)$$

where  $\mathbf{p}$  is the momentum operator taken in the direction of the electric field. Expression (7-67) can be decomposed into two contributions by operating on the two factors, and only one contribution is relevant so that

$$a_{if} \simeq \int |\psi(\mathbf{k}_0, \mathbf{r})|^2 \varphi_i^*(\mathbf{r}) \mathbf{p} \varphi_f(\mathbf{r}) d\mathbf{r}; \quad (7-68a)$$

because of the usual argument developed in Section 7-3b to justify the effective mass approximation,

$$a_{if} \simeq \int \varphi_i^*(\mathbf{r}) \mathbf{p} \varphi_f(\mathbf{r}) d\mathbf{r}. \quad (7-68b)$$

In the isotropic case we obtain the usual selection rules which apply in atomic physics. In the case of anisotropic uniaxial crystals the envelope function has cylindrical symmetry and we obtain different selection rules depending on the polarization of light with respect to the  $c$  axis,  $\Delta m = 0$  for linearly polarized light, and  $\Delta m = \pm 1$  for right or left circularly polarized light, the parity being changed with the transition. In the case of transitions originating in cubic crystals with minima away from  $\mathbf{k} = 0$ , all equivalent points contribute to the transition and cubic symmetry is restored. In the case of intervalley mixing the states are still classified according to the cubic symmetry, and the perturbation  $H_{eR}$  belongs to  $\Gamma_{15}$ , so that under no circumstances is dichroism present in cubic symmetry.

When band mixing occurs, the ground state of the impurity is formed by wave functions of type (7-20), where the contribution from different critical points is present as indicated in (7-59). As a consequence we may have optical transitions between the ground state and states associated to higher minima, which are resonant states in the continuum. By substituting (7-20) into the amplitude probability we obtain, instead of (7-68), the expression

$$a_{if} \simeq \int d\mathbf{k} \varphi_i^*(\mathbf{k}) \varphi_f(\mathbf{k}) C(\mathbf{k}), \quad (7-69a)$$

where

$$C(\mathbf{k}) \simeq \int d\mathbf{r} \psi_{in}^*(\mathbf{k}, \mathbf{r}) \mathbf{p} \psi_{fm}(\mathbf{k}, \mathbf{r}) \quad (7-69b)$$

if we consider contributions originating from different points of the Brillouin zone, and

$$C(\mathbf{k}) \simeq \int d\mathbf{r} \psi_{in}^*(\mathbf{k}, \mathbf{r}) \mathbf{p} \psi_{fm}(\mathbf{k}, \mathbf{r}) \quad (7-69c)$$

if we consider contributions originating from different bands at the same  $\mathbf{k}$  point. Interband mixing in the ground state is required to have transitions to resonant states,

## ELECTRONIC STATES AND OPTICAL TRANSITIONS

as shown in Fig. 7-6, because otherwise the integral over  $\mathbf{k}$  space (7-69a) would be zero because  $\varphi_i^*(\mathbf{k})$  would not overlap at all in  $\mathbf{k}$  space with  $\varphi_f(\mathbf{k})$ .

Until now we have considered transitions between impurity levels, but we may easily extend (7-69) to the continuum to obtain a transition probability from localized impurity states to the band states of the continuum, or vice versa. If the effective mass approximation is valid we can have transitions only to a continuum very near the critical point because one of the two  $\varphi(\mathbf{k})$  is extremely localized in a small region of  $\mathbf{k}$  space and that is the only region which contributes to (7-69). On the contrary, when the impurity wave function is localized in space, as is the case for isoelectronic impurities, we may have transitions to a large number of points of the Brillouin zone because the impurity envelope wave function extends in  $\mathbf{k}$  space and the integral (7-69a) includes contributions from a large number of  $\mathbf{k}$  values. This is the reason why, for instance, one can have zero phonon indirect transitions between an acceptor localized level near  $\Gamma$  and minima in the conduction band at  $X$ .

Before closing this chapter we must mention a very important phenomenon which takes place when light is emitted or absorbed (usually emitted) between two different impurities—a donor and an acceptor—which are close enough that their wave functions may overlap and a tunnelling process can take place. The suggestion that recombination of donor–acceptor pairs takes place has been made by Williams to explain the luminescence of ZnS but has been later verified in most semiconductors where large number of emission lines were observed.<sup>[48]</sup> More recently it has been demonstrated in GaP that a very large number of emission lines can be interpreted<sup>[49]</sup> by taking into account the Coulomb interaction between donor and deep acceptor centres after recombination with the expression

$$\hbar\omega = E_d - E_a - E_c + \frac{e^2}{\epsilon R}, \quad (7-70)$$

where  $E_d$  and  $E_a$  denote the absolute values of the donor and acceptor states binding energies, and  $R$  indicates all possible lattice separations between pairs. We will not dwell any further into this active field for which we refer the reader to specialized articles.<sup>[44, 50]</sup>

To conclude this chapter we wish to mention that, in considering transitions between localized states, account must be taken of the effect of the nuclear positions on the electronic energies, or in other words, of the phonon contribution to the total energy of a given electronic state. This is done by assuming that during the absorption the nuclear positions do not have time to change, but before emission they have relaxed to the equilibrium position appropriate to the excited state and the electron energy has changed. This is known as the Frank–Condon principle and is visually indicated in Fig. 7-8 to explain the large red shift of the luminescence for deep impurity states, particularly in ionic crystals.<sup>[47]</sup> Such an effect is not confined to impurity states. Also excitons can change their energy after formation because of lattice relaxation, thus becoming self-trapped; as a consequence the luminescence frequency of exciton annihilation shows a red shift with respect to the excitation frequency. This effect is particularly strong in ionic crystals because of the large interaction of the electrons with the optical phonons. To exemplify the type of problems here involved we refer the reader to some recent experimental results for the case of CsI,<sup>[51]</sup> whose exciton states we discussed in Section 6-3d.

## References and notes

- [1] See, for instance: M. HAMERMESH, *Group Theory and its Applications to Physical Problems* (Addison-Wesley, 1962); R. S. KNOX and A. GOLD, *Symmetry in the Solid State*, (Benjamin, New York, 1965).
- [2] H. A. BETHE, *Annln. Physik* **3**, 133 (1929).
- [3] W. OPECHOWSKI, *Physica* **7**, 552 (1940).
- [4] W. LOW, Paramagnetic resonance in solids, in *Solid State Physics* (edited by H. EHRENREICH, F. SEITZ and D. TURNBULL, Academic Press, 1960), Suppl. 2.
- [5] W. DE WETTE and B. R. A. NIJBOER, *Physica* **23**, 309 (1957).
- [6] See, for instance: G. BURNS, *Phys. Rev.* **128**, 2121 (1962); M. T. HUTCHINGS and D. K. RAY, *Proc. Phys. Soc. (London)* **81**, 633 (1963).
- [7] See, for instance, E. M. CONDON and G. H. SHORTLY, *The Theory of Atomic Spectra* (Cambridge University Press, 1967).
- [8] G. VETRI and F. BASSANI, *Nuovo Cimento* **55B**, 504 (1968).
- [9] D. S. MCCLURE, Electronic spectra of molecules and ions, in *Solid State Physics* (edited by H. EHRENREICH, F. SEITZ, and D. TURNBULL, Academic Press, 1969), vol. 9, p. 399.
- [10] M. T. HUTCHINGS, Point charge calculations of energy levels of magnetic ions in crystalline electric fields, in *Solid State Physics* (edited by H. EHRENREICH, F. SEITZ, and D. TURNBULL, Academic Press, 1954), vol. 16, p. 227.
- [11] J. H. VAN VLECK, *J. Chem. Phys.* **7**, 72 (1939); J. H. VAN VLECK, *J. Chem. Phys.* **8**, 790 (1940).
- [12] F. C. VON DER LAGE and H. A. BETHE, *Phys. Rev.* **71**, 612 (1947); D. G. BELL, *Rev. Mod. Phys.* **26**, 311 (1964); S. L. ALTMANN and C. J. BRADLEY, *Rev. Mod. Physics* **32**, 33 (1965).
- [13] D. L. WOOD and W. KEISER, *Phys. Rev.* **130**, 945 (1963).
- [14] C. J. BALLHAUSEN, *Introduction to Ligand Field Theory*, (McGraw-Hill, New York 1962).
- [15] W. KOHN, Shallow impurity states in Si and Ge, in *Solid State Physics* (edited by H. EHRENREICH, F. SEITZ and D. TURNBULL, Academic Press, New York, 1957), vol. 5.
- [16] R. L. AGGARWAL, P. FISHER, V. MOURZINE, and A. K. RAMDAS, *Phys. Rev. Letters* **4**, 173 (1960); J. H. REUSZER and P. FISHER, *Phys. Rev.* **135**, A 1125 (1964); R. L. AGGARWAL and A. K. RAMDAS, *Phys. Rev.* **137**, A 602 (1965); B. T. ALBURN and A. K. RAMDAS, *Phys. Rev.* **167**, 717 (1968).
- [17] P. FISHER and H. Y. FAN, *Phys. Rev. Letters* **2**, 456 (1959); R. L. JONES and P. FISHER, *J. Phys. Chem. Solids* **26**, 1125 (1965); A. ONTON, P. FISHER, and A. K. RAMDAS, *Phys. Rev.* **163**, 686 (1967); R. J. STIRN and W. M. BECKER, *Phys. Rev.* **148**, 907 (1966); B. T. ALBURN and A. K. RAMDAS, *Phys. Rev.* **187**, 932 (1969); P. J. DEAN, C. J. FROSH, and C. H. HENRY, *J. Applied Phys.* **39**, 563 (1968).
- [18] S. ZWERDLING, K. J. BUTTON, B. LAX, and L. M. ROTH, *Phys. Rev. Letters* **4**, 173 (1960); A. ONTON, P. FISHER, and A. K. RAMDAS, *Phys. Rev.* **163**, 868 (1967).
- [19] B. B. KOSICKI and W. PAUL, *Phys. Rev. Letters* **17**, 246 (1966); W. PAUL, *Proceedings of the IX International Conference on the Physics of Semiconductors*, (Publishing House Nauka, Moscow, 1968), vol. I, p. 16; A. ONTON, *Phys. Rev. B* **4**, 4449 (1971); A. ONTON, Y. YACOBY, and R. J. CHICOTKA, *Phys. Rev. Letters* **28**, 966 (1972).
- [20] R. PEIERLS, *Z. Physik* **80**, 763 (1933).
- [21] G. WANNIER, *Phys. Rev.* **52**, 191 (1937).
- [22] E. N. ADAMS, *J. Chemical Phys.* **21**, 2013 (1937).
- [23] C. KITTEL and A. H. MITCHELL; *Phys. Rev.* **96**, 1488 (1954).
- [24] J. M. LUTTINGER and W. KOHN, *Phys. Rev.* **97**, 869 (1955); W. KOHN and J. M. LUTTINGER, *Phys. Rev.* **98**, 915 (1955).
- [25] G. A. PETERSON, *Proceedings of VII International Conference on the Physics of Semiconductors* (Dunod, Paris, 1964), p. 771.
- [26] G. IADONISI and B. PREZIOSI, *Phys. Status Solidi* **37**, 281 (1970).
- [27] G. F. KOSTER and J. C. SLATER, *Phys. Rev.* **96**, 439 (1954). See also the Appendix 2 in the book *Insulator, Semiconductors and Metals* by J. C. SLATER (McGraw-Hill, New York 1967).
- [28] L. LIU and D. BRUST, *Phys. Rev.* **157**, 627 (1967).
- [29] J. CALLAWAY, *J. Math. Phys.* **5**, 783 (1964).
- [30] F. BASSANI, G. IADONISI, and B. PREZIOSI, *Phys. Rev.* **186**, 735 (1969).
- [31] M. ALTARELLI and G. IADONISI, *Nuovo Cimento* **5B**, 21 and 36 (1971); M. COSTATO, F. MANCINELLI, and L. REGGIANI, *Solid State Commun.* **9**, 1335 (1971).

## ELECTRONIC STATES AND OPTICAL TRANSITIONS

- [32] F. BASSANI, G. IADONISI, and B. PREZIOSI, Electronic impurity levels in semiconductors, *Reports on Progress in Physics* (1974) to appear.
- [33] See, for instance: I. M. LIFSHITZ and M. I. KAGANOV, *Soviet Physics Uspekhi*, **1-L**, 831 (1959); B. A. LIPPMANN and J. SCHWINGER, *Phys. Rev.* **79**, 469 (1963); R. G. NEWTON, *Scattering Theory of Waves and Particles* (McGraw-Hill, New York, 1966). About the causality condition, see B. PREZIOSI, *Nuovo Cimento* **6B**, 131 (1971).
- [34] J. HERMANSON and J. C. PHILLIPS, *Phys. Rev.* **150**, 652 (1966); J. C. PHILLIPS, *Phys. Rev.* **1** 1540 (1970) and **1**, 1545 (1970) and related references.
- [35] R. A. FAULKNER, *Phys. Rev.* **184**, 713 (1969).
- [36] A. BALDERESCHI and M. DIAZ, *Nuovo Cimento* **68B**, 217 (1970); J. A. DEVERIN, *Nuovo Cimento* **63B**, 1 (1969) and related references.
- [37] A. MORITA and H. NARA, *J. Phys. Soc. Japan (Suppl.)* **21**, 234 (1966) and related references.
- [38] A. BALDERESCHI, *Phys. Rev.* **1B**, 4673 (1970) and related references. See also: T. G. CASTNER, *Phys. Rev.* **2B**, 4911 (1970); T. G. CASTNER, W. KÄNZIG, and T. O. WOODRUFF, *Phys. Rev. Letters* **8**, 13 (1962).
- [39] See, for instance, E. KANE, The  $k \cdot p$  method, in *Semiconductors and Semimetals* (edited by R. K. WILLARDSON and A. C. BEER, Academic Press, 1966), vol. 1, p. 75.
- [40] G. DRESSELHAUS, A. F. KIP, and C. KITTEL, *Phys. Rev.* **98**, 368 (1955); For valence and band parameters, see P. LAWAETZ, *Phys. Rev.* **B4**, 3460 (1971); J. M. LUTTINGER, *Phys. Rev.* **102**, 1030 (1956).
- [41] W. KOHN and D. SCHECTER, *Phys. Rev.* **99**, 1903 (1955); D. SCHECTER, *J. Phys. Chem. Solids* **23**, 237 (1962); K. S. MENDELSON and H. M. JAMES, *J. Phys. Chem. Solids* **25**, 729 (1964); A. BALDERESCHI and N. LIPARI, *Phys. Rev. Letters* **25**, 1660 (1970); *Phys. Rev.* **9B**, 1525 (1924); W. CZAJA, *Phys. Condens. Matter* **12**, 226 (1971).
- [42] See, for instance: I. M. LIFSHITZ, *Advances in Physics* **13**, 483 (1964); V. L. BONCH BRUEVICH, Effect of heavy doping in the semiconductor band structure, in *Semiconductors and Semimetals* (edited by R. K. WILLARDSON and A. C. BEER, Academic Press, 1966), vol. 1.
- [43] R. A. FAULKNER, *Phys. Rev.* **175**, 991 (1968); A. BALDERESCHI and J. J. HOPFIELD, *Phys. Rev. Letters* **28**, 171 (1972); and *Proceedings to the XI International Conference on the Physics of Semiconductors* (Warsaw, 1972).
- [44] W. CZAJA, Isoelectronic impurities in semiconductors, in *Festkörperprobleme* 65 (edited by O. MADELUNG, Vietweg, Braunschweig, 1971), vol. XI, p. 65.
- [45] G. CHIAROTTI and M. GRASSANO, *Nuovo Cimento* **46B**, 78 (1966); S. I. PECKAR, *Nuovo Cimento* **60B**, 291 (1969).
- [46] W. D. COMPTON and J. H. SHULMAN, *Colour Centres in Solids* (Pergamon, New York, 1962); W. B. FOWLER, *Physics of Colour Centres* (edited by W. B. FOWLER, Academic Press, New York, 1968).
- [47] See, for instance, D. L. DEXTER, Theory of the optical properties of imperfections in nonmetals, in *Solid State Physics* (edited by H. EHRENREICH, F. SEITZ and D. TURNBULL, Academic Press, New York, 1958), vol. 5.
- [48] J. S. PRENER and F. E. WILLIAMS, *Phys. Rev.* **101**, 1427 (1956); F. E. WILLIAMS, *J. Phys. Chem. Solids* **12**, 265 (1960); D. G. THOMAS, M. GERSHENZON, and F. A. TRUMBORE, *Phys. Rev.* **133**, A269 (1964).
- [49] P. J. DEAN, C. H. HENRY, and C. J. FROSH, *Phys. Rev.* **168**, 812 (1968).
- [50] See, for instance: P. J. DEAN, *J. Luminescence* **1**, 398 (1970); T. N. MORGAN and H. MAIER, *Phys. Rev. Letters* **27**, 1200 (1971); D. S. NEDZVETSKII, S. I. RADANTSAN, and YU. I. MAKSIMOV, *Fizika Iverd. Tela* **14**, 643 (1972) (English translation: *Sov. Phys., Solid State* **14**, 551 (1972)), and quoted references.
- [51] See, for instance: H. LAMATSCH, J. ROSSEL, and E. SAURER, *Phys. Status Solidi* **41**, 605 (1970); **48B**, 311 (1971); **49B**, 311 (1972).

SIQUE  
Fédérale  
Ecole Polytechnique  
CH - 1015 LAUSANNE Suisse  
Té.: 021-47 11 11

D  
Eu

CH - 915

Tél. 21 47 11 11

ISAN

## CHAPTER 8

### EFFECTS OF EXTERNAL PERTURBATIONS

#### 8-1 Introduction and general remarks

Just as the interpretation of the optical spectra in atomic spectroscopy was obtained from studies of the Stark and Zeeman effects,<sup>[1]</sup> the interpretation of the optical excitation spectrum in solids cannot be complete unless it is put to the test by applying external perturbations. The advantage of these studies is twofold. First of all the external perturbations are artificially produced and can be controlled and continuously varied, which is not the case for intrinsic perturbations like impurities or excitons discussed in the two previous chapters. Secondly, the effect of external perturbations can be predicted on the basis of the electronic structure as computed for the perfect lattice, and the comparison between theoretical prediction and experiment may be taken as a test of the accuracy of the electronic structure itself.

A further advantage, which although experimental in nature is nevertheless of great importance, concerns the possibility of producing periodic variations of the external perturbation and measuring physical quantities with the same phase and periodicity. In this way a direct measurement of the variation of a physical property due to the perturbation is obtained with an improvement of several orders of magnitude in the signal-to-noise ratio. Such a type of technique was first applied in the microwave region for paramagnetic resonance experiments, but it has recently become very popular in the optical region where it has quickly produced a number of very interesting results, particularly in non-metals. For further information on this topic we refer the reader to the excellent book by Cardona<sup>[2]</sup> and to some review articles,<sup>[3]</sup> while a summary of the basic developments and perspectives for future applications in this field will be found in the forthcoming *Proceedings of the First International Conference on Modulation Spectroscopy*.<sup>[3]</sup>

The external perturbations can be classified according to whether or not they change the symmetry of the Hamiltonian. Perturbations such as hydrostatic pressure do not modify the symmetry of the Hamiltonian; shifts of the electronic states occur, but all degeneracies and selection rules for electronic transitions remain unchanged. Perturbations such as uniaxial stresses, external electric fields, and magnetic fields do modify the symmetry of the Hamiltonian and therefore produce also splittings of degeneracies and change the selection rules.

The magnetic field is a particularly interesting type of perturbation for another reason besides the ones just mentioned. It introduces new quantizations of the electronic states which may produce a discrete spectrum in place of a continuous one. One only

## ELECTRONIC STATES AND OPTICAL TRANSITIONS

has to think of the Landau quantization of free electrons in a constant magnetic field to have an immediate example of the above effect.<sup>[4]</sup>

In the following sections we shall briefly examine the effects on the electronic structure of different types of perturbations and their implications to the optical properties. We shall not give a review of the enormous literature in this field, but will occasionally mention some specific results to illustrate our discussion.

### 8-2 Effect of hydrostatic pressure and alloying

A modification of the crystal lattice which does not change its symmetry properties can be obtained by applying hydrostatic pressure to the crystal. A pressure changes the lattice parameters and, hence, produces shifts of the electronic states in the crystal. For every single electron state with vector  $\mathbf{k}$  in the band  $n$ , one can define the pressure coefficient

$$C_p(\mathbf{k}, n) = \frac{\partial E_n(\mathbf{k})}{\partial p}$$

as the change of the band energy  $E_n(\mathbf{k})$  with pressure; equivalent expressions can be defined in terms of the lattice parameter when the compressibility is known. The pressure coefficient is in general different for different electronic states in the Brillouin zone and can have either sign.

Pressure provides a convenient technique for shifting the relative positions of some energy levels by a controlled amount.<sup>[5]</sup> In Table 8-1 we give the experimental pressure

TABLE 8-1. Pressure coefficients for relevant valence to conduction band transitions in some group IV and III-V semiconductors. The symbols  $v$  and  $c$  denote valence and conduction respectively (from ref. [5]).

Transition	Group IV element	Pressure coefficients in $10^{-6}$ eV/bar					
		Group III-V compound	Ge	Si	GaP	InAs	GaSb
$\Gamma_{25}^v \rightarrow \Gamma_2^c$		$\Gamma_{15}^v \rightarrow \Gamma_1^c$	13		11	10	14
$A_3^v \rightarrow A_1^c$		$A_3^v \rightarrow A_1^c$	7.5			7	7
$\Gamma_{25}^v \rightarrow \Gamma_{15}^c$				5	6		
$\Gamma_{25}^v \rightarrow L_1^c$		$\Gamma_{15}^v \rightarrow L_1^c$	5				$\sim 5$
$\Gamma_{25}^v \rightarrow A_1^c$		$\Gamma_{15}^v \rightarrow X_1^c$	-1.5	-1.5	-1.1		

coefficients of relevant valence to conduction band transitions for a number of semiconductors with diamond and zincblende structures. Every transition can be seen to be characterized by a typical pressure coefficient which is only slightly changed from one

substance to another. It is also evident that by applying sufficient pressure one can change the band extrema from one point of the Brillouin zone to another. For instance, the minimum of the conduction band of germanium (Fig. 4-4) will be at  $\Delta_1$ , as in silicon (Fig. 4-3), for pressures larger than  $\approx 50$  Kbar.

We can interpret the effect of pressure very well by using the knowledge that some energy levels depend more critically than others on small variations of the lattice parameter. This was first discussed by Herman<sup>[6]</sup> in connection with the OPW method. The variation of relevant energy levels with the lattice constant in germanium has been calculated by Bassani and Brust;<sup>[7]</sup> the conduction levels  $I'_2$  and  $L_1$  are found to be sensitive levels, whereas the level of the conduction state  $X_1$  is found to be insensitive to small changes in the crystal potential or lattice parameter.

In the case of group IV semiconductors it is easy to establish the connection between the symmetry of a level and its dependence on pressure by considering the pseudopotential approximation discussed at the end of Section 3-4. In this scheme, the diagonalization of the pseudopotential Hamiltonian

$$H_p = -\frac{\hbar^2}{2m} \nabla^2 + V_p \quad (8-1a)$$

amongst plane waves leads to a determinantal equation whose matrix elements  $M_{ij}$  are given by

$$M_{ij} = \langle W_{k_i} | H_p - E | W_{k_j} \rangle = \left( \frac{\hbar^2 k_i^2}{2m} - E \right) \delta_{ij} + \sum_{\mu} e^{-i(\mathbf{h}_i - \mathbf{h}_j) \cdot \mathbf{d}_{\mu}} V_{p,\mu}(\mathbf{h}_i - \mathbf{h}_j) \quad (8-1b)$$

where the notations used are the same as those of Section 3-4. The matrix element  $M_{ij}$  contains the Fourier transform of the pseudopotential with reciprocal lattice vector  $\mathbf{h}_i - \mathbf{h}_j$ . The dependence of  $V_p(|h|)$  on  $|h|$  is a typical function. As  $|h|$  increases,  $V_p(|h|)$  goes rapidly to zero because of the cancellation due to the orthogonality to core states discussed in Section 3-4, and it has been proved<sup>[8]</sup> that one can describe with sufficient accuracy the valence and conduction states of group IV semiconductors by assuming:

$V_p(|h|^2) = 0$  for  $(a/2\pi)^2 h^2 > 11$ , and by choosing appropriate values for  $V_p(3)$ ,  $V_p(8)$ , and  $V_p(11)$ . (For instance in germanium  $V_p(3) = -0.23$  Ry,  $V_p(8) = 0$ ,  $V_p(11) = 0.06$  Ry, and in silicon  $V_p(3) = -0.22$  Ry,  $V_p(8) = 0.04$  Ry,  $V_p(11) = 0.08$  Ry).

A schematic visualization of the pseudopotential Fourier transforms  $V_p(|h|)$  is shown in Fig. 8-1 for the case of germanium to show clearly the typical behaviour illustrated above. Cohen and Heine<sup>[8]</sup> give similar pseudopotential curves for a large number of substances and establish their connection to the resulting band structure. Such quantities can also be connected to Fourier transforms of pseudopotentials appropriate to free atoms as originally suggested by Heine and Abarenkov and discussed in Section 3-4; in this way one obtains the advantage that appropriate scaling of the value of  $\hbar$  and  $\Omega$  can give pseudopotential Fourier coefficients for the same atom in different compounds from a single curve of type (8-1).

To investigate how a change in the lattice constant influences a state of given symmetry, we use a number of symmetrized combinations of plane waves, construct the secular

## ELECTRONIC STATES AND OPTICAL TRANSITIONS

equation (8-1 b) with Hamiltonian (8-1 a), and, finally, we show how the eigenvalues change when

$$a \rightarrow a(1 - \delta), \quad (8-2 \text{ a})$$

and consequently when

$$V_p(h) \rightarrow V_p(h) + \Delta V_p(h). \quad (8-2 \text{ b})$$

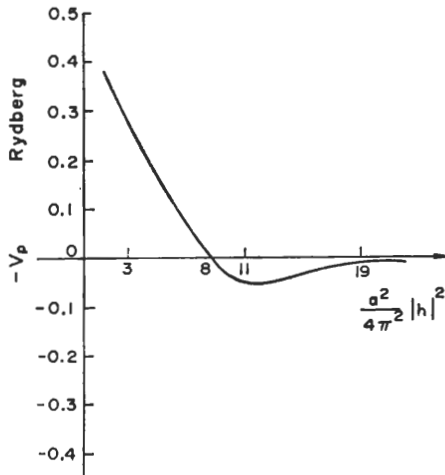


FIG. 8-1. Typical dependence of the pseudopotential Fourier transforms  $V_p(|h|)$  on  $|h|^2$  redundant, measured in units of  $(2\pi/a)^2$ . The case reported here refers to germanium (after Bassani and Celli, ref. [8]). The potential is given in the ordinate with opposite sign (in Rydberg units).

Calculations of this type have been made with considerable success.<sup>[7]</sup> We can appreciate the sort of results which we could expect by means of a simplified analysis. From Table 4-1 we can see that the state  $\Gamma'_{25}$  is formed mainly from combinations of plane waves of energy 3 and energy 4 (in units  $(\hbar^2/2m)(4\pi^2/a^2)$ ). Appropriate combinations of plane waves belonging to the same row of  $\Gamma'_{25}$  are obtained using the standard group theory procedures described in Sections 1-3 and 4-1; they are given by

$$\begin{aligned} & \frac{1}{\sqrt{8}} \{ \langle 111 \rangle + \langle 1\bar{1}\bar{1} \rangle + \langle \bar{1}1\bar{1} \rangle - \langle \bar{1}\bar{1}1 \rangle + \langle \bar{1}\bar{1}\bar{1} \rangle \\ & \quad + \langle \bar{1}11 \rangle + \langle 1\bar{1}1 \rangle - \langle 11\bar{1} \rangle \} \end{aligned} \quad (8-3 \text{ a})$$

and

$$\frac{1}{\sqrt{2}} \{ \langle 002 \rangle + \langle 00\bar{2} \rangle \}, \quad (8-3 \text{ b})$$

where  $\langle l_1 l_2 l_3 \rangle$  stands for

$$\langle l_1 l_2 l_3 \rangle = \frac{1}{\sqrt{(N\Omega)}} e^{i(2\pi/a)(l_1x+l_2y+l_3z)}.$$

The determinant equation obtained by diagonalizing the Hamiltonian (8-1) in the space of the symmetrized combinations of plane waves (8-3) is

$$\begin{vmatrix} 3 \frac{\hbar^2}{2m} \left( \frac{2\pi}{a} \right)^2 + V_p(0) - V_p(8) - E & \sqrt{2} [V_p(3) - V_p(11)] \\ \sqrt{2} [V_p(3) - V_p(11)] & 4 \frac{\hbar^2}{2m} \left( \frac{2\pi}{a} \right)^2 + V_p(0) - E \end{vmatrix} = 0, \quad (8-4a)$$

where  $V_p(g)$  indicates the Fourier transform of the atomic like pseudopotential with vector  $\mathbf{h}$  such that  $|\mathbf{h}|^2 = g(2\pi/a)^2$ . To study the position of the valence state  $\Gamma'_{2s}$  we should have included more symmetrized combinations of plane waves in addition to (8-3), but since our purpose is to determine qualitatively the change of the level  $\Gamma'_{2s}$  when the lattice parameter, and consequently the Fourier transforms, are changed, eq. (8-4a) is sufficient. We can calculate the change  $\Delta E_{\Gamma'_{2s}}$  of  $E_{\Gamma'_{2s}}$  with lattice parameter by substituting (8-2a) and (8-2b) into the lowest eigenvalue of (8-4a) and by expanding in terms of  $\delta$  and  $\Delta V_p(\mathbf{h})$ .

Similar simple results can be immediately obtained in the same way for other states of interest, in particular for the states  $\Gamma'_2$ ,  $X_1$ , and  $L_1$  of the lowest conduction band. We may show, for instance, that  $\Gamma'_2$  is given by the lowest root of the determinant equation

$$\begin{vmatrix} 3 \frac{\hbar^2}{2m} \left( \frac{2\pi}{a} \right)^2 + V_p(0) + 3V_p(8) - E & \sqrt{6} [V_p(3) + V_p(11)] \\ \sqrt{6} [V_p(3) + V_p(11)] & 4 \frac{\hbar^2}{2m} \left( \frac{2\pi}{a} \right)^2 + V_p(0) + 4V_p(8) - E \end{vmatrix} = 0, \quad (8-4b)$$

and  $X_1$  by the highest root of the determinant equation

$$\begin{vmatrix} \frac{\hbar^2}{2m} \left( \frac{2\pi}{a} \right)^2 + V_p(0) - E & \sqrt{2} V_p(3) \\ \sqrt{2} V_p(3) & 2 \frac{\hbar^2}{2m} \left( \frac{2\pi}{a} \right)^2 + V_p(0) + V_p(8) - E \end{vmatrix} = 0, \quad (8-4c)$$

always with corrections due to the contribution of higher plane waves, which, however, are not essential for our present purposes.

To estimate the pressure shifts of the energy levels we must decide how  $\Delta V_p(|\mathbf{h}|)$  of (8-2b) depends on  $\delta$  of (8-2a) and then substitute the new expressions in the secular equations. We can observe that the variations  $\Delta V_p(|\mathbf{h}|)$  tend to be positive under pressure for all the parameters involved, and in general, for pseudopotential curves with the shape of Fig. 8-1, the variation will be the largest near the point where the curve crosses the  $|\mathbf{h}|^2$  axis because its slope is larger. In fact, a simple scaling of the pseudopotential curve by changing  $|\mathbf{h}|^2$ , as would result from the assumption of atomic form factors, would shift it to the right, producing a positive  $\Delta V_p(|\mathbf{h}|)$  for the parameters of interest. The same result follows from explicating the dependence on  $a$  (lattice constant) of the attractive part and of the repulsive orthogonalization part of (3-37b) as done by Bassani and Brust, who computed the values of  $\Delta V_p(|\mathbf{h}|)$  as functions of  $\delta$ , and thus determined numerical values of the pressure coefficients  $C_p(n, \mathbf{k})$  for the case of germanium. The important thing we wish to remark here is that one can understand why

the pressure coefficient are nearly the same for the same symmetry states of different substances as shown in Table 8-1. The reason is that the qualitative behaviour of the various states for positive  $\delta$  and consequently positive values of  $\Delta V_p(|h|)$  is basically determined by their symmetry structure, as can be seen by considering a small number of plane waves. For instance, in the case of the states considered above we can solve eq. (8-4) and expand to low order in  $\delta$  and  $\Delta V_p(|h|)$ . We then obtain

$$\begin{aligned} \Delta E_{\Gamma_{25}'} &\simeq 7\delta \frac{\hbar^2}{2m} \left( \frac{2\pi}{a} \right)^2 + \Delta V_p(0) - \frac{\Delta V_p(8)}{2} \\ &- \frac{\left[ \frac{\hbar^2}{2m} \left( \frac{2\pi}{a} \right)^2 + V_p(8) \right] [2\delta + \Delta V_p(8)] + 8[V_p(3) - V_p(11)][\Delta V_p(3) - \Delta V_p(11)]}{\sqrt{\left[ \frac{\hbar^2}{2m} \left( \frac{2\pi}{a} \right)^2 + V_p(8) \right]^2 + 8[V_p(3) - V_p(11)]^2}}, \end{aligned} \quad (8-5a)$$

$$\begin{aligned} \Delta E_{\Gamma_2'} &\simeq 7\delta \frac{\hbar^2}{2m} \left( \frac{2\pi}{a} \right)^2 + \Delta V_p(0) + \frac{7}{2} \Delta V_p(8) \\ &- \frac{\left[ \frac{\hbar^2}{2m} \left( \frac{2\pi}{a} \right)^2 + V_p(8) \right] [2\delta + \Delta V_p(8)] + 24[V_p(3) + V_p(11)][\Delta V_p(3) + \Delta V_p(11)]}{\sqrt{\left[ \frac{\hbar^2}{2m} \left( \frac{2\pi}{a} \right)^2 + V_p(8) \right]^2 + 24[V_p(3) + V_p(11)]^2}}, \end{aligned} \quad (8-5b)$$

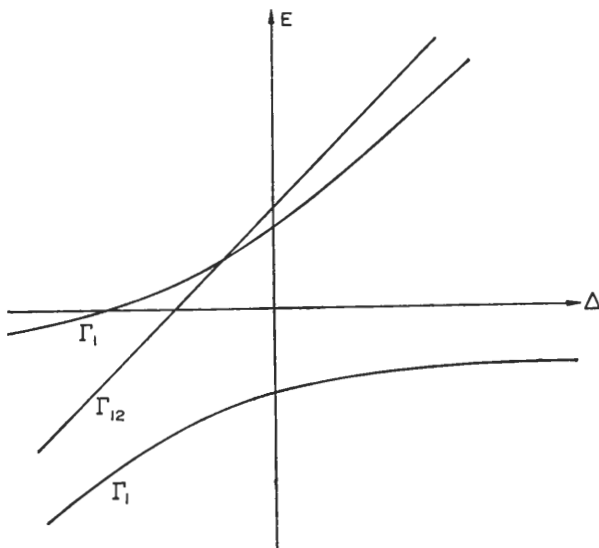
and

$$\begin{aligned} \Delta E_{X_1} &\simeq 3\delta \frac{\hbar^2}{2m} \left( \frac{2\pi}{a} \right)^2 + \Delta V_p(0) + \frac{\Delta V_p(8)}{2} \\ &+ \frac{\left[ \frac{\hbar^2}{2m} \left( \frac{2\pi}{a} \right)^2 + V_p(8) \right] [2\delta + \Delta V_p(8)] + 8V_p(3)\Delta V_p(3)}{\sqrt{\left[ \frac{\hbar^2}{2m} \left( \frac{2\pi}{a} \right)^2 + V_p(8) \right]^2 + 8[V_p(3)]^2}}. \end{aligned} \quad (8-5c)$$

When we substitute into the above expressions the values of  $\delta$  appropriate to a given pressure and the corresponding positive values of  $\Delta V_p(|h|)$ , we can find the energy shifts and, what is more important, the shifts relative to the positions of the top valence band  $\Gamma'_{25}$ . The most important relative contribution is  $\Delta V_p(8)$ , which gives a large positive shift for  $\Gamma'_2$ . The state  $X_1$  is nearly constant with respect to  $\Gamma'_{25}$  because the different contributions to  $\Delta E_{X_1} - \Delta E_{\Gamma_{25}'}$  tend to cancel. We notice, in particular, by subtracting (8-5a) from (8-5b), that the separation  $E_{\Gamma_2'} - E_{\Gamma_{25}'}$  increases with pressure with a pressure coefficient of the order of  $10 \times 10^{-6}$  eV/bar for all substances. By subtracting (8-5c) from (8-5a) we can see that the separation  $E_{X_1} - E_{\Gamma_{25}'}$  remains nearly constant with pressure, in qualitative agreement with the experimental results of Table 8-1.

We should like to point out that pressure also influences the shallow impurity states associated with band extrema in the Brillouin zone discussed in Section 7-3. In GaAs, for instance (see the band structure of Fig. 4-7), the ground state of donor impurities

is the state  $\Gamma_1$  associated with the principal minimum at  $\mathbf{k} = 0$ . Below the higher minimum  $X_1$  there is a resonant ground state split into the two states  $\Gamma_1$  and  $\Gamma_{12}$  by inter-valley interaction (see Section 7-3e). With increasing pressure, the separation  $\Delta$  between the principal minimum and the secondary minimum decreases down to negative values and the impurity states change their energy accordingly. A strong interaction takes place only between the two  $\Gamma_1$  states which cannot cross because they have the same symmetry, while the state  $\Gamma_{12}$  decreases linearly with increasing pressure. Detailed calculations have been performed by Altarelli and Iadonisi,<sup>[9]</sup> and their results are shown in Fig. 8-2 to illustrate the above considerations.



S.I. INSTITUÉ DU  
 DÉPARTEMENT DE PHYSIQUE  
 Ecole Polytechnique Fédérale  
 PHB - Ecublens  
 CH - 1015 LAUSANNE Suisse  
 Tél. 021-47 11 11

FIG. 8-2. Schematic representation of the dependence of bound and resonant states in GaAs on the separation  $\Delta$  between the principal minimum  $\Gamma_1$  and the secondary minimum  $X_1$ . For positive and large values of  $\Delta$  the lowest  $\Gamma_1$  is a bound state and the higher  $\Gamma_1, \Gamma_{12}$  are resonant states. As  $\Delta$  decreases we have appreciable band mixing and the role of the band extrema at  $X$  and at  $\Gamma$  in determining the wave function of the ground impurity state  $\Gamma_1$  is inverted. Such a decrease in  $\Delta$  can be obtained with pressure or alloying. (After Altarelli and Iadonisi, ref. [9].)

Another technique which also varies the lattice parameter consists in alloying one semiconductor with another. The lattice parameter of the alloy varies linearly with concentration and this has the most important effect on the band structure. In this case, however, the pseudopotential parameters also depend on the type of alloying element because of its intrinsic pseudopotential. In fact, Parmenter<sup>[10]</sup> has shown that to first order an alloy preserves the band structure of the perfect crystal with a new lattice constant and an average crystal potential. Bassani and Brust<sup>[7]</sup> performed detailed computations on the Si-Ge alloys and compared the effect of alloying with the effect of pressure. Already by comparing the pseudopotential parameters  $V_p(|\mathbf{h}|)$  given above for germanium and silicon, one can observe that their change going from germanium to silicon is qualitatively similar to that obtained by applying pressure to

## ELECTRONIC STATES AND OPTICAL TRANSITIONS

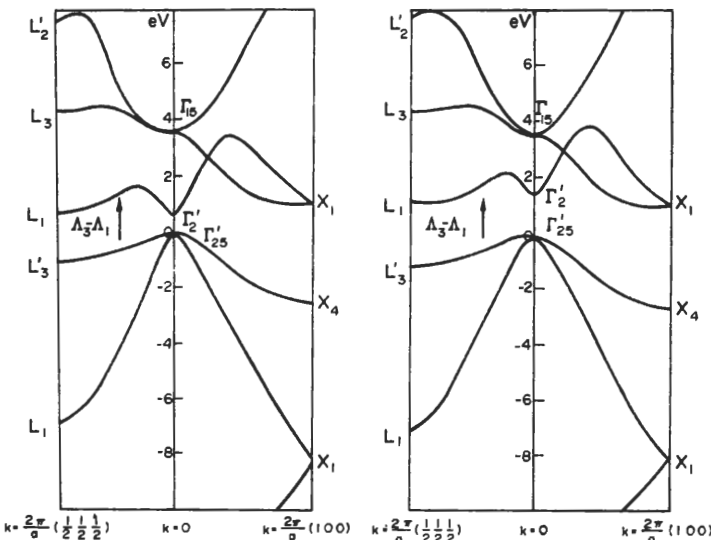


FIG. 8-3. Typical band structure of germanium alloyed with silicon. The case of pure germanium is given (on the left) and by comparison the case of the semiconductor alloy with 20 per cent silicon (on the right). All energies are referred to the top valence state  $\Gamma'_2$ . (After Bassani and Brust, ref. [7].)

germanium. It is not surprising, therefore, to find that the effect of alloying is rather similar to that of pressure. We show in Fig. 8-3 the band structure obtained with a 20 per cent silicon concentration in germanium and for comparison the band structure of pure germanium. The average pseudopotential has been obtained by interpolating between the pseudopotentials of germanium and silicon with the expression

$$V_p^{\text{alloy}}(|\hbar|) = V_p^{\text{Ge}}(|\hbar|)(1-x) + xV_p^{\text{Si}}(|\hbar|),$$

which is just the average potential as defined in the virtual crystal model<sup>[10]</sup>, where  $x$  denotes the concentration of silicon. The dependence of relevant energy states on pressure and on alloying for the case of germanium are given in Fig. 8-4. It can be observed that the sensitive levels  $\Gamma'_2$  and  $L_1$  are the only ones to be critically affected in both cases.

The results described in detail for germanium and silicon above can be easily extended to all zincblende structure semiconductors by considering also an antisymmetric part of the potential  $V_B(|\hbar|) - V_A(|\hbar|)$ , for the two atoms  $A$  and  $B$  of the unit cell as shown in Chapter 4. The explicit form of the matrix elements given in Table VIII of ref. [11] can be used, and similar considerations can be made. It is found in general that the symmetry of the energy states is the dominant factor in determining their sensitivity to pressure and alloying. When account is taken of both lattice parameter and pseudopotential magnitude, variation of the energy gap and of relevant band transitions from one compound to another one with the same symmetry can then be qualitatively understood. One can expect that as the lattice parameter decreases the direct gap and the transition  $L_3 \rightarrow L_1$  will increase so that the absolute minimum of the conduction band tends to shift to state  $X_1$  (as happens going from GaAs to GaP, for instance).

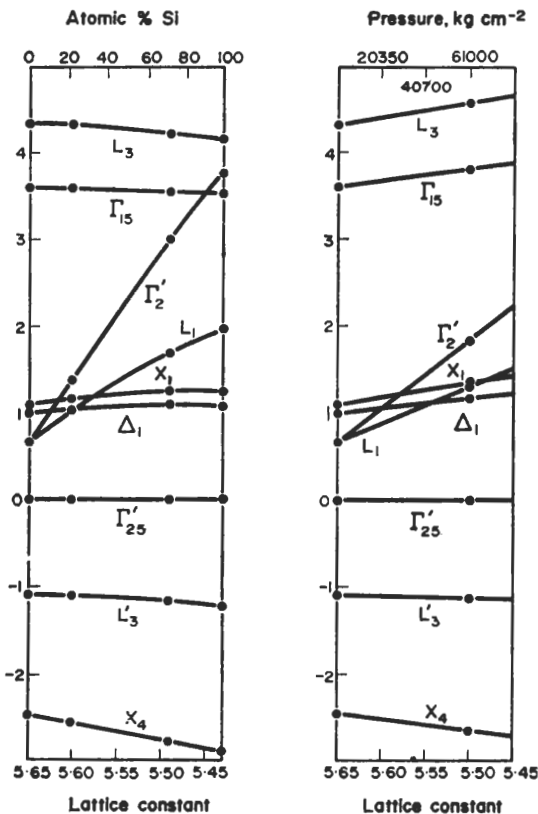


FIG. 8-4. Variation of the energies (in electron volts) of relevant electronic states in germanium as function of alloying (drawing on the left) and of pressure (drawing on the right). All levels are referred to the top of the valence band  $\Gamma'_{25}$ . (After Bassani and Brust, ref. [7].) Note: It can be observed that the sensitive states  $\Gamma'_2$  and  $L_1$  have similar behaviour with alloying and pressure. The energy gap behaviour is obtained by following the energy transition  $\Gamma'_{25} \rightarrow L_1$  and  $\Gamma'_{25} \rightarrow X_1$ .

Relativistic effects tend to decrease the pseudopotential parameters so that the gap decreases and one can obtain an inversion of the states  $\Gamma_6$  and  $\Gamma_8$  which produces zero gap semiconductors (HgTe and cubic tin, for instance, as shown in Section 4-4).

It should be mentioned that the virtual crystal model is valid only to first order of perturbation theory. To second order the presence of randomly distributed atoms of different kinds produces deviations from linearity in the dependence of the energy levels on the lattice parameter, and also produces a tail in the absorption coefficient below the gap.<sup>[12]</sup>

### 8-3 Effect of uniaxial stresses

Although hydrostatic pressure does not change the symmetry of the lattice, uniaxial stress will lower the symmetry of the system and consequently will produce splittings of otherwise degenerate states. The new symmetry of the crystal under stress depends

## ELECTRONIC STATES AND OPTICAL TRANSITIONS

furthermore on the direction in which the stress is applied, and this information can be used as a check of the nature of the critical point to which the optical transition has been attributed.

A uniaxial stress has two main effects on the energy band structure of a given crystal. First of all we notice that the small group of  $\mathbf{k}$  of the deformed crystal is a subgroup of the small group of  $\mathbf{k}$  of the undeformed crystal. At a given  $\mathbf{k}$  vector the original states are split into a number of states as determined by the compatibility relations (Section 2-2) between the groups of  $\mathbf{k}$  for the deformed and undeformed crystal. A second and perhaps more important effect is due to the change in the symmetry of the Brillouin zone, which changes the number of points belonging to the same star of  $\mathbf{k}$ . In this case, when some  $\mathbf{k}$  points are no longer equivalent, an additional splitting may be produced upon application of the stress. Quantitatively the effect of a unidirectional stress can be computed from an energy band calculation by placing the nuclei in the new equilibrium positions.

As an example let us consider the case of a cubic crystal with symmetry operations given in Table 2-3. If the stress is applied along one of the cubic axes, for instance the  $x$ -axis, the symmetry group of the deformed crystal is given by the operations of Table 2-3 which change  $x$  into itself or into  $-x$ . In this situation the symmetry group of the deformed crystal is  $D_{4h}$ . If the stress is applied along one of the cube diagonals the subgroup invariant under stress is  $D_{3d}$  and is obtained from Table 2-3 by considering the operations which interchange the axes ( $x, y, z$ ) amongst themselves and their products with the inversion. At the point  $\Gamma(\mathbf{k} = (0, 0, 0))$  the splitting effect of pressure on degenerate levels can be established by considering the compatibility relations between the irreducible representations of the group  $O_h$  (Table 1-4) and the irreducible representations of the group  $D_{4h}$  (Table 1-8) or  $D_{3d}$  (Table 1-6) for stress along one cubic axis or a cubic diagonal respectively. We notice immediately that all states of degeneracy 3 will split since no irreducible representation of order 3 is possible in the new symmetry groups. At other symmetry points away from the centre of the Brillouin zone, besides the eventual splitting of the energy bands, we have to take into account the change in the symmetry of the Brillouin zone. For instance in the undeformed cubic crystal the six vectors  $(k_0, 0, 0)$ ,  $(\bar{k}_0, 0, 0)$ ,  $(0, k_0, 0)$ ,  $(0, \bar{k}_0, 0)$ ,  $(0, 0, k_0)$ ,  $(0, 0, \bar{k}_0)$  are all equivalent. If we apply a stress in the  $x$  direction the vectors

$$(k_0, 0, 0), (\bar{k}_0, 0, 0) \quad (8-6a)$$

are no longer equivalent to the other four vectors

$$(0, k_0, 0), (0, \bar{k}_0, 0), (0, 0, k_0), (0, 0, \bar{k}_0). \quad (8-6b)$$

If we apply a stress along a cube diagonal, the six vectors of (8-6a, b) belong again to the same star, and the corresponding band energies are the same.

All the above considerations have been tested in great detail by optical piezoabsorption at the transition edge and by piezoreflectance measurements at the other critical points. The interpretation of the absorption edge in germanium and silicon with the minima of the conduction band at the point  $L$  and along the  $\Delta$  direction, respectively, has been fully confirmed also by this technique.<sup>[12]</sup>

We now wish to briefly discuss the effect of uniaxial stresses on the exciton states and impurity states considered in Chapters 6 and 7 respectively. In the case of tightly bound states we can consider the small change produced on the lattice by the applied stress as a further perturbation with reduced symmetry. If we consider, for instance,

## EFFECTS OF EXTERNAL PERTURBATIONS

the crystal field splitting of  $d$  states described in Section 7-2, we notice that a uniaxial stress will produce a further splitting of the threefold degenerate state  $\Gamma'_{2s}$ . In the case of shallow impurity states or of weakly bound excitons, we must first of all consider the effects on the band structure. Then we must examine the consequences of this on the bound states originating from the different critical points. In the case of shallow impurity states in silicon with stress applied in the  $x$  direction, for example, we shall

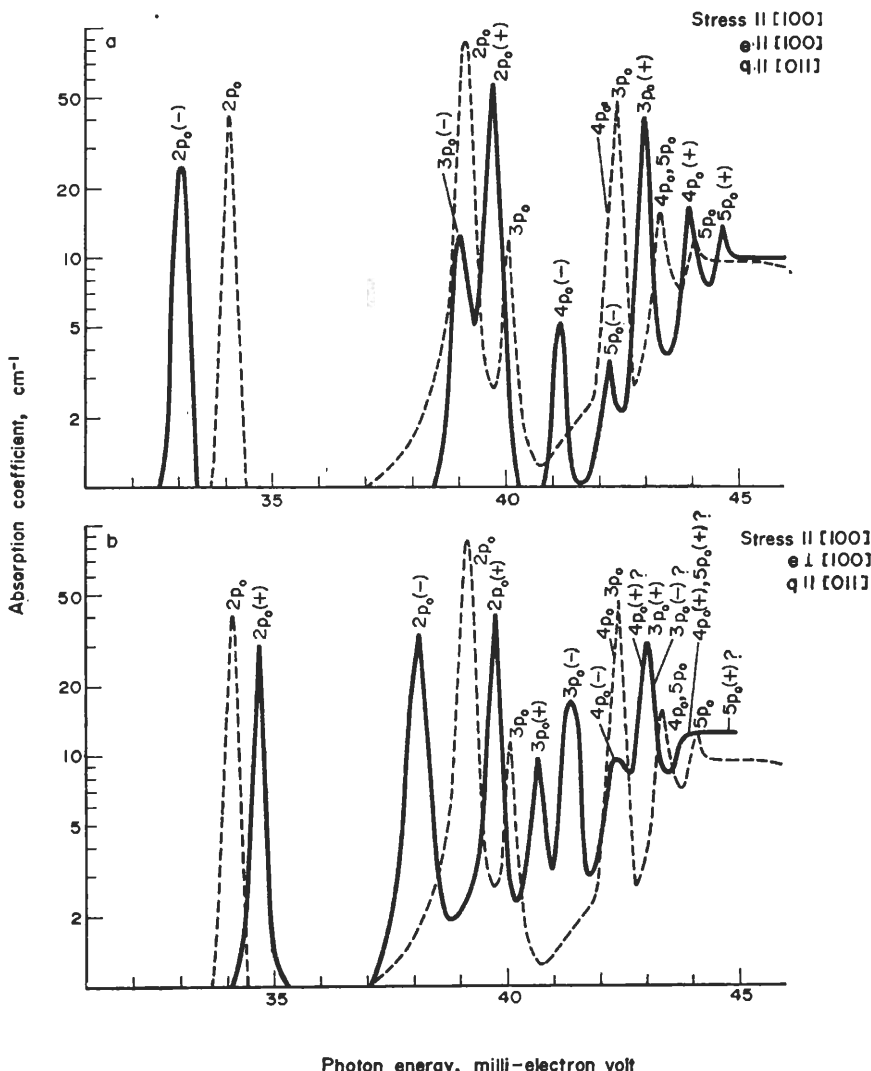


FIG. 8-5. Excitation spectrum of the donor phosphorus in silicon under uniaxial stress in the [100] direction;  $e$  and  $q$  denote the vectors of polarization and propagation of light respectively. The excitation spectrum for zero stress is indicated by dashed lines. (After Aggarwal and Ramdas, ref. [13].) Note the splitting of the effective mass states, due to the separation of equivalent minima, and observe the role of polarization dependent selection rules.

## ELECTRONIC STATES AND OPTICAL TRANSITIONS

have two sets of effective mass equation—one relative to the minima

$$(k_0, 0, 0), \quad (\bar{k}_0, 0, 0),$$

and one relative to the other four minima

$$(0, k_0, 0), \quad (0, \bar{k}_0, 0), \quad (0, 0, k_0), \quad (0, 0, \bar{k}_0),$$

which are now displaced in energy because of stress. Consequently the impurity states are split by the stress into two states of degeneracy 2 and 4. If the stress is applied along a cube diagonal, the six minima (8-6 a, b) are still equivalent and the impurity states are not split. We shall therefore obtain only a small shift of the energy in this case.

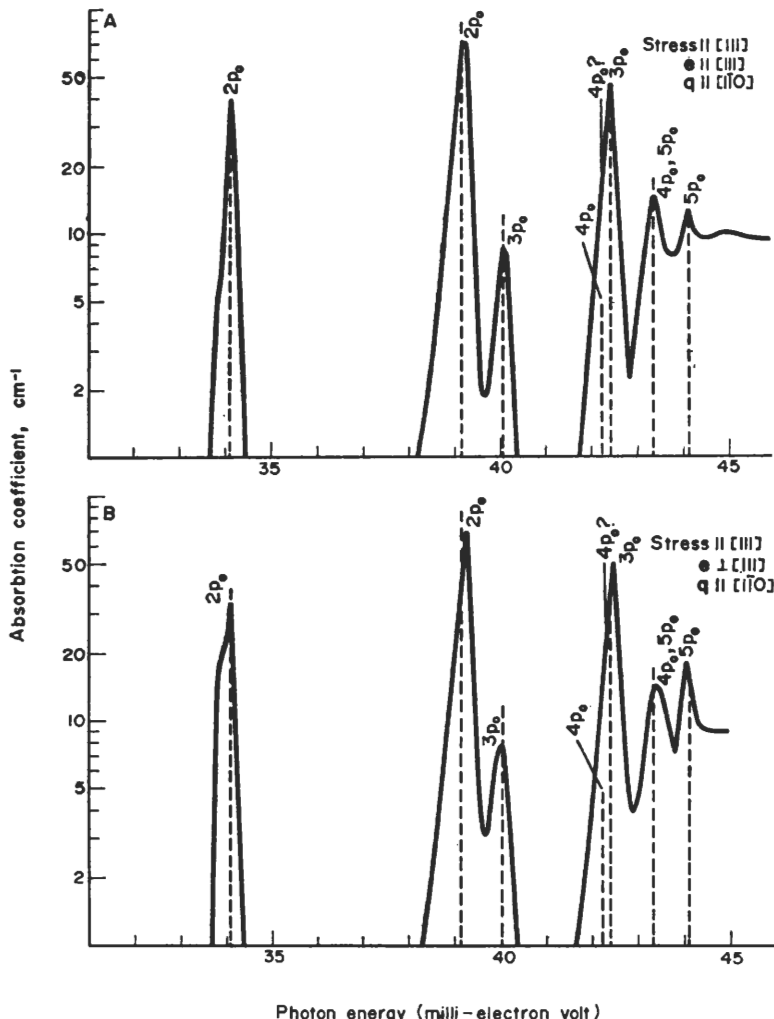


FIG. 8-6. Excitation spectrum of the donor phosphorus in silicon under uniaxial compression in the [111] direction;  $e$  and  $q$  denote the vectors of polarization and propagation of light respectively. The positions of the peaks in the excitation spectrum for zero stress are indicated by dashed lines. (After Aggarwal and Ramdas, ref. [13].) Note the absence of any splitting and of any polarization dependence.

From the many experiments performed we should like to mention those by Aggarwal and Ramdas<sup>[13]</sup> on the excitation spectrum of phosphorus impurity in silicon under compression. In Fig. 8-5 the excitation spectrum for impurity states in the presence of stress applied in the [1, 0, 0] direction is given. In Fig. 8-5(a) the polarization vector  $\mathbf{e}$  of the incident light is parallel to the stress; in Fig. 8-5(b)  $\mathbf{e}$  is perpendicular to the stress. By comparing the excitation spectrum for undeformed crystals, we find that for stress in the [1, 0, 0] direction, every excitation line  $1s \rightarrow np^{0,\pm 1}$  splits into two component lines with strong polarization effects; the splitting of the  $s \rightarrow p$  transitions is essentially due to the different energy shifts of the minima  $(k_0, 0, 0)$ ,  $(\bar{k}_0, 0, 0)$  with respect to the other minima  $(0, k_0, 0)$ ,  $(0, \bar{k}_0, 0)$ ,  $(0, 0, k_0)$ ,  $(0, 0, \bar{k}_0)$ .<sup>[13]</sup> The ground state  $1s(\Gamma_1)$  is practically unaffected by the small changes in the band structure while the excited states obey the effective mass equation (7-38) and follow the minima of the band. In Fig. 8-6 the excitation spectrum for impurity states of phosphorus in silicon with stress in the [111] direction is given. In this case no splitting occurs because the six valleys are still equivalent under stress.

Before closing this section on the effect of uniaxial stress on impurity states we would like to mention that the effect of stress is expected to be stronger the more the impurity potential and wave function are localized, because in this case the resulting binding energies are more strongly dependent on the arrangements of the nearest atoms or ions than on band shifts, as implied in the analysis of Section 7-4. In fact, particularly strong energy shifts and degeneracy splittings due to uniaxial stress have been recently observed in the case of electronic states bound to isoelectronic impurities and on the states of the  $F$  centre in alkali-halides. We refer the reader to the paper by Merz *et al.* and quoted references for further details on this point.<sup>[13]</sup>

## 8-4 Electronic states and optical constants of crystals in an electric field

### 8-4a General remarks

Another powerful tool in the investigation of energy band structure is a study of the effects of an external electric field. They were considered for some time as too small to be experimentally detected, but after the development of the technique of small modulations a tremendous amount of information has been obtained on a number of semiconductors by electroabsorption and electroreflectance measurements.<sup>[2,3]</sup>

An external electric field modifies the optical properties because it produces both a change in the electronic levels and a change in the transition probabilities. In the case of atomic spectroscopy the former is the important process, giving rise to the splitting of spectroscopic lines known as the Stark effect.<sup>[1]</sup> In crystals we are generally considering continuous states, and we may have a modification of the optical properties simply due to a change in transition probability. This effect, known as the Franz-Keldish effect,<sup>[14]</sup> was first discovered theoretically by them in 1958, and was later observed experimentally by a large number of other workers.<sup>[15]</sup> It can be thought of as a tunnelling<sup>[16]</sup> of an electron between the top of the valence band and the bottom of the conduction band due to the external electric field in the presence of a photon. In effect, all energies are possible for the electron in the presence of the electric field, and along the direction of the electric field the energy gap between valence and conduction

states is transformed into a triangular potential barrier whose height is the energy gap and whose width is  $z = E_G/(eF)$ , where  $F$  is the electric field. In the presence of a photon of energy  $h\nu$  the height of the effective barrier becomes  $E_G - h\nu$  and the tunnelling, or transition probability, to the conduction band depends exponentially on the above quantity. Consequently, even when  $h\nu < E_G$ , there is a finite transition probability for the electron to jump from the valence to the conduction band. This is the main effect on the optical properties of semiconductors which we can expect from an electric field.

The analogue of the Stark effect in crystals would be a change in the energy band structure due to the fact that the component of the wave vector  $\mathbf{k}$  in the direction of the electric field is no longer a quantum number. As a consequence, it can be proved that the energy should have a linear dependence on the electric field, with discrete states separated by  $Fea$ ,  $a$  being the lattice parameter.<sup>[17]</sup> Since the maximum values of the electric field one can use in crystals are of the order of  $10^5 \text{ V cm}^{-1}$  and  $a$  is of the order of an angstrom, the fine structure introduced by the electric field has a separation of about  $10^{-3} \text{ eV}$  and does not seem to be of any relevance, vibrational broadening being sufficient to eliminate such a structure. Callaway<sup>[17]</sup> has taken this effect into account in his discussion of the optical properties of crystals, but in the following we shall neglect it completely.

Another type of change in the band structure is only indirectly produced by the electric field. It is due to the displacements of the lattice ions to new equilibrium positions which in turn modify the electron eigenvalues according to the Born-Oppenheimer approximation. This effect is of relevance only in ionic crystals, and it becomes the dominant effect in ferroelectric crystals because the positions of the ions are shifted by large amounts by an electric field.<sup>[18]</sup>

In the following we shall confine our attention to the Franz-Keldish effect because it seems more directly related to the electronic band structure. After the original papers by Franz and Keldish,<sup>[14]</sup> extensions have been made and transitions have been considered at all critical points of the Brillouin zone. Seraphin and Hess<sup>[19]</sup> first observed oscillations in the reflectivity in correspondence to the  $M_1$  transition in germanium, and Phillips and Seraphin<sup>[20]</sup> interpreted the shape of the peak in terms of interband transitions in an electric field. Aspnes<sup>[21]</sup> has provided a general and very elegant method of computing field effects at all critical points using an extension of the Elliott<sup>[22]</sup> procedure (see Section 6-3c), previously adapted to the electric field problem by Tharmalingam.<sup>[23]</sup> Aymerich and Bassani,<sup>[24]</sup> within the framework laid down by Keldish,<sup>[14]</sup> obtained the same results and proved in addition why electric field effects occur only at critical points. They also considered the anisotropy with respect to the direction of the electric field and the dichroism in the absorption coefficient produced by the combined effect of all the equivalent critical points of the Brillouin zone. Extensions of the theory to treat indirect transitions have also been considered,<sup>[25]</sup> and detailed analysis of the role of field inhomogeneities near the surface has been developed by Frova and Aspnes.<sup>[26]</sup>

In the very last few years, as experiments became more and more precise, other effects which modify the line shape of the basic Franz-Keldish effect were considered, namely electron-hole interaction and lifetime broadening. For a detailed calculation of the electron-hole interaction effects we refer the reader to a recent analysis by Lao *et al.*<sup>[27]</sup> For a study of broadening effects in the low field limit, where an accurate line shape analysis has been shown to give a third derivative relationship between the unperturbed

dielectric function and its field induced change, we refer the reader to a number of papers<sup>[28]</sup> and particularly to the paper by Aspnes and Row.

We shall concentrate in the following mainly on the basic principles of the Franz-Keldish effect. For a detailed analysis of recent developments we refer the reader to the recent review article by Fisher and Aspnes.<sup>[29]</sup>

#### 8-4b Theory of electric field effects on interband transitions

The time dependent Schrödinger equation for an electron in a crystal in the presence of an electric field can be written as

$$[H_0 + e\mathbf{F} \cdot \mathbf{r}] \psi = i\hbar \frac{\partial \psi}{\partial t}, \quad (8-7)$$

where  $H_0$  is the crystal Hamiltonian,  $e$  is the modulus of the electron charge, and the displacements of nuclei due to the electric field have been neglected. The time evolution of the wave function, which at the time  $t = 0$  is the Bloch function  $\psi_n(\mathbf{k}_0, \mathbf{r})$ , is given by

$$\psi(\mathbf{r}, t) = e^{-i(Ht/\hbar)} \psi_n(\mathbf{k}_0, \mathbf{r}) \quad (8-8a)$$

with

$$H = H_0 + e\mathbf{F} \cdot \mathbf{r}. \quad (8-8b)$$

Following Houston,<sup>[17]</sup> an important property of  $\psi(\mathbf{r}, t)$  can be obtained by applying a crystal translation  $\tau$  to (8-8a). We obtain

$$\begin{aligned} \psi(\mathbf{r} + \tau, t) &= e^{-i(e\mathbf{F} \cdot \tau/\hbar)} e^{i\mathbf{k}_0 \cdot \tau} \psi(\mathbf{r}, t) \\ &= \exp\left[i\left(\mathbf{k}_0 - \frac{e\mathbf{F}}{\hbar} t\right) \cdot \tau\right] \psi(\mathbf{r}, t). \end{aligned}$$

The wave function (8-8a) is therefore a Bloch function at any time, but its  $\mathbf{k}$  vector has a time dependent component in the direction of the electric field

$$\mathbf{k}(t) = \mathbf{k}_0 - \frac{e\mathbf{F}}{\hbar} t. \quad (8-9)$$

Because of the above property we can always expand  $e^{-iHt/\hbar} \psi_n(\mathbf{k}_0, \mathbf{r})$  in Bloch functions with vector  $\mathbf{k}$  given by (8-9). If we make the further restriction that the band under consideration is well separated in energy from all the other bands so that "tunnelling" to other bands can be neglected, we have that

$$e^{-i(Ht/\hbar)} \psi_n(\mathbf{k}_0, \mathbf{r})$$

can differ at most by a phase factor from the Bloch function

$$\psi_n\left(\mathbf{k}_0 - \frac{e\mathbf{F}t}{\hbar}, \mathbf{r}\right).$$

We can thus write

$$\psi_n(\mathbf{k}, \mathbf{r}, t) \equiv e^{-iHt/\hbar} \psi_n(\mathbf{k}_0, \mathbf{r}) \simeq e^{-i\varphi(t)} \psi_n\left(\mathbf{k}_0 - \frac{e\mathbf{F}t}{\hbar}, \mathbf{r}\right) \quad (8-10)$$

## ELECTRONIC STATES AND OPTICAL TRANSITIONS

with  $\varphi(t)$  a real quantity and  $\varphi(0) = 0$ . In order to fix  $\varphi(t)$ , we differentiate the above equation with respect to time:

$$-\frac{iH}{\hbar} e^{-iHt/\hbar} \psi_n(\mathbf{k}_0, \mathbf{r}) \simeq -i \frac{d\varphi}{dt} e^{-i\varphi(t)} \psi_n\left(\mathbf{k}_0 - \frac{e\mathbf{F}t}{\hbar}, \mathbf{r}\right) - \frac{e\mathbf{F}}{\hbar} \frac{\partial}{\partial \mathbf{k}} \psi_n(\mathbf{k}, \mathbf{r}) e^{-i\varphi(t)},$$

with  $\mathbf{k}$  given by (8-9). Using (8-10),

$$-\frac{iH}{\hbar} \psi_n(\mathbf{k}, \mathbf{r}, t) \simeq -i \frac{d\varphi}{dt} \psi_n(\mathbf{k}, \mathbf{r}, t) - \frac{e\mathbf{F}}{\hbar} \frac{\partial}{\partial \mathbf{k}} \psi_n(\mathbf{k}, \mathbf{r}, t). \quad (8-11)$$

From (8-8b)

$$H\psi_n(\mathbf{k}, \mathbf{r}, t) = E_n(\mathbf{k}) \psi_n(\mathbf{k}, \mathbf{r}, t) + e\mathbf{F} \cdot \mathbf{r} \psi_n(\mathbf{k}, \mathbf{r}, t),$$

and (8-11) becomes

$$\frac{1}{\hbar} \left[ E_n(\mathbf{k}) + e\mathbf{F} \cdot \left( \mathbf{r} + i \frac{\partial}{\partial \mathbf{k}} \right) \right] \psi_n(\mathbf{k}, \mathbf{r}, t) \simeq \frac{d\varphi}{dt} \psi_n(\mathbf{r}, \mathbf{k}, t). \quad (8-12)$$

Substituting the expression (8-10), in the form

$$\psi_n(\mathbf{k}, \mathbf{r}, t) = e^{-i\varphi(t)} e^{i\mathbf{k} \cdot \mathbf{r}} u_{\mathbf{k}}(\mathbf{r}),$$

into (8-12), and neglecting the  $\mathbf{k}$  dependence of the periodic function  $u_{\mathbf{k}}(\mathbf{r})$

$$\frac{d\varphi(t)}{dt} = \frac{E_n(\mathbf{k})}{\hbar}.$$

Hence with (8-10) the important result follows that the solution (8-8a) of the time dependent Schrödinger equation (8-7) can be approximately written as

$$\psi_n(\mathbf{k}, \mathbf{r}, t) \simeq \exp \left[ -\frac{i}{\hbar} \int_0^t E_n(\mathbf{k}) dt \right] \psi_n(\mathbf{k}, \mathbf{r}), \quad (8-13)$$

with  $\mathbf{k}$  given by (8-9).

We can now determine the optical constants of a crystal in the presence of an electric field, using procedures similar to those of Section 5-1, by taking into account the time dependence of the solutions (8-13). In the dipole approximation, we obtain for the imaginary part of the dielectric function due to a pair of valence and conduction bands:

$$\epsilon_2(\omega, \mathbf{F}) = \frac{4\pi e^2}{\hbar m^2 \omega^2} \int_{BZ} \frac{d\mathbf{k}}{(2\pi)^3} |\mathbf{e} \cdot \mathbf{M}_{cv}(\mathbf{k})|^2 \frac{1}{T} \left| \int_0^T dt' \exp \left[ \int_0^{t'} \frac{i}{\hbar} (E_c(\mathbf{k}) - E_v(\mathbf{k}) - \hbar\omega) dt \right] \right|^2, \quad (8-14)$$

where  $T$  indicates a time sufficiently long with respect to the period of the radiation field  $2\pi/\omega$ , the notations are the same as those of (5-14), and the time integral replaces the  $\delta$  function of (5-14).

We notice that (8-14) reduces to the usual (5-14a) when the electric field is absent and  $\mathbf{k}$  does not depend on  $t$ . In fact in such a case the time integral in (8-14) can be immediately performed to give

$$\frac{1}{T} \left| \int_0^T dt' \exp \left[ \int_0^{t'} \frac{i}{\hbar} [E_c(\mathbf{k}) - E_v(\mathbf{k}) - \hbar\omega] dt \right] \right|^2 = 2\pi\hbar\delta(E_c(\mathbf{k}) - E_v(\mathbf{k}) - \hbar\omega). \quad (8-15)$$

Aymerich and Bassani<sup>[24]</sup> have also shown that this same expression is true when  $E_c(\mathbf{k}) - E_v(\mathbf{k})$ , expanded as a function of  $\mathbf{k}$ , contains a dominant linear term in the direction of the dielectric field. Hence the effect of the electric field on the optical properties is of importance only at the critical points of the Brillouin zone, where the energy difference  $E_c(\mathbf{k}) - E_v(\mathbf{k})$  is a quadratic function of  $\mathbf{k}$ .

We can now discuss the effect of an electric field on the different types of critical points by proceeding to an explicit evaluation of (8-14). We give the detailed calculations only for the point  $M_0$  and discuss only the results for other cases. For allowed transitions it is possible to consider as usual the dipole matrix elements  $\mathbf{e} \cdot \mathbf{M}_{cv}$  in the vicinity of a critical point as being constant.

From (8-14)

$$\varepsilon_2(\omega, \mathbf{F}) = \frac{8\pi^2 e^2}{m^2 \omega^2} |\mathbf{e} \cdot \mathbf{M}_{cv}|^2 J_{cv}(\omega, \mathbf{F}), \quad (8-16a)$$

with

$$J_{cv}(\omega, \mathbf{F}) = \frac{1}{2\pi\hbar} \int_{BZ} \frac{d\mathbf{k}}{(2\pi)^3} \frac{1}{T} \left| \int_0^T dt' \exp \left\{ \frac{i}{\hbar} \int_0^{t'} [E_c(\mathbf{k}) - E_v(\mathbf{k}) - \hbar\omega] dt' \right\} \right|^2. \quad (8-16b)$$

The effect of the electric field on the joint density of states (8-16b) is contained in the  $\mathbf{F}$  dependence of the vector  $\mathbf{k}$ , given by (8-9).

#### *Isotropic $M_0$ critical point*

In the simplest case for the isotropic critical point  $M_0$  we may write

$$E_c(\mathbf{k}) - E_v(\mathbf{k}) = E_0 + \frac{\hbar^2}{2\mu} (k_x^2 + k_y^2 + k_z^2),$$

where  $\mu$  is the reduced mass of the electron and hole pair and  $E_0$  is the energy of the critical point. Because of the isotropy, we can assume, without loss of generality, that  $\mathbf{F}$  is directed along the  $z$  axis. Equation (8-16b) becomes

$$J_{cv}(\omega, F) = \frac{1}{2\pi\hbar} \int_{BZ} \frac{d\mathbf{k}}{(2\pi)^3} \frac{\hbar}{eFh_z} \left| \int_{-h_z/2}^{h_z/2} dk_z \times \exp \left\{ \frac{i}{eF} \left[ \frac{\hbar^2}{2\mu} \frac{k_z^3}{3} + \left( \frac{\hbar^2}{2\mu} k_x^2 + \frac{\hbar^2}{2\mu} k_y^2 + E_0 - \hbar\omega \right) k_z \right] \right\} \right|^2, \quad (8-17)$$

where we have chosen

$$T = \frac{\hbar h_z}{eF} \quad (8-18)$$

as a time sufficiently long compared with the transition time,  $h_z$  being the component of the reciprocal lattice vector in the  $z$ -direction. Expression (8-18) gives the time taken for an electron to again assume the original vector  $\mathbf{k}_0$ .

It is convenient to transform the integral appearing in (8-17) using the dimensionless variable

$$u = \left( \frac{2\mu e F}{\hbar^2} \right)^{1/3} k_z.$$

The integral on  $k_z$  in (8-17) can then be transformed into an integral between  $-u(h_z)$  and  $+u(h_z)$ , and, for large values of the electric field as are attainable in a crystal, it is a good approximation to extend the limits of the integration over  $u$  from  $-\infty$  to  $+\infty$ .

This approximation is a consequence of the behaviour of the integrand as function of  $k_z$  in (8-17) and its validity can be verified numerically. The main advantage is that in the high field limit one can represent the integral over  $k_z$  with a well known mathematical function which depends on the other variables only. This is the Airy function, whose mathematical properties are given explicitly in Appendix 8A. Making use of the Airy function as defined in (8A-5), in the high field limit eq. (8-17) becomes

$$J_{cv}(\omega, F) = \frac{1}{(2\pi)^2} \frac{1}{(eF)^{1/3} (\hbar^2/2\mu)^{2/3} h_z} \int_{BZ} d\mathbf{k} \left| Ai \left[ \frac{E_0 + (\hbar^2/2\mu)(k_x^2 + k_y^2) - \hbar\omega}{(\hbar^2/2\mu)^{1/3}(eF)^{2/3}} \right] \right|^2.$$

Since the Airy function does not depend on  $k_z$  the effect of the integration over  $k_z$  is just to cancel the reciprocal vector  $h_z$ . Furthermore the integration over  $k_x$  and  $k_y$  can be simplified by introducing polar coordinates in the space  $(k_x, k_y)$ . Finally,

$$\varepsilon_2(\omega, F) = \frac{2e^2 |\mathbf{e} \cdot \mathbf{M}_{cv}|^2}{\mu^2 \hbar \omega^2} \left( \frac{2\mu}{\hbar} \right)^{3/2} \theta_F^{1/2} \int_{(\omega_0 - \omega)/\theta_F}^{\infty} Ai^2(x) dx, \quad (8-19)$$

where for convenience we have introduced the variables

$$\theta_F = \frac{(eF)^{2/3}}{(2\mu\hbar)^{1/3}},$$

$$\omega_0 = \frac{E_0}{\hbar},$$

$$x = \frac{E_0 + (\hbar^2 k^2 / 2\mu) - \hbar\omega}{\hbar\theta_F}.$$

Expression (8-19) was first obtained by Tharmalingam.<sup>[23]</sup> The integration can be carried out using expression (8A-8) and we obtain

$$\varepsilon_2(\omega, F) = R\theta_F^{1/2} \left[ -\frac{\omega_0 - \omega}{\theta_F} Ai^2 \left( \frac{\omega_0 - \omega}{\theta_F} \right) + Ai'^2 \left( \frac{\omega_0 - \omega}{\theta_F} \right) \right], \quad (8-20a)$$

with

$$R = \frac{2e^2}{\mu^2 \hbar \omega^2} \left( \frac{2\mu}{\hbar} \right)^{3/2} |\mathbf{e} \cdot \mathbf{M}_{cv}|^2. \quad (8-20b)$$

It is instructive to study the behaviour of  $\varepsilon_2(\omega)$  in the regions far from the absorption edge using the asymptotic expressions for the Airy functions given in the Appendix. Using (8A-7) we find for  $\omega \gg \omega_0$  that

$$\varepsilon_2(\omega, F) \approx R(\omega - \omega_0)^{1/2}$$

which coincides with the expression in Table 5-1 corresponding to the absence of the electric field; this signifies that the effect dies out as one goes away from the critical point. Using (8A-6) we find for  $\omega \ll \omega_0$  that

$$\varepsilon_2(\omega, F) \approx R\theta_F^{1/2} \frac{1}{8(\omega_0 - \omega)} \exp \left[ -\frac{4}{3} \left( \frac{\omega_0 - \omega}{\theta_F} \right)^{3/2} \right],$$

which gives the exponential type absorption tail in the gap originally found by Franz and Keldish.<sup>[14]</sup> Finally, we should like to point out that expression (8-19) for  $\omega > \omega_0$  shows oscillations about the zero field values; the amplitude of the oscillations decreases away from the critical point and their period depends on  $F$  and on the reduced mass  $\mu$ , and is given by

$$\left( \frac{9\pi^2\hbar^2e^2}{8} \frac{F^2}{\mu} \right)^{1/3}.$$

#### *General critical point*

The explicit integration of (8-16) for the dielectric function  $\epsilon_2(\omega, F)$  can be carried out at all critical points<sup>[21,24]</sup> using procedures similar to those used for the isotropic  $M_0$  point. We shall not give explicit expressions, but merely illustrate some of the results by figures. Figure 8-7 shows the joint density of states  $J_{cv}(\omega, F)$  for an anisotropic  $M_0$  point and for two directions of the electric field. The energy expansion is supposed to have the form

$$E_c(\mathbf{k}) - E_0(\mathbf{k}) = E_0 + \frac{\hbar^2}{2\mu_x} k_x^2 + \frac{\hbar^2}{2\mu_y} k_y^2 + \frac{\hbar^2}{2\mu_z} k_z^2,$$

with  $\mu_x = \mu_y \neq \mu_z$ . From Fig. 8-7, it can be seen that the joint density of states depends also on the direction of the electric field. The oscillation period for  $\omega > \omega_0$  is given by

$$\left( \frac{9\pi^2\hbar^2e^2}{8} \frac{F^2}{\mu_{||}} \right)^{1/3},$$

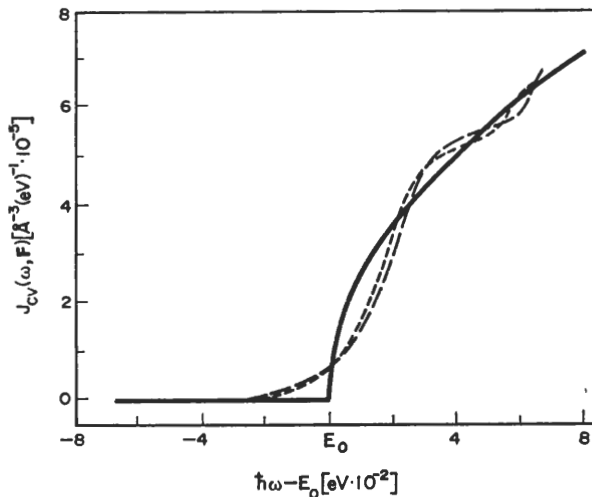


FIG. 8-7. Joint density of states in the presence of an electric field for an anisotropic transition edge  $M_0$  compared to the joint density of states at zero field. The continuous line refers to zero field. The dotted line refers to the  $z$  direction (anisotropy axis). The dashed line refers to the field perpendicular to the  $z$  direction. The values used in the calculation are  $F = 5 \times 10^4 \text{ V cm}^{-1}$ ,  $\hbar^2/2\mu_x = \hbar^2/2\mu_y = 1.24 \times 10^{-3}$ ,  $\hbar^2/2\mu_z = 1.53 \times 10^{-3}$ , (in  $\text{eV}^2 \text{ s}^2 \text{ g}^{-1}$ ). (After Aymerich and Bassani, ref. [24].)

where  $\mu_{||}$  is the projection of the effective mass on the direction of the electric field

$$\frac{1}{\mu_{||}} = \frac{1}{\mu_x} l_x^2 + \frac{1}{\mu_y} l_y^2 + \frac{1}{\mu_z} l_z^2, \quad (8-21)$$

and  $l_x, l_y, l_z$  are the direction cosines of the electric field  $\mathbf{F}$  with respect to the principal axes  $k_x, k_y, k_z$ .

DÉPARTEMENT DE PHYSIQUE DU  
 École Polytechnique Fédérale de Lausanne  
 CH - 1015 LAUSANNE Suisse  
 Tél. 021-47 11 11

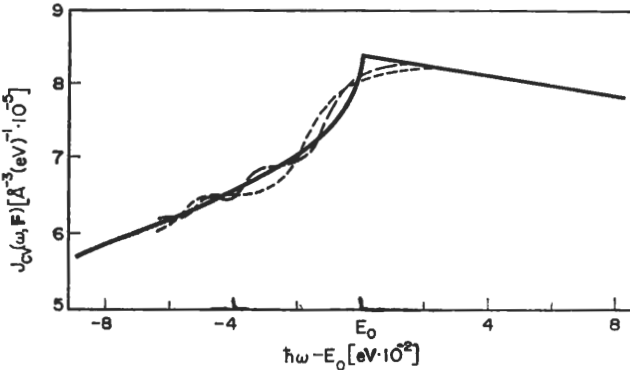


FIG. 8-8. Joint density of states in presence of an electric field at a critical point  $M_1$  compared to the joint density of states at zero field. The values of the parameters are  $\hbar^2/2\mu_x = \hbar^2/2\mu_y = 3.62 \times 10^{-3} \text{ eV}^2 \text{ s}^2 \text{ g}^{-1}$ ,  $\hbar^2/2\mu_z = -0.95 \times 10^{-3} \text{ eV}^2 \text{ s}^2 \text{ g}^{-1}$ . The continuous line gives the result for  $F = 0$ . The dotted line gives the result for  $(\hbar^2/2\mu_{||})^{1/3} (eF)^{2/3} = -0.80 \times 10^{-2} \text{ eV}$ . The dashed line gives the result for  $(\hbar^2/2\mu_{||})^{1/3} (eF) = -1.25 \times 10^{-2} \text{ eV}$ . (After Aymerich and Bassani, ref. [24].) Note that the negative value of the mass projection  $1/\mu_{||}$  gives oscillations for  $\hbar\omega < E_0$ .

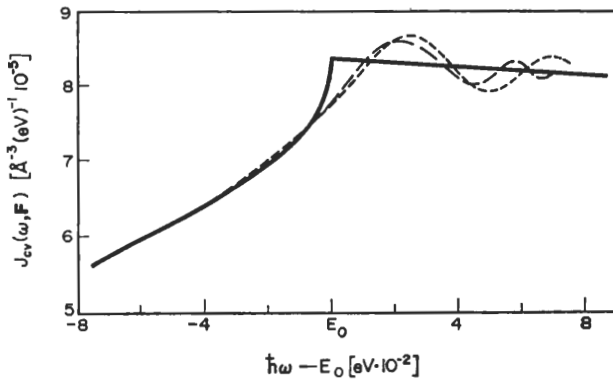


FIG. 8-9. Joint density of states in presence of an electric field at a critical point  $M_1$  and value at zero field for comparison. The values of the parameters are  $\hbar^2/2\mu_x = \hbar^2/2\mu_y = 3.62 \times 10^{-3} \text{ eV}^2 \text{ s}^2 \text{ g}^{-1}$ ,  $\hbar^2/2\mu_z = -0.95 \times 10^{-3} \text{ eV}^2 \text{ s}^2 \text{ g}^{-1}$ . The continuous line gives the result for  $\xi = 0$ . The dotted line gives the result for  $(\hbar^2/2\mu_{||})^{1/3} (eF)^{2/3} = 1.53 \times 10^{-2} \text{ eV}$ . The dashed line gives the result for  $(\hbar^2/2\mu_{||})^{1/3} (eF)^{2/3} = 1.78 \times 10^{-2} \text{ eV}$ . (After Aymerich and Bassani, ref. [24].) Note that the positive value of  $1/\mu_{||}$  results in oscillations for  $\hbar\omega > E_0$ .

Directional effects on the joint density of states are even more important for a critical point  $M_1$ . Typical results are shown in Figs. 8-8 and 8-9, where we notice a damping on one side of the critical point and periodic oscillations on the other. On which side the oscillations actually occur depends on the direction of the electric field through the relation (8-21). The oscillations are at energies lower than  $E_0$  when  $1/\mu_{\parallel} < 0$  and at energies larger than  $E_0$  if  $1/\mu_{\parallel} > 0$ .

#### *Dicroism in optical transitions in presence of an electric field*

So far we have only considered the effect of the electric field on the joint density of states. We wish now to discuss expression (8-16) further in order to show that even for cubic crystals there is a dicroism in optical transitions corresponding to critical points away from the centre of the Brillouin zone. In general, we must sum the contributions from all equivalent critical points when they are located away from the centre of the Brillouin zone. The density of states without the electric field is the same at all equivalent critical points, so even when the matrix elements  $|e \cdot M_{cv}|^2$  are different for equivalent points, their sum is a constant, independent of polarization. In the presence of the electric field, each matrix element  $|e \cdot M_{cv}|^2$  must be multiplied by a different factor (8-16b) because the direction of the external electric field is different relative to the intrinsic axes of any equivalent critical point, so that a dicroism in the optical constants may result.

A detailed analysis of polarization effects for a critical point  $M_1$  in the [111] direction in a cubic semiconductor has been developed by Aymerich and Bassani.<sup>[24]</sup> They discuss the polarization dependence of the  $\epsilon_2(\omega, F)$  on the direction of the external electric field. We immediately see that when the external field is in the direction [100], it forms the same angle with all the directions [111] and therefore the coefficient which multiplies the matrix elements  $|e \cdot M_{cv}|^2$  in (8-16a) is the same for all equivalent points and the dicroism disappears. This suggests another very nice method of locating the position of saddle points in the Brillouin zone, by an analysis of the dicroism in electro-reflectance for different directions of the electric field.

Polarization dicroism at saddle points has been observed by a number of people<sup>[30]</sup> and the results have confirmed very nicely the possibility of obtaining symmetry assignments of the critical point transitions by the polarization dependence of the electro-reflectance amplitude versus field orientation. In principle the period of the experimentally observed oscillations could be used to determine the reduced masses as well if the value of the field were known. The effective masses obtained in this way, however, are generally not very accurate, and further refinements are required to bring theory and experiment into quantitative agreement. Field inhomogeneities near the surface have been shown to introduce significant corrections on the theoretical effect, and lifetime broadening also influences the line shape.<sup>[26]</sup> The effect of the electron-hole interaction will also modify line shapes and periodicity of the oscillations,<sup>[27]</sup> with strong effects very near the edge where exciton states have to be considered. For an extensive analysis of such effects we refer the reader to the paper by Bottka and Fisher.<sup>[31]</sup> For a detailed study of the experimental situation and of the accuracy that one can obtain in the determination of band parameters, we refer the reader to the review articles by Seraphin<sup>[31]</sup> and by Rehn.<sup>[30]</sup>

The effect of an electric field on localized states like deep excitons, deep impurity states, and colour centres cannot be developed along the present lines because in that case the Stark effect, rather than the electric field influence on the density of states, has to be considered. We shall not discuss this point in detail; in the effective mass

approximation the Stark effect is basically the same as in atomic physics and for deep states it must be developed in a similar way, using the wave functions described in Chapter 7. We refer the reader who is interested in this specific problem to a forthcoming review article on impurity states.<sup>[32]</sup>

## 8-5 Electronic states and optical constants in a magnetic field

### 8-5a General remarks and effective mass formulation

In crystals, as in atomic spectroscopy, the magnetic field is also one of the most effective external perturbations for investigating the electronic band structure. In atomic spectroscopy the effect of the magnetic field is generally treated as a perturbation, but this cannot be appropriate for electrons in crystals because of the continuous distribution of states in the energy bands. The problem of the effect of a magnetic field on electrons in crystals is more strictly connected with that of the quantization of free electrons by the magnetic field which was discovered by Landau.<sup>[4]</sup> A similar quantization exists also for electrons in the energy bands of a crystal, and this produces a peculiar structure in the optical constants due to interband transitions. In addition one might have electronic transitions between magnetic levels of the same band (cyclotron resonance), which have been very useful in the determination of effective masses for semiconductors and metals. We should mention that magnetic quantization effects play a very important role in all transport properties and produce oscillations due to the condensation of the density of states at the quantum levels,<sup>[33]</sup> but shall confine ourselves to the quantum theory of the electronic states and to interband optical transitions in order to be consistent with the general framework of this book.

The general scheme in which to work is very similar to that discussed for shallow impurity states in Section 7-3 and for weakly bound excitons in Section 6-3. In the presence of an external magnetic field, the one electron Hamiltonian becomes

$$H = \frac{1}{2m} \left( \mathbf{p} + \frac{e}{c} \mathbf{A} \right)^2 + V_c(\mathbf{r}), \quad (8-22)$$

where  $V_c(\mathbf{r})$  is the crystal potential,  $\mathbf{A}$  is the vector potential of the uniform magnetic field, and  $e$  the modulus of the electron charge. Following the procedure of Luttinger and Kohn, discussed in Section 7-3b for shallow impurity states, we expand the eigenfunctions of the operator (8-22) in the Bloch representation, assuming that the crystal wave functions  $\psi_n(\mathbf{k}, \mathbf{r})$  and the crystal energy bands  $E_n(\mathbf{k})$  are known. Following a procedure similar to that described in the two proceeding chapters we can simplify the Schrödinger equation in the Bloch representation and reduce it to an effective mass equation. In the vicinity of a critical point  $\mathbf{k}_c$  the band energy is a quadratic expansion in  $\mathbf{k}' = \mathbf{k} - \mathbf{k}_c$ ,

$$E_n(\mathbf{k}') = E_0 + \hbar^2 (\alpha'_x k_x'^2 + \alpha'_y k_y'^2 + \alpha'_z k_z'^2), \quad (8-23)$$

with  $\alpha'_i = 1/(2m_i)$ , and  $m_i$  effective masses which can be positive or negative.

The effective mass equation is then

$$\left[ \alpha'_x \left( p_x + \frac{e}{c} A_x \right)^2 + \alpha'_y \left( p_y + \frac{e}{c} A_y \right)^2 + \alpha'_z \left( p_z + \frac{e}{c} A_z \right)^2 \right] F(\mathbf{r}) = (E - E_0) F(\mathbf{r}), \quad (8-24)$$

where  $\mathbf{p}$  indicates the usual operator  $-i\hbar\nabla$ . The function  $F(\mathbf{r})$  is the Fourier transform of  $F(\mathbf{k})$  which expands the eigenfunctions of (8-22) in the set of Bloch functions  $\psi_n(\mathbf{k}, \mathbf{r})$ ,

$$\psi(\mathbf{r}, \mathbf{H}) = \int_{BZ} d\mathbf{k} F(\mathbf{k}) \psi_n(\mathbf{k}, \mathbf{r}). \quad (8-25a)$$

As shown in Section 7-3c, expression (8-25a) can be written to first order as

$$\psi(\mathbf{r}, \mathbf{H}) \simeq F(\mathbf{r}) \psi_n(\mathbf{k}_c, \mathbf{r}). \quad (8-25b)$$

Equation (8-24) is, of course, an approximation which assumes no coupling between different bands and also assumes the validity of the quadratic expansion. We shall briefly mention at the end of this section the case of degenerate bands at the critical point, but for the time being we will consider the case of non degenerate bands.

We have neglected so far the interaction of the spin magnetic moment with the magnetic field. We can consider this interaction separately every time it is required by adding to the Hamiltonian (8-22) the term  $g\mu_B \sigma \cdot \mathbf{H}$ , where  $\sigma$  is the Pauli spin operator,  $\mu_B = e\hbar/(2mc)$  is the Bohr magneton, and the  $g$  factor takes appropriate values which are related to the energy structure<sup>[34]</sup> (for free electrons  $g = 2$ ).

### 8-5b Magnetic quantum levels

Equation (8-24) can be solved exactly in terms of the direction of the magnetic field in the case of isotropic and anisotropic effective mass tensor and for all types of critical points, as shown by Baldereschi and Bassani.<sup>[35]</sup> The isotropic case, with a change of masses, reduces to the case of the free electron in magnetic field solved by Landau.<sup>[4]</sup> More generally, let  $\theta, \varphi$  denote the polar angles of the constant magnetic field  $\mathbf{H}$  with respect to the principal axes  $k'_x, k'_y, k'_z$  of the critical point. It is convenient to perform a rotation by an angle  $\varphi$  about the  $k'_x$  axis in such a way that  $\mathbf{H}$  will belong to the new  $k_x, k_z$  plane. The relation between the  $k'_x, k'_y, k'_z$  axes and the new axes  $k_x, k_y, k_z$  is given by

$$\begin{aligned} k'_z &= k_z, \\ k'_x &= k_x \cos \varphi - k_y \sin \varphi, \\ k'_y &= k_x \sin \varphi + k_y \cos \varphi. \end{aligned}$$

Expression (8-23) then becomes

$$E_n(\mathbf{k}) = E_0 + \hbar^2(\alpha_x k_x^2 + \alpha_{xy} k_x k_y + \alpha_y k_y^2 + \alpha_z k_z^2). \quad (8-26a)$$

with

$$\left. \begin{aligned} \alpha_z &= \alpha'_z, \\ \alpha_x &= \alpha'_x \cos^2 \varphi + \alpha'_y \sin^2 \varphi, \\ \alpha_{xy} &= (\alpha'_y - \alpha'_x) \sin \varphi \cos \varphi, \\ \alpha_y &= \alpha'_x \sin^2 \varphi + \alpha'_y \cos^2 \varphi. \end{aligned} \right\} \quad (8-26b)$$

In the new axes  $H_y$  is zero, and we can choose the gauge so that the vector potential is defined as follows:

$$\mathbf{A} = (-H_z y, 0, H_x y).$$

## ELECTRONIC STATES AND OPTICAL TRANSITIONS

From (8-26a) the effective mass equation for the envelope function is

$$\left[ \alpha_x \left( p_x - \frac{e}{c} H_z y \right)^2 + \alpha_{xy} \left( p_x - \frac{e}{c} H_z y \right) p_y + \alpha_y p_y^2 + \alpha_z \left( p_z + \frac{e}{c} H_x y \right)^2 \right] F(\mathbf{r}) = (E - E_0) F(\mathbf{r}). \quad (8-27)$$

Using the fact that  $p_x$  and  $p_z$  are constants of motion since they commute with the Hamiltonian (8-27), we can reduce the Hamiltonian to a quadratic form which depends only on two canonically conjugate variables  $q, p$  ( $[q, p] = i\hbar$ ). They can be defined by

$$\left. \begin{aligned} q &= y - \frac{c}{eH_z} p_x + \frac{c}{e} \frac{\alpha_y \alpha_z}{\alpha} \frac{H_x}{H_z} S, \\ p &= p_y - \frac{e}{c} H_z \frac{\alpha_{xy}}{\alpha_y} y + \frac{\alpha_{xy}}{\alpha_y} p_x, \end{aligned} \right\} \quad (8-28a)$$

where, without loss of generality, we can suppose  $H_z \neq 0$  since the case  $H_z = 0$  can be handled by a change of axes. In (8-28a) the symbols have been defined as follows:

$$S = H_x p_x + H_z p_z \quad (8-28b)$$

and

$$\alpha = \alpha'_x \alpha'_y H_z'^2 + \alpha'_y \alpha'_z H_x'^2 + \alpha'_z \alpha'_x H_y'^2, \quad (8-28c)$$

$H'_x, H'_y, H'_z$  being the components of  $\mathbf{H}$  in the original frame  $k'_x, k'_y, k'_z$ . Note that the operator

$$S = \left( \mathbf{p} + \frac{e}{c} \mathbf{A} \right) \cdot \mathbf{H}$$

is in general a constant of motion since it represents the projection of the velocity along the magnetic field; in the present case because of the rotation of coordinates, which implies  $H_y = 0$ , and of the choice of gauge, the operator  $S$  has the particularly simple form (8-28b). With the canonical transformation (8-28a), the Hamiltonian of eq. (8-27) becomes

$$H = \alpha_y p^2 + \frac{e^2}{c^2} \frac{\alpha}{\alpha_y} q^2 + \frac{\beta}{\alpha} S^2, \quad (8-29a)$$

with

$$\beta = \alpha'_x \alpha'_y \alpha'_z. \quad (8-29b)$$

When  $\alpha > 0$ , the Hamiltonian (8-29a) is that of an harmonic oscillator, and the eigenvalues are

$$E_{ns} = E_0 + \left( n + \frac{1}{2} \right) \frac{\alpha_y}{|\alpha_y|} \frac{2e\hbar}{c} \sqrt{\alpha} + \frac{\beta}{\alpha} s^2, \quad (8-30)$$

where  $s$  is the eigenvalue of the operator  $S$  defined in (8-28b) and  $\alpha$  and  $\alpha_y$  are defined in (8-28c) and (8-26b) respectively. The corresponding eigenfunctions are obtained as the product of the eigenfunctions of  $p_x$  and  $p_z$ , which are constants of motion, with the eigenfunctions of an harmonic oscillator canonically transformed by (8-28). They are

$$\begin{aligned} F_{nk_xk_z}(\mathbf{r}, \mathbf{H}) &= \frac{1}{\sqrt{L_x}} e^{ik_x x} \frac{1}{\sqrt{L_z}} e^{ik_z z} \exp -i \left[ \frac{e}{2\hbar c} H_z \frac{\alpha_{xy}}{\alpha_y} \left( y - \frac{\hbar c}{eH_z} k_x \right)^2 \right] \\ &\times \varphi_n \left( y - \frac{\hbar c}{eH_z} k_x + \frac{c}{e} \frac{\alpha_y \alpha_z}{\alpha} \frac{H_x}{H_z} s \right), \end{aligned} \quad (8-31)$$

where the plane waves are normalized on the length of the crystal  $L_x$  and  $L_y$  in the  $x$  and  $y$  directions respectively, and  $\varphi_n(q)$  is the wave function of the harmonic oscillator with typical frequency  $(2e/c)\sqrt{\alpha}$ , which depends, through  $\alpha$ , on the effective masses and on the magnetic field  $\mathbf{H}$ .

When  $\alpha < 0$  the Hamiltonian (8-29a) does not admit quantized levels, and all values of energy are allowed. Such a case can occur only if one or two of the effective masses are negative (saddle points  $M_1$  or  $M_2$ ), and is realized when the magnetic field forms an angle larger than a critical angle  $\theta$  with the direction of the axis of negative ( $M_1$ ) or positive ( $M_2$ ) effective mass ( $\tan\theta = \sqrt{(m_z/m_x)}$ , when  $m_x = m_z$ ). Consequently magnetic quantization will occur also at saddle points  $M_1$  provided that the direction of the magnetic field is inside a cone of angle  $\theta$  around the principal axis of the critical point.

When Landau quantization exists ( $\alpha > 0$ ) any state (8-30) with a given  $n$  and  $s$  has degeneracy

$$\frac{eH_z L_x L_y}{2\pi\hbar c}, \quad (8-32)$$

where  $L_x$  and  $L_y$  are the dimensions of the crystal in the  $x$  and  $y$  directions respectively. This result can be obtained by noting that the argument of  $\varphi_n$  is such that the quantity  $(\hbar c/eH_z) k_x$  can vary by at most  $L_y$ , because the electron has to be inside the crystal and the separation between the values of  $k_x$  is  $2\pi/L_x$ .

In the case of a critical point  $M_0$  with cylindrical symmetry about the  $k_z$  axis, formula (8-30) indicates that the dependence of the quantum levels on the longitudinal ( $m_x = m_z$ ) and transverse ( $m_x = m_y = m_t$ ) effective masses and on the direction and magnitude of the magnetic field, can be expressed as a function of an effective cyclotron frequency

$$\omega_c^{\text{eff}}(\mathbf{H}) = \frac{eH}{m_{\text{eff}}c}, \quad (8-33a)$$

where

$$\frac{1}{m_{\text{eff}}} = \sqrt{\left( \frac{1}{m_t^2} \cos^2 \theta + \frac{1}{m_e m_t} \sin^2 \theta \right)}, \quad (8-33b)$$

$\theta$  being the angle between the magnetic field and the  $z$  axis. In fact, by substituting into (8-30) the magnetic field components  $(H \sin \theta, 0, H \cos \theta)$  and the appropriate expressions for  $\alpha$  and  $\beta$ , we find a Landau type solution

$$E_n(\mathbf{H}) = E_0 + \left( n + \frac{1}{2} \right) \hbar \omega_c^{\text{eff}}(\mathbf{H}) + \frac{1}{2} \frac{(\sin \theta \hbar k_x + \cos \theta \hbar k_y)^2}{m_t \cos^2 \theta + m_t \sin^2 \theta}. \quad (8-33c)$$

The above eqs. (8-33) find an important use in cyclotron resonance of electrons in semiconductors like silicon and germanium where the effective mass is anisotropic. They can also be used to obtain the spacing of the levels at saddle points  $M_1$  or  $M_2$  provided  $m_t$  or  $m_z$  is taken negative.

It is instructive to apply the above results to the case of an isotropic minimum to recover the well known Landau levels. In this case, without loss of generality we can suppose  $\mathbf{H} = (0, 0, H_z)$ , and we easily obtain from (8-30)

$$E_{nk_z} = E_0 + \left( n + \frac{1}{2} \right) \hbar \omega_c + \frac{\hbar^2 k_z^2}{2m^*} \quad (8-34a)$$

with Landau functions

$$F_{nk_xk_z}(\mathbf{r}) = \frac{1}{\sqrt{(L_x L_z)}} e^{ik_x x} e^{ik_z z} \varphi_n \left( y - \frac{\hbar c}{eH_z} k_x \right), \quad (8-34b)$$

where  $\omega_c$  is the usual cyclotron frequency  $\omega_c = eH/(m^*c)$ . Expression (8-34) also applies near the top of the valence band by formally taking  $m^*$  and consequently  $\omega_c$  to have a negative sign.

The density of states in a magnetic field can be immediately obtained by the procedure described in Section 5-2a, using formulae (8-30) and (8-32). For simplicity, from (8-34) we give the density of states  $J(E, H)$  for the isotropic case

$$J(E, H) = \frac{[2eH]}{\hbar^2 c} (2m^*)^{1/2} \sum_n \left[ E - E_0 - \hbar\omega_c \left( n + \frac{1}{2} \right) \right]^{-1/2}. \quad (8-35)$$

The density of states is sharply peaked around the values  $(n + \frac{1}{2})\hbar\omega_c$  as can be seen from Fig. 8-10. This is the reason for many oscillatory effects found in transport properties in the presence of a magnetic field and for the peaks in the optical constants corresponding to transitions between Landau levels. In effect, by applying a magnetic field we have produced a series of one-dimensional critical points which give singularities in the density of states.

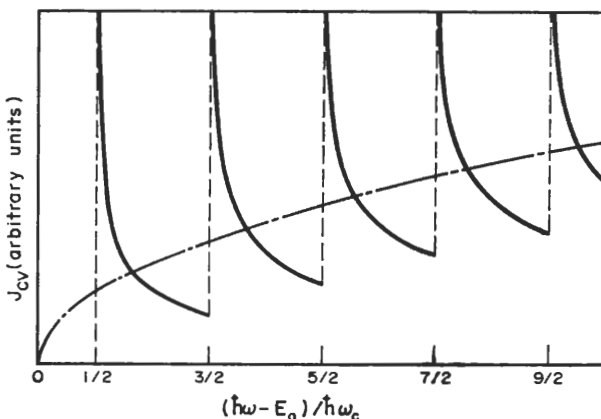


FIG. 8-10. Joint density of states in the presence of a magnetic field at an isotropic critical point  $M_0$ . The dotted line gives the result for zero magnetic field and the continuous line the result with a magnetic field, neglecting lifetime broadening.

An interesting result of the present general treatment is that quantization may exist also at saddle points, the spacing between the levels depending on the direction of the magnetic field. We note that, when the critical point is away from the centre of the Brillouin zone there is a number of equivalent critical points which are obtained one from the other by an appropriate operation of the crystal point group. In the presence of a magnetic field the above critical points are no longer equivalent because the magnetic field has a different orientation relative to each of them. Therefore in any physical effect we must compute their separate contributions similarly to the case discussed

for the electric field effect. It is noted that one does not need to consider intervalley coupling, because this has been shown to be negligible for all attainable values of the magnetic field.<sup>[35]</sup>

### 8-5c Interband transitions in a magnetic field and selection rules

We can study the interband transitions in the presence of a magnetic field using the procedure described in Section 5-1. In the dipole approximation, the perturbation due to an electromagnetic field on the Hamiltonian (8-22) is

$$\frac{e}{mc} \left( \mathbf{p} + \frac{e}{c} \mathbf{A}_{\text{ext}} \right) \cdot \mathbf{A}_{\text{em}}.$$

where  $\mathbf{A}_{\text{ext}}$  is the vector potential of the constant magnetic field and  $\mathbf{A}_{\text{em}}$  is the time dependent vector potential of the radiation field. With procedures similar to those used in obtaining (5-14), we obtain for a pair of valence and conduction bands,

$$\epsilon_2(\omega, \mathbf{H}) = \frac{4\pi^2 e^2}{m^2 \omega^2} \sum_{\text{all possible states}} |\mathbf{e} \cdot \mathbf{M}_{cv}(\mathbf{H})|^2 \delta(E_c(\mathbf{H}) - E_v(\mathbf{H}) - \hbar\omega), \quad (8-36a)$$

where

$$\mathbf{e} \cdot \mathbf{M}_{cv}(\mathbf{H}) = \int \psi_c^*(\mathbf{r}, \mathbf{H}) \mathbf{e} \cdot \left( \mathbf{p} + \frac{e}{c} \mathbf{A}_{\text{ext}} \right) \psi_v(\mathbf{r}, \mathbf{H}) d\mathbf{r}, \quad (8-36b)$$

and  $\psi_c(\mathbf{r}, \mathbf{H})$ ,  $\psi_v(\mathbf{r}, \mathbf{H})$ ,  $E_c(\mathbf{H})$ , and  $E_v(\mathbf{H})$  indicate the band wave functions and energies in the presence of the constant external magnetic field.

The effect of the magnetic field on the matrix elements can be seen very easily to first order by neglecting  $\mathbf{A}_{\text{ext}}$  in (8-36b) and employing (8-25a).

$$\begin{aligned} \mathbf{e} \cdot \mathbf{M}_{cv}(\mathbf{H}) &= \int \left[ \sum_{\mathbf{k}} F_c(\mathbf{k}) \psi_c(\mathbf{k}, \mathbf{r}) \right]^* \mathbf{e} \cdot \mathbf{p} \left[ \sum_{\mathbf{k}'} F_v(\mathbf{k}') \psi_v(\mathbf{k}', \mathbf{r}) \right] d\mathbf{r} \\ &= \sum_{\mathbf{k}\mathbf{k}'} F_c^*(\mathbf{k}) F_v(\mathbf{k}') \mathbf{e} \cdot \mathbf{M}_{cv}(\mathbf{k}) \delta(\mathbf{k} - \mathbf{k}'), \end{aligned} \quad (8-37)$$

where we have used the interband selection rule  $\Delta\mathbf{k} = 0$ . Since near the critical point the matrix element  $\mathbf{M}_{cv}(\mathbf{k})$  can be taken to be independent of  $\mathbf{k}$  for allowed transitions, we can simplify (8-37) and obtain

$$\mathbf{e} \cdot \mathbf{M}_{cv}(\mathbf{H}) = \mathbf{e} \cdot \mathbf{M}_{cv} \int F_{cn'k_x'k_z'}^*(\mathbf{r}) F_{vnk_xk_z}(\mathbf{r}) d\mathbf{r}, \quad (8-38)$$

where we have also transformed the summation over  $\mathbf{k}$  into an integral over  $\mathbf{r}$  by expanding the  $\delta$  function of (8-37) in plane waves and using the definition that the envelope function  $F(\mathbf{r})$  (given by 8-31 in the most general case) is the Fourier transform of  $F(\mathbf{k})$ .

In the case of isotropic energy bands or in the case of cylindrical symmetry with respect to the magnetic field in the direction of the  $z$  axis, the envelope functions for the harmonic oscillators in the valence and conduction band belong to proportional Hamiltonians and are orthonormal giving the new selection rule

$$\Delta n = 0, \quad (8-39a)$$

besides the usual selection rules

$$\Delta k_x = \Delta k_z = 0. \quad (8-39\text{b})$$

Less restrictive selection rules than (8-39a) apply when the symmetry is reduced. In the case of energy bands with cylindrical symmetry and the magnetic field perpendicular to the symmetry axis we would obtain the selection rule<sup>[35]</sup>

$$\Delta n = \text{even number}.$$

In the case of transitions which would be forbidden in the absence of a magnetic field we should express  $\mathbf{M}_{cv}(\mathbf{k})$  in (8-37) as a function linearly dependent on  $\mathbf{k}$ . Transforming integrals over  $\mathbf{k}$  into integrals over  $\mathbf{r}$  and expanding the  $\delta$  function in plane waves, we obtain

$$\mathbf{e} \cdot \mathbf{M}_{cv}(\mathbf{H}) \doteq \int F_{cn'k_x'k_z'}^*(\mathbf{r}) \mathbf{e} \cdot \nabla F_{vnk_xk_z}(\mathbf{r}) d\mathbf{r},$$

which in the isotropic case gives the selection rule  $\Delta n = \pm 1$ .

While the matrix elements described above give the strength of the optical transition, the sum over the  $\delta$  functions in (8-36a) gives the joint density of states, which determines the shape of the transition. This can be computed by taking into account the selection rules described above and considering the energy difference between the magnetic quantum levels of the conduction and valence bands. The joint density of states for the isotropic case is given by [see (8-35)]

$$J_{cv}(E, \mathbf{H}) = \frac{2eH}{\hbar^2 c} (2\mu)^{1/2} \sum_n \left[ E - E_G - \hbar\omega_c \left( n + \frac{1}{2} \right) \right]^{-1/2}, \quad (8-40)$$

with  $\omega_0 = eH/(\mu c)$ ,  $\mu$  being the reduced hole-electron effective mass, and  $E_G$  the energy gap between valence and conduction band.

The imaginary part of the dielectric function (8-36a) can now be written explicitly near an allowed transition edge using the selection rules (8-39) and the joint density of states (8-40)

$$\varepsilon_2(\omega, \mathbf{H}) = \frac{4\pi^2 e^2}{m^2 \omega^2} \frac{2eH}{\hbar^2 c} (2\mu)^{1/2} |\mathbf{e} \cdot \mathbf{M}_{cv}|^2 \sum_n \left[ \hbar\omega - E_G - \hbar\omega_c \left( n + \frac{1}{2} \right) \right]^{-1/2}.$$

The above expression exhibits very sharp singularities corresponding to transitions between the magnetic quantum levels, as can be visually seen in Fig. 8-10.

The spacings of the singularities will give the reduced effective mass. The energy gap  $E_G$  can also be obtained by plotting the position of the absorption peaks as a function of  $H$  and extrapolating for  $H \rightarrow 0$ . For an extensive description of magneto-optics effects at the absorption edge, we refer the reader to some review papers.<sup>[36]</sup>

Similar results can be obtained in the same way for the anisotropic case, and in particular for saddle point transitions, in which case the shape of the joint density of states is shown in Fig. 8-11. The appearance of Landau peaks in correspondence to singularities above the absorption edge has been recently found by Sari<sup>[37]</sup> in a number of semiconductors, along the lines here discussed, providing a very nice experimental verification of the all theory.

We also wish to point out that the theory of two-photon transitions discussed in Section 5-3 can be extended to the case of magnetic levels, the most important consequence being a modification of the selection rules.<sup>[38]</sup> Since two-photon transitions are a second-order process, their probability is determined by the product of matrix elements

$$\langle \psi_c(\mathbf{H}, \mathbf{r}) | \mathbf{A}_1 \cdot \mathbf{p} | \psi_{\text{int}}(\mathbf{H}, \mathbf{r}) \rangle \langle \psi_{\text{int}}(\mathbf{H}, \mathbf{r}) | \mathbf{A}_2 \cdot \mathbf{p} | \psi_v(\mathbf{H}, \mathbf{r}) \rangle,$$

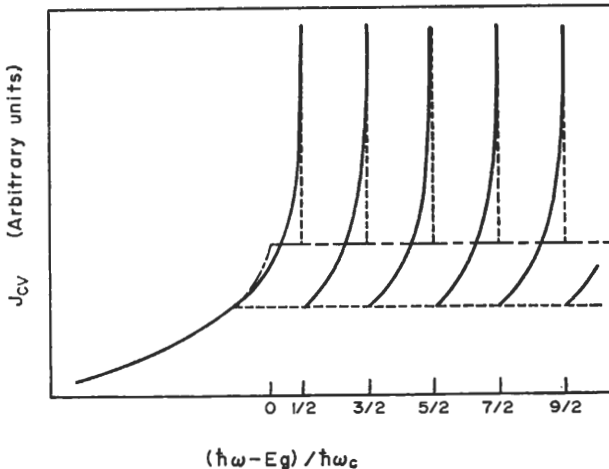


FIG. 8-11. Joint density of states at a critical point  $M_1$  with cylindrical symmetry and in presence of a magnetic field oriented along the symmetry axis. The cyclotron energy  $\hbar\omega_c$  is the one appropriate to reduced transverse mass. The broken line indicates the zero field case. (After Baldereschi and Bassani, ref. [35].)

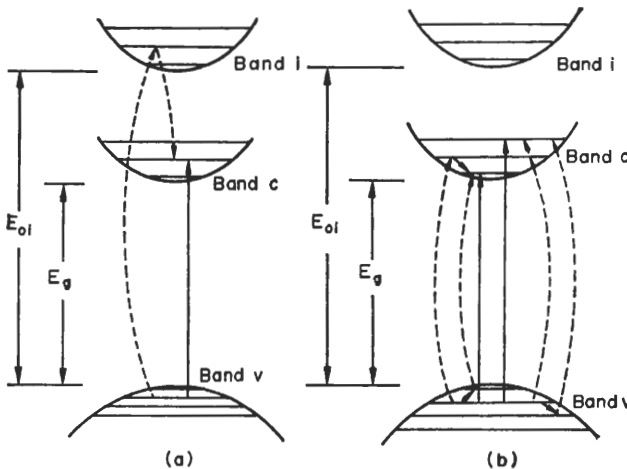


FIG. 8-12. Different processes for two-photon transitions between Landau levels of the valence and the conduction bands: (a) indicates inter-inter transitions in which both photons produce interband transitions. If one of the two photons produces an intraband transition, the process (b) occurs. (After Bassani and Girlanda, ref. [38].)

where the indices 1 and 2 refer to the two photons and  $\psi_{int}$  represent a general intermediate state. Two different processes can occur depending on the choice of intermediate state and also on the polarization of the light with respect to the magnetic field. If the intermediate state does not belong to the same band as the initial or final states, the selection rules  $\Delta n = 0$  still holds because it holds for each matrix element. If the intermediate state is a different magnetic level in the same band to which the initial or the final states belong, then, when at least one of two photons is polarized perpendicularly to the magnetic field, we also have allowed transitions with  $\Delta n = \pm 1$  as illustrated in

## ELECTRONIC STATES AND OPTICAL TRANSITIONS

Fig. 8-12. A typical two-photon interband magneto-optical experiment should then give transitions with both  $\Delta n = 0$  and  $\Delta n = \pm 1$ , so that in principle a measurement of both electron and hole effective masses can be obtained.

### 8-5d Degenerate bands and interband coupling

As discussed in Chapters 6 and 7 in connection with excitons and impurity states, also in this case coupling between different bands must be considered when band degeneracy occurs at the critical point, as is the case for the valence bands of cubic semiconductors and for semimetals. To account for such coupling a procedure very similar to the one described in Section 7-3d must be carried out except that one has to substitute  $\hbar\mathbf{k}$  with  $\hbar\mathbf{k}' = [\mathbf{p} + (e/c)\mathbf{A}]$  and to take into account the new commutation rules  $[k'_x, k'_y] = (e/ie\hbar) H_z$ , and cyclic permutations. A Hamiltonian matrix results which produces a system of coupled differential equations on the envelope functions at the extremum.

If we consider the valence band of a cubic semiconductor, we have threefold degeneracy which is doubled by including spin. If we now take into account the electron spin and the spin-orbit interaction, the sixfold degenerate valence band state splits into an upper fourfold degenerate state and a lower twofold state. Limiting ourselves to the top valence band with degeneracy 4, we have to consider a 4 by 4 matrix equation. As discussed in Section 7-3d, it is convenient to introduce the 4 by 4 matrices  $J_x$ ,  $J_y$ , and  $J_z$  which describe an angular momentum  $3/2$ . In terms of these matrices and of the operator  $\hbar\mathbf{k}'$ , the 4 by 4 Hamiltonian matrix can be written in compact form as<sup>[39]</sup>

$$H' = \frac{\hbar^2}{m} \left\{ \left( \gamma_1 + \frac{5}{2} \gamma_2 \right) \frac{k'^2}{2} - \gamma_2 (k'_x^2 J_x^2 + k'_y^2 J_y^2 + k'_z^2 J_z^2) \right. \\ - 2\gamma_3 [\{k'_x, k'_y\} \{J_x, J_y\} + \{k'_y, k'_z\} \{J_y, J_z\} + \{k'_z, k'_x\} \{J_z, J_x\}] \\ \left. + \frac{e}{c} \mathbf{k} \cdot \mathbf{H} + \frac{e}{c} q (J_x^3 H_x + J_y^3 H_y + J_z^3 H_z) \right\}, \quad (8-41)$$

where the parameters  $\gamma_i$  are the same as those of the previous chapter and two new parameters  $k$  and  $q$  are introduced,  $k$  being due to new commutation rules and  $q$  to the spin-orbit interaction. Since the value of  $q$  is generally very small, the last term in (8-41) is generally neglected.

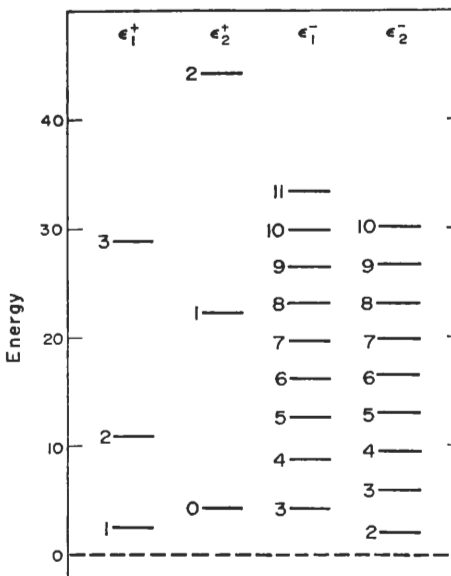
Eigenvalues and eigenfunctions of Hamiltonian (8-41) have been found in terms of the Landau functions (8-34b) by performing suitable linear transformations. It is generally considered a good approximation to assume that  $\gamma_2 \approx \gamma_3 \approx \bar{\gamma}$ , in which case Hamiltonian (8-41) is spherically symmetric in the absence of the magnetic field. Under this assumption the solution of the matrix equation

$$H'_{\alpha\beta} \psi_\beta = (E - E_0) \psi_\alpha \quad (8-42a)$$

is of the form

$$\begin{bmatrix} \psi_{l=1} \\ \psi_{l=2} \\ \psi_{l=3} \\ \psi_{l=4} \end{bmatrix} = \begin{bmatrix} c_1 \psi_{m-3} \\ c_2 \psi_{m-1} \\ c_3 \psi_{m-2} \\ c_4 \psi_m \end{bmatrix}, \quad (8-42b)$$

where the functions that appear on the right hand side are Landau functions  $\psi_m(k_x, k_z)$ . Expression (8-42) describes the coupling between Landau levels of different degenerate bands. The effect of this coupling on the eigenvalues has been obtained by Wallis and Bowlden.<sup>[40]</sup> We report in Fig. 8-13 the position of the levels calculated by Wallis and Bowlden for germanium in the limit  $k_z = 0$ . From the results of Fig. 8-13 we can observe that for large values of  $m$  the bands are decoupled (light and heavy mass Landau levels), while for small values of  $m$  coupling effects give large shifts of the magnetic quantum levels.



DEPARTEMENT D'ÉTUDES PHYSIQUES  
 ÉCOL. POLYTECHNIQUE FÉDÉRALE  
 DE LAUSANNE  
 CH-1015 LAUSANNE Suisse  
 Réf. 521-47111

FIG. 8-13. Magnetic energy levels in the valence band of germanium in the spherical model and neglecting the kinetic energy in the direction of the field. The values of the valence band parameters are  $\gamma_1 = 13.2$ ,  $\gamma_2 = \gamma_3 = 4.92$ , and  $k = 3.3$ . The energies are measured from the band edge in units of  $(eH)/mc$ . (After Wallis and Bowlden, ref. [40].)

For an accurate interpretation of the experimental results one generally has to go beyond the spherical approximation and consider the general case  $\gamma_2 \neq \gamma_3$ . Under these circumstances the energy spectrum depends on the direction of the magnetic field and must be obtained by numerical integration.<sup>[40]</sup> The energy spectra obtained in this way show some anisotropy, but do not differ qualitatively from those obtained using the spherical model.

The procedure outlined above for degenerate bands can also be applied to consider magnetic coupling between non-degenerate bands. In the case of small gap semiconductors, for instance, the magnetic field produces a strong coupling between valence and conduction bands. The extension of this procedure in order to include such coupling has been carried out by Pidgeon and Brown.<sup>[41]</sup>

When the bands are degenerate at the critical point, the selection rule  $\Delta n = 0$  is still valid for interband transitions in cubic semiconductors, but since interband coupling mixes different Landau levels as indicated by (8-42), more transitions are in general allowed. For instance, in the case of cubic semiconductors with a non-degenerate

conduction band, interband transitions to a certain Landau level  $n$  in the conduction band are allowed only from initial states in the valence band which contains contribution of the same harmonic oscillator  $n$ . In the spherical model approximation, for instance, the Landau level  $n = 0$  in the conduction band can be reached from the states  $m = 0, 1, 2$ , and 3 in the valence band, as indicated by (8-42).

### 8-6 Excitons in a magnetic field

In the previous section we studied interband transitions in a magnetic field without considering the effective electron-hole interaction which is responsible for the creation of localized states in the energy gap (see Chapter 6). When the binding energies of exciton states are much larger than the energy  $\hbar\omega_c$  of the magnetic states, we can consider the magnetic field as a small perturbation, and we handle the problem using standard perturbation theory. This is the case with the Zeeman effect of atomic spectroscopy.<sup>[1]</sup> However, in semiconductors the electron-hole interaction is screened by the dielectric function and is much weaker than the attractive potential of an electron in an atom so that by comparison the magnetic field effect are not small. We are then faced with the problem of determining the solution of Schrödinger's equation for an hydrogenic atom in a magnetic field, which has never been solved exactly because the equation is non-separable.

To illustrate some approximate solutions of this problem, we start by considering the effective mass equation for the envelope function  $F(\mathbf{r}_e, \mathbf{r}_h)$ , which depends on both electron and hole coordinates in the presence of both a constant magnetic field and electron-hole interaction. We have

$$\left[ \frac{1}{2m_e^*} \left( \mathbf{p}_e + \frac{e}{c} \mathbf{A}(\mathbf{r}_e) \right)^2 + \frac{1}{2m_h^*} \left( \mathbf{p}_h - \frac{e}{c} \mathbf{A}(\mathbf{r}_h) \right)^2 - \frac{e^2}{\epsilon |\mathbf{r}_e - \mathbf{r}_h|} \right] F(\mathbf{r}_e, \mathbf{r}_h) = (E - E_0) F(\mathbf{r}_e, \mathbf{r}_h), \quad (8-43)$$

where for simplicity we consider the case of the model semiconductor with isotropic effective masses of Fig. 6-3. In the absence of a magnetic field eq. (8-43) separates using the relative coordinate

$$\mathbf{r} = \mathbf{r}_e - \mathbf{r}_h$$

and the centre of mass coordinate

$$\mathbf{R} = \frac{m_e^* \mathbf{r}_e + m_h^* \mathbf{r}_h}{m_e^* + m_h^*}.$$

With the magnetic field we make use of the coordinates  $\mathbf{r}$  and  $\mathbf{R}$ , and in addition we perform the canonical transformation<sup>[42]</sup>

$$F(\mathbf{r}_e, \mathbf{r}_h) = \exp \left\{ i \left[ \mathbf{k} + \frac{e}{\hbar c} \mathbf{A}(\mathbf{r}) \right] \cdot \mathbf{R} \right\} \Phi(\mathbf{r}).$$

We obtain

$$\begin{aligned} \left[ \frac{\mathbf{p}^2}{2\mu} + \frac{e}{c} \left( \frac{1}{m_h^*} - \frac{1}{m_e^*} \right) \mathbf{A} \cdot \mathbf{p} + \frac{e^2}{2\mu c^2} \mathbf{A}^2(r) - \frac{e^2}{\epsilon r} + \frac{\hbar^2 k^2}{2M} - \frac{2e\hbar}{Mc} \mathbf{k} \cdot \mathbf{A}(\mathbf{r}) \right] \Phi(\mathbf{r}) \\ = (E - E_0) \Phi(\mathbf{r}), \end{aligned} \quad (8-44)$$

where  $M$  is the total mass,  $\mu$  the reduced mass, and  $\mathbf{k}$  the momentum eigenvalue of the centre of mass motion. In (8-44)  $\mathbf{p}^2/2\mu$  gives the kinetic energy of the relative motion. The quantity

$$\frac{e}{c} \left( \frac{1}{m_h^*} - \frac{1}{m_e^*} \right) \mathbf{A} \cdot \mathbf{p}$$

is the Zeeman term, as can be seen immediately by taking the symmetric gauge

$$\mathbf{A} = \frac{1}{2} \mathbf{H} \wedge \mathbf{r}.$$

Next we have the diamagnetic term  $(e^2/2\mu c^2) \mathbf{A}^2(\mathbf{r})$ , the electron-hole interaction  $-e^2/\epsilon r$ , and the kinetic energy  $\hbar^2 k^2/2M$  of the centre of mass motion. The final term  $-(2e\hbar/Mc) \mathbf{k} \cdot \mathbf{A}$  gives a coupling between the centre of mass motion and the magnetic field and is equivalent to the effect of an electric field of magnitude  $-(e\hbar/Mc) \mathbf{k} \wedge \mathbf{H}$  acting on the electron and the hole as can be immediately seen from the symmetric gauge. This latter term can be neglected for  $\mathbf{k}$  sufficiently small, and is exactly zero when  $\mathbf{H}$  and  $\mathbf{k}$  are in the same direction. Using measurements of this term, Thomas and Hopfield<sup>[42]</sup> were able to give proof of exciton motion, but for the interpretation of magneto-optical experiments it can be neglected. The kinetic energy of the centre of mass and the Zeeman term are constants of motion, and we can write (8-44) in the form

$$\left[ \frac{\mathbf{p}^2}{2\mu} - \frac{e^2}{\epsilon r} + \frac{e^2}{8\mu c^2} H^2(x^2 + y^2) \right] \Phi(\mathbf{r}) = E' \Phi(\mathbf{r}), \quad (8-45a)$$

where we have taken the direction of the magnetic field to lie along the  $z$  axis, and we have defined

$$E' = E - E_0 - \frac{\hbar^2 k^2}{2M} - \frac{e}{2c} \left( \frac{1}{m_h^*} - \frac{1}{m_e^*} \right) H m \hbar. \quad (8-45b)$$

Many attempts have been made to solve eq. (8-45) by perturbation theory, by the adiabatic approximation and by variational methods. We cannot discuss the details but may perhaps indicate some of the results so far obtained. For further information we refer the reader to some papers which deal with this problem.<sup>[43]</sup>

It is convenient to choose as unit of energy the effective Rydberg

$$R^* = \frac{\mu e^4}{2\hbar^2 \epsilon^2},$$

and to introduce a dimensionless parameter  $\gamma$  to indicate the relative strengths of the magnetic field effect and Coulomb interaction

$$\gamma = \frac{\hbar \omega_c}{2R^*}.$$

For large values of the magnetic fields ( $\gamma \gg 1$ ) the adiabatic approximation can be used. It consists in writing  $\Phi(\mathbf{r})$  in the form  $\Phi(\mathbf{r}) = e^{im\varphi} f(\varrho, z) g(z)$ ,  $\varphi$ ,  $\varrho$  and  $z$  being cylindrical coordinates, and assuming the  $z$  dependence of the function  $f(\varrho, z)$  to be very small

so that we may neglect the terms  $(\partial/\partial z)f(\varrho, z)$  and  $(\partial/\partial z^2)f(\varrho, z)$ . We then obtain

$$\left[ -\frac{\partial^2}{\partial \varrho^2} - \frac{1}{\varrho} \frac{\partial}{\partial \varrho} - \frac{2}{\sqrt{(\varrho^2 + z^2)}} + \frac{\gamma^2}{4} \varrho^2 \right] f_n(\varrho, z) = W_n(z) f_n(\varrho, z), \quad (8-46a)$$

$$\left[ -\frac{d^2}{dz^2} + W_n(z) \right] g_i(z) = E_{n,i} g_i(z), \quad (8-46b)$$

where the  $\varphi$  dependence has been neglected since only totally symmetric states  $\Sigma_g$  (with  $m = 0$ ) do not vanish at the origin and have non-zero dipole transition probability. We may mention at this point that the symmetry group of the total Hamiltonian of (8-43) is  $D_{\infty h}$  since it contains all rotations about the magnetic field and a reflection  $\sigma_h$  in the plane perpendicular to  $H$ , while the symmetry of  $\Phi$  in (8-45) also contains inversion. Equation (8-46a) gives a  $z$  dependent eigenvalue  $W_n(z)$  for every Landau level because in the limit  $z \rightarrow \infty$  we have

$$W_n(z \rightarrow \infty) = (n + \frac{1}{2}) 2\gamma, \quad (8-47)$$

as it can be immediately obtained by noticing that the electron-hole interaction is then absent.<sup>[4]</sup> As  $z$  decreases,  $W_n(z)$  decreases with respect to (8-47) resulting in an attractive potential which produces bound states when substituted into (8-46b). The effect of the Coulomb interaction is then to produce bound states below every Landau level. Detailed solutions of (8-46) have been obtained by the WKB approximation, by perturbation theory, and also by direct numerical integration.<sup>[43]</sup> It has been shown by Baldereschi and Bassani<sup>[43]</sup> that the adiabatic method is valid down to  $\gamma \approx 1$  for the lowest state and to smaller values of  $\gamma$  for the excited states. We show in Fig. 8-14

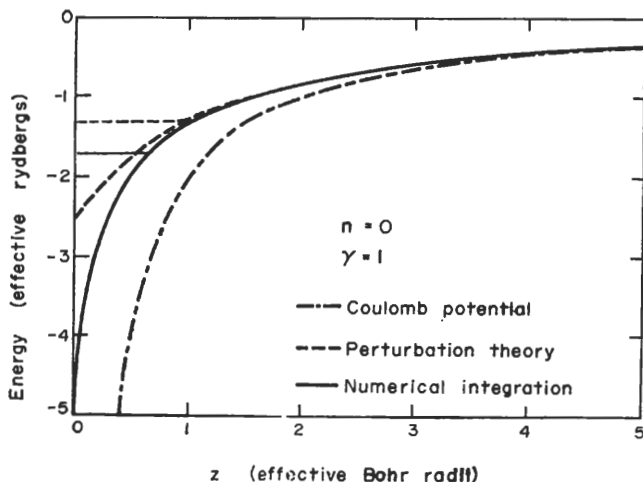


FIG. 8-14. Adiabatic potential  $W_0(z)$  in the direction of the magnetic field for the lowest Landau level. The energy position of the lowest bound state ( $n = 0, i = 0$ ) is indicated by an horizontal line. The magnetic field is chosen so that the ratio  $\gamma = (\hbar\omega_c)/2Ry^* = 1$ . Note: The results one would obtain by a one-dimensional Coulomb potential and by perturbation theory with the perturbing Coulomb potential (Elliott and Loudon) are shown for comparison. (After Bassani and Baldereschi, ref. [43].)



a typical curve  $W_n(z)$  with  $\gamma = 1$ , obtained with different approximations, and its lowest bound state  $i = 0$ . We can thus conclude that the effect of the Coulomb interaction is to quantize the one-dimensional continuum in the direction of the magnetic field and to produce a set of sublevels  $E'_{n,i}$  below each of the Landau bands. The only true bound states are those associated with the  $n = 0$  level; those associated with larger values of  $n$  are resonant states because they are degenerate with the continuum of the lower values of  $n$ .

For small values of the magnetic field, perturbation theory on the low lying hydrogenic states  $u_{nlo}$  can be applied using the perturbation  $(\gamma^2/4) \rho^2$ . So far reasonable results have been obtained only for the few lowest states with values of  $\gamma$  up to about 0.5; for higher exciton states the low field limit is still an open problem because perturbation theory breaks down for much smaller values of  $\gamma$ .

A problem still remains in connecting the states for very small values of  $\gamma$ , which are classified according to the hydrogenic quantum numbers  $n, l, m = 0$  to the states for large values of  $\gamma$  which are classified according to the quantum numbers  $n, i, m = 0$ . This problem is of practical importance since most of the experimental results occur in the region of intermediate magnetic fields where detailed solutions are currently not available. Figure 8-15 illustrates the above results with the beautiful experimental

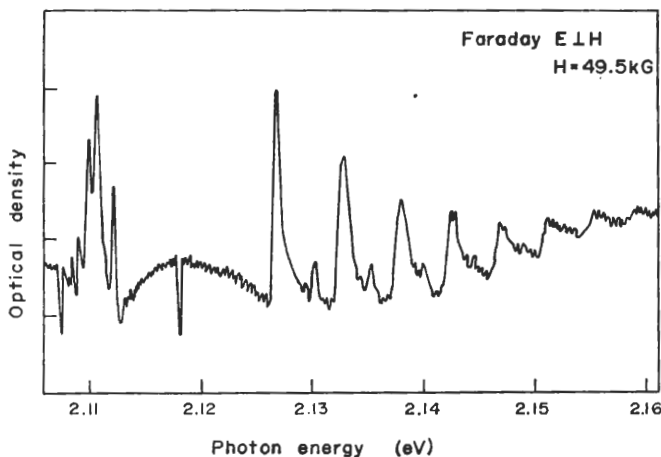


FIG. 8-15. Magneto-absorption spectrum of GaSe in the Faraday geometry (propagation vector of the light  $\mathbf{q}$  parallel to the magnetic field) and for field oriented along the  $c$ -axis. Note the transition from the exciton-like spectrum at lower energies to the Landau-type spectrum at higher energies. Note also the weaker satellite structures above each strong  $(n, 0)$  peak. (After Brebner *et al.*, ref. [44].)

evidence of the satellite structure below the Landau levels in the case of GaSe.<sup>[44]</sup> The position of the lowest energy peaks are shown as functions of the magnetic field strength in Fig. 8-16, where, for comparison, the theoretical results for the lowest levels obtained using perturbation theory at low magnetic fields and the adiabatic approximation at higher magnetic fields are also indicated. The comparison indicates the type of problems one encounters in connecting exciton quantum levels at low and high magnetic fields. The experimental evidence (see Fig. 8-15) indicates that the oscillator strength associated with the state  $(n = 1, i = 0)$  is much larger than that

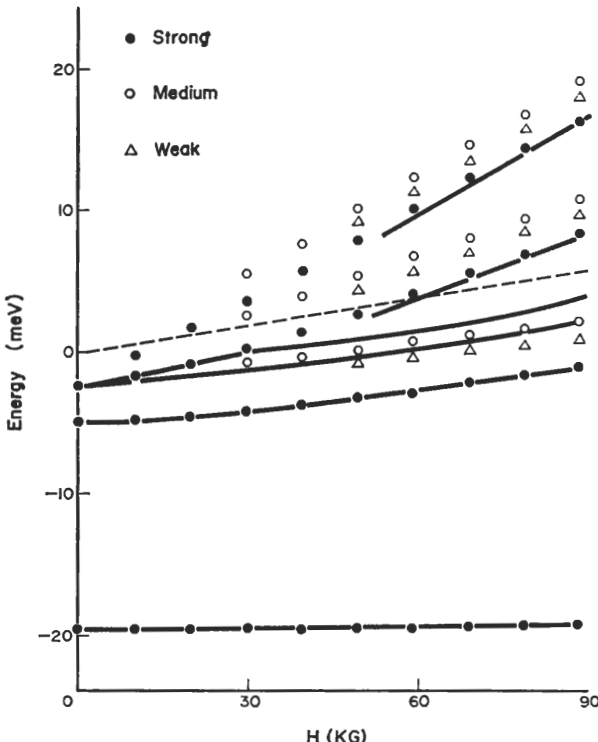


FIG. 8-16. Energies of the magneto-absorption peaks in GaSe as a function of the magnetic field which is oriented parallel to the *c*-axis. The energies are measured relative to the energy gap. The lines represent the theoretical energy spectrum. After Bassani and Baldereschi, ref. [43]. The experimental data are from ref. [44].

of the state ( $n = 0, i = 2$ ) in spite of the fact that the non-crossing rule connects ( $n = 0, i = 2$ ) to the  $2s$  exciton. This is due to the transfer of oscillator strength to the resonant ( $n > 0, i = 0$ ) states as the field increases.

It should also be mentioned that the complete interpretation of the optical spectra in a magnetic field requires the consideration of states with  $m = 1$ , and in some cases  $m = 2$ . As we have seen in the case of second class excitons, magneto-optical states corresponding to dipole forbidden interband transitions will be of types  $\Sigma$ ,  $\Pi^\pm$ , and  $\Delta^\pm$ . Very detailed experimental studies have been performed on the exciton states of CuCl and Cu<sub>2</sub>O on the region of low and intermediate magnetic fields,<sup>[45]</sup> but their detailed interpretation along the lines indicated above has not yet been attempted.

We have presented the optical spectra in GaSe as an example of interband transitions in a magnetic field because in this material we have the advantage that both valence and conduction bands are non-degenerate at their extrema. In cubic semiconductors the valence band is generally fourfold degenerate at the critical point, and we have seen that this produces strong effects on the Landau levels for small values of  $n$ . In this case the inclusion of the Coulomb interaction is more complex, but one can follow an approach similar to that discussed for non-degenerate bands. Using the adiabatic ap-

proximation, Rees<sup>[46]</sup> obtained a system of coupled differential equations and estimated the Coulomb shift or the lowest level in high fields. Altarelli and Lipari<sup>[46]</sup> have recently computed the same shift in the low field limit using perturbation theory.

The electron-hole interaction should also affect magneto-optical transitions at saddle points and quantize the one-dimensional continuum. Such an effect appears in the magnetic field dependence of the lowest energy transitions in Sari's experiments.<sup>[37]</sup>

Another problem to be considered is that of magnetic field effects on the localized impurity states described in Chapter 7. In this case the Zeeman term is the most important because we do not have the selection rule  $m = 0$ , which is valid for allowed excitons. The diamagnetic term must also be considered, but the most important effect is the splitting of the  $m$  degeneracy. In the case of impurity states originating from non-degenerate bands the treatment is similar to that of atomic spectroscopy.<sup>[11]</sup> In cases like those of acceptor states in cubic semiconductors, the problem is still far from being solved, though progress is being made.<sup>[47]</sup>

A last point we like to briefly mention is that a strong magnetic field can be produced inside some complex semiconductors like the rare earth chalcogenides (EuS for instance) or chromium spinels ( $\text{Hg}_2\text{CrO}_4$  for instance), by lowering the temperature below the Curie temperature, thus making the crystal ferromagnetic. This produces band shifts and interesting luminescence effects which cannot be understood solely in terms of the simple Landau quantization based on the effective mass approximation.<sup>[48]</sup>

## APPENDIX 8A

### Electron in a uniform electric field

Let us consider the Schrödinger equation for one electron in a uniform electric field

$$\left[ \frac{\mathbf{p}^2}{2m} + eFz \right] F(\mathbf{r}) = EF(\mathbf{r}), \quad (8A-1)$$

where  $e$  indicates the modulus of the electron charge, and the electric field  $F$  is taken to be in the  $z$  direction. Since  $p_x$  and  $p_y$  are constants of motion, we can perform the canonical transformation

$$F(\mathbf{r}) = e^{ik_xx} e^{ik_yy} Z(z).$$

Equation (8A-1) becomes

$$-\frac{\hbar^2}{2m} \frac{d^2Z(z)}{dz^2} + eFzZ(z) = \varepsilon_z Z(z), \quad (8A-2)$$

where

$$\varepsilon_z = E - \frac{\hbar^2}{2m} (k_x^2 + k_y^2).$$

Introducing the dimensionless variable

$$\xi = \left( z - \frac{\varepsilon_z}{eF} \right) \left( \frac{2mFe}{\hbar^2} \right)^{1/3}, \quad (8A-3)$$

## ELECTRONIC STATES AND OPTICAL TRANSITIONS

we can transform (8A-2) to the standard form

$$\frac{d^2 Z(\xi)}{d\xi^2} - \xi Z(\xi) = 0. \quad (8A-4)$$

The solution of this equation which is regular at the origin is the well known Airy function<sup>[42]</sup>  $Ai(\xi)$ . The eigenvalues of (8A-1) are continuous and given by

$$E = \frac{\hbar^2}{2m} (k_x^2 + k_y^2) + \varepsilon_z,$$

where  $\varepsilon_z$  satisfies (8-A2).

The corresponding eigenfunctions are

$$F(\mathbf{r}) = N e^{i(k_x x + k_y y)} Ai(\xi),$$

where  $N$  is the normalization factor  $(2m)^{1/3}/\pi^{1/2}(eF)^{1/6}\hbar^{2/3}$  required to normalize the probability current density.

We wish here to summarize some mathematical properties of the Airy function. A general definition simpler than (8A-4) is<sup>[48]</sup>

$$Ai(x) = \frac{1}{2\pi} \int_{-\infty}^{+\infty} du \exp \left[ i \left( \frac{u^3}{3} + ux \right) \right]. \quad (8A-5)$$

The asymptotic expression of  $Ai(x)$  for large positive values of  $x$  is

$$Ai(x) \approx \frac{1}{2} x^{-1/4} e^{-(2/3)x^{3/2}}. \quad (8A-6)$$

Thus for large positive values of the argument the Airy function decreases exponentially.

The asymptotic expression of  $Ai(x)$  for large negative values of  $x$  is

$$Ai(x) \approx |x|^{-1/4} \sin \left( \frac{2}{3} |x|^{3/2} + \frac{\pi}{4} \right), \quad (8A-7)$$

which describes a damped oscillatory function with zeroes at

$$x_n = [\frac{3}{2}(n - \frac{1}{4})\pi]^{2/3}, \quad n = 1, 2, 3, \dots$$

A further result which is often used is

$$\int_{\beta}^{\infty} Ai^2(x) dx = -\beta Ai^2(\beta) + Ai'^2(\beta). \quad (8A-8)$$

### References and notes

[1] See, for example: H. E. WHITE, *Introduction to Atomic Spectra* (McGraw-Hill, 1934); E. U. CONDON and G. H. SHORTLEY, *The Theory of Atomic Spectra*, (Cambridge University Press, 1935); G. HERZBERG, *Atomic Spectra and Atomic Structure* (Dover Publications, 1937).

[2] M. CARDONA, Modulation spectroscopy, in *Solid State Physics* (edited by H. EHRENREICH, F. SEITZ, and D. TURNBULL, Academic Press, 1969), suppl. 11.

[3] B. O. SERAPHIN, in *Semiconductors and Semimetals* (edited by R. K. WILLARDSON and A. C. BEER, Academic Press, 1970), vol. 8; D. E. ASPNES and N. BOTTKA, in *Semiconductors and Semimetals* (edited by R. K. WILLARDSON and A. C. BEER, Academic Press, 1970), vol. 9; *Proceedings of the First International Conference on Modulation Spectroscopy* (edited by B. O. SERAPHIN) (North-Holland, 1973).

- [4] L. D. LANDAU, *Z. Physik* **64**, 629 (1930); L. D. LANDAU and E. M. LIFSHITZ, *Quantum Mechanics*. (Pergamon Press, 1958), vol. 3.
- [5] W. PAUL, *J. Appl. Phys. Suppl.* **32**, 2082 (1961). See also the chapter by W. PAUL and D. M. WARSCHAUER in *Solids Under Pressure* (edited by W. PAUL and D. M. WARSCHAUER, McGraw-Hill, 1963); H. G. DRICKAMER, The effects of high pressure on the electronic structure of solid, in *Solid State Physics* (edited by E. EHRENREICH, F. SEITZ, and D. TURNBULL, Academic Press, 1965), vol. 17; W. PAUL, *Proceedings of the International School of Physics "Enrico Fermi"*, course XXXIV on the optical properties of solids (Academic Press 1966), p. 257; R. ZALLEN and W. PAUL, *Phys. Rev.* **134A**, 1628 (1964); **155**, 703 (1967); L. D. LAUDE, M. CARDONA, and F. H. POLLAK, *Phys. Rev.* **1B**, 1436 (1970).
- [6] F. HERMAN, *Proceedings of the Vth International Conference on the Physics of Semiconductors Prague*, 1960, p. 20-28.
- [7] F. BASSANI and D. BRUST, *Phys. Rev.* **131**, 1524 (1963); I. GOROFF and L. KLEINMAN, *Phys. Rev.* **132**, 1080 (1963). For the calculation of the dependence of band structure on the lattice parameter, see also: M. CARDONA and F. H. POLLAK, *Phys. Rev.* **142**, 530 (1966); F. HERMAN, R. L. KORTUM, C. D. KUGLIN, and R. A. SHORT, in *Quantum Theory of Atoms, Molecules and the Solid States* (edited by P. LÖWDIN, Academic Press, 1966).
- [8] F. BASSANI and V. CELLI, *J. Phys. Chem. Solids* **20**, 64 (1961); D. BRUST, J. C. PHILLIPS, and F. BASSANI, *Phys. Rev. Letters* **9**, 94 (1962). See also M. L. COHEN and V. HEINE, Fitting of pseudopotentials to experimental data and applications, in *Solid State Physics*, (edited by H. EHRENREICH, F. SEITZ, and D. TURNBULL, Academic Press, 1970), vol. 24.
- [9] M. ALTARELLI and G. IADONISI, *Il Nuovo Cimento* **5B**, 21 (1971); M. COSTATO, F. MANCINELLI, and L. REGGIANI, *Solid State Commun.* **9**, 1335 (1971).
- [10] R. H. PARMENTER, *Phys. Rev.* **97**, 587 (1955); R. BRAUNSTEIN, A. R. MOORE, and F. HERMAN, *Phys. Rev.* **109**, 695 (1958); M. CARDONA, *Phys. Rev.* **129**, 69 (1963). See also ref. [42] of Chapter 7.
- [11] F. BASSANI, Methods of band calculations applicable to III-V compounds, in *Semiconductors and Semimetals*, (edited by R. K. WILLARDSON and A. C. BEER, Academic Press, 1966), vol. 1, p. 21.
- [12] See, for example, the discussion contained in Chapter 7 of D. L. GRENNAWAY and G. HARBEKE, *Optical Properties and Band Structure of Semiconductors* (Pergamon Press, 1968).
- [13] R. L. AGGARWAL and A. K. RAMDAS, *Phys. Rev.* **137A**, 602 (1965); J. L. MERZ, A. BALDERESCHI, and A. M. SERGENT, *Phys. Rev. B*, **6**, 3082 (1972); L. MARTINELLI and G. SANI, *Solid State Commun.* **12**, 639 (1973).
- [14] W. FRANZ, *Z. Naturf.* **13**, 484 (1958); L. V. KELDISH, *Zh. eksp. teor. Fiz.* **34**, 1138 (1958) (English trans., *Sov. Phys. JETP* **7**, 788 (1958)).
- [15] See, for example: V. S. VAVILOV and K. I. BRITSYN, *Fizika tverd. Tela* **2**, 1937 (1960) (English trans., *Sov. Phys. Solid State*) **2**, 1746 (1961); R. WILLIAMS, *Phys. Rev.* **117**, 1487 (1960); **126**, 442 (1962); T. S. MOSS, *J. Appl. Phys.* **32**, 2136 (1962); A. FROVA and P. HANDLER, *Phys. Rev.* **137A**, 1857 (1965); P. H. WENDLAND and M. CHESTER, *Phys. Rev.* **140A**, 1384 (1965); A. FROVA, P. HANDLER, F. A. GERMANO, and D. E. ASPNES, *Phys. Rev.* **145**, 575 (1966).
- [16] For a general review of tunnelling in solid, see C. B. DUKE, in *Solid State Physics* (Academic Press, 1969), S10.
- [17] W. V. HOUSTON, *Phys. Rev.* **57**, 184 (1940); G. H. WANNIER, *Rev. Mod. Phys.* **34**, 645 (1962); J. CALLAWAY, *Phys. Rev.* **130**, 549 (1963); **134A**, 998 (1964).
- [18] See, for example: A. H. KAHN and A. J. LEYENDECKER, *Phys. Rev.* **135A**, 1321 (1964); A. FROVA and P. J. BODDY, *Phys. Rev.* **153**, 606 (1967); C. GÄHWILLER and G. HARBEKE, *Phys. Rev.* **185**, 1141 (1969).
- [19] B. O. SERAPHIN and R. B. HESS, *Phys. Rev. Letters* **14**, 138 (1965).
- [20] J. C. PHILLIPS and B. O. SERAPHIN, *Phys. Rev. Letters* **15**, 107 (1965).
- [21] D. E. ASPNES, *Phys. Rev.* **147**, 554 (1966).
- [22] R. J. ELLIOTT, *Phys. Rev.* **108**, 1384 (1957).
- [23] K. THARMALINGAM, *Phys. Rev.* **130**, 2204 (1963).
- [24] F. AYMERICH and F. BASSANI, *Nuovo Cimento* **48**, 358 (1967); **56B**, 295 (1968). See also N. BOTTKA and V. ROESSLER, *Sol. State Commun.* **5**, 939 (1967).
- [25] C. PENCHINA, *Phys. Rev.* **138A**, 924 (1965); M. CHESTER and L. FRITSCH, *Phys. Rev.* **139A**, 518 (1965); L. FRITSCH, *Phys. Status Solidi* **11**, 381 (1965); Y. YACOBY, *Phys. Rev.* **140A**, 263 (1965).
- [26] A. FROVA and D. E. ASPNES, *Phys. Rev.* **182**, 795 (1969); M. OKUYAMA, T. NISHINO, and Y. HAMAKAWA, *Jap. J. Appl. Physics* **11**, 1002 (1972).
- [27] B. Y. LAO, J. O. DOW, and F. C. WEINSTEIN, *Phys. Rev. B* **4**, 4424 (1971) and quoted references.

## ELECTRONIC STATES AND OPTICAL TRANSITIONS

- [28] D. E. ASPNES, P. HANDLER, and D. F. BLOSSEY, *Phys. Rev.* **166**, 921 (1968); D. E. ASPNES and J. E. ROW, *Phys. Rev. B5*, 4022 (1972) and related references.
- [29] J. E. FISHER and D. E. ASPNES, *Phys. Status Solidi B* **55**, 9 (1973).
- [30] M. CARDONA, K. L. SHAKLEE, and F. H. POLLAK, Proceedings of the International Conference on Physics of Semiconductors, in *J. Soc. Japan*, vol. 21. Suppl. 89 (1966); V. REHN and D. S. KYSER, *Phys. Rev. Letters* **18**, 848 (1967); D. S. KYSER and V. REHN, *Solid State Commun.* **8**, 1437 (1970); V. REHN and D. S. KYSER, *Phys. Rev. Letters* **28**, 494 (1972). See the critical review by V. REHN, Interband critical-point symmetry from electroreflectance spectra, in *Proceedings of the First International Conference on Modulation Spectroscopy* (edited by B. C. SERAPHIN) (North-Holland, 1973).
- [31] N. BOTTKA and J. E. FISHER, *Phys. Rev. B3*, 2514 (1971).
- [32] F. BASSANI, G. IADONISI, and B. PREZIOSI, *Theory of Impurity States in Semiconductors*, Reports on Progress in Physics (to appear).
- [33] See, for example: J. M. ZIMAN, *Principles of the Theory of Solids* (Cambridge University Press, 1972); C. KITTEL, *Introduction to Solid State Physics* (Wiley 1970).
- [34] See, for example, Y. YAFET, in *Solid State Physics* (edited by H. EHRENREICH, F. SEITZ and D. TURNBULL, Academic Press, 1963), vol. 14, p. 1.
- [35] A. BALDERESCHI and F. BASSANI, *Phys. Rev. Letters* **19**, 66 (1967); *Proceedings of the International Conference on the Physics of Semiconductors. Moscow*, 1968, p. 280. F. BASSANI and M. CINI, to be published.
- [36] B. LAX and J. C. MAVROIDES, in *Solid State Physics* (edited by H. EHRENREICH, F. SEITZ and D. TURNBULL, Academic Press 1960), vol. 11, p. 261; S. D. SMITH, in *Light and Matters* (edited by S. FLÜGGE) (1967), p. 234; L. M. ROTH and P. N. ARGYRES, in *Semiconductors and Semimetals* (edited by R. K. WILLARDSON and A. C. BEER, Academic Press, 1966), vol. 1, p. 159.
- [37] S. O. SARI, *Phys. Rev. B6*, 2304 (1972).
- [38] W. ZAWADSKI, E. HANAMURA, and B. LAX, *Bull. Am. Phys. Soc.* **12**, 100 (1967); F. BASSANI, and R. GIRLANDA, *Optics Communications* **1**, 359 (1970); R. GIRLANDA, *Nuovo Cimento* **6B**, 53 (1971).
- [39] J. M. LUTTINGER, *Phys. Rev.* **102**, 1030 (1956). See also the review article by E. O. KANE in *Semiconductors and Semimetals* (edited by R. K. WILLARDSON and A. C. BEER, Academic Press, 1966), vol. 1, p. 75.
- [40] R. F. WALLIS and H. J. BOWLDEN, *Phys. Rev.* **118**, 456 (1960); R. R. GOODMAN, *Phys. Rev.* **122**, 397 (1961); V. EVTUHOV, *Phys. Rev.* **125**, 1869 (1962).
- [41] C. R. PIDGEON and R. N. BROWN, *Phys. Rev.* **146**, 575 (1966).
- [42] See, for example: R. S. KNOX, Theory of excitons, in *Solid State Physics* (edited by H. EHRENREICH, F. SEITZ and D. TURNBULL, Academic Press, 1963), suppl. 5, p. 79; J. O. DIMMOCK, Introduction to the theory of exciton states in semiconductors, in *Semiconductors and Semimetals* (edited by R. K. WILLARDSON and A. C. BEER, Academic Press, 1967), vol. 3, p. 259; D. G. THOMAS and J. J. HOPFIELD, *Phys. Rev.* **124**, 657 (1961).
- [43] L. J. SCHIFF and H. SNYDER, *Phys. Rev.* **55**, 59 (1938); R. J. WALLIS and H. J. BOWLDEN, *J. Phys. Chem. Solids* **7**, 78 (1958); R. J. ELLIOTT and R. LOUDON, *J. Phys. Chem. Solids* **15**, 196 (1959); O. AKIMOTO and H. HASEGAWA, *J. Phys. Soc. Japan* **22**, 181 (1966); A. G. ZILICH and B. S. MONOZON, *Fizika tverd. Tela* **8**, 3559 (1966) (English trans., *Sov. Phys. Solid State* **8**, 2846 (1967); D. M. LARSEN, *J. Phys. Chem. Solids* **29**, 271 (1968); I. FRITSCHE, *Phys. Status Solidi* **34**, 195 (1969); A. BALDERESCHI and F. BASSANI, *Proceedings of the Xth International Conference on the Physics of Semiconductors* (Cambridge, Mass., 1970), p. 191; D. CABIB, E. FABRI, and G. FIORIO, *Nuovo Cimento* **10B**, 185 (1972). For a recent review of this field, see also F. BASSANI and A. BALDERESCHI, in *Proceedings of the First International Conference on Modulation Spectroscopy Surface Science* **37**, 304 (1973).
- [44] J. L. BREBNER, J. HALPERN, and E. MOOSER, *Helv. phys. Acta* **40**, 385 (1967); J. L. BREBNER, E. MOOSER and M. SCHLÜTER, *Nuovo Cimento* **18 B**, 164 (1973).
- [45] For experimental evidence of exciton transitions in magnetic fields, see, for example: M. CERTIER, C. WECKER and S. NIKITINE, *J. Phys. Chem. Solids* **30**, 1181 (1969); C. WECKER and S. NIKITINE *J. Phys. Chem. Solids* **30**, 2135 (1969); W. STAUDE, *Phys. Letters* **29**, 228 (1969); M. CERTIER, C. WECKER, S. NIKITINE and J. C. MERLE, *Phys. Letters* **33A**, 270 (1970).
- [46] G. J. REES, *J. Physics C*, **5**, 549 (1972); M. ALTARELLI and N. O. LIPARI, *Phys. Rev. B* **9B**, 1733 (1974).
- [47] P. J. LIN-CHUNG and R. F. WALLIS, *J. Phys. Chem. Solids*, **30**, 1453 (1969); W. J. MOORE, *J. Phys. Chem. Solids*, **32**, 93 (1971).
- [48] See, for example: P. WACHER, *Critical Reviews in Solid State Sciences* **3**, 189 (1972); H. W. LEHMAN, G. HARBEKE, and H. PINCH, *J. de Phys.*, Suppl. to Fol. 32, C 1-932 (1971), and related references.

## SUBJECT INDEX

BIBLIOTHÈQUE  
DÉPARTEMENT D'ÉLECTRONIQUE  
Ecole Polytechnique Fédérale  
1015 Lausanne  
CH - 1015 LAUSANNE Suisse  
Tél. 021-471111

Abelian group 2, 41  
 Absorption coefficient 153, 154, 165ff., 170ff.,  
 200, 208ff., 265, 266  
 Acceptors and acceptor levels 242ff., 244, 247  
*see also* Impurity states  
 Accidental degeneracy 17  
 Adiabatic approximation 68ff., 168, 195ff., 287ff.  
 AgCl 141  
 Airy function 272, 292  
 Alkali halides 138ff.  
 Alkali metals  
     band structure 145ff.  
     effective masses 96ff.  
 AlSb 244  
 Angular momentum operators 25, 101  
 Anisotropic crystals 120ff., 134ff., 162ff., 200ff.  
 Annihilation operators 169  
 Anti-linear operator 33  
 Anti-symmetric product representation 39, 66  
 Anti-unitary operator 33  
 APW method 89ff., 145  
 Argon  
     electronic states 138ff., 204  
     excitons 103ff.  
 Axioms for a group 1, 2

Band approximation 70  
 Band structure methods of calculation  
     augmented plane wave 89ff.  
     cellular 86ff.  
     Green's function 91ff.  
      $k \cdot p$  94ff.  
     mixed basis 81  
     molecular tight binding 77, 142ff.  
     orthogonalized plane wave 77ff.  
     perturbative approach to OPW 81ff.  
     pseudopotential 83ff.  
     quantum defect 93ff.  
     relativistic generalizations 97ff., 100ff.  
     tight binding 71ff.  
 Band structures  
     AgCl 141  
     alkali halides 138ff., 197ff.  
     alkali metals 144ff.

Band structures (cont.)  
     alloys 261ff.  
     argon 138ff., 204  
     BN 120ff., 127ff.  
     caesium 146  
     CsI 197ff.  
     diamond 104ff., 108ff.  
     GaAs 118, 247  
     germanium 110ff.  
     graphite 120ff., 125ff.  
     grey tin 115ff.  
     hydrogen 143  
     KCl 142  
     krypton 139  
     layer type crystals 120ff.  
     linear chain type crystals 134ff.  
     lithium 144  
     molecular crystals 142ff.  
     potassium 146  
     selenium 134ff.  
     silicon 110ff.  
     silver halides 138ff., 141  
     simple metals 143ff.  
     sodium 145  
     rare gases 138ff., 204  
     tellurium 134ff.  
     zincblende structure compounds 117ff.  
     III-V compounds 117ff.  
 Basis functions 16ff.  
     for the rotation group 20ff.  
     for the double rotation group 25ff.  
 Bloch functions 43, 70ff.  
 Bloch's theorem 43  
 Bloch sums 71ff.  
 BN 120ff., 127ff.  
 Body centred cubic lattice 144  
 Born-Von Karman cyclic boundary conditions  
     41  
 Born-Oppenheimer approximation 68ff.  
 Bose-Einstein distribution 170, 209  
 Brillouin zone 41ff.  
     body centred cubic lattice 144  
     face centred cubic lattice 46  
     graphite lattice 121, 130  
     simple cubic lattice 198

## SUBJECT INDEX

- Caesium 96ff., 146  
 $\text{CaF}_2$  227  
 Cancellation theorem 84ff.  
 Canonical transformation 168, 278  
 $\text{CdS}$  168, 206  
 $\text{CdTe}$  115  
 Cellular method 86ff.  
 Character of a representation 7  
 Character tables for irreducible representations 8ff., 46ff.  
 BN structure 123ff.  
 diamond structure 49ff., 56ff.  
 graphite structure 123ff.  
 point groups 9ff., 27ff., 201, 221  
 rotation and rotation-inversion group 20ff., 30  
 selenium structure 137  
 translation group 42ff.  
 zincblende structure 116  
 Charge density distribution 133ff.  
 Chemical potential *see* Fermi energy  
 Chemical shift 243  
 Class 2  
 Class product 2, 5, 9  
 Clebsch-Gordon coefficients 226, 229  
 Colour centres 249ff., 267  
 Common group 64ff.  
 Compatibility relations 15, 55, 60  
 Complex conjugate representations 14, 26, 36ff., 61ff.  
 Conduction bands *see* Band structures  
 Core shift 74, 140ff.  
 Core wave functions 74, 78ff.  
 Coset 2ff., 47  
 Coulomb interaction 67ff., 174ff., 178ff., 186ff., 202ff., 211ff., 235ff., 239, 286ff.  
 Covalent bond 107ff., 126ff., 132ff., 141  
 Creation operators 169  
 Critical points 155ff., 160ff., 166ff., 194ff., 273ff., 277ff., 283  
 Crystal field splittings 74, 224, 225ff., 229ff.  
 Crystal momentum representation 232ff.  
 Crystal potential 70, 73ff., 80ff., 88, 117, 129, 219, 232  
 Crystal symmetry 41ff.  
*see also* Little group, Point group, Space group, Translation group  
 $\text{CsI}$   
 band structure 199  
 excitons 197ff., 252  
 Cubic group 3ff.  
 Cubic harmonics 24  
 $\text{CuBr}$  119  
 $\text{CuCl}$  290  
 $\text{Cu}_2\text{O}$  193, 206, 209ff., 290  
 Cyclic group 2, 12, 41ff.  
 Cyclotron frequency 279ff.  
 Darwin term 97ff., 100  
 Davydov splitting 183  
 d-bands 141, 145  
 Degeneracy 16ff.  
*see also* Accidental degeneracy, Essential degeneracy  
 Density of states 155ff., 283  
*see also* Joint density of states  
 Determinantal wave function 69, 151, 172ff., 179ff., 184ff.  
 Diamond  
 band structure 108ff.  
 structure 49ff., 104  
 Dielectric function 153ff., 160ff., 188ff., 204ff., 215, 237ff., 270ff., 281  
 Dielectric screening 70, 204ff., 239  
 d-impurity levels 224, 228  
 Dipole approximation 152  
 Dipole-dipole coupling term 182ff., 196, 202, 214  
 Dirac equation 97ff.  
 Direct product of groups 3, 14ff.  
 Direct product of representations 13ff.  
 Direct transitions 150ff.  
*see also* Optical transitions  
 Dispersion relations 154  
 Distorted orbitals 76  
 Donors and donor levels 237ff., 240ff., 247, 261, 265ff.  
*see also* Impurity states  
 Double group 26ff.  
 Double space group 56ff., 113ff.  
 Effective mass 96ff.  
 Effective mass equation  
 excitons 186ff., 196ff., 215, 286ff.  
 impurities 235ff.  
 in magnetic fields 276ff.  
 Eigenfunctions 15ff., 68ff., 151, 178ff., 232ff., 278ff.  
 Electric field effects 267ff.  
 Electron-electron interaction 67ff.  
 Electron-hole interaction 175, 181, 186, 202, 215, 286  
 Electronic band structure *see* Band structures  
 Electron-phonon interaction 168ff., 206ff.  
 Element of a group 1ff.  
 Empty lattice 82, 88, 105ff.  
 Energy bands *see* Band structures  
 Equivalent representations 6ff., 36, 61  
 Essential degeneracy 16, 17  
 Exchange interaction 69ff., 174ff., 181, 186, 196, 202, 215  
 Excitons 177ff.  
 argon 203ff.  
 $\text{CsI}$  198ff., 200  
 $\text{Cu}_2\text{O}$  193ff., 209ff.

- Excitons (cont.)**
- effective mass approximation 186ff., 196ff.
  - GaSe 189ff., 200, 289
  - indirect transitions 205ff.
  - intermediately bound 201ff.
  - lifetime broadening 206, 211
  - magnetic field effects 286ff.
  - MoS<sub>2</sub> 189ff.
  - optical processes 183ff., 190ff., 205ff., 206ff., 286ff.
  - PbI<sub>2</sub> 201
  - saddle point 195ff.
  - tight binding 178ff., 211ff.
  - two-photon transitions 205ff.
  - weak binding 184ff.
- Extended zone scheme 43, 233
- 
- Face centred cubic lattice 45ff., 104ff.
- Factor group 3, 47, 56
- Faithful representation 6
- f-bands 145
- Fermi energy 106, 114, 143
- Fermi surface 145
- f-impurity levels 224, 228, 229
- Finite group 2
- Forbidden transitions 168, 190
- see also* Selection rules
- Fourier transforms
- crystal potential 78
  - envelope functions 186, 215, 233
  - impurity potential 239
  - pseudopotential 85, 257ff.
- Franck-Condon principle 250, 252
- Franz-Keldish effect 268
- Free electron model 105
- see also* Empty lattice
- Frenkel-Peierls exciton 177ff.
- Frobenius-Schur test 14
- Fundamental unit cell 46, 49
- 
- GaAs
- band structure 118ff.
  - impurity states 244, 247, 261
- GaP 244, 249, 252, 262
- GaS 133
- GaSe 133ff., 189, 200, 289
- Germanium
- acceptor levels 244
  - band structure 112ff., 262
  - donor levels 238
  - indirect transitions 172
  - optical excitation spectrum 160ff.
- Germanium-silicon alloys 262ff.
- g-factor 177
- Graphite 120ff., 162ff.
- 
- Green's function method
- band calculations 91ff.
  - impurities 234ff.
- Group 1ff.
- see also* Abelian group, Character tables for irreducible representations, Cyclic group, Double group, Finite group, Point group, Representation of a group, Rotation group, Space group, Subgroup, Translation group
- Group of the wave vector
- see* Little group
- 
- Hamiltonian operator 1, 15ff., 67ff., 178ff., 218ff., 276ff.
- Hartree-Fock equations 69
- Herring's test 61ff.
- Hexagonal lattice 120ff.
- HF 143
- HgTe 115
- Hydrostatic pressure 156ff.
- H<sub>2</sub> 143
- H<sub>2</sub>O 143
- 
- Identical representation 6
- Identity element 1, 27
- Improper rotations 21
- Impurity states 218ff.
- acceptor 242ff., 244, 247
  - donor 237ff., 240ff., 247, 261, 265ff.
  - effective mass approximation 235ff.
  - intermediately bound 248ff.
  - isoelectronic 249
  - optical processes 251ff., 265ff.
  - resonant 246ff.
  - Sm<sup>++</sup> in SrF<sub>2</sub> 229
  - tightly bound 219ff.
  - weakly bound 231ff.
- Index of refraction 153
- Indirect band-to-band transitions 168ff.
- Indirect exciton transitions 206ff.
- Infinitesimal rotation operator 25
- Inner product 2
- InSb 244
- Insulators 108ff., 138ff.
- Interband transitions 150ff.
- Intermediately bound excitons 201ff.
- see also* Excitons
- Intermediately bound impurities 248ff.
- see also* Impurity states
- Intervalley interaction 240ff., 281
- Invariant subgroup 3, 47ff.
- Inverse of an element 2, 47
- Inversion symmetry 3, 20ff., 26
- Ionic crystals 138ff., 199, 203
- Irreducible representations 6ff.
- see also* Character tables for irreducible representations

## SUBJECT INDEX

- Isoelectronic impurities 248ff.  
Isoelectronic sequence 117ff., 129  
Isomorphic group 2
- Joint density of states 155ff., 160ff., 271ff., 280, 282ff.
- KCl 142  
Kernel 202, 232ff.  
KKR method  
    *see* Green's function method  
Koopman's approximation 150, 174ff., 213  
Koster-Slater model 196  
 $k \cdot p$  method 94ff.  
Kramers-Kronig relations 154  
Kramer's theorem 35ff., 45  
Krypton 139ff.  
Kronecker product of matrices 13  
 $k$  vector 42ff.
- Landau levels 277ff.  
Layer compounds 120ff., 130ff.  
Lifetime broadening 206, 211, 245  
Ligand field mixing 230  
Line of symmetry 47ff., 51, 55  
Linear chain type crystals 134ff.  
Lithium 96ff., 144  
Little group 48ff.  
    BN structure 123ff.  
    diamond structure 49ff., 56ff.  
    graphite structure 123ff.  
    selenium structure 137  
    zincblende structure 116  
Localized functions 71ff., 76, 178, 218ff.  
Logarithmic singularity, density of states 159, 162  
Longitudinal-transverse exciton splitting 183, 196, 202, 214  
Luttinger-Kohn representation 231ff.
- Madelung shift 140ff.  
Magneto-optical effects 276ff.  
Many-body effects 67ff., 70, 204ff., 239  
Metals 143ff.  
Metastable excitons 195ff.  
Methane 143  
Mixed-basis method 81  
Model potential 85  
Molecular crystals 143  
Molecular tight binding method 77, 142ff.  
Momentum matrix elements 95, 152ff., 165ff., 190ff., 251, 281ff.  
MoS<sub>2</sub> 189, 220  
Muffin-tin potential 88ff.  
Multiphoton absorption 164ff., 205ff.
- NaCl 227  
Nearly free electron approximation 86, 145  
Neon 138  
Non-singular matrix 5  
Non-symmorphic space group 47
- One-electron approximation 69  
Optical constants 153ff.  
    *see also* Dielectric function  
Optical transitions 149ff.  
    argon 203  
    CsI 200  
    Cu<sub>2</sub>O 193, 209ff.  
    direct 150ff.  
    electric field effects 272ff.  
    exciton effects 183ff., 190ff., 205ff., 206ff., 286ff.  
    GaSe 200, 289  
    germanium 160ff., 168, 206  
    graphite 162ff.  
    impurities 251ff., 265ff.  
    indirect 168ff., 206ff.  
    magnetic field effects 281ff., 286ff.  
    multiphoton 164ff., 205ff., 281ff.  
    pressure effects 261ff., 265ff.  
OPW method 77ff., 108ff.  
Order of a group 2  
Orthogonality coefficients 79  
Orthogonality theorem  
    irreducible representations 7  
    partner functions 17ff.  
Oscillator strength 194, 289ff.  
Overlap integrals 72ff.
- Parity 9, 19  
Partner functions 17ff.  
Pauli exclusion principle 69, 143ff., 151, 179ff.  
Pauli matrices 23, 97ff.  
PbI<sub>2</sub> 133, 201  
Periodic boundary conditions 41  
Perturbative approach to OPW method 81ff.  
Phonons 168ff., 206ff.  
Plane of symmetry 122ff., 162, 167  
Plane wave expansion 77ff., 79, 85ff., 89, 105ff., 258  
Plasma frequency 154  
Point group 47ff.  
Point impurities *see* Impurity states  
Polarization screening 70, 204ff., 239  
Polarization vector 151ff., 164ff., 184, 190ff., 265ff.  
Polytype 129ff., 130ff.  
Potassium 96ff., 146  
Pressure coefficients 256ff.  
Pressure effects 256ff.  
Primitive lattice translations 42

- Primitive unit cell 46  
 Principal axes 156ff., 186ff., 235ff., 273ff., 276ff.  
 Projection operator 17ff., 75, 79ff., 101  
 Propagation vector 151ff., 164  
 Proper rotation 20  
 Pseudopotential approximation 85ff., 257ff.  
 Pseudopotential method 83ff.  
 Pseudowave functions 83ff., 133ff.
- Quantum defect method 93ff., 145ff.
- Random-phase approximation 204  
 Rare gases 138ff., 203ff.  
 Reality of representations 14, 61  
 Reciprocal lattice 42, 46, 121, 136  
 Reduced effective masses 156ff., 166ff., 186ff., 271ff., 276ff., 287ff.  
 Reduced zone scheme 43, 233  
 Reducible representation 6ff., 38ff., 63ff., 196  
 Refractive index 153  
 Relativistic effects 97ff., 113ff., 118, 137, 198ff., 204, 224ff., 242ff., 284ff.  
 Representation of a group 5ff.  
*see also* Character tables for irreducible representations  
 Repulsive potential 84ff.  
 Resonant states 211, 244ff.  
 Rotation and rotation-inversion group 20ff., 23ff.  
 Rubidium 96ff., 146
- Saddle point 156ff., 160ff., 167, 195ff., 273ff., 277ff.  
 Saddle point excitons 195ff.  
 Schrödinger equation 15ff., 68, 218ff.  
 Schur's lemma 7  
 Screening *see* Dielectric screening  
 Seitz space group symbols 41ff., 46ff.  
 Selection rules 38ff., 63ff., 152, 162ff., 166ff., 172, 197, 251, 281ff.  
 Selenium 134ff.  
 Semiconductors 110ff., 132ff., 134ff., 160ff., 189ff., 237ff., 256ff., 284ff.  
 Semimetals 114ff., 125ff., 162ff.  
 Silicon  
 acceptor levels 244  
 band structure 112ff., 262  
 donor levels 238, 265ff.  
 indirect transitions 172  
 optical properties 161  
 Silicon-germanium alloys 262ff.  
 Silver halides 141  
 Simple cubic lattice 197ff.  
 Simple group 26  
 Simple metals 96ff., 143ff.
- Slater determinant  
*see* Determinantal wave function  
 Slater exchange 69  
 $\text{Sm}^{++}$  in  $\text{SrF}_2$  (impurity states) 227ff., 229  
 Sodium 96ff., 145  
 Space group 46ff.  
 Spherical harmonics 20ff., 24, 79, 86, 89, 226  
 Spin functions 23ff.  
 Spin-orbit interaction 97ff., 113ff., 197ff., 203, 224, 228ff., 284  
 Stark effect 267ff.  
 Stresses  
*see* Pressure and Uniaxial stresses  
 Subgroup 2ff., 15  
 Sum rules 154ff.  
 Symmetric product representation 39, 66  
 Symmetry adapted functions 17ff.  
 augmented plane waves 90  
 Bloch sums 75ff., 101, 107, 108, 126ff.  
 orthogonalized plane waves 80  
 plane waves 79ff., 105ff., 258ff.  
 spherical harmonics 24, 87  
 Symmetry group 3ff., 41ff., 46ff.  
 Symmorphic space group 47
- Tellurium 137ff.  
 Three-photon transitions 168  
 Tight binding  
 band calculation 71ff., 125ff., 138ff.  
 excitons 178ff., 211ff.  
*see also* Excitons  
 impurities 219ff.  
*see also* Impurity states  
 Time reversal symmetry 31ff., 44, 45, 58ff., 65  
 Tin, grey 114ff.  
 Trace (of a matrix) 6  
 Transfer model for excitons 183  
 Transition metals 145  
 Transition probability rate 150ff.  
*see also* Optical transitions  
 Translation group 41ff., 46ff.  
 Transverse excitons 183, 196, 202, 214  
 Tunneling 267ff.  
 Two-centre integrals 73ff.  
 Two-dimensional lattice 120ff.  
 Two-photon transitions 164ff., 205ff.
- Unfaithful representation 6  
 Uniaxial stresses 263ff.  
 Unit cell 46  
 Unitary matrix 6  
 Unitary representation 6ff.  
 Unitary transformation 71, 179
- Valence bands *see* Band structures  
 Van der Waals binding 120

## SUBJECT INDEX

- Van Hove singularities 155ff.  
*see also* Critical points
- Variational principle 69, 72, 77, 78, 90
- Vector potential, electromagnetic 149ff., 164ff.
- Vertical transitions 153  
*see also* Optical transitions
- Wannier-Mott excitons 177, 184ff.
- Wannier functions 71ff., 179ff., 201ff., 234ff.
- Wave functions *see* Eigenfunctions
- Wave vector 42ff.
- Weak binding excitons 184ff.  
*see also* Excitons
- Weak binding impurities 231ff.  
*see also* Impurity states
- Wigner coefficients *see* Clebsch-Gordon coefficients
- Wigner's rules 36
- Wigner-Seitz cell 86ff., 89
- Wigner-Seitz spherical approximation 87ff.
- Xenon 138
- Zeeman effect 255
- Zincblende isoelectronic sequence 117ff.
- ZnS 249, 252
- ZnSe 119